Advancing Profile-Based Curl-and-Warp Analysis Using LTPP Profile Data

PUBLICATION NO. FHWA-HRT-20-066

APRIL 2023

U.S. Department of Transportation
Federal Highway Administration

Research, Development, and Technology
Turner-Fairbank Highway Research Center
6300 Georgetown Pike
McLean, VA 22101-2296

FOREWORD

This report is focused on predicting and quantifying curling and warping of jointed portland cement concrete pavements. Researchers used the comprehensive research-quality datasets available through the Long-Term Pavement Performance (LTPP) program, supplemented by additional datasets collected by other Federal Highway Administration studies. The analyzed test sections are part of either the Specific Pavement Studies-2 or General Pavement Studies-3 LTPP experiments.

Researchers assessed the impact of curl and warp on fluctuations of the International Roughness Index (IRI); generalized relationships between the IRI and pseudostrain gradient (PSG) to less robust datasets (i.e., datasets typically available to State highway agencies); correlated PSG values to environmental factors, falling weight deflectometer results, and measured roughness; and examined the implications of short- and long-term changes in IRI in the appearance of areas of localized roughness. This report is intended for highway pavement engineers and researchers involved in performance analysis of concrete pavements.

Jean A. Nehme, Ph.D., P.E.
Director, Office of Infrastructure
Research and Development

Recommended citation: Federal Highway Administration, *Advancing Profile-Based Curl-and-Warp Analysis Using LTPP Profile Data* (Washington, DC: 2023) https://doi.org/10.21949/1521638

TECHNICAL REPORT DOCUMENTATION PAGE

1. Report No. FHWA-HRT-20-066	2. Government Accession No.	3. Recipient's Catalog No.	
4. Title and Subtitle Advancing Profile-Based Curl-and-Warp Analysis Using LTPP Profile Data		5. Report Date April 2023 6. Performing Organization Code	
7. Author(s) S. M. Karamihas (ORCID: 0000-0002-7480-3952), T. Punnackal, N. Dufalla, K. Senn		8. Performing Organization Report No.	
9. Performing Organization Name and Address NCE 1885 S. Arlington Avenue, Suite 111 Reno, NV 89509		10. Work Unit No. 11. Contract or Grant No. DTFH6114C00015	
12. Sponsoring Agency Name and Address U.S. Department of Transportation Federal Highway Administration Office of Infrastructure Research and Development 6300 Georgetown Pike McLean, VA 22101		13. Type of Report and Period Covered Final Report May 2014–November 2018 14. Sponsoring Agency Code HRDI-30	
15. Supplementary Notes The Contracting Officer's Representative was Larry Wiser (ORCID: 0000-0002-6916-1369), HRDI-30.			
16. Abstract This report is focused on predicting and quantifying curling and warping of jointed portland cement concrete pavements. Researchers used the comprehensive research-quality datasets available through the Long-Term Pavement Performance (LTPP) program, supplemented by additional datasets collected by other Federal Highway Administration studies. The analyzed test sections are part of either the Specific Pavement Studies-2 or General Pavement Studies-3 LTPP experiments. Researchers assessed the impact of curl and warp on fluctuations of the International Roughness Index (IRI); generalized IRI and pseudostrain gradient (PSG) relationships to less-robust datasets (i.e., datasets typically available to State highway agencies); correlated PSG to environmental factors, falling weight deflectometer results, and measured roughness; and examined the implications of short- and long-term changes in IRI in the appearance of areas of localized roughness. Researchers also completed a literature review describing work on profile-based estimates of curl and warp and the influence of curl and warp on the IRI. Theoretical and analytical modeling showed that the original hypothesis of a direct relationship between PSG and IRI was valid, but that the assumption of a linear relationship was incorrect. Researchers proposed an alternative model that produced a high correlation between IRI and PSG on field data with diurnal and seasonal changes in curl and warp.			
17. Keywords Road roughness, longitudinal profile, International Roughness Index, LTPP, pavement testing, pavement rehabilitation, jointed concrete pavement, slab curl and warp, pseudostrain gradient, falling weight deflectometer testing, temperature gradient, load-transfer efficiency, areas of localized roughness		18. Distribution Statement No restrictions. This document is available to the public through the National Technical Information Service, Springfield, VA 22161. http://www.ntis.gov	
19. Security Classif. (of this report) Unclassified	20. Security Classif. (of this page) Unclassified	21. No. of Pages 461	22. Price N/A

Form DOT F 1700.7 (8-72) Reproduction of completed page authorized.

SI* (MODERN METRIC) CONVERSION FACTORS				
APPROXIMATE CONVERSIONS TO SI UNITS				
Symbol	**When You Know**	**Multiply By**	**To Find**	**Symbol**
		LENGTH		
in	inches	25.4	millimeters	mm
ft	feet	0.305	meters	m
yd	yards	0.914	meters	m
mi	miles	1.61	kilometers	km
		AREA		
in^2	square inches	645.2	square millimeters	mm^2
ft^2	square feet	0.093	square meters	m^2
yd^2	square yard	0.836	square meters	m^2
ac	acres	0.405	hectares	ha
mi^2	square miles	2.59	square kilometers	km^2
		VOLUME		
fl oz	fluid ounces	29.57	milliliters	mL
gal	gallons	3.785	liters	L
ft^3	cubic feet	0.028	cubic meters	m^3
yd^3	cubic yards	0.765	cubic meters	m^3
		NOTE: volumes greater than 1,000 L shall be shown in m^3		
		MASS		
oz	ounces	28.35	grams	g
lb	pounds	0.454	kilograms	kg
T	short tons (2,000 lb)	0.907	megagrams (or "metric ton")	Mg (or "t")
		TEMPERATURE (exact degrees)		
°F	Fahrenheit	5 (F-32)/9 or (F-32)/1.8	Celsius	°C
		ILLUMINATION		
fc	foot-candles	10.76	lux	lx
fl	foot-Lamberts	3.426	candela/m^2	cd/m^2
		FORCE and PRESSURE or STRESS		
lbf	poundforce	4.45	newtons	N
lbf/in^2	poundforce per square inch	6.89	kilopascals	kPa
APPROXIMATE CONVERSIONS FROM SI UNITS				
Symbol	**When You Know**	**Multiply By**	**To Find**	**Symbol**
		LENGTH		
mm	millimeters	0.039	inches	in
m	meters	3.28	feet	ft
m	meters	1.09	yards	yd
km	kilometers	0.621	miles	mi
		AREA		
mm^2	square millimeters	0.0016	square inches	in^2
m^2	square meters	10.764	square feet	ft^2
m^2	square meters	1.195	square yards	yd^2
ha	hectares	2.47	acres	ac
km^2	square kilometers	0.386	square miles	mi^2
		VOLUME		
mL	milliliters	0.034	fluid ounces	fl oz
L	liters	0.264	gallons	gal
m^3	cubic meters	35.314	cubic feet	ft^3
m^3	cubic meters	1.307	cubic yards	yd^3
		MASS		
g	grams	0.035	ounces	oz
kg	kilograms	2.202	pounds	lb
Mg (or "t")	megagrams (or "metric ton")	1.103	short tons (2,000 lb)	T
		TEMPERATURE (exact degrees)		
°C	Celsius	1.8C+32	Fahrenheit	°F
		ILLUMINATION		
lx	lux	0.0929	foot-candles	fc
cd/m^2	candela/m2	0.2919	foot-Lamberts	fl
		FORCE and PRESSURE or STRESS		
N	newtons	2.225	poundforce	lbf
kPa	kilopascals	0.145	poundforce per square inch	lbf/in^2

*SI is the symbol for International System of Units. Appropriate rounding should be made to comply with Section 4 of ASTM E380.
(Revised March 2003)

TABLE OF CONTENTS

LIST OF FIGURES

LIST OF TABLES

LIST OF ABBREVIATIONS

AASHTO	American Association of State Highway and Transportation Officials
AC	asphalt concrete
ALR	area of localized roughness
BCI	Byrum curvature index
CI	curvature index
DI	deflection intercept
DMI	distance-measurement instrument
DOT	department of transportation
ER	excess roughness
FHWA	Federal Highway Administration
FWD	falling weight deflectometer
GB	granular base
GPS	General Pavement Studies
HHT	Hilbert–Huang Transform
HRI	Half-car Roughness Index
IMF	intrinsic mode function
IRI	International Roughness Index
JPCP	jointed plain concrete pavement
LCB	lean concrete base
LTE	load-transfer efficiency
LTPP	Long-Term Pavement Performance
MERRA	Modern-Era Retrospective Analysis for Research and Applications
MRI	Mean Roughness Index
PATB	permeable-asphalt-treated base
PCC	portland cement concrete
PSG	pseudostrain gradient
RMS	root mean square
SD	standard deviation
SMP	seasonal monitoring program
SPS	Specific Pavement Studies
TER	total excess roughness

LIST OF SYMBOLS

b	slab length
c_λ	cosine of λ
ch_λ	hyperbolic cosine of λ
$curvature_n$	Three-point estimate of curvature at point n
d_0	deflection measured at the center of the load plate
d_0^*	nondimensional deflection coefficient at the center of the load plate
d_x	peak deflection in inches at sensor offset
h	slab thickness
h_B	average layer thickness of base
h_{GB}	average layer thickness of GB
h_{GS}	average layer thickness of granular subbase
h_{LCB}	average layer thickness of LCB
h_{PATB}	average layer thickness of PATB
h_{PC}	average layer thickness of PCC
h_{TS}	average layer thickness of treated subbase
k	modulus of subgrade reaction
k_{est}	estimated modulus of subgrade reaction
l	radius of relative stiffness
l_{est}	estimated radius of relative stiffness
s_λ	sine of λ
sh_λ	hyperbolic sine of λ
$slope_n$	two-point estimate of slope at point n
x	distance along the slab relative to the slab center
$y(x)$	fitted displacement profile
z	vertical deformation
z_0	uplift at slab ends
A	adjustment factor for nonrandom roughness
AF_{d_0}	adjustment factor for d_0
$AF_{l_{est}}$	adjustment factor for l_{est}
$AREA_7$	deflection basin parameter for the seven-sensor configuration
DI_{J1}	deflection intercept at the slab center
DI_{J2}	deflection intercept at the slab corner
E	elastic modulus of the PCC slab
F	estimated PCC flexural strength
H_0	average relative humidity in the first month after construction
H_1	average relative humidity in the first 10 years after construction
IRI_{Back}	superimposed background roughness.
IRI_{Comb}	IRI of the combined profile
IRI_{Curl}	IRI of the synthetic profile of curl and warp
L	square slab size
L_{slab}	average slab length
L_S	section length
LTE_i	LTE intercept using data from the first 10 years after construction

LTE_s	LTE slope using data from the first 10 years after construction
N	number of points in the roughness profile
N_E	index of the last value above the threshold for the area of localized roughness
N_S	index of the first value above the threshold for the area of localized roughness
P	load magnitude
PSG_i	initial PSG value after construction
PSG_s	rate of change in PSG value after construction
PV	estimated PCC paste volume
R_i	roughness profile at point i
$R_{E,i}$	sum of the ER at point i in the profile
R_T	roughness threshold
T_0	average temperature in the first month after construction
T_1	average temperature in the first 10 years after construction
W_{slab}	average slab width
$\alpha\Delta T/h$	temperature gradient
κ	curvature
λ	nondimensional trigonometric and hyperbolic function argument
μ	Poisson's ratio
Δ_{H0}	average difference between the maximum and minimum daily relative humidity in the first month after construction
Δ_{H1}	average difference between the maximum and minimum daily relative humidity in the first 10 years after construction
Δ_{T0}	average difference between the maximum and minimum daily temperature in the first month after construction
Δ_{T1}	average difference between the maximum and minimum daily temperature in the first 10 years after construction
Δx	profile sample spacing, profile recording interval
Δz	relative uplift
ΔDI	difference between deflection intercept at the slab center and the slab center
ΔDI_i	ΔDI intercept
ΔDI_s	ΔDI slope
ΔT	temperature gradient
$\Delta\varepsilon_{sh}/h$	moisture gradient

CHAPTER 1. INTRODUCTION

This study applied profile-based curl-and-warp analysis to longitudinal profile data from jointed plain concrete pavement (JPCP) test sections within the Long-Term Pavement Performance (LTPP) program. The LTPP program was initiated in 1986 by the Strategic Highway Research Program to collect high-quality performance data for various pavement experiments under varying traffic and environmental conditions. LTPP experiments include General Pavement Studies (GPS) and Specific Pavement Studies (SPS). GPS experiments are divided into types of pavement, including JPCP, which is designated as GPS-3. SPS experiments have multiple test sections per project, and each test section has unique structural factors. SPS-2 projects include JPCP test sections with 12 core test sections and several agency-specified supplemental sections. The core test sections have a unique combination of structural factors as defined by the SPS-2 experimental design and research plan.(1) Supplemental sections typically have unique design properties specified by the local agency. LTPP data have been used to demonstrate the behavior of pavements regarding environmental factors, structural design, and construction practices.

The Federal Highway Administration (FHWA) report, *Curl and Warp Analysis of the LTPP SPS-2 Site in Arizona* (FHWA-HRT-12-068), proposed a method for estimating curl and warp of jointed portland cement concrete (PCC) pavements using the longitudinal profile.(2) The report showed that fluctuations in the measured profile caused by curl and warp, as well as the long-term changes in the profile caused by warp, exhibited a strong statistical correlation to changes in the International Roughness Index (IRI). Consequently, the method for estimating curl and warp of jointed PCC pavements using the longitudinal profile provided a technique to separate roughness associated with curl and warp from long-term changes in roughness caused by other factors. For the low-strength sections within the Arizona LTPP SPS-2 site, this method provided a much clearer view of the structural and functional status throughout the monitoring history than the IRI alone.

The method quantified curl and warp using a pseudostrain gradient (PSG).(3) Researchers assigned PSG values to individual slabs by fitting their measured slab profiles to the profiles produced using the Westergaard solution for determining slab deformation using pavement structural properties. The PSG represents the linear strain gradient required to deform the slab into the measured shape. The average PSG value for all slabs within a test section summarized curl and warp for each profile measurement. The method established site-specific linear relationships between changes in IRI and changes in average PSG using profile measurements from multiple monitoring visits.

The method was successful on the Arizona LTPP SPS-2 site.(2) The method's application, however, required profile measurements on the site over several seasonal and diurnal cycles. The quality of the statistical relationship between PSG and IRI depended on observing large changes in PSG, and a different relationship between IRI and PSG was observed on each test section.

This research applied the PSG-based curl-and-warp analysis to a wider range of LTPP test sections over a more diverse range of climates in support of three lines of investigation, which include the following:

1. Advancement of the profile analysis algorithms and statistical procedures from FHWA-HRT-12-068.[2]
2. Application of the PSG method to investigations of the curl-and-warp phenomena related to structural behavior.
3. Examination of the effect of curl and warp on areas of localized roughness (ALRs).

Each line of investigation depended on a large volume of profile analysis results. This report describes major tasks and analyses performed in support of the research; additional details are presented in the appendices. Chapter 11 provides key findings and recommendations across all elements of the study.

PROFILE ANALYSIS ALGORITHMS

The project team selected five SPS-2 sites and five GPS-3 test sections for analysis based on geographic distribution, life span, and available seasonal data. Chapter 2 describes the SPS-2 and GPS-3 test sections for analysis. Appendix B provides a detailed list of design features and profile-measurement history for each test section.

The research team created a rigorously synchronized profile dataset for iterative and efficient application of the curl-and-warp algorithm. The process for data-quality screening and synchronization ensured consistent placement of joint locations for all profile measurements throughout the monitoring of each test section. Chapter 4 summarizes each stage of the profile data preparation and analysis, including synchronization, data-quality screening, roughness-index calculation, joint finding, and PSG calculation. Appendix A describes a literature review that revisited key references pertaining to estimates of curl and warp based on changes in surface profile and the influence of curl and warp on the IRI. Appendices C through H describe the calculation algorithms and present the outputs of the analyses in detail.

Advancing the profile analysis algorithms and statistical procedures included demonstrations of using PSG to examine curl-and-warp behavior. Chapter 5 demonstrates methods of using PSG to examine changes with time, spatial variations, and differences in behavior among test sections. Advancement of the curl-and-warp analysis also included a detailed examination of the relationship between IRI and PSG for the 83 PCC test sections selected for this study. The linear relationship proposed in FHWA-HRT-12-068 did not adequately describe the relationship between IRI and PSG for the broader dataset used in this research. As such, researchers developed an alternative. Chapter 6 proposes an empirical model that relates IRI and PSG based on theoretical numerical simulation, and chapter 7 presents results from the application of the model to the measured profile data.

INVESTIGATIONS OF STRUCTURAL BEHAVIOR

The investigations related to structural behavior and the profile-based analyses are interrelated because the procedure for estimating PSG requires estimates of pavement structural properties as inputs. Investigations of the curl-and-warp phenomena included correlation to environmental factors and falling weight deflectometer (FWD) results for which PSG estimates functioned as an independent variable. The following research tasks are described in chapters 3, 8, and 9, respectively:

- Estimation of structural factors: structural factors that are required for the calculation of the PSG include layer thicknesses, Poisson's ratio, the elastic modulus of the PCC, and the modulus of subgrade reaction or the composite reaction of base and subgrade layers. These moduli of subgrade reaction, however, were measured from remolding soil samples, which may not accurately represent in-situ conditions. This task, therefore, employed an algorithm provided in *AASHTO Guide for Design of Pavement Structures*, (circa 1993) published by American Association of State Highway and Transportation Officials (AASHTO), which combined the given moduli for each layer into a single composite modulus.[4] Additionally, backcalculation results from *Long-Term Pavement Performance Program Determination of In-Place Elastic Layer Modulus: Backcalculation Methodology and Procedures* (FHWA-HRT-15-036) were available and FWD data were used to backcalculate modulus values.[5] Researchers collected information from these multiple sources and selected the values that represented these variables to be used in the estimation of structural factors.
- Correlation of curl and warp to environmental factors: PSG derived from the profile quantified the level of curvature present in pavement slabs but did not directly imply a climatic cause. The PSG values were correlated to environmental factors to evaluate the effects of climatic factors on pavement curl and warp. Typically, curling is considered a response to differential thermal expansion caused by a temperature gradient. Alternatively, warping is considered the result of differential drying shrinkage resulting from a moisture gradient. This analysis examined the correlation of PSG to available environmental measurements that affect curl, such as temperature gradient, average temperature, and average relative humidity. Detailed results and models produced in this task are provided in appendix I.
- FWD analyses: deflection measurements from FWD testing have the potential to indicate the amount of deflection from curling of pavement. Typically, there is a linear relationship between the load applied at the plate and the deflection of the pavement under the plate. This linear elastic relationship was modeled using deflection measurements at three load levels used in LTPP FWD testing. Linear regression showed that the intercept value typically was not zero, implying an initial deflection was present in the slab prior to loading. This intercept value indicated the presence of uplift in the PCC pavement from curling. FWD analysis explored the relationship between deflection intercept (DI) from FWD testing and PSG values from profile-processing methods. The analysis also compared the relationship between load-transfer efficiency (LTE) and PSG values.

ALR

The analyses described in chapters 5 through 7 demonstrated short- and long-term changes in average IRI values due to curl and warp, as well as long-term changes in roughness caused by other factors. Chapter 10 examines the implications of those changes to the appearance of ALR. The study proposes several methods of quantifying and displaying changes in ALR in terms of location, length, and severity. These methods are used to demonstrate the effect of curl and warp on short- and long-term changes in ALR, persistence and growth of ALR that appears early in the service life of pavement sections, and repeatability of placement and severity of ALR among multiple profile-measurement passes. Appendix J provides a detailed background and analysis of the results.

CHAPTER 2. TEST SECTIONS

Researchers performed the profile measurements analysis on five SPS-2 test sites and five GPS-3 test sections.

Table 1 lists the SPS-2 sites used in this study. SPS-2 sites were selected based on long-term, consistent monitoring of profiles within the LTPP program; diversity of climate; and availability of additional seasonal and diurnal profile measurements from a previous curl-and-warp study performed by FHWA.[6]

Table 1. SPS-2 sites.

State	Climate	Test Sections	Monitoring Duration (Years)	Profile-Measurement Visits	Additional FHWA Visits
Arizona	DNF	21	22	23	Seasonal, diurnal
Kansas	DF	13	23	24	Seasonal, diurnal
North Carolina	WNF	14	21	30	Diurnal
Ohio	WF	19	18	21	Seasonal, diurnal
Washington	DF	13	20	21	Diurnal

DNF = dry/no freeze; DF = dry freeze; WNF = wet/no freeze; WF = wet/freeze.

Table 1 provides the number of test sections at each site. Each site includes 12 core test sections with variations in slab thickness, PCC flexural strength, base design, and slab width that contribute to a broader factorial matrix for the LTPP SPS-2 experiment.[7] Each site also includes supplemental test sections selected by State departments of transportation (DOTs) for comparison to a standard local design or to augment the core matrix.

One site from each of the LTPP climate zones was included. The climate at each site was verified using average monthly rainfall and temperature from the LTPP database. The Kansas site experienced more rainfall than expected for the dry/freeze region.

Table 1 lists total monitoring duration in years and the number of LTPP profile-measurement visits to each site included in this study. Many of the sites were in service when the analysis was completed and were monitored beyond the duration included in this research. The profile measurements at the sites in North Carolina, Ohio, and Washington included three visits over a 24-hour cycle in 2014. Monitoring the North Carolina site included seasonal visits over three annual cycles starting in fall 1997, fall 1999, and fall 2000.

In addition to LTPP profile measurements, the analysis for this study incorporated profile measurements from another FHWA curl-and-warp study.[6] FHWA profile data included diurnal measurements of all five sites listed in table 1 and seasonal measurements of three sites. Diurnal measurements occurred before sunrise, after sunrise, at midafternoon, and after sunset over a single 24-hour cycle. Seasonal measurements occurred once per season over a 1-year cycle, and each seasonal measurement visit included measurements over a diurnal cycle.

Table 2 lists the sections from the seasonal monitoring program (SMP). Additional profile-measurement visits were available from each section. For example, the 38 additional visits to Arizona section 040215 included 19 cases when the section was visited twice in the same day. Thirty-four additional visits to North Carolina section 370201 formed 18 daily groups and completed seasonal measurement cycles from fall 2001 through summer 2003. The 18 daily groups include 11 pairs of visits from the same day and 7 instances when the section was visited 3 times on the same day. The 15 additional visits to section 390204 completed seasonal measurement cycles from winter 1997 through fall 2000.

Table 2. Seasonal monitoring sections.

State	Section	Additional Visits	Daily Groups
Arizona	040215	38	19
North Carolina	370201	34	18
North Carolina	370205	4	3
North Carolina	370208	3	2
North Carolina	370212	2	1
Ohio	390204	15	7

Table 3 lists the GPS-3 test sections. The five GPS-3 sections listed offered geographic diversity, consistent long-term monitoring of profile within the LTPP program, and seasonal and diurnal monitoring within the FHWA study of curl and warp. Sections 063021, 133019, 183002, and 493011 were included in the SMP.

Table 3. GPS-3 sections.

State	Section	Climate	Monitoring Duration (Years)	Profile-Measurement Visits	Additional FHWA Visits
California	063021	DNF	25	21	Seasonal, diurnal
Georgia	133019	WNF	24	39	Seasonal, diurnal
Indiana	183002	WF	25	31	Diurnal
Minnesota	273003	WF	18	12	Seasonal, diurnal
Utah	493011	DF	26	31	Seasonal, diurnal

DNF = dry/no freeze; DF = dry freeze; WNF = wet/no freeze; WF = wet/freeze.

Thirty-nine visits to section 133019 included seasonal visits over 4 annual cycles starting in spring 1992, starting in winter 1996, starting in fall 1997, and starting in spring 2000. Visits were made in 11 pairs, meaning that 2 visits were performed at different times on the same day. Thirty-one visits to section 183002 included seasonal visits over 1 annual cycle starting in fall 1997. The visits also included four pairs of visits performed at two different times of the day and three other groups of visits performed at three different times on the same day. Thirty-one visits to section 493011 included seasonal visits over 4 annual cycles starting in fall 1993, starting in fall 1994, and starting in fall 1996. The visits also included five pairs of visits performed at two different times of the day. Appendix B provides a detailed listing of design features and a profile-measurement history for each test section.

CHAPTER 3. METHODS FOR ESTIMATING STRUCTURAL FACTORS

The PSG value is empirically estimated using profile data and the Westergaard curve-fitting procedure. This procedure assumes an idealized profile based on assumptions of linear temperature and moisture gradient throughout the full depth of the slab, which has ends that are unrestrained and a width that is infinite along the undeformed axis. The PSG is then estimated as the value required for the idealized profile to fit the measure profile along each slab.(2)

To calculate PSG, certain structural factors for each section needed to be estimated as inputs for the Westergaard procedure: elastic modulus of the PCC slab (E), Poisson's ratio (μ), modulus of subgrade reaction (k), and PCC slab thickness (h). This analysis used both AREA and Best Fit methods for estimating structural factors, k and E, which were evaluated in *Long-Term Pavement Performance Program Determination of In-Place Elastic Layer Modulus: Backcalculation Methodology and Procedures* (FHWA-HRT-15-036).(5) The analysis resulted in two sets of structural factors used to compute PSG values.

ESTIMATING LAYER THICKNESS AND POISSON'S RATIO

AREA and Best Fit methods used the same PCC layer thickness and assumed a μ of 0.15. Generally, μ for PCC ranges from 0.15 to 0.20; 0.15 typically represents concrete with a higher stiffness. Assuming the value of μ is reasonable, as minor changes in μ would not result in significant error in calculating the shape of the Westergaard idealized profile. The other structural factors (E, k, and h) were more significant in determining the PSG.

The value for h was taken from data table TST_L05B of the LTPP InfoPave™ database.(8) This value is the representative thickness of the PCC layer and is usually estimated based on pavement cores taken before and after each test section. The pavement cores were measured in accordance with LTPP protocol AC01.(8) The thickness of a pavement layer from the beginning of a test section to its end is not perfectly uniform; averages from core measurements typically provide the best representation for the section as a whole.

ESTIMATING STRUCTURAL FACTORS

Most test sections in the LTPP program have been sampled and have undergone laboratory material testing using LTPP testing protocols.(8) LTPP data, however, do not provide information on the stiffness of treated bases. Material testing on treated bases was limited to compressive strength testing and was only performed on four SPS-2 test sections in Michigan. The stiffness of treated bases was necessary to estimate the modulus of subgrade reaction of a composite pavement. Additionally, the modulus of subgrade reaction was measured by remolding soil samples, which may not represent the in-situ condition of the material. Therefore, estimations of material properties using FWD backcalculation were used to provide consistent data. However, there is a small source of error that inevitably occurs with FWD backcalculation because of the compensating layer effect. This effect is common in pavements with layers that are not clearly defined, undistressed, and homogenous, and results in the modulus of layers being overestimated or underestimated relative to the modulus of an adjacent layer. This research evaluated the results from two methods, AREA and Best Fit, for estimating E and k.

ESTIMATING STRUCTURAL FACTORS USING THE AREA METHOD

The AREA method uses a backcalculation algorithm to estimate the radius of relative stiffness (l), k, and E. Unlike the Best Fit method, the AREA method is not iterative and is based on the AREA parameter.[9] In either method, both E and k values have an inverse relationship in determining the FWD deflection basin because of the compensating layer effect. The following equations (figure 1 through Figure 8) were used to estimate k and E.

The deflection basin parameter for the seven-sensor configuration ($AREA_7$) is the stiffness of the pavement layer relative to the subgrade. The value is computed using deflection measured by seven sensors at various offsets from the center of the load plate. Early FWD testing was performed using seven sensors with typical offsets of 0, 8, 12, 18, 24, 36, and 60 inches. The sensor at 8 inches would sometimes be moved to −12 (before the plate) for LTE testing. However, in 1999, the LTPP FWD equipment changed to nine sensors with typical offsets of −12 (before the plate), 8, 12, 18, 24, 36, 48, and 60 inches. For consistency, the $AREA_7$ did not consider sensor offsets that only appear after 1999. The value is normalized to the deflection measured at the center of the load plate (d_0), as shown in figure 1.

$$\boldsymbol{AREA_7 = 4 + 6\left(\frac{d_8}{d_0}\right) + 5\left(\frac{d_{12}}{d_0}\right) + 6\left(\frac{d_{18}}{d_0}\right) + 9\left(\frac{d_{24}}{d_0}\right) + 18\left(\frac{d_{36}}{d_0}\right) + 12\left(\frac{d_{60}}{d_0}\right)}$$

Figure 1. Equation. Calculation of the $AREA_7$ parameter.

Where:

d_x = peak deflection in inches at sensor offset.

$AREA_7$ = a maximum value of 60, which would be an extremely stiff pavement. A minimum value of 4 would be an extremely soft pavement. However, the minimum and maximum values would be too extreme to be achievable for actual pavement.

The equation in figure 2 is an empirical computation for the estimated radius of relative stiffness (l_{est}) and is based on correlation to the $AREA_7$ value. Both l_{est} and $AREA_7$ are values that express the relative stiffness between the pavement and the subgrade. Westergaard's idealized profile computes l_{est} from E, k, μ, and h. In theory, the l_{est} value estimated from the $AREA_7$ value could be input directly in Westergaard's curve-fitting procedure, which would minimize the error in the idealized profile created from the compensating layer effect between E and k. For this reason, there is an expectation that PSG values derived from the AREA method would be more accurate than those derived using the Best Fit method because l_{est} is derived from the shape of the deflection basin. The AREA method, however, relies on empirical data that precede LTPP. Therefore, the values produced by both methods were compared.

$$\boldsymbol{l_{est} = \left[\frac{\ln\left(\frac{60 - AREA_7}{289.708}\right)}{-0.698}\right]^{2.566}}$$

Figure 2. Equation. Calculation of l_{est}.

Figure 3 shows the equation for the nondimensional deflection coefficient at the center of the load plate (d_0^*). The equation is used to estimate the modulus of subgrade reaction and the nondimensional deflection under the center of loading plates based on the radius of relative stiffness.

$$d_0^* = 0.1245e^{\left[-0.14707e^{(-0.07565l_{est})}\right]}$$

Figure 3. Equation. Calculation of d_0^*.

Figure 4 shows the equation for the estimated modulus of subgrade reaction (k_{est}). P is load magnitude. The equation is used to estimate the dynamic subgrade modulus estimated from the deflection measured at d_0.

$$k_{est} = \frac{Pd_0^*}{d_0 {l_{est}}^2}$$

Figure 4. Equation. Calculation of k_{est}.

The adjustment factor equation for d_0 (AF_{d_0}) is presented in figure 5. L equals square slab size. This equation is based on d_0 and used to correct the estimated modulus of subgrade reaction for slab size, which was assumed to be an infinite plate in the Westergaard solution.

$$AF_{d_0} = 1 - 1.15085e^{-0.71878\left(\frac{L}{l_{est}}\right)^{0.80151}}$$

Figure 5. Equation. Calculation of AF_{d_0}.

Figure 6 shows the adjustment factor equation for l_{est} ($AF_{l_{est}}$). The equation is based on l_{est} and used to correct the estimated k for slab size, which was assumed to be an infinite plate in the Westergaard solution.

$$AF_{l_{est}} = 1 - 0.89434e^{-0.61662\left(\frac{L}{l_{est}}\right)^{1.04831}}$$

Figure 6. Equation. Calculation of $AF_{l_{est}}$.

Figure 7 shows the equation for k. The equation is used to correct slab size and addresses the generalized limitations of Westergaard's infinite slab solution by correcting to a solution for a finite circular slab.

$$k = \frac{k_{est}}{\left(AF_{l_{est}}\right)^2 AF_{d_0}}$$

Figure 7. Equation. Calculation of the corrected k.

Figure 8 shows the equation for E. The value of μ is assumed to be 0.15, and h is the representative thickness of the PCC pavement.

$$E = \frac{12(1-\mu^2){l_{est}}^4 k}{h^3}$$

Figure 8. Equation. Calculation of *E*.

ESTIMATING STRUCTURAL FACTORS USING THE BEST FIT METHOD

The *k* and *E* using the Best Fit method is a computed parameter from the data table BAKCAL_BEST_FIT_SECTION_LAYER in the LTPP database.(8) The computed unbonded modulus of the PCC layer was averaged to represent *E* in this dataset.

The Best Fit method iterates through predicted deflection basins computed from *k* and *l*. The Best Fit method solves for *k* and *l* values that show the best agreement between the profile of the measured and predicted deflection basins.(10)

In contrast to the AREA method, the Best Fit method does not rely on empirical data. The structural factors are estimated in the Best Fit method so that errors in the predicted deflection are minimized.

COMPARING AREA AND BEST FIT METHODS

Figure 9 plots the *k* values estimated from the AREA and Best Fit methods. The two methods produced similar *k* values. The *k* values from the AREA method were slightly higher than the values from the Best Fit method.

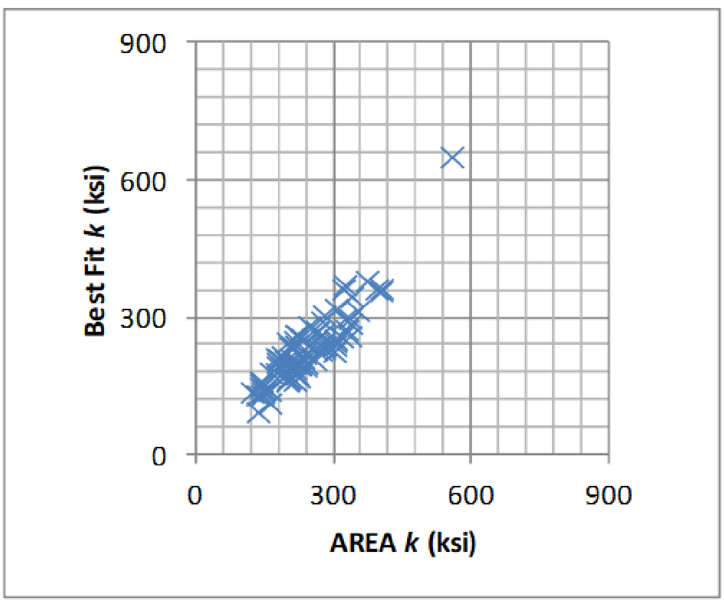

Source: FHWA.

Figure 9. Graph. AREA versus Best Fit method for estimating *k*.

Figure 10 plots the *E* estimated from the AREA and Best Fit methods. In several cases, *E* was estimated by the AREA and Best Fit methods to be similar in value. However, in several other cases, *E* was estimated to be slightly higher when using the Best Fit method than when using the

AREA method. This relationship is the opposite of *k*, but that was expected because *E* and *k* have a compensating effect on the deflection basin. The outliers in figure 10 indicated the AREA method overestimated *E* compared to the Best Fit method. The difference in estimated values appeared more often in pavements with a lean concrete base (LCB). The *E*, *k*, and l_{est} values for each section can be found in appendix F. Both Best Fit and AREA methods have estimated *E* values higher than the expected average of 4,000 ksi and in some cases higher than the expected maximum of 10,000 ksi.

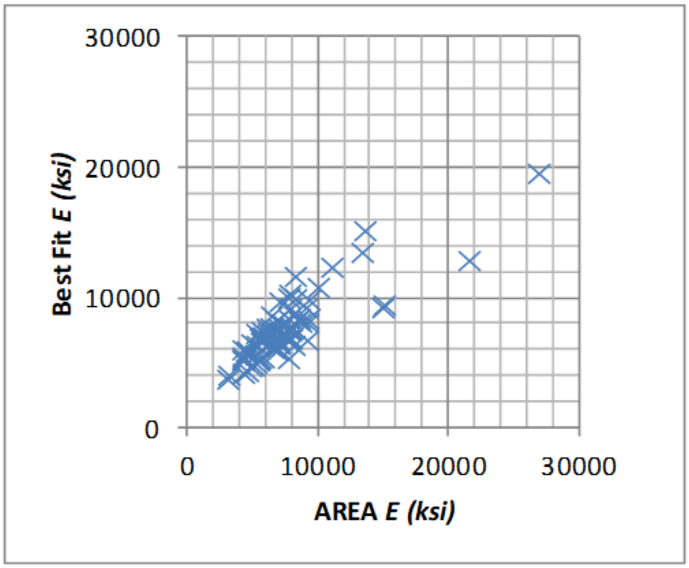

Source: FHWA.

Figure 10. Graph. AREA versus Best Fit method for estimating *E*.

Figure 11 plots the *l* values from the AREA and Best Fit methods. The plot illustrates the level of consistency between the two methods, especially considering the compensating effect between *E* and *k*. The PSG value derived by fitting to a measured slab profile varies approximately with the inverse of the square of radius of relative stiffness for a given level of uplift at the slab ends (see Figure 14 for the equation to compute uplift at the slab ends). However, in terms of uplift, the curve-fitting results vary slightly for the differences between the AREA and Best Fit methods as shown in figure 11.

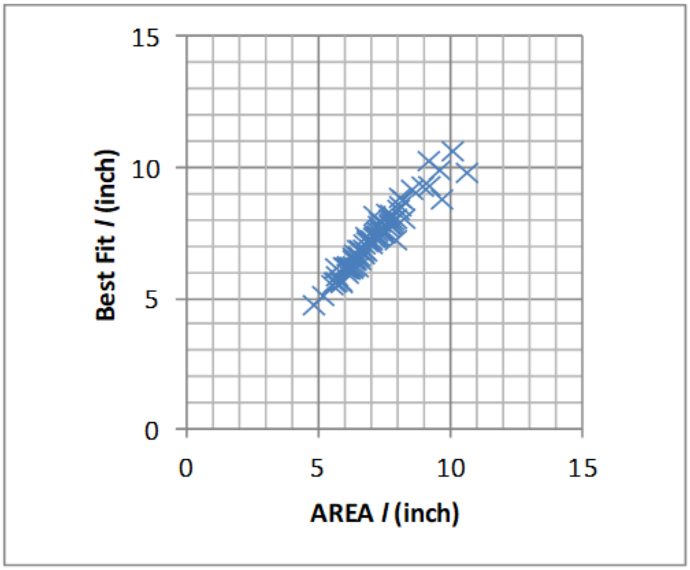

Source: FHWA.

Figure 11. Graph. AREA versus Best Fit method for estimating *l*.

CHAPTER 4. PROFILE DATA ANALYSIS

SYNCHRONIZATION

Profiles were extracted directly from the raw measurements and aligned using automated synchronization to an initial basis profile. In automated synchronization, each candidate profile is aligned to a basis measurement using cross-correlation. The procedure iteratively searched for the longitudinal offset and longitudinal distance-measurement scale factor that maximized the correlation between the candidate profile and the basis measurement. Computer programs used for automated synchronization performed cross-correlation after applying the IRI algorithm to the candidate and basis profiles.

Researchers used an automated synchronization procedure in these studies similar to a procedure applied in other studies of long-term roughness progression on LTPP SPS sites.(2,11–13) In those studies, the procedure aligned the profiles by adjusting their longitudinal offset. In this study, the procedure aligned the profiles over their entire extent by adjusting the longitudinal offset and applying a scale factor to the recording interval of each candidate measurement. This procedure ensured consistency of joint locations over the complete monitoring of each section, which expedited joint finding and curl-and-warp analysis.

Table 4 lists the source (i.e., section or site) of the initial basis profiles by visit number, measurement date, and repeat number for each GPS-3 section and SPS-2 site. Appendix B provides additional information on visit numbers. A basis profile for each section was selected from raw profile data recorded at an interval of 1 inch or less. Profile data were collected at an interval of 1 inch or less starting in late 1996.(14) For each SPS-2 site, basis profiles were selected from a profile measurement for which a complete set of event markers for section starting points were stored within the raw data. Spacing of event markers reconciled closely with the test section layout published in the construction reports.(15–19)

Table 4. Source of initial basis profiles.

Section/Site	Visit	Measurement Date	Repeat
Section 063021	13	04-Dec-2004	1
Section 133019	15	16-Oct-1997	1
Section 183002	14	05-Dec-1997	1
Section 273003	06	01-Aug-1997	1
Section 493011	12	05-Dec-1996	1
Site 040200	08	08-Nov-2001	1
Site 200200	06	03-Mar-1997	2
Site 370200	12	14-Jul-2001	7
Site 390200	03	08-Dec-1997	2
Site 530200	03	15-May-1998	1

For visits listed in Table 4, profiles of the remaining repeat measurements were automatically synchronized to the initial basis profiles. For subsequent visits, profiles were extracted from raw measurements of each test section using the following steps:

1. Synchronize profiles from the current visit to the basis measurement from the previous visit.
2. Designate the repeat measurement from the current visit with the highest correlation to the basis measurement from the previous visit as the basis measurement from the current visit.
3. Synchronize profiles from the current visit to the basis measurement from the current visit.
4. Repeat steps 1 through 3 until the final visit is complete.

Progress backward through the visits that precede the initial basis measurement using steps 1 through 4.

Before extracting the individual profiles as described in steps 1 through 4, the longitudinal offset and recording interval of raw measurements over SPS-2 test sites were automatically adjusted to improve their compatibility with the raw measurement designated for extracting initial basis measurements. The adjustment reduced the computation time needed during the iterative portion of the automatic synchronization process.

QUALITY SCREENING

Visits to each test section included up to nine repeat profile measurements. Researchers selected the five measurements that exhibited the best agreement with each other for further analysis. Agreement between two profiles was judged by cross-correlating the profiles after applying the IRI filter. The average correlation level produced by these calculations provided a quantitative assessment of the repeatability within each set of repeat measurements. Overall, the selected data included 9,570 profiles from 1,941 section visits. Appendix C includes a list of the five selected repeat measurements from each visit to each section and a detailed description of the selection process.

SUMMARY ROUGHNESS VALUES

Appendix D provides roughness progression plots for the 85 test sections included in this study. These plots show the left and right IRI values from each visit during the monitoring period. Appendix D also lists the Mean Roughness Index (MRI) and Half-car Roughness Index (HRI) of each section for each visit. These IRI, MRI, and HRI values are the average of the five repeat measurements selected in the quality screening. Appendix D also provides the standard deviation (SD) of the IRI for the five repeat measurements. High SD values help identify erratic roughness values resulting from transverse variations in the pavement surface caused by surface distresses.

JOINT FINDING

Estimating curl and warp required isolating individual slab profiles by identifying joint locations. Researchers needed to identify joint locations consistently to help ensure changes in estimates of curl and warp were caused by genuine changes in slab movement rather than inconsistencies in the assumed slab boundaries. Precise identification (to the extent possible) of joint locations helped incorporate as much of the longitudinal range of profile within a slab as possible, particularly at slab ends where changes in elevation because of curl and warp are often the largest.

The algorithm for finding joint used in this research was similar to the algorithm applied in the Arizona SPS-2 site study of curl and warp.[2] The method identified potential joint locations by seeking narrow downward spikes in each profile, prioritized locations where the spikes appeared consistently in repeated profile measurements and on both sides of the lane with provisions for skewed joints, and sought the set of prioritized locations that best approximated a known joint spacing or saw-cut spacing pattern. Appendix E describes the application of the method in detail.

The algorithm succeeded in locating all joints for profiles collected from December 1996 through January 2013 because those profiles were measured using narrow footprint-height sensors. A narrow footprint height sensor detects the height of the road surface by projecting (and detecting) light over a relatively small area on the pavement surface. As a result, narrow spikes appeared within the profiles at the locations of joint openings. Profile data collected before December 1996 were measured using height sensors with wider footprints and recorded after the application of low-pass filtering. Narrow spikes did not appear in the joints within in these profiles, and joint locations were assumed to be the same as the nearest visit for which the spike-detection algorithm succeeded. The profile synchronization process, described in the beginning of chapter 4, enforced consistency in longitudinal distance measurement for all profiles throughout the monitoring history of each section.

After January 2013, high-speed profilers recorded the profile measurements after applying low-pass filtering, which removed more short-wavelength content than the high-speed profilers used before January 2013. Downward spikes that appear in measured profiles at the joints did not stand out relative to other content within from the Washington SPS-2 site because those test sections included coarse surface texture. Joint locations for profiles collected after January 2013 at the Washington site were assumed to be the same as the last visit from before January 2013.

In some cases, the curl-and-warp analysis was terminated prior to the end of the monitoring period because of changes in the structural status of the test section. These changes included the installation of wide patches at joints on sections 200205 and 493011, diamond grinding of section 200210, patching and slab replacement on sections 390208 and 390212, and placement of an asphalt overlay on section 183002.

CURL-AND-WARP ANALYSIS

Curl-and-warp levels present within each profile were estimated using slab-by-slab analysis of local profile segments. The procedure quantified the level of curl and warp on each slab using PSG. PSG is the gross strain gradient required to deform a slab into the shape that appears within the measured slab profile from a flat baseline. The PSG value for each slab was derived using a curve fit between the measured profile and an assumed slab shape predicted by the Westergaard equation.[20] Appendix F presents the Westergaard equation and details about the curve-fitting procedure.

The Westergaard equation predicts the change in slab profile that has deformed in response to a linear strain gradient throughout its depth. The underlying model assumes that the slab rests on a dense liquid foundation. The equation includes slab length, Poisson's ratio, and radius of relative stiffness. In turn, radius of relative stiffness depends on elastic modulus, slab thickness, modulus of subgrade reaction, and Poisson's ratio.

For this study, material properties were assumed to be constant for a given section throughout the section's distance and monitoring history. LTPP database table L05B provided slab thickness values, which were primarily based on cores collected at the ends of each section. Elastic modulus and modulus of subgrade reaction were derived from FWD testing using two methods of analysis: AREA and Best Fit. Appendix F provides the material properties derived from each method.

The analysis for the structural properties produced a PSG value for each slab with every profiler's pass over an individual test section. Depending on the test section, this included 24 to 42 slabs that were within the test section boundaries. The analysis also included slabs at each end of the test section that were partially within the test section boundaries. A typical test section with 15-ft-long slabs included either 32 or 33 slabs that were completely within the test section boundaries. The analysis was applied to 876,211 slab profiles.

PSG values for a given profile-measurement visit were analyzed by examining the distribution of PSG values within a test section and the spatial variation within a test section. The PSG values for a given slab were summarized by averaging PSG values for the five (or fewer, in some cases) repeat profile measurements from each visit to a test section. Sectionwide PSG averages were examined for long-term changes, diurnal variations, and seasonal variations over multiple visits.

CHAPTER 5. CURL-AND-WARP BEHAVIOR

DETAILED VIEW

Figure 12 shows a detailed view of the curl-and-warp behavior evident in the left profiles of section 133019 throughout that section's monitoring history. The figure shows whisker plots of PSG values from each set of five repeated profiler passes. PSG values were derived using an estimate of *l* of 34.1 inches, which was produced by the Best Fit method. Positive PSG values correspond to downward curl.

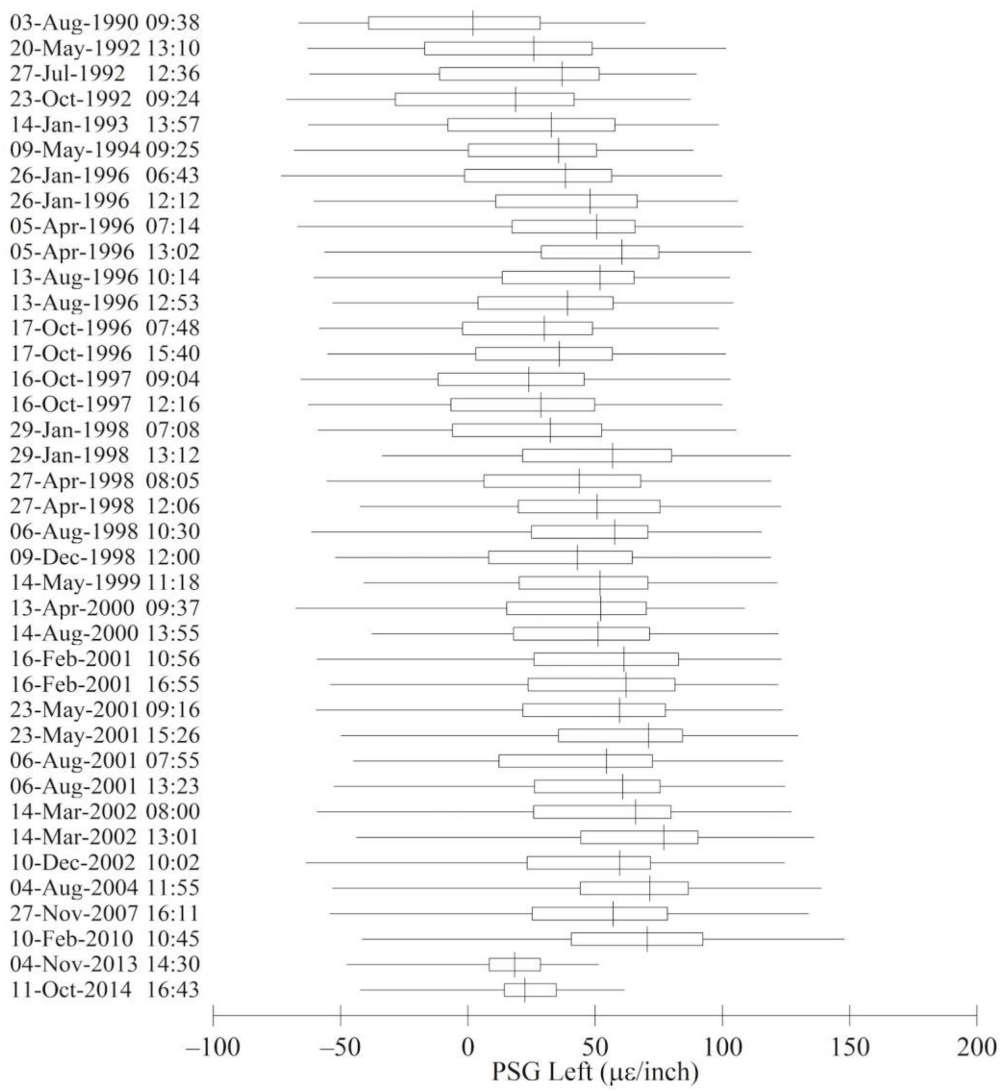

Source: FHWA.

Figure 12. Graph. Detailed view of curl-and-warp behavior in left profiles of section 133019.

Each row in figure 12 shows the minimum, 25th percentile, median, 75th percentile, and maximum PSG value for 120 slab profiles. The 120 slab profiles correspond to 24 slabs within the test section and 5 passes over the section per visit. The figure lists the date of each visit and the time of the first profiler pass. PSG values from individual slabs do not necessarily characterize curl-and-warp behavior because the profile of each slab includes other sources of irregularity, such as construction defects, grade changes, and distress. However, the median PSG values shown for each visit are associated with the amount of curl and warp present at the time because the influence of other irregularities is compensated over many slabs. Differences in median PSG values between visits are of interest because the differences are associated with cyclic and long-term changes in curl and warp.

Figure 12 illustrates several aspects about the curl-and-warp behavior of section 133019. First, the prevailing curl and warp on section 133019 is downward. The median value of the PSG is near zero for the first monitoring visit and is positive for all subsequent visits, which corresponds to downward curl. Second, the downward curl increases unsteadily over the first 20 years of monitoring. The overall increase in median PSG may have implications to the structural status of the section but is obscured by short-term changes. Third, section 133019 exhibits diurnal changes in slab curl. For example, figure 12 includes nine visits that occurred prior to 9:30 a.m. followed by a subsequent visit in the afternoon the same day. In every case, the median PSG value was higher in the afternoon, which is associated with an increase in downward curl caused by an increase in surface temperature. The two diurnal pairs shown in figure 12 with an initial visit after 10 a.m. did not follow this trend. Fourth, section 133019 may exhibit seasonal changes in curl.

Figure 12 includes seasonal measurements in 1996, 1998, and 2001. Median PSG values fluctuated throughout each interval, and fluctuations were the largest in 1996. However, explicitly distinguishing diurnal, seasonal, and long-term changes in PSG required knowledge of the temperature and moisture environment of the slab.

Finally, the magnitude of curl detected in the last two visits is reduced. Surface grinding performed in late 2010 reduced the roughness on this section. The postgrind PSG values are shown in figure 12 to illustrate the change in apparent slab curl. The difference in pregrind and postgrind PSG values does not, however, imply a change in the internal stress state of the pavement.

TRENDS WITH TIME FOR SECTIONWIDE CURL

Figure 13 summarizes the trends in prevailing curl and warp with time on section 133019. The figure shows a weighted average of PSG values from each profile-measurement visit. Like the data in figure 12, PSG values were derived using an *l* value produced by the Best Fit method. The weighted average incorporates slab-by-slab PSG values from repeat passes (typically five passes) selected for each monitoring visit. The contribution of the PSG value from each slab profile is weighted by slab length, which has a constant nominal value on section 133019. Figure 13 expresses the age of section 133019 in years since the date of construction for each visit.

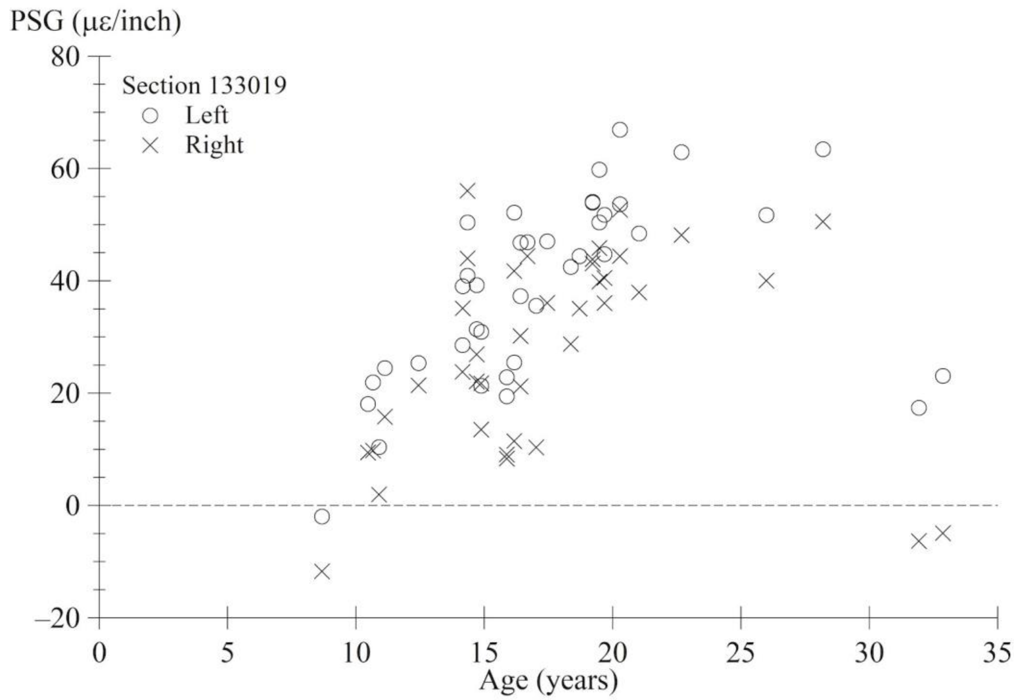

Source: FHWA.

Figure 13. Graph. Average PSG values versus time using Best Fit method for section 133019.

Figure 13 illustrates the direction of slab curl and warp observed in section 133019 and the long-term trend. The figure also demonstrates the magnitude of seasonal and diurnal changes in curl relative to the prevailing level. Appendices G and H provide plots in the same format as Figure 13 for PSG values derived using the Best Fit and AREA methods, respectively, for each test section.

The trends in PSG derived using the Best Fit and AREA methods were similar. In the Westergaard deflection equation used to produce curve fits for estimating PSG, the uplift at the slab ends (z_0) is proportional to the product of PSG and l^2, as shown in Figure 14.

$$z_0 = -PSG(1+\mu)l^2$$

Figure 14. Equation. Uplift at slab ends.

Poisson's ratio (μ) was assumed to be 0.15.

Fitted PSG values from the Best Fit and AREA methods correlate closely when they are scaled by the square of their respective estimates of l. Values of slab-end uplift for fitted profiles were closely correlated between the two methods. For example, plots in appendices G and H each include 1,877 PSG values for the left-side profiles. The corresponding uplift values range from −0.21 to 0.19 inches, and the largest difference between the AREA and Best Fit methods is 0.0026 inches. Therefore, results are provided for the Best Fit method only in the remainder of this discussion.

Figure 15 through Figure 20 summarize the curl-and-warp behavior of the test sections included in this study. The figures group SPS-2 test sections by site; the five GPS-3 sections appear in the same figure. These figures show the weighted PSG ranges observed over the monitoring period for each section included in this study. The figures show PSG values derived using the *l* value produced by the Best Fit method.

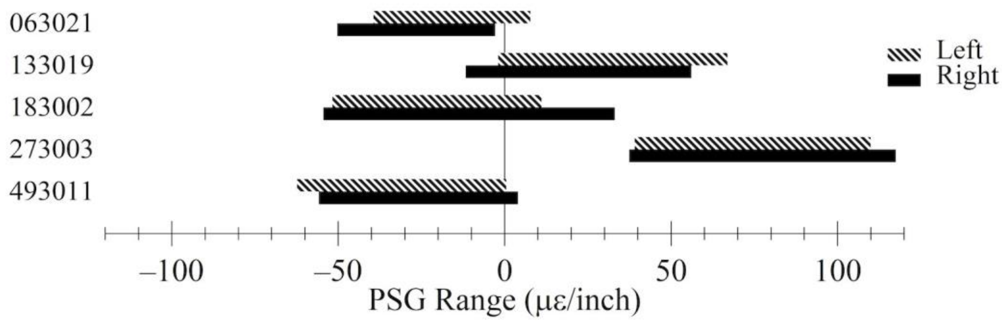

Source: FHWA.

Figure 15. Graph. Weighted PSG ranges for GPS-3 test sections.

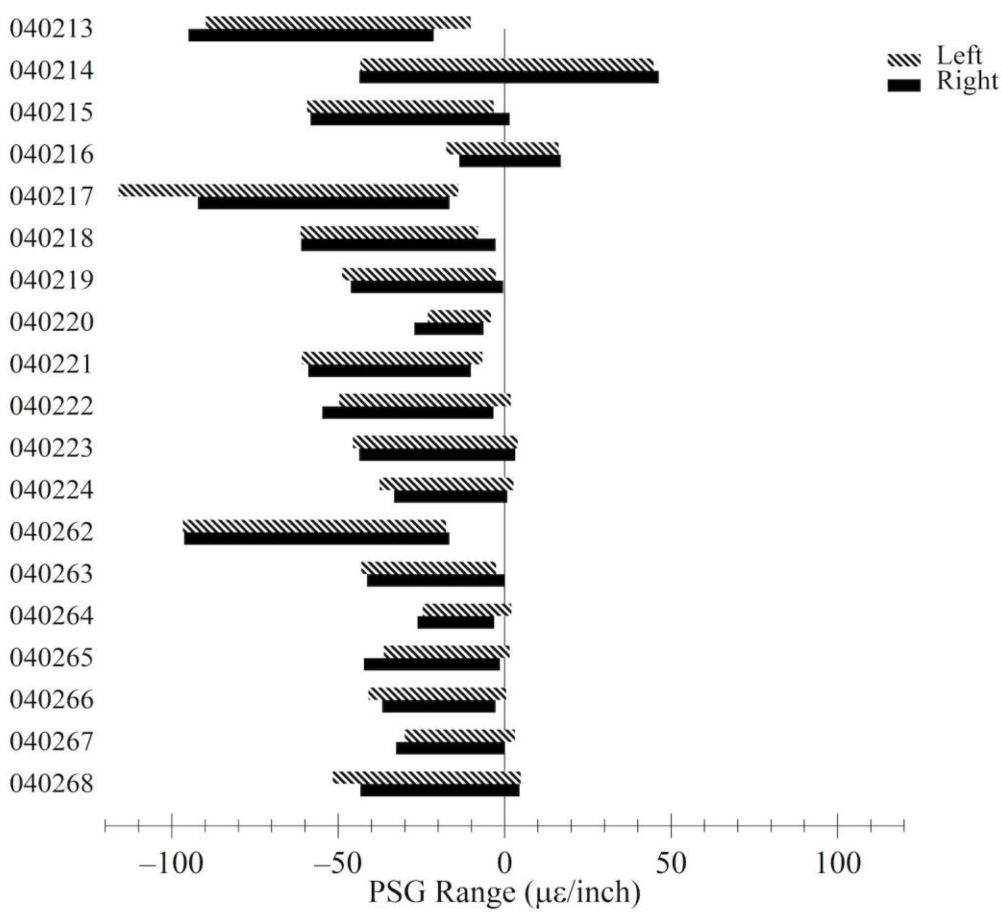

Source: FHWA.

Figure 16. Graph. Weighted PSG ranges for Arizona SPS-2 test sections.

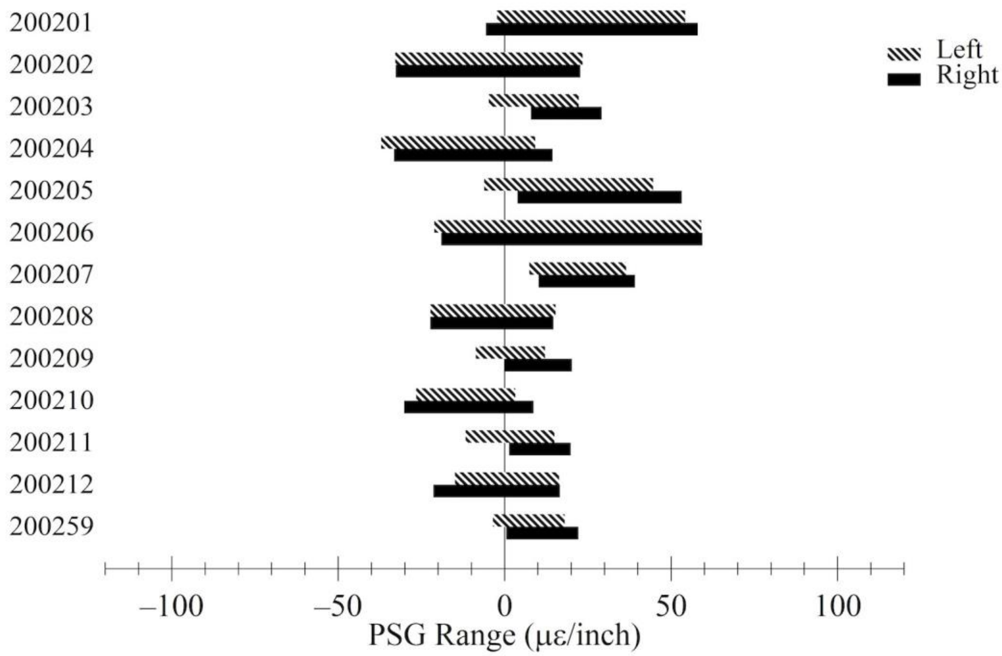

Source: FHWA.

Figure 17. Graph. Weighted PSG ranges for Kansas SPS-2 test sections.

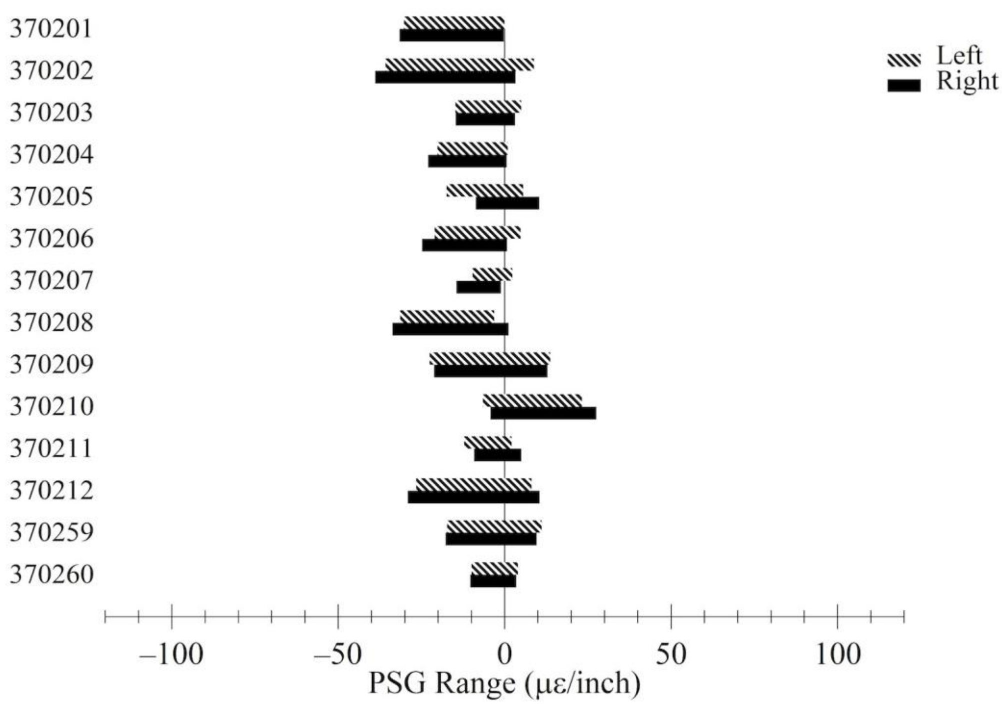

Source: FHWA.

Figure 18. Graph. Weighted PSG ranges for North Carolina SPS-2 test sections.

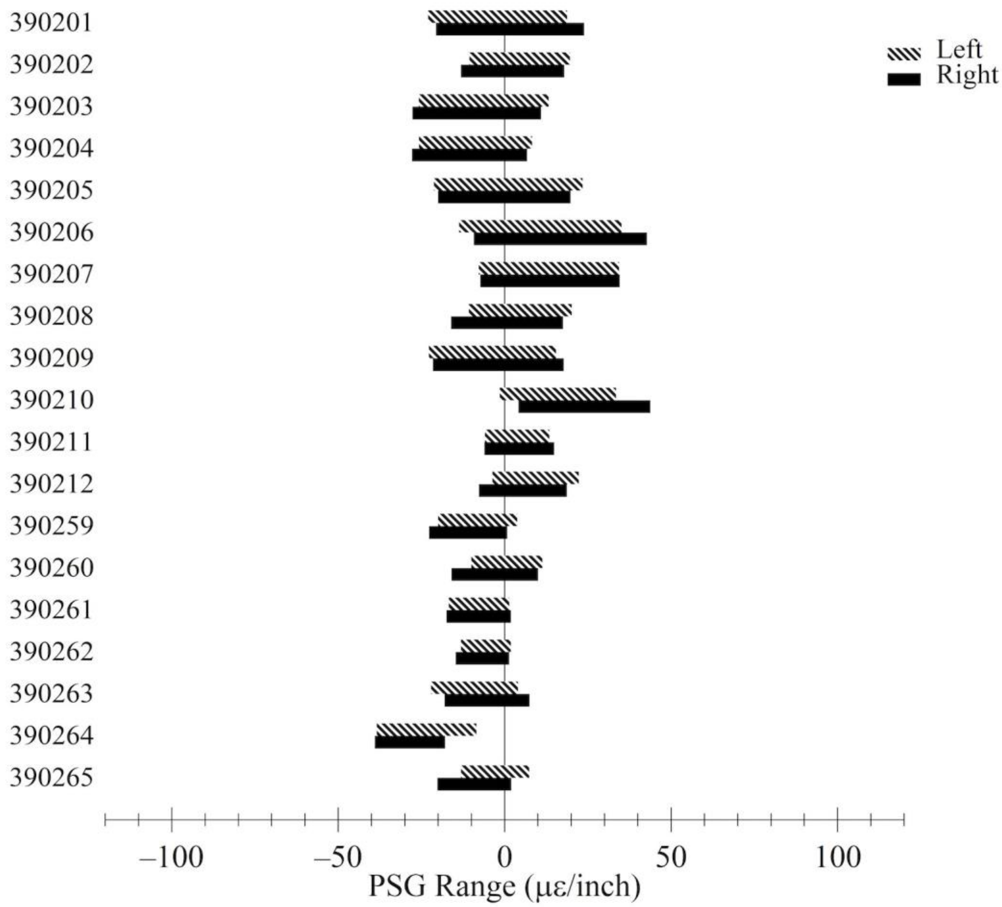

Source: FHWA.

Figure 19. Graph. Weighted PSG ranges for Ohio SPS-2 test sections.

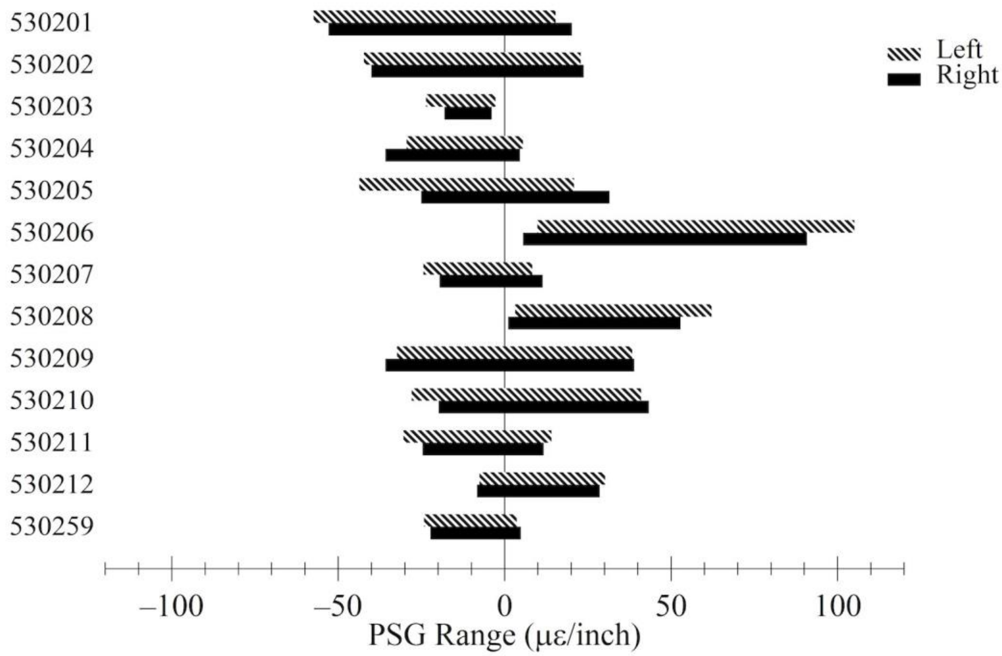

Source: FHWA.

Figure 20. Graph. Weighted PSG ranges for Washington SPS-2 test sections.

SPATIAL TRENDS

Some test sections exhibited spatial changes in PSG values. Figure 21 shows left PSG values for 34 slabs in section 040214. Each value in the figure is the average over five repeated passes. PSG values transition from upward curl (negative values) at the start of the test section to values near zero at the end of the test section in profiles measured in winter 1994. These profiles were measured less than 4 months from the date the site was opened to traffic. Profiles measured in winter 2004 transition from downward curl (positive values) to upward curl (negative values) at the end of the test section. Karamihas and Senn illustrated the transition from downward curl to upward curl for the right PSG values from the same test section.[2]

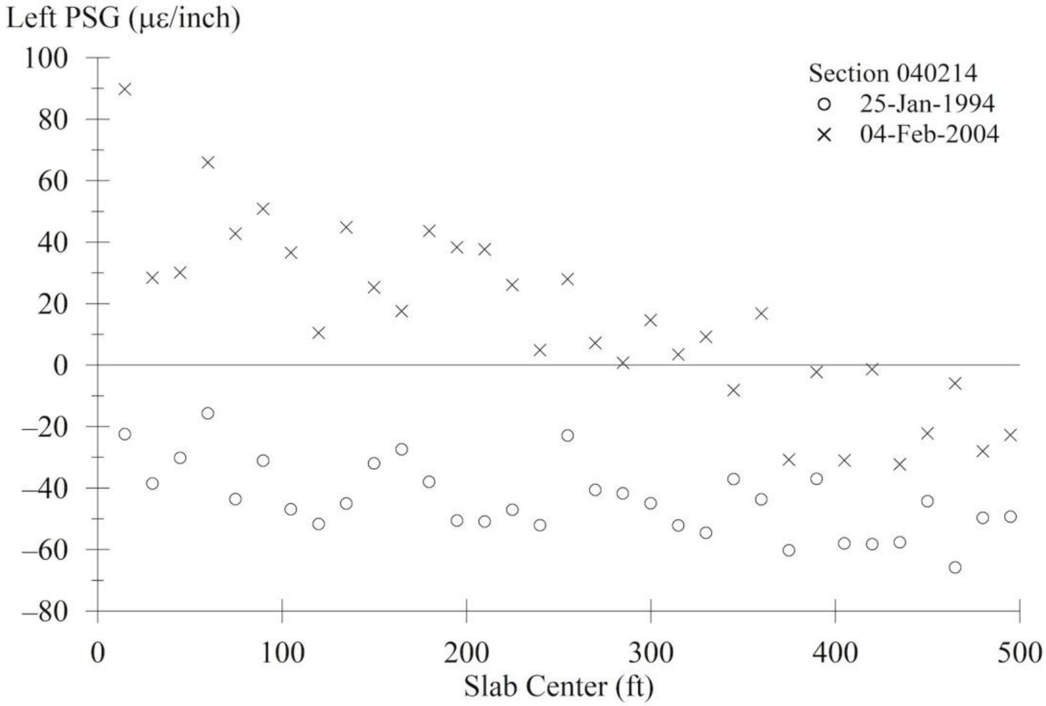

Source: FHWA.

Figure 21. Graph. Spatial variation in left PSG values for section 040214.

Figure 22 shows the spatial trend in left PSG values for profiles measured on section 040220. These profiles were measured 18.2 years after the site was opened to traffic. The transition toward a reduction in upward curl along section 040220 appeared in profiles from both sides. The reduction in upward curling was small early in the life of this section, increased over the first 18.2 years, and held steady over the rest of the monitoring period.

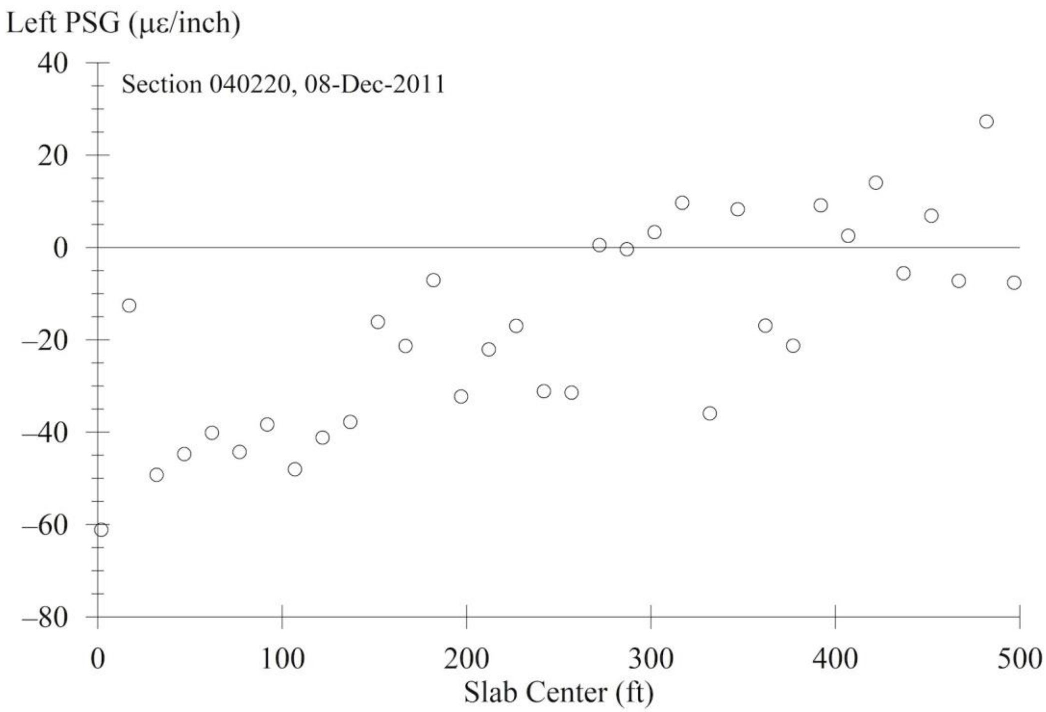

Source: FHWA.

Figure 22. Graph. Spatial variation in left PSG values for section 040220.

Figure 23 shows the spatial trend in left PSG values for profiles measured on section 200201. These profiles were measured 13.8 years after the site was opened to traffic. The negative PSG values over the last 60 ft of the section were observed on replacement slabs. The two slabs closest to the end of the section were replaced 3.4 years after the site was opened to traffic, and the two adjacent slabs upstream were replaced 10.1 years after the site was opened to traffic.

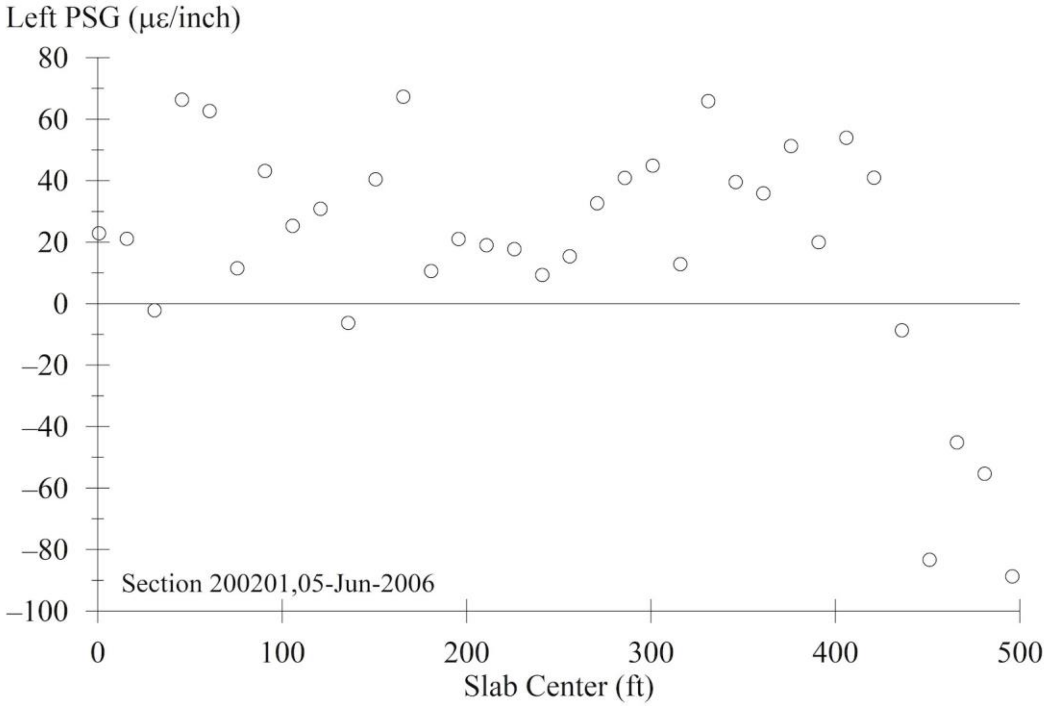

Source: FHWA.

Figure 23. Graph. Spatial variation in left PSG values for section 200201.

Additional examples of spatial trends in PSG are included in the following list:

- Section 133019 exhibited an increase in downward curl along its length throughout its monitoring history, except for when profile measurements were collected after surface grinding. The magnitude of the trend was strongest for right-side profiles.
- Section 183002 exhibited a decrease in upward curl along its length throughout the monitoring period. The magnitude of the trend was larger for left-side profiles than right-side profiles. The magnitude of the trend also increased for left-side profiles over the first 24 years of the monitoring period and was steady for several visits afterward.
- Section 200206 exhibited a decrease in downward curl along its length for part of the monitoring period for left-side profiles. The magnitude of the trend increased from 11 to 21 years after the date the site was opened to traffic and held steady afterward.

CHAPTER 6. THEORETICAL IRI–PSG RELATIONSHIP

This section illustrates the relationship between IRI and PSG values using synthesized profiles. Synthesized profiles with curling are created using the Westergaard deflection equations. The relationship between IRI and PSG values is examined in the absence of other sources of roughness using the synthesized profiles. This section also examines the IRI–PSG relationship for profiles with curling and other sources of roughness by superimposing synthesized background roughness on the idealized deflection profiles.

SYNTHESIZED PROFILES FOR CURL ONLY

Synthetic profiles of curl and warp are based are created using the Westergaard deflection equation in a repeating pattern. Figure 24 shows an example with a 15-ft slab length (*b*), *l* of 40 inches, μ of 0.15, and PSG of 100 με/inch. The IRI of this profile is 207.6 inches/mi.

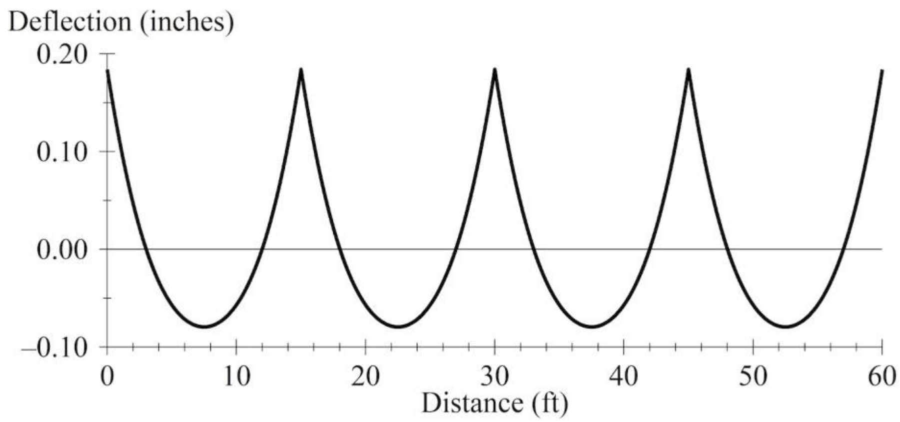

Source: FHWA.

Figure 24. Graph. Idealized profile with curling.

Figure 25 shows the variation in IRI with PSG for idealized profiles with a *b* value of 15 ft and *l* values of 25, 40, and 60 inches. As shown, IRI varies in proportion to the magnitude of PSG for a given combination of *l* and *b*. This magnitude of the slope for a given combination of *b* and *l* is the same for negative values of PSG. This would not be the case, however, when the influence of faulting and downward spikes at joints are added.

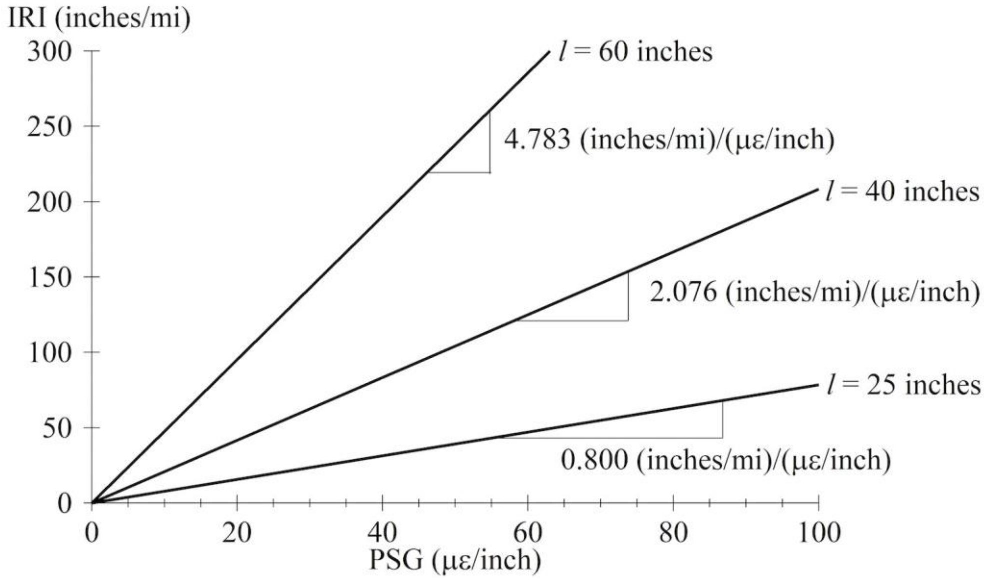

Source: FHWA.

Figure 25. Graph. IRI versus PSG for various values of *l*.

The slope defining the increase in IRI with PSG depends heavily on *l*. Figure 26 shows a reduced version of the Westergaard deflection equation.

$$z(x) = z_0 f(x,l,b) = -PSG(1+\mu)l^2 f(x,l,b)$$

Figure 26. Equation. Simplified Westergaard equation for slab deflection.

Idealized slab profiles have a shape that is a function of *b*, *l*, and distance along the slab (*x*). The function *f* has a unit upward deflection at the slab ends. The value of z_0 scales in proportion to PSG and in proportion to l^2.

Figure 27 demonstrates this relationship for *b* values of 12, 15, and 20 ft. The figure shows the variation in IRI versus PSG slope with *l*. For each value of *b*, the IRI versus PSG slope varies in approximate proportion to l^2. Changes in the shape of slab profiles with *l* cause minor deviations from a squared relationship not visible in figure 27. However, the squared relationship between *l* and z_0 translates to an approximately squared relationship between the *l* and the IRI versus PSG slope.

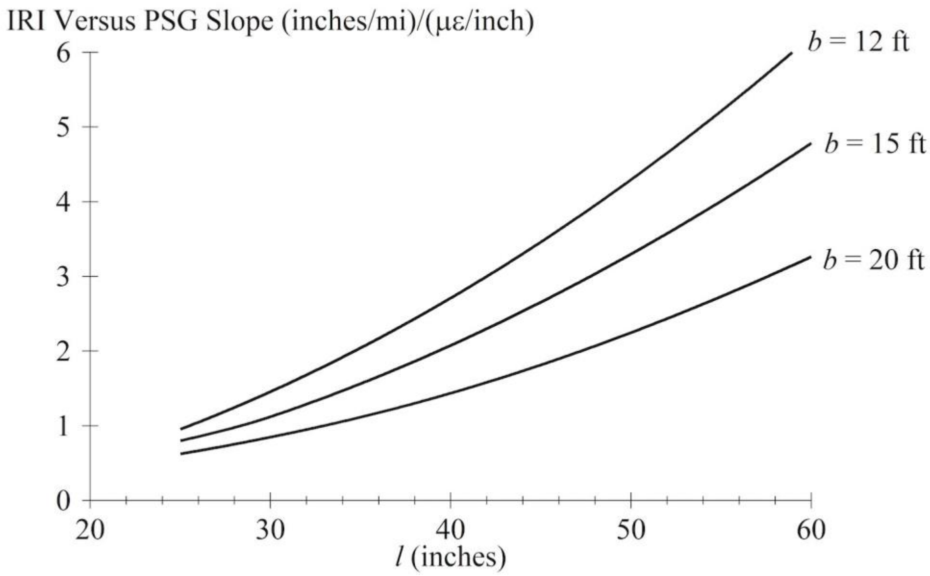

Source: FHWA.

Figure 27. Graph. IRI versus PSG slope versus *l*.

For an evaluation of curl and warp that involves structural behavior, using PSG is a convenient way to quantify slab deformation because it offers a potential link to changes in the slab stress state at various times and absolute stress state in some cases. For the evaluation of functional behavior, such as evaluation of changes in IRI versus time, uplift provides a more convenient quantification of curl and warp. Uplift (z_0), as defined implicitly in Figure 26, provides the upward deflection at the slab ends. For this discussion, the research team defines relative uplift (Δz) for the Westergaard deflection equation as uplift relative to the slab center. As shown in Figure 24, the slab center also deflects. Δz is defined as shown in figure 28, where s_λ, c_λ, sh_λ, and ch_λ are trigonometric and hyperbolic functions of the argument λ.

$$\Delta z = z(b/2) - z(0) = -PSG(1+\mu)l^2\left(1 - \frac{s_\lambda ch_\lambda - c_\lambda sh_\lambda}{s_\lambda c_\lambda - sh_\lambda ch_\lambda}\right)$$

Figure 28. Equation. Δ*z*.

Figure 29 shows the equation for λ.

$$\lambda = \frac{b}{l\sqrt{8}}$$

Figure 29. Equation. *λ*.

Figure 30 shows the IRI for 0.01 inches of Δz as a function of l for b values of 12, 15, and 20 ft. Figure 30 also shows that IRI increases as b decreases for a given amount of Δz because an approximately equal amount of slope variation is concentrated within a shorter distance when the slab is shorter. For each value of b, the IRI for a given amount of Δz changes with l because of changes in the shape of the slab deflection profiles. As l reduces in relation to b, the deflection profiles transition from an approximate parabolic shape to a profile that flattens in the middle. The result is a relative increase in the short-wavelength variation that contributes to the IRI.

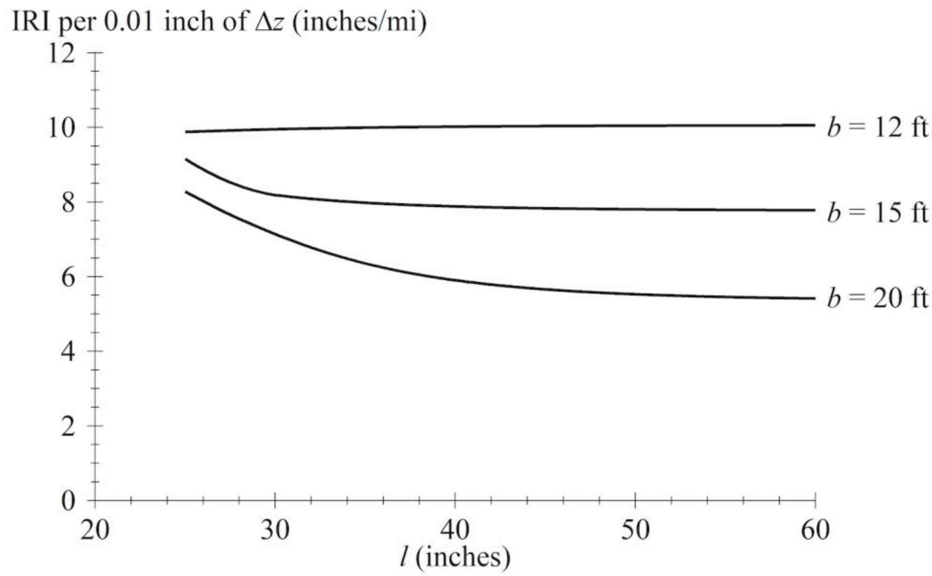

Source: FHWA.

Figure 30. Graph. IRI per 0.01 inch of Δ*z*.

SYNTHESIZED PROFILES WITH BACKGROUND ROUGHNESS

When deflection caused by curl and warp and other sources of roughness are superimposed to establish a combined profile, some cancellation between the two sources of roughness occurs. In addition, variations of the apparent PSG values for individual slabs occur around the nominal value. This section demonstrates these phenomena by combining synthesized slab profiles with curling and profiles with nonperiodic background roughness. As in the previous discussion on synthesized profiles for curl, profiles are synthesized using the Westergaard deflection equation.

Systematic Effects

Figure 31 shows the IRI versus PSG for profiles that combine synthesized profiles with slab curl and background roughness. The profiles were synthesized for 15-ft-long slabs and *l* of 40 inches, which are shown in Figure 24. Background roughness was synthesized with IRI values of 50, 80, and 110 inches/mi. The line in Figure 31 that represents 0 inches/mi shows the relationship between IRI and PSG for synthesized profiles with no background roughness added. This corresponds to the middle line in Figure 25.

Each point in Figure 31 shows the average IRI versus the average PSG for 15,000 simulated test sections. Each test section included thirty-three 15-ft-long slabs totaling 495 ft. For each point, the simulation superimposed synthesized deflection profiles over 100 realizations of white noise slope, which were each 75,000-ft long. This length includes 150 test sections with 33 slabs each and an additional 50 slabs for at the start. As described in the following sections, the IRI and PSG values for individual test sections vary around the averaged values shown in Figure 31 for individual sections.

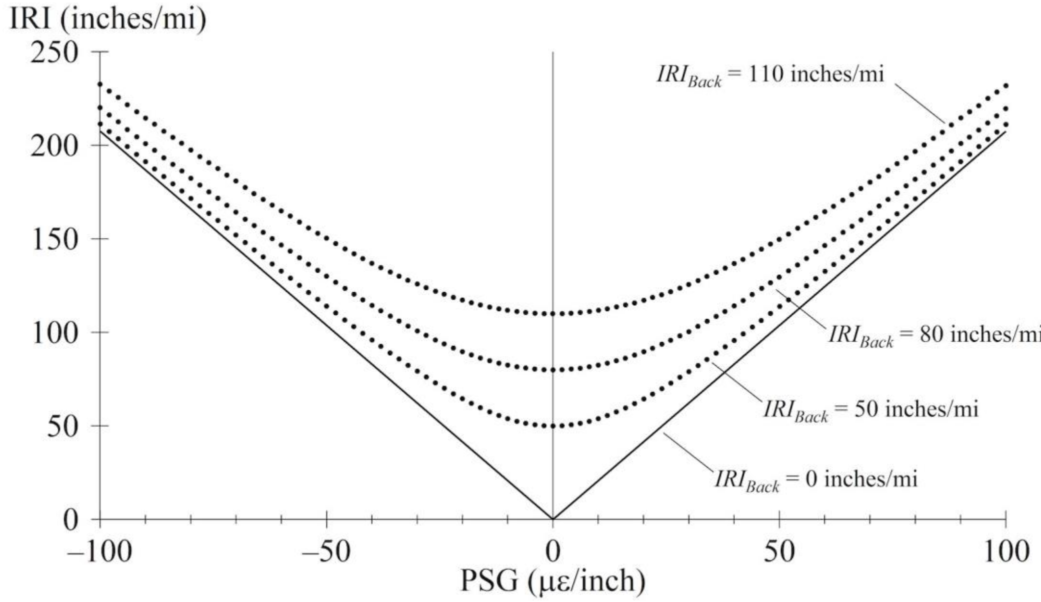

Source: FHWA.

Figure 31. Graph. Average IRI versus PSG for curl and background roughness.

Previous research into the application of PSG proposed a linear relationship between IRI and PSG.(2,3) Figure 31 shows that a linear fit approximates the relationship between IRI and PSG values when curl and warp account for a majority of the roughness. However, a linear fit does not approximate the relationship between IRI and PSG values when the magnitude of curl and warp is relatively low. Additionally, extrapolation of the IRI versus PSG slope from a range with substantial curl and warp to estimate the background roughness is not accurate.

If both profile components were random, Gaussian signals, a sum-of-squares model approximates the IRI of the combined profile (IRI_{Comb}) as shown in figure 32.

$$IRI_{Comb} = \sqrt{IRI_{Curl}^2 + IRI_{Back}^2}$$

Figure 32. Equation. Simple expression for IRI_{Comb}.

Where:

IRI_{Curl} = the IRI of the synthetic profile of curl and warp, shown in the lower trace of Figure 31.

IRI_{Back} = the superimposed background roughness.

When IRI_{Comb} is estimated using PSG, the equation in figure 32 becomes the equation shown in figure 33.

$$IRI_{Comb} = \sqrt{\left(PSG\frac{dIRI}{dPSG}\right)^2 + IRI_{Back}^2}$$

Figure 33. Equation. Estimated IRI_{Comb}.

The derivative of IRI with respect to PSG (*dIRI*/*dPSG*) is the theoretical IRI versus PSG slope established using synthetic profile of curl and warp, as shown in Figure 25. The equation in Figure 32 estimated IRI_{Comb} to within 1.4 percent or less using the data from Figure 31. However, the equation in figure 33 overestimated IRI_{Comb} with a systematic residual that increased with PSG because the synthetic profiles of curl and warp were not Gaussian. Less cancellation of roughness occurs when the profiles are combined than if both profile components were Gaussian. The equation in figure 34 estimates IRI_{Comb} with absolute residual values of 0.60 inches/mi or less and an SD of 0.21 inches/mi when using data points from Figure 31.

$$IRI_{Comb} = \sqrt{0.97347\left(PSG\frac{dIRI}{dPSG}\right)^2 + IRI_{Back}^2}$$

Figure 34. Equation. *IRI_{Comb}* empirically estimated using PSG.

However, the factor applied to IRI_{Curl} required to create the best fit may depend on *b* and *l*.

The research in this report is concerned with predicting the roughness not caused by curl and warp (i.e., IRI_{Back}) using the overall IRI (i.e., IRI_{Comb}) and values of PSG derived from the profile in figure 35.

$$IRI_{Back} = \sqrt{IRI_{Comb}^2 - A\left(PSG\frac{dIRI}{dPSG}\right)^2}$$

Figure 35. Equation. *IRI_{Back}* empirically estimated using PSG.

Factor A is introduced because the profile content caused by curl and warp is not random or Gaussian. The error in the sum-of-squares approximation is low for predictions of IRI_{Comb} based on PSG and IRI_{Back}. Prediction of IRI_{Back} from PSG and IRI_{Comb}, however, can yield a high systematic error when the background roughness is low relative to the roughness caused by curl and warp.

Figure 36 shows the prediction of background roughness by using the equation in figure 35 for combined profiles produced with actual IRI_{Back} of 50 inches/mi. With no adjustment to account for non-Gaussian content (i.e., $A = 1$), the error grows in approximate proportion to PSG squared. For higher values of IRI_{Back}, the error is lower. The absolute error in IRI reduced in inverse proportion to IRI_{Back} and the percentage error in IRI reduced in inverse proportion to the square of IRI_{Back}. As shown in figure 36, the error is much lower with the adjustment applied (i.e., $A = 0.97347$).

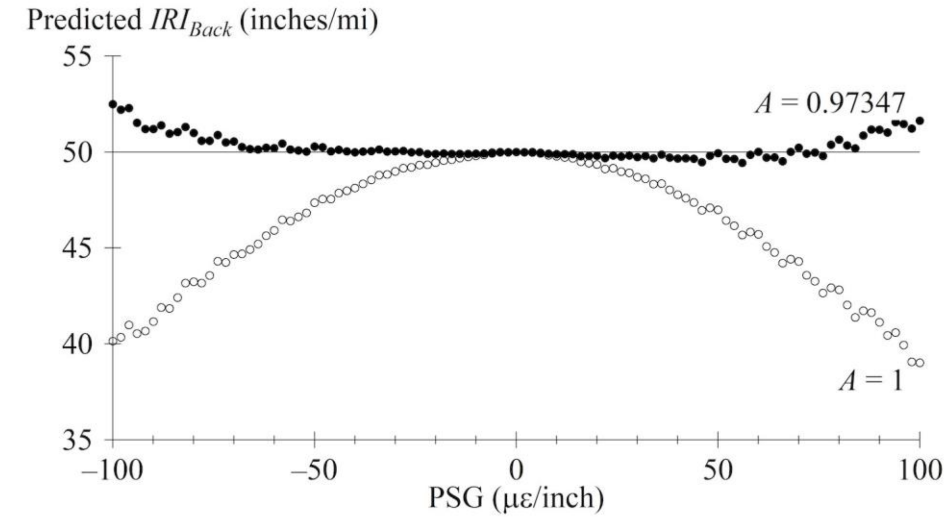

Source: FHWA.

Figure 36. Graph. IRI_{Back} prediction.

Random Effects

With background roughness added, PSG values for individual slabs vary from the nominal value. For the simulations used to produce the graph in Figure 31, the white noise slope profile with an IRI of 50 inches/mi introduced slab-by-slab variation in PSG with an SD of 10.78 με/inch. This corresponds to a *b* value of 15 ft and an *l* value of 40 inches. The distribution closely approximated a Gaussian distribution and produced a value of 0.0035 in a Komoglorov−Smirnov test for the 495,000 simulated slabs.

The slab-by-slab variation in PSG values caused by background roughness averages out over many slabs. Figure 37 shows the result when 495,000 slabs are divided into 15,000 test sections containing 33 slabs each. The figure shows the distribution in sectionwide PSG for groups containing 33 slabs when IRI_{Back} is 50 inches/mi and the nominal PSG value is −50 με/inch. For this distribution, the average is −50.02 με/inch and the SD is 2.4 με/inch. Using an average of 33 slabs, which equals 495 ft, some of the scatter was eliminated.

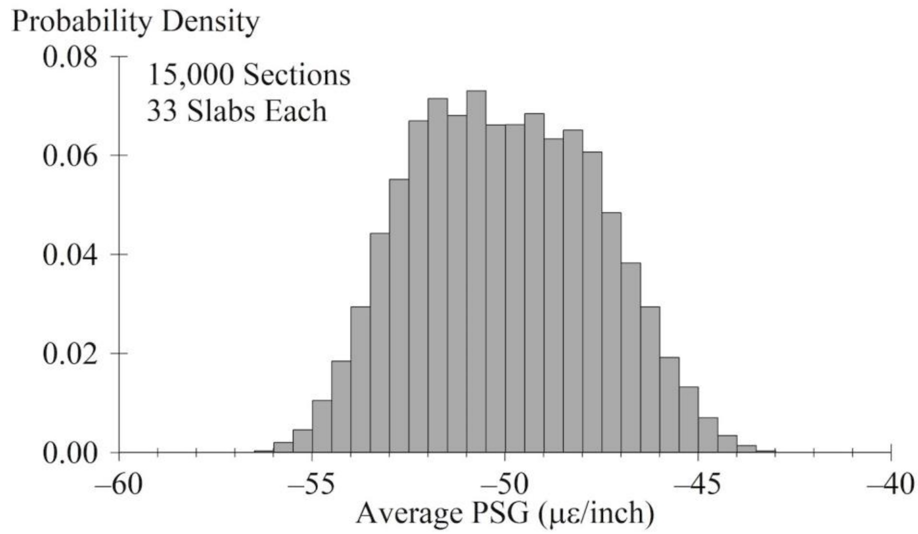

Source: FHWA.

Figure 37. Graph. PSG distribution with background roughness for 15,000 test sections.

For the simulations used to produce the graph in Figure 31, the variation in PSG grew in proportion to the IRI_{Back}. However, the variation did not depend on the nominal PSG value. For PSG values ranging from −100 to 100 με/inch, the SD of sectionwide PSG values (averaged over 33 slabs) ranged from 2.36 to 2.42 με/inch with IRI_{Back} of 50 inches/mi. At 80 inches/mi, the SD ranged from 3.78 to 3.87 με/inch, and at 100 inches/mi, the SD ranged from 5.20 to 5.33 με/inch. For longer sections, the variation in sectionwide averages decreased. For example, with IRI_{Back} equal to 50 inches/mi, the SD in sectionwide PSG averaged over 66 slabs (i.e., a section length of 990 ft) was 1.11 με/inch, and the SD in sectionwide PSG averaged over 165 slabs (i.e., a section length of 2,475 ft) was 0.66 με/inch.

CHAPTER 7. OBSERVATIONS OF THE IRI−PSG RELATIONSHIP

A goal of this research was to examine whether the relationship between IRI and PSG could be generalized. For example, if field observations using FHWA and LTPP data analyzed in this work demonstrated agreement with the analytical results previously presented, the measurement effort needed to infer the contribution of curl and warp to the overall roughness of a test section would be reduced. Alternatively, if observations of the change in IRI with PSG values demonstrated a consistent relationship among the test sections analyzed in this study, some generalizations would be possible. This, however, was not the case. Although the sum-of-squared model fits the IRI versus PSG data well for cases that had sufficient data to capture short-term changes in curl and warp, the fitting coefficients were not consistent among test sections with the same slab length.

Figure 38 shows a curve fit produced by the sum-of-squares model for profiles in section 040213 of the FHWA dataset. The figure compares IRI to PSG for the right-side profiles measured during 16 seasonal and diurnal measurement visits to the section.

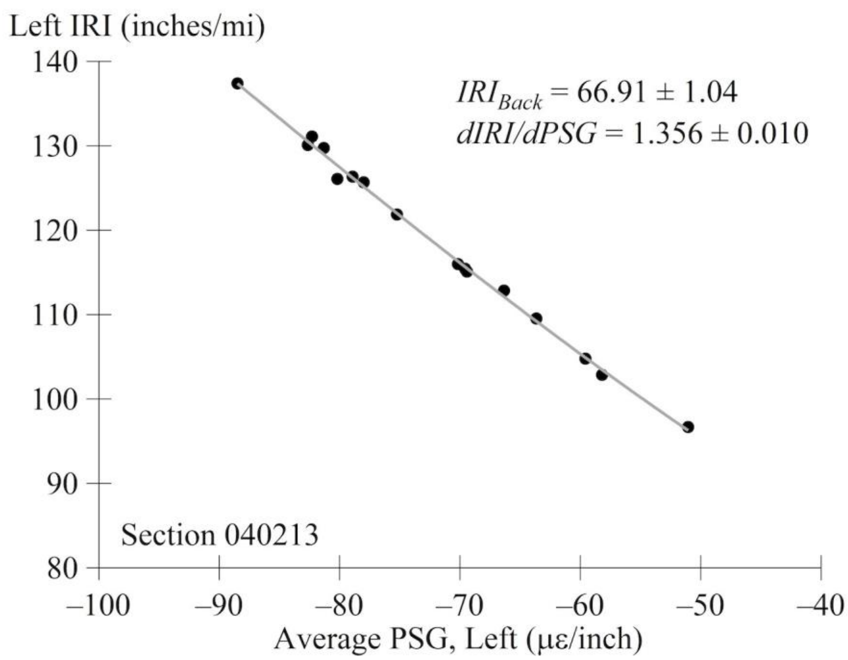

Source: FHWA.

Figure 38. Graph. Sample IRI versus PSG fit for the sum-of-squares model.

The fitted curve in Figure 38 was produced using the Levenberg–Marquardt algorithm for a nonlinear, least squares fit to the function shown in Figure 39.

$$IRI = \sqrt{\left(PSG\frac{dIRI}{dPSG}\right)^2 + IRI_{Back}^2}$$

Figure 39. Equation. Fitting function for IRI versus PSG.

In the equation in Figure 39, IRI and PSG are measured. IRI_{Back} and $dIRI/dPSG$ are fitted parameters. IRI_{Back} represents a prediction of the IRI that would occur in the absence of slab curl and warp (i.e., background roughness). The coefficient $dIRI/dPSG$ represents an empirical estimate of the IRI versus PSG slope that would exist in the absence of background roughness.

Table 5 shows the results for 38 curve fits applied to the FHWA dataset. The table includes only test sections monitored seasonally and diurnally and only with a nominal slab length of 15 ft, which are sections within the core experiment from SPS-2 sites. Table 5 lists cases in which the curve fit produced a residual less than 2.4 inches/mi and the 95-percent confidence interval for the IRI versus PSG slope was less than 10 percent of the fitted value. Table 5 also lists the two fitted coefficients and their 95-percent confidence intervals and the high and low PSG values included in the observations. Most of the excluded data produced high 95-percent confidence intervals because the PSG values were low or changed very little.

Table 5 also includes the coefficients produced by fitting the IRI to relative uplift (Δz) using the sum-of-squares model (Figure 40).

$$IRI = \sqrt{\left(\Delta z \frac{dIRI}{d\Delta z}\right)^2 + IRI_{Back}^2}$$

Figure 40. Equation. Fitting function for IRI versus Δz.

In the equation in figure 40, $dIRI/d\Delta z$ is a fitted value that represents the IRI versus relative uplift slope that would exist without other sources of roughness. Figure 40 provides the relationship between Δz, PSG, and l. Unlike the IRI versus PSG slope, the slope between IRI and Δz does not vary in proportion to the square of l.

As shown in Figure 30, the fitted value of $dIRI/d\Delta z$ is expected to be consistent over a large range of l values and have a value near 800 inches/mi/inch. It is not consistent, which shows that the relationship between the IRI and curl and warp cannot be generalized solely on structural properties. The individual curve fits often produced low residuals for individual sections when observations over a sufficient range of PSG values were available (Table 5). The data characterize the relationship between IRI and curl and warp for the individual test sections that produced the data.

Table 5. IRI versus PSG fitted coefficients.

Section	Side	IRI_{Back} (Inches/mi)	*dIRI/dPSG* (Inches/mi)/ (με/Inch)	PSG Range (με/Inch)	*dIRI/dΔz* (Inches/mi)/ (Inch)
040213	Left	66.91 ± 1.04	1.356 ± 0.010	−88.5 to −51.0	702 ± 5
040215	Right	91.26 ± 2.13	1.970 ± 0.051	−50.9 to −30.7	734 ± 19
040215	Left	85.25 ± 1.34	1.821 ± 0.029	−54.5 to −32.5	678 ± 11
040217	Right	62.82 ± 0.94	0.881 ± 0.019	−92.2 to −19.4	842 ± 18
040217	Left	68.95 ± 1.08	0.848 ± 0.015	−116.1 to −39.1	811 ± 14
040218	Right	58.92 ± 0.97	1.567 ± 0.072	−32.4 to −4.4	986 ± 45
040219	Right	91.78 ± 0.92	2.454 ± 0.036	−46.3 to −12.8	891 ± 13
040220	Right	66.69 ± 0.91	2.249 ± 0.086	−27.2 to −6.3	814 ± 31
040221	Right	54.37 ± 1.80	1.665 ± 0.035	−59.0 to −25.4	776 ± 16
040221	Left	60.87 ± 0.92	1.537 ± 0.020	−61.0 to −24.6	716 ± 9
040222	Right	52.68 ± 0.85	1.353 ± 0.025	−54.8 to −9.1	684 ± 13
040223	Right	78.30 ± 0.93	2.211 ± 0.033	−43.8 to −17.0	765 ± 11
040223	Left	69.40 ± 1.51	2.147 ± 0.048	−42.2 to −17.3	743 ± 17
040224	Right	69.67 ± 0.44	1.667 ± 0.051	−28.3 to −2.1	561 ± 17
200201	Left	118.46 ± 0.62	1.931 ± 0.109	−2.4 to 29.2	1006 ± 57
200202	Left	60.96 ± 0.58	1.355 ± 0.062	−32.9 to 4.5	699 ± 32
200203	Right	85.82 ± 0.35	2.270 ± 0.048	10.8 to 23.9	826 ± 17
200204	Right	77.57 ± 0.90	2.028 ± 0.060	−31.3 to −12.1	626 ± 18
200204	Left	71.08 ± 0.94	2.237 ± 0.031	−37.1 to −20.5	690 ± 10
200205	Left	96.69 ± 0.63	2.515 ± 0.165	−6.2 to 18.6	1268 ± 83
200207	Right	91.82 ± 1.05	2.871 ± 0.106	12.9 to 23.4	860 ± 32
200211	Right	81.34 ± 0.44	3.004 ± 0.085	1.4 to 18.9	934 ± 26
390201	Left	98.65 ± 0.74	2.271 ± 0.110	−23.0 to 13.8	1021 ± 49
390203	Right	68.46 ± 0.44	2.045 ± 0.038	−27.7 to 5.4	666 ± 12
390203	Left	72.67 ± 0.41	2.009 ± 0.042	−25.8 to 4.9	654 ± 14
390204	Left	60.56 ± 0.72	2.407 ± 0.058	−25.8 to −1.1	851 ± 20
390207	Right	79.83 ± 0.61	2.550 ± 0.064	1.3 to 28.0	839 ± 21
390207	Left	84.17 ± 0.40	2.307 ± 0.052	1.5 to 26.4	759 ± 17
390208	Right	84.36 ± 0.93	2.456 ± 0.218	−16.1 to 15.8	738 ± 66
390209	Right	73.70 ± 0.45	1.679 ± 0.097	−19.5 to 12.1	780 ± 45
390209	Left	78.78 ± 0.25	1.358 ± 0.055	−22.8 to 8.7	631 ± 25
390210	Left	72.73 ± 0.57	1.327 ± 0.111	−1.5 to 28.5	702 ± 59
390212	Left	66.50 ± 0.38	2.336 ± 0.105	−3.7 to 17.8	753 ± 34
390261	Right	70.86 ± 0.24	2.350 ± 0.059	−17.5 to 1.0	623 ± 16
390261	Left	81.88 ± 0.49	2.363 ± 0.136	−16.8 to 0.0	627 ± 36
390262	Right	68.02 ± 0.44	2.003 ± 0.139	−14.7 to −1.3	476 ± 33
390263	Right	81.20 ± 0.55	2.648 ± 0.102	−18.1 to 5.7	779 ± 30

CHAPTER 8. CORRELATION TO ENVIRONMENTAL FACTORS

The curl-and-warp response in PCC pavements has been attributed to temperature and moisture gradients. Pavement surface is directly exposed to temperature and moisture from sunlight and precipitation, either of which can then permeate the pavement. Moisture can also permeate upward from the ground and become trapped underneath the pavement. In either case, the top and bottom of the PCC pavement layers are exposed to different environmental conditions. This difference in conditions is measured using a temperature or moisture gradient that expresses a change in temperature or moisture relative to the depth of the pavement.

The relationship of moisture and temperature to pavement depth is not perfectly linear, and the gradients produced in each slab are not identical. The design of a test section assumes a certain amount of uniformity. However, there are variations in construction methods (e.g., finishing and curing), subpavement conditions, and drainage that affect individual slabs. Researchers have observed that some slabs in a test section may curl up while others curl down. Some slabs may crack and some may have voids underneath the pavement. Portions of this study assume that the average curling across a test section should reflect the behavior of most slabs. However, in sections with near equal amounts of slabs curled up and curled down, averaging PSG over the test section may introduce variability into the correlation analyses.

PCC has higher compressive strength than tensile strength. Accordingly, PCC's design is typically controlled by its flexural strength. Internal stresses from curling and warping can magnify external bending stresses and cause different types of slab failures. Changes in temperature can cause concrete to expand or contract, and evaporation of moisture in the concrete can cause shrinkage. When the top or bottom of concrete pavement expands, contracts, or shrinks at a faster rate than the other side, the shape of the pavement curls or warps from uneven internal stresses. An upward curl can cause corner breaks from high stress at the top of a slab. A downward curl may result in transverse cracking from high stress at the bottom of a slab.

An upward pavement curl from temperature gradients usually occurs at night when the temperature at the bottom of a slab is greater than the temperature at the surface. This happens because pavement stores heat during the day but at night the surface of the pavement cools faster than the bottom of the pavement, which creates a temperature differential. By the next morning, the bottom of the pavement would have cooled off in time to have the pavement surface heat again from daytime temperatures. During the day, the temperature at the top of the pavement is higher than at the bottom, which causes a downward curl. Concrete pavement can cycle between relatively upward- and downward-curl behavior through daily temperature fluctuations (diurnal cycling). Curling is not typically considered to cause permanent curvature but is unknown how it might interact with drying shrinkage on a seasonal cycle. Seasonal temperature variation adds yet another level to this trend as hot summer days will create higher temperature differentials than colder winter days.

Warping caused by the moisture gradient in concrete pavements is typically upward. The moisture gradient occurs due to a cycle of wetting and drying at the top of the slab while the bottom of the slab remains saturated. Downward warping may occur in rare occasions where the moisture content is higher at the top of the slab than at the bottom, such as wetting of the pavement surface following a long dry period. As the concrete dries, it shrinks, and when one side (i.e., top or bottom) shrinks more than the other side, internal stresses cause curvature. The shrinkage that occurs through each cycle of wetting and drying is partly irreversible, which could cause the pavement to incur permanent and incremental changes in the slab curvature.

Slab curvature can occur over time and at the time of construction because there are two types of shrinkage—drying and autogenous—with different mechanisms that can cause the slab to warp. Drying shrinkage happens over time as the pavement undergoes wetting and drying from changes in relative humidity. Autogenous shrinkage can cause the pavement to warp while it cures during construction. Autogenous shrinkage occurs while the pavement has yet to set; therefore, the built-in curvature that is initially observed in a new pavement is expected to flatten because of concrete creep (the permanent deformation of concrete from persistent loading). Drying shrinkage is driven by the loss of capillary water through evaporation. Water in the capillaries becomes saturated from the humidity in air-entraining voids. When the water in the capillaries evaporates, the hydrate particles contract, causing tensile stress.

Shrinkage in concrete pavements transpires exclusively in the paste component of the mixture and not the chemically inert aggregate. The paste is made from water and cement that undergoes hydration, causing the concrete to harden. Differences in moisture and temperature during the initial curing process cause the concrete to form an initial curvature. High-strength concrete with higher volumes of paste can cause even higher amounts of autogenous shrinkage, thus resulting in more-significant curvature. The use of curing compounds and methods and construction practices can also affect the initial curl. The initial curing process can also impact how the pavement behaves over time by altering its shrinkage potential.

Minor variability in construction methods, subsurface nonuniformity, and localized environmental conditions can often enforce a butterfly effect, which compels slabs that were designed equally to behave differently over time. This analysis generalized the initial curl and change in curl over time of a test section and correlated these two measures of curl to environmental and structural-design factors.

DETERMINING PSG PREDICTION VALUES

Time-series analysis of PSG values suggested that pavements tend to start out at an initial curl-and-warp state and steadily change in curl-and-warp amount as the pavement ages. After approximately 10 years, the change in the amount of warping either plateaued or became highly variable. The reasons for this variability include slabs reaching a maximum amount of permanent warp and cracking from distress. Figure 41 demonstrates this trend in eight randomly chosen sections. Of the 83 test sections evaluated, data typically showed a linear trend in PSG values in the first 10 years of the pavement's life. This is a general observation and varies depending on the performance and shrinkage potential of specific sections or slabs. In some cases, this trend is less obvious, as seen in sections 390263 and 493011. In the case of section 133019, a 10-year trend does not exist because this section entered the LTPP program several years after construction. Of the five GPS-3 sections selected for analysis, only 273003 and 493011 entered the LTPP program in time for FWD testing to occur within the first 10 years. Table 31 in appendix B includes the construction dates of the selected GPS-3 test sections.

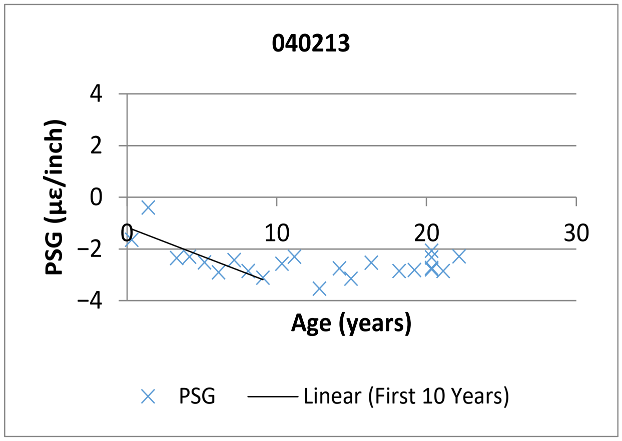

Source: FHWA.

A. Example of PSG over time for section 040213.

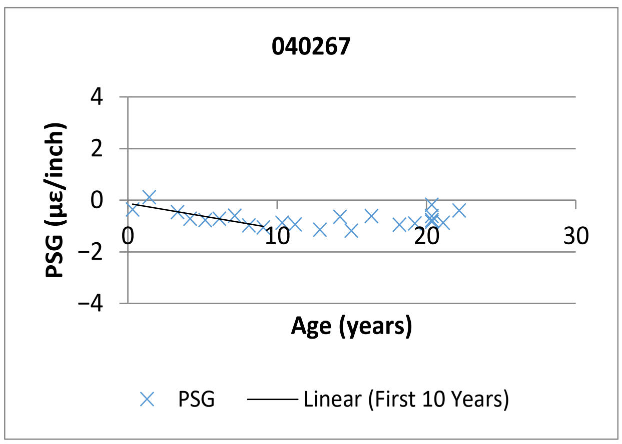

Source: FHWA.

B. Example of PSG over time for section 040267.

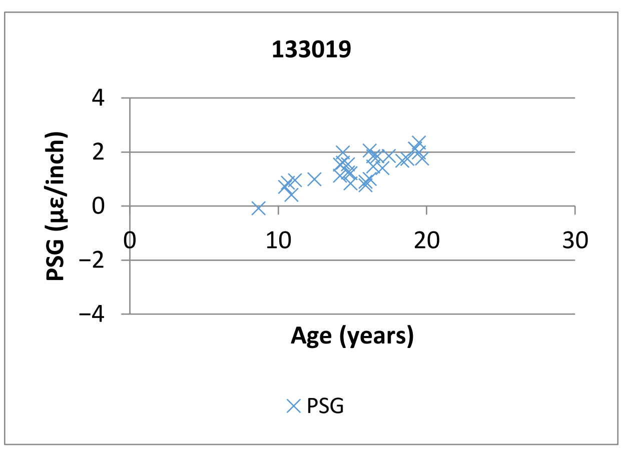

Source: FHWA.

C. Example of PSG over time for section 133019.

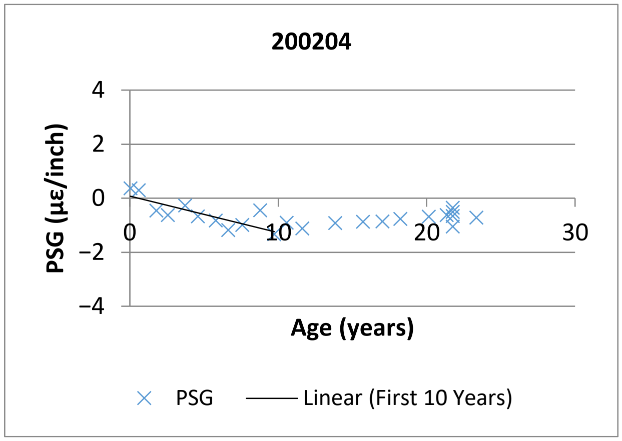

Source: FHWA.

D. Example of PSG over time for section 200204.

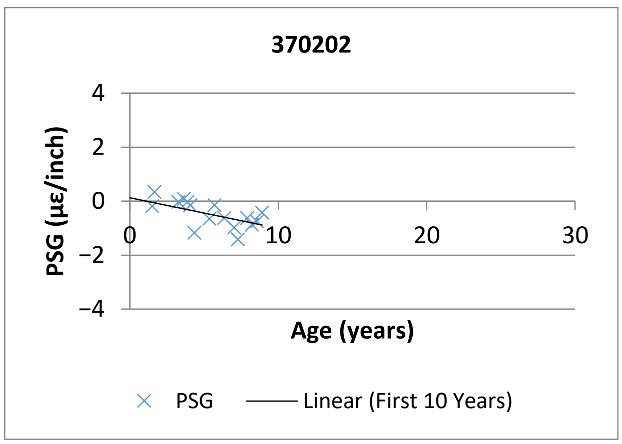

Source: FHWA.

E. Example of PSG over time for section 370202.

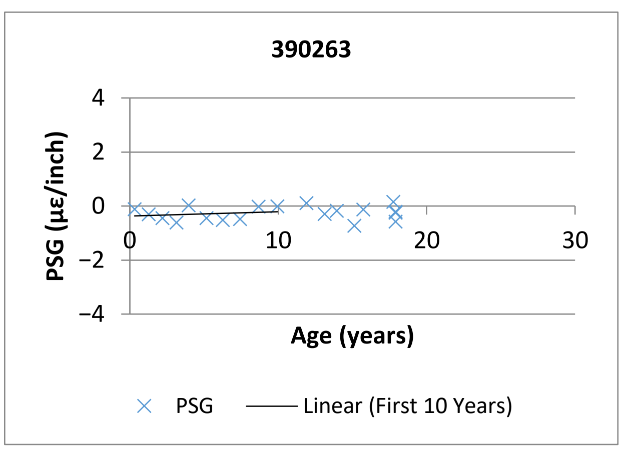

Source: FHWA.

F. Example of PSG over time for section 390263.

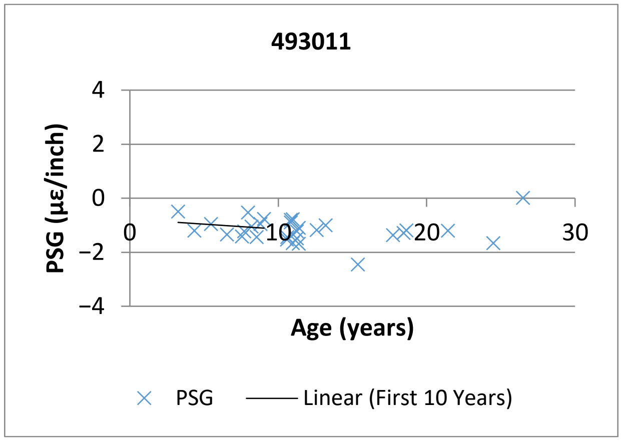

Source: FHWA.

G. Example of PSG over time for section 493011.

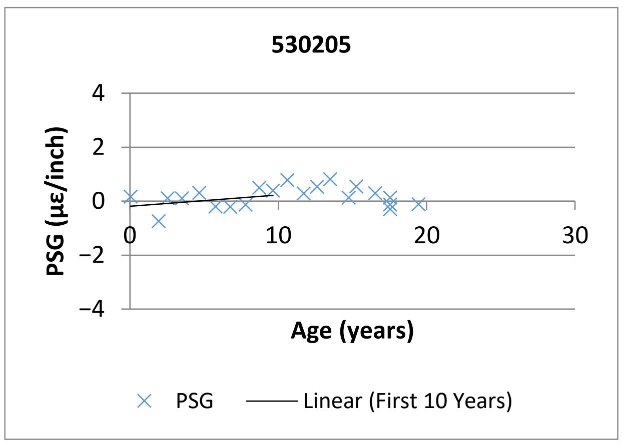

Source: FHWA.

H. Example of PSG over time for section 530205.

Figure 41. Graphs. Examples of PSG values over time for specific sections.

PSG values were averaged from each slab within a test section. Individual slabs deteriorated at different rates and caused variability in the average PSG for each section. The slabs also curled at different rates or directions, likely because of variations in construction or environmental factors. Additionally, the profile measurements used to compute PSG were measured at different times of the day or during different seasons, which caused variations in temperature and moisture gradient. Given these sources of variability, researchers found it difficult to observe a continuous trend in PSG. However, this variability became more significant as the pavement aged.

For this analysis, linear regression of PSG was performed on data from the first 10 years after construction. The regression intercept was the initial PSG value after construction (PSG_i) and the regression slope was the rate of change in PSG value after construction (PSG_s). Figure 42 and Figure 43 show a histogram of PSG intercept and slope by site with average annual temperature and relative humidity. The PSG regression values for each test section can be found in appendix I.

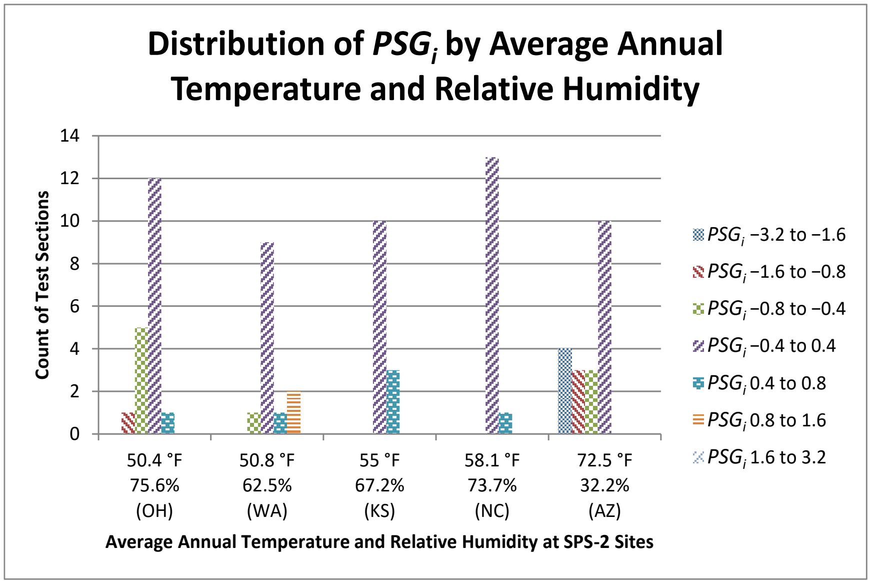

Source: FHWA.

Figure 42. Graph. PSG intercept histogram by SPS-2 site.

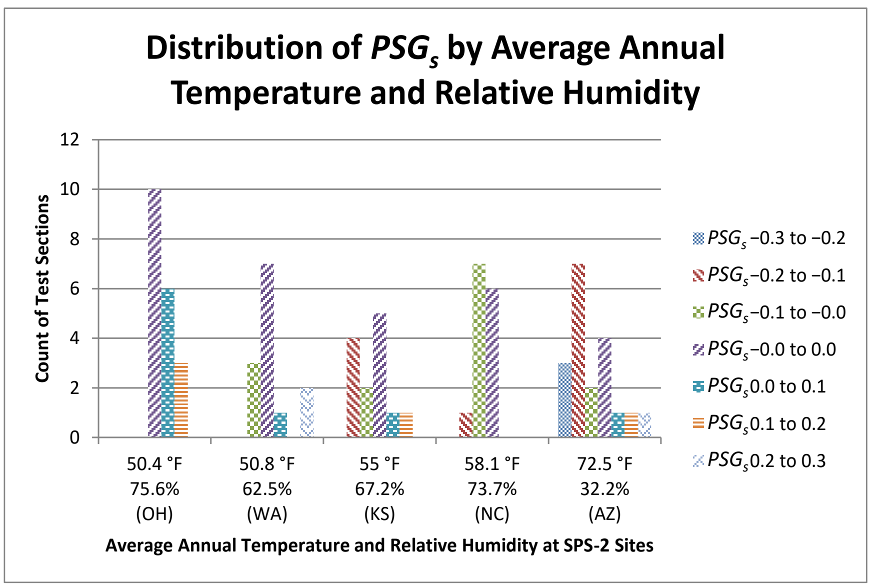

Source: FHWA.

Figure 43. Graph. PSG slope histogram by SPS-2 site.

The data showed that most test sections, regardless of climatic condition, started out with no initial curvature. However, there were multiple test sections that had an initial curvature. Arizona had multiple sections that started with strong upward curvature. Ohio also had a few sections with moderate upward curvature. Kansas had three sections with slight downward initial curvature.

Sites with high relative humidity and low temperatures showed less long-term change in PSG than sites with low humidity and high temperatures. Several Arizona sites showed an increase in upward curl over time. As the average annual temperature decreased, the number of sites with a negative value for PSG_s (indicating an upward change in curvature) decreased. Ohio had the most sites with a positive value for PSG_s (indicating a downward change in curvature). Nonzero PSG_s values imply that periodic incremental permanent changes in curvature occurred over 10 years. Warping is the expected cause of permanent changes in curvature, which theoretically should be upward because of shrinkage from the evaporation of moisture. However, several test sections curled downward as the annual average temperature decreased. This suggests two possibilities: downward curling commonly associated with the temperature gradient can contribute to permanent curvature in colder regions, or the moisture gradient that causes permanent warping tends to be inverted in colder regions. It is also possible that this trend was coincidental because of the limited number of test sites in the study.

DETERMINING ENVIRONMENTAL FACTORS

Temperature gradient (ΔT) was estimated as the average linear regression slope of temperature measurements taken at various pavement depths. These subsurface measurements were obtained from the LTPP database and taken during FWD testing. Table 6 shows how the temperature and humidity data were summarized from the Modern-Era Retrospective Analysis for Research and Applications (MERRA) climate database.[21] Climate factors for each SPS-2 site can be found in table 54 and table 55 in appendix I. Several climate indices were also analyzed, including annual precipitation and freezing index. These factors, however, did not show significant correlation to PSG. The average annual precipitation and freezing index were of interest to researchers because LTPP defines climatic region using criteria for these indices.

Table 6. Climatic factors and their variables for PSG correlation.

Climatic Factors	In the First Month After Construction	In the First 10 Years After Construction
Average temperature	T_0	T_1
Average relative humidity	H_0	H_1
Average difference between the maximum and minimum daily temperature	Δ_{T0}	Δ_{T1}
Average difference between the maximum and minimum daily relative humidity	Δ_{H0}	Δ_{H1}

Table 7 shows the structural design factors considered in the analysis. Paste volume was of interest because the shrinkage in the paste causes warping. Paste volume was expressed as percentage of the total mix. The total quantity of paste depended on the dimensions of the slab (i.e., length, width, and thickness). Thickness of base layers, elastic modulus of the PCC, and flexural strength of PCC were also considered in the analyses.

Table 7. Climate analysis: structural design factors for PSG correlation.

Design Factor	Variable
Average slab width (ft)	W_{slab}
Average slab length (ft)	L_{slab}
Average layer thickness of PCC (inch)	h_{PC}
Average layer thickness of base (inch)	h_B
Average layer thickness of GB (inch)	h_{GB}
Average layer thickness of PATB (inch)	h_{PATB}
Average layer thickness of LCB (inch)	h_{LCB}
Average layer thickness of granular subbase (inch)	h_{GS}
Average layer thickness of treated subbase (inch)	h_{TS}
Estimated PCC paste volume (percent)	PV
Estimated PCC flexural strength (ksi)	F
Estimated PCC elastic modulus (ksi)	E

CORRELATING PSG AND ENVIRONMENTAL FACTORS

Predicting initial PSG values using all identified coefficients showed poor correlation. The RStudio® software was used for linear regression analysis and results can be found in appendix I.[22] RStudio identified the most significant coefficients but was unable to provide a solution with a good fit. The model for PSG_i and PSG_s had R-squared values that ranged from 0.60 and 0.47. The most significant coefficients for PSG_i were humidity and PCC/permeable-asphalt-treated base (PATB) layer thicknesses. For PSG_s, the most significant coefficients were paste volume, PCC elastic modulus, and LCB layer thickness.

Treated-base (i.e., PATB and LCB) thickness had a significant impact in the all-inclusive model; therefore, researchers determined that base type was potentially a classifier for the prediction model. Therefore, three prediction models were developed for each base type: granular base (GB), LCB, and PATB. Separating the models by base type produced models with significantly better fits; it also established that base type plays an important role in determining curling-and-warping behavior. The analysis resulted in the following linear models.

Figure 44 and Figure 45 show models for predicting PSG_i (i.e., initial curvature) and PSG_s (i.e., change in curvature after construction) using climatic and structural factors.

Table 8 describes the linear regression coefficients in Figure 44 and Table 9 describes the linear regression coefficients in Figure 45.

Table 8. Correlation of linear regression coefficients for *PSGi*.

Variables	GB	PATB	LCB
h_B	h_{GB}	h_{PATB}	h_{LCB}
x_1	−8.722E+00	−6.047E+00	−4.766E+01
x_2	2.344E−02	−1.709E−02	−5.899E−02
x_3	2.759E−01	1.314E−01	9.638E−02
x_4	8.845E−02	4.063E−02	7.194E−02
x_5	−9.592E−02	−3.494E−02	−6.759E−02
x_6	6.088E−02	4.125E−02	1.106E−01
x_7	−7.825E−01	−5.206E−02	9.587E+00
x_8	1.960E−01	8.286E−02	8.880E−02
x_9	1.259E−01	2.809E−01	2.459E−01
x_{10}	1.405E−02	5.537E−04	−4.156E−02
x_{11}	4.430E−02	4.419E−02	7.129E−02
x_{12}	−4.540E−03	2.761E−02	−2.999E−02
x_{13}	4.533E−04	−2.032E−04	−4.672E−04
x_{14}	−2.708E−07	9.288E−08	3.459E−07
x_{15}	−2.986E−01	−1.034E−01	1.489E−01

$$\begin{aligned}(PSG_i)_B = x_1 + x_2 T_0 + x_3 H_0 + x_4 \Delta_{T0} + x_5 \Delta_{H0} + x_6 W_{slab} \\ + x_7 L_{slab} + x_8 h_{PC} + x_9 h_B + x_{10} h_{GS} + x_{11} h_{TS} + x_{12} PV \\ + x_{13} F + x_{14} E + x_{15} \Delta T\end{aligned}$$

Figure 44. Equation. Calculation of the change in *PSGi* using climatic and structural factors.

Table 9. Correlation of linear regression coefficients for *PSGs*.

Variables	GB	PATB	LCB
h_B	h_{GB}	h_{PATB}	h_{LCB}
x_1	−9.055E+00	1.314E+00	1.623E+00
x_2	−1.263E−01	4.998E−03	8.846E−03
x_3	6.536E−01	−5.076E−02	−7.783E−02
x_4	5.891E−02	−4.385E−03	−1.624E−02
x_5	−3.412E−02	−2.928E−03	3.277E−02
x_6	−2.896E−02	−5.074E−03	−6.427E−03
x_7	1.433E−01	−1.573E−04	−5.811E−02
x_8	4.817E−03	−5.466E−03	−2.028E−02
x_9	4.353E−02	1.382E−02	5.206E−03
x_{10}	−9.524E−04	1.147E−04	−1.646E−03
x_{11}	−3.683E−02	2.970E−03	−2.011E−02
x_{12}	1.373E−02	−8.084E−04	9.411E−03
x_{13}	−3.263E−04	6.176E−05	−1.122E−04
x_{14}	−2.119E−07	−2.142E−08	−6.196E−08
x_{15}	−5.627E−02	1.183E−02	6.397E−02

$$(PSG_s)_B = x_1 + x_2T_1 + x_3H_1 + x_4\Delta_{T1} + x_5\Delta_{H1} + x_6W_{slab} + x_7L_{slab} + x_8h_{PC} + x_9h_B + x_{10}h_{GS} + x_{11}h_{TS} + x_{12}PV + x_{13}F + x_{14}E + x_{15}\Delta T$$

Figure 45. Equation. Calculation of the change in *PSGs* using climatic and structural factors.

Table 10 summarizes the statistical outputs for all prediction models identified in appendix I. Two key observations can be made from the regression statistics in Table 10:

- When predicting PSG_i, the model for GBs had the least error and the model for PATBs had the most error.
- When predicting PSG_s, the model for GBs had the most error and the model for treated bases (i.e., PATB and LCB) had the least error.

These observations imply that autogenous shrinkage had more predictable effects on pavements with GBs and that drying shrinkage had more predictable effects on pavements with treated bases. The observations also mean the material properties of bases can change over time, causing models for PSG_s to be more unpredictable in the case of GBs, which are typically more erodible than treated bases.

Table 10. Climate analysis: summary of prediction model statistics.

Model Statistic	GB Base Type	PATB Base Type	LCB Base Type
PSG_i model – Residual standard error	0.355	0.359	0.486
PSG_i model – Multiple R-squared	0.805	0.673	0.780
PSG_i model – Adjusted R-squared	0.502	0.368	0.437
PSG_i model – F-statistic	2.654	2.205	2.273
PSG_i model – p-value	0.072	0.070	0.109
PSG_s model – Residual standard error	0.109	0.033	0.072
PSG_s model – Multiple R-squared	0.576	0.810	0.751
PSG_s model – Adjusted R-squared	−0.083	0.632	0.363
PSG_s model – F-statistic	0.875	4.563	1.938
PSG_s model – p-value	0.603	0.003	0.160

Figure 46 shows the plots by base type comparing predicted PSG_i and PSG_s (from environmental/structural factors) to the measured PSG_s (from profile analysis). The poorest prediction was the PSG_s of pavements with GB. Several GB sections with large amounts of upward or downward curl tended to show poor correlation to climatic factors.

In contrast, the PSG_s predictions for pavements with treated bases were significantly better, which indicates that climatic factors have a more consistent effect on the curl and warp of pavements with treated bases. Pavements with treated bases tended to have more downward than upward curvature over time. Upward curvature is typically driven by the moisture gradient;

therefore, downward curvature may be the result of another factor that contributed to warping in treated base pavements.

It was more difficult to determine how the predicted value compared to the measured value in the case of the PSG_i because for most sections the amount of initial curvature was not significant. There were a few sections in which initial curvature was significantly upward. These sections had granular or LCBs and had better prediction models because the spread of initial PSG_i values was wider.

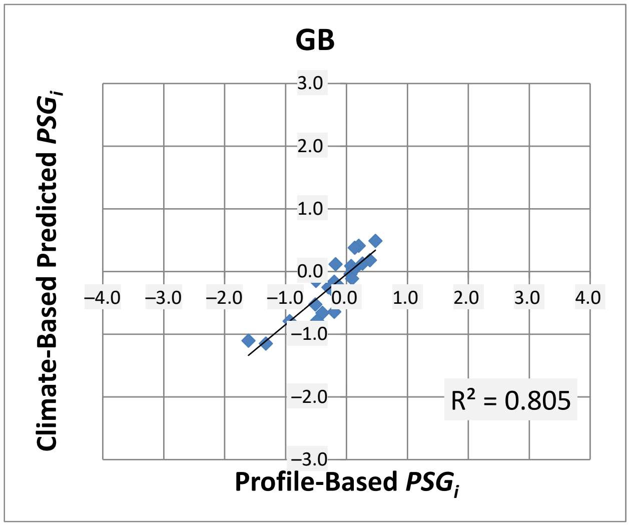

Source: FHWA.

A. Comparing predicted and measured PSG_i on pavements with GB.

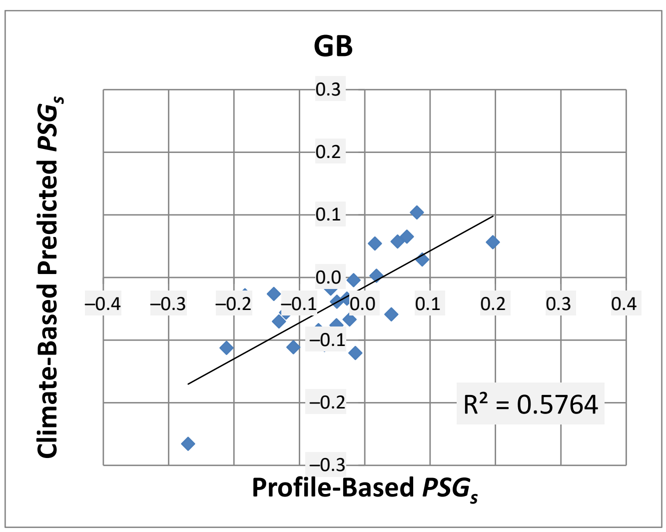

Source: FHWA.

B. Comparing predicted and measured PSG_s on pavements with GB.

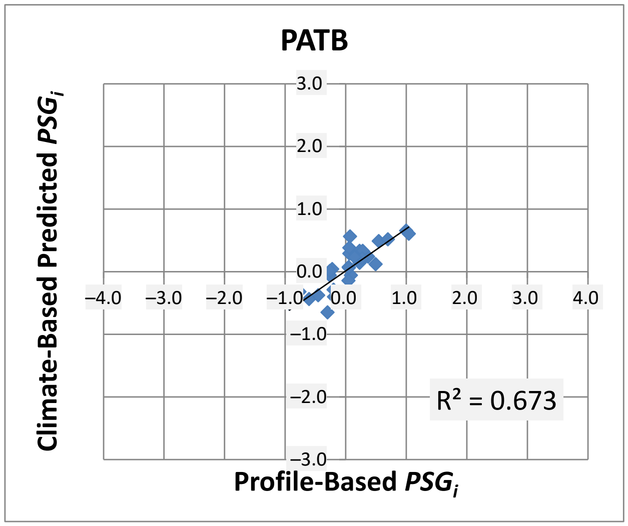

Source: FHWA.

C. Comparing predicted and measured PSG_i on pavements with PATB.

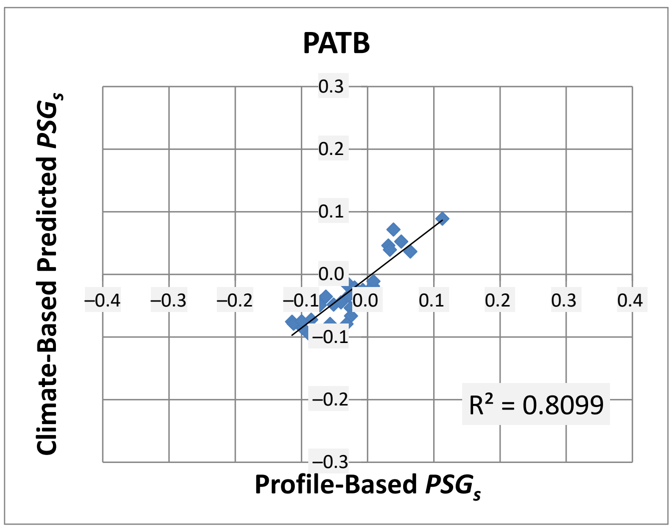

Source: FHWA.

D. Comparing predicted and measured PSG_s on pavements with PATB.

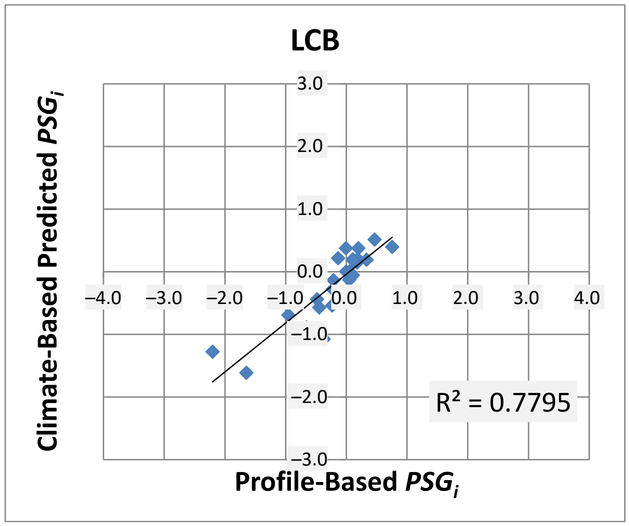

Source: FHWA.

E. Comparing predicted and measured PSG_i on pavements with LCB.

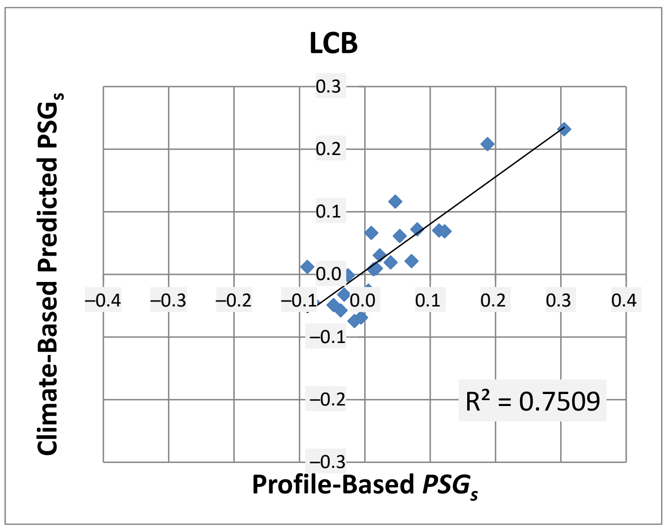

Source: FHWA.

F. Comparing predicted and measured PSG_s on pavements with LCB.

Figure 46. Graphs. Climate analysis of predicted PSG_i and PSG_s versus measured PSG_i and PSG_s.

SIGNIFICANCE OF ENVIRONMENTAL FACTORS

Based on the *p*-values of the prediction model, Table 11 shows coefficients that have the most significance in predicting PSG_i and PSG_s. The thicknesses of certain layers had significant influence on the prediction model. Paste volume and PCC modulus also had a significant effect for pavements with GB and PATB. However, for pavements with LCBs, temperature and humidity coefficients were more significant.

The coefficients that had the most significance in determining the PSG prediction models were identified using the Pr(>|*t*|) value (*p*-value in RStudio for the *t*-test) shown in Table 11. The *p*-value determines the chance the result was obtained by random error. For example, a *p*-value of 0.1 indicates there was less than a 10-percent chance that the result is from random error. *p*-values greater than 0.1 are usually interpreted as having no evidence that the null hypothesis holds, which means that there was a good chance the result was from random error. However, this interpretation could also have been an oversimplification and high *p*-values could result from having a small sample size (i.e., low degrees of freedom). The following observations were made using the *p*-values from PSG_i and PSG_s prediction models:

- **GB**: The PSG_i was mostly controlled by the thickness of the base and treated subbase layers, the dimensions (length and width) of the PCC slab, the paste volume, and flexural strength. The PSG_s was mostly controlled by the stiffness of the PCC slab, the thickness of the granular subbase and treated subbase layers, and paste volume. The model for PSG_i had lower R-squared values than the model for PSG_s (0.805 versus 0.576), suggesting that the initial curl was easier to predict than the change in curl over time for pavements with a GB.

- **PATB**: The PSG_i was mostly controlled by the paste volume and the thickness of the PCC slab and base layers. The PSG_s was mostly controlled by the thickness of the PCC slab, base, and subbase layers. The model for PSG_i has higher R-squared values than the model for PSG_s (0.673 versus 0.810), suggesting that the change in curl over time was easier to predict than the initial curl for pavements with PATB.

- **LCB**: The PSG_i was mostly controlled by the PCC slab stiffness, temperature gradient, and thickness of the granular base layers. The PSG_s was mostly controlled by the average annual relative humidity and temperature, average daily difference between maximum and minimum temperature and humidity, and thickness of the slab length. The model for PSG_i has higher R-squared values than the model for PSG_s (0.780 versus 0.751), suggesting that the initial curl was easier to predict than the change in curl over time for pavements with LCB.

The best prediction model was for the change in PSG of pavements with LCBs. This model met the expectation that temperature and humidity controlled the long-term curling and warping behavior of a PCC pavement. Slab length also showed good correlation in predicting PSG_s for pavements with LCBs. The *p*-values on these coefficients were all less than 0.01, which indicated that there was strong evidence the null hypothesis did not hold. The other PSG prediction models depended mostly on the structural factors of the pavement (e.g., layer thickness, stiffness, paste volume). Compared to the impact of structural factors, climatic factors had a secondary impact on PSG prediction models.

In the case of structural factors, *p*-values were typically larger than 0.1 and indicated either that the model likely resulted from random errors or the sample size was not large enough. These structural properties likely contributed to an unknown structural parameter of mechanical behavior. The significance of the thickness of pavement layers may indicate that the dynamics of the pavement structure played some role in the curl behavior. The significance of pavement-layer thickness was especially true for pavements with more flexible base types, such as GB and

PATB. The change in PSG of pavements with LCB was strongly controlled by climatic effects of humidity, temperature, and slab length.

Table 11. Climate analysis: correlation coefficients with the lowest *p*-value per model.

Predicted Curling	Coefficient for GB	*Pr*(>|*t*|) for GB	Coefficient for PATB	Pr(>|*t*|) for PATB	Coefficient for LCB	Pr(>|*t*|) for LCB
PSG_i	h_{PC}	0.030	h_{PC}	0.193	h_{GS}	0.218
PSG_i	h_{GS}	0.122	(Intercept)	0.205	h_{LCB}	0.219
PSG_i	H_0	0.130	H_0	0.299	H_0	0.270
PSG_i	Δ_{T0}	0.162	PV	0.318	(Intercept)	0.276
PSG_i	L_{slab}	0.162	h_{PATB}	0.339	L_{slab}	0.300
PSG_i	ΔT	0.173	Δ_{T0}	0.392	h_{PC}	0.370
PSG_i	(Intercept)	0.196	Δ_{H0}	0.467	T_0	0.385
PSG_i	Δ_{H0}	0.222	—	—	Δ_{H0}	0.425
PSG_i	T_0	0.377	—	—	E	0.471
PSG_s	E	0.126	h_{PC}	0.349	h_{PC}	0.183
PSG_s	PV	0.142	E	0.386	PV	0.342
PSG_s	h_{TS}	0.189	W_{slab}	0.485	h_{TS}	0.357
PSG_s	T_0	0.199	—	—	E	0.389
PSG_s	Δ_{T0}	0.205	—	—	ΔT	0.396
PSG_s	(Intercept)	0.217	—	—	—	—
PSG_s	H_0	0.241	—	—	—	—
PSG_s	W_{slab}	0.320	—	—	—	—
PSG_s	F	0.334	—	—	—	—

—No data.

SUMMARY OF FINDINGS

Researchers developed six models to predict the initial curl and warp of test sections of different base types and the rate of change in curl and warp in the first 10 years after construction. The simple linear regression analysis produced interesting results that described curl-and-warp behavior in LTPP concrete pavements. The models were developed using RStudio software, and results of the linear regression analysis can be found in the climate analysis section of appendix I.[(22)]

The initial curvature of many of the test sections was not overly significant, which could be because of the effect of concrete creep while the pavement was curing. Some pavements started out with an upward curvature; these pavement sections had either granular or LCBs. Pavements with PATBs typically had very little initial curvature. Humidity affected initial curvature for all bases types (the third most significant coefficient), but initial curvature was primarily controlled by nonclimatic structural factors (i.e., layer thickness, paste volume, stiffness). However, the *p*-values of coefficients in the prediction models were typically high, suggesting that correlations could result from random error. For example, paste volume only appeared to have significance in the model for PATB pavements (when predicting PSG_i), but the effect of paste volume may have been coincidental since *p*-values were slightly high. In general, these models indicated that base type, pavement structure, and humidity strongly impact the built-in curvature in PCC slabs, and pavements typically start out with little curvature.

The change in PSG over time was the best way to identify curling behavior. Models that predicted this change were consistent for pavements with treated bases (i.e., PATB and LCB). PCC elastic moduli were significant in the PSG_s models for GB, PATB, and LCB pavements. Paste volume was significant only in GB and LCB pavements. The thickness of the PCC layer was significant in test sections with treated bases. Temperature and humidity were significant for GB test sections only, and the temperature gradient had a minor effect for LCB test sections. In general, these results indicated the stiffness of the PCC was the most common coefficient with significance. The effect of base types caused certain factors to have more influence on the prediction model than other factors. The PSG_s models for treated bases had the least amount of error and the primary coefficient in those models was PCC thickness. In the case of test sections with GBs, PCC thickness was not as significant as climatic factors; therefore, the model was less reliable.

Other climatic factors considered included the total annual precipitation and the freezing index, but these factors had no effect in the linear regression analysis. The precipitation amount and days below freezing were not as important to curl-and-warp behavior as the annual average temperature and humidity. To predict initial curling in a pavement, researchers determined that climate data (temperature and humidity) averaged over the first month after construction had a better correlation than climate data averaged over the first 10 years. Likewise, prediction models for the change in curl over time were better when using climate data averages from the first 10 years after construction rather than the first month.

CHAPTER 9. CORRELATION OF PSG TO FWD RESULTS

Pavements with uplift from curl and warp can behave differently than level pavements that are fully supported by their base when a load is applied. The uplift often causes a void or soft soil underneath the pavement at the raised part of the slab. When a load is applied to the uplifted part of the slab, the slab can deflect freely until it contacts the underlying layer. Once the pavement is supported by the underlying layer, the pavement structure can act in unison to resist the applied load. While under load, the total deflection of the slab is partly due to the uplifted deflection of the curled slab and partly to the deflection from loading the pavement.

The unloaded deflection should remain constant regardless of the amount of load being applied, but the deflection from loading should be proportional to the applied load. Analyzing FWD testing data at different load levels produced the amount of linear elastic deflection in proportion to the applied load and distinguished the amount of unloaded deflection from the loaded deflection. This unloaded deflection was correlated to PSG, an indicator of the tensile strain in the slab resulting from curl and warp.

DEVELOPING DIs

Per LTPP tests and protocols, FWD testing on rigid pavements was performed at three load levels.(23) Typically, as the load level increases, the amount of deflection in the pavement proportionally increases. Performing linear regression analyses on the loads and deflections yielded a slope and an intercept. The DI is the unloaded deflection of the pavement. In theory, pavements with an upward curl should have an unloaded deflection near the edge of the slab, and pavements with a downward curl should have an unloaded deflection near the center of the slab. However, this assumption also assumes the pavement and underlying layers are not significantly deteriorated. Cracked slabs, air voids, or soft soils could also impact the DI value.

Figure 47 demonstrates how error can be introduced into the DI value depending on the actual relationship curve between load and deflection. The calculated DI may result partly from the uplift from curl and warp and partly from the reaction of the base or subgrade. Soil liquefaction may cause soil to lose stiffness in proportion to the applied load, resulting in higher deflections. Liquefaction is especially common in freeze-thaw areas, where thawed subgrade may be sandwiched between the pavement and frozen subgrade. The viscoelastic nature of asphalt-bound layers may cause asphalt-treated bases in concrete test sections to increase in stiffness with repeated loading. The load shown in Figure 47 is the net of the applied dynamic load from the FWD and the uplift force from the curvature of the slab. This uplift force is unique to each slab and test point. Uplift at the slab corner may react differently than uplift at the center. When at the corner, doweling and aggregate interlock between the adjacent slab and the shoulder may influence the DI value. Because of these potential sources of error, the DI value may be subject to interpretation based on the structural properties of the slab and not purely the curvature from curl and warp.

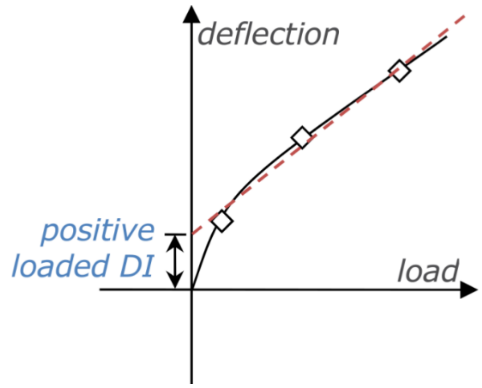

Source: FHWA.

A. Diagram of positive-loaded DIs.

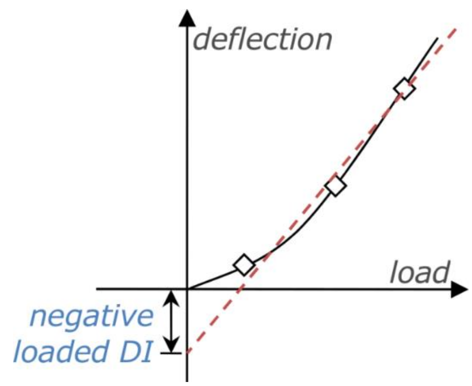

Source: FHWA.

B. Diagram of negative-loaded DIs.

Figure 47. Illustrations. Demonstration of error in the linear elastic calculation of DIs when there is a nonlinear relationship between deflection and load.

LTPP FWD testing is performed at specific locations with respect to the slab. This testing allows for a DI value to be calculated for each location on the slab. Figure 48 shows a diagram of FWD test location relative to the slab. Table 12 describes the location of FWD test point IDs relative to the JPCP slab. However, because FWD testing is performed in order of test point type and not slab-by-slab, a time gap exists between tests performed at each location on the slab. The time gap can be an issue if temperature or other environmental conditions change during the day and cause a change in the curl state of the slab. For example, the curl state of the slab may be slightly different when FWD testing was conducted at the midslab location than when testing was conducted at the corner. Depending on the lane width of the test section, FWD testing on a 500-ft SPS-2 section will typically take 1 to 5 hours. Table 12 describes the location of each FWD test point ID illustrated in Figure 48.

Table 12. FWD test point IDs and locations.

Test Point ID	Location
J1	Midlane, midslab
J2	Pavement edge, approach joint edge
J3	Pavement edge, midslab
J5	Outer wheel path, approach joint edge

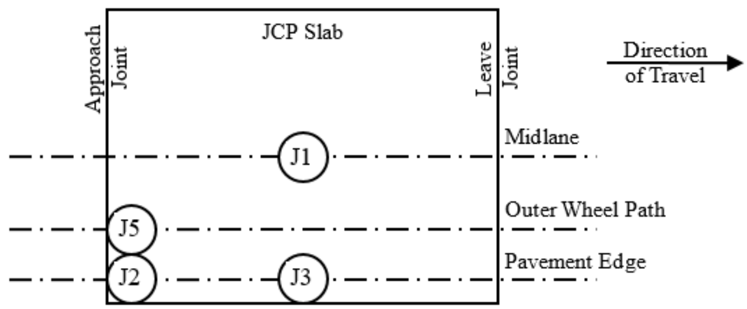

Source: FHWA.

Figure 48. Illustration. FWD test-point locations relative to the slab.

CURL AND WARP IN DIs

In most cases, time-series plots of DI values did not provide sufficient information to identify the curl state of the pavement. Intervals between FWD tests ranged from 4 months to 12 years (3.2 years on average). Testing occurred in different seasons or at different times during the day. Testing interval variations resulted in different temperature and humidity conditions for each test. FWD testing was typically not performed in concurrence with profile testing; therefore, each form of pavement testing was typically performed in different environmental conditions—conditions that are known to cause diurnal and seasonal fluctuations in a pavement's curl-and-warp state. Additionally, the curling of each slab in a section may affect the DI values to a different extent. Compounding all these factors of variability added significant background noise to trend analysis using only the DI value.

CORRELATING PSG AND DIs

A positive DI value at J1 (slab center) indicates the amount of downward curl, and a positive DI value at J2 (slab corner) indicates the amount of upward curl. Therefore, the difference between DI_{J1} and DI_{J2} will indicate the overall curl direction, as shown in Figure 49. A positive ΔDI indicates a downward curl and a negative ΔDI indicates an upward curl.

$$\boldsymbol{\Delta DI = DI_{J1} - DI_{J2}}$$

Figure 49. Equation. Calculation of Δ*DI*.

Where:

DI_{J1} = DI at FWD test point J1 (slab center).

DI_{J2} = DI at FWD test point J2 (slab corner).

The DI values at J3 and J5 were also evaluated but no significant trends were found. Test point J2 is farther from the pavement's center than J3 and provided more pronounced and consistent DI values. The DI values at J5 also did not provide any meaningful trends in relation to the curl state. The uplift from curling is more prominent across the length of the slab than the width; therefore, a common mitigation for pavement curling has been to design a pavement using shorter slab lengths.

Certain SPS-2 test sections have 14-ft-wide slabs that included additional test points: J7 and J8. These slabs were typically wider than the travel lane and extend into the shoulder. At widened test sections, J2 is the corner at the travel lane edge and J7 is farther out at the corner of the pavement edge. Likewise, J8 is farther out than J3. However, because only half of the SPS-2 test sections had 14-ft-wide slabs, the DI values at J7 and J8 were not evaluated for a comprehensive trend analysis. Slab width may affect curvature; therefore, evaluating test points at different locations relative to the slab midpoint could potentially skew the results. Based on a quick investigation, deflections at J7 and J8 were similar enough to deflections at J2 and J3 that that these values did not have a significant difference in how they should be interpreted.

Figure 50 shows the distribution of DI values evaluated at FWD test locations. DI values at J1 (slab center) were typically lower than at other locations. Because of this, DI_{J2} usually controls the computed value of ΔDI. The DI at J2 typically had higher absolute values than other locations (except J7). J2 and J7 followed the same distribution of DI values. The only major difference between J2 and J7 was that twice as many tests were performed on J2; the same difference also applied to J3 and J8. DI values followed the same distribution and twice as many tests were performed on J3 than J8. The distributions in J2 and J3 followed a similar pattern, but the absolute DI values at J2 were typically larger than at J3.

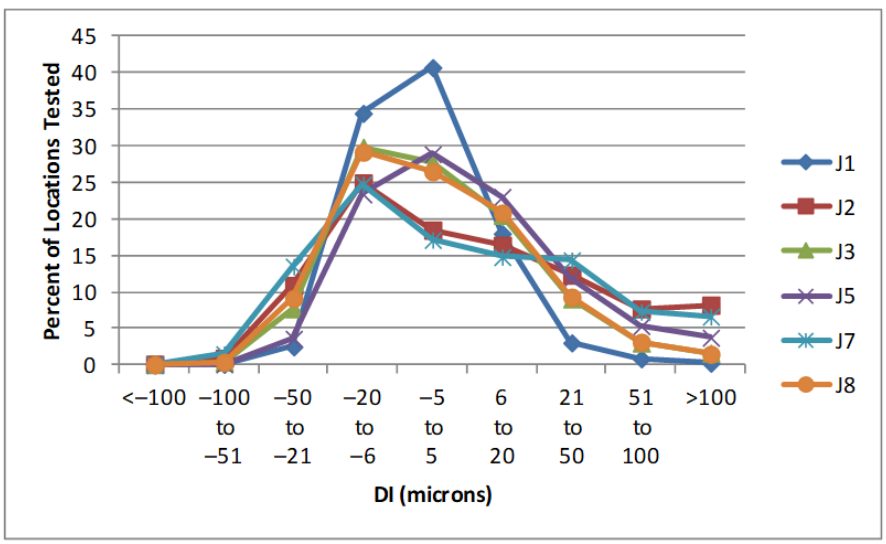

Source: FHWA.

Figure 50. Graph. Distribution of DI values by FWD test-point location.

Figure 50 also describes the characteristic differences between slabs that are curled up and curled down. Assuming DI values near zero represent slab without curvature, the distribution of DI values for slabs that curled up was different from the distribution of slab were curled down.

These distributions suggested the true DI value for a slab with no curvature is slightly negative and not zero. Slabs that curled up (positive DI_{J2} and negative DI_{J1}) have larger absolute DI values than slabs that curled down (negative DI_{J2} and positive DI_{J1}). This finding suggested that the degree of curvature for slabs that curled up was typically greater than the amount of curvature in slabs that curled down.

Figure 51 through Figure 53 show the trend of DIs and PSG values of three test sections (these sections were selected from examples discussed in Figure 41). From Figure 51 through Figure 53, two observations can be made that reflect trends seen in the DI data.

- The slope of DI_{J1} in these examples was close to zero, while the slope of DI_{J2} was positive.
- The slope of ΔDI and PSG did not always indicate the same direction of curvature.

These initial observations were examined by performing linear regression analysis on DI_{J1}, DI_{J2}, ΔDI, and PSG for all test sections.

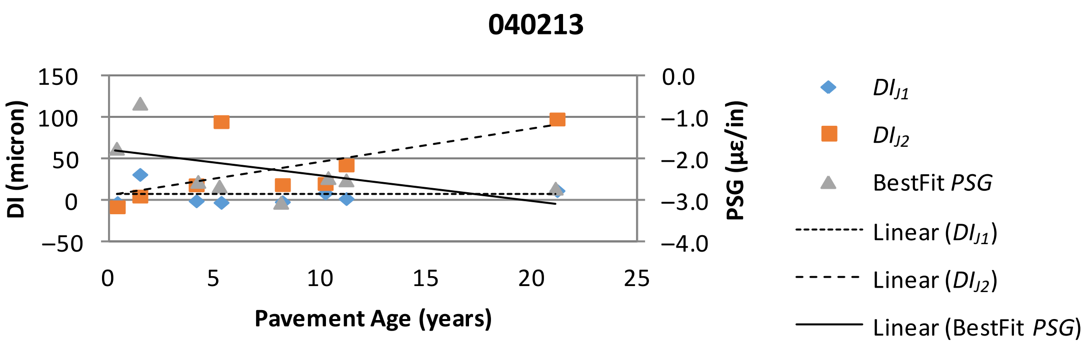

Source: FHWA.

A. Trend in DI_{J1}, DI_{J2}, and PSG at test section 040213.

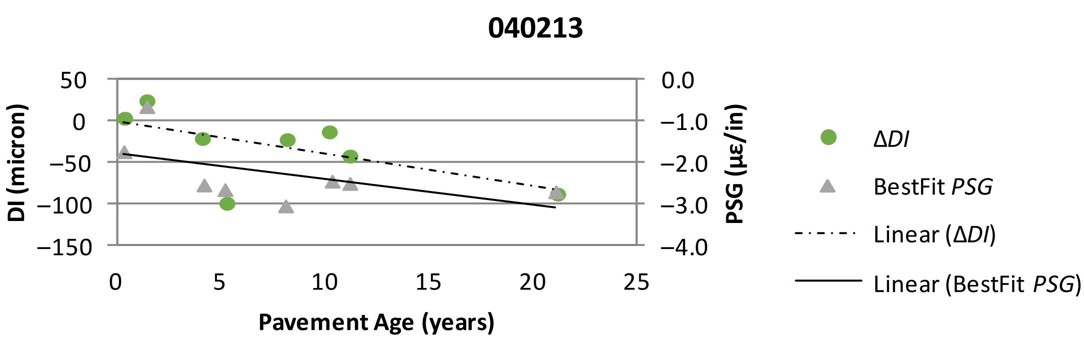

Source: FHWA.

B. Trend in ΔDI and PSG at test section 040213.

Figure 51. Graphs. DI and PSG trends over time using test section 040213.

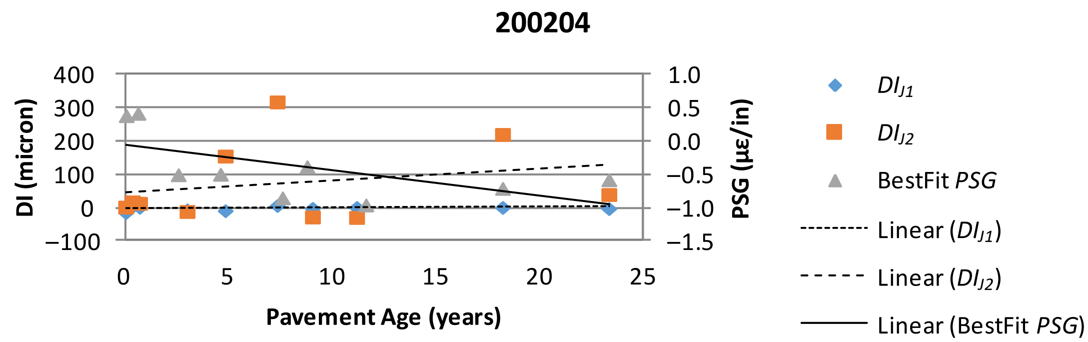

Source: FHWA.

A. Trend in DI_{J1}, DI_{J2}, and PSG at test section 200204.

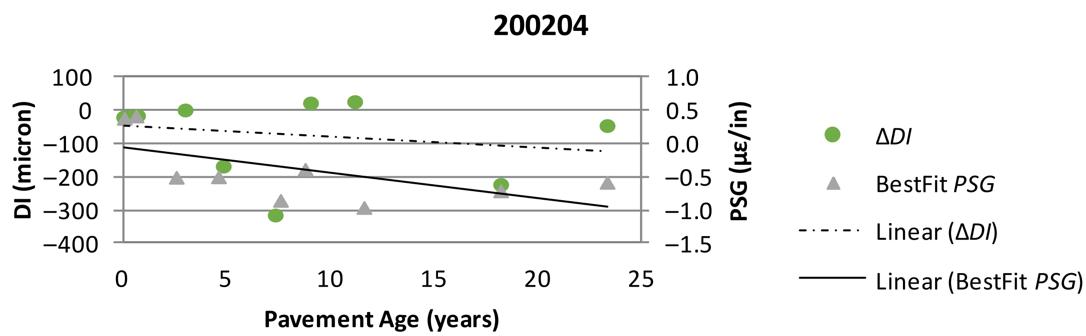

Source: FHWA.

B. Trend in ΔDI and PSG at test section 200204.

Figure 52. Graphs. DI and PSG trends using test section 200204.

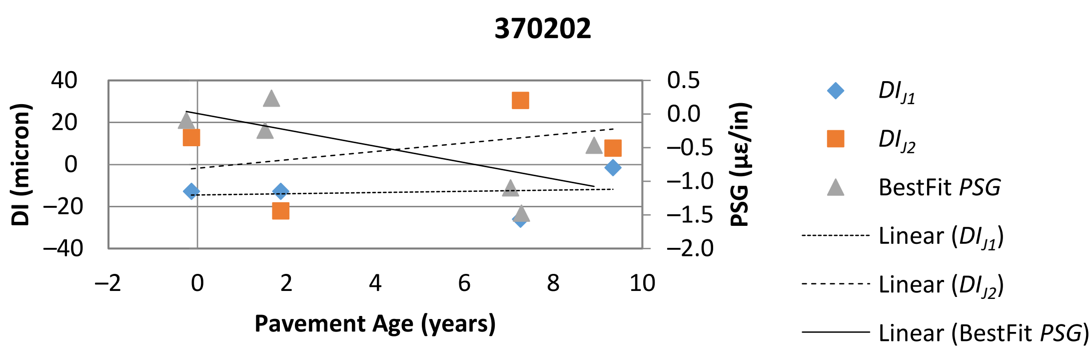

Source: FHWA.

A. Trend in DI_{J1}, DI_{J2}, and PSG at test section 370202.

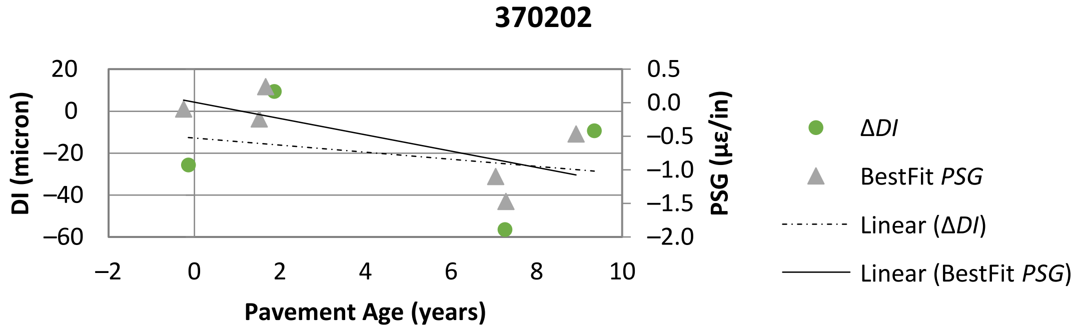

Source: FHWA.

B. Trend in ΔDI and PSG at test section 370202.

Figure 53. Graphs. DI and PSG trends using test section 370202.

Intercept of DI_{J1} (DI_{J1i}), slope of DI_{J1} (DI_{J1s}), intercept of DI_{J2} (DI_{J2i}), and slope of DI_{J2} (DI_{J2s}) resulted from regression analysis of DIs at locations J1 and J2. Figure 54 shows the number of test sections for which the slopes of DI_{J1} and DI_{J2} were inversely related (one was positive and one was negative) and for which the slopes of DI_{J1} and DI_{J2} were the same (either both were positive or both were negative). DI_{J1} and DI_{J2} had an inverse relationship in about half of the evaluated test sections. The average slope of ΔDI (the difference between DI_{J1} and DI_{J2}) was much more significant when DI_{J1} and DI_{J2} were both positive. This significance suggests the relationship between DI_{J1} and DI_{J2} may be relative to each other and not to a slope of zero. In other words, a zero DI value at J1 or J2 did not necessarily mean that the amount of slab uplift at this FWD test point location was also zero. The use of ΔDI mitigated this issue because ΔDI was the difference between DI values.

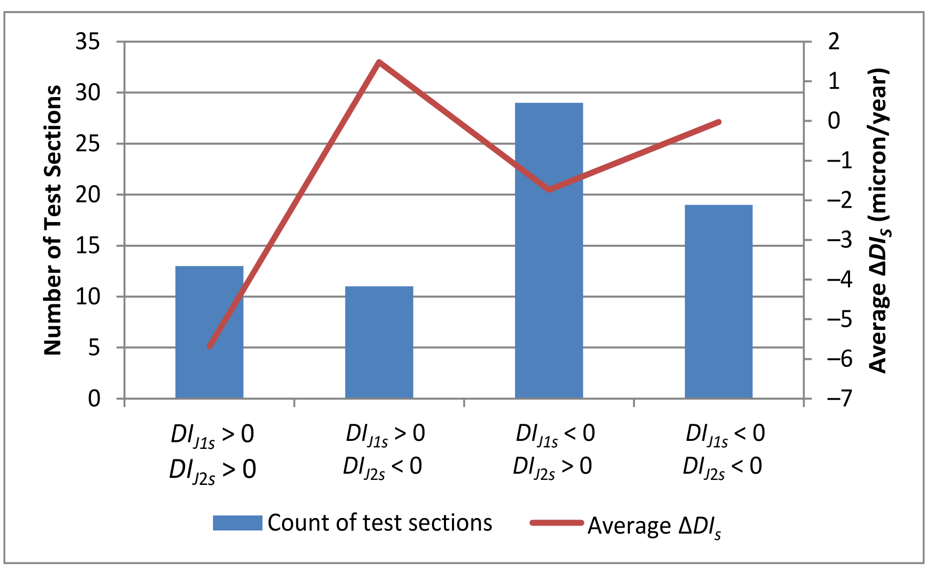

Source: FHWA.

Figure 54. Graph. Categorizing the regression slope of DI_{J1} and DI_{J2}.

Linear regression analysis of ΔDI yielded an intercept (ΔDI_i) and a slope (ΔDI_s). Values for each test section can be found in appendix G. Figure 55 and figure 56 compare these ΔDI regression values to PSG_i and PSG_s respectively. Like the climate-based PSG regression analysis, FWD testing performed only in the first 10 years after construction was considered for regression analysis. *PSG* and *DI* values became highly variable after 10 years and were not useful for trend analysis.

The section-by-section comparisons found that ΔDI regression values very often did not agree with the trends in PSG regression values. For example, a zero PSG value indicated that no curvature was present in the slab, but ΔDI often indicated the presence of some slab uplift with either a positive or negative value. Voids, soft soils, liquefaction, and dowel socketing can affect DI; therefore, it was difficult to directly compare one section to another section. The ΔDI values were influenced by structural and environmental factors, which needed to be considered when comparing the sections.

Figure 55 shows that the initial curvature of the pavement had more agreement in warm, dry climates than in cool, wet climates. Figure 56 shows the change in curvature over time that, regardless of climate, about half the test sections had ΔDI_s with the same direction of curling as PSG_s and about half did not. Test sections in North Carolina were the only exception as ΔDI_s and PSG_s agreed with each other more frequently. If PSG was to be used as the baseline for the true direction of curvature, then ΔDI_s was not able to predict the correct curl-and-warp direction by itself because DI_{J1} and DI_{J2} were weighted equally in the computation ΔDI_s. The DI values at the slab corner and slab center need to be weighted differently to predict PSG. Linear regression analysis was performed to predict PSG depending on the base type and other structural factors that may affect curl-and-warp behavior.

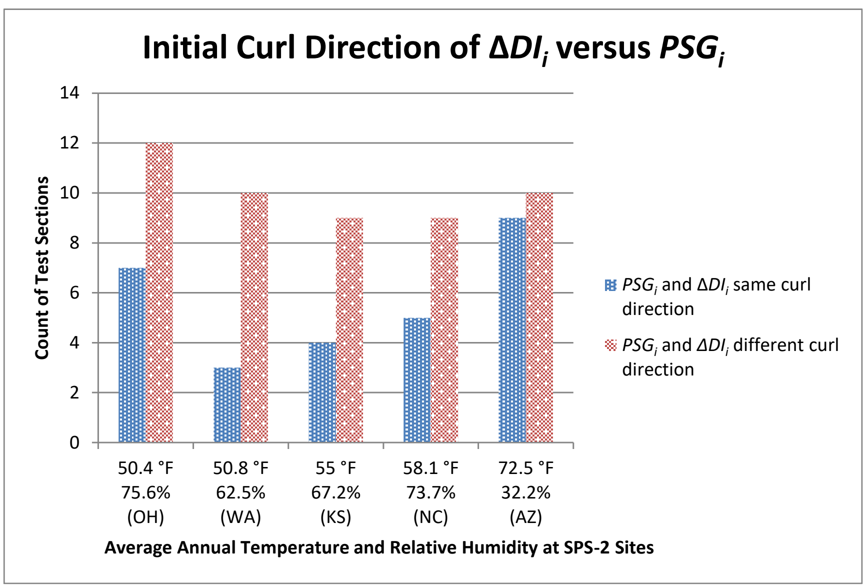

Source: FHWA.

Figure 55. Graph. Initial curvature direction (up or down) of ΔDI_i versus PSG_i.

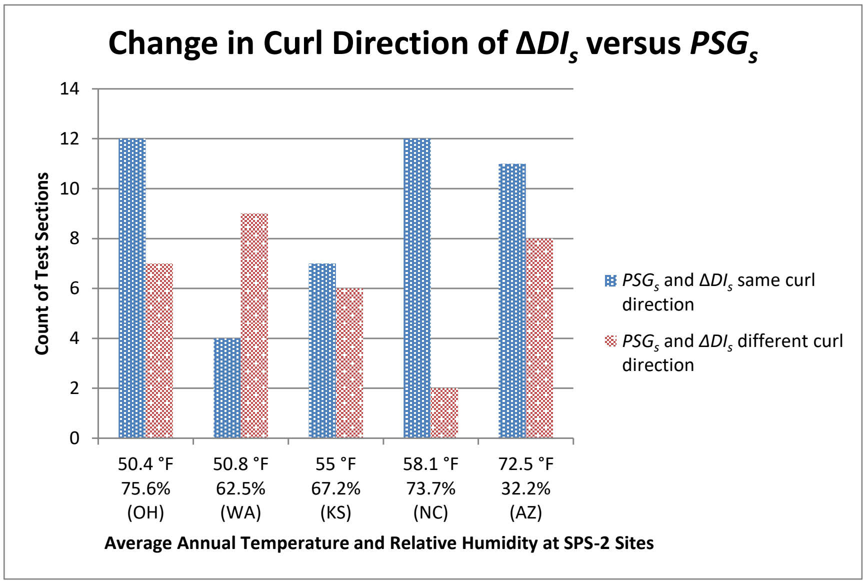

Source: FHWA.

Figure 56. Graph. Change over time in curvature direction (up or down) of ΔDI_s versus PSG_s.

To determine how structural factors influence the interpretation of ΔDI, researchers performed linear regression analysis using the structural factors defined in Table 13 (i.e., slab width, slab length, layer thicknesses, paste volume, flexural strength, and elastic modulus). The analysis also considered the average temperature gradient (ΔT) and regression coefficients (intercept and slope) of DI_{J1} and DI_{J2}. The DI at test points J1 (slab center) and J2 (slab corner) may be interpreted differently depending on base type. Granular and flexible bases are more likely to deform to fit the curvature of a curled or warped slab, while rigid bases are more likely to retain their shape or form their own curvature because of curl and warp.

Table 13. DI analysis: structural design factors for PSG correlation.

Design Factor	Variable
Average slab width (ft)	W_{slab}
Average slab length (ft)	L_{slab}
Average layer thickness of PCC (inch)	h_{PC}
Average layer thickness of base (inch)	h_B
Average layer thickness of GB (inch)	h_{GB}
Average layer thickness of PATB (inch)	h_{PATB}
Average layer thickness of LCB (inch)	h_{LCB}
Average layer thickness of granular subbase (inch)	h_{GS}
Average layer thickness of treated subbase (inch)	h_{TS}
Estimated PCC paste volume (percent)	PV
Estimated PCC flexural strength (ksi)	F
Estimated PCC elastic modulus (ksi)	E
Average temperature gradient (°F/inch)	ΔT

Figure 57 and Figure 58 show models for predicting PSG_i and PSG_s using DI and structural factors. Table 14 describes the linear regression coefficients in Figure 57 and table 15 describes the linear regression coefficients in Figure 58.

Table 14. DI analysis: linear regression coefficients for PSG_i.

Variable	GB	PATB	LCB
h_B	h_{GB}	h_{PATB}	h_{LCB}
x_1	−2.772E+00	−3.159E+00	−3.521E+01
x_2	1.913E−03	1.628E−02	6.997E−02
x_3	6.160E−02	2.978E−03	4.351E−01
x_4	−2.672E−02	−2.144E−02	−9.576E−02
x_5	−1.247E−01	5.418E−02	−4.803E−01
x_6	3.549E−03	2.319E−02	6.678E−02
x_7	7.384E−02	2.949E−02	4.426E−01
x_8	1.855E−01	1.742E−01	−6.267E−02
x_9	−3.346E−01	−2.423E−01	7.586E+00
x_{10}	2.049E−01	5.361E−02	3.056E−02
x_{11}	−9.189E−02	1.442E−01	8.421E−02
x_{12}	1.223E−02	6.437E−03	9.356E−03
x_{13}	1.415E−01	4.943E−02	1.398E−01
x_{14}	−1.253E−02	2.873E−02	−5.009E−03
x_{15}	7.779E−04	3.039E−04	−1.754E−04
x_{16}	−2.394E−07	−1.563E−07	1.093E−07
x_{17}	−3.271E−01	−1.545E−01	6.994E−01

$$\begin{aligned}(\boldsymbol{PSG_i})_{\boldsymbol{B}} = {} & \boldsymbol{x_1 + x_2 \Delta DI_i + x_3 \Delta DI_s + x_4 (DI_{J1})_i + x_5 (DI_{J1})_s} \\ & \boldsymbol{+ x_6 (DI_{J2})_i + x_7 (DI_{J2})_s + x_8 W_{slab} + x_9 L_{slab} + x_{10} h_{PC}} \\ & \boldsymbol{+ x_{11} h_B + x_{12} h_{GS} + x_{13} h_{TS} + x_{14} PV + x_{15} F + x_{16} E + x_{17} \Delta T}\end{aligned}$$

Figure 57. Equation. Calculation of PSG_i using DI and structural factors.

Table 15. DI analysis: linear regression coefficients for PSG_s.

Variable	GB	PATB	LCB
h_B	h_{GB}	h_{PATB}	h_{LCB}
x_1	−1.133E+00	4.358E−01	5.934E−01
x_2	6.087E−03	1.232E−03	−3.804E−03
x_3	2.905E−02	1.974E−03	−2.029E−02
x_4	−6.447E−03	−1.923E−03	5.906E−03
x_5	−7.694E−03	−2.322E−02	2.023E−02
x_6	5.584E−03	−7.790E−04	−3.769E−03
x_7	2.999E−02	−9.947E−03	−2.152E−02
x_8	1.181E−02	−1.912E−02	−9.838E−03
x_9	3.053E−01	2.289E−02	−6.043E−02
x_{10}	−7.708E−03	−3.904E−03	−2.362E−02

Variable	GB	PATB	LCB
x_{11}	−1.485E−02	−9.838E−03	2.185E−02
x_{12}	−5.543E−04	−6.330E−04	2.420E−03
x_{13}	−1.502E−03	−1.856E−03	−1.033E−02
x_{14}	4.687E−04	6.303E−04	8.473E−03
x_{15}	−1.108E−04	−6.565E−05	−6.934E−05
x_{16}	−5.924E−08	−4.763E−08	−3.622E−08
x_{17}	6.327E−03	−1.075E−02	8.179E−02

$$
\begin{aligned}
(\boldsymbol{PSG_s})_{\boldsymbol{B}} = {} & \boldsymbol{x_1} + \boldsymbol{x_2}\Delta\boldsymbol{DI_i} + \boldsymbol{x_3}\Delta\boldsymbol{DI_s} + \boldsymbol{x_4}(\boldsymbol{DI_{J1}})_{\boldsymbol{i}} + \boldsymbol{x_5}(\boldsymbol{DI_{J1}})_{\boldsymbol{s}} \\
& + \boldsymbol{x_6}(\boldsymbol{DI_{J2}})_{\boldsymbol{i}} + \boldsymbol{x_7}(\boldsymbol{DI_{J2}})_{\boldsymbol{s}} + \boldsymbol{x_8}\boldsymbol{W_{slab}} + \boldsymbol{x_9}\boldsymbol{L_{slab}} + \boldsymbol{x_{10}}\boldsymbol{h_{PC}} \\
& + \boldsymbol{x_{11}}\boldsymbol{h_B} + \boldsymbol{x_{12}}\boldsymbol{h_{GS}} + \boldsymbol{x_{13}}\boldsymbol{h_{TS}} + \boldsymbol{x_{14}}\boldsymbol{PV} + \boldsymbol{x_{15}}\boldsymbol{F} + \boldsymbol{x_{16}}\boldsymbol{E} + \boldsymbol{x_{17}}\Delta\boldsymbol{T}
\end{aligned}
$$

Figure 58. Equation. Calculation of PSG_s using DI and structural factors.

In terms of base type, the results from these prediction models shared several similarities to the climate-based prediction models developed in climate analysis, which can be found in chapter 8.

Table 16 shows a summary of residual standard errors, R-squared values, F-statistic values, and *p*-values for each model. The prediction model for PSG_i had a better fit in test sections with GBs than in sections with treated bases. In contrast, the prediction model for PSG_s had a better fit for treated base test sections than GB test sections.

Table 16. DI analysis: summary of prediction model statistics.

Model Statistic	GB Base Type	PATB Base Type	LCB Base Type
PSG_i Model – Residual standard error	0.4106	0.38550	0.67190
PSG_i Model – Multiple R-squared	0.7970	0.68450	0.67190
PSG_i Model – Adjusted R-squared	0.3331	0.26380	−0.07795
PSG_i Model – F-statistic	1.7180	1.62700	0.89610
PSG_i Model – *p*-value	0.2392	0.19900	0.59990
PSG_s Model – Residual standard error	0.1157	0.03316	0.08809
PSG_s Model – Multiple R-squared	0.6307	0.84010	0.71380
PSG_s Model – Adjusted R-squared	−0.2134	0.62690	0.05974
PSG_s Model – F-statistic	0.7471	3.94100	1.09100
PSG_s Model – *p*-value	0.7043	0.01033	0.48090

Figure 59 shows the plots by base type comparing predicted PSG_s (from DI regression coefficients and structural factors) and measured PSG_s (from profile analysis). The following similarities between this regression analysis and the analysis performed on climatic factors (Figure 46) were determined as follows:

- GB test sections had a good prediction for PSG_i but a poor prediction for the PSG_s.
- PATB test sections had a satisfactory prediction for PSG_i and a good prediction for PSG_s. PSG_i in PATB test sections were not very large.

- LCB test sections had a satisfactory prediction for both PSG_i and PSG_s.

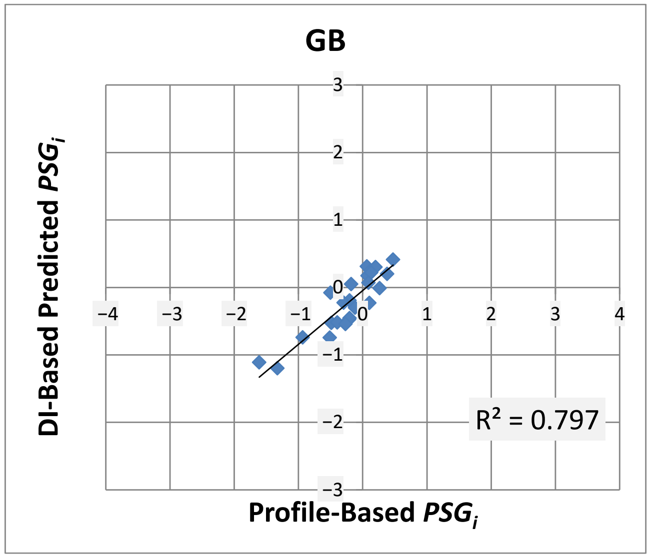

Source: FHWA.

A. Predicted and measured PSG_i on pavements with GB.

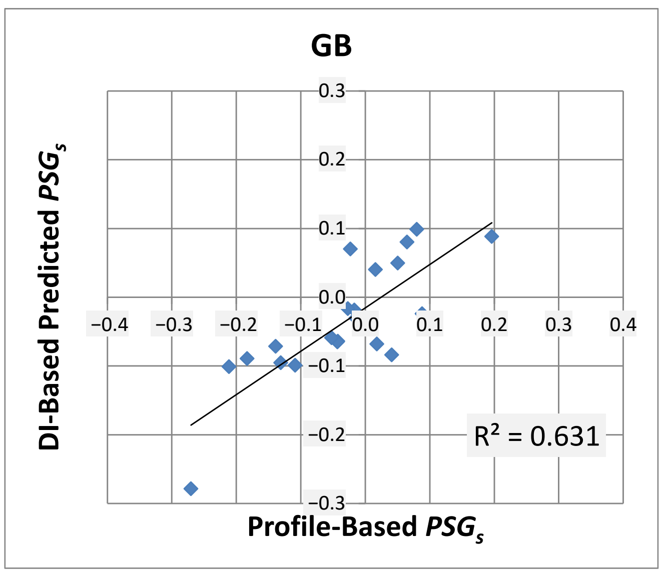

Source: FHWA.

B. Predicted and measured PSG_s on pavements with GB.

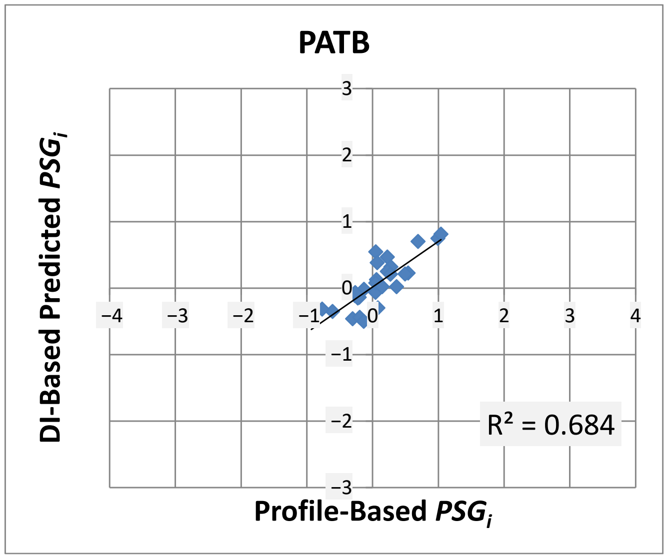

Source: FHWA.

C. Predicted and measured PSG_i on pavements with PATB.

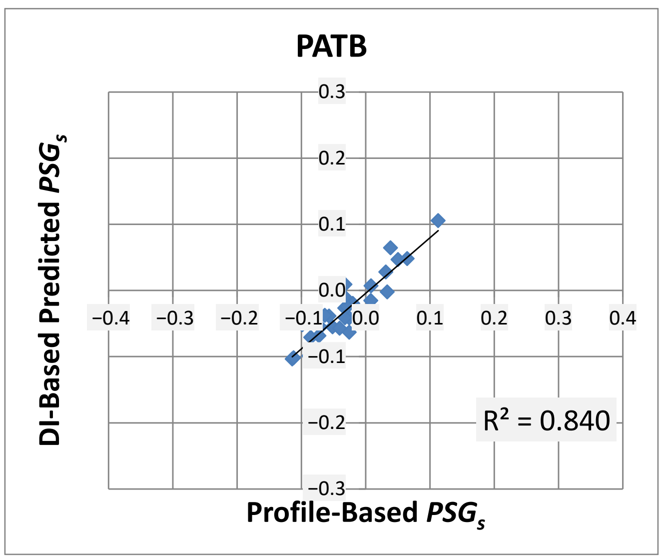

Source: FHWA.

D. Predicted and measured PSG_s on pavements with PATB.

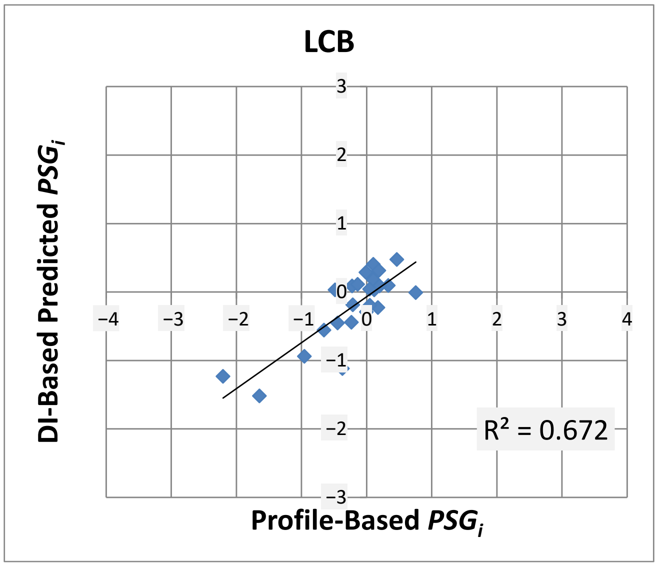

Source: FHWA.

E. Predicted and measured PSG_i on pavements with LCB.

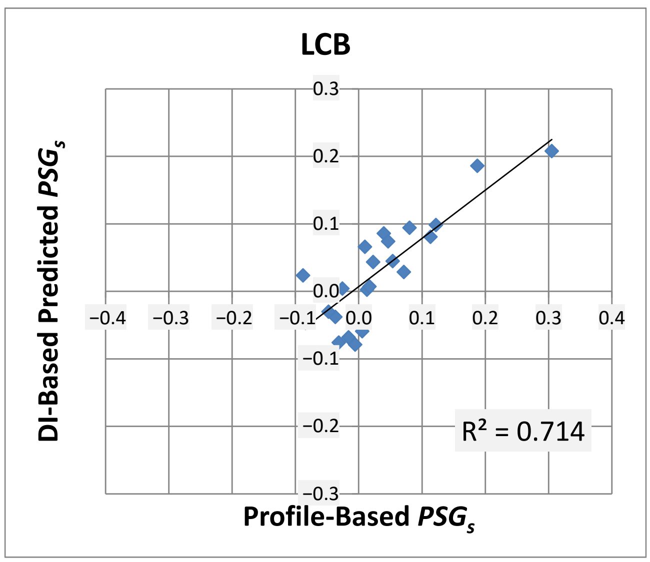

Source: FHWA.

F. Predicted and measured PSG_s on pavements with LCB.

Figure 59. Graphs. DI analysis showing predicted PSG_i and PSG_s versus measured PSG_i and PSG_s.

Table 17 shows the coefficients with the most significance in developing their respective prediction models. Several of the *p*-values for coefficients were high, which means the significance of some coefficients may have been caused by random error.

Table 17. DI analysis: correlation coefficients with the lowest *p*-value per model.

Predicted Curling	Coefficient for GB	Pr(>|*t*|) for GB	Coefficient for PATB	Pr(>|*t*|) for PATB	Coefficient for LCB	Pr(>|*t*|) for LCB
PSG_i	h_{TS}	0.024	W_{slab}	0.173	h_{TS}	0.117
PSG_i	h_{PC}	0.098	(Intercept)	0.215	ΔDI_i	0.322
PSG_i	ΔT	0.205	h_{TS}	0.236	DI_{J2i}	0.372
PSG_i	h_{GS}	0.212	PV	0.294	ΔDI_s	0.380
PSG_i	W_{slab}	0.253	DI_{J2i}	0.323	DI_{J2s}	0.384
PSG_i	DI_{J1s}	0.374	ΔDI_i	0.341	ΔT	0.429
PSG_i	E	0.398	DI_{J1i}	0.363	(Intercept)	0.457
PSG_i	DI_{J1i}	0.405	h_{GS}	0.370	L_{slab}	0.468
PSG_i	—	—	h_{PATB}	0.415	DI_{J1i}	0.474
PSG_s	L_{slab}	0.250	(Intercept)	0.058	h_{PC}	0.243
PSG_s	ΔDI_s	0.400	E	0.053	h_{GS}	0.289
PSG_s	(Intercept)	0.402	W_{slab}	0.090	h_{TS}	0.348
PSG_s	DI_{J2s}	0.418	DI_{J1s}	0.167	PV	0.352
PSG_s	E	0.456	h_{GS}	0.308	ΔT	0.478
PSG_s	DI_{J1i}	0.473	DI_{J1i}	0.343	—	—
PSG_s	—	—	ΔDI_i	0.400	—	—
PSG_s	—	—	L_{slab}	0.491	—	—
PSG_s	—	—	—	—	—	—

—No data.

The results were mixed on which coefficients were most significant for predicting PSG_i. The thicknesses of treated subbases were a significant factor. Only the test sections located in Kansas and North Carolina (31 percent of all selected SPS-2 test sections) had treated subbases with typical thickness between 6 and 8 inches. Whether a test section had a treated subbase had some control over how DI values correlated to PSG. However, this may not necessarily be because of the subbase but possibly related to environmental conditions that Kansas and North Carolina may share. Temperature gradient was significant for test sections with GB and LCB. Paste volume was more significant in PATB sections. The following DI regression values were found to have some significance in all PSG_i models but the significance of specific DI coefficients depended on the base type:

- GB test sections were more controlled by the slope and intercept of DI_{J1}.
- PATB test sections were more controlled by intercept of DI_{J1}, DI_{J2}, and ΔDI. In other words, the initial DI conditions controlled the prediction of the initial PSG condition.
- LCB test sections were more controlled by the slope and intercept of DI_{J2}.

Most test sections had a PSG_i that was close to zero, especially the PATB sections. A few GB and LCB test sections had an initial upward curl. When the slab curls upward, the corners of the slab were expected to rise slightly off the base. Researchers observed the rise on LCB test sections where the PSG_i correlated better with the DI at the slab corner. However, on GB test sections, the upward curl correlated better to the DI at the slab center. A large DI at the slab center should be more indicative of a downward curl. Results shows that several test sections began with an upward curl curled downward over time. The GB may have conformed to the initial upward curl (bowl shape) of the slab, but as the slab curled downward, uplift was created at the slab center.

For predicting PSG_s, the coefficients that have significance vary considerably depending on the base type. There were low *p*-values for the coefficients of elastic modulus and slab width in the PATB model. The coefficients in other models commonly have slightly higher *p*-values. Slab dimensions (i.e., width, length, and thickness) are significant coefficients just as they were in the climate analysis. The following DI coefficients also had significance, but this could be due to random error because their *p*-values were slightly high:

- GB test sections were more controlled by the slope of ΔDI and DI_{J2}.
- PATB test sections were more controlled by the slope and intercept of DI_{J1} and the intercept of ΔDI.
- LCB test sections were more controlled by layer thickness, paste volume, and temperature gradient.

Changes in DI at the slab corner indicated slabs curled upward over time or there was a void at the slab edge. Similarly, DI changes at the slab center showed slabs may have curled downward or there was a void under the center of the slab. ΔDI was also significant because it is a function of DI at the slab center and corner. Test sections with GB curled either upward or downward over time, as shown in Figure 59. The predictive models for PSG_s showed that GB test sections were sensitive to the initial DI at the slab center and the change in DI at the slab corner. This indicated some slabs that may have started out curled in one direction might have curled in the opposite direction over time. PATB test sections were more sensitive to the initial DI and the change in DI at only the slab center. PATB test sections; therefore, tended to curl downward creating uplift at the slab center. The PSG_s of LCB test sections, on the other hand, did not correlate well to DI values. The LCB test section tended to curl downward over time; therefore, PSG_s should have been sensitive to DI at the slab center but DI values were generally random and inconsistent with PSG. It is possible the lack of correlation between DI and PSG was caused by curvature in the LCB.

RELATING AVERAGE TEMPERATURE GRADIENT AND ΔDI

The relationship between ΔDI and average temperature gradient (ΔT) can be placed into two main categories: parabolic and linear. Fifty-five percent of the test sections exhibited a parabolic relationship between ΔDI and average temperature gradient, many of which show negative ΔDI values corresponding to positive average temperature gradient values. Forty-five percent of the test sections showed a linear relationship, where ΔDI decreased as average temperature gradient increased.

The value of ΔDI is the difference between DI values at the slab center and the slab corner. Testing at these two locations usually occurred nonconsecutively; therefore, the temperature gradient at the time of testing was different for the slab center than the slab edge. Because of this difference, an average of these temperature gradients was used for comparison to the ΔDI value. Figure 60 shows how much temperature gradient can change as the duration of FWD testing increases. Since most FWD testing is completed within 1 to 5 hours, the fluctuation in temperature gradients may cause the DI for a slab to change during FWD testing.

Figure 61 shows the parabolic or linear model that describes the relationship between ΔDI and temperature gradient can possess very low R-squared values due slab-by-slab fluctuation of temperature gradient and DI during FWD testing.

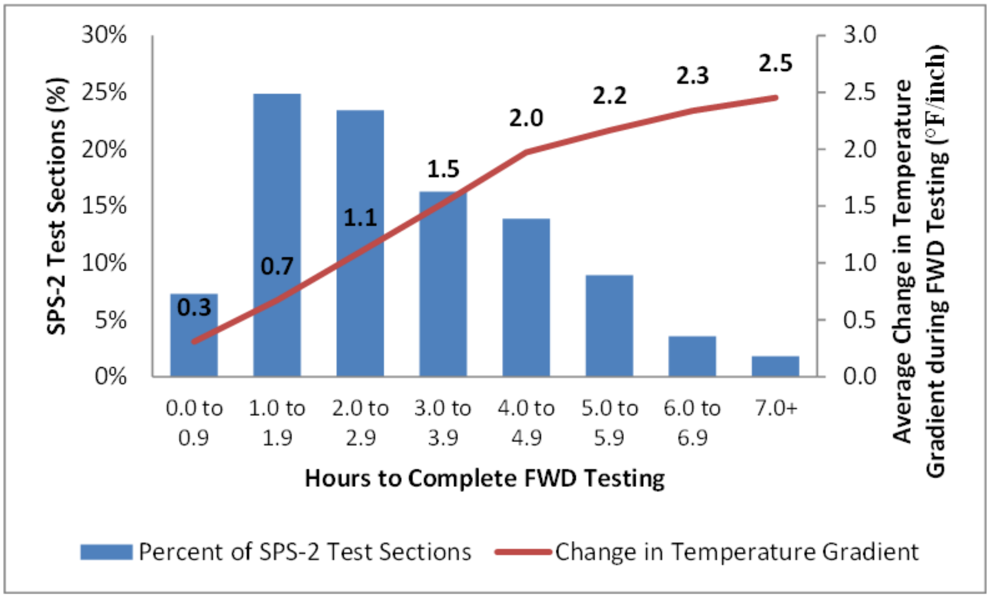

Source: FHWA.

Figure 60. Graph. Change in temperature gradient with the duration of FWD testing.

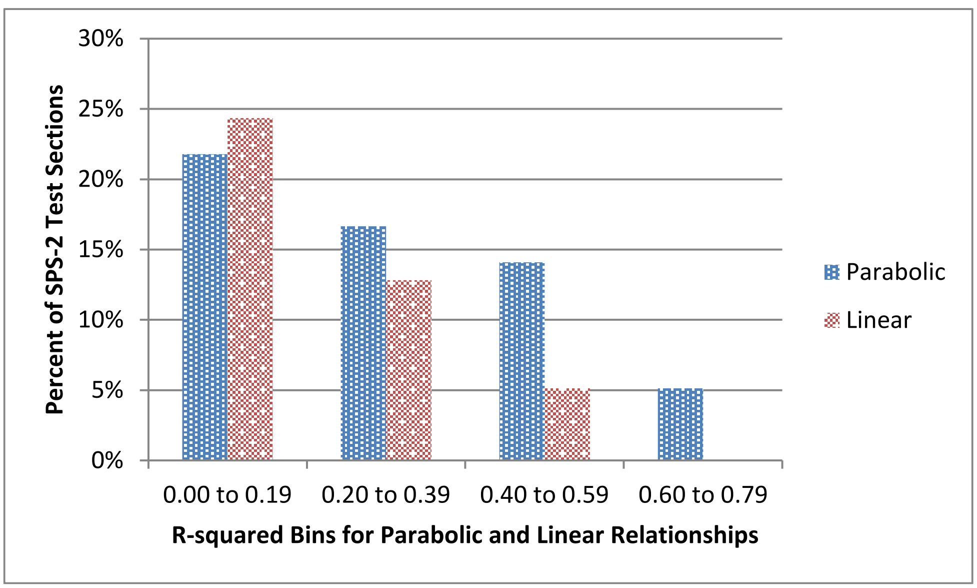

Source: FHWA.

Figure 61. Graph. R-squared value of parabolic and linear relationships between ΔDI and ΔT.

There were linear relationships between ΔDI and the average temperature gradient in half of the test sections. In these cases, as average temperature gradient increased, ΔDI typically decreased. Figure 62 shows test section plot with a linear relationship between ΔDI and ΔT. In this figure, test section 370201 shows that as the average temperature gradient became positive, Δ*DI* became negative. Both a positive Δ*DI* and a negative Δ*T* indicated that slabs had a downward curl. The R-squared value in this example is 0.059 because of the variation in slabs and the time of testing.

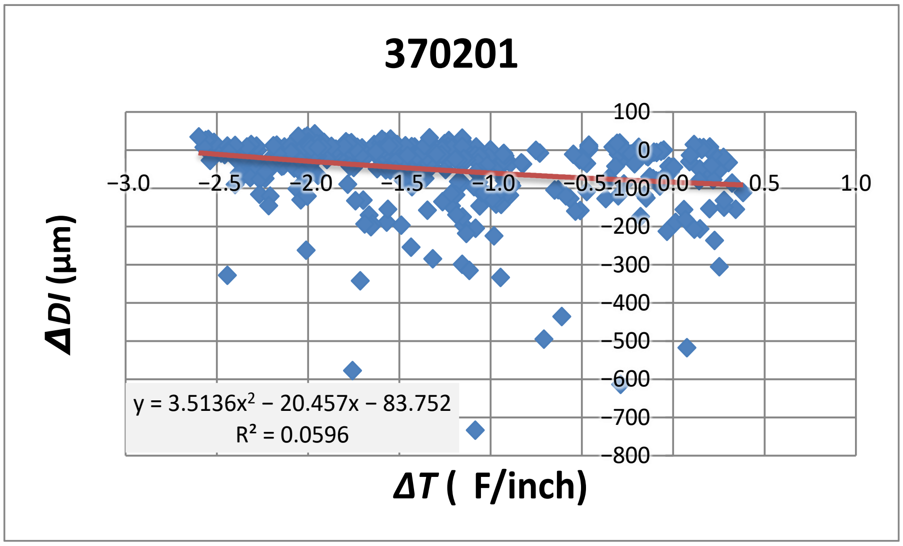

Source: FHWA.

Figure 62. Graph. Δ*DI* versus average temperature gradient of section 370201.

The other half of the test sections exhibited a parabolic relationship between Δ*DI* and the average temperature gradient. For these test sections, the vertex of the parabola occurred at an average temperature gradient of −1.5 ± 1 °F/inch. Therefore, for an average temperature gradient of −1.5 ± 1 °F/inch, Δ*DI* is at its highest point. As average temperature gradient continued to decrease, there was a slight decrease in Δ*DI*. This decrease occurred at an average temperature gradient of −2.5 ± 1 °F/inch. To the right of the vertex, as the average temperature gradient became positive, there was a greater decrease in Δ*DI*. Figure 63 shows test section 040213, which is an example of this parabolic relationship.

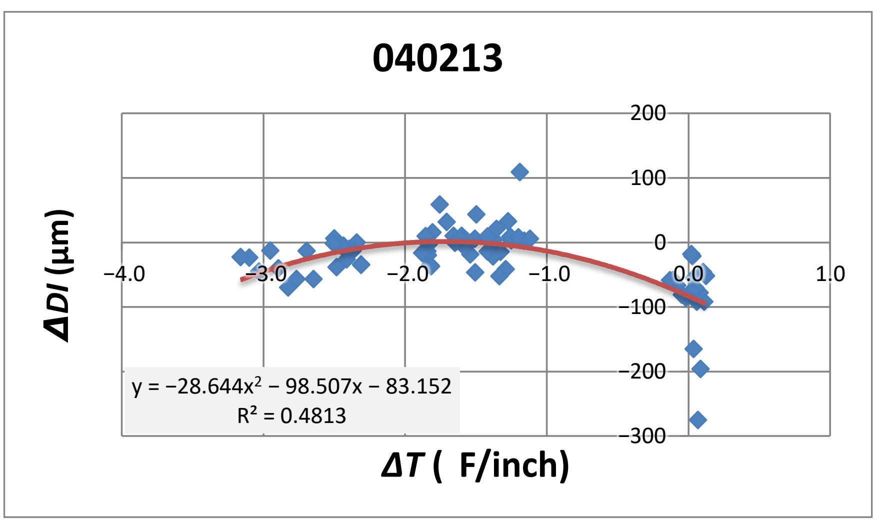

Source: FHWA.

Figure 63. Graph. Δ*DI* versus average temperature gradient of section 040213.

For many of the sections that showed a parabolic relationship between average temperature and ΔDI, the vertex often had a positive ΔDI value, which means the DI at the panel center was greater than the DI at the panel corner. Therefore, the panel was curling downward at a temperature gradient between −1.5 ± 1 °F/inch. These positive ΔDI values correspond with negative average temperature gradient values. A negative temperature gradient indicated the panel had a higher temperature at the top and a lower temperature on the bottom, meaning the panel would likely curl downward. Figure 64 demonstrates how ΔDI and ΔT agreed with each other. This figure also shows how ΔDI became more unpredictable as ΔT increased, which was a typical behavior in all test sections with a parabolic relationship.

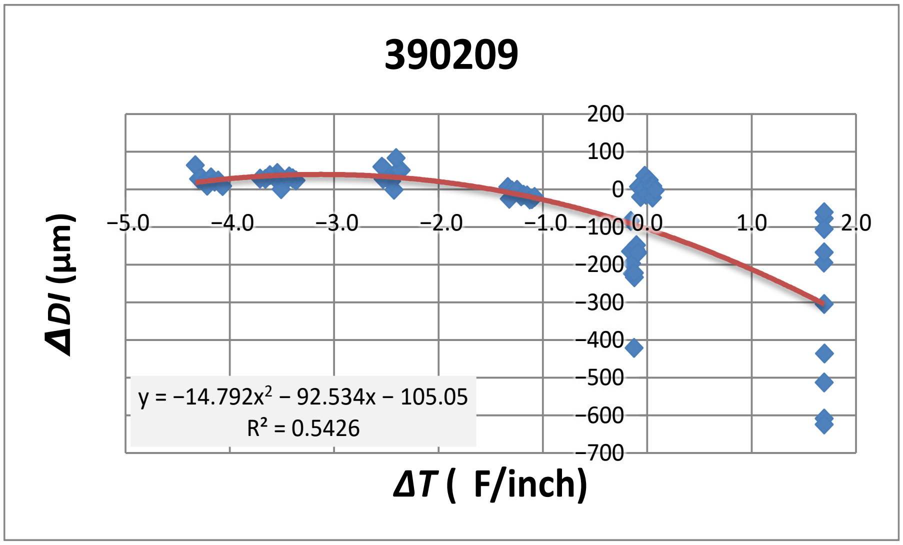

Source: FHWA.

Figure 64. Graph. ΔDI versus average temperature gradient of section 390209.

This analysis was not able to conclusively determine why some sections had a linear relationship and others had a parabolic relationship. However, observations suggested the type of relationship between ΔDI and ΔT was based on the amount of warping present in the slab during testing. Slabs that had parabolic relationships typically had little curvature (PSG values near zero) and linear relationships were seen more often in slabs that were warped upward or downward. This may be similar to how the relationship between IRI and PSG was not linear at low magnitudes of curl and warp in the PSG analysis.

CORRELATING PSG AND LEAVE SLAB LTE

LTE is a measurement of the percentage of a load that is transferred from the approach slab to the leave slab through dowels and aggregate interlock. Poor LTE is likely to result in various distresses, such as pumping, corner breaks, and faulting. Some factors that reduce LTE include voids under the slab joint, socketing of dowel bars, and polished aggregates in the aggregate interlock. Figure 65 shows how measurements of LTE typically reduced over time despite the direction of curvature in PSG. The figure illustrates that both PSG and LTE had some variability in their measurement, which was expected because both were affected by seasonal variations in climate; therefore, relative changes in PSG were reflected in relative changes in LTE.

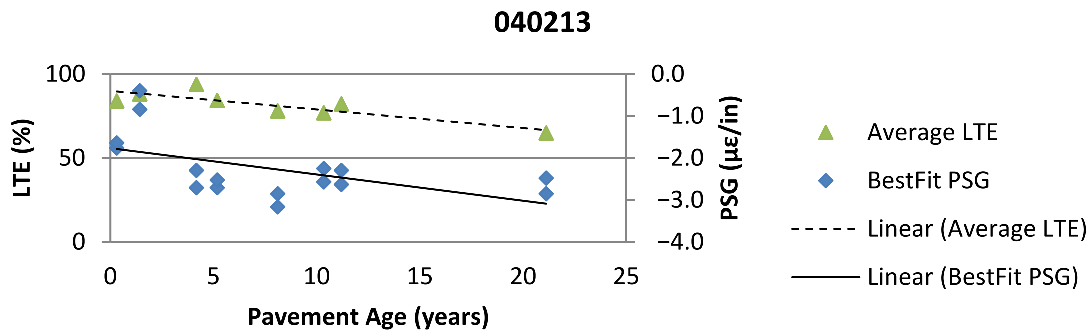

Source: FHWA.

A. Example for test section 040213.

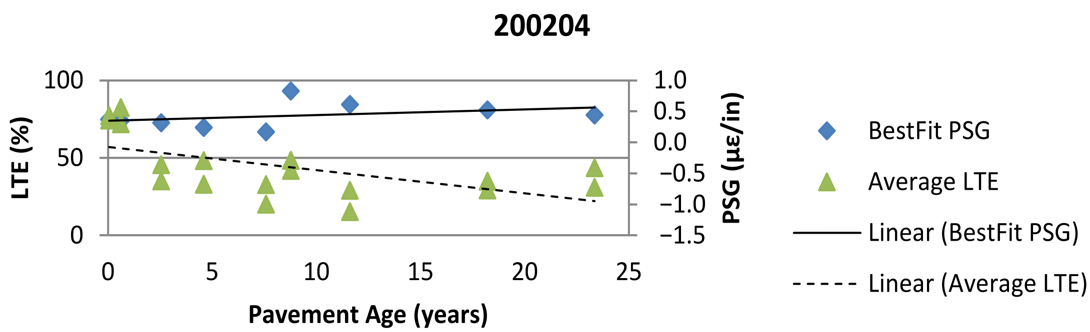

Source: FHWA.

B. Example for test section 200204.

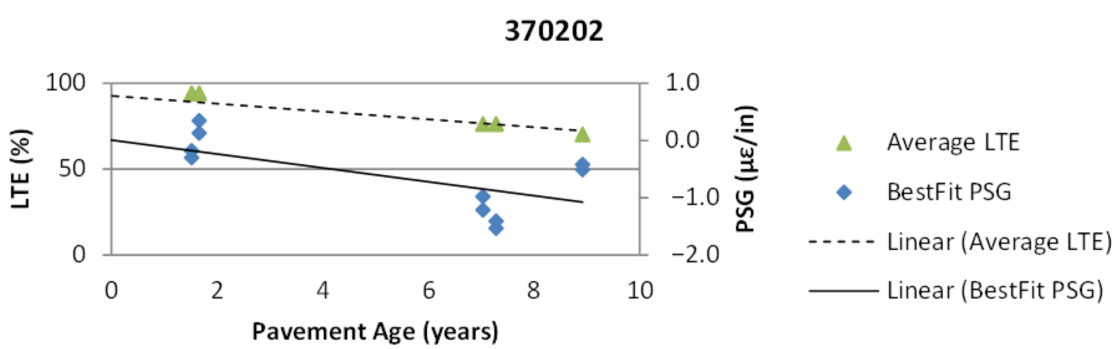

Source: FHWA.

C. Example for test section 370202.

Figure 65. Graphs. Examples of LTE and PSG measurements over time.

The variability in the PSG trend was a combination of the effects of curling and warping. Warping was controlled by seasonal changes in relative humidity caused by drying shrinkage in the cement paste. In contrast, curling was controlled by seasonal and daily variations in temperature that caused differential thermal expansion in the aggregate component. LTE was also influenced by seasonal and daily temperature variations; temperature variations that caused thermal expansion to control the effectiveness of aggregate interlock between slabs.

Figure 66 shows the categorization of test sections by the linear regression slope of PSG and LTE (i.e., PSG_s and LTE_s) using data from the first 10 years after construction. Approximately half of all test sections had positive PSG slopes and the other half had negative PSG slopes. The average PSG slopes in these categories were between 0.03 and 0.04. This indicates that in most cases, the change in PSG per year was very subtle. A positive slope meant that slabs in the test section curled downward on average and a negative slope meant they curled upward. When the PSG slope was positive, the number of test sections that had a positive or negative LTE slope was about the same. When the PSG slope was negative, there were more test sections that had a negative LTE slope than sections with a positive LTE slope. LTE does not normally increase over time. When LTE slope was positive, the average gain in LTE was 0.4 percent per year, a very minor increase that may be within the margin of error due to seasonal variations in LTE. A positive LTE slope typically meant that the test section maintained its original LTE value over time. A negative LTE slope indicated that the LTE decreased over time. In cases where LTE slope was negative and PSG slope was positive (downward curling), the average LTE slope was −0.5 percent per year. Compared to the positive LTE slope, this amount of change in LTE was within the margin of error due to seasonal variation and may reflect that in most case the LTE did not reduce over time. However, when both LTE and PSG slope were negative (decreasing LTE and upward curling slabs), the average LTE slope was slightly lower at −1.5 percent per year. As slabs curled upward, voids were potentially created at the uplifted edge. These voids may have contributed to a reduction in LTE.

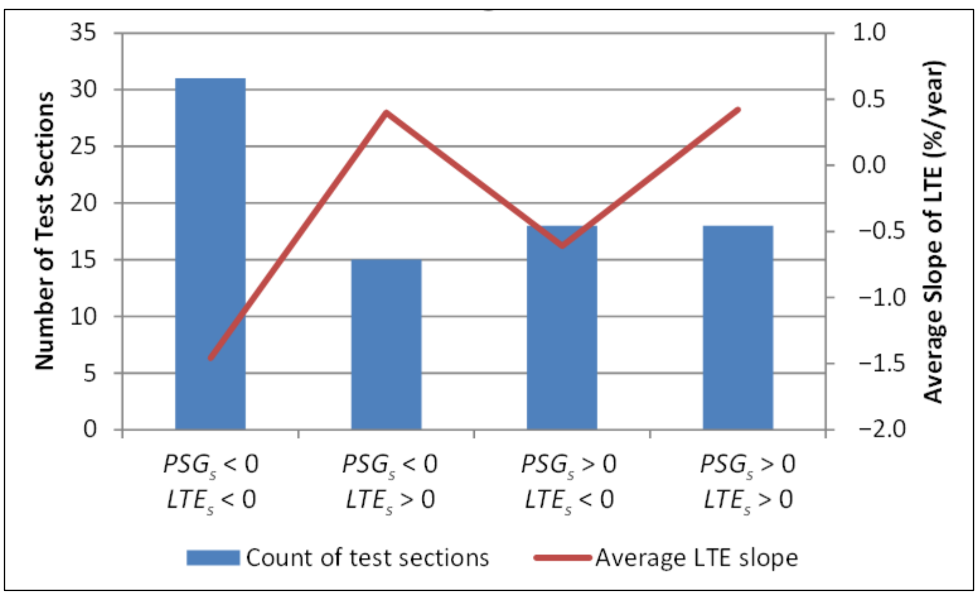

Source: FHWA.

Figure 66. Graph. Categorizing the regression slope of PSG and LTE.

PSG and LTE did not directly correlate; therefore, linear regression analysis was performed to determine if consideration of structural factors could improve correlation between PSG and LTE.

The following PSG prediction models were developed using LTE_i and LTE_s (LTE regression intercept and slope using data from the first 10 years after construction) and test section structural factors as defined in Table 13.

Figure 67 and Figure 68 show models for predicting PSG_i and PSG_s using LTE_i, LTE_s, and structural factors. Table 18 describes the linear regression coefficients in Figure 67 and Table 19 describes the linear regression coefficients in Figure 68.

Table 18. LTE analysis: linear regression coefficients for *PSG_i*.

Variable	GB	PATB	LCB
h_B	h_{GB}	h_{PATB}	h_{LCB}
x_1	−6.312E−01	−4.129E+00	−4.127E+01
x_2	−1.794E−02	2.487E−02	2.608E−02
x_3	−1.018E−01	−2.640E−03	1.777E−01
x_4	1.411E−01	8.649E−02	2.965E−02
x_5	−9.829E−02	−1.896E−01	7.981E+00
x_6	1.855E−01	5.797E−02	2.944E−02
x_7	−7.182E−02	1.190E−02	3.692E−01
x_8	1.619E−02	1.092E−02	4.813E−03
x_9	1.424E−01	4.285E−02	1.045E−01
x_{10}	−2.074E−02	3.026E−02	−4.006E−03
x_{11}	8.004E−04	−3.912E−04	−5.590E−04
x_{12}	−3.755E−07	4.644E−08	1.865E−08
x_{13}	−2.530E−01	−2.012E−01	2.441E−01

$$\begin{aligned}(PSG_i)_B = x_1 + x_2 LTE_i + x_3 LTE_s + x_4 W_{slab} + x_5 L_{slab} + x_6 h_{PC} \\ + x_7 h_B + x_8 h_{GS} + x_9 h_{TS} + x_{10} PV + x_{11} F + x_{12} E + x_{13} \Delta T\end{aligned}$$

Figure 67. Equation. Calculation of PSG_i using LTE and structural factors.

Table 19. LTE analysis: linear regression coefficients for PSG_s.

Base Type	GB	PATB	LCB
h_B	h_{GB}	h_{PATB}	h_{LCB}
x_1	−5.562E−02	1.498E−01	3.874E−01
x_2	2.019E−03	2.651E−03	2.617E−04
x_3	2.778E−02	5.444E−03	−3.868E−03
x_4	−3.243E−02	−6.950E−03	−1.409E−02
x_5	7.359E−02	−8.880E−03	−1.116E−02
x_6	2.312E−03	−5.500E−03	−2.189E−02
x_7	1.224E−02	7.667E−04	6.982E−03
x_8	−1.131E−03	2.200E−04	2.331E−03
x_9	−8.287E−03	−8.380E−04	−9.440E−03
x_{10}	5.240E−03	7.143E−04	7.837E−03
x_{11}	−8.368E−05	−1.235E−05	−4.472E−05
x_{12}	−6.258E−08	−5.434E−08	−1.825E−08
x_{13}	−2.909E−02	−5.039E−03	9.846E−02

$$\begin{aligned}(\boldsymbol{PSG_s})_{\boldsymbol{B}} = {} & \boldsymbol{x_1} + \boldsymbol{x_2 LTE_i} + \boldsymbol{x_3 LTE_s} + \boldsymbol{x_4 W_{slab}} + \boldsymbol{x_5 L_{slab}} + \boldsymbol{x_6 h_{PC}} \\ & + \boldsymbol{x_7 h_B} + \boldsymbol{x_8 h_{GS}} + \boldsymbol{x_9 h_{TS}} + \boldsymbol{x_{10} PV} + \boldsymbol{x_{11} F} + \boldsymbol{x_{12} E} + \boldsymbol{x_{13} \Delta T}\end{aligned}$$

Figure 68. Equation. Calculation of PSG_s using LTE and structural factors.

Table 20 shows statistics of the prediction models for the LTE analysis. Overall, R-squared values ranged from 0.493 to 0.780 and the *p*-values ranged from 0.002 to 0.579. The best prediction model was the PSG_s for PATB test sections. The poorest prediction model was for the PSG_s of granular base pavements. The other prediction models had satisfactory results, but the relatively high *p*-values on the LCB prediction models indicated that the correlation likely resulted from random error.

Table 20. LTE analysis: summary of prediction model statistics.

Model Statistic	GB Base Type	PATB Base Type	LCB Base Type
PSG_i model—Residual standard error	0.366	0.355	0.567
PSG_i model—Multiple R-squared	0.746	0.643	0.633
PSG_i model—Adjusted R-squared	0.469	0.375	0.234
PSG_i model—F-statistic	2.695	2.400	1.584
PSG_i model—*p*-value	0.056	0.052	0.227
PSG_s model—Residual standard error	0.108	0.034	0.073
PSG_s model—Multiple R-squared	0.493	0.780	0.693
PSG_s model—Adjusted R-squared	−0.060	0.615	0.358
PSG_s model—F-statistic	0.891	4.733	2.068
PSG_s model—*p*-value	0.579	0.002	0.120

Figure 69 shows the plots by base type comparing predicted PSG_i and PSG_s from LTE and structural factors to measured PSG_i and PSG_s from profile analysis. The following findings were similar to the previous climate and DI analysis:

- GB test sections had a better prediction for the PSG_i than PSG_s.
- PATB sections had a better prediction for the change in curvature than the initial curvature.
- LCB test sections had a satisfactory prediction for both the initial slab curvature and the change in slab.

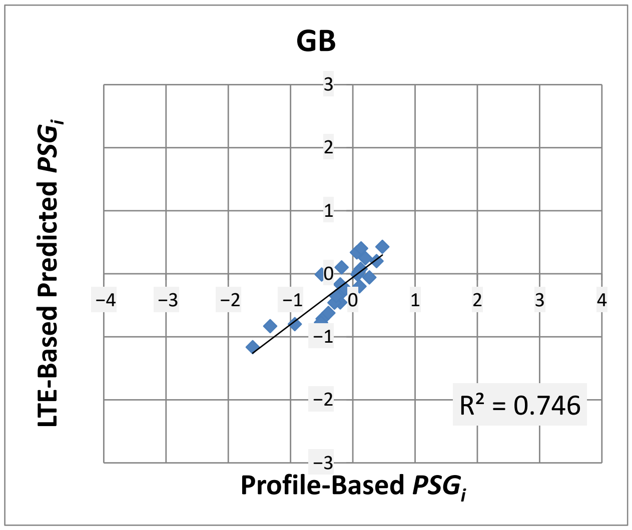

Source: FHWA.

A. Predicted and measured PSG_i on pavements with GB.

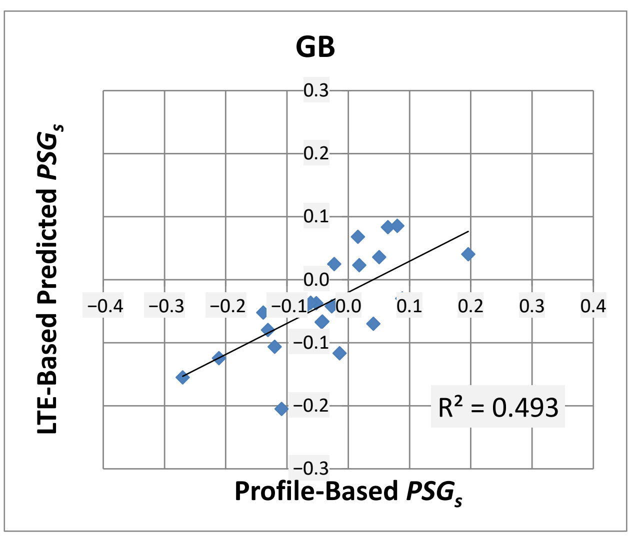

Source: FHWA.

B. Predicted and measured PSG_s on pavements with GB.

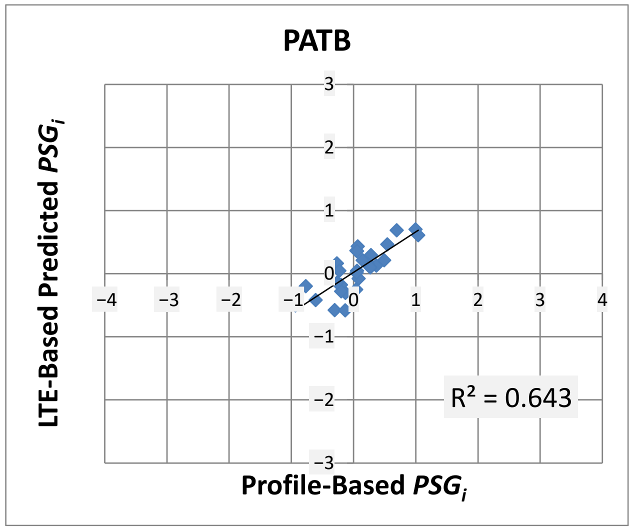

Source: FHWA.

C. Predicted and measured PSG_i on pavements with PATB.

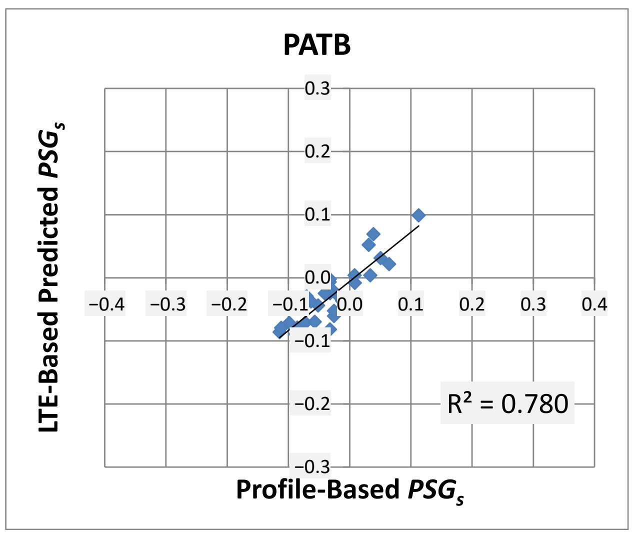

Source: FHWA.

D. Predicted and measured PSG_s on pavements with PATB.

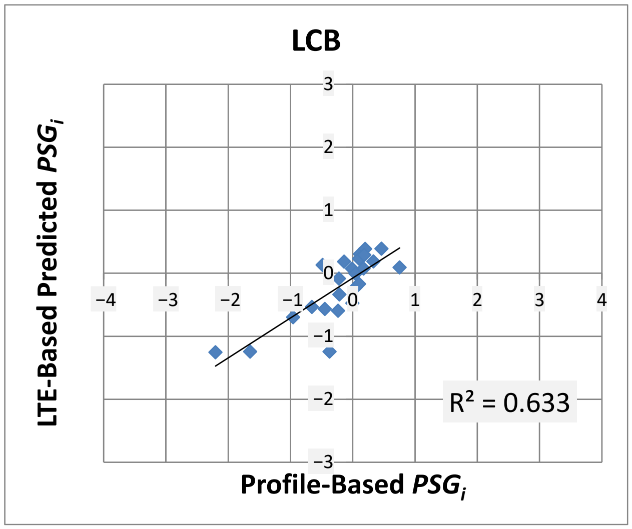

Source: FHWA.

E. Predicted and measured PSG_i on pavements with LCB.

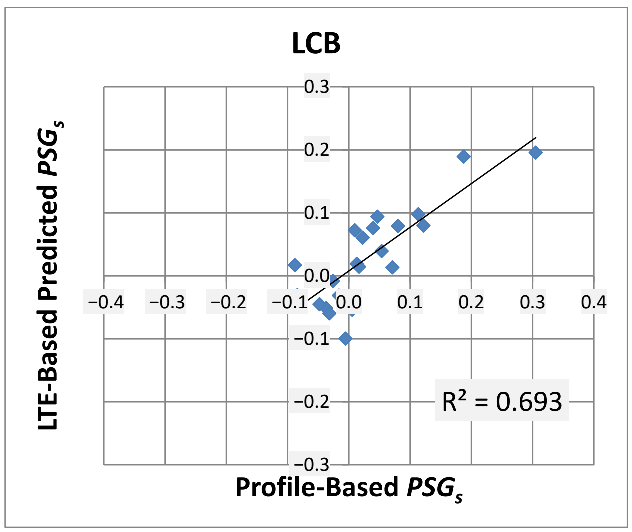

Source: FHWA.

F. Predicted and measured PSG_s on pavements with LCB.

Figure 69. Graphs. LTE analysis of predicted PSG_i and PSG_s versus measured PSG_i and PSG_s.

Table 21 shows the coefficient that had the most significance in developing the prediction models. Lower *p*-values (typically less than 0.1) indicate the significance of coefficients is less likely to be the result of random error.

Table 21. LTE analysis: correlation coefficients with the lowest *p*-value per model.

Predicted Curling	Coefficient for GB	Pr(>|t|) for GB	Coefficient for PATB	Pr(>|t|) for PATB	Coefficient for LCB	Pr(>|t|) for LCB
PSG_i	h_{TS}	0.002	h_{GS}	0.012	h_{TS}	0.085
PSG_i	h_{GS}	0.006	(Intercept)	0.083	h_{LCB}	0.134
PSG_i	h_{PC}	0.019	LTE_i	0.097	LTE_i	0.200
PSG_i	W_{slab}	0.179	PV	0.216	LTE_s	0.201
PSG_i	E	0.188	W_{slab}	0.229	(Intercept)	0.330
PSG_i	ΔT	0.191	h_{TS}	0.237	L_{slab}	0.379
PSG_i	LTE_s	0.383	h_{PC}	0.294	—	—
PSG_i	PV	0.404	ΔT	0.419	—	—
PSG_i	—	—	L_{slab}	0.469	—	—
PSG_s	W_{slab}	0.287	E	0.002	h_{GS}	0.077
PSG_s	LTE_s	0.419	LTE_i	0.065	h_{PC}	0.091
PSG_s	h_{GS}	0.435	h_{PC}	0.293	ΔT	0.148
PSG_s	h_{TS}	0.438	W_{slab}	0.305	PV	0.163
PSG_s	E	0.445	LTE_s	0.322	h_{TS}	0.210
PSG_s	PV	0.473	(Intercept)	0.490	—	—
PSG_s	—	—	—	—	—	—
PSG_s	—	—	—	—	—	—
PSG_s	—	—	—	—	—	—

—No data.

For predicting PSG_i, coefficients of layer thickness had the lowest *p*-values. These layers typically were granular and treated subbase layers. Test sections with treated subbase were only present in SPS-2 projects in Kansas and North Carolina. Granular subbases were present in test sections in all States, but Washington had particularly thick granular subbase layers (50–70 inches). The thickness of the subbase may affect prediction of PSG, but it is also likely that the subbase layer thickness coefficient was classifying projects by the environmental conditions at the sites where subbases were present. Treated subbase thickness had relatively low significance in the model for PATB test sections. Granular subbase thickness did not have significance in the model for LCB test sections. Base thickness did have significance in the LCB model but not in the GB or PATB models for predicting initial curvature, PSG_i. The following describe the models by base type:

- **GB:** The most significant coefficients for this model were the thickness of the subbase layers and the PCC layer. The thickness of the GB was not significant. The PCC slab width, elastic modulus, temperature gradient, and paste volume had some minor significance, but this may be the result of random error. The initial LTE had no significance, and the LTE slope value had minor significance. Based on this dataset, LTE did not correlate well to PSG on test sections with GBs.

- **PATB:** Granular subbase thickness had the lowest *p*-value, but the initial LTE was also significant in predicting the initial PSG. Other factors that had relatively high *p*-values included paste volume, slab width, layer thickness, and temperature gradient.

- **LCB:** The thickness of treated subbase was the most significant coefficient. The LCB model was the only model for which the thickness of the base layer was also significant. Both the initial LTE and the LTE slope had significance in predicting the initial PSG, which suggests that in test sections with LCB, there might be a relationship between the initial slab curvature and the initial LTE and change in LTE over time.

*S*ome coefficients of layer thickness were also significant for predicting PSG_s, which is similar to the prediction model for PSG_i. The layer thickness of granular and treated subbases may be significant because they classified the environmental condition of test sections by the project location where those subbases were present. Treated subbases were found only in North Carolina and Kansas and extremely thick GBs were found only in Washington; therefore, these coefficients may act as indicators of environmental conditions at these project locations. Slab width, *h*, elastic modulus, and paste volume have also shown significance, in addition to layer thickness. Each model for PSG_s is described by base type as follows:

- **GB:** This model showed poor correlation. Most coefficients in this model showed high *p*-values and suggested the correlation may be from random error. The most significant coefficient was slab width, with a *p*-value of 0.287. The LTE slope might have some relationship with the PSG slope, but the *p*-value for it was slightly too high.

- **PATB:** This model was better than the models for the other two base types. It showed the PCC elastic modulus and the initial LTE strongly controlled the change in PSG over time. A few other coefficients had minor significance, including slab width, slab thickness, and change in LTE over time.

- **LCB:** The model LCB pavements were strongly controlled by non-LTE coefficients, including granular subbase thickness, slab thickness, temperature gradient, paste volume, and treated subbase thickness. This model suggests that LTE did not relate to PSG in this dataset of LCB test sections.

SUMMARY OF FINDINGS

FWD testing provides valuable information on the physical properties of pavements. FWD is typically performed on LTPP test sections every 1 to 6 years. Analyzing these data provided insight into how FWD testing may be affected by the curl and warp of concrete pavements. The analysis was divided into three parts: (1) the development and evaluation of DIs, (2) correlation of DIs to PSG and temperature gradient, and (3) correlation of LTE to PSG.

DIs were expected to express the amount of deflection at an FWD testing point that was not from linear elastic loading of the pavement slab. The DI values were calculated based on regression of three deflection measurements at different load levels. Ninety-nine percent of the regressions performed had R-squared values of 0.98 or greater. Despite the good correlation between deflection and loading, the actual relationship between pavement deflection and loading was nonlinear. The simplification of the linear elastic model may have slightly skewed the DI. Because of this skew, the DIs may not have reflected the actual uplift of the slab at some locations. This nonlinear relationship between pavement deflection and loading explains why DIs can be negative even though the uplift of a slab cannot be a negative value. DIs were not only the result of the uplift of a slab, but also affected by the reaction from the base or by internal stresses within the slab.

Many sources of variability made clear trends in the relationship between DI and PSG difficult to observe. In addition to the ambiguous interpretation of DI, PSG values were also subject to seasonal variability and they were based on profile testing performed at different times and frequencies than FWD testing. The DI analysis focused on potential factors that may have influenced the relationship between a linear 10-year trend between DI and PSG values. The same approach was used to analyze the relationship between LTE and PSG values because LTE is based on FWD data.

The DI analysis first determined that there was no direct correlation between DI and PSG. The climate analysis established that PSG was predictable based on climatic and structural factors. To avoid biasing the correlation between DI and PSG with climatic data, only structural factors were considered in the DI analysis. The structural factors included base type, layer thickness, PCC slab width, slab length, elastic modulus, modulus of rupture, and paste volume. Temperature gradient was also included because it was based on FWD testing data.

The PSG prediction models using DI values had slightly less error than models based on climatic factors or models based on LTE values. All PSG prediction models had R-squared values between 0.84 and 0.49, suggesting most models provided a satisfactory fit to actual PSG values. The *p*-value of most coefficients in these models was typically high, but there were a few cases for which coefficients had low *p*-values. Comparing the results from PSG prediction models from the climate analysis, DI analysis, and LTE analysis led to the following observations:

- Models with the lowest correlation between coefficients and PSG predicted the change in PSG over time on test sections with GBs. The R-squared values of these models in the LTE, climate, and DI analyses were 0.49, 0.58, and 0.63, respectively. There are two possible reasons for this low correlation: (1) the data for these test sections were more unpredictable and subject to higher variability than test sections with treated bases and (2) test sections with GBs were by nature more difficult to predict warping because of physical properties of the unbound material, such as stiffness, erodibility, drainage, swelling, liquefaction, freeze-thaw, and deformation.

- Models with the highest correlation between coefficients and PSG predicted the change in PSG over time for test sections with PATBs. The R-squared values of these models were 0.81 and 0.84 in the climate and DI analyses, respectively. Base type is a major distinguishing feature between models with poor correlation and good correlation; therefore, physical properties of the base are more likely to influence the predictability of PSG over time.

- Models with the second highest correlation between coefficients and PSG predicted the initial PSG for test sections with GBs. The R-squared values of these models were 0.78 and 0.80 in the DI and climate analyses, respectively. Despite the difficulty in predicting the change in PSG over time in GB test sections, the initial curvature assigned to autogenous shrinkage was easier to predict. The base type was the distinguishing feature in the PSG's predictability. The built-in PSG occurred over a short time period; therefore, material properties that change over time will likely have less influence on the PSG. This could be the reason for a good prediction of initial PSG and a poor prediction of change in PSG.

Change in PSG over time is typically controlled by warping resulting from differential drying shrinkage. Curling was initially thought to provide nonpermanent seasonal variation in the curvature. The most significant coefficient for predicting the change in PSG over time was the elastic modulus (stiffness) of the PCC slab. The second most significant coefficients were the thickness and width of slabs, followed by treated base thickness, initial DI at the slab center, change in LTE over time, paste volume, and granular subbase thickness.

In the case of prediction models for initial PSG, the coefficient with lowest *p*-value (most significance) was typically the average relative humidity. This was followed by the initial LTE, thickness of treated and granular subbases, PCC thickness, intercept value, and average daily difference in relative humidity.

Coefficients that had low significance in predicting the initial PSG include modulus of rupture, most DI coefficients, PCC elastic modulus, and paste volume. Only the modulus of rupture had low significance in both models for predicting initial PSG and change in PSG; however, it is not clear why the significance is low. The significance of most other coefficients typically varied depending on what was being predicted. These variances suggested the mechanism that caused the initial PSG was different from the mechanism that caused the change in PSG.

The thickness of treated and granular subbases was unusually significant in prediction models. Only two projects had treated subbases; one of them had an unusually thick treated granular subbase. Two possible reasons for the significance of these coefficients include the presence of certain subbases that influenced both the initial and change in PSG, which seems unlikely because the base thickness had low significance in predicting PSG and these coefficients are project specific; therefore, there may be unknown environmental, material, or construction-related factors present that have coincidentally been classified by the presence of subbases found in these projects.

Aside from base thicknesses, other coefficients with low significance for predicting the change in PSG include the modulus of rupture and slab length. Low significance does not mean the modulus of rupture and slab length coefficients had no effect on the amount of curling due to seasonal cycles, but they were not significant for predicting the yearly change in PSG.

While a formal sensitivity analysis was not performed to determine whether certain factors could be adjusted to improve the correlation in prediction models, in earlier iterations of this analysis, erroneous values were used in the calculation of granular subbase thickness. These erroneous values, however, had improved correlations in some cases. It is possible the inputs used to develop prediction models could be refined further to provide a better fit. Temperature gradient, for example, was found to have a parabolic relationship to DI in about half of all test slabs. Other factors with similar nonlinear relationships could have improved the overall fit of prediction models, which could be an opportunity for a future study.

CHAPTER 10. ALR

This report presents detailed information about changes in sectionwide roughness using IRI values and slab curl and warp using PSG. The distribution of roughness is an aspect of longitudinal road profiles that relates to functional and structural performance. The ALR may degrade ride quality disproportionately and may indicate the presence of surface defects or surface distress. Per AASHTO R54, ALRs are defined as any region where the IRI averaged over a 25-ft base length is greater than a specified threshold.(24) ALR is generally defined as a range within a pavement section where the roughness profile with a specific base length has a magnitude above a given threshold.

Figure 70 shows the right roughness profile for section 040213 collected 14.2 years after the section opened to traffic. This roughness profile uses an averaging base length of 25 ft. As such, each point in the roughness profile is the IRI averaged over a 25-ft interval, which has boundaries 12.5 ft upstream and 12.5 ft downstream. The figure also marks a threshold of 150 inches/mi using a horizontal line.

With a base length of 25 ft and a threshold of 150 inches/mi, this profile has seven ALRs with an area of 157.9 ft. The largest ALR with the highest peaks appear at 36.6–53.5, 121.2–174.6, 177.0–206.7, and 310.2–345.5 ft. These ALRs correspond to locations where the profiler passed over wide longitudinal cracks in the right wheel path. The remaining areas do not correspond to any known surface distress; rather, they are areas where the severity of upward slab curl exacerbated the roughness sufficiently to raise the roughness profile above 150 inches/mi. These ALRs may grow or decrease in range and severity with seasonal or diurnal changes in slab curl. The ALR at 247.8–249.0 ft, which has a peak roughness just above 150 inches/mi, will have a roughness level below the threshold if the severity of upward curl decreases. Alternatively, additional ALRs may appear if the severity of upward curl increases.

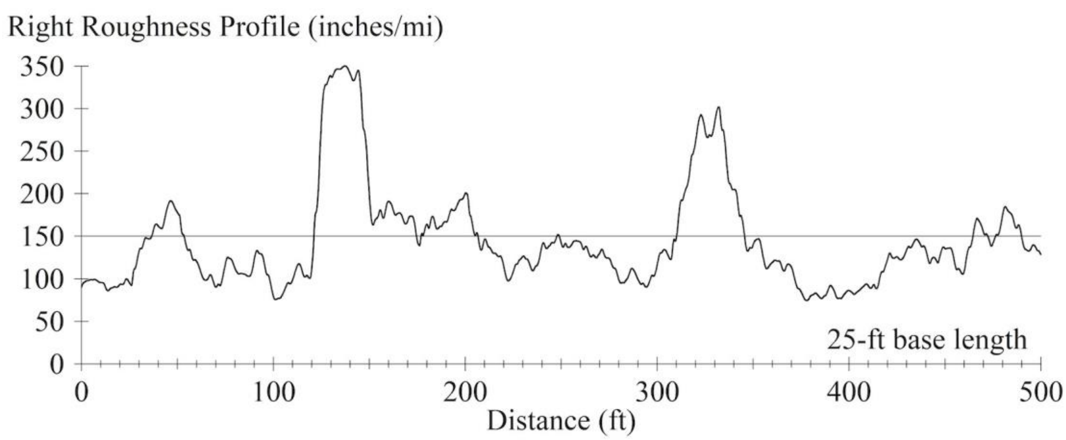

Source: FHWA.

Figure 70. Graph. Right roughness profile of section 040213 at 14.2 years.

Figure 71 demonstrates short-term changes in ALRs caused by changes in curl and warp. The figure marks ALRs in the right wheel path for each of five repeat passes over section 040213 in diurnal visits conducted over four seasons. These data were collected 9.9 to 10.7 years after the open-to-traffic date. For each pass, figure 71 marks any area where the IRI is above 160 inches/mi in the right roughness profile for a base length of 25 ft. Two items in the figure stand out. First, the location and extent of the ALR is similar but not exact for all five repeat passes within each set. Second, the nominal level of ALR exhibits seasonal and diurnal changes, which are attributed to curl and warp.

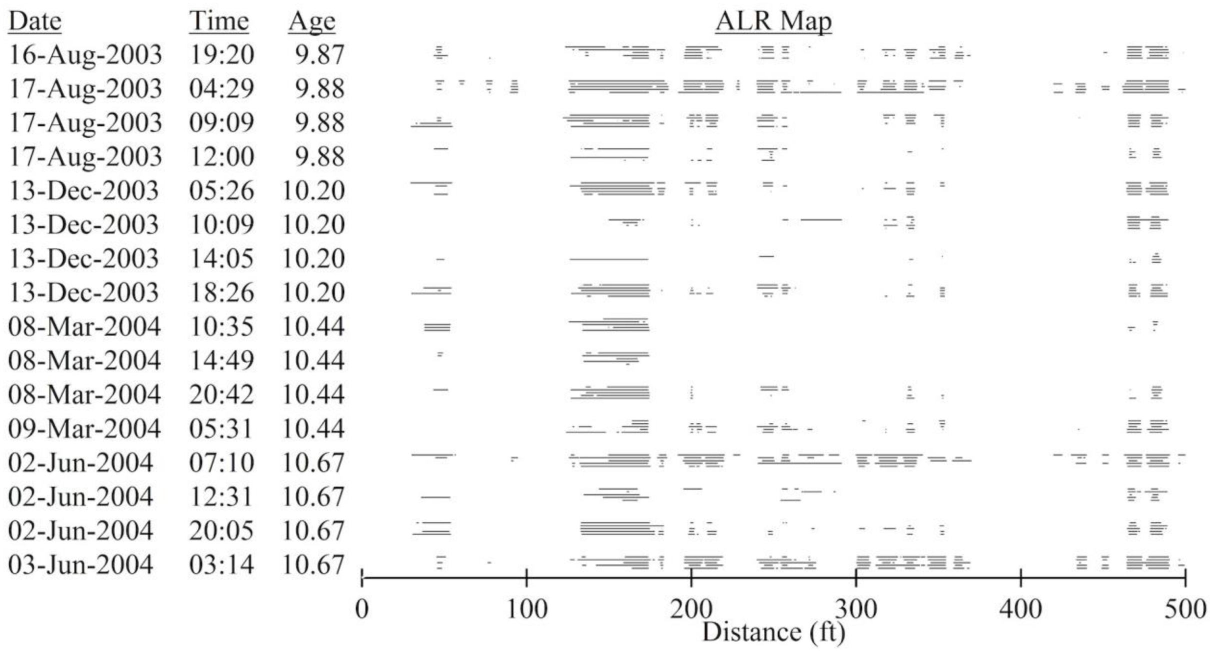

Source: FHWA.

Figure 71. Graph. Section 040213 ALR for seasonal, diurnal, and repeated passes.

Figure 72 summarizes the diurnal and seasonal changes in ALR on the right side of section 040213. The figure shows the average extent of ALR for each of the 16 visits. Note that in August 2003 and June 2004, the extent of ALRs is greater than in December 2003 and March 2004. The ground under the pavement is warmer compared to December 2003 and March 2004, which promoted upward curling. Also, within each seasonal group, the total extent of ALR is highest in the early morning hours and lowest in midafternoon because the upward slab curl is the most severe before sunrise and the least severe at midday.

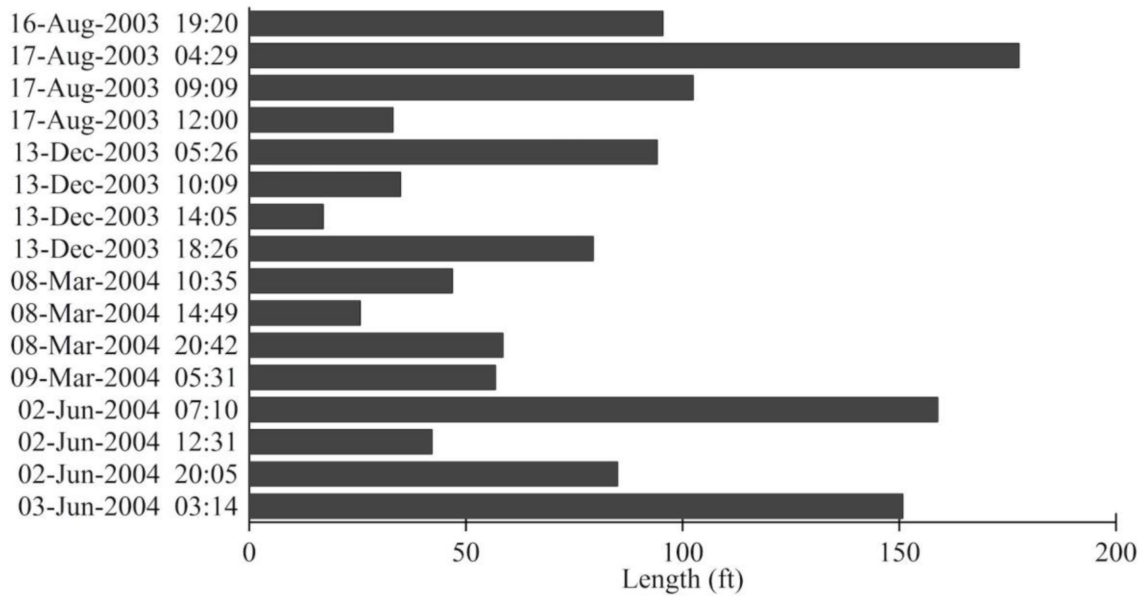

Source: FHWA.

Figure 72. Graph. Section 040213 average ALR for seasonal and diurnal visits.

Figure 73 demonstrates long-term changes in ALR on section 040213 using a base length of 25 ft and a threshold of 160 inches/mi. The figure marks ALR for each repeat measurement over the section over the monitoring history for LTPP. The figure also lists the age of the test section relative to the date the section opened to traffic. The figure shows a growth in ALR over the first 16 years, which includes an increase in the extent of ALR as longitudinal cracking appears in the right wheel path. However, the trend is most likely confounded by seasonal and diurnal changes in curl and warp as the extent of ALR for a specific visit is affected by environmental conditions at the time. The ALR that is registered in areas with longitudinal cracking also depends on the transverse positioning of the profiler within the lane.

Figure 70 through Figure 73 provide a detailed analysis of ALR for the right side of section 040213. The LTPP and FHWA profile datasets offer an unusual opportunity to examine ALR of jointed concrete pavements in detail. For this study, the longitudinal profiles were synchronized throughout their entire monitoring period, such that their starting locations and accumulation of longitudinal distance is consistent beyond what was possible with careful field procedures. These data were used to study short- and long-term changes in ALR of the 83 test sections included in this research.

The study also included an examination of the extent and severity of ALR repeatability, which was performed using well-synchronized data. The data were accurately aligned; therefore, changes in ALR are attributed to tracking variations and other sources of profile-measurement uncertainty not related to measurement of longitudinal distance. Variations in ALR location were also addressed using unsynchronized measurements.

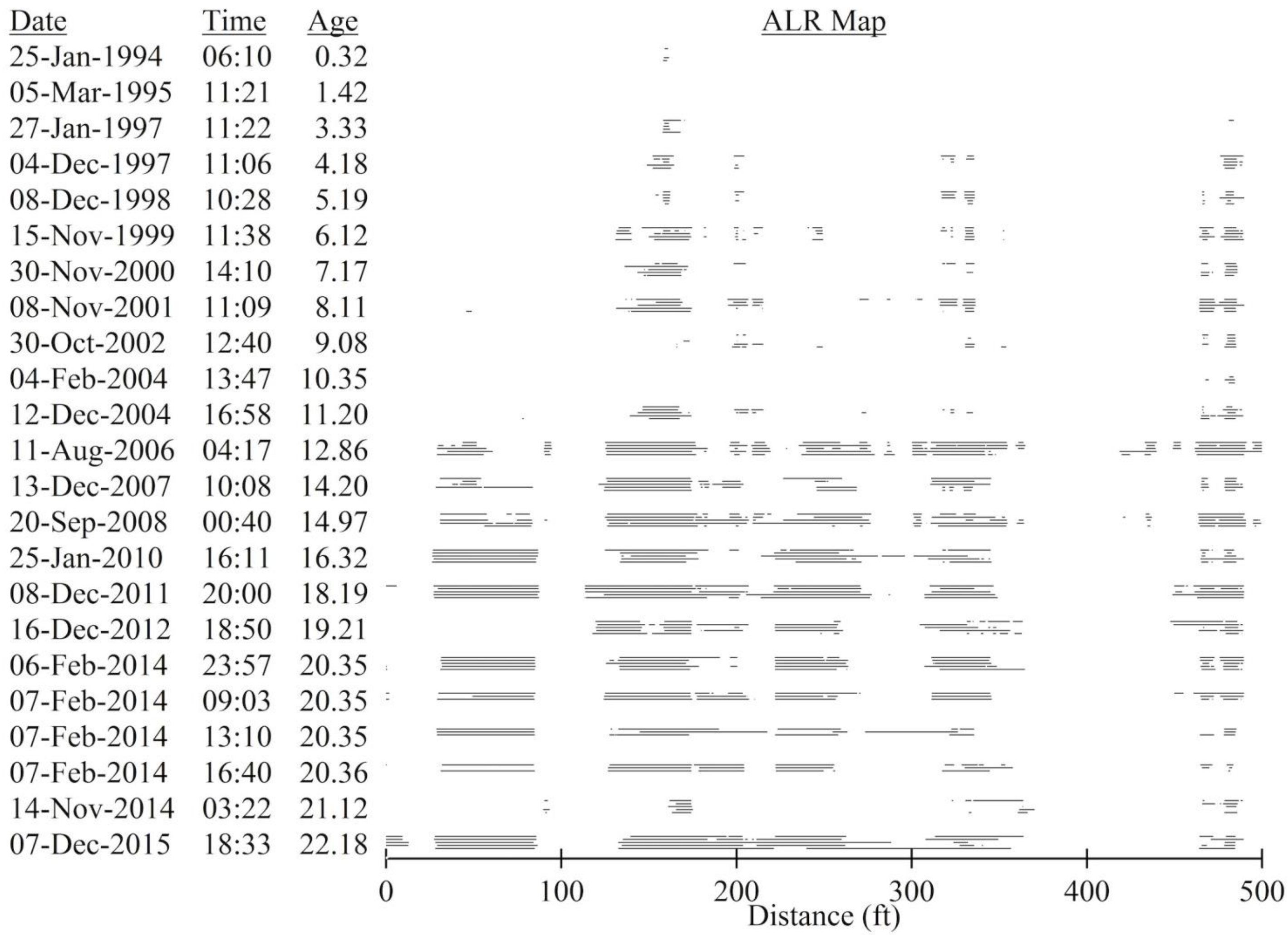

Source: FHWA.

Figure 73. Graph. ALRs long-term changes of section 040213.

Appendix J provides results of ALR analysis of several test sections. Like section 040213, many test sections included short-term variations in ALR caused by changes in curl and warp. All test sections exhibited long-term changes in ALR. These effects included long-term growth in roughness, the confounding effects of changes in curl and warp, increased roughness at locations with distress, and changes in roughness caused by maintenance. Overall, the analysis showed that the potential influence of curl and warp must be considered when interpreting ALR on jointed concrete pavements. Timing and prevailing environmental conditions must be reported with ALR measurements and considered when interpreting the results or comparing ALR extent and severity.

Appendix J describes other effects of practical concern, including the following:

- ALR depends on index type. For example, using MRI, which is the average of the left and right IRI, in place of individual wheel tracks moderates the most extreme areas of roughness. Using HRI, which is based on averaging the left and right profile before computing the roughness, universally reduces ALR.

- Roughness threshold strongly affects ALR. ALR increases as the threshold value decreases. When the average roughness approaches the ALR threshold, evaluation of ALR becomes less meaningful, and a threshold proportional to the sectionwide average may be more useful for some applications.

- Base length affects the severity of roughness. As base length decreases, peak roughness values grow in severity and highly localized features are easier to pinpoint. However, a base length lower than 25 ft may fail to capture the entire contribution to roughness of a localized feature.

- Severity of an ALR is as important as its extent. ALR with the same extent included a wide range of peak values. Further, several ALR were detected that barely exceeded the threshold or included very low extent. For some applications, an index is proposed that quantifies the extent and severity of ALR.

- ALR length and severity vary more widely than IRI between repeat passes. Several instances were observed where repeated passes were not needed to obtain an accurate measurement of overall IRI, but multiple passes were needed to assess ALR length and severity.

CHAPTER 11. CONCLUSIONS AND RECOMMENDATIONS

Throughout this study, researchers learned what could—and in some cases could not—be quantified or related to curl and warp on jointed concrete pavements. Key findings regarding the various analysis efforts are summarized in the following sections, and some promising areas for future research are identified.

This research demonstrated detailed analyses of road profiles for detection of jointed concrete curl and warp, changes in curl and warp, and estimation of the influence of curl and warp on the IRI. The research examined the relationship between the IRI and curl and warp quantified using the average PSG over the slabs within a test section, which was done to quantify cyclic and long-term changes in curl and warp and corresponding changes in IRI. The report demonstrates the use of this framework to quantify the effect of curl and warp on the IRI of 83 LTPP test sections, including long- and short-term changes and spatial variation within a test section.

The research sought to estimate the portion of roughness from sources other than curl and warp (i.e., background roughness) using a linear fit between observations of IRI versus PSG over the short term (e.g., diurnal and seasonal changes) and extrapolation to a condition with no curl. Theoretical modeling combined with simulations of random roughness mixed with idealized profiles of curl and warp showed that a linear fit was not appropriate for extrapolation.

An alternative method was proposed based on the assumption that the square of the total roughness was approximated by the sum of the square of background roughness and the square of the roughness caused by curl and warp. Fitting this model to data for individual test sections quantified the influence of curl and warp on the IRI for test sections where large changes in curl and warp were present. However, the PSG–IRI relationship could not be generalized because the PSG–IRI relationship for individual test sections was not consistent enough to justify using the fitted model from one test section to infer the effects of curl and warp on roughness of another test section.

Seasonal and diurnal measurement of jointed concrete test sections is recommended for test sections that require quantifying curl and warp. The diurnal measurements should include four series of passes:

1. Predawn, preferably just before sunrise or when air temperature is at a minimum.
2. At least 2 hours after sunrise.
3. Late afternoon, preferably after solar radiation has maximized for the afternoon and when air temperature is at a maximum.
4. After sunset.

Whenever possible, these measurements should be conducted on a clear day to maximize solar radiation to the pavement surface. The timing of seasonal measurements should favor extremes in daily average solar radiation and extremes in the expected temperature and moisture at the slab underside.

In support of the curl-and-warp analysis, the research demonstrated a methodology for selecting five repeat passes from a larger group of raw profile measurements based on mutual cross-correlation of IRI-filtered profile traces. This methodology is proposed for any application that emphasizes the effect of specific profile features on the IRI and the distribution of roughness within a test section.

The research also applied an algorithm for isolating the location of transverse joints by identifying narrow downward spikes that appear with the expected spacing. The algorithm is the most successful when repeat profile measurements are available over the same test sections and when narrow downward spikes at the joints are not eliminated from the stored profile by low-pass filtering. Researchers recommend that profile measurements collected for the study of curl and warp include at least three repeat passes for every measurement visit. Further, measurement protocols should include specification of height-sensor footprint, low-pass filtering, and data-recording intervals that facilitate joint finding without introducing spurious (i.e., aliased) short-wavelength content into the profile.

A direct correlation between PSG and climatic factors—such as average temperature and relative humidity—could not be established. However, the following general observations can be made based on the analysis:

- Base type had influence on the correlation of climatic factors to PSG.
- Humidity had the effect on the initial pavement curvature.
- Stiffness of the PCC affected the PSG.
- Correlation with PSG improved with more-refined climate factors.

Recommendations for further investigation of the correlation between climate and PSG include:

- Consider climatic factor that describes seasonal variation.
- Factor the climate during profile testing into correlation analysis.
- Explore nonlinear relationships between climatic factors and PSG.

DI and LTE are parameters derived from FWD testing and were considered to have potential as predictors of PSG and the curl state of the slab. DI and LTE was computed and compared to PSG but were found not to have a correlation. Additionally, DI values at various FWD test points and the relative difference between these DI values were also evaluated and found not to have a correlation to PSG. Structural design factors, such as layer thicknesses, base type, slab dimensions, and paste volume were included in the correlation analysis as coefficients in the regression models developed by researchers. While these models showed good R-squared values, the number of degrees of freedom was low, and these models required additional data to validate. The models did indicate, however, that FWD data alone were not sufficient to compute PSG or evaluate curl state.

The FWD analysis lacked enough established knowledge on the mechanisms affecting curl-and-warp behavior. Researchers made assumptions on what factors were of potential importance to curl and warp and how to compute and interpret these factors. The curl-and-warp indices, such as PSG, DI, and LTE, were also subject to interpretation without sufficient means to validate the interpretation. Curl-and-warp indices varied; therefore, in the analysis, trends were generalized to develop correlations. This generalization reduced the size of the dataset and consequently the degree of freedom in correlations.

Findings from the FWD analysis include the following:

- DI could be developed using LTPP FWD data.
- Interpretation of DI was subject to FWD testing location, curl state of the slab, the base type, and other structural factors.
- Direct relationships between averages of DI and PSG could not be established.
- Change in curl was more difficult to correlate in test sections with GBs than test sections with treated bases.
- Structural properties of the slab influenced the correlation between DI and PSG.
- Unknown factors specific to the site location may have influenced the correlation between DI and PSG or LTE and PSG.

The FWD analysis was not able to establish a correlation between DI and PSG, but the analysis showed that a relationship could potentially exist. Recommendations based on this analysis for further investigation include the following:

- Correlation between ΔDI and z_0.
- Nonlinear relationship between DI, LTE, and PSG.
- Slab-by-slab analysis or site-specific analysis on the correlation between DI and PSG.
- Sensitivity analysis on parameters that affect the correlation between DI and PSG.

The potential influence of curl and warp was shown to affect the interpretation of ALR on jointed concrete pavements. Timing and prevailing environmental conditions must be reported with ALR measurements and considered when interpreting the results or comparing ALR extent and severity. Other practical concerns regarding the interpretation of ALRs include the following:

- ALR's dependence on index type.
- Effects of roughness threshold on ALR.
- Effects of base length on the severity of roughness.
- Importance of the severity of ALR compared to the extent of ALR.

APPENDIX A. LITERATURE REVIEW

INTRODUCTION

This appendix provides a literature review related to experimental determination of jointed-concrete pavement curl and warp using pavement-surface elevation measurements. Separate discussions are provided for various types of measurement technology, but each discussion emphasizes techniques for quantifying curl and warp using field measurements. Many of the cited references also describe background and research findings relevant to a pavement's response to moisture, thermal, and applied loads not described in this appendix.

CURL-AND-WARP MEASUREMENT

Graphical Demonstration

Early studies of jointed-concrete behavior used plots of responses from roughness devices measured along longitudinal tracks to graphically demonstrate curl and warp.

Stanton demonstrated seasonal and diurnal changes in profilograph traces measured on various experimental in-service jointed-concrete pavements in California.(25) Stanton noted "the difference in curvature between morning and afternoon in warm weather and the decreased curvature in the damp cool weather of the rainy season." Hveem showed seasonal, diurnal, and early-age changes to profilograph traces; sensitivity of behavior to soil type; and long-term changes in profilograph traces on the same experimental pavements.(26–28) Tremper and Spellman showed profilograph traces from a later study of concrete shrinkage due to moisture loss and identified curl graphically as shown in figure 74.(29)

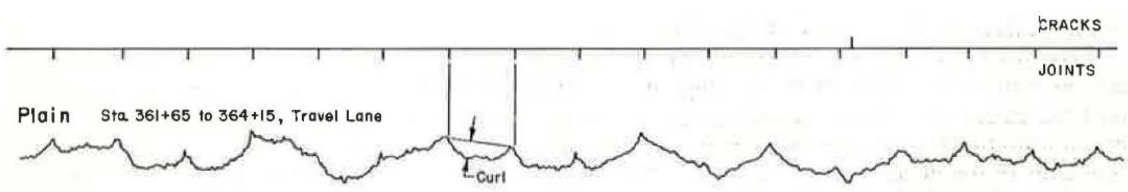

Figure 74. Graph. Representation of curling using a profilograph trace.(29)

Moyer showed traces from a response-type road-roughness measurement system for a segment of road that was "badly warped at the joints."(30) Housel demonstrated seasonal changes in in-service pavements caused by "curling at the joints combined with frost action in the granular base" using traces measured by a truck-mounted profilograph.(31)

Direct Elevation Measurement

Several studies monitored the curl and warp of in-service test pavements by directly measuring elevation changes at critical locations on selected slabs. The instrumentation included a surveyor's rod and level,(32,33) dial gauges,(34–37) slip-pin deflectometers,(38,39) multidepth deflectometers,(40,41) or linear variable differential transformers.(42–45)

Evans and Drake cited the difference between elevation at joints and slab midpoints as a measure of warping, and the State Highway Commission of Kansas defined "warping factor" similarly.(32,33) Spellman, Stoker, and Neal described the measurement of vertical "movements of slab corners to temperature and moisture changes (curl)."(39)

Armaghani, Larsen, and Smith presented slab center, edge, and corner deflections over a 48-hour cycle for comparison to slab temperature and temperature differential.(42) Goldsberry presented slab center, edge, and corner deflections for comparison to thermal loading over several diurnal cycles for multiple seasons.(43) Poblete et al. compared changes in slab corner elevations, which were expressed as uplift, to changes in thermal gradient over diurnal cycles in multiple seasons.(44) Jeong and Zollinger demonstrated the difference between two curing methods on early-age slab behavior through the first seven diurnal cycles by comparing vertical corner displacement to measurements of dowel-bar bending moment and slab material strain.(36) Rao and Roesler and Rao presented changes in edge and corner deflection over 24 hours.(41,46) These studies examined the behavior of instrumented slabs under changes in thermal loading as a basis for explaining behavior under load.

Researchers compared slab deformation to thermal loading using values of curl calculated from measured elevations at critical locations. Lowrie and Nowlen presented "changes in curl" using averaged corner and edge deflections over multiple test slabs.(38) Ardani reported values of curl measured every 30 minutes from early morning until late afternoon, which were defined as the difference in elevation between the corners and slab center.(37) Yu et al. defined curl as the deflection at slab edges and slab corners relative to the slab center.(35) Values were reported for comparison to temperature gradient over two diurnal cycles.

Inclinometer-Based Slab Profiles

Teller and Sutherland used a precision clinometer to measure deflections caused by temperature warping and displayed deflection profiles along slab edges and slab longitudinal and transverse centerlines.(47,48) Several modern studies, which are cited in this section, monitored the curl and warp of in-service jointed-concrete pavements using low-speed, inclinometer-based profiles along key lines over selected slabs. In these studies, profiles of relative elevation versus position were collected diagonally and along transverse edges and longitudinal edges. In a few cases, roughness for longitudinal profiles were reported in terms of the IRI to examine early-age behavior or changes at various times of day.(49–51) Curl and warp was typically quantified by direct analysis of measured profiles and related to measurements of slab temperature at various depths, material strain, or other quantities pertinent to structural response.

Rao et al. emphasized early-age and long-term causes of slab deformation and, using profiles collected along slab diagonals, characterized curl as the elevation difference between slab corners and slab center.(52)

In some cases, selected locations on in-service pavements were monitored to explain premature cracking. Hansen et al. applied a second-order curve fit to profiles measured along longitudinal tracks and reported edge-to-center elevation difference from the best-fit curve.(53) Yu and Khazanovich and Beckemeyer, Khazanovich, and Yu measured profiles along longitudinal slab edges and applied a quadratic fit to the profiles after "adjustment for longitudinal slope."(45,54) Yu and Khazanovich and Beckemeyer, Khazanovich, and Yu defined the amount of curling as the difference between vertical deflections at the corners to deflection at the slab center. All three studies applied the curve fit as a way to eliminate the effect of surface irregularities on the results.

Vandenbossche measured profiles along transverse edges, longitudinal edges, and a diagonal of selected slabs at several test sites.(55) In the description of analysis methods, Vandenbossche observed that slab profiles "contained the geometric pavement slope and surface irregularities." Analysis of slab profiles included a zeroing procedure to mitigate the effects of slope. Each profile was adjusted by subtracting the profile measured along the same track under specific environmental conditions. Curvature (κ) was approximated from the resulting displacement profiles using a second-order curve fit, as shown in figure 75 and figure 76.

$$y(x) = Ax^2 + Bx + C$$

Figure 75. Equation. Second-order curve fit.

$$\kappa = \frac{\dfrac{\partial^2 y}{\partial x^2}}{\left[1+\left(\dfrac{\partial y}{\partial x}\right)^2\right]^{3/2}} = \frac{2A}{\left[1+(2Ax+B)^2\right]}$$

Figure 76. Equation. Curvature derived from a second-order curve fit.

In figure 75, y(x) is the fitted displacement profile as a function of distance along the slab diagonal; A, B, and C are fitted coefficients. Figure 76 shows that curvature derived from a second-order polynomial is not constant across the entire slab. All reported curvature values, however, were less than 0.0006 1/ft and the longest test slab was 24 ft. For these parameters, the curvature varies across the fitted curve by less than 0.06 percent, and curvature may be estimated solely based on A.

The studies by Vandenbossche included three technical observations with important implications to quantifying curl and warp from measured longitudinal profile. The observations include the following:

- Using a single parameter to characterize curl was advantageous if it could be justified.
- "Identifying a single parameter that can characterize the measured profile, or slab shape, is beneficial when making comparisons for a range of temperature conditions between cells and within cells. The parameter chosen to characterize the shape of the slab was curvature."(55)
- Predicting measured curvature depended on radius of relative stiffness and slab length, in addition to thermal loading.
- Using a curve fit over the entire length of the slab profile achieved satisfactory results, but curvature may vary within a given slab because of the influence of gravity and load-transfer devices.

In a study of early-age behavior, Wells, Phillips, and Vandenbossche monitored selected slab groups with and without dowel and tie bars for the first 72 hours after construction.(56) This study used processing techniques described by Vandenbossche and quantified slab curvature using the value 1 ft into the slab from the edge.(55) Subsequently, Asbahan and Vandenbossche monitored the same slabs over 2 years to quantify the relative influence of temperature gradient, moisture gradient, and restraint at the joints on slab deformation.(57) This study applied the zeroing procedure previously described and quantified curvature using the second derivative of the fitted second-order curve (i.e., *2A* from figure 76).

Kim monitored selected slab groups on two newly constructed pavements for 7 days following construction.(58) The study included measuring profiles along diagonals and transverse edges and reported curvature using Vandenbossche's analysis procedure for profiles along diagonals and transverse edges. Ceylan et al. characterized slab deformation in related work from the same field sites using the relative corner-to-center elevation changes from profiles measured along slab diagonals.(50,59)

Chen, Nassiri, and Umeyer monitored the deformation of several transverse profiles on five test sections that had been in service for 24 years or more and processed the profiles using a second-order curve fit.(60) Slab deformation was quantified using the fitted polynomial in two ways: differential deflection between the edges and the center of the slab and curvature estimated using the second derivative.

Custom Devices

Early studies of slab warp used custom mechanical devices to record the movement of slab edges relative to a fixed external reference over time or the elevation at transverse joints relative to the slab interior.(61,62) Ceylan et al. proposed a low-cost device for the measurement of slab-deflection profiles along a selected line using a stretched wire and either a custom gauge block or a digital depth gauge to measure the gap to the slab surface at various locations along the wire.(63)

Lederle, Lothschutz, and Hiller analyzed transverse profiles measured at multiple longitudinal positions on several instrumented test slabs at the MnROAD research facility using the Automated Laser Profile System 2.(64) The system includes a laser that sweeps along a long rigid beam and collects a relative profile along a selected line. Lederle quantified curl and warp by associating properties of the measured transverse profiles with surface profiles predicted by ISLAB2000 for differences in temperature across the depth of the slab.(65) This association produced an empirical estimate of the curl and warp of each measured profile regarding the temperature difference in the predicted profile that produced the best match. After removing the prevailing linear trend (i.e., cross slope) and extraneous points from each transverse profile, researchers used the following three methods of relating measured and predicted profiles:

- Polynomial Curvature Method: A polynomial curve fit was applied to predicted and measured profiles, which were associated with a predicted counterpart based on curvature versus distance across the slab derived from the fitted polynomial.
- Δh Method: Measured profiles were associated with a predicted counterpart based on the difference between the slab midpoint and the edges.

- Minimum Error Method: A polynomial curve fit was applied to the measured profiles, which were associated with a predicted counterpart based on a direct fit to the predicted profiles.

Lederle found that agreement between the model and measured profiles was better at the slab center than near the joints because of the restraint placed on vertical movement caused by friction at joints between other slabs or shoulders.[65] The Polynomial Curvature Method and Minimum Error Method were each applied five times using polynomial fits with orders of two through six. The analysis did not produce consistent results for various polynomial orders, and the results for lower-order polynomials were deemed more realistic and more physically relevant. The inconsistency in results for higher-order polynomials illustrates the potential confounding influence of roughness in measured profiles (i.e., curvature and curvature changes) unrelated to slab curl and warp and the importance of fitting the measured profiles directly to an assumed function that corresponds to a structural model of slab deformation.

Ceylan et al. measured curling and warping of slabs on six in-service pavements in Iowa at various times of day using LiDAR scans.[66] The LiDAR scans produced point clouds, which were processed to produce three-dimensional surface profiles for each test slab. Surface profiles were fitted to a general bivariate quadratic function (i.e., elevation was cast as a second-order function of transverse and longitudinal position). Curling and warping was reported in terms of relative deflection for two-dimensional slices along transverse slab edges, longitudinal slab edges, and the two slab diagonals that connect the corners. Relative deflection along each slice was defined as the difference between the fitted profile and a reference line connecting the two ends.

Inertial Profilers

Darlington and Milliman envisioned "a study of 24-hour slab movement recording actual slab curling" as an application of inertial profilers early in their adoption for use in pavement-network management.[67] Some researchers demonstrated the effect of curl and warp on road profiles using filtered elevation plots and power spectral density plots. (See references 68 through 73.) Other research studies have attributed changes in IRI measured by inertial profilers to changes in curl and warp over daily and seasonal cycles or used changes in IRI measured by inertial profilers to investigate early-age behavior.[70,73,74] Byrum and Sixbey et al. first proposed algorithms for directly quantifying slab curl and warp using inertial profile measurements.[75,76] This section describes several proposed methods for quantifying curl and warp using inertial profiler measurements.

Byrum Curvature Index

Byrum proposed and demonstrated a curvature index (CI) using high-speed inertial profile measurements collected for the LTPP study on GPS-3 and GPS-4 test sections.[77,78] CI combines discrete curvature estimates calculated from as shown in the equation in Figure 77.

$$curvature_n = \frac{slope_{n+i} - slope_n}{x_{n+i} - x_n},\ slope_n = \frac{y_{n+i} - y_n}{x_{n+i} - x_n}$$

Figure 77. Equation. Discrete curvature estimates.

In Figure 77, *y* and *x* are the values of profile elevation and longitudinal distance, respectively, at sample points indicted by the subscripts. These expressions reduce algebraically to a form related to midchord deviation and calculation of vertical acceleration from a profile corresponding to a particular interval (i.e., base length).[79,80]

In figure 78, Δx is the profile recording interval, $i\Delta x$ is the interval over which slope is calculated, and $curvature_n$ is a three-point estimate of curvature for the corresponding interval.

$$curvature_n = \frac{y_{n+2i} - 2y_{n+i} + y_n}{(i\Delta x)^2}$$

Figure 78. Equation. Discrete curvature estimates, constant interval.[77]

When CI was first proposed, LTPP profile data were stored at a sample spacing of 6 inches, which determined the values of interval available for computing curvature estimates.

The overall value of CI for a wheel path included a sum of the average curvature estimates calculated over intervals of 6, 24, and 48 inches (i.e., for $i = 1$, 4, and 8). Byrum recognized the potential variation in curvature within long slabs:

> One complication in the processing is related to long slab behavior. In this case, the portion of the slab near a joint would have curvature. However, the middle portion of the slab remains flat because of physical and geometric confinement.[75]

As such, CI also included additional terms that averaged the 6-inch interval curvature estimates for approach and leave areas within 15 ft of joints or cracks.

Byrum isolated slabs from joints and cracks using a curvature-variation threshold. Points within the profile with relatively high levels of curvature were marked as imperfections, and the areas within 2 ft of imperfections were excluded from the calculation of CI. This approach for detecting joints and cracks was subsequently applied in studies of other behaviors in jointed-concrete pavements, such as rocking and pumping and faulting.[81,82]

Byrum demonstrated a model that correlated to the IRI of a 500-ft-long profile to a linear combination of CI, the number of imperfections found, the average severity of the imperfections, the SD of curvature estimates with 6- and 48-inch intervals and the average curvature estimate with a 48-inch interval.[77] The model predicted IRI with a standard error of 9.75 inches/mi.

Byrum later compared several methods of quantifying slab curvature, including three-point curvature estimates, polynomial curve fits, and fitting to an assumed slab profile.[83] The comparison included a detailed description of the Byrum Curvature Index (BCI) method. In addition to CI and the underlying curvature estimates, the BCI method includes the report of the average, SD, and standard error for a suite of curvature estimates using intervals of 6 through 48 inches (i.e., $i = 1$ through 8), a companion set of estimates taken from the profile after the application of a cubic spline filter, and several combinations thereof aggregated for all points within slab boundaries, and within joint-and-crack approach and leave areas.

The comparison included three important observations that translate to other methods of processing profile data to obtain curvature estimates. First, analysis of many slabs over a uniform pavement segment is advantageous because using many slabs reduces variations in curvature estimates caused by confounding variations, such as other sources of roughness. Second, fitting a profile over the length of a slab to an assumed shape may fail to accurately capture an estimate of slope at the slab ends. Third, an algebraic relationship exists between many of the prevailing choices for quantifying slab curl from profile (e.g., center versus edge deformation, differences in slope at slab ends, polynomial curve fits, and fitting to a structural model).

Curve Fitting

Sixbey et al. analyzed profiles of 65 lane-miles of in-service jointed concrete with premature transverse cracking.(76) Profiles were collected in four passes on the same day, starting in the early morning and ending in the early evening. The research characterized curvature of individual slab profiles using the maximum deformation. The profile-analysis procedure normalized the measured traces into a deformation profile by removing the trend along the slab. This procedure applied a third-order fit to slab-wide profiles and removed a linear trend from the fitted and measured profiles. From the graphical demonstration, plots appeared to show that both fitted and measured profiles were adjusted equally, such that values of zero deformation would appear in the fitted profile at the slab boundaries. Maximum deformation was read from the measured deformation profile at the location where the fitted deformation profile had the largest absolute value.

The work by Sixbey et al. applied curve fitting to reduce the sensitivity of the process to irregularities within each slab.(76) In a subsequent description of the work by Sixbey et al., Gagarin and Mekemson explained that "the curvature of the surface profile is not necessarily equivalent to slab curvature," and concluded that for individual slabs, the relevant measure was changes in deformation.(84) Sixbey et al. characterized the overall behavior of the pavement using the distribution of maximum deformation values for all slabs at a given time and by observing changes throughout the day.(76)

Sixbey et al. and Gagarin and Mekemson did not provide details of the procedure for identifying the boundaries of each slab.(76,84) However, researchers recommended using a recording interval 0.2 inches or shorter. Gagarin and Mekemson cited the need to overcome inconsistencies in the measurement of longitudinal distance between multiple runs over the same pavement section.(84)

Fitting to an Assumed Slab Profile

Chang et al. studied seasonal and diurnal profile changes in 19 test sections and diurnal profile changes in 19 additional test sections throughout the United States. Diurnal testing included repeated profile measurements collected during four time periods throughout a 24-hour cycle: early morning, midmorning, early afternoon, and late afternoon. Seasonal testing required diurnal testing once per season yearly.(85)

Chang et al. quantified the level of curl and warp in measured profiles by fitting profiles of individual slabs to an assumed shape predicted by the Westergaard equation.(3,20) The

Westergaard equation predicts vertical deformation caused by a constant strain gradient throughout the depth of a slab using structural properties, b, l, and μ.

In the procedure used in Chang et al., researchers isolated individual slab profiles by searching for narrow spikes that appeared in the profiles at the joints. This procedure depended on the availability of up to 10 repeat profile measurements collected at each visit and data collected with a narrow height-sensor footprint (i.e., a point laser) and recorded at short intervals (i.e., 0.25 inches). Slab profiles were preprocessed by eliminating a length of profile not exceeding 2 inches at each end and by removing the linear trend.

The fitting procedure, show in in Figure 79, sought a scale factor that produced the best fit between the measured profile and the assumed slab shape.

$$z(x) = -z_0 f(x,b,l)$$

Figure 79. Equation. Slab profile fitting function.

In the equation in Figure 79, $z(x)$ is the fitted displacement function, and x is the distance along the slab with its origin at the slab center. The function f defines the shape of the slab. It is symmetric about the slab center with a value of one at the slab ends. The fitted scale factor is the uplift at the slab ends (z_0) in the fitted function. Results were expressed in terms of the strain gradient required to deform a slab into measured shape, as shown in the equation in Figure 80.

$$PSG = {}^{-z_0}\!\big/_{(1+\mu)l^2}$$

Figure 80. Equation. PSG.

In Figure 80, PSG is measured in units of strain per inch of depth, proportional to magnitude of deformation.

Chang et al. reported the level of curl and warp for slabs within a given road segment in terms of the distribution of PSG values and related changes in HRI for the measured profiles to the average PSG.[3,6] Chang et al. reported diurnal changes in HRI as high as 40 inches/mi.[3] Chang et al. observed that for test sections with large changes in PSG, a strong linear relationship existed between HRI and average PSG and demonstrated extrapolation of the linear fit for estimating the HRI that would exist without slab curl.

Karamihas and Senn applied the method to profiles from the LTPP SPS-2 site in Arizona over the first 16 years of its monitoring history.[12] The study demonstrated a close linear relationship between IRI and average PSG for low-strength sections in which large diurnal and seasonal changes in IRI were observed but not for high-strength sections in which changes in IRI were small. For the low-strength sections, linear regression produced standard estimate of error values ranging from 1.19 to 4.64 inches/mi.

Ruiz et al. applied the method to diagnose the cause of premature slab cracking to in-service pavements in Bolivia.[86] The study examined variations in PSG within a test section and changes in PSG between profiles measured in the morning and afternoon. Merritt et al. applied the method to investigate undesirable roughness of a jointed-concrete pavement in Colorado.[87] The study included diurnal profile measurements in February and August of the same year and confirmed the presence of curl in pavements in both directions. The results included changes in HRI of more than 20 inches/mi on some test segments and attributed up to 40 inches/mi to slab curl in profile collected in the early morning.

Profile Decomposition

Siddique proposed the separation of a curled profile from components unrelated to curl using a fast Fourier transform algorithm. Siddique attributed roughness at wavelengths equal to the slab length and integer fractions of the slab length (e.g., a half, a third) to slab curl.[88] The fast Fourier transform algorithm was applied to the measured profile. The Fourier coefficients were split into two sets: one for wavenumbers that correspond to the slab length and upper harmonics and another for the remaining wavenumbers. An inverse Fourier transform produces a separate profile for each set of coefficients. The effects of curling were reported for the reduction in the IRI of the profile without the components associated with curl relative to the IRI of the original profile. Siddique provides an example with 9-percent reduction in the IRI when the curling contribution was removed.

Adu-Gyamfi, Attoh-Okine, and Ayenu-Prah proposed using the Hilbert–Huang Transform (HHT) as a tool for characterizing road roughness using measured profiles.[89] The HHT includes decomposition of profiles into intrinsic mode functions (IMFs). Unlike the Fourier transform, shapes of the IMFs depend empirically on the properties of the measured signal. The HHT is best suited for applications for which the signal under study includes changes in the severity of the measured fluctuations or changes in the contributing frequencies.

Gagarin et al. illustrated the use of the HHT as a filtering tool on a jointed-concrete pavement profile.[90] The example showed plots of IMF combinations that helped distinguish slab curling from other content, such as texture and narrow dips at joints. Franta described a method for separating a profile into the following three components using the HHT: noise/surface texture, curl, and base trends.[91] Each component included contributions from several IMFs produced by the transform. Franta provides an example of quantifying the curl of a slab in terms of temperature gradient in which the curl and base trend components are compared to slab deformation profiles predicted by ISLAB2005.

Assessment

The literature reviewed in appendix A included the following findings pertinent to the research examined in the report:

- Curvature caused by curl and warp varies throughout the length of concrete slabs. Curvature at slab ends may disagree with simple slab models because of loss of contact with the subgrade, friction between adjacent slabs, and load-transfer devices.

- Variations in the curvature of measured slab profiles caused by sources other than curl and warp necessitate the use of smoothing, a curve fit, or some analysis technique that minimizes sensitivity to surface irregularities. Although curl and warp contributes to the absolute curvature of slabs, the only justified assumption is that changes in curvature of a slab profile relate primarily to changes in curl and warp.

- Characterization of the status of a road segment by averaging the severity of curl and warp over many slabs reduces the influence of confounding variables. The distribution of values from individual slabs is also informative.

- Use of a single parameter to characterize curl and warp is advantageous if the use can be justified by a theoretical or experimental link to structural behavior. Measures that easily translate to an estimate of equivalent linear temperature gradient facilitate comparisons with past research and existing design practice.

- Under certain conditions, a statistical link exists between measures of curl and warp and measures of roughness, such as the IRI.

- Processing data for many slabs measured by an inertial profiler requires a reliable, preferably automated, method of detecting the location of joints.

APPENDIX B. DESIGN FEATURES, MAINTENANCE HISTORY, AND PROFILE-MEASUREMENT HISTORY

DESIGN FEATURES

SPS-2 Sites

This section provides relevant information about SPS-2 sites provided in construction reports, a description of the LTPP SPS-2 core experiment, and a description of a proposed SPS-2 pavement-preservation experiment. (See references 7, 15, 19, and 92.)

Table 22 lists the variations in structural factors that appear at LTPP SPS-2 sites. These 24 combinations make up a factorial matrix with 2 values of slab thickness, 2 values of PCC flexural strength, 3 base designs, and 2 values of slab width. Each site includes 12 core sections. The sites in Kansas, North Carolina, Ohio, and Washington include sections 0201–0212, and the site in Arizona includes sections 0213–0224. The two groups have the same combinations of slab thickness, PCC flexural strength, and base design but have the opposite pairing of each combination with slab width.

The subgrade is silty sand with gravel at the Arizona site, silty clay at the Kansas site, primarily silty clay at the North Carolina site, silty clay at the Ohio site, and fine-grained sandy-silt material at the Washington site.

Table 23 lists the supplemental sections at each site and the structural factors known about each site. The Kansas, North Carolina, and Washington sites include control sections that were built using the State DOT's standard design. The control section in Kansas (200259) has a 6-inch-thick stabilized base above a 6-inch-thick modified fly ash subbase. The control section in North Carolina (370259) has a 4-inch PATB and includes a section (370260) that substitutes a 5-inch-thick asphalt-treated base for the LCB on section 370207 for comparison. The control section in Washington (530259) has a 3-inch-thick asphalt-treated base over a 2-inch-thick crushed surfacing base course.

The Arizona site includes four undoweled sections with skewed joints (040262–040265). Their doweled counterparts are 040213, 040221, 040223, and 040215, respectively. Three additional sections of doweled jointed plain concrete (040266–040268) were included with specialized designs of interest to the Arizona DOT. The Arizona site also includes two asphalt concrete (AC) sections (040260 and 040261).

The Ohio site includes seven supplemental sections with the same PCC thickness and various combinations of base designs and mix designs of interest to the Ohio DOT. Even-numbered sections were built using a higher-strength mix than odd-numbered sections.

Table 22. SPS-2 core experiment structural factors.

Section	Slab Width (ft)	PCC Flexural Strength (psi)	Layer 1 Thickness (Inches)	Layer 2 Thickness (Inches)	Layer 3 Thickness (Inches)	Layer 1 Type	Layer 2 Type	Layer 3 Type
0201	12	550	8	6	—	PCC	DGAB	—
0202	14	900	8	6	—	PCC	DGAB	—
0203	14	550	11	6	—	PCC	DGAB	—
0204	12	900	11	6	—	PCC	DGAB	—
0205	12	550	8	6	—	PCC	LCB	—
0206	14	900	8	6	—	PCC	LCB	—
0207	14	550	11	6	—	PCC	LCB	—
0208	12	900	11	6	—	PCC	LCB	—
0209	12	550	8	4	4	PCC	PATB	DGAB
0210	14	900	8	4	4	PCC	PATB	DGAB
0211	14	550	11	4	4	PCC	PATB	DGAB
0212	12	900	11	4	4	PCC	PATB	DGAB
0213	14	550	8	6	—	PCC	DGAB	—
0214	12	900	8	6	—	PCC	DGAB	—
0215	12	550	11	6	—	PCC	DGAB	—
0216	14	900	11	6	—	PCC	DGAB	—
0217	14	550	8	6	—	PCC	LCB	—
0218	12	900	8	6	—	PCC	LCB	—
0219	12	550	11	6	—	PCC	LCB	—
0220	14	900	11	6	—	PCC	LCB	—
0221	14	550	8	4	4	PCC	PATB	DGAB
0222	12	900	8	4	4	PCC	PATB	DGAB
0223	12	550	11	4	4	PCC	PATB	DGAB
0224	14	900	11	4	4	PCC	PATB	DGAB

—No layer.
DGAB = dense-graded aggregate base.

Table 23. Supplemental section structural factors.

Section	Slab Width (ft)	PCC Flexural Strength (psi)	Layer 1 Thickness (Inches)	Layer 2 Thickness (Inches)	Layer 3 Thickness (Inches)	Layer 1 Type	Layer 2 Type	Layer 3 Type
040260	—	—	8.5	4	—	AC	DGAB	—
040261	—	—	8.5	4	—	AC	DGAB	—
040262	14	550	8.0	6	—	PCC	DGAB	—
040263	14	550	8.0	4	4	PCC	PATB	DGAB
040264	12	550	8.5	4	4	PCC	PATB	DGAB
040265	12	550	8.5	6	—	PCC	DGAB	—
040266	14	550	12.5	4	—	PCC	DGAB	—
040267	14	550	11.0	4	—	PCC	ATB	—
040268	14	550	8.0	4	—	PCC	ATB	—
200259	12	600	12.0	6	6	PCC	unk	unk
370259	12	unk	10.0	4	—	PCC	PATB	—
370260	14	550	11.0	5	—	PCC	ATB	—
390259	12	unk	11.0	6	—	PCC	AB	—
390260	12	unk	11.0	4	4	PCC	PATB	AB
390261	14	unk	11.0	4	4	PCC	CTFDB	AB
390262	12	unk	11.0	4	4	PCC	CTFDB	AB
390263	14	unk	11.0	6	—	PCC	AB	—
390264	12	unk	11.0	6	—	PCC	AB	—
390265	14	550	11.0	4	4	PCC	PATB	AB
530259	14	650	10.0	3	2	PCC	ATB	DGAB

—Not applicable.
AB = aggregate base; ATB = asphalt-treated base; CTFDB = cement-treated free-drainage base; DGAB = dense-graded aggregate base; unk = unknown.

GPS-3 Sections

Table 24 provides information about the structural design of GPS-3 sections included in this study. The bound treated base for sections 063021 and 493011 were composed of a cement-aggregate mixture. All five sections had an untreated GB and an untreated subgrade. Table 25 provides more detail about the unbound base and subgrade of each section.

Table 24. GPS-3 section structural factors.

Section	28-Day Flexural Strength (psi)	Layer 1 Thickness (Inches)	Layer 2 Thickness (Inches)	Layer 3 Thickness (Inches)	Layer 1 Type	Layer 2 Type	Layer 3 Type
063021	550	8.1	5.4	5.5	PCC	BTB	UGB
133019	550	8.9	7.2	—	PCC	UGB	—
183002	546	9.5	5.5	—	PCC	UGB	—
273003	unk	7.8	5	—	PCC	UGB	—
493011	487	10.2	4	3.2	PCC	BTB	UGB

—Not applicable.
BTB = bound-treated base; UGB = unbound granular base; unk = unknown.

Table 25. GPS-3 section base layer materials.

Section	Untreated Base	Subgrade
063021	Aggregate mixture, primarily fine-grained	Silty sand with gravel
133019	Coarse-grained aggregate	Sandy lean clay
183002	Crushed stone	Sandy lean clay
273003	Gravel	Sandy lean clay
493011	Crushed gravel	Clayey gravel with sand

CONSTRUCTION AND MAINTENANCE HISTORY

SPS-2 Sections

Table 26 lists the date each site was opened to traffic and the source. These dates are used as a reference for determining a value of age in other parts of this report.

Table 26. SPS-2 site open to traffic dates.

Site	Open to Traffic Date
Arizona	01-Oct-1993[7]
Kansas	13-Jul-1992[15]
North Carolina	01-Jul-1994[18]
Ohio	01-Oct-1996[7]
Washington	21-Nov-1995[16]

Some SPS-2 test sections were taken out of the LTPP study primarily because of rehabilitation to address pavement deterioration. The sections removed from the study and the date of removal include the following:

- 31-Dec-2003—sections 370201, 370202, 370205, 370206, 370209, and 370210.
- 16-Feb-2007—sections 390201, 390202, 390204, 390205, 390206, 390210, and 390259.
- 01-Sep-2012—sections 390209 and 390264.

All other test sections in North Carolina and Ohio and all test sections at the Arizona, Kansas, and Washington sites were included in the study over the entire interval.

Table 27 through table 30 list maintenance and rehabilitation performed on each test section that may affect the test section’s measured roughness. Maintenance and rehabilitation were not performed at the Washington site.

Table 27. Maintenance and rehabilitation for Arizona SPS-2 sections.

Section	Approximate Date	Description
040213	Aug-2009	Partial-depth patching at joints and elsewhere
040217	Aug-2009	Partial-depth patching at joints and elsewhere
040218	Jul-2007	Partial-depth patching at joints and elsewhere
040221	Jul-2007	Partial-depth patching at joints
040260	Aug-2005	Patch potholes
040260	Aug-2007	Patch potholes
040260	Aug-2009	Patch potholes
040260	Jan-2013	Patch potholes
040260	Mar-2015	Crack sealing
040261	Dec-2004	Patch potholes
040261	Aug-2009	Patch potholes
040261	Aug-2011	Patch potholes
040261	Mar-2015	Crack sealing
040262	Aug-2009	Partial-depth patching at locations away from joints
040262	Jan-2013	Partial-depth patching at joints
040263	Jan-2013	Partial-depth patching at joints
040264	Jan-2013	Partial-depth patching at joints
040267	Nov-2007	Grinding surface

Table 28. Maintenance and rehabilitation for North Carolina SPS-2 sections.

Section	Approximate Date	Description
370210	Jun-1995	Partial-depth patching at joints
370212	Jun-2015	Patch potholes
370259	Jun-1995	Partial-depth patching at joints

Table 29. Maintenance and rehabilitation for Kansas SPS-2 sections.

Section	Approximate Date	Description
200201	Dec-1995	Slab replacement Partial-depth patching at joints
200201	Jun-2002	Slab replacement
200201	Aug-2004	Slab replacement
200201	Mar-2005	Transverse joint sealing
200201	Jun-2011	Full-depth transverse-joint-repair patching Full-depth patching away from joints
200202	Mar-2005	Transverse joint sealing
200202	Jun-2011	Full-depth transverse-joint-repair patching Full-depth patching away from joints
200203	Mar-2005	Transverse joint sealing
200204	Jun-1995	Partial-depth patching at joints
200204	Apr-1997	Partial-depth patching at joints
200204	Mar-2005	Transverse joint sealing
200204	Jun-2011	Full-depth transverse-joint-repair patching
200205	Mar-2005	Transverse joint sealing
200205	Jun-2008	Partial-depth patching at joints
200205	Jun-2010	Partial-depth patching at joints
200205	Jun-2011	Full-depth transverse-joint-repair patching Full-depth patching away from joints
200205	Jun-2014	Partial-depth patching at joints
200206	Mar-2005	Transverse joint sealing
200206	Jun-2011	Slab replacement

Section	Approximate Date	Description
200207	Mar-2005	Transverse joint sealing
200207	Jun-2008	Partial-depth patching at joints
200207	Jun-2011	Full-depth transverse-joint-repair patching Full-depth patching away from joints
200208	Mar-2005	Transverse joint sealing
200209	Mar-2005	Transverse joint sealing
200209	Jun-2011	Full-depth transverse-joint-repair patching Full-depth patching away from joints
200210	Mar-2005	Transverse joint sealing
200210	Jun-2011	Full-depth transverse-joint-repair patching
200211	Mar-2005	Transverse joint sealing
200211	Jun-2011	Full-depth transverse-joint-repair patching
200212	Mar-2005	Transverse joint sealing
200259	Mar-2005	Transverse joint sealing
200259	Jun-2011	Full-depth patching away from joints

Table 30. Maintenance and rehabilitation for Ohio SPS-2 sections.

Section	Approximate Date	Description
390203	Jun-2013	Grinding surface
390207	Aug-2012	Full-depth transverse-joint-repair patching Full-depth patching away from joints Joint load-transfer restoration
390207	Jun-2013	Slab replacement
390208	Jun-2007	Full-depth transverse-joint-repair patching Joint load-transfer restoration
390208	Aug-2012	Full-depth transverse-joint-repair patching Full-depth patching away from joints Joint load-transfer restoration
390208	Jun-2013	Full-depth patching away from joints Slab replacement
390209	Jun-2007	Full-depth transverse-joint-repair patching
390212	Jun-2007	Full-depth transverse-joint-repair patching Joint load-transfer restoration
390212	Jun-2010	Partial-depth patching at locations away from joints
390212	Jun-2012	Partial-depth patching at locations away from joints
390212	Aug-2012	Full-depth transverse-joint-repair patching Full-depth patching away from joints Joint load-transfer restoration
390212	Jun-2013	Slab replacement
390261	Jun-2013	Grinding surface
390262	Jun-2013	Grinding surface
390263	Jun-2013	Grinding surface
390264	Jun-2007	Full-depth transverse-joint-repair patching

GPS-3 Sections

Table 31 lists the section number, construction date, and the date each section was incorporated into the LTPP program for each GPS-3 section included in this study. The construction date for each section is used as a reference for determining a value of age in other parts of this report. Section 273003 was removed from the LTPP study on 01-Jul-2010. The other sections were still active when this research was performed. The curl-and-warp analysis of section 183002, however, was terminated after July 2014 because it received an AC overlay.

Section	Construction Date	Date Included in LTPP
063021	01-Apr-1974	28-Jan-1988
133019	01-Dec-1981	01-Jan-1987
183002	01-Aug-1976	01-Jan-1987
273003	01-Oct-1985	01-Jan-1987
493011	01-May-1986	05-Apr-1989

Table 32 lists major maintenance and rehabilitation performed on each section.

Table 31. Dates of construction and incorporation into LTPP for GPS-3 sections.

Section	Construction Date	Date Included in LTPP
063021	01-Apr-1974	28-Jan-1988
133019	01-Dec-1981	01-Jan-1987
183002	01-Aug-1976	01-Jan-1987
273003	01-Oct-1985	01-Jan-1987
493011	01-May-1986	05-Apr-1989

Table 32. Maintenance and rehabilitation for GPS-3 sections.

Section	Approximate Date	Description
063021	Aug-2008	Crack sealing
063021	Jun-2011	Grinding
063021	Jun-2012	AC shoulder restoration
133019	Dec-2010	Grinding and transverse joint sealing
183002	May-1996	Partial-depth patching at joints and elsewhere
183002	Jun-2000	Partial-depth patching at joints
183002	Jun-2002	Partial-depth patching at joints
183002	Jun-2004	Partial-depth patching at joints
183002	June-2006	Partial-depth patching at joints and elsewhere
183002	June-2013	Partial-depth patching at joints and elsewhere
183002	July-2014	AC overlay
273003	June-2007	Partial-depth patching at joints
493011	Aug-1996	Transverse joint sealing
493011	May-2012	Grinding, transverse joint sealing Joint load-transfer restoration Partial-depth patching at joints

PROFILE-MONITORING HISTORY

SPS-2 Sections

Table 33 through

table 37 list the visit number, measurement date, ranges of time, number of repeat measurements, and section details for each profile-measurement visit to the SPS-2 site. Visit numbers are assigned to each sequence of visits for reference in other parts of this report. In some cases (e.g., visit 02 to the Arizona site), the tables list only a single value for time because the same measurement time was recorded for the entire set of repeat measurements.

In many cases, all test sections were included in a single set of passes over the site (e.g., visits 01 through 11 to the Arizona site). In other cases, portions of a site, including one or more test sections, were measured in separate sets of passes (e.g., visits 12 through 22 to the Arizona site). These cases are listed separately in Table 33 through

Table 37 because the timing of the measurements is different. Some sections do not appear in later visits because they had been taken out of the LTPP study.

Table 33. Profile-measurement history for Arizona SPS-2 site.

Visit	Date	Time	Repeats	Sections
01	25-Jan-1994	06:10–08:14	9	All
02	05-Mar-1995	11:21	9	All
03	27-Jan-1997	11:22–12:49	9	All
04	04-Dec-1997	11:06–13:07	7	All
05	08-Dec-1998	10:28–11:27	7	All
06	15-Nov-1999	11:38–12:38	7	All
07	05-Dec-2000	13:37–15:01	9	All
08	08-Nov-2001	11:09–12:39	9	All
09	30-Oct-2002	12:40–14:07	9	All
10	04-Feb-2004	13:47–15:12	9	All
11	12-Dec-2004	16:15–18:37	9	All
12	13-Aug-2006	00:13–01:39	9	0215, 0216, 0219, 0223, 0224
12	13-Aug-2006	04:17–06:26	9	0213, 0217, 0221, 0262, 0263
12	13-Aug-2006	03:00–03:30	9	0214, 0261
12	13-Aug-2006	00:17–01:33	9	0260, 0264–0268
12	13-Aug-2006	03:35–04:28	9	0218, 0220, 0222
13	13-Dec-2007	11:54–13:12	9	0215, 0216, 0219, 0223, 0224
13	13-Dec-2007	10:08–11:37	9	0213, 0217, 0221, 0262, 0263
13	13-Dec-2007	10:05–11:27	9	0214, 0218, 0220, 0222, 0261
13	13-Dec-2007	11:59–13:21	9	0260, 0264–0268
14	20-Sep-2008	02:06–03:32	9	0215, 0216, 0219, 0223, 0224
14	20-Sep-2008	00:40–01:53	9	0213, 0217, 0221, 0262, 0263
14	20-Sep-2008	00:37–01:50	9	0214, 0218, 0220, 0222, 0261
14	20-Sep-2008	02:10–03:35	9	0260, 0264–0268
15	25-Jan-2010	17:37–18:56	9	0215, 0216, 0219, 0223, 0224
15	25-Jan-2010	16:11–17:23	9	0213, 0217, 0221, 0262, 0263
15	25-Jan-2010	16:08–17:20	9	0214, 0218, 0220, 0222, 0261
15	25-Jan-2010	17:42–19:00	9	0260, 0264–0268
16	08-Dec-2011	21:26–22:37	9	0215, 0216, 0219, 0223, 0224
16	08-Dec-2011	20:00–21:07	9	0213, 0217, 0221, 0262, 0263
16	08-Dec-2011	19:57–21:04	9	0214, 0218, 0220, 0222, 0261
16	08-Dec-2011	21:28–22:39	9	0260, 0264–0268
17	16-Dec-2012	19:46–21:04	9	0215, 0216, 0219, 0223, 0224
17	16-Dec-2012	18:09–19:35	9	0213, 0217, 0221, 0262, 0263
17	16-Dec-2012	18:06–19:33	9	0214, 0218, 0220, 0222, 0261
17	16-Dec-2012	19:48–21:07	9	0260, 0264–0268
18	06-Feb-2014	21:58–22:52	9	0215, 0216, 0219, 0223, 0224
18	06-Feb-2014	23:02–23:49	9	0213, 0217, 0221, 0262, 0263
18	06-Feb-2014	23:57–00:56	9	0214, 0218, 0220, 0222, 0261
18	07-Feb-2014	01:01–01:42	9	0260, 0264–0268
19	07-Feb-2014	08:39–08:53	3	0214–0216, 0218–0220, 0222–0224, 0261
19	07-Feb-2014	09:03–09:23	3	0213, 0217, 0221, 0260, 0262–0268
20	07-Feb-2014	12:48–13:01	3	0214–0216, 0218–0220, 0222–0224, 0261
20	07-Feb-2014	13:10–13:29	3	0213, 0217, 0221, 0260, 0262–0268
21	07-Feb-2014	16:21–16:34	3	0214–0216, 0218–0220, 0222–0224, 0261
21	07-Feb-2014	16:40–16:59	3	0213, 0217, 0221, 0260, 0262–0268
22	14-Nov-2014	00:27–01:16	9	0214, 0218, 0220, 0222, 0261
22	14-Nov-2014	01:24–02:03	9	0215, 0216, 0219, 0223, 0224
22	14-Nov-2014	03:10–04:02	9	0213, 0217, 0221, 0262, 0263
22	14-Nov-2014	04:06–04:53	9	0260, 0264–0268
23	07-Dec-2015	18:23–19:44	9	All

Table 34. Profile-measurement history for Kansas SPS-2 site.

Visit	Date	Time	Repeats	Sections
01	14-Aug-1992	12:52–15:38	8	0201–0212
02	10-Mar-1993	11:05–12:39	9	All
03	15-May-1994	10:10–11:00	9	All
04	18-Feb-1995	09:12	8	All
05	20-Apr-1996	13:31	7	All
06	03-Mar-1997	11:40–13:37	7	All
07	15-May-1998	10:26–11:32	7	All
08	15-Mar-1999	08:34–09:38	5	All
09	01-Mar-2000	11:25–12:45	7	All
10	10-May-2001	14:08–15:17	7	All
11	21-Apr-2002	08:01–09:05	7	All
12	20-Feb-2003	10:31–11:34	7	All
13	12-Mar-2004	17:04–18:28	9	All
14	05-Jun-2006	12:58–14:53	7	All
15	19-Apr-2008	09:42–11:08	9	All
16	07-Aug-2009	09:23–10:58	9	All
17	19-Oct-2010	15:49–17:10	9	All
18	21-Sep-2012	13:58–15:30	9	All
19	03-Dec-2013	16:25–17:45	9	All
20	05-May-2014	14:17–15:58	9	All
21	06-May-2014	06:57–07:39	5	All
22	06-May-2014	13:53–15:29	8	All
23	06-May-2014	20:25–21:29	5	All
24	09-Dec-2015	13:08–14:24	7	All

Table 35. Profile-measurement history for Ohio SPS-2 site.

Visit	Date	Time	Repeats	Sections
02	27-Dec-1996	10:22–11:43	7	All
03	8-Dec-1997	09:21–10:27	7	All
04	12-Nov-1998	09:24–10:38	7	All
05	20-Oct-1999	08:44–09:40	7	All
06	16-Aug-2000	09:17–10:58	7	All
07	4-Nov-2001	07:59–09:15	7	All
08	6-Dec-2002	11:26–12:28	7	All
09	29-Apr-2003	14:15–15:41	9	0201–0212, 0259–0261, 0265
10	4-Feb-2004	14:54–16:12	9	All
11	5-May-2005	12:20–13:30	9	All
12	8-Aug-2006	11:39–13:24	9	0201–0212, 0260–0263, 0265
13	23-Jul-2008	14:13–15:21	9	0203, 0207–0209, 0211, 0260–0263, 0265
14	21-Oct-2009	14:32–15:37	9	0203, 0207–0209, 0211, 0260–0263, 0265
15	11-Aug-2010	10:40–14:09	9	0203, 0207–0209, 0211, 0260–0263, 0265
16	18-Oct-2011	10:34–11:32	9	0203, 0207–0209, 0211, 0260–0263, 0265
17	22-May-2012	13:37–14:41	9	0203, 0207–0209, 0211, 0212, 0260–0265
18	3-Jun-2014	14:27–15:49	7	0203, 0207, 0208, 0211, 0212, 0260–0263, 0265
19	29-Jul-2014	19:55–20:36	5–6	0203, 0207, 0208, 0211, 0212, 0260–0263, 0265
20	30-Jul-2014	05:57–06:54	6	0203, 0207, 0208, 0211, 0212, 0260–0263, 0265
21	30-Jul-2014	13:01–13:42	5–6	0203, 0207, 0208, 0211, 0212, 0260–0263, 0265

Table 36. Profile-measurement history for North Carolina SPS-2 site.

Visit	Date	Time	Repeats	Sections
01	30-Mar-1994	10:28	9	All
02	06-Jan-1996	05:46	9	0201–0203, 0205–0212, 0259, 0260
03	28-Feb-1996	10:43–14:21	9	0201–0203, 0205–0212, 0259, 0260
03	28-Feb-1996	10:53–14:33	7	0204
04	07-Oct-1997	13:36–15:30	7	0201–0203, 0205–0212, 0259, 0260
04	07-Oct-1997	13:43–15:36	7	0204
05	18-Feb-1998	13:23–15:04	7	0201–0203, 0205–0212, 0259, 0260
05	18-Feb-1998	13:28–15:09	7	0204
06	19-May-1998	10:36–13:48	9	0201–0203, 0205–0212, 0259, 0260
06	19-May-1998	10:41–11:44	5	0204
07	24-Jul-1998	11:14–12:54	7	0201–0203, 0205–0212, 0259, 0260
07	24-Jul-1998	11:19–12:42	6	0204
07	24-Jul-1998	14:35–14:47	2	0202, 0203, 0206–0208, 0210–0212, 0260
08	04-Nov-1998	08:45–11:25	6	0201–0203, 0205–0212, 0259, 0260
08	04-Nov-1998	11:47–12:28	6	0204
09	10-Nov-1999	23:54–01:14	9	0201–0203, 0205–0212, 0259, 0260
09	10-Nov-1999	04:17–04:46	5	0204
10	13-Mar-2000	14:02–17:36	9	0201–0203, 0205–0212, 0259, 0260
10	13-Mar-2000	17:46–18:19	5	0204
11	08-Nov-2000	11:16–12:26	9	0201–0203, 0205–0212, 0259, 0260
11	08-Nov-2000	12:57–12:57	5	0204
12	14-Jul-2001	09:11–10:19	9	0201–0203, 0205–0212, 0259, 0260
12	14-Jul-2001	10:39–11:18	7	0204
13	11-Oct-2001	08:45–12:43	7	All
14	23-May-2002	10:07–11:02	9	All
15	19-Sep-2002	17:31–19:41	9	All
16	22-Jan-2003	15:42–17:53	9	All
17	01-Jun-2003	11:28–12:50	9	0201–0203, 0205–0212, 0259, 0260
17	01-Jun-2003	08:03–08:47	7	0204
18	07-Nov-2003	09:16–10:38	9	0203, 0207, 0208, 0211, 0212, 0260
18	08-Nov-2003	13:59–14:28	5	0204
18	08-Nov-2003	12:57–13:40	5	0259
19	14-Nov-2004	15:48–17:10	9	0203, 0207, 0208, 0211, 0212, 0260
19	14-Nov-2004	11:02–11:57	9	0204
19	14-Nov-2004	15:46–17:08	9	0259
20	14-Jun-2006	15:42–17:52	9	0203, 0204, 0207, 0208, 0211, 0212, 0259, 0260
21	30-Nov-2006	12:41–14:41	9	0203, 0204, 0207, 0208, 0211, 0212, 0259, 0260
22	18-Mar-2009	15:51–17:52	9	0203, 0204, 0207, 0208, 0211, 0212, 0259, 0260
23	18-Apr-2010	15:03–16:35	9	0203, 0204, 0207, 0208, 0211, 0212, 0259, 0260
24	27-Apr-2011	19:38–21:56	9	0203, 0204, 0207, 0208, 0211, 0212, 0259, 0260
25	10-Dec-2012	13:24–15:15	7	0203, 0207, 0208, 0211, 0212, 0260
25	10-Dec-2012	13:30–15:17	7	0204
25	10-Dec-2012	13:20–15:28	7	0259
26	24-Jun-2014	13:23–14:27	5	0203, 0204, 0207, 0208, 0211, 0212, 0259, 0260
27	24-Jun-2014	16:42–18:31	6	0203, 0204, 0207, 0208, 0211, 0212, 0259, 0260
28	24-Jun-2014	19:20–20:17	5	0203, 0204, 0207, 0208, 0211, 0212, 0259, 0260
29	25-Jun-2014	18:08–18:51	4	0203, 0204, 0207, 0208, 0211, 0212, 0259, 0260
30	09-Mar-2015	16:33–18:12	7	0203, 0204, 0207, 0208, 0211, 0212, 0259, 0260

Table 37. Profile-measurement history for Washington SPS-2 site.

Visit	Date	Time	Repeats	Sections
01	18-Nov-1995	13:18–14:18	9	All
02	06-Oct-1997	16:48–17:20	5	All
03	15-May-1998	14:14–15:19	7	All
04	07-May-1999	12:52–13:52	7	All
05	29-Jun-2000	13:13–15:01	9	All
06	07-Aug-2001	10:33–11:53	9	All
07	05-Aug-2002	10:46–12:09	9	All
08	20-Aug-2003	15:16–16:40	9	All
09	23-Jul-2004	13:41–15:02	9	All
10	24-Jun-2005	18:21–21:04	9	All
11	07-Jun-2006	17:59–19:23	9	All
12	19-Jul-2007	17:55–19:20	9	All
13	12-Jun-2008	13:24–14:44	9	0201, 0205–0208
13	12-Jun-2008	12:24–13:11	9	0202–0204, 0209–0212, 0259
14	30-Apr-2009	14:30–15:54	9	0201, 0205–0208
14	30-Apr-2009	13:33–14:17	9	0202–0204, 0209–0212, 0259
15	29-Jul-2010	11:08–12:22	9	0201, 0205–0208
15	29-Jul-2010	10:08–10:51	9	0202–0204, 0209–0212, 0259
16	05-Feb-2011	12:33–13:52	9	0201, 0205–0208
16	05-Feb-2011	11:45–12:26	9	0202–0204, 0209–0212, 0259
17	14-May-2012	21:48–23:18	9	0201, 0205–0208
17	14-May-2012	20:52–21:34	9	0202–0204, 0209–0212, 0259
18	16-May-2013	06:43–08:38	9	0201, 0205–0208
18	16-May-2013	06:53–08:02	9	0202–0204, 0209–0212, 0259
19	16-May-2013	10:05–11:46	9	0201, 0205–0208
19	16-May-2013	10:01–11:07	9	0202–0204, 0209–0212, 0259
20	16-May-2013	15:04–16:43	9	All
21	16-Apr-2015	00:21–01:44	9	All

Table 38 through table 40 list the visit number of the seasonal measurement program, measurement date, ranges of time, and number of repeat measurements for SMP sections 040215, 370201, 370205, 370208, 370212, and 390204. Table 39 lists measurements of sections 370209, 370210, and 370259. These measurements were not SMP sections, but sections 370209, 370210, and 370259 were contained within the range of raw profile measurements that were collected during some visits to SMP sections. A second set of profile measurements was collected on section 040267 in the midafternoon following visit 12 to the Arizona SPS-2 site. These measurements were included in the analysis as visit S01 to section 040267.

Table 38. Profile-measurement history for SMP section 390204.

Visit	Date	Time	Repeats
S01	15-Aug-1996	13:15	7
S02	07-Mar-1998	06:12–06:23	5
S03	07-Mar-1998	11:20–11:31	5
S04	07-Mar-1998	15:06–15:17	5
S05	28-May-1998	06:19–06:44	7
S06	28-May-1998	15:06–15:33	7
S07	13-Aug-1998	03:22–03:41	7
S08	13-Aug-1998	07:29–07:44	7
S09	12-Nov-1998	15:01–15:21	7
S10	10-Mar-1999	06:25–06:39	5
S11	10-Mar-1999	14:00–14:19	5
S12	22-Jun-1999	06:14–06:38	7
S13	22-Jun-1999	15:23–15:42	7
S14	17-Jun-2000	05:23–06:47	7
S15	17-Jun-2000	14:35–15:01	7

Table 39. Profile-measurement history for North Carolina SMP sections.

Visit	Date	Time	Repeats	Sections
S01	06-Jan-1996	04:35	4	0201
S02	28-Feb-1996	09:38	5	0201
S03	28-Feb-1996	18:16	6	0201, 0205, 0209, 0210, 0259
S03	28-Feb-1996	18:22–19:33	7	0208
S04	23-Apr-1996	06:57	5	0201
S05	07-Oct-1997	07:38–08:18	5	0201
S06	17-Jan-1998	08:48–09:51	6	0201
S07	28-Feb-1998	07:18–07:58	5	0201
S08	19-May-1998	08:14–09:17	6	0201
S09	19-May-1998	14:43–16:10	8	0201, 0205, 0209, 0210
S10	24-Jul-1998	08:07–08:45	5	0201
S11	04-Nov-1998	14:03–14:55	6	0201
S12	13-Mar-2000	07:45–09:35	9	0201
S13	06-Jul-2000	12:30	5	0201
S14	23-Jan-2001	07:49–08:38	7	0201
S15	23-Jan-2001	14:49–15:42	7	0201
S16	17-May-2001	07:09	5–7	0201, 0205, 0208, 0212
S17	17-May-2001	13:28–14:06	5–7	0201, 0205, 0208, 0212
S18	14-Jul-2001	07:11–08:00	6	0201
S19	14-Jul-2001	13:31–13:39	5	0201
S20	11-Oct-2001	06:56	5	0201
S21	11-Oct-2001	14:03–14:57	7	0201
S22	10-Jan-2002	06:32–07:38	7	0201
S23	10-Jan-2002	13:07–14:00	7	0201
S24	23-May-2002	08:02–08:31	7	0201
S25	23-May-2002	13:43	5	0201
S26	16-Aug-2002	06:08	7	0201
S27	16-Aug-2002	13:30	5	0201
S28	18-Sep-2002	06:25–07:40	9	0201
S29	18-Dec-2002	06:55–07:46	7	0201
S30	18-Dec-2002	12:54–13:30	5	0201
S31	22-Jan-2003	07:20–08:39	7	0201

Visit	Date	Time	Repeats	Sections
S32	22-Jan-2003	12:51–13:28	5	0201
S33	01-Jun-2003	06:01–07:02	7	0201
S34	01-Jun-2003	13:15–14:28	7	0201

Table 40. Profile-measurement history for SMP section 040215.

Visit	Date	Time	Repeats
S01	05-Dec-1995	09:14	7
S02	05-Dec-1995	14:56	7
S03	02-May-1996	09:30	7
S04	02-May-1996	14:58–15:42	7
S05	12-Aug-1996	09:40–11:26	9
S06	12-Aug-1996	14:15	9
S07	15-Jan-1998	11:33–11:52	7
S08	15-Jan-1998	16:43–16:52	5
S09	13-Apr-1998	10:13–10:29	5
S10	13-Apr-1998	15:19–15:30	5
S11	09-Jul-1998	08:22–08:45	5
S12	09-Jul-1998	12:10–12:25	5
S13	30-Sep-1998	11:58–12:14	5
S14	30-Sep-1998	14:35–15:05	7
S15	09-Dec-2001	09:20–09:45	7
S16	09-Dec-2001	14:57–15:29	9
S17	24-Jan-2002	10:12–10:38	7
S18	24-Jan-2002	14:55–15:33	9
S19	15-Mar-2002	09:40–10:11	7
S20	15-Mar-2002	14:30–15:01	7
S21	09-Oct-2002	08:42–09:33	9
S22	09-Oct-2002	13:46–14:34	9
S23	20-Dec-2002	09:05–09:43	9
S24	20-Dec-2002	13:23–14:07	9
S25	07-Mar-2003	09:24–09:53	9
S26	07-Mar-2003	13:56–14:37	9
S27	25-Jul-2003	04:24–05:06	9
S28	25-Jul-2003	08:34–09:11	9
S29	24-Nov-2003	09:32–10:17	9
S30	24-Nov-2003	14:22–15:03	9
S31	14-Dec-2003	10:32–11:10	9
S32	14-Dec-2003	15:16–15:55	9
S33	22-Apr-2004	04:58–05:38	9
S34	22-Apr-2004	09:48–10:24	9
S35	15-Jul-2004	04:17–04:49	9
S36	15-Jul-2004	09:02–09:40	9
S37	09-Sep-2004	03:52–04:24	9
S38	09-Sep-2004	08:34–09:05	9

GPS-3 Sections

Table 41 through table 45 list the visit numbers, measurement dates, ranges of time, and number of repeat measurements for each profile-measurement visit for each GPS-3 section. Visit numbers are assigned to each sequence of visits for reference in other parts of this report. In some cases (e.g., visit 01 to section 063021), the tables list only a single value for time because the profile data headers recorded the same measurement time for the entire set of repeat measurements.

Table 41. Profile-measurement history for GPS section 063021.

Visit	Date	Time	Repeats
01	01-Feb-1990	17:20	5
02	20-Sep-1990	11:09–11:58	7
03	12-Mar-1991	14:23–14:23	5
04	29-Feb-1992	17:03–17:41	6
05	02-Mar-1993	16:15–17:53	9
06	02-Mar-1993	18:33	5
07	10-Apr-1995	12:34–14:12	9
08	24-Feb-1997	10:36–12:01	9
09	16-Feb-1998	12:02–13:16	7
10	10-Mar-1999	12:53–13:37	7
11	15-Feb-2001	12:00–13:45	9
12	14-Nov-2002	13:16–14:32	9
13	04-Dec-2004	09:15–11:27	9
14	07-Dec-2004	09:49–12:08	9
15	29-Jan-2007	16:08–16:34	9
16	05-Nov-2009	15:11–15:37	9
17	08-Mar-2011	15:01–15:30	9
18	10-Mar-2012	14:30–14:58	9
19	23-Jan-2013	17:14–17:40	9
20	17-Mar-2014	19:45–20:18	9
21	15-Jan-2015	18:47–19:19	9

Table 42. Profile-measurement history for GPS section 133019.

Visit	Date	Time	Repeats
01	03-Aug-1990	09:38–10:19	9
02	20-May-1992	13:10–15:37	9
03	27-Jul-1992	12:36	7
04	23-Oct-1992	09:24	0
05	14-Jan-1993	13:57	0
06	09-May-1994	09:25	0
07	26-Jan-1996	06:43	0
08	26-Jan-1996	12:12	0
09	05-Apr-1996	07:14	5
10	05-Apr-1996	13:02	9
11	13-Aug-1996	10:14	9
12	13-Aug-1996	12:53–13:30	9
13	17-Oct-1996	07:48	9
14	17-Oct-1996	15:40–16:11	9
15	16-Oct-1997	09:04–09:20	5
16	16-Oct-1997	12:16–12:32	5
17	29-Jan-1998	07:13–07:33	6
18	29-Jan-1998	13:12–13:27	5
19	27-Apr-1998	08:05–08:26	5
20	27-Apr-1998	12:06–12:23	5
21	06-Aug-1998	10:29–10:42	7
22	09-Dec-1998	11:55–12:19	7
23	14-May-1999	10:41–11:42	8

Visit	Date	Time	Repeats
24	13-Apr-2000	09:37–10:05	7
25	14-Aug-2000	13:45–14:17	7
26	16-Feb-2001	10:56–11:40	7
27	16-Feb-2001	16:55–17:27	7
28	23-May-2001	09:06–09:42	7
29	23-May-2001	15:21–15:50	7
30	6-Aug-2001	07:55–08:31	7
31	6-Aug-2001	13:23–13:52	7
32	14-Mar-2002	07:57–08:11	6
33	14-Mar-2002	13:01–13:18	7
34	10-Dec-2002	10:00–10:21	7
35	4-Aug-2004	11:50-12:35	9
36	27-Nov-2007	16:11–16:51	9
37	10-Feb-2010	10:45–11:09	9
38	4-Nov-2013	14:24–15:06	9
39	11-Oct-2014	16:43–17:29	9

Table 43. Profile-measurement history for GPS section 183002.

Visit	Date	Time	Repeats
01	23-Aug-1990	10:48	5
02	10-Sep-1991	11:00	7
03	04-Oct-1992	15:37	6
04	11-Jan-1994	18:41	9
05	16-Mar-1995	08:26	9
06	24-Oct-1995	07:48	5
07	24-Oct-1995	11:42	5
08	24-Oct-1995	16:01	5
09	03-Apr-1996	07:23	5
10	03-Apr-1996	11:36	5
11	03-Apr-1996	15:45	5
12	06-Sep-1996	16:39	5
13	22-May-1997	07:41–08:01	7
14	05-Dec-1997	08:31–08:46	7
15	05-Dec-1997	14:37–14:51	7
16	05-Feb-1998	14:29–14:43	7
17	06-Feb-1998	06:49–07:05	7
18	26-May-1998	07:59–08:09	5
19	26-May-1998	15:13–15:22	5
20	16-Aug-1998	08:01–08:16	7
21	17-Aug-1998	13:07–13:30	7
22	29-Oct-1999	13:06–13:25	7
23	23-Aug-2000	13:56–14:10	7
24	11-Nov-2001	11:59–12:13	7
25	24-Nov-2003	17:08–17:25	9
26	26-Jul-2004	16:06–16:18	7
27	17-Oct-2007	12:34–12:59	9
28	20-Jul-2010	11:46–11:57	6
29	26-Apr-2011	14:37–15:00	9
30	24-Jul-2012	12:41–12:59	9
31	29-Apr-2015	17:26–17:48	7

Table 44. Profile-measurement history for GPS section 273003.

Visit	Date	Time	Repeats
01	20-Jun-1990	17:08	5
02	10-Aug-1991	11:49	5
03	03-Aug-1992	17:00	9
04	23-Nov-1993	19:10	9
05	30-Jul-1994	14:33	5
06	01-Aug-1997	06:41–06:58	7
07	03-Oct-1998	14:37–14:47	5
08	14-Jun-1999	13:24–13:36	7
09	27-Jul-2000	09:28–09:37	5
10	22-Aug-2001	16:57–17:06	6
11	16-Oct-2004	12:26–12:42	9
12	28-Jul-2009	16:53–17:26	9

Table 45. Profile-measurement history for GPS section 493011.

Visit	Date	Time	Repeats
01	02-Aug-1989	11:56	5
02	01-Sep-1990	07:49	9
03	22-Oct-1991	15:37	6
04	12-Nov-1992	17:06	7
05	15-Nov-1993	15:53	9
06	13-Jan-1994	10:52	7
07	16-Apr-1994	01:18	9
08	14-Jul-1994	20:39–22:33	9
09	13-Nov-1994	13:54	9
10	15-Feb-1995	12:39	7
11	18-May-1995	07:05–14:55	9
12	05-Dec-1996	07:49–08:33	9
13	05-Dec-1996	13:56–14:39	9
14	02-Mar-1997	09:34–10:11	9
15	02-Mar-1997	13:56–14:35	9
16	25-Apr-1997	07:09–07:45	9
17	25-Apr-1997	12:00–12:38	9
18	01-Aug-1997	09:21–09:44	5
19	01-Aug-1997	14:28–14:52	5
20	17-Sep-1997	09:15–09:41	5
21	17-Sep-1997	12:42–13:11	5
22	01-Dec-1998	11:55–12:26	7
23	13-Jul-1999	14:26–15:16	7
24	09-Sep-2001	07:52–08:21	7
25	26-Jan-2004	16:11–16:48	9
26	06-Oct-2004	13:47–14:43	9
27	20-Dec-2004	11:53–12:44	9
28	09-Oct-2007	15:01–15:42	9
29	26-Oct-2010	14:00–14:38	9
30	23-Oct-2012	16:15–16:54	9
31	20-May-2014	21:25–21:55	9
32	18-May-2015	19:53–20:25	9

APPENDIX C. DATA-QUALITY SCREENING

Researchers performed a screening process to select five repeat profile measurements from each visit to each section. The five measurements among the group of up to nine available passes within a visit were selected that exhibited best agreement with each other. Agreement between any pair of profile measurements was judged by cross-correlating the measurements after applying the IRI filter. The details of this method are described in Karamihas.(93) Researchers applied the IRI filter to the profiles before cross correlating them.

High cross correlation between the IRI-filtered profiles requires that their overall roughness is in agreement, as well as the details of the profile shape that affect the IRI, including the severity and distribution of roughness within the section. When 9 repeat profile measurements (i.e., passes) were available, cross-correlating all possible profile pairs produced a total of 36 correlation values for left-side profiles and 36 correlation values for the right. Researchers summarized the composite correlation level for a given set of 5 profiles using an average of the 20 appropriate cross correlation values. The subgroup that produced the highest composite correlation was selected; the other repeat profile measurements were excluded from the analyses discussed in this report. In a few cases, the cross correlation was based on left-side profiles because only left-side profiles were available.

Table 46 lists the results for each visit of each section. The table provides the time and date of the first selected pass, number of available passes, selected pass numbers, and their composite correlation. For visits with five or fewer available passes, all passes were included. Visits 19 through 21 to the SPS-2 site in Arizona included three passes; seasonal visit S01 to section 370201 included four passes; visit 29 to the SPS-2 site in North Carolina included four passes. Pass four over the North Carolina SPS-2 site in visit 26 did not include profiles for the right side.

Overall, 9,570 passes in 1,941 sets of up to 5 repeats comprise the dataset listed in this appendix.

Table 46. Selected repeats.

Section	Visit	Date	Time	Available Repeats	Selected Repeats	Composite Correlation
040213	01	25-Jan-1994	06:10	9	2, 3, 6, 7, 8	0.936
040213	02	05-Mar-1995	11:21	9	2, 5, 6, 7, 9	0.902
040213	03	27-Jan-1997	11:22	9	1, 3, 5, 6, 8	0.971
040213	04	04-Dec-1997	11:06	7	1, 3, 4, 5, 7	0.953
040213	05	08-Dec-1998	10:28	7	1, 2, 5, 6, 7	0.966
040213	06	15-Nov-1999	11:38	7	1, 2, 3, 4, 6	0.961
040213	07	30-Nov-2000	14:10	9	4, 5, 6, 7, 9	0.946
040213	08	08-Nov-2001	11:09	9	1, 2, 4, 7, 9	0.933
040213	09	30-Oct-2002	12:40	9	1, 3, 4, 5, 7	0.949
040213	10	04-Feb-2004	13:47	9	1, 2, 6, 7, 8	0.947
040213	11	12-Dec-2004	16:58	9	3, 4, 7, 8, 9	0.899
040213	12	11-Aug-2006	04:17	9	1, 4, 5, 7, 8	0.848
040213	13	13-Dec-2007	10:08	9	1, 2, 3, 4, 5	0.809
040213	14	20-Sep-2008	00:40	9	1, 3, 4, 5, 6	0.770
040213	15	25-Jan-2010	16:11	9	1, 4, 5, 7, 9	0.763
040213	16	08-Dec-2011	20:00	9	1, 4, 6, 7, 9	0.790

Section	Visit	Date	Time	Available Repeats	Selected Repeats	Composite Correlation
040213	17	16-Dec-2012	18:50	9	4, 5, 6, 7, 9	0.720
040213	18	06-Feb-2014	23:57	9	1, 4, 6, 8, 9	0.897
040213	19	07-Feb-2014	09:03	3	1, 2, 3	0.901
040213	20	07-Feb-2014	13:10	3	1, 2, 3	0.723
040213	21	07-Feb-2014	16:40	3	1, 2, 3	0.819
040213	22	14-Nov-2014	03:22	9	3, 6, 7, 8, 9	0.931
040213	23	07-Dec-2015	18:33	9	2, 4, 5, 6, 8	0.682
040214	01	25-Jan-1994	06:10	9	2, 3, 5, 6, 8	0.908
040214	02	05-Mar-1995	11:21	9	2, 4, 6, 7, 8	0.823
040214	03	27-Jan-1997	11:38	9	2, 3, 4, 5, 8	0.910
040214	04	04-Dec-1997	11:06	7	1, 3, 4, 5, 7	0.902
040214	05	08-Dec-1998	10:28	7	1, 2, 3, 6, 7	0.908
040214	06	15-Nov-1999	11:38	7	1, 2, 4, 5, 7	0.926
040214	07	30-Nov-2000	13:37	9	1, 2, 5, 6, 8	0.952
040214	08	08-Nov-2001	11:09	9	1, 2, 5, 6, 7	0.952
040214	09	30-Oct-2002	12:40	9	1, 3, 5, 6, 8	0.938
040214	10	04-Feb-2004	13:57	9	2, 3, 5, 6, 8	0.935
040214	11	12-Dec-2004	17:14	9	4, 5, 6, 7, 8	0.928
040214	12	13-Aug-2006	03:02	9	2, 3, 4, 7, 8	0.949
040214	13	13-Dec-2007	10:35	9	4, 5, 6, 8, 9	0.960
040214	14	20-Sep-2008	00:37	9	1, 2, 4, 7, 8	0.932
040214	15	25-Jan-2010	16:08	9	1, 2, 4, 5, 6	0.955
040214	16	08-Dec-2011	19:57	9	1, 2, 4, 5, 7	0.941
040214	17	16-Dec-2012	18:47	9	4, 5, 6, 8, 9	0.938
040214	18	06-Feb-2014	21:58	9	1, 2, 4, 8, 9	0.973
040214	19	07-Feb-2014	08:39	3	1, 2, 3	0.933
040214	20	07-Feb-2014	12:48	3	1, 2, 3	0.907
040214	21	07-Feb-2014	16:21	3	1, 2, 3	0.955
040214	22	14-Nov-2014	00:37	9	2, 3, 4, 5, 7	0.968
040214	23	07-Dec-2015	18:33	9	2, 5, 6, 7, 9	0.960
040215	01	25-Jan-1994	06:10	9	1, 3, 4, 5, 8	0.933
040215	02	05-Mar-1995	11:21	9	1, 3, 5, 7, 8	0.920
040215	S01	05-Dec-1995	09:14	7	1, 3, 5, 6, 7	0.942
040215	S02	05-Dec-1995	14:56	7	1, 2, 3, 4, 6	0.912
040215	S03	02-May-1996	09:30	7	1, 2, 3, 4, 5	0.942
040215	S04	02-May-1996	14:58	7	1, 2, 3, 5, 7	0.933
040215	S05	12-Aug-1996	09:40	9	1, 2, 6, 7, 9	0.898
040215	S06	12-Aug-1996	14:15	9	4, 5, 6, 7, 9	0.910
040215	03	27-Jan-1997	12:11	9	5, 6, 7, 8, 9	0.961
040215	04	04-Dec-1997	11:06	7	1, 3, 4, 5, 7	0.920
040215	S07	15-Jan-1998	11:35	7	2, 3, 4, 5, 7	0.934
040215	S08	15-Jan-1998	16:43	5	1, 2, 3, 4, 5	0.964
040215	S09	13-Apr-1998	10:13	5	1, 2, 3, 4, 5	0.954
040215	S10	13-Apr-1998	15:19	5	1, 2, 3, 4, 5	0.920
040215	S11	09-Jul-1998	08:22	5	1, 2, 3, 4, 5	0.935
040215	S12	09-Jul-1998	12:10	5	1, 2, 3, 4, 5	0.957
040215	S13	30-Sep-1998	11:58	5	1, 2, 3, 4, 5	0.936
040215	S14	30-Sep-1998	14:39	7	2, 3, 4, 5, 6	0.957
040215	05	08-Dec-1998	10:28	7	1, 2, 4, 6, 7	0.965
040215	06	15-Nov-1999	11:38	7	1, 2, 4, 6, 7	0.953
040215	07	30-Nov-2000	13:37	9	1, 3, 5, 6, 7	0.976

Section	Visit	Date	Time	Available Repeats	Selected Repeats	Composite Correlation
040215	08	08-Nov-2001	11:48	9	4, 5, 6, 7, 9	0.985
040215	S15	09-Dec-2001	09:20	7	1, 2, 3, 4, 7	0.977
040215	S16	09-Dec-2001	14:57	9	1, 3, 4, 5, 9	0.971
040215	S17	24-Jan-2002	10:16	7	2, 3, 5, 6, 7	0.978
040215	S18	24-Jan-2002	15:00	9	2, 3, 5, 6, 8	0.982
040215	S19	15-Mar-2002	09:40	7	1, 3, 4, 5, 7	0.978
040215	S20	15-Mar-2002	14:34	7	2, 3, 5, 6, 7	0.965
040215	S21	09-Oct-2002	09:00	9	4, 5, 6, 7, 9	0.960
040215	S22	09-Oct-2002	13:46	9	1, 2, 3, 4, 5	0.966
040215	09	30-Oct-2002	13:06	9	3, 5, 6, 7, 8	0.942
040215	S23	20-Dec-2002	09:05	9	1, 2, 3, 4, 6	0.974
040215	S24	20-Dec-2002	13:23	9	1, 4, 7, 8, 9	0.944
040215	S25	07-Mar-2003	09:28	9	2, 3, 5, 6, 9	0.963
040215	S26	07-Mar-2003	13:59	9	2, 4, 6, 7, 9	0.959
040215	S27	25-Jul-2003	04:24	9	1, 3, 4, 5, 6	0.972
040215	S28	25-Jul-2003	08:42	9	3, 4, 6, 7, 9	0.974
040215	S29	24-Nov-2003	09:41	9	3, 4, 5, 8, 9	0.964
040215	S30	24-Nov-2003	14:22	9	1, 4, 5, 6, 9	0.956
040215	S31	14-Dec-2003	10:32	9	1, 2, 4, 7, 9	0.975
040215	S32	14-Dec-2003	15:16	9	1, 4, 5, 6, 9	0.973
040215	10	04-Feb-2004	13:47	9	1, 3, 5, 8, 9	0.931
040215	S33	22-Apr-2004	04:58	9	1, 2, 3, 8, 9	0.972
040215	S34	22-Apr-2004	10:01	9	4, 6, 7, 8, 9	0.961
040215	S35	15-Jul-2004	04:17	9	1, 2, 3, 4, 8	0.973
040215	S36	15-Jul-2004	09:07	9	2, 4, 6, 7, 8	0.977
040215	S37	09-Sep-2004	04:01	9	3, 4, 6, 7, 8	0.977
040215	S38	09-Sep-2004	08:34	9	1, 2, 3, 4, 6	0.976
040215	11	12-Dec-2004	16:15	9	1, 2, 3, 5, 7	0.948
040215	12	13-Aug-2006	00:24	9	2, 4, 5, 6, 7	0.980
040215	13	13-Dec-2007	12:08	9	2, 3, 4, 7, 9	0.974
040215	14	20-Sep-2008	02:06	9	1, 2, 7, 8, 9	0.970
040215	15	25-Jan-2010	17:50	9	2, 3, 4, 5, 8	0.964
040215	16	08-Dec-2011	21:26	9	1, 3, 4, 8, 9	0.970
040215	17	16-Dec-2012	19:55	9	2, 5, 6, 8, 9	0.969
040215	18	06-Feb-2014	23:02	9	1, 3, 6, 7, 9	0.975
040215	19	07-Feb-2014	08:39	3	1, 2, 3	0.948
040215	20	07-Feb-2014	12:48	3	1, 2, 3	0.970
040215	21	07-Feb-2014	16:21	3	1, 2, 3	0.928
040215	22	14-Nov-2014	01:24	9	1, 6, 7, 8, 9	0.972
040215	23	07-Dec-2015	18:23	9	1, 3, 4, 6, 8	0.959
040216	01	25-Jan-1994	06:10	9	1, 3, 5, 8, 9	0.920
040216	02	05-Mar-1995	11:21	9	3, 5, 7, 8, 9	0.892
040216	03	27-Jan-1997	11:22	9	1, 2, 3, 5, 7	0.926
040216	04	04-Dec-1997	11:06	7	1, 2, 4, 5, 6	0.928
040216	05	08-Dec-1998	10:28	7	1, 2, 3, 5, 6	0.949
040216	06	15-Nov-1999	11:48	7	2, 3, 4, 5, 6	0.946
040216	07	30-Nov-2000	13:49	9	2, 3, 4, 6, 9	0.967
040216	08	08-Nov-2001	11:28	9	2, 3, 4, 6, 8	0.956
040216	09	30-Oct-2002	12:40	9	1, 2, 4, 5, 8	0.931
040216	10	04-Feb-2004	13:47	9	1, 3, 4, 6, 7	0.937
040216	11	12-Dec-2004	16:15	9	1, 5, 6, 8, 9	0.910

Section	Visit	Date	Time	Available Repeats	Selected Repeats	Composite Correlation
040216	12	13-Aug-2006	00:13	9	1, 4, 6, 7, 8	0.948
040216	13	13-Dec-2007	12:08	9	2, 4, 7, 8, 9	0.953
040216	14	20-Sep-2008	02:16	9	2, 3, 6, 8, 9	0.938
040216	15	25-Jan-2010	17:37	9	1, 2, 3, 4, 8	0.947
040216	16	08-Dec-2011	21:44	9	3, 4, 5, 7, 8	0.959
040216	17	16-Dec-2012	19:46	9	1, 3, 4, 5, 7	0.955
040216	18	06-Feb-2014	23:08	9	2, 3, 5, 8, 9	0.967
040216	19	07-Feb-2014	08:39	3	1, 2, 3	0.955
040216	20	07-Feb-2014	12:48	3	1, 2, 3	0.912
040216	21	07-Feb-2014	16:21	3	1, 2, 3	0.904
040216	22	14-Nov-2014	01:24	9	1, 5, 6, 8, 9	0.962
040216	23	07-Dec-2015	18:43	9	3, 5, 6, 8, 9	0.935
040217	01	25-Jan-1994	06:10	9	4, 6, 7, 8, 9	0.928
040217	02	05-Mar-1995	11:21	9	1, 4, 5, 6, 8	0.872
040217	03	27-Jan-1997	11:48	9	3, 4, 6, 8, 9	0.956
040217	04	04-Dec-1997	11:40	7	2, 3, 4, 6, 7	0.913
040217	05	08-Dec-1998	10:28	7	1, 2, 3, 6, 7	0.913
040217	06	15-Nov-1999	11:38	7	1, 2, 4, 5, 7	0.938
040217	07	30-Nov-2000	14:10	9	4, 5, 6, 8, 9	0.963
040217	08	08-Nov-2001	11:09	9	1, 2, 3, 6, 9	0.955
040217	09	30-Oct-2002	12:40	9	1, 2, 3, 4, 5	0.921
040217	10	04-Feb-2004	13:47	9	1, 2, 3, 7, 9	0.911
040217	11	12-Dec-2004	16:15	9	1, 2, 6, 7, 9	0.880
040217	12	11-Aug-2006	04:17	9	1, 3, 5, 6, 7	0.958
040217	13	13-Dec-2007	10:18	9	2, 3, 4, 6, 9	0.922
040217	14	20-Sep-2008	00:40	9	1, 2, 5, 7, 9	0.934
040217	15	25-Jan-2010	16:11	9	1, 5, 6, 7, 9	0.840
040217	16	08-Dec-2011	20:25	9	4, 5, 6, 8, 9	0.886
040217	17	16-Dec-2012	18:09	9	1, 2, 4, 5, 9	0.897
040217	18	07-Feb-2014	00:04	9	2, 4, 6, 8, 9	0.899
040217	19	07-Feb-2014	09:03	3	1, 2, 3	0.907
040217	20	07-Feb-2014	13:10	3	1, 2, 3	0.817
040217	21	07-Feb-2014	16:40	3	1, 2, 3	0.866
040217	22	14-Nov-2014	03:22	9	3, 4, 5, 6, 8	0.914
040217	23	07-Dec-2015	18:33	9	2, 3, 6, 7, 8	0.892
040218	01	25-Jan-1994	06:10	9	1, 2, 5, 7, 9	0.894
040218	02	05-Mar-1995	11:21	9	2, 3, 4, 8, 9	0.815
040218	03	27-Jan-1997	11:22	9	1, 3, 6, 7, 9	0.907
040218	04	04-Dec-1997	11:06	7	1, 3, 4, 5, 7	0.888
040218	05	08-Dec-1998	10:28	7	1, 2, 3, 4, 5	0.887
040218	06	15-Nov-1999	11:48	7	2, 3, 4, 6, 7	0.923
040218	07	30-Nov-2000	14:00	9	3, 4, 5, 8, 9	0.943
040218	08	08-Nov-2001	11:09	9	1, 3, 4, 7, 8	0.950
040218	09	30-Oct-2002	12:55	9	2, 3, 5, 6, 7	0.892
040218	10	04-Feb-2004	13:47	9	1, 2, 4, 7, 9	0.905
040218	11	12-Dec-2004	16:15	9	1, 2, 3, 6, 7	0.888
040218	12	13-Aug-2006	03:51	9	4, 5, 6, 7, 9	0.927
040218	13	13-Dec-2007	10:14	9	2, 3, 6, 8, 9	0.930
040218	14	20-Sep-2008	00:37	9	1, 3, 7, 8, 9	0.949
040218	15	25-Jan-2010	16:08	9	1, 3, 6, 7, 8	0.921
040218	16	08-Dec-2011	19:57	9	1, 3, 4, 5, 7	0.962

Section	Visit	Date	Time	Available Repeats	Selected Repeats	Composite Correlation
040218	17	16-Dec-2012	18:30	9	2, 3, 4, 7, 8	0.952
040218	18	06-Feb-2014	22:21	9	4, 5, 6, 7, 8	0.969
040218	19	07-Feb-2014	08:39	3	1, 2, 3	0.949
040218	20	07-Feb-2014	12:48	3	1, 2, 3	0.830
040218	21	07-Feb-2014	16:21	3	1, 2, 3	0.859
040218	22	14-Nov-2014	00:27	9	1, 2, 4, 6, 8	0.944
040218	23	07-Dec-2015	18:33	9	2, 3, 7, 8, 9	0.948
040219	01	25-Jan-1994	06:10	9	3, 5, 6, 7, 9	0.902
040219	02	05-Mar-1995	11:21	9	1, 2, 5, 6, 8	0.875
040219	03	27-Jan-1997	11:38	9	2, 4, 7, 8, 9	0.931
040219	04	04-Dec-1997	11:06	7	1, 3, 4, 6, 7	0.921
040219	05	08-Dec-1998	10:28	7	1, 2, 3, 6, 7	0.926
040219	06	15-Nov-1999	11:48	7	2, 3, 4, 6, 7	0.941
040219	07	30-Nov-2000	13:49	9	2, 4, 6, 8, 9	0.953
040219	08	08-Nov-2001	11:09	9	1, 2, 5, 6, 8	0.953
040219	09	30-Oct-2002	12:40	9	1, 2, 3, 7, 9	0.920
040219	10	04-Feb-2004	13:47	9	1, 2, 5, 6, 8	0.929
040219	11	12-Dec-2004	17:14	9	4, 5, 6, 7, 8	0.936
040219	12	13-Aug-2006	00:13	9	1, 4, 6, 7, 8	0.969
040219	13	13-Dec-2007	12:08	9	2, 3, 4, 8, 9	0.952
040219	14	20-Sep-2008	02:06	9	1, 3, 4, 5, 6	0.951
040219	15	25-Jan-2010	18:09	9	4, 5, 6, 7, 9	0.932
040219	16	08-Dec-2011	21:35	9	2, 5, 6, 7, 9	0.961
040219	17	16-Dec-2012	19:55	9	2, 3, 6, 7, 8	0.955
040219	18	06-Feb-2014	23:02	9	1, 3, 4, 6, 8	0.946
040219	19	07-Feb-2014	08:39	3	1, 2, 3	0.945
040219	20	07-Feb-2014	12:48	3	1, 2, 3	0.935
040219	21	07-Feb-2014	16:21	3	1, 2, 3	0.915
040219	22	14-Nov-2014	01:24	9	1, 2, 3, 8, 9	0.961
040219	23	07-Dec-2015	18:33	9	2, 3, 4, 8, 9	0.941
040220	01	25-Jan-1994	06:10	9	5, 6, 7, 8, 9	0.912
040220	02	05-Mar-1995	11:21	9	3, 4, 5, 6, 9	0.872
040220	03	27-Jan-1997	11:22	9	1, 2, 6, 7, 8	0.912
040220	04	04-Dec-1997	11:06	7	1, 3, 4, 6, 7	0.900
040220	05	08-Dec-1998	10:38	7	2, 3, 4, 6, 7	0.948
040220	06	15-Nov-1999	11:38	7	1, 2, 5, 6, 7	0.950
040220	07	30-Nov-2000	13:37	9	1, 2, 5, 7, 9	0.933
040220	08	08-Nov-2001	11:09	9	1, 2, 3, 4, 5	0.954
040220	09	30-Oct-2002	12:40	9	1, 2, 3, 6, 8	0.910
040220	10	04-Feb-2004	13:57	9	2, 3, 4, 6, 7	0.927
040220	11	12-Dec-2004	16:15	9	1, 2, 5, 6, 9	0.938
040220	12	13-Aug-2006	03:46	9	3, 4, 6, 7, 8	0.933
040220	13	13-Dec-2007	10:14	9	2, 3, 6, 7, 9	0.933
040220	14	20-Sep-2008	00:47	9	2, 4, 5, 6, 7	0.940
040220	15	25-Jan-2010	16:08	9	1, 3, 6, 8, 9	0.935
040220	16	08-Dec-2011	20:13	9	3, 5, 6, 7, 8	0.957
040220	17	16-Dec-2012	18:30	9	2, 4, 5, 6, 7	0.936
040220	18	06-Feb-2014	21:58	9	1, 2, 4, 6, 8	0.957
040220	19	07-Feb-2014	08:39	3	1, 2, 3	0.927
040220	20	07-Feb-2014	12:48	3	1, 2, 3	0.925
040220	21	07-Feb-2014	16:21	3	1, 2, 3	0.870

Section	Visit	Date	Time	Available Repeats	Selected Repeats	Composite Correlation
040220	22	14-Nov-2014	00:37	9	2, 3, 5, 6, 9	0.928
040220	23	07-Dec-2015	18:43	9	3, 6, 7, 8, 9	0.928
040221	01	25-Jan-1994	06:10	9	1, 4, 6, 8, 9	0.895
040221	02	05-Mar-1995	11:21	9	4, 6, 7, 8, 9	0.838
040221	03	27-Jan-1997	11:22	9	1, 2, 4, 6, 9	0.901
040221	04	04-Dec-1997	11:06	7	1, 2, 4, 5, 6	0.878
040221	05	08-Dec-1998	10:28	7	1, 2, 3, 4, 5	0.936
040221	06	15-Nov-1999	11:38	7	1, 2, 4, 5, 7	0.948
040221	07	30-Nov-2000	13:37	9	1, 2, 5, 6, 9	0.933
040221	08	08-Nov-2001	11:09	9	1, 5, 6, 8, 9	0.947
040221	09	30-Oct-2002	12:40	9	1, 5, 6, 7, 8	0.821
040221	10	04-Feb-2004	13:47	9	1, 3, 4, 6, 8	0.863
040221	11	12-Dec-2004	16:44	9	2, 4, 5, 6, 7	0.858
040221	12	11-Aug-2006	04:17	9	1, 3, 5, 6, 7	0.945
040221	13	13-Dec-2007	10:08	9	1, 2, 3, 5, 6	0.907
040221	14	20-Sep-2008	00:40	9	1, 2, 3, 4, 6	0.950
040221	15	25-Jan-2010	16:19	9	2, 5, 7, 8, 9	0.935
040221	16	08-Dec-2011	20:17	9	3, 4, 6, 7, 9	0.917
040221	17	16-Dec-2012	18:57	9	5, 6, 7, 8, 9	0.938
040221	18	07-Feb-2014	00:18	9	4, 5, 6, 7, 8	0.931
040221	19	07-Feb-2014	09:03	3	1, 2, 3	0.852
040221	20	07-Feb-2014	13:10	3	1, 2, 3	0.815
040221	21	07-Feb-2014	16:40	3	1, 2, 3	0.802
040221	22	14-Nov-2014	03:10	9	1, 2, 3, 5, 9	0.941
040221	23	07-Dec-2015	18:23	9	1, 3, 4, 5, 6	0.841
040222	01	25-Jan-1994	06:10	9	4, 5, 6, 8, 9	0.897
040222	02	05-Mar-1995	11:21	9	1, 4, 5, 6, 7	0.814
040222	03	27-Jan-1997	11:22	9	1, 3, 5, 6, 9	0.941
040222	04	04-Dec-1997	11:06	7	1, 3, 5, 6, 7	0.856
040222	05	08-Dec-1998	10:38	7	2, 3, 4, 6, 7	0.927
040222	06	15-Nov-1999	12:00	7	3, 4, 5, 6, 7	0.920
040222	07	30-Nov-2000	13:49	9	2, 4, 5, 6, 8	0.941
040222	08	08-Nov-2001	11:28	9	2, 4, 5, 7, 8	0.950
040222	09	30-Oct-2002	12:40	9	1, 2, 4, 6, 7	0.901
040222	10	04-Feb-2004	13:47	9	1, 2, 3, 4, 5	0.878
040222	11	12-Dec-2004	16:44	9	2, 3, 4, 6, 8	0.851
040222	12	13-Aug-2006	03:46	9	3, 4, 6, 7, 8	0.935
040222	13	13-Dec-2007	10:14	9	2, 3, 5, 6, 9	0.931
040222	14	20-Sep-2008	00:47	9	2, 3, 4, 6, 7	0.913
040222	15	25-Jan-2010	16:17	9	2, 6, 7, 8, 9	0.910
040222	16	08-Dec-2011	19:57	9	1, 3, 6, 7, 9	0.943
040222	17	16-Dec-2012	18:30	9	2, 3, 6, 7, 9	0.932
040222	18	06-Feb-2014	22:05	9	2, 3, 4, 6, 9	0.971
040222	19	07-Feb-2014	08:39	3	1, 2, 3	0.878
040222	20	07-Feb-2014	12:48	3	1, 2, 3	0.918
040222	21	07-Feb-2014	16:21	3	1, 2, 3	0.943
040222	22	14-Nov-2014	00:43	9	3, 4, 6, 8, 9	0.959
040222	23	07-Dec-2015	19:04	9	5, 6, 7, 8, 9	0.949
040223	01	25-Jan-1994	06:10	9	1, 2, 6, 7, 9	0.890
040223	02	05-Mar-1995	11:21	9	1, 3, 4, 8, 9	0.894
040223	03	27-Jan-1997	12:01	9	4, 5, 6, 7, 9	0.932

Section	Visit	Date	Time	Available Repeats	Selected Repeats	Composite Correlation
040223	04	04-Dec-1997	11:06	7	1, 4, 5, 6, 7	0.946
040223	05	08-Dec-1998	10:28	7	1, 2, 3, 6, 7	0.942
040223	06	15-Nov-1999	11:38	7	1, 2, 3, 4, 6	0.952
040223	07	30-Nov-2000	13:37	9	1, 2, 3, 6, 8	0.955
040223	08	08-Nov-2001	11:38	9	3, 4, 5, 6, 9	0.958
040223	09	30-Oct-2002	12:55	9	2, 3, 6, 7, 8	0.949
040223	10	04-Feb-2004	13:57	9	2, 4, 6, 7, 9	0.913
040223	11	12-Dec-2004	17:28	9	5, 6, 7, 8, 9	0.944
040223	12	13-Aug-2006	00:24	9	2, 4, 5, 6, 9	0.972
040223	13	13-Dec-2007	12:08	9	2, 3, 4, 8, 9	0.953
040223	14	20-Sep-2008	02:27	9	3, 5, 6, 8, 9	0.965
040223	15	25-Jan-2010	18:00	9	3, 4, 6, 8, 9	0.950
040223	16	08-Dec-2011	21:26	9	1, 2, 3, 5, 8	0.968
040223	17	16-Dec-2012	19:46	9	1, 2, 5, 6, 9	0.961
040223	18	06-Feb-2014	23:02	9	1, 2, 3, 7, 9	0.975
040223	19	07-Feb-2014	08:39	3	1, 2, 3	0.948
040223	20	07-Feb-2014	12:48	3	1, 2, 3	0.963
040223	21	07-Feb-2014	16:21	3	1, 2, 3	0.932
040223	22	14-Nov-2014	01:29	9	2, 3, 5, 7, 8	0.959
040223	23	07-Dec-2015	18:23	9	1, 2, 3, 4, 8	0.940
040224	01	25-Jan-1994	06:10	9	3, 4, 6, 8, 9	0.897
040224	02	05-Mar-1995	11:21	9	2, 4, 5, 6, 8	0.836
040224	03	27-Jan-1997	11:38	9	2, 3, 4, 6, 7	0.908
040224	04	04-Dec-1997	11:06	7	1, 2, 3, 4, 5	0.861
040224	05	08-Dec-1998	10:28	7	1, 2, 3, 6, 7	0.873
040224	06	15-Nov-1999	11:48	7	2, 3, 5, 6, 7	0.921
040224	07	30-Nov-2000	13:49	9	2, 3, 5, 6, 7	0.939
040224	08	08-Nov-2001	11:28	9	2, 4, 6, 7, 8	0.933
040224	09	30-Oct-2002	12:40	9	1, 2, 4, 5, 8	0.917
040224	10	04-Feb-2004	13:57	9	2, 3, 4, 6, 9	0.959
040224	11	12-Dec-2004	16:15	9	1, 2, 4, 7, 9	0.875
040224	12	13-Aug-2006	00:13	9	1, 2, 6, 7, 8	0.939
040224	13	13-Dec-2007	12:17	9	3, 6, 7, 8, 9	0.949
040224	14	20-Sep-2008	02:41	9	4, 6, 7, 8, 9	0.903
040224	15	25-Jan-2010	17:37	9	1, 2, 3, 5, 9	0.917
040224	16	08-Dec-2011	21:44	9	3, 6, 7, 8, 9	0.964
040224	17	16-Dec-2012	19:46	9	1, 2, 3, 6, 7	0.972
040224	18	06-Feb-2014	23:08	9	2, 3, 4, 8, 9	0.977
040224	19	07-Feb-2014	08:39	3	1, 2, 3	0.955
040224	20	07-Feb-2014	12:48	3	1, 2, 3	0.919
040224	21	07-Feb-2014	16:21	3	1, 2, 3	0.879
040224	22	14-Nov-2014	01:39	9	4, 5, 6, 7, 9	0.959
040224	23	07-Dec-2015	18:43	9	3, 4, 7, 8, 9	0.932
040260	01	25-Jan-1994	06:10	9	1, 2, 3, 4, 7	0.939
040260	02	05-Mar-1995	11:21	9	3, 5, 6, 8, 9	0.903
040260	03	27-Jan-1997	11:22	9	1, 2, 5, 6, 8	0.930
040260	04	04-Dec-1997	12:13	7	3, 4, 5, 6, 7	0.886
040260	05	08-Dec-1998	10:28	7	1, 2, 4, 5, 7	0.919
040260	06	15-Nov-1999	11:48	7	2, 4, 5, 6, 7	0.919
040260	07	30-Nov-2000	13:37	9	1, 3, 4, 6, 9	0.952
040260	08	08-Nov-2001	11:28	9	2, 3, 6, 7, 9	0.963

Section	Visit	Date	Time	Available Repeats	Selected Repeats	Composite Correlation
040260	09	30-Oct-2002	12:40	9	1, 3, 4, 6, 8	0.921
040260	10	04-Feb-2004	13:47	9	1, 2, 5, 7, 8	0.899
040260	11	12-Dec-2004	16:15	9	1, 3, 5, 7, 9	0.881
040260	12	13-Aug-2006	00:17	9	1, 3, 4, 6, 8	0.887
040260	13	13-Dec-2007	11:59	9	1, 3, 5, 6, 8	0.788
040260	14	20-Sep-2008	02:10	9	1, 2, 3, 4, 6	0.878
040260	15	25-Jan-2010	17:42	9	1, 3, 4, 5, 6	0.867
040260	16	08-Dec-2011	21:28	9	1, 3, 4, 8, 9	0.900
040260	17	16-Dec-2012	19:48	9	1, 4, 7, 8, 9	0.800
040260	18	07-Feb-2014	01:16	9	4, 5, 7, 8, 9	0.913
040260	19	07-Feb-2014	09:03	3	1, 2, 3	0.836
040260	20	07-Feb-2014	13:10	3	1, 2, 3	0.795
040260	21	07-Feb-2014	16:40	3	1, 2, 3	0.753
040260	22	14-Nov-2014	04:06	9	1, 2, 5, 6, 7	0.769
040260	23	07-Dec-2015	18:43	9	3, 4, 5, 6, 8	0.851
040261	01	25-Jan-1994	06:10	9	3, 5, 6, 8, 9	0.909
040261	02	05-Mar-1995	11:21	9	2, 4, 6, 7, 9	0.861
040261	03	27-Jan-1997	12:11	9	5, 6, 7, 8, 9	0.904
040261	04	04-Dec-1997	11:06	7	1, 3, 5, 6, 7	0.838
040261	05	08-Dec-1998	10:48	7	3, 4, 5, 6, 7	0.914
040261	06	15-Nov-1999	11:38	7	1, 2, 4, 5, 7	0.895
040261	07	30-Nov-2000	14:00	9	3, 4, 5, 6, 7	0.933
040261	08	08-Nov-2001	11:09	9	1, 3, 4, 6, 7	0.934
040261	09	30-Oct-2002	12:40	9	1, 2, 3, 4, 9	0.869
040261	10	04-Feb-2004	13:47	9	1, 2, 5, 6, 7	0.866
040261	11	12-Dec-2004	16:15	9	1, 4, 5, 6, 7	0.761
040261	12	13-Aug-2006	03:10	9	4, 5, 6, 8, 9	0.882
040261	13	13-Dec-2007	10:14	9	2, 3, 4, 7, 9	0.898
040261	14	20-Sep-2008	00:37	9	1, 2, 3, 6, 7	0.881
040261	15	25-Jan-2010	16:08	9	1, 2, 3, 5, 9	0.921
040261	16	08-Dec-2011	20:13	9	3, 5, 7, 8, 9	0.891
040261	17	16-Dec-2012	18:30	9	2, 3, 4, 5, 9	0.934
040261	18	06-Feb-2014	21:58	9	1, 2, 3, 7, 9	0.948
040261	19	07-Feb-2014	08:39	3	1, 2, 3	0.833
040261	20	07-Feb-2014	12:48	3	1, 2, 3	0.921
040261	21	07-Feb-2014	16:21	3	1, 2, 3	0.935
040261	22	14-Nov-2014	00:27	9	1, 2, 3, 7, 9	0.947
040261	23	07-Dec-2015	18:33	9	2, 4, 6, 7, 8	0.945
040262	01	25-Jan-1994	06:10	9	4, 5, 6, 8, 9	0.870
040262	02	05-Mar-1995	11:21	9	1, 4, 5, 7, 9	0.865
040262	03	27-Jan-1997	11:38	9	2, 3, 5, 6, 7	0.964
040262	04	04-Dec-1997	11:40	7	2, 3, 4, 5, 7	0.968
040262	05	08-Dec-1998	10:28	7	1, 2, 3, 4, 5	0.979
040262	06	15-Nov-1999	11:48	7	2, 3, 4, 5, 6	0.980
040262	07	30-Nov-2000	13:49	9	2, 5, 6, 8, 9	0.979
040262	08	08-Nov-2001	11:28	9	2, 3, 5, 8, 9	0.986
040262	09	30-Oct-2002	12:40	9	1, 2, 3, 4, 6	0.976
040262	10	04-Feb-2004	13:57	9	2, 3, 4, 6, 7	0.974
040262	11	12-Dec-2004	16:44	9	2, 3, 4, 6, 7	0.975
040262	12	11-Aug-2006	04:17	9	1, 4, 5, 8, 9	0.982
040262	13	13-Dec-2007	10:18	9	2, 3, 5, 7, 9	0.948

Section	Visit	Date	Time	Available Repeats	Selected Repeats	Composite Correlation
040262	14	20-Sep-2008	00:40	9	1, 4, 7, 8, 9	0.957
040262	15	25-Jan-2010	16:11	9	1, 2, 5, 8, 9	0.974
040262	16	08-Dec-2011	20:08	9	2, 5, 7, 8, 9	0.941
040262	17	16-Dec-2012	18:09	9	1, 2, 3, 4, 8	0.966
040262	18	06-Feb-2014	23:57	9	1, 4, 5, 6, 9	0.967
040262	19	07-Feb-2014	09:03	3	1, 2, 3	0.961
040262	20	07-Feb-2014	13:10	3	1, 2, 3	0.933
040262	21	07-Feb-2014	16:40	3	1, 2, 3	0.970
040262	22	14-Nov-2014	03:10	9	1, 6, 7, 8, 9	0.938
040262	23	07-Dec-2015	18:33	9	2, 5, 7, 8, 9	0.916
040263	01	25-Jan-1994	06:10	9	3, 6, 7, 8, 9	0.845
040263	02	05-Mar-1995	11:21	9	1, 6, 7, 8, 9	0.815
040263	03	27-Jan-1997	11:22	9	1, 2, 3, 5, 9	0.939
040263	04	04-Dec-1997	11:06	7	1, 2, 3, 4, 5	0.935
040263	05	08-Dec-1998	10:38	7	2, 3, 4, 5, 7	0.938
040263	06	15-Nov-1999	11:38	7	1, 2, 3, 4, 6	0.941
040263	07	30-Nov-2000	13:37	9	1, 3, 5, 7, 9	0.946
040263	08	08-Nov-2001	11:28	9	2, 3, 5, 7, 9	0.944
040263	09	30-Oct-2002	12:55	9	2, 5, 6, 7, 8	0.884
040263	10	04-Feb-2004	13:47	9	1, 2, 4, 5, 9	0.929
040263	11	12-Dec-2004	16:15	9	1, 2, 4, 5, 7	0.856
040263	12	11-Aug-2006	04:32	9	2, 3, 4, 6, 7	0.949
040263	13	13-Dec-2007	10:18	9	2, 4, 5, 6, 8	0.942
040263	14	20-Sep-2008	00:50	9	2, 3, 5, 7, 8	0.939
040263	15	25-Jan-2010	16:19	9	2, 3, 4, 5, 6	0.902
040263	16	08-Dec-2011	20:08	9	2, 4, 6, 7, 9	0.943
040263	17	16-Dec-2012	18:09	9	1, 3, 5, 7, 9	0.925
040263	18	07-Feb-2014	00:04	9	2, 4, 5, 7, 8	0.927
040263	19	07-Feb-2014	09:03	3	1, 2, 3	0.879
040263	20	07-Feb-2014	13:10	3	1, 2, 3	0.880
040263	21	07-Feb-2014	16:40	3	1, 2, 3	0.826
040263	22	14-Nov-2014	03:10	9	1, 2, 3, 4, 9	0.927
040263	23	07-Dec-2015	18:53	9	4, 5, 6, 7, 9	0.923
040264	01	25-Jan-1994	06:10	9	2, 3, 4, 5, 8	0.905
040264	02	05-Mar-1995	11:21	9	1, 5, 6, 7, 8	0.931
040264	03	27-Jan-1997	11:22	9	1, 2, 4, 6, 8	0.937
040264	04	04-Dec-1997	11:40	7	2, 3, 4, 5, 6	0.938
040264	05	08-Dec-1998	10:38	7	2, 3, 5, 6, 7	0.962
040264	06	15-Nov-1999	11:38	7	1, 2, 3, 6, 7	0.950
040264	07	30-Nov-2000	13:37	9	1, 2, 5, 6, 8	0.960
040264	08	08-Nov-2001	11:09	9	1, 4, 5, 6, 7	0.969
040264	09	30-Oct-2002	12:40	9	1, 3, 4, 7, 8	0.901
040264	10	04-Feb-2004	14:08	9	3, 4, 5, 7, 8	0.892
040264	11	12-Dec-2004	16:15	9	1, 2, 4, 5, 6	0.909
040264	12	13-Aug-2006	00:17	9	1, 3, 6, 8, 9	0.967
040264	13	13-Dec-2007	12:11	9	2, 4, 6, 8, 9	0.945
040264	14	20-Sep-2008	02:10	9	1, 2, 4, 6, 7	0.960
040264	15	25-Jan-2010	17:42	9	1, 2, 3, 4, 5	0.937
040264	16	08-Dec-2011	21:46	9	3, 6, 7, 8, 9	0.960
040264	17	16-Dec-2012	19:48	9	1, 4, 5, 6, 9	0.951
040264	18	07-Feb-2014	01:01	9	1, 2, 3, 4, 8	0.958

Section	Visit	Date	Time	Available Repeats	Selected Repeats	Composite Correlation
040264	19	07-Feb-2014	09:03	3	1, 2, 3	0.961
040264	20	07-Feb-2014	13:10	3	1, 2, 3	0.911
040264	21	07-Feb-2014	16:40	3	1, 2, 3	0.950
040264	22	14-Nov-2014	04:11	9	2, 4, 6, 8, 9	0.959
040264	23	07-Dec-2015	18:23	9	1, 4, 5, 8, 9	0.946
040265	01	25-Jan-1994	06:10	9	1, 2, 4, 5, 8	0.910
040265	02	05-Mar-1995	11:21	9	4, 5, 6, 7, 9	0.882
040265	03	27-Jan-1997	11:22	9	1, 3, 4, 6, 7	0.955
040265	04	04-Dec-1997	12:13	7	3, 4, 5, 6, 7	0.924
040265	05	08-Dec-1998	10:28	7	1, 4, 5, 6, 7	0.949
040265	06	15-Nov-1999	11:38	7	1, 2, 4, 6, 7	0.936
040265	07	30-Nov-2000	13:49	9	2, 4, 6, 7, 8	0.976
040265	08	08-Nov-2001	11:28	9	2, 3, 4, 5, 6	0.963
040265	09	30-Oct-2002	12:55	9	2, 3, 4, 5, 7	0.922
040265	10	04-Feb-2004	14:08	9	3, 6, 7, 8, 9	0.934
040265	11	12-Dec-2004	16:15	9	1, 2, 4, 6, 7	0.914
040265	12	13-Aug-2006	00:27	9	2, 3, 7, 8, 9	0.976
040265	13	13-Dec-2007	12:20	9	3, 4, 6, 8, 9	0.966
040265	14	20-Sep-2008	02:10	9	1, 2, 4, 6, 7	0.963
040265	15	25-Jan-2010	17:42	9	1, 2, 3, 6, 7	0.977
040265	16	08-Dec-2011	21:28	9	1, 4, 5, 6, 9	0.972
040265	17	16-Dec-2012	19:48	9	1, 2, 3, 5, 9	0.968
040265	18	07-Feb-2014	01:01	9	1, 4, 7, 8, 9	0.973
040265	19	07-Feb-2014	09:03	3	1, 2, 3	0.948
040265	20	07-Feb-2014	13:10	3	1, 2, 3	0.943
040265	21	07-Feb-2014	16:40	3	1, 2, 3	0.965
040265	22	14-Nov-2014	04:06	9	1, 5, 7, 8, 9	0.966
040265	23	07-Dec-2015	18:33	9	2, 4, 5, 6, 9	0.968
040266	01	25-Jan-1994	06:10	9	1, 4, 6, 7, 9	0.890
040266	02	05-Mar-1995	11:21	9	1, 2, 3, 5, 6	0.887
040266	03	27-Jan-1997	11:22	9	1, 2, 7, 8, 9	0.943
040266	04	04-Dec-1997	11:06	7	1, 2, 3, 4, 6	0.902
040266	05	08-Dec-1998	10:28	7	1, 2, 3, 4, 6	0.972
040266	06	15-Nov-1999	11:38	7	1, 2, 3, 5, 6	0.944
040266	07	30-Nov-2000	13:37	9	1, 4, 6, 7, 8	0.957
040266	08	08-Nov-2001	11:28	9	2, 3, 4, 6, 7	0.965
040266	09	30-Oct-2002	13:06	9	3, 4, 7, 8, 9	0.901
040266	10	04-Feb-2004	13:47	9	1, 3, 4, 5, 7	0.950
040266	11	12-Dec-2004	16:15	9	1, 4, 5, 7, 9	0.937
040266	12	13-Aug-2006	00:17	9	1, 2, 5, 6, 9	0.947
040266	13	13-Dec-2007	11:59	9	1, 2, 4, 5, 8	0.961
040266	14	20-Sep-2008	02:10	9	1, 3, 4, 5, 8	0.953
040266	15	25-Jan-2010	17:42	9	1, 3, 4, 5, 6	0.938
040266	16	08-Dec-2011	21:38	9	2, 4, 5, 7, 9	0.954
040266	17	16-Dec-2012	19:48	9	1, 2, 5, 7, 9	0.948
040266	18	07-Feb-2014	01:01	9	1, 3, 4, 6, 9	0.961
040266	19	07-Feb-2014	09:03	3	1, 2, 3	0.970
040266	20	07-Feb-2014	13:10	3	1, 2, 3	0.914
040266	21	07-Feb-2014	16:40	3	1, 2, 3	0.943
040266	22	14-Nov-2014	04:06	9	1, 2, 5, 7, 9	0.940
040266	23	07-Dec-2015	18:33	9	2, 3, 5, 8, 9	0.945

Section	Visit	Date	Time	Available Repeats	Selected Repeats	Composite Correlation
040267	01	25-Jan-1994	06:10	9	1, 3, 6, 7, 9	0.888
040267	02	05-Mar-1995	11:21	9	4, 5, 6, 7, 8	0.879
040267	03	27-Jan-1997	12:01	9	4, 5, 6, 8, 9	0.922
040267	04	04-Dec-1997	11:06	7	1, 2, 3, 4, 6	0.873
040267	05	08-Dec-1998	10:28	7	1, 2, 4, 5, 6	0.922
040267	06	15-Nov-1999	11:48	7	2, 3, 4, 5, 7	0.949
040267	07	30-Nov-2000	13:37	9	1, 2, 3, 7, 9	0.954
040267	08	08-Nov-2001	11:09	9	1, 4, 6, 7, 9	0.960
040267	09	30-Oct-2002	12:55	9	2, 3, 5, 6, 8	0.876
040267	10	04-Feb-2004	13:57	9	2, 3, 5, 7, 9	0.930
040267	11	12-Dec-2004	16:15	9	1, 2, 5, 6, 7	0.926
040267	12	13-Aug-2006	00:17	9	1, 2, 4, 6, 9	0.866
040267	S01	13-Aug-2006	02:01	9	1, 4, 5, 7, 9	0.859
040267	13	13-Dec-2007	11:59	9	1, 4, 6, 7, 8	0.879
040267	14	20-Sep-2008	02:10	9	1, 2, 4, 5, 6	0.906
040267	15	25-Jan-2010	17:42	9	1, 2, 3, 4, 6	0.910
040267	16	08-Dec-2011	22:03	9	5, 6, 7, 8, 9	0.894
040267	17	16-Dec-2012	19:58	9	2, 4, 7, 8, 9	0.909
040267	18	07-Feb-2014	01:01	9	1, 2, 6, 8, 9	0.925
040267	19	07-Feb-2014	09:03	3	1, 2, 3	0.807
040267	20	07-Feb-2014	13:10	3	1, 2, 3	0.780
040267	21	07-Feb-2014	16:40	3	1, 2, 3	0.758
040267	22	14-Nov-2014	04:06	9	1, 2, 3, 6, 7	0.876
040267	23	07-Dec-2015	18:23	9	1, 4, 5, 6, 9	0.889
040268	01	25-Jan-1994	06:10	9	1, 2, 5, 6, 9	0.852
040268	02	05-Mar-1995	11:21	9	1, 3, 5, 6, 8	0.814
040268	03	27-Jan-1997	12:01	9	4, 5, 7, 8, 9	0.917
040268	04	04-Dec-1997	11:06	7	1, 2, 4, 6, 7	0.861
040268	05	08-Dec-1998	10:28	7	1, 2, 4, 5, 6	0.905
040268	06	15-Nov-1999	11:48	7	2, 3, 5, 6, 7	0.955
040268	07	30-Nov-2000	13:37	9	1, 3, 4, 8, 9	0.932
040268	08	08-Nov-2001	11:28	9	2, 3, 6, 7, 9	0.947
040268	09	30-Oct-2002	12:40	9	1, 2, 3, 5, 6	0.827
040268	10	04-Feb-2004	13:47	9	1, 5, 6, 8, 9	0.924
040268	11	12-Dec-2004	16:58	9	3, 4, 6, 7, 9	0.874
040268	12	13-Aug-2006	00:27	9	2, 3, 6, 7, 8	0.939
040268	13	13-Dec-2007	12:20	9	3, 4, 5, 7, 9	0.931
040268	14	20-Sep-2008	02:10	9	1, 2, 5, 6, 9	0.884
040268	15	25-Jan-2010	17:53	9	2, 3, 4, 6, 9	0.874
040268	16	08-Dec-2011	21:38	9	2, 5, 6, 8, 9	0.938
040268	17	16-Dec-2012	19:58	9	2, 3, 5, 6, 7	0.931
040268	18	07-Feb-2014	01:01	9	1, 2, 3, 6, 7	0.922
040268	19	07-Feb-2014	09:03	3	1, 2, 3	0.845
040268	20	07-Feb-2014	13:10	3	1, 2, 3	0.850
040268	21	07-Feb-2014	16:40	3	1, 2, 3	0.825
040268	22	14-Nov-2014	04:17	9	3, 6, 7, 8, 9	0.908
040268	23	07-Dec-2015	18:33	9	2, 3, 4, 6, 9	0.915
063021	01	01-Feb-1990	17:20	5	1, 2, 3, 4, 5	0.935
063021	02	20-Sep-1990	11:25	7	3, 4, 5, 6, 7	0.938
063021	03	12-Mar-1991	14:23	5	1, 2, 3, 4, 5	0.911
063021	04	29-Feb-1992	17:03	6	1, 3, 4, 5, 6	0.941

Section	Visit	Date	Time	Available Repeats	Selected Repeats	Composite Correlation
063021	05	02-Mar-1993	17:04	9	4, 5, 7, 8, 9	0.916
063021	06	02-Mar-1993	18:33	5	1, 2, 3, 4, 5	0.941
063021	07	10-Apr-1995	12:34	9	1, 2, 5, 6, 8	0.942
063021	08	24-Feb-1997	11:11	9	3, 4, 7, 8, 9	0.957
063021	09	16-Feb-1998	12:02	7	1, 2, 4, 5, 7	0.937
063021	10	10-Mar-1999	12:53	7	1, 2, 3, 5, 7	0.928
063021	11	15-Feb-2001	12:27	9	3, 6, 7, 8, 9	0.950
063021	12	14-Nov-2002	13:24	9	2, 3, 7, 8, 9	0.887
063021	13	04-Dec-2004	09:47	9	2, 4, 5, 6, 7	0.881
063021	14	07-Dec-2004	10:36	9	3, 4, 6, 7, 8	0.888
063021	15	29-Jan-2007	16:08	9	1, 3, 7, 8, 9	0.888
063021	16	05-Nov-2009	15:11	9	1, 4, 5, 6, 9	0.909
063021	17	08-Mar-2011	15:05	9	2, 3, 7, 8, 9	0.894
063021	18	10-Mar-2012	14:34	9	2, 4, 5, 8, 9	0.480
063021	19	23-Jan-2013	17:14	9	1, 2, 4, 7, 9	0.545
063021	20	17-Mar-2014	19:50	9	2, 3, 5, 8, 9	0.652
063021	21	15-Jan-2015	18:52	9	2, 6, 7, 8, 9	0.707
133019	01	03-Aug-1990	09:38	9	1, 2, 3, 5, 9	0.977
133019	02	20-May-1992	13:10	9	2, 3, 4, 5, 9	0.967
133019	03	27-Jul-1992	12:36	7	2, 3, 4, 6, 7	0.977
133019	04	23-Oct-1992	09:24	9	2, 4, 5, 6, 8	0.966
133019	05	14-Jan-1993	13:57	9	2, 3, 4, 5, 8	0.968
133019	06	09-May-1994	09:25	9	1, 3, 5, 6, 8	0.969
133019	07	26-Jan-1996	06:43	9	2, 3, 4, 5, 7	0.953
133019	08	26-Jan-1996	12:12	9	1, 2, 3, 4, 5	0.955
133019	09	05-Apr-1996	07:14	5	1, 2, 3, 4, 5	0.888
133019	10	05-Apr-1996	13:02	9	1, 2, 3, 6, 7	0.927
133019	11	13-Aug-1996	10:14	9	2, 4, 5, 6, 8	0.964
133019	12	13-Aug-1996	12:53	9	1, 2, 5, 6, 8	0.943
133019	13	17-Oct-1996	07:48	9	1, 3, 4, 6, 8	0.951
133019	14	17-Oct-1996	15:40	9	2, 6, 7, 8, 9	0.930
133019	15	16-Oct-1997	09:04	5	1, 2, 3, 4, 5	0.967
133019	16	16-Oct-1997	12:16	5	1, 2, 3, 4, 5	0.956
133019	17	29-Jan-1998	07:33	6	1, 2, 4, 5, 6	0.973
133019	18	29-Jan-1998	13:12	5	1, 2, 3, 4, 5	0.965
133019	19	27-Apr-1998	08:05	5	1, 2, 3, 4, 5	0.935
133019	20	27-Apr-1998	12:06	5	1, 2, 3, 4, 5	0.944
133019	21	06-Aug-1998	10:30	7	2, 4, 5, 6, 7	0.960
133019	22	09-Dec-1998	12:00	7	2, 3, 4, 5, 6	0.946
133019	23	14-May-1999	11:18	8	3, 4, 6, 7, 8	0.961
133019	24	13-Apr-2000	09:37	7	1, 2, 3, 4, 5	0.962
133019	25	14-Aug-2000	13:55	7	2, 3, 4, 5, 7	0.972
133019	26	16-Feb-2001	10:56	7	1, 2, 5, 6, 7	0.977
133019	27	16-Feb-2001	16:55	7	1, 3, 4, 6, 7	0.962
133019	28	23-May-2001	09:16	7	2, 3, 4, 6, 7	0.971
133019	29	23-May-2001	15:26	7	2, 3, 4, 5, 7	0.947
133019	30	06-Aug-2001	07:55	7	1, 2, 3, 6, 7	0.973
133019	31	06-Aug-2001	13:23	7	1, 4, 5, 6, 7	0.958
133019	32	14-Mar-2002	08:00	6	2, 3, 4, 5, 6	0.973
133019	33	14-Mar-2002	13:01	7	1, 2, 3, 4, 7	0.968
133019	34	10-Dec-2002	10:02	7	2, 4, 5, 6, 7	0.959

Section	Visit	Date	Time	Available Repeats	Selected Repeats	Composite Correlation
133019	35	04-Aug-2004	11:55	9	2, 5, 7, 8, 9	0.963
133019	36	27-Nov-2007	16:11	9	1, 2, 4, 8, 9	0.940
133019	37	10-Feb-2010	10:45	9	1, 3, 4, 8, 9	0.947
133019	38	04-Nov-2013	14:30	9	2, 4, 6, 7, 8	0.819
133019	39	11-Oct-2014	16:43	9	1, 2, 5, 6, 7	0.835
183002	01	23-Aug-1990	10:48	5	1, 2, 3, 4, 5	0.943
183002	02	10-Sep-1991	11:00	7	1, 3, 4, 6, 7	0.929
183002	03	04-Oct-1992	15:37	6	1, 2, 4, 5, 6	0.961
183002	04	11-Jan-1994	18:41	9	1, 3, 4, 6, 7	0.959
183002	05	16-Mar-1995	08:26	9	2, 4, 5, 6, 9	0.956
183002	06	24-Oct-1995	07:48	5	1, 5, 7, 8, 9	0.975
183002	07	24-Oct-1995	11:42	5	1, 2, 4, 6, 9	0.965
183002	08	24-Oct-1995	16:01	5	1, 2, 5, 7, 8	0.960
183002	09	04-Mar-1996	07:23	5	1, 2, 4, 5, 6	0.929
183002	10	04-Mar-1996	11:36	5	4, 5, 6, 7, 9	0.933
183002	11	04-Mar-1996	15:45	5	1, 3, 4, 5, 8	0.652
183002	12	06-Sep-1996	16:39	5	1, 2, 3, 4, 9	0.922
183002	13	22-May-1997	07:44	7	2, 3, 4, 5, 6	0.981
183002	14	05-Dec-1997	08:36	7	3, 4, 5, 6, 7	0.984
183002	15	05-Dec-1997	14:37	7	1, 2, 3, 4, 6	0.983
183002	16	05-Feb-1998	14:29	7	1, 3, 4, 6, 7	0.974
183002	17	06-Feb-1998	06:53	7	2, 3, 4, 5, 6	0.979
183002	18	26-May-1998	07:59	5	1, 2, 3, 4, 5	0.975
183002	19	26-May-1998	15:13	5	1, 2, 3, 4, 5	0.961
183002	20	16-Aug-1998	08:01	7	1, 2, 4, 5, 6	0.981
183002	21	17-Aug-1998	13:07	7	1, 2, 4, 6, 7	0.961
183002	22	29-Oct-1999	13:06	7	1, 2, 5, 6, 7	0.968
183002	23	23-Aug-2000	13:59	7	2, 3, 5, 6, 7	0.977
183002	24	11-Nov-2001	11:59	7	1, 2, 3, 6, 7	0.960
183002	25	24-Nov-2003	17:09	9	2, 3, 4, 6, 8	0.963
183002	26	26-Jul-2004	16:06	7	1, 2, 3, 6, 7	0.960
183002	27	17-Oct-2007	12:34	9	1, 2, 5, 7, 9	0.960
183002	28	20-Jul-2010	11:46	6	4, 6, 7, 8, 9	0.956
183002	29	26-Apr-2011	14:37	9	1, 3, 5, 7, 8	0.959
183002	30	24-Jul-2012	12:43	9	2, 3, 6, 7, 9	0.968
183002	31	29-Apr-2015	17:26	7	1, 3, 4, 6, 7	0.926
200201	01	14-Aug-1992	13:17	8	3, 4, 6, 7, 8	0.925
200201	02	10-Mar-1993	11:05	5	1, 2, 3, 4, 5	0.891
200201	03	15-May-1994	10:10	8	1, 3, 6, 7, 8	0.933
200201	04	18-Feb-1995	09:12	7	1, 2, 4, 5, 7	0.942
200201	05	20-Apr-1996	13:31	7	1, 3, 4, 5, 7	0.876
200201	06	03-Mar-1997	11:40	7	1, 2, 4, 6, 7	0.954
200201	07	15-May-1998	10:37	7	2, 3, 4, 6, 7	0.964
200201	08	15-Mar-1999	08:34	5	1, 2, 3, 4, 5	0.923
200201	09	01-Mar-2000	11:25	5	1, 2, 3, 4, 5	0.971
200201	10	10-May-2001	14:20	6	2, 3, 4, 5, 6	0.974
200201	11	21-Apr-2002	08:22	7	3, 4, 5, 6, 7	0.957
200201	12	20-Feb-2003	10:52	7	3, 4, 5, 6, 7	0.973
200201	13	12-Mar-2004	17:04	8	1, 3, 4, 5, 8	0.963
200201	14	05-Jun-2006	13:24	7	3, 4, 5, 6, 7	0.949
200201	15	19-Apr-2008	09:42	8	1, 5, 6, 7, 8	0.966

Section	Visit	Date	Time	Available Repeats	Selected Repeats	Composite Correlation
200201	16	07-Aug-2009	10:01	9	4, 5, 7, 8, 9	0.962
200201	17	19-Oct-2010	15:49	9	1, 3, 4, 6, 9	0.962
200201	18	21-Sep-2012	14:08	8	2, 3, 4, 5, 8	0.966
200201	19	03-Dec-2013	16:25	6	1, 2, 3, 4, 6	0.972
200201	20	05-May-2014	14:45	7	3, 4, 5, 6, 7	0.963
200201	21	06-May-2014	06:57	5	1, 2, 3, 4, 5	0.953
200201	22	06-May-2014	14:10	7	1, 2, 3, 6, 7	0.972
200201	23	06-May-2014	20:25	5	1, 2, 3, 4, 5	0.957
200201	24	09-Dec-2015	13:08	7	1, 2, 3, 4, 7	0.957
200202	01	14-Aug-1992	13:17	8	4, 5, 6, 7, 8	0.939
200202	02	10-Mar-1993	11:26	9	2, 6, 7, 8, 9	0.898
200202	03	15-May-1994	10:10	8	2, 4, 6, 7, 8	0.920
200202	04	18-Feb-1995	09:12	7	1, 3, 5, 6, 7	0.852
200202	05	20-Apr-1996	13:31	7	2, 3, 5, 6, 7	0.729
200202	06	03-Mar-1997	11:40	7	1, 2, 3, 6, 7	0.925
200202	07	15-May-1998	10:26	5	1, 2, 3, 4, 5	0.922
200202	08	15-Mar-1999	08:34	5	1, 2, 3, 4, 5	0.921
200202	09	01-Mar-2000	11:25	7	1, 2, 4, 6, 7	0.962
200202	10	10-May-2001	14:08	7	1, 2, 3, 4, 7	0.943
200202	11	21-Apr-2002	08:01	7	1, 4, 5, 6, 7	0.898
200202	12	20-Feb-2003	10:31	7	1, 2, 4, 5, 7	0.931
200202	13	12-Mar-2004	17:15	8	2, 3, 4, 5, 8	0.943
200202	14	05-Jun-2006	12:58	7	1, 2, 3, 4, 7	0.940
200202	15	19-Apr-2008	09:52	9	2, 3, 4, 7, 9	0.962
200202	16	07-Aug-2009	09:23	8	1, 2, 4, 5, 8	0.950
200202	17	19-Oct-2010	15:59	8	2, 5, 6, 7, 8	0.966
200202	18	21-Sep-2012	13:58	9	1, 3, 4, 8, 9	0.957
200202	19	03-Dec-2013	16:25	9	1, 4, 6, 7, 9	0.977
200202	20	05-May-2014	14:35	9	2, 6, 7, 8, 9	0.973
200202	21	06-May-2014	06:57	5	1, 2, 3, 4, 5	0.946
200202	22	06-May-2014	13:53	6	0, 1, 4, 5, 6	0.980
200202	23	06-May-2014	20:25	5	1, 2, 3, 4, 5	0.966
200202	24	09-Dec-2015	13:23	7	2, 3, 5, 6, 7	0.976
200203	01	14-Aug-1992	13:17	8	2, 4, 6, 7, 8	0.895
200203	02	10-Mar-1993	11:41	9	4, 5, 6, 7, 9	0.857
200203	03	15-May-1994	10:10	8	1, 4, 6, 7, 8	0.925
200203	04	18-Feb-1995	09:12	7	1, 3, 4, 6, 7	0.921
200203	05	20-Apr-1996	13:31	7	3, 4, 5, 6, 7	0.887
200203	06	03-Mar-1997	11:52	7	2, 4, 5, 6, 7	0.954
200203	07	15-May-1998	10:37	7	2, 3, 5, 6, 7	0.941
200203	08	15-Mar-1999	08:34	5	1, 2, 3, 4, 5	0.934
200203	09	01-Mar-2000	11:25	7	1, 2, 3, 4, 7	0.966
200203	10	10-May-2001	14:08	6	1, 2, 3, 5, 6	0.958
200203	11	21-Apr-2002	08:01	7	1, 4, 5, 6, 7	0.907
200203	12	20-Feb-2003	10:31	6	1, 2, 3, 4, 6	0.939
200203	13	12-Mar-2004	17:04	9	1, 6, 7, 8, 9	0.942
200203	14	05-Jun-2006	13:14	6	2, 3, 4, 5, 6	0.944
200203	15	19-Apr-2008	10:03	8	3, 4, 5, 7, 8	0.955
200203	16	07-Aug-2009	09:34	9	2, 3, 4, 7, 9	0.944
200203	17	19-Oct-2010	15:49	9	1, 2, 3, 5, 9	0.948
200203	18	21-Sep-2012	13:58	9	1, 3, 4, 8, 9	0.954

Section	Visit	Date	Time	Available Repeats	Selected Repeats	Composite Correlation
200203	19	03-Dec-2013	16:25	9	1, 2, 6, 8, 9	0.957
200203	20	05-May-2014	14:17	9	1, 5, 6, 8, 9	0.959
200203	21	06-May-2014	06:57	5	1, 2, 3, 4, 5	0.917
200203	22	06-May-2014	14:34	7	3, 4, 5, 6, 7	0.957
200203	23	06-May-2014	20:25	5	1, 2, 3, 4, 5	0.941
200203	24	09-Dec-2015	13:08	7	1, 3, 4, 6, 7	0.964
200204	01	14-Aug-1992	13:17	8	3, 4, 5, 6, 8	0.946
200204	02	10-Mar-1993	11:05	5	1, 2, 3, 4, 5	0.906
200204	03	15-May-1994	10:10	8	1, 4, 5, 6, 8	0.926
200204	04	18-Feb-1995	09:12	8	1, 3, 4, 6, 8	0.931
200204	05	20-Apr-1996	13:31	5	1, 2, 3, 4, 5	0.815
200204	06	03-Mar-1997	11:40	5	1, 2, 3, 4, 5	0.956
200204	07	15-May-1998	10:49	7	3, 4, 5, 6, 7	0.947
200204	08	15-Mar-1999	08:34	5	1, 2, 3, 4, 5	0.934
200204	09	01-Mar-2000	11:25	6	1, 2, 3, 5, 6	0.957
200204	10	10-May-2001	14:20	7	2, 3, 4, 6, 7	0.954
200204	11	21-Apr-2002	08:01	7	1, 4, 5, 6, 7	0.926
200204	12	20-Feb-2003	10:41	7	2, 3, 5, 6, 7	0.942
200204	13	12-Mar-2004	17:45	9	5, 6, 7, 8, 9	0.939
200204	14	05-Jun-2006	12:58	5	1, 2, 3, 4, 5	0.956
200204	15	19-Apr-2008	10:13	9	4, 6, 7, 8, 9	0.951
200204	16	07-Aug-2009	09:23	5	1, 2, 3, 4, 5	0.940
200204	17	19-Oct-2010	15:49	9	1, 3, 7, 8, 9	0.949
200204	18	21-Sep-2012	13:58	9	1, 2, 6, 8, 9	0.959
200204	19	03-Dec-2013	16:25	9	1, 2, 5, 8, 9	0.950
200204	20	05-May-2014	14:35	7	2, 3, 4, 6, 7	0.960
200204	21	06-May-2014	06:57	5	1, 2, 3, 4, 5	0.948
200204	22	06-May-2014	13:53	6	0, 1, 4, 5, 6	0.955
200204	23	06-May-2014	20:25	5	1, 2, 3, 4, 5	0.936
200204	24	09-Dec-2015	13:08	6	1, 2, 3, 4, 6	0.959
200205	01	14-Aug-1992	13:17	8	2, 5, 6, 7, 8	0.926
200205	02	10-Mar-1993	11:05	9	1, 6, 7, 8, 9	0.879
200205	03	15-May-1994	10:10	8	4, 5, 6, 7, 8	0.943
200205	04	18-Feb-1995	09:12	8	1, 3, 5, 7, 8	0.926
200205	05	20-Apr-1996	13:31	7	2, 3, 5, 6, 7	0.869
200205	06	03-Mar-1997	12:02	7	3, 4, 5, 6, 7	0.962
200205	07	15-May-1998	10:26	6	1, 2, 3, 5, 6	0.942
200205	08	15-Mar-1999	08:34	5	1, 2, 3, 4, 5	0.934
200205	09	01-Mar-2000	11:25	7	1, 2, 3, 4, 7	0.917
200205	10	10-May-2001	14:20	7	2, 3, 5, 6, 7	0.963
200205	11	21-Apr-2002	08:01	7	1, 4, 5, 6, 7	0.885
200205	12	20-Feb-2003	10:41	7	2, 3, 4, 5, 7	0.938
200205	13	12-Mar-2004	17:15	9	2, 5, 6, 7, 9	0.943
200205	14	05-Jun-2006	12:58	5	1, 2, 3, 4, 5	0.957
200205	15	19-Apr-2008	09:42	8	1, 2, 3, 4, 8	0.951
200205	16	07-Aug-2009	09:23	7	1, 2, 4, 5, 7	0.919
200205	17	19-Oct-2010	15:49	8	1, 2, 3, 4, 8	0.955
200205	18	21-Sep-2012	14:08	9	2, 3, 5, 8, 9	0.933
200205	19	03-Dec-2013	16:25	8	1, 2, 3, 7, 8	0.920
200205	20	05-May-2014	14:17	9	1, 2, 3, 6, 9	0.897
200205	21	06-May-2014	06:57	5	1, 2, 3, 4, 5	0.745

Section	Visit	Date	Time	Available Repeats	Selected Repeats	Composite Correlation
200205	22	06-May-2014	13:53	7	0, 3, 4, 6, 7	0.852
200205	23	06-May-2014	20:25	5	1, 2, 3, 4, 5	0.858
200205	24	09-Dec-2015	13:08	7	1, 2, 3, 5, 7	0.899
200206	01	14-Aug-1992	13:17	8	3, 4, 5, 6, 8	0.954
200206	02	10-Mar-1993	11:05	6	1, 2, 3, 5, 6	0.907
200206	03	15-May-1994	10:10	9	1, 3, 5, 8, 9	0.938
200206	04	18-Feb-1995	09:12	7	1, 2, 3, 5, 7	0.916
200206	05	20-Apr-1996	13:31	7	2, 3, 4, 5, 7	0.862
200206	06	03-Mar-1997	11:52	7	2, 4, 5, 6, 7	0.953
200206	07	15-May-1998	10:26	7	1, 2, 4, 5, 7	0.933
200206	08	15-Mar-1999	08:34	5	1, 2, 3, 4, 5	0.918
200206	09	01-Mar-2000	11:25	7	1, 3, 4, 6, 7	0.949
200206	10	10-May-2001	14:20	7	2, 3, 5, 6, 7	0.945
200206	11	21-Apr-2002	08:01	7	1, 3, 5, 6, 7	0.898
200206	12	20-Feb-2003	10:31	6	1, 3, 4, 5, 6	0.957
200206	13	12-Mar-2004	17:04	9	1, 2, 5, 8, 9	0.925
200206	14	05-Jun-2006	12:58	7	1, 2, 4, 5, 7	0.970
200206	15	19-Apr-2008	09:42	6	1, 2, 4, 5, 6	0.969
200206	16	07-Aug-2009	10:01	8	4, 5, 6, 7, 8	0.965
200206	17	19-Oct-2010	15:59	9	2, 4, 5, 8, 9	0.975
200206	18	21-Sep-2012	14:08	9	2, 4, 5, 8, 9	0.966
200206	19	03-Dec-2013	16:45	9	3, 4, 5, 6, 9	0.971
200206	20	05-May-2014	14:17	9	1, 4, 6, 7, 9	0.978
200206	21	06-May-2014	06:57	5	1, 2, 3, 4, 5	0.949
200206	22	06-May-2014	13:53	6	0, 2, 3, 4, 6	0.983
200206	23	06-May-2014	20:25	5	1, 2, 3, 4, 5	0.941
200206	24	09-Dec-2015	13:08	7	1, 3, 4, 5, 7	0.973
200207	01	14-Aug-1992	13:17	8	4, 5, 6, 7, 8	0.934
200207	02	10-Mar-1993	11:05	9	1, 2, 3, 7, 9	0.891
200207	03	15-May-1994	10:10	8	3, 4, 5, 7, 8	0.956
200207	04	18-Feb-1995	09:12	8	2, 3, 4, 6, 8	0.940
200207	05	20-Apr-1996	13:31	7	1, 2, 5, 6, 7	0.861
200207	06	03-Mar-1997	11:52	7	2, 3, 5, 6, 7	0.934
200207	07	15-May-1998	10:37	6	2, 3, 4, 5, 6	0.948
200207	08	15-Mar-1999	08:34	5	1, 2, 3, 4, 5	0.922
200207	09	01-Mar-2000	11:25	7	1, 2, 3, 4, 7	0.953
200207	10	10-May-2001	14:08	6	1, 2, 4, 5, 6	0.962
200207	11	21-Apr-2002	08:01	7	1, 4, 5, 6, 7	0.901
200207	12	20-Feb-2003	10:41	7	2, 4, 5, 6, 7	0.945
200207	13	12-Mar-2004	17:04	8	1, 5, 6, 7, 8	0.958
200207	14	05-Jun-2006	12:58	5	1, 2, 3, 4, 5	0.952
200207	15	19-Apr-2008	10:03	8	3, 5, 6, 7, 8	0.960
200207	16	07-Aug-2009	09:23	9	1, 3, 6, 7, 9	0.946
200207	17	19-Oct-2010	15:49	7	1, 4, 5, 6, 7	0.965
200207	18	21-Sep-2012	13:58	9	1, 2, 5, 8, 9	0.965
200207	19	03-Dec-2013	16:25	9	1, 2, 6, 7, 9	0.961
200207	20	05-May-2014	14:17	9	1, 3, 5, 7, 9	0.974
200207	21	06-May-2014	06:57	5	1, 2, 3, 4, 5	0.949
200207	22	06-May-2014	13:53	6	0, 1, 3, 5, 6	0.972
200207	23	06-May-2014	20:25	5	1, 2, 3, 4, 5	0.954
200207	24	09-Dec-2015	13:08	7	1, 2, 4, 6, 7	0.966

Section	Visit	Date	Time	Available Repeats	Selected Repeats	Composite Correlation
200208	01	14-Aug-1992	13:17	8	3, 5, 6, 7, 8	0.960
200208	02	10-Mar-1993	11:05	5	1, 2, 3, 4, 5	0.911
200208	03	15-May-1994	11:00	9	5, 6, 7, 8, 9	0.961
200208	04	18-Feb-1995	09:12	8	1, 2, 3, 5, 8	0.967
200208	05	20-Apr-1996	13:31	7	1, 3, 4, 6, 7	0.861
200208	06	03-Mar-1997	11:40	6	1, 2, 3, 4, 6	0.973
200208	07	15-May-1998	10:49	7	3, 4, 5, 6, 7	0.954
200208	08	15-Mar-1999	08:34	5	1, 2, 3, 4, 5	0.947
200208	09	01-Mar-2000	11:25	7	1, 2, 3, 5, 7	0.966
200208	10	10-May-2001	14:08	7	1, 3, 4, 6, 7	0.946
200208	11	21-Apr-2002	08:01	7	1, 4, 5, 6, 7	0.925
200208	12	20-Feb-2003	10:31	7	1, 2, 4, 5, 7	0.961
200208	13	12-Mar-2004	17:04	8	1, 2, 3, 6, 8	0.965
200208	14	05-Jun-2006	12:58	7	1, 2, 3, 6, 7	0.961
200208	15	19-Apr-2008	10:03	8	3, 4, 5, 6, 8	0.979
200208	16	07-Aug-2009	09:23	9	1, 4, 5, 7, 9	0.958
200208	17	19-Oct-2010	15:49	9	1, 5, 7, 8, 9	0.968
200208	18	21-Sep-2012	14:08	8	2, 3, 4, 7, 8	0.978
200208	19	03-Dec-2013	16:25	9	1, 3, 5, 7, 9	0.970
200208	20	05-May-2014	14:35	9	2, 3, 7, 8, 9	0.975
200208	21	06-May-2014	06:57	5	1, 2, 3, 4, 5	0.940
200208	22	06-May-2014	13:53	6	0, 1, 2, 5, 6	0.970
200208	23	06-May-2014	20:25	5	1, 2, 3, 4, 5	0.949
200208	24	09-Dec-2015	13:08	7	1, 2, 4, 5, 7	0.958
200209	01	14-Aug-1992	13:17	8	3, 4, 5, 6, 8	0.901
200209	02	10-Mar-1993	11:05	5	1, 2, 3, 4, 5	0.881
200209	03	15-May-1994	10:10	5	1, 2, 3, 4, 5	0.917
200209	04	18-Feb-1995	09:12	8	1, 3, 6, 7, 8	0.901
200209	05	20-Apr-1996	13:31	7	2, 3, 4, 5, 7	0.803
200209	06	03-Mar-1997	11:40	6	1, 3, 4, 5, 6	0.958
200209	07	15-May-1998	10:26	7	1, 3, 4, 6, 7	0.912
200209	08	15-Mar-1999	08:34	5	1, 2, 3, 4, 5	0.891
200209	09	01-Mar-2000	11:25	7	1, 3, 5, 6, 7	0.939
200209	10	10-May-2001	14:08	5	1, 2, 3, 4, 5	0.914
200209	11	21-Apr-2002	08:01	7	1, 4, 5, 6, 7	0.887
200209	12	20-Feb-2003	10:41	6	2, 3, 4, 5, 6	0.912
200209	13	12-Mar-2004	17:15	9	2, 3, 5, 8, 9	0.936
200209	14	05-Jun-2006	12:58	6	1, 2, 4, 5, 6	0.915
200209	15	19-Apr-2008	09:42	7	1, 2, 3, 4, 7	0.940
200209	16	07-Aug-2009	09:44	7	3, 4, 5, 6, 7	0.905
200209	17	19-Oct-2010	16:28	9	5, 6, 7, 8, 9	0.920
200209	18	21-Sep-2012	14:20	9	3, 6, 7, 8, 9	0.929
200209	19	03-Dec-2013	16:25	9	1, 2, 3, 5, 9	0.929
200209	20	05-May-2014	14:17	9	1, 2, 3, 7, 9	0.937
200209	21	06-May-2014	06:57	5	1, 2, 3, 4, 5	0.882
200209	22	06-May-2014	14:23	7	2, 3, 5, 6, 7	0.948
200209	23	06-May-2014	20:25	5	1, 2, 3, 4, 5	0.907
200209	24	09-Dec-2015	13:08	5	1, 2, 3, 4, 5	0.945
200210	01	14-Aug-1992	12:52	7	1, 3, 4, 6, 7	0.929
200210	02	10-Mar-1993	11:05	9	1, 6, 7, 8, 9	0.925
200210	03	15-May-1994	10:10	9	4, 5, 6, 7, 9	0.959

Section	Visit	Date	Time	Available Repeats	Selected Repeats	Composite Correlation
200210	04	18-Feb-1995	09:12	8	1, 3, 6, 7, 8	0.937
200210	05	20-Apr-1996	13:31	6	2, 3, 4, 5, 6	0.827
200210	06	03-Mar-1997	11:52	6	2, 3, 4, 5, 6	0.957
200210	07	15-May-1998	10:26	7	1, 2, 5, 6, 7	0.933
200210	08	15-Mar-1999	08:34	5	1, 2, 3, 4, 5	0.908
200210	09	01-Mar-2000	11:52	7	2, 3, 4, 6, 7	0.945
200210	10	10-May-2001	14:08	7	1, 2, 3, 4, 7	0.943
200210	11	21-Apr-2002	08:01	7	1, 4, 5, 6, 7	0.908
200210	12	20-Feb-2003	10:41	7	2, 4, 5, 6, 7	0.912
200210	13	12-Mar-2004	17:24	9	3, 4, 5, 8, 9	0.928
200210	14	05-Jun-2006	12:58	5	1, 2, 3, 4, 5	0.939
200210	15	19-Apr-2008	09:52	8	2, 3, 4, 7, 8	0.941
200210	16	07-Aug-2009	09:34	6	2, 3, 4, 5, 6	0.924
200210	17	19-Oct-2010	15:59	9	2, 4, 6, 7, 9	0.932
200210	18	21-Sep-2012	14:45	9	5, 6, 7, 8, 9	0.950
200210	19	03-Dec-2013	16:25	7	1, 2, 3, 6, 7	0.945
200210	20	05-May-2014	14:45	7	3, 4, 5, 6, 7	0.952
200210	21	06-May-2014	06:57	5	1, 2, 3, 4, 5	0.947
200210	22	06-May-2014	13:53	6	0, 1, 2, 5, 6	0.921
200210	23	06-May-2014	20:25	5	1, 2, 3, 4, 5	0.830
200210	24	09-Dec-2015	13:08	6	1, 2, 3, 5, 6	0.929
200211	01	14-Aug-1992	13:17	7	2, 3, 5, 6, 7	0.919
200211	02	10-Mar-1993	11:05	9	1, 6, 7, 8, 9	0.892
200211	03	15-May-1994	10:10	9	1, 3, 4, 7, 9	0.906
200211	04	18-Feb-1995	09:12	7	1, 3, 4, 5, 7	0.919
200211	05	20-Apr-1996	13:31	7	1, 2, 4, 5, 7	0.840
200211	06	03-Mar-1997	11:40	7	1, 2, 3, 5, 7	0.933
200211	07	15-May-1998	10:26	7	1, 2, 4, 5, 7	0.933
200211	08	15-Mar-1999	08:34	5	1, 2, 3, 4, 5	0.918
200211	09	01-Mar-2000	11:25	6	1, 2, 3, 5, 6	0.919
200211	10	10-May-2001	14:20	7	2, 4, 5, 6, 7	0.961
200211	11	21-Apr-2002	08:01	7	1, 4, 5, 6, 7	0.886
200211	12	20-Feb-2003	10:31	6	1, 3, 4, 5, 6	0.920
200211	13	12-Mar-2004	17:15	9	2, 4, 5, 7, 9	0.912
200211	14	05-Jun-2006	12:58	7	1, 2, 4, 6, 7	0.932
200211	15	19-Apr-2008	09:42	7	1, 2, 4, 5, 7	0.944
200211	16	07-Aug-2009	10:01	9	4, 5, 6, 7, 9	0.915
200211	17	19-Oct-2010	16:09	9	3, 4, 7, 8, 9	0.927
200211	18	21-Sep-2012	14:08	8	2, 3, 6, 7, 8	0.934
200211	19	03-Dec-2013	16:56	8	4, 5, 6, 7, 8	0.941
200211	20	05-May-2014	14:17	7	1, 2, 3, 4, 7	0.955
200211	21	06-May-2014	06:57	5	1, 2, 3, 4, 5	0.895
200211	22	06-May-2014	14:10	6	1, 2, 3, 4, 6	0.948
200211	23	06-May-2014	20:25	5	1, 2, 3, 4, 5	0.840
200211	24	09-Dec-2015	13:08	5	1, 2, 3, 4, 5	0.896
200212	01	14-Aug-1992	13:17	8	3, 5, 6, 7, 8	0.932
200212	02	10-Mar-1993	11:05	9	1, 6, 7, 8, 9	0.909
200212	03	15-May-1994	10:10	9	2, 4, 5, 7, 9	0.956
200212	04	18-Feb-1995	09:12	8	2, 3, 4, 5, 8	0.942
200212	05	20-Apr-1996	13:31	7	3, 4, 5, 6, 7	0.906
200212	06	03-Mar-1997	12:02	7	3, 4, 5, 6, 7	0.947

Section	Visit	Date	Time	Available Repeats	Selected Repeats	Composite Correlation
200212	07	15-May-1998	10:26	6	1, 2, 3, 5, 6	0.943
200212	08	15-Mar-1999	08:34	5	1, 2, 3, 4, 5	0.914
200212	09	01-Mar-2000	11:25	7	1, 3, 4, 6, 7	0.956
200212	10	10-May-2001	14:08	7	1, 2, 4, 5, 7	0.967
200212	11	21-Apr-2002	08:01	6	1, 3, 4, 5, 6	0.924
200212	12	20-Feb-2003	10:41	7	2, 3, 4, 6, 7	0.950
200212	13	12-Mar-2004	17:15	8	2, 3, 5, 7, 8	0.965
200212	14	05-Jun-2006	12:58	6	1, 2, 3, 4, 6	0.970
200212	15	19-Apr-2008	09:42	6	1, 2, 3, 4, 6	0.972
200212	16	07-Aug-2009	10:01	9	4, 5, 7, 8, 9	0.947
200212	17	19-Oct-2010	15:49	9	1, 2, 3, 8, 9	0.964
200212	18	21-Sep-2012	13:58	9	1, 4, 5, 7, 9	0.974
200212	19	03-Dec-2013	16:35	7	2, 3, 5, 6, 7	0.966
200212	20	05-May-2014	14:45	9	3, 4, 6, 8, 9	0.973
200212	21	06-May-2014	06:57	5	1, 2, 3, 4, 5	0.948
200212	22	06-May-2014	13:53	7	0, 1, 3, 6, 7	0.971
200212	23	06-May-2014	20:25	5	1, 2, 3, 4, 5	0.949
200212	24	09-Dec-2015	13:23	7	2, 4, 5, 6, 7	0.956
200259	02	10-Mar-1993	11:05	9	1, 6, 7, 8, 9	0.891
200259	03	15-May-1994	10:10	9	4, 5, 6, 7, 9	0.940
200259	04	18-Feb-1995	09:12	8	4, 5, 6, 7, 8	0.932
200259	05	20-Apr-1996	13:31	6	2, 3, 4, 5, 6	0.860
200259	06	03-Mar-1997	11:40	7	1, 2, 3, 4, 7	0.949
200259	07	15-May-1998	10:49	7	3, 4, 5, 6, 7	0.941
200259	08	15-Mar-1999	08:34	5	1, 2, 3, 4, 5	0.919
200259	09	01-Mar-2000	11:25	6	1, 2, 3, 5, 6	0.959
200259	10	10-May-2001	14:08	5	1, 2, 3, 4, 5	0.955
200259	11	21-Apr-2002	08:01	7	1, 4, 5, 6, 7	0.905
200259	12	20-Feb-2003	10:31	7	1, 2, 4, 6, 7	0.943
200259	13	12-Mar-2004	17:04	9	1, 3, 4, 8, 9	0.934
200259	14	05-Jun-2006	13:14	7	2, 3, 4, 5, 7	0.951
200259	15	19-Apr-2008	09:52	8	2, 3, 5, 7, 8	0.952
200259	16	07-Aug-2009	09:23	9	1, 3, 4, 5, 9	0.927
200259	17	19-Oct-2010	15:59	8	2, 4, 6, 7, 8	0.925
200259	18	21-Sep-2012	14:20	9	3, 6, 7, 8, 9	0.931
200259	19	03-Dec-2013	16:25	9	1, 2, 3, 4, 9	0.948
200259	20	05-May-2014	14:17	9	1, 3, 6, 8, 9	0.952
200259	21	06-May-2014	06:57	5	1, 2, 3, 4, 5	0.951
200259	22	06-May-2014	14:10	6	1, 3, 4, 5, 6	0.964
200259	23	06-May-2014	20:25	5	1, 2, 3, 4, 5	0.946
200259	24	09-Dec-2015	13:08	7	1, 2, 4, 5, 7	0.958
273003	01	20-Jun-1990	17:08	5	1, 2, 3, 4, 5	0.958
273003	02	10-Aug-1991	11:49	5	2, 3, 4, 8, 9	0.957
273003	03	03-Aug-1992	17:00	9	4, 5, 6, 8, 9	0.942
273003	04	23-Nov-1993	19:10	9	2, 4, 5, 6, 8	0.936
273003	05	30-Jul-1994	14:33	5	1, 2, 3, 4, 5	0.965
273003	06	01-Aug-1997	06:43	7	2, 3, 4, 5, 7	0.983
273003	07	03-Oct-1998	14:37	5	1, 2, 3, 4, 5	0.972
273003	08	14-Jun-1999	13:24	7	1, 2, 4, 5, 6	0.990
273003	09	27-Jul-2000	09:28	5	1, 2, 3, 4, 5	0.969
273003	10	22-Aug-2001	17:00	6	2, 3, 4, 5, 6	0.981

Section	Visit	Date	Time	Available Repeats	Selected Repeats	Composite Correlation
273003	11	16-Oct-2004	12:26	9	1, 5, 6, 7, 9	0.960
273003	12	28-Jul-2009	16:53	9	1, 3, 4, 6, 7	0.970
370201	01	30-Mar-1994	10:28	9	2, 3, 4, 8, 9	0.889
370201	S01	06-Jan-1996	04:35	4	2, 3, 4, 5	0.923
370201	02	06-Jan-1996	05:46	9	3, 4, 6, 8, 9	0.953
370201	S02	28-Feb-1996	09:38	5	1, 2, 3, 4, 5	0.925
370201	03	28-Feb-1996	10:43	9	1, 2, 3, 7, 9	0.937
370201	S03	28-Feb-1996	18:26	6	2, 3, 4, 5, 6	0.935
370201	S04	23-Apr-1996	06:57	5	1, 2, 3, 6, 7	0.920
370201	S05	07-Oct-1997	07:38	5	1, 2, 3, 4, 5	0.916
370201	04	07-Oct-1997	13:36	7	1, 3, 4, 6, 7	0.940
370201	S06	17-Jan-1998	08:48	6	1, 2, 3, 4, 5	0.907
370201	S07	18-Feb-1998	07:18	5	1, 2, 3, 4, 5	0.890
370201	05	18-Feb-1998	13:23	7	1, 3, 5, 6, 7	0.943
370201	S08	19-May-1998	08:14	6	1, 2, 3, 4, 6	0.940
370201	06	19-May-1998	11:08	9	3, 4, 6, 7, 8	0.931
370201	S09	19-May-1998	14:43	8	1, 3, 4, 7, 8	0.932
370201	S10	24-Jul-1998	08:07	5	1, 2, 3, 4, 5	0.933
370201	07	24-Jul-1998	11:46	7	3, 4, 5, 6, 7	0.940
370201	08	04-Nov-1998	08:45	6	1, 2, 3, 4, 5	0.961
370201	S11	04-Nov-1998	14:03	6	1, 2, 3, 5, 6	0.962
370201	09	11-Nov-1999	00:14	9	3, 4, 5, 6, 9	0.936
370201	S12	13-Mar-2000	08:06	9	3, 4, 5, 6, 7	0.942
370201	10	13-Mar-2000	14:02	9	1, 3, 4, 5, 6	0.943
370201	S13	06-Jul-2000	12:30	5	1, 2, 3, 4, 5	0.908
370201	11	08-Nov-2000	11:28	9	2, 4, 5, 7, 8	0.945
370201	S14	23-Jan-2001	07:49	7	2, 3, 4, 6, 7	0.962
370201	S15	23-Jan-2001	14:49	7	1, 2, 3, 4, 5	0.947
370201	S16	17-May-2001	07:09	7	2, 4, 5, 6, 7	0.952
370201	S17	17-May-2001	13:28	7	1, 3, 4, 5, 6	0.954
370201	S18	14-Jul-2001	07:11	6	1, 2, 4, 5, 6	0.945
370201	12	14-Jul-2001	09:11	9	1, 3, 4, 6, 9	0.948
370201	S19	14-Jul-2001	13:31	5	1, 2, 3, 4, 5	0.944
370201	S20	11-Oct-2001	06:56	5	1, 2, 3, 4, 5	0.948
370201	13	11-Oct-2001	08:45	7	1, 2, 3, 4, 5	0.951
370201	S21	11-Oct-2001	14:03	7	1, 3, 5, 6, 7	0.936
370201	S22	10-Jan-2002	07:00	7	3, 4, 5, 6, 7	0.931
370201	S23	10-Jan-2002	13:18	7	2, 3, 4, 5, 7	0.940
370201	S24	23-May-2002	08:02	7	1, 2, 3, 4, 5	0.900
370201	14	23-May-2002	11:02	9	3, 5, 6, 7, 8	0.933
370201	S25	23-May-2002	13:43	5	1, 2, 3, 4, 5	0.893
370201	S26	16-Aug-2002	06:08	7	1, 2, 3, 4, 6	0.907
370201	S27	16-Aug-2002	13:30	5	1, 2, 3, 4, 5	0.933
370201	S28	18-Sep-2002	06:25	9	1, 4, 5, 8, 9	0.954
370201	15	19-Sep-2002	17:31	9	1, 4, 5, 6, 8	0.917
370201	S29	18-Dec-2002	06:55	7	1, 2, 3, 6, 7	0.916
370201	S30	18-Dec-2002	12:54	5	1, 2, 3, 4, 5	0.888
370201	S31	22-Jan-2003	07:29	7	2, 3, 4, 6, 7	0.924
370201	S32	22-Jan-2003	12:51	5	1, 2, 3, 4, 5	0.876
370201	16	22-Jan-2003	15:42	9	1, 2, 7, 8, 9	0.933
370201	S33	01-Jun-2003	06:11	7	2, 4, 5, 6, 7	0.929

Section	Visit	Date	Time	Available Repeats	Selected Repeats	Composite Correlation
370201	17	01-Jun-2003	11:38	9	2, 3, 5, 6, 9	0.958
370201	S34	01-Jun-2003	13:25	7	2, 3, 5, 6, 7	0.940
370202	01	30-Mar-1994	10:28	9	2, 3, 4, 7, 9	0.822
370202	02	06-Jan-1996	05:46	9	2, 3, 4, 6, 8	0.948
370202	03	28-Feb-1996	10:58	9	2, 3, 4, 6, 7	0.932
370202	04	07-Oct-1997	13:36	7	1, 3, 4, 5, 7	0.953
370202	05	18-Feb-1998	13:57	7	3, 4, 5, 6, 7	0.934
370202	06	19-May-1998	10:36	9	1, 2, 4, 5, 9	0.932
370202	07	24-Jul-1998	12:02	9	4, 5, 6, 8, 9	0.941
370202	08	04-Nov-1998	08:45	6	1, 2, 3, 4, 5	0.954
370202	09	10-Nov-1999	23:54	9	1, 3, 6, 7, 9	0.965
370202	10	13-Mar-2000	14:02	9	1, 2, 3, 4, 5	0.944
370202	11	08-Nov-2000	11:28	9	4, 5, 6, 7, 8	0.949
370202	12	14-Jul-2001	09:11	9	1, 2, 3, 4, 5	0.949
370202	13	11-Oct-2001	08:45	7	1, 2, 3, 4, 5	0.945
370202	14	23-May-2002	11:02	9	3, 4, 5, 6, 7	0.923
370202	15	19-Sep-2002	17:48	9	2, 5, 6, 7, 8	0.950
370202	16	22-Jan-2003	15:42	9	1, 2, 3, 4, 6	0.947
370202	17	01-Jun-2003	11:38	9	2, 4, 6, 7, 8	0.954
370203	01	30-Mar-1994	10:28	9	2, 3, 4, 8, 9	0.923
370203	02	06-Jan-1996	05:46	9	1, 4, 5, 7, 8	0.972
370203	03	28-Feb-1996	10:58	9	2, 3, 4, 5, 6	0.967
370203	04	07-Oct-1997	13:36	7	1, 2, 3, 4, 7	0.963
370203	05	18-Feb-1998	13:40	7	2, 3, 4, 6, 7	0.965
370203	06	19-May-1998	11:23	9	4, 5, 7, 8, 9	0.957
370203	07	24-Jul-1998	11:31	9	2, 3, 4, 8, 9	0.968
370203	08	04-Nov-1998	08:45	6	1, 2, 3, 4, 5	0.961
370203	09	11-Nov-1999	00:14	9	3, 4, 5, 7, 8	0.973
370203	10	13-Mar-2000	14:24	9	3, 5, 6, 7, 9	0.962
370203	11	08-Nov-2000	11:28	9	2, 3, 4, 5, 8	0.967
370203	12	14-Jul-2001	09:19	9	3, 4, 5, 6, 7	0.972
370203	13	11-Oct-2001	08:45	7	1, 2, 3, 4, 5	0.952
370203	14	23-May-2002	10:07	9	2, 3, 4, 5, 6	0.933
370203	15	19-Sep-2002	17:31	9	1, 3, 4, 6, 9	0.966
370203	16	22-Jan-2003	15:42	9	1, 2, 3, 4, 5	0.938
370203	17	01-Jun-2003	11:28	9	1, 3, 6, 7, 8	0.954
370203	18	07-Nov-2003	09:16	9	1, 3, 5, 8, 9	0.947
370203	19	14-Nov-2004	16:09	9	3, 4, 5, 7, 9	0.966
370203	20	14-Jun-2006	16:16	9	3, 4, 5, 7, 9	0.969
370203	21	30-Nov-2006	12:41	9	1, 5, 6, 7, 8	0.940
370203	22	18-Mar-2009	15:51	9	1, 3, 4, 7, 8	0.973
370203	23	18-Apr-2010	15:03	9	1, 4, 5, 6, 7	0.980
370203	24	27-Apr-2011	19:38	9	1, 3, 4, 5, 6	0.959
370203	25	10-Dec-2012	13:24	7	1, 4, 5, 6, 7	0.969
370203	26	24-Jun-2014	13:23	5	1, 2, 3, 4, 5	0.942
370203	27	24-Jun-2014	16:42	6	1, 3, 4, 5, 6	0.936
370203	28	24-Jun-2014	19:20	5	1, 2, 3, 4, 5	0.925
370203	29	25-Jun-2014	06:08	4	1, 2, 3, 4	0.964
370203	30	09-Mar-2015	16:52	7	2, 3, 4, 5, 7	0.973
370204	01	30-Mar-1994	10:28	9	1, 2, 7, 8, 9	0.881
370204	03	28-Feb-1996	10:53	7	1, 2, 3, 4, 7	0.894

Section	Visit	Date	Time	Available Repeats	Selected Repeats	Composite Correlation
370204	04	07-Oct-1997	13:43	7	1, 2, 4, 5, 6	0.952
370204	05	18-Feb-1998	13:45	7	2, 3, 4, 5, 6	0.961
370204	06	19-May-1998	10:41	5	1, 2, 3, 4, 5	0.881
370204	07	24-Jul-1998	11:19	6	1, 3, 4, 5, 6	0.952
370204	08	04-Nov-1998	11:47	6	1, 2, 4, 5, 6	0.966
370204	09	11-Nov-1999	04:17	5	1, 2, 3, 4, 5	0.932
370204	10	13-Mar-2000	17:46	5	1, 2, 3, 4, 5	0.963
370204	11	08-Nov-2000	12:57	5	1, 2, 3, 4, 5	0.956
370204	12	14-Jul-2001	10:39	7	1, 4, 5, 6, 7	0.926
370204	13	11-Oct-2001	08:45	7	1, 2, 3, 4, 5	0.959
370204	14	23-May-2002	11:02	9	5, 6, 7, 8, 9	0.930
370204	15	19-Sep-2002	18:15	9	4, 5, 6, 7, 9	0.958
370204	16	22-Jan-2003	16:27	9	4, 5, 6, 7, 9	0.952
370204	17	01-Jun-2003	08:03	7	1, 2, 4, 5, 7	0.948
370204	18	08-Nov-2003	13:59	5	1, 2, 3, 4, 5	0.924
370204	19	14-Nov-2004	11:02	9	1, 2, 3, 6, 7	0.964
370204	20	14-Jun-2006	16:01	9	2, 3, 4, 5, 8	0.966
370204	21	30-Nov-2006	13:01	9	2, 3, 5, 6, 9	0.933
370204	22	18-Mar-2009	16:21	9	3, 4, 5, 6, 7	0.974
370204	23	18-Apr-2010	15:03	9	1, 3, 4, 5, 7	0.964
370204	24	27-Apr-2011	19:38	9	1, 2, 3, 5, 7	0.964
370204	25	10-Dec-2012	13:30	7	1, 2, 3, 4, 6	0.976
370204	26	24-Jun-2014	13:23	5	1, 2, 3, 4, 5	0.938
370204	27	24-Jun-2014	16:42	6	1, 2, 3, 4, 6	0.957
370204	28	24-Jun-2014	19:20	5	1, 2, 3, 4, 5	0.918
370204	29	25-Jun-2014	06:08	4	1, 2, 3, 4	0.964
370204	30	09-Mar-2015	16:33	7	1, 2, 5, 6, 7	0.974
370205	01	30-Mar-1994	10:28	9	2, 3, 4, 8, 9	0.886
370205	02	06-Jan-1996	05:46	9	2, 3, 4, 6, 7	0.942
370205	03	28-Feb-1996	10:43	9	1, 4, 7, 8, 9	0.926
370205	S03	28-Feb-1996	18:16	6	1, 3, 4, 5, 6	0.906
370205	04	07-Oct-1997	13:36	9	1, 2, 4, 5, 6	0.906
370205	05	18-Feb-1998	13:23	7	1, 3, 4, 5, 6	0.923
370205	06	19-May-1998	11:08	9	3, 4, 5, 7, 8	0.916
370205	S09	19-May-1998	14:43	8	1, 3, 4, 6, 7	0.910
370205	07	24-Jul-1998	11:14	7	1, 2, 3, 4, 5	0.911
370205	08	04-Nov-1998	08:45	6	1, 2, 4, 5, 6	0.910
370205	09	10-Nov-1999	23:54	9	1, 4, 5, 6, 9	0.906
370205	10	13-Mar-2000	14:14	9	2, 3, 4, 6, 7	0.884
370205	11	08-Nov-2000	11:16	9	1, 3, 5, 8, 9	0.878
370205	S16	17-May-2001	07:09	7	1, 2, 3, 4, 5	0.945
370205	S17	17-May-2001	13:28	7	1, 3, 4, 5, 7	0.944
370205	12	14-Jul-2001	09:11	9	1, 2, 4, 6, 7	0.922
370205	13	11-Oct-2001	08:45	7	1, 2, 3, 4, 7	0.913
370205	14	23-May-2002	10:07	9	1, 3, 5, 6, 8	0.853
370205	15	19-Sep-2002	17:31	9	1, 3, 6, 8, 9	0.845
370205	16	22-Jan-2003	15:42	9	1, 2, 3, 7, 8	0.900
370205	17	01-Jun-2003	11:38	9	2, 4, 5, 7, 8	0.933
370206	01	30-Mar-1994	10:28	9	1, 2, 3, 4, 5	0.867
370206	02	06-Jan-1996	05:46	9	1, 2, 4, 5, 7	0.941
370206	03	28-Feb-1996	10:43	9	1, 2, 3, 4, 9	0.930

Section	Visit	Date	Time	Available Repeats	Selected Repeats	Composite Correlation
370206	04	07-Oct-1997	13:36	7	1, 2, 4, 5, 7	0.934
370206	05	18-Feb-1998	13:57	7	3, 4, 5, 6, 7	0.905
370206	06	19-May-1998	10:36	9	1, 2, 3, 7, 8	0.928
370206	07	24-Jul-1998	11:14	9	1, 2, 4, 6, 9	0.936
370206	08	04-Nov-1998	08:45	6	1, 2, 3, 4, 6	0.939
370206	09	10-Nov-1999	23:54	9	1, 2, 5, 7, 9	0.940
370206	10	13-Mar-2000	14:02	9	1, 2, 3, 4, 5	0.921
370206	11	08-Nov-2000	11:16	9	1, 2, 4, 5, 8	0.930
370206	12	14-Jul-2001	09:11	9	1, 2, 3, 4, 5	0.933
370206	13	11-Oct-2001	08:45	7	1, 2, 3, 4, 5	0.921
370206	14	23-May-2002	10:07	9	2, 3, 4, 8, 9	0.905
370206	15	19-Sep-2002	17:31	9	1, 3, 4, 5, 6	0.944
370206	16	22-Jan-2003	15:57	9	2, 3, 4, 6, 8	0.935
370206	17	01-Jun-2003	12:08	9	5, 6, 7, 8, 9	0.922
370207	01	30-Mar-1994	10:28	9	3, 4, 5, 8, 9	0.944
370207	02	06-Jan-1996	05:46	9	1, 2, 3, 5, 8	0.973
370207	03	28-Feb-1996	10:58	9	2, 6, 7, 8, 9	0.974
370207	04	07-Oct-1997	13:55	7	2, 4, 5, 6, 7	0.966
370207	05	18-Feb-1998	13:40	7	2, 3, 5, 6, 7	0.967
370207	06	19-May-1998	11:08	9	3, 4, 6, 8, 9	0.953
370207	07	24-Jul-1998	11:46	9	3, 6, 7, 8, 9	0.964
370207	08	04-Nov-1998	08:45	6	1, 2, 3, 4, 6	0.972
370207	09	10-Nov-1999	23:54	9	1, 3, 4, 8, 9	0.970
370207	10	13-Mar-2000	14:24	9	3, 4, 5, 7, 8	0.959
370207	11	08-Nov-2000	11:28	9	2, 4, 6, 8, 9	0.960
370207	12	14-Jul-2001	09:19	9	3, 4, 5, 6, 9	0.951
370207	13	11-Oct-2001	08:45	7	1, 2, 3, 4, 5	0.969
370207	14	23-May-2002	11:02	9	4, 6, 7, 8, 9	0.938
370207	15	19-Sep-2002	18:01	9	3, 5, 7, 8, 9	0.965
370207	16	22-Jan-2003	15:42	9	1, 2, 3, 4, 5	0.952
370207	17	01-Jun-2003	11:28	9	1, 4, 7, 8, 9	0.963
370207	18	07-Nov-2003	09:16	9	1, 2, 3, 4, 5	0.949
370207	19	14-Nov-2004	16:29	9	5, 6, 7, 8, 9	0.963
370207	20	14-Jun-2006	16:16	9	3, 5, 6, 7, 8	0.945
370207	21	30-Nov-2006	12:41	9	1, 3, 4, 5, 7	0.959
370207	22	18-Mar-2009	15:51	9	1, 2, 3, 5, 6	0.962
370207	23	18-Apr-2010	15:26	9	3, 6, 7, 8, 9	0.971
370207	24	27-Apr-2011	19:53	9	2, 3, 7, 8, 9	0.960
370207	25	10-Dec-2012	13:24	7	1, 3, 4, 5, 7	0.961
370207	26	24-Jun-2014	13:23	5	1, 2, 3, 4, 5	0.944
370207	27	24-Jun-2014	16:42	6	1, 2, 3, 4, 6	0.926
370207	28	24-Jun-2014	19:20	5	1, 2, 3, 4, 5	0.932
370207	29	25-Jun-2014	06:08	4	1, 2, 3, 4	0.975
370207	30	09-Mar-2015	16:33	7	1, 3, 5, 6, 7	0.956
370208	01	30-Mar-1994	10:28	9	1, 6, 7, 8, 9	0.867
370208	02	06-Jan-1996	05:46	9	2, 3, 5, 7, 9	0.961
370208	03	28-Feb-1996	10:43	9	1, 2, 5, 7, 8	0.952
370208	S03	28-Feb-1996	18:22	7	1, 2, 5, 6, 7	0.944
370208	04	07-Oct-1997	14:12	7	3, 4, 5, 6, 7	0.943
370208	05	18-Feb-1998	13:23	7	1, 2, 4, 6, 7	0.933
370208	06	19-May-1998	10:36	9	1, 4, 6, 8, 9	0.949

Section	Visit	Date	Time	Available Repeats	Selected Repeats	Composite Correlation
370208	07	24-Jul-1998	11:31	9	2, 3, 4, 6, 7	0.938
370208	08	04-Nov-1998	08:45	6	1, 2, 3, 4, 5	0.928
370208	09	10-Nov-1999	23:54	9	1, 3, 4, 5, 8	0.946
370208	10	13-Mar-2000	14:14	9	2, 3, 4, 5, 8	0.930
370208	11	08-Nov-2000	11:16	9	1, 2, 4, 7, 9	0.944
370208	S16	17-May-2001	08:37	5	1, 2, 3, 4, 5	0.962
370208	S17	17-May-2001	13:35	5	1, 2, 3, 4, 5	0.926
370208	12	14-Jul-2001	09:19	9	3, 4, 5, 6, 9	0.939
370208	13	11-Oct-2001	08:45	7	1, 2, 3, 4, 5	0.944
370208	14	23-May-2002	11:02	9	3, 4, 6, 7, 9	0.914
370208	15	19-Sep-2002	17:31	9	1, 2, 3, 6, 9	0.941
370208	16	22-Jan-2003	15:42	9	1, 2, 3, 6, 9	0.927
370208	17	01-Jun-2003	11:28	9	1, 2, 5, 7, 8	0.953
370208	18	07-Nov-2003	09:27	9	2, 3, 4, 8, 9	0.927
370208	19	14-Nov-2004	15:58	9	2, 4, 5, 6, 7	0.950
370208	20	14-Jun-2006	16:01	9	2, 4, 6, 7, 8	0.927
370208	21	30-Nov-2006	13:43	9	5, 6, 7, 8, 9	0.922
370208	22	18-Mar-2009	15:51	9	1, 2, 5, 6, 7	0.952
370208	23	18-Apr-2010	15:03	9	1, 2, 3, 5, 8	0.942
370208	24	27-Apr-2011	19:38	9	1, 2, 3, 4, 5	0.973
370208	25	10-Dec-2012	13:24	7	1, 2, 4, 6, 7	0.944
370208	26	24-Jun-2014	13:23	5	1, 2, 3, 4, 5	0.902
370208	27	24-Jun-2014	16:57	6	2, 3, 4, 5, 6	0.942
370208	28	24-Jun-2014	19:20	5	1, 2, 3, 4, 5	0.952
370208	29	25-Jun-2014	06:08	4	1, 2, 3, 4	0.964
370208	30	09-Mar-2015	16:33	7	1, 3, 4, 6, 7	0.930
370209	01	30-Mar-1994	10:28	9	2, 3, 4, 8, 9	0.889
370209	02	06-Jan-1996	05:46	9	2, 3, 5, 8, 9	0.938
370209	03	28-Feb-1996	10:58	9	2, 4, 5, 6, 7	0.927
370209	S03	28-Feb-1996	18:16	6	1, 2, 3, 4, 5	0.919
370209	04	07-Oct-1997	13:36	7	1, 3, 4, 5, 7	0.919
370209	05	18-Feb-1998	13:40	7	2, 3, 4, 5, 6	0.917
370209	06	19-May-1998	11:08	9	3, 4, 5, 8, 9	0.903
370209	S09	19-May-1998	14:43	8	1, 3, 5, 7, 8	0.907
370209	07	24-Jul-1998	11:14	7	1, 2, 4, 5, 6	0.932
370209	08	04-Nov-1998	08:45	6	1, 2, 4, 5, 6	0.909
370209	09	10-Nov-1999	23:54	9	1, 2, 5, 7, 8	0.925
370209	10	13-Mar-2000	14:14	9	2, 3, 4, 5, 7	0.940
370209	11	08-Nov-2000	11:16	9	1, 3, 4, 7, 8	0.908
370209	12	14-Jul-2001	09:19	9	3, 4, 6, 7, 9	0.931
370209	13	11-Oct-2001	08:45	7	1, 2, 3, 4, 5	0.901
370209	14	23-May-2002	10:07	9	2, 3, 6, 7, 9	0.923
370209	15	19-Sep-2002	17:48	9	2, 4, 6, 8, 9	0.927
370209	16	22-Jan-2003	15:57	9	2, 3, 7, 8, 9	0.918
370209	17	01-Jun-2003	11:28	9	1, 2, 5, 6, 9	0.935
370210	01	30-Mar-1994	10:28	9	2, 3, 5, 8, 9	0.861
370210	02	06-Jan-1996	05:46	9	3, 6, 7, 8, 9	0.953
370210	03	28-Feb-1996	11:31	9	4, 6, 7, 8, 9	0.935
370210	S03	28-Feb-1996	18:16	6	1, 3, 4, 5, 6	0.918
370210	04	07-Oct-1997	14:12	7	3, 4, 5, 6, 7	0.951
370210	05	18-Feb-1998	13:40	7	2, 3, 5, 6, 7	0.934

Section	Visit	Date	Time	Available Repeats	Selected Repeats	Composite Correlation
370210	06	19-May-1998	11:39	9	5, 6, 7, 8, 9	0.931
370210	S09	19-May-1998	14:43	8	1, 2, 3, 5, 8	0.944
370210	07	24-Jul-1998	11:14	9	1, 2, 4, 6, 8	0.935
370210	08	04-Nov-1998	08:45	6	1, 2, 4, 5, 6	0.932
370210	09	10-Nov-1999	23:54	9	1, 4, 5, 6, 9	0.948
370210	10	13-Mar-2000	14:02	9	1, 2, 3, 4, 5	0.922
370210	11	08-Nov-2000	11:28	9	4, 5, 7, 8, 9	0.939
370210	12	14-Jul-2001	09:11	9	1, 3, 4, 5, 6	0.935
370210	13	11-Oct-2001	08:45	7	1, 2, 3, 4, 5	0.917
370210	14	23-May-2002	11:02	9	4, 6, 7, 8, 9	0.910
370210	15	19-Sep-2002	17:48	9	2, 3, 4, 5, 6	0.923
370210	16	22-Jan-2003	15:42	9	1, 2, 4, 7, 8	0.925
370210	17	01-Jun-2003	11:28	9	1, 2, 3, 4, 7	0.948
370211	01	30-Mar-1994	10:28	9	2, 3, 5, 7, 9	0.936
370211	02	06-Jan-1996	05:46	9	1, 2, 3, 4, 8	0.948
370211	03	28-Feb-1996	10:58	9	2, 3, 4, 7, 8	0.951
370211	04	07-Oct-1997	13:36	7	1, 2, 3, 4, 5	0.939
370211	05	18-Feb-1998	13:40	7	2, 3, 4, 5, 6	0.950
370211	06	19-May-1998	10:52	9	2, 3, 4, 6, 9	0.934
370211	07	24-Jul-1998	11:31	9	2, 3, 4, 7, 8	0.962
370211	08	04-Nov-1998	08:45	6	1, 3, 4, 5, 6	0.936
370211	09	10-Nov-1999	23:54	9	1, 2, 6, 7, 9	0.942
370211	10	13-Mar-2000	14:02	9	1, 3, 4, 5, 9	0.921
370211	11	08-Nov-2000	11:16	9	1, 2, 3, 7, 9	0.935
370211	12	14-Jul-2001	09:11	9	1, 3, 4, 7, 9	0.947
370211	13	11-Oct-2001	08:45	7	1, 2, 3, 4, 5	0.960
370211	14	23-May-2002	10:07	9	1, 2, 5, 7, 8	0.881
370211	15	19-Sep-2002	17:31	9	1, 2, 3, 4, 5	0.920
370211	16	22-Jan-2003	15:42	9	1, 3, 4, 6, 9	0.913
370211	17	01-Jun-2003	11:28	9	1, 2, 3, 4, 8	0.932
370211	18	07-Nov-2003	09:16	9	1, 2, 3, 4, 9	0.940
370211	19	14-Nov-2004	15:58	9	2, 3, 4, 6, 8	0.928
370211	20	14-Jun-2006	16:16	9	3, 4, 5, 6, 7	0.907
370211	21	30-Nov-2006	12:41	9	1, 3, 5, 7, 9	0.812
370211	22	18-Mar-2009	16:21	9	3, 4, 6, 8, 9	0.952
370211	23	18-Apr-2010	15:03	9	1, 2, 5, 6, 9	0.947
370211	24	27-Apr-2011	19:38	9	1, 2, 6, 7, 9	0.922
370211	25	10-Dec-2012	13:24	7	1, 2, 3, 4, 7	0.920
370211	26	24-Jun-2014	13:23	5	1, 2, 3, 4, 5	0.880
370211	27	24-Jun-2014	16:42	6	1, 2, 4, 5, 6	0.890
370211	28	24-Jun-2014	19:20	5	1, 2, 3, 4, 5	0.908
370211	29	25-Jun-2014	06:08	4	1, 2, 3, 4	0.876
370211	30	09-Mar-2015	16:33	7	1, 4, 5, 6, 7	0.902
370212	01	30-Mar-1994	10:28	9	2, 3, 6, 8, 9	0.880
370212	02	06-Jan-1996	05:46	9	1, 3, 4, 6, 8	0.931
370212	03	28-Feb-1996	10:43	9	1, 2, 7, 8, 9	0.912
370212	04	07-Oct-1997	14:12	7	3, 4, 5, 6, 7	0.900
370212	05	18-Feb-1998	13:23	7	1, 2, 3, 6, 7	0.917
370212	06	19-May-1998	10:36	9	1, 2, 5, 7, 9	0.903
370212	07	24-Jul-1998	11:31	9	2, 3, 4, 6, 7	0.919
370212	08	04-Nov-1998	08:45	6	1, 2, 3, 4, 5	0.918

Section	Visit	Date	Time	Available Repeats	Selected Repeats	Composite Correlation
370212	09	10-Nov-1999	23:54	9	1, 2, 3, 4, 9	0.920
370212	10	13-Mar-2000	14:02	9	1, 2, 3, 4, 5	0.909
370212	11	08-Nov-2000	11:16	9	1, 3, 6, 7, 8	0.876
370212	S16	17-May-2001	08:37	5	1, 2, 3, 4, 5	0.940
370212	S17	17-May-2001	13:35	5	1, 2, 3, 4, 5	0.961
370212	12	14-Jul-2001	09:19	9	3, 5, 6, 8, 9	0.904
370212	13	11-Oct-2001	08:45	7	1, 2, 3, 4, 5	0.935
370212	14	23-May-2002	10:07	9	1, 2, 3, 5, 7	0.892
370212	15	19-Sep-2002	17:48	9	2, 3, 4, 6, 7	0.947
370212	16	22-Jan-2003	15:42	9	1, 2, 3, 4, 5	0.903
370212	17	01-Jun-2003	11:38	9	2, 3, 4, 6, 7	0.910
370212	18	07-Nov-2003	09:16	9	1, 2, 3, 4, 5	0.884
370212	19	14-Nov-2004	15:48	9	1, 3, 4, 6, 8	0.923
370212	20	14-Jun-2006	16:31	9	4, 5, 7, 8, 9	0.933
370212	21	30-Nov-2006	12:41	9	1, 3, 4, 5, 7	0.889
370212	22	18-Mar-2009	16:37	9	4, 5, 7, 8, 9	0.906
370212	23	18-Apr-2010	15:14	9	2, 3, 4, 6, 8	0.905
370212	24	27-Apr-2011	19:38	9	1, 2, 3, 4, 6	0.935
370212	25	10-Dec-2012	13:24	7	1, 2, 3, 5, 6	0.902
370212	26	24-Jun-2014	13:23	5	1, 2, 3, 4, 5	0.875
370212	27	24-Jun-2014	16:42	6	1, 2, 4, 5, 6	0.904
370212	28	24-Jun-2014	19:20	5	1, 2, 3, 4, 5	0.865
370212	29	25-Jun-2014	06:08	4	1, 2, 3, 4	0.926
370212	30	09-Mar-2015	16:33	7	1, 2, 4, 6, 7	0.938
370259	01	30-Mar-1994	10:28	9	5, 6, 7, 8, 9	0.850
370259	02	06-Jan-1996	05:46	9	1, 3, 5, 8, 9	0.937
370259	03	28-Feb-1996	10:43	9	1, 3, 4, 5, 7	0.933
370259	S03	28-Feb-1996	18:16	6	1, 2, 3, 4, 6	0.931
370259	04	07-Oct-1997	13:55	7	2, 3, 4, 6, 7	0.957
370259	05	18-Feb-1998	13:23	7	1, 2, 5, 6, 7	0.940
370259	06	19-May-1998	10:36	9	1, 2, 4, 5, 7	0.911
370259	07	24-Jul-1998	11:31	7	2, 3, 4, 5, 6	0.947
370259	08	04-Nov-1998	08:45	6	1, 2, 3, 4, 5	0.956
370259	09	10-Nov-1999	23:54	9	1, 2, 3, 4, 8	0.924
370259	10	13-Mar-2000	14:24	9	3, 5, 6, 7, 9	0.904
370259	11	08-Nov-2000	11:16	9	1, 4, 5, 6, 9	0.914
370259	12	14-Jul-2001	09:19	9	3, 4, 6, 7, 8	0.931
370259	13	11-Oct-2001	08:45	7	1, 2, 3, 4, 5	0.955
370259	14	23-May-2002	10:07	9	1, 2, 3, 4, 7	0.929
370259	15	19-Sep-2002	17:31	9	1, 3, 4, 5, 8	0.893
370259	16	22-Jan-2003	15:57	9	2, 3, 6, 7, 8	0.884
370259	17	01-Jun-2003	11:28	9	1, 4, 5, 6, 8	0.935
370259	18	08-Nov-2003	12:57	5	1, 2, 3, 4, 5	0.929
370259	19	14-Nov-2004	15:46	9	1, 2, 3, 5, 8	0.943
370259	20	14-Jun-2006	16:01	9	2, 3, 5, 6, 7	0.952
370259	21	30-Nov-2006	12:41	9	1, 3, 4, 8, 9	0.879
370259	22	18-Mar-2009	15:51	9	1, 2, 4, 6, 7	0.949
370259	23	18-Apr-2010	15:14	9	2, 4, 5, 6, 7	0.939
370259	24	27-Apr-2011	19:53	9	2, 3, 4, 5, 9	0.918
370259	25	10-Dec-2012	13:20	7	1, 3, 5, 6, 7	0.938
370259	26	24-Jun-2014	13:23	5	1, 2, 3, 4, 5	0.905

Section	Visit	Date	Time	Available Repeats	Selected Repeats	Composite Correlation
370259	27	24-Jun-2014	16:42	6	1, 2, 3, 4, 5	0.884
370259	28	24-Jun-2014	19:20	5	1, 2, 3, 4, 5	0.898
370259	29	25-Jun-2014	06:08	4	1, 2, 3, 4	0.856
370259	30	09-Mar-2015	16:33	7	1, 4, 5, 6, 7	0.937
370260	01	30-Mar-1994	10:28	9	1, 2, 4, 5, 8	0.952
370260	02	06-Jan-1996	05:46	9	1, 2, 4, 8, 9	0.971
370260	03	28-Feb-1996	10:43	9	1, 3, 4, 7, 9	0.957
370260	04	07-Oct-1997	13:55	7	2, 3, 4, 5, 7	0.941
370260	05	18-Feb-1998	13:23	7	1, 2, 5, 6, 7	0.972
370260	06	19-May-1998	10:52	9	2, 6, 7, 8, 9	0.947
370260	07	24-Jul-1998	11:14	9	1, 2, 4, 7, 8	0.963
370260	08	04-Nov-1998	08:45	6	1, 2, 3, 4, 5	0.943
370260	09	11-Nov-1999	00:04	9	2, 3, 4, 5, 9	0.965
370260	10	13-Mar-2000	14:02	9	1, 3, 5, 6, 8	0.957
370260	11	08-Nov-2000	11:16	9	1, 3, 4, 5, 8	0.951
370260	12	14-Jul-2001	09:19	9	3, 4, 6, 7, 9	0.951
370260	13	11-Oct-2001	08:45	7	1, 2, 3, 4, 5	0.958
370260	14	23-May-2002	10:07	9	2, 3, 4, 6, 7	0.939
370260	15	19-Sep-2002	17:31	9	1, 4, 5, 6, 7	0.958
370260	16	22-Jan-2003	15:42	9	1, 3, 4, 6, 9	0.937
370260	17	01-Jun-2003	11:58	9	4, 5, 6, 7, 8	0.943
370260	18	07-Nov-2003	09:36	9	3, 4, 5, 8, 9	0.927
370260	19	14-Nov-2004	15:58	9	2, 6, 7, 8, 9	0.961
370260	20	14-Jun-2006	15:42	9	1, 3, 7, 8, 9	0.964
370260	21	30-Nov-2006	12:41	9	1, 3, 5, 6, 9	0.925
370260	22	18-Mar-2009	15:51	9	1, 2, 3, 5, 7	0.955
370260	23	18-Apr-2010	15:14	9	2, 3, 4, 6, 8	0.953
370260	24	27-Apr-2011	19:38	9	1, 3, 5, 6, 7	0.957
370260	25	10-Dec-2012	13:24	7	1, 2, 5, 6, 7	0.951
370260	26	24-Jun-2014	13:23	5	1, 2, 3, 4, 5	0.932
370260	27	24-Jun-2014	16:42	6	1, 2, 4, 5, 6	0.928
370260	28	24-Jun-2014	19:20	5	1, 2, 3, 4, 5	0.824
370260	29	25-Jun-2014	06:08	4	1, 2, 3, 4	0.934
370260	30	09-Mar-2015	16:33	7	1, 3, 5, 6, 7	0.931
390201	02	27-Dec-1996	10:22	7	1, 3, 5, 6, 7	0.957
390201	03	08-Dec-1997	09:21	7	1, 3, 4, 5, 7	0.966
390201	04	12-Nov-1998	09:39	7	2, 3, 4, 5, 7	0.973
390201	05	20-Oct-1999	08:44	7	1, 2, 3, 4, 5	0.954
390201	06	16-Aug-2000	09:17	7	1, 2, 3, 4, 5	0.966
390201	07	04-Nov-2001	08:30	7	3, 4, 5, 6, 7	0.970
390201	08	06-Dec-2002	11:26	7	1, 2, 3, 4, 6	0.978
390201	09	29-Apr-2003	14:15	9	1, 2, 3, 8, 9	0.976
390201	10	04-Feb-2004	15:12	9	3, 6, 7, 8, 9	0.976
390201	11	05-May-2005	12:20	9	1, 3, 5, 6, 8	0.975
390201	12	08-Aug-2006	12:10	9	2, 3, 4, 5, 6	0.977
390202	02	27-Dec-1996	10:35	7	2, 3, 5, 6, 7	0.945
390202	03	08-Dec-1997	09:21	7	1, 2, 3, 4, 6	0.965
390202	04	12-Nov-1998	09:39	7	2, 3, 4, 5, 6	0.978
390202	05	20-Oct-1999	09:04	7	3, 4, 5, 6, 7	0.976
390202	06	16-Aug-2000	09:55	7	2, 3, 4, 5, 7	0.977
390202	07	04-Nov-2001	08:18	7	2, 3, 4, 5, 6	0.969

Section	Visit	Date	Time	Available Repeats	Selected Repeats	Composite Correlation
390202	08	06-Dec-2002	11:26	7	1, 2, 4, 6, 7	0.982
390202	09	29-Apr-2003	14:19	9	2, 4, 5, 7, 8	0.981
390202	10	04-Feb-2004	14:54	9	1, 5, 7, 8, 9	0.987
390202	11	05-May-2005	12:29	9	2, 3, 4, 6, 8	0.981
390202	12	08-Aug-2006	12:10	9	2, 4, 7, 8, 9	0.980
390203	02	27-Dec-1996	10:35	7	2, 3, 4, 6, 7	0.922
390203	03	08-Dec-1997	09:21	7	1, 2, 5, 6, 7	0.959
390203	04	12-Nov-1998	09:24	7	1, 2, 4, 6, 7	0.948
390203	05	20-Oct-1999	08:44	7	1, 3, 4, 5, 6	0.953
390203	06	16-Aug-2000	09:17	7	1, 2, 4, 5, 6	0.944
390203	07	04-Nov-2001	08:18	7	2, 3, 4, 6, 7	0.937
390203	08	06-Dec-2002	11:26	7	1, 3, 4, 5, 6	0.958
390203	09	29-Apr-2003	14:15	9	1, 2, 4, 6, 7	0.947
390203	10	04-Feb-2004	15:20	9	4, 5, 6, 7, 8	0.964
390203	11	05-May-2005	12:29	9	2, 3, 4, 5, 8	0.939
390203	12	08-Aug-2006	12:21	9	3, 5, 6, 7, 8	0.935
390203	13	23-Jul-2008	14:21	9	2, 3, 4, 6, 9	0.940
390203	14	21-Oct-2009	14:32	9	1, 4, 5, 6, 8	0.939
390203	15	11-Aug-2010	10:58	9	3, 4, 5, 8, 9	0.969
390203	16	18-Oct-2011	10:41	9	2, 3, 5, 7, 8	0.964
390203	17	22-May-2012	13:37	9	1, 3, 5, 6, 7	0.955
390203	18	03-Jun-2014	14:27	7	1, 3, 4, 5, 6	0.944
390203	19	29-Jul-2014	19:55	5	1, 2, 3, 4, 5	0.940
390203	20	30-Jul-2014	06:06	6	2, 3, 4, 5, 6	0.944
390203	21	30-Jul-2014	13:01	5	1, 2, 3, 4, 5	0.915
390204	S01	15-Aug-1996	13:15	7	2, 3, 4, 5, 7	0.923
390204	02	27-Dec-1996	10:22	7	1, 2, 3, 5, 7	0.911
390204	03	08-Dec-1997	09:34	7	2, 3, 5, 6, 7	0.938
390204	S02	07-Mar-1998	06:12	5	1, 2, 3, 4, 5	0.937
390204	S03	07-Mar-1998	11:20	5	1, 2, 3, 4, 5	0.920
390204	S04	07-Mar-1998	15:06	5	1, 2, 3, 4, 5	0.941
390204	S05	28-May-1998	06:23	7	2, 3, 4, 6, 7	0.954
390204	S06	28-May-1998	15:06	7	1, 2, 4, 5, 7	0.934
390204	S07	13-Aug-1998	03:22	7	1, 3, 4, 5, 6	0.946
390204	S08	13-Aug-1998	07:31	7	2, 3, 4, 6, 7	0.945
390204	04	12-Nov-1998	09:24	7	1, 2, 3, 4, 5	0.958
390204	S09	12-Nov-1998	15:01	7	1, 3, 4, 6, 7	0.946
390204	S10	10-Mar-1999	06:25	5	1, 2, 3, 4, 5	0.909
390204	S11	10-Mar-1999	14:00	5	1, 2, 3, 4, 5	0.949
390204	S12	22-Jun-1999	06:14	7	1, 3, 4, 5, 7	0.927
390204	S13	22-Jun-1999	15:32	7	3, 4, 5, 6, 7	0.953
390204	05	20-Oct-1999	08:54	7	2, 3, 4, 5, 6	0.964
390204	S14	17-Jun-2000	05:23	7	1, 4, 5, 6, 7	0.957
390204	S15	17-Jun-2000	14:35	7	1, 4, 5, 6, 7	0.964
390204	06	16-Aug-2000	09:17	7	1, 2, 3, 4, 6	0.956
390204	07	04-Nov-2001	08:30	7	3, 4, 5, 6, 7	0.955
390204	08	06-Dec-2002	11:36	7	2, 3, 4, 5, 7	0.967
390204	09	29-Apr-2003	14:19	9	2, 4, 5, 6, 9	0.943
390204	10	04-Feb-2004	15:12	9	3, 4, 6, 7, 8	0.961
390204	11	05-May-2005	12:37	9	3, 4, 5, 7, 8	0.957
390204	12	08-Aug-2006	12:10	9	2, 4, 5, 7, 8	0.957

Section	Visit	Date	Time	Available Repeats	Selected Repeats	Composite Correlation
390205	02	27-Dec-1996	10:22	7	1, 2, 3, 6, 7	0.932
390205	03	08-Dec-1997	09:21	7	1, 2, 3, 4, 5	0.955
390205	04	12-Nov-1998	09:24	7	1, 2, 3, 4, 5	0.965
390205	05	20-Oct-1999	08:44	7	1, 2, 3, 4, 5	0.968
390205	06	16-Aug-2000	09:17	7	1, 3, 4, 5, 7	0.974
390205	07	04-Nov-2001	07:59	7	1, 3, 4, 5, 6	0.968
390205	08	06-Dec-2002	11:26	7	1, 2, 4, 6, 7	0.963
390205	09	29-Apr-2003	14:15	9	1, 3, 4, 5, 7	0.977
390205	10	04-Feb-2004	14:54	9	1, 3, 5, 6, 7	0.976
390205	11	05-May-2005	12:20	9	1, 2, 4, 7, 8	0.968
390205	12	08-Aug-2006	12:10	9	2, 4, 5, 6, 7	0.969
390206	02	27-Dec-1996	10:22	7	1, 2, 4, 5, 6	0.937
390206	03	08-Dec-1997	09:21	7	1, 2, 3, 4, 7	0.963
390206	04	12-Nov-1998	09:24	7	1, 3, 4, 5, 7	0.976
390206	05	20-Oct-1999	08:44	7	1, 2, 3, 4, 6	0.964
390206	06	16-Aug-2000	09:17	7	1, 3, 4, 5, 7	0.953
390206	07	04-Nov-2001	07:59	7	1, 2, 3, 4, 5	0.950
390206	08	06-Dec-2002	11:26	7	1, 2, 3, 5, 6	0.891
390206	09	29-Apr-2003	14:19	9	2, 3, 4, 6, 7	0.919
390206	10	04-Feb-2004	14:54	9	1, 3, 4, 6, 7	0.936
390206	11	05-May-2005	12:20	9	1, 2, 5, 7, 8	0.900
390206	12	08-Aug-2006	11:39	9	1, 2, 3, 6, 8	0.813
390207	02	27-Dec-1996	10:22	7	1, 2, 3, 5, 7	0.946
390207	03	08-Dec-1997	09:21	7	1, 2, 4, 5, 7	0.965
390207	04	12-Nov-1998	09:24	7	1, 2, 3, 4, 5	0.964
390207	05	20-Oct-1999	08:44	7	1, 2, 3, 5, 7	0.966
390207	06	16-Aug-2000	09:55	7	2, 3, 4, 5, 6	0.966
390207	07	04-Nov-2001	07:59	7	1, 2, 3, 4, 5	0.943
390207	08	06-Dec-2002	11:46	7	3, 4, 5, 6, 7	0.956
390207	09	29-Apr-2003	14:15	9	1, 2, 7, 8, 9	0.958
390207	10	04-Feb-2004	14:54	9	1, 5, 6, 8, 9	0.932
390207	11	05-May-2005	12:37	9	3, 4, 6, 8, 9	0.964
390207	12	08-Aug-2006	12:10	9	2, 4, 5, 7, 8	0.956
390207	13	23-Jul-2008	14:13	9	1, 2, 4, 5, 7	0.955
390207	14	21-Oct-2009	14:32	9	1, 3, 4, 8, 9	0.944
390207	15	11-Aug-2010	10:40	9	1, 3, 5, 7, 8	0.975
390207	16	18-Oct-2011	10:48	9	3, 4, 6, 8, 9	0.967
390207	17	22-May-2012	13:37	9	1, 4, 6, 8, 9	0.966
390207	18	03-Jun-2014	14:27	7	1, 2, 3, 4, 5	0.968
390207	19	29-Jul-2014	19:55	6	1, 2, 4, 5, 6	0.941
390207	20	30-Jul-2014	05:57	6	1, 2, 4, 5, 6	0.949
390207	21	30-Jul-2014	13:01	5	1, 2, 3, 4, 5	0.954
390208	02	27-Dec-1996	10:35	7	2, 4, 5, 6, 7	0.944
390208	03	08-Dec-1997	09:34	7	2, 3, 4, 5, 7	0.959
390208	04	12-Nov-1998	09:24	7	1, 3, 4, 6, 7	0.950
390208	05	20-Oct-1999	08:44	7	1, 3, 5, 6, 7	0.957
390208	06	16-Aug-2000	09:17	7	1, 3, 4, 5, 7	0.958
390208	07	04-Nov-2001	08:30	7	3, 4, 5, 6, 7	0.949
390208	08	06-Dec-2002	11:26	7	1, 2, 5, 6, 7	0.945
390208	09	29-Apr-2003	14:19	9	2, 3, 5, 6, 9	0.968
390208	10	04-Feb-2004	15:12	9	3, 5, 6, 8, 9	0.970

Section	Visit	Date	Time	Available Repeats	Selected Repeats	Composite Correlation
390208	11	05-May-2005	12:29	9	2, 4, 5, 6, 8	0.945
390208	12	08-Aug-2006	12:10	9	2, 4, 5, 6, 7	0.947
390208	13	23-Jul-2008	14:13	9	1, 2, 4, 5, 9	0.938
390208	14	21-Oct-2009	14:46	9	2, 3, 4, 6, 8	0.912
390208	15	11-Aug-2010	10:58	9	3, 5, 7, 8, 9	0.962
390208	16	18-Oct-2011	10:34	9	1, 6, 7, 8, 9	0.959
390208	17	22-May-2012	13:37	9	1, 4, 7, 8, 9	0.955
390208	18	03-Jun-2014	14:27	7	1, 2, 3, 4, 7	0.961
390208	19	29-Jul-2014	19:55	6	1, 2, 3, 5, 6	0.968
390208	20	30-Jul-2014	05:57	6	1, 2, 3, 5, 6	0.941
390208	21	30-Jul-2014	13:01	6	1, 3, 4, 5, 6	0.948
390209	02	27-Dec-1996	10:22	7	1, 3, 4, 6, 7	0.915
390209	03	08-Dec-1997	09:21	7	1, 2, 4, 5, 7	0.941
390209	04	12-Nov-1998	09:24	7	1, 2, 3, 4, 6	0.943
390209	05	20-Oct-1999	08:44	7	1, 2, 3, 5, 6	0.935
390209	06	16-Aug-2000	09:17	7	1, 2, 4, 6, 7	0.945
390209	07	04-Nov-2001	08:30	7	3, 4, 5, 6, 7	0.942
390209	08	06-Dec-2002	11:36	7	2, 3, 4, 6, 7	0.935
390209	09	29-Apr-2003	14:37	9	3, 4, 6, 8, 9	0.947
390209	10	04-Feb-2004	15:01	9	2, 3, 4, 5, 6	0.943
390209	11	05-May-2005	12:20	9	1, 3, 5, 7, 9	0.953
390209	12	08-Aug-2006	12:10	9	2, 3, 4, 6, 9	0.952
390209	13	23-Jul-2008	14:13	9	1, 4, 5, 8, 9	0.943
390209	14	21-Oct-2009	14:53	9	3, 4, 5, 6, 8	0.952
390209	15	11-Aug-2010	10:40	9	1, 2, 3, 7, 8	0.961
390209	16	18-Oct-2011	10:34	9	1, 5, 7, 8, 9	0.963
390209	17	22-May-2012	13:37	9	1, 5, 7, 8, 9	0.974
390210	02	27-Dec-1996	10:22	7	1, 2, 3, 4, 7	0.931
390210	03	08-Dec-1997	09:21	7	1, 3, 4, 5, 7	0.970
390210	04	12-Nov-1998	09:24	7	1, 2, 5, 6, 7	0.932
390210	05	20-Oct-1999	08:44	7	1, 3, 5, 6, 7	0.945
390210	06	16-Aug-2000	09:17	7	1, 2, 3, 5, 7	0.945
390210	07	04-Nov-2001	07:59	7	1, 2, 3, 5, 6	0.950
390210	08	06-Dec-2002	11:26	7	1, 2, 4, 5, 6	0.940
390210	09	29-Apr-2003	14:44	9	4, 5, 7, 8, 9	0.964
390210	10	04-Feb-2004	15:20	9	4, 5, 6, 7, 8	0.947
390210	11	05-May-2005	12:20	9	1, 4, 6, 7, 8	0.946
390210	12	08-Aug-2006	12:21	9	3, 4, 5, 7, 8	0.947
390211	02	27-Dec-1996	10:22	7	1, 2, 3, 4, 5	0.940
390211	03	08-Dec-1997	09:21	7	1, 2, 4, 5, 7	0.955
390211	04	12-Nov-1998	09:24	7	1, 2, 3, 4, 5	0.973
390211	05	20-Oct-1999	08:44	7	1, 3, 4, 5, 7	0.961
390211	06	16-Aug-2000	09:17	7	1, 3, 4, 6, 7	0.955
390211	07	04-Nov-2001	08:30	7	3, 4, 5, 6, 7	0.962
390211	08	06-Dec-2002	11:26	7	1, 3, 4, 6, 7	0.961
390211	09	29-Apr-2003	14:37	9	3, 4, 6, 8, 9	0.955
390211	10	04-Feb-2004	15:01	9	2, 3, 6, 7, 9	0.951
390211	11	05-May-2005	12:37	9	3, 5, 6, 7, 9	0.964
390211	12	08-Aug-2006	11:39	9	1, 2, 4, 7, 8	0.943
390211	13	23-Jul-2008	14:13	9	1, 3, 4, 5, 9	0.974
390211	14	21-Oct-2009	14:32	9	1, 3, 5, 6, 9	0.949

Section	Visit	Date	Time	Available Repeats	Selected Repeats	Composite Correlation
390211	15	11-Aug-2010	10:50	9	2, 5, 6, 7, 8	0.973
390211	16	18-Oct-2011	10:34	9	1, 3, 6, 7, 9	0.959
390211	17	22-May-2012	13:44	9	2, 3, 5, 7, 9	0.961
390211	18	03-Jun-2014	14:27	7	1, 3, 4, 5, 6	0.969
390211	19	29-Jul-2014	19:55	5	1, 2, 3, 4, 5	0.953
390211	20	30-Jul-2014	05:57	6	1, 2, 3, 4, 5	0.949
390211	21	30-Jul-2014	13:01	5	1, 2, 3, 4, 5	0.950
390212	02	27-Dec-1996	10:22	7	1, 2, 3, 6, 7	0.938
390212	03	08-Dec-1997	09:34	7	2, 3, 4, 5, 6	0.964
390212	04	12-Nov-1998	09:24	7	1, 2, 3, 4, 5	0.956
390212	05	20-Oct-1999	08:44	7	1, 2, 3, 4, 7	0.944
390212	06	16-Aug-2000	10:08	7	3, 4, 5, 6, 7	0.952
390212	07	04-Nov-2001	08:18	7	2, 4, 5, 6, 7	0.963
390212	08	06-Dec-2002	11:36	7	2, 3, 4, 6, 7	0.939
390212	09	29-Apr-2003	14:15	9	1, 4, 5, 7, 9	0.962
390212	10	04-Feb-2004	14:54	9	1, 2, 3, 4, 5	0.952
390212	11	05-May-2005	12:29	9	2, 3, 5, 6, 8	0.958
390212	12	08-Aug-2006	12:21	9	3, 5, 6, 7, 8	0.949
390212	17	22-May-2012	13:37	9	1, 2, 6, 8, 9	0.956
390212	18	03-Jun-2014	14:27	7	1, 2, 3, 4, 5	0.904
390212	19	29-Jul-2014	19:55	6	1, 2, 4, 5, 6	0.958
390212	20	30-Jul-2014	05:57	6	1, 2, 3, 4, 6	0.930
390212	21	30-Jul-2014	13:01	6	1, 2, 3, 5, 6	0.959
390259	02	27-Dec-1996	10:35	7	2, 3, 4, 5, 7	0.913
390259	03	08-Dec-1997	09:21	7	1, 3, 5, 6, 7	0.941
390259	04	12-Nov-1998	09:24	7	1, 2, 3, 4, 5	0.944
390259	05	20-Oct-1999	09:04	7	3, 4, 5, 6, 7	0.947
390259	06	16-Aug-2000	09:55	7	2, 4, 5, 6, 7	0.947
390259	07	04-Nov-2001	08:18	7	2, 3, 4, 5, 6	0.937
390259	08	06-Dec-2002	11:46	7	3, 4, 5, 6, 7	0.934
390259	09	29-Apr-2003	14:44	9	4, 5, 6, 7, 8	0.934
390259	10	04-Feb-2004	15:12	9	3, 4, 5, 7, 8	0.952
390259	11	05-May-2005	12:37	9	3, 4, 5, 7, 9	0.960
390260	02	27-Dec-1996	10:22	7	1, 2, 3, 4, 7	0.946
390260	03	08-Dec-1997	09:21	7	1, 2, 3, 4, 6	0.955
390260	04	12-Nov-1998	09:24	7	1, 3, 4, 6, 7	0.947
390260	05	20-Oct-1999	08:44	7	1, 2, 4, 6, 7	0.949
390260	06	16-Aug-2000	09:17	7	1, 2, 3, 4, 6	0.943
390260	07	04-Nov-2001	07:59	7	1, 2, 4, 5, 6	0.948
390260	08	06-Dec-2002	11:26	7	1, 3, 4, 6, 7	0.944
390260	09	29-Apr-2003	14:15	9	1, 2, 3, 6, 8	0.943
390260	10	04-Feb-2004	15:12	9	3, 4, 5, 7, 9	0.956
390260	11	05-May-2005	12:37	9	3, 5, 6, 8, 9	0.953
390260	12	08-Aug-2006	12:21	9	3, 4, 6, 7, 9	0.938
390260	13	23-Jul-2008	14:21	9	2, 5, 6, 7, 9	0.947
390260	14	21-Oct-2009	14:32	9	1, 2, 3, 7, 9	0.924
390260	15	11-Aug-2010	10:50	9	2, 3, 4, 7, 8	0.951
390260	16	18-Oct-2011	10:41	9	2, 3, 4, 7, 9	0.941
390260	17	22-May-2012	13:37	9	1, 2, 3, 4, 8	0.941
390260	18	03-Jun-2014	14:27	7	1, 3, 4, 5, 6	0.942
390260	19	29-Jul-2014	20:06	6	2, 3, 4, 5, 6	0.953

Section	Visit	Date	Time	Available Repeats	Selected Repeats	Composite Correlation
390260	20	30-Jul-2014	05:57	6	1, 2, 3, 4, 6	0.949
390260	21	30-Jul-2014	13:01	6	1, 2, 3, 5, 6	0.958
390261	02	27-Dec-1996	10:22	7	1, 4, 5, 6, 7	0.938
390261	03	08-Dec-1997	09:34	7	2, 4, 5, 6, 7	0.965
390261	04	12-Nov-1998	09:24	7	1, 2, 4, 5, 6	0.944
390261	05	20-Oct-1999	09:04	7	3, 4, 5, 6, 7	0.966
390261	06	16-Aug-2000	09:17	7	1, 3, 4, 5, 6	0.950
390261	07	04-Nov-2001	07:59	7	1, 2, 3, 4, 7	0.951
390261	08	06-Dec-2002	11:36	7	2, 3, 4, 5, 6	0.959
390261	09	29-Apr-2003	14:15	9	1, 4, 5, 6, 7	0.949
390261	10	04-Feb-2004	14:54	9	1, 2, 3, 5, 7	0.964
390261	11	05-May-2005	12:29	9	2, 3, 5, 7, 9	0.967
390261	12	08-Aug-2006	12:10	9	2, 4, 6, 8, 9	0.939
390261	13	23-Jul-2008	14:13	9	1, 3, 5, 6, 9	0.963
390261	14	21-Oct-2009	14:32	9	1, 2, 7, 8, 9	0.943
390261	15	11-Aug-2010	11:16	9	5, 6, 7, 8, 9	0.966
390261	16	18-Oct-2011	10:34	9	1, 3, 5, 6, 7	0.961
390261	17	22-May-2012	13:37	9	1, 3, 4, 6, 7	0.966
390261	18	03-Jun-2014	14:27	7	1, 2, 3, 6, 7	0.968
390261	19	29-Jul-2014	19:55	5	1, 2, 3, 4, 5	0.940
390261	20	30-Jul-2014	05:57	6	1, 2, 3, 4, 6	0.954
390261	21	30-Jul-2014	13:01	5	1, 2, 3, 4, 5	0.943
390262	02	27-Dec-1996	10:22	7	1, 2, 4, 5, 6	0.928
390262	03	08-Dec-1997	09:42	7	3, 4, 5, 6, 7	0.960
390262	04	12-Nov-1998	09:24	7	1, 2, 3, 6, 7	0.955
390262	05	20-Oct-1999	09:04	7	3, 4, 5, 6, 7	0.952
390262	06	16-Aug-2000	09:55	7	2, 3, 4, 6, 7	0.953
390262	07	04-Nov-2001	08:18	7	2, 4, 5, 6, 7	0.950
390262	08	06-Dec-2002	11:36	7	2, 3, 4, 6, 7	0.920
390262	10	04-Feb-2004	15:29	9	5, 6, 7, 8, 9	0.956
390262	11	05-May-2005	12:29	9	2, 4, 5, 8, 9	0.950
390262	12	08-Aug-2006	12:21	9	3, 4, 6, 8, 9	0.886
390262	13	23-Jul-2008	14:13	9	1, 2, 3, 5, 6	0.917
390262	14	21-Oct-2009	14:32	9	1, 4, 5, 6, 7	0.933
390262	15	11-Aug-2010	10:40	9	1, 2, 3, 5, 9	0.941
390262	16	18-Oct-2011	10:34	9	1, 2, 4, 5, 7	0.934
390262	17	22-May-2012	13:37	9	1, 3, 4, 5, 9	0.938
390262	18	03-Jun-2014	14:27	7	1, 2, 3, 4, 5	0.928
390262	19	29-Jul-2014	20:06	6	2, 3, 4, 5, 6	0.933
390262	20	30-Jul-2014	05:57	6	1, 2, 3, 5, 6	0.926
390262	21	30-Jul-2014	13:01	6	1, 3, 4, 5, 6	0.941
390263	02	27-Dec-1996	10:22	7	1, 2, 3, 5, 7	0.917
390263	03	08-Dec-1997	09:34	7	2, 4, 5, 6, 7	0.955
390263	04	12-Nov-1998	09:24	7	1, 2, 4, 5, 6	0.950
390263	05	20-Oct-1999	08:54	7	2, 3, 4, 5, 6	0.943
390263	06	16-Aug-2000	09:17	7	1, 3, 4, 6, 7	0.951
390263	07	04-Nov-2001	08:18	7	2, 4, 5, 6, 7	0.955
390263	08	06-Dec-2002	11:26	7	1, 2, 3, 6, 7	0.951
390263	10	04-Feb-2004	14:54	9	1, 5, 7, 8, 9	0.968
390263	11	05-May-2005	12:37	9	3, 5, 6, 7, 8	0.954
390263	12	08-Aug-2006	12:10	9	2, 3, 4, 7, 8	0.950

Section	Visit	Date	Time	Available Repeats	Selected Repeats	Composite Correlation
390263	13	23-Jul-2008	14:13	9	1, 2, 3, 7, 9	0.943
390263	14	21-Oct-2009	14:46	9	2, 3, 6, 8, 9	0.944
390263	15	11-Aug-2010	10:50	9	2, 6, 7, 8, 9	0.959
390263	16	18-Oct-2011	10:41	9	2, 3, 6, 7, 8	0.962
390263	17	22-May-2012	13:37	9	1, 2, 4, 5, 9	0.956
390263	18	03-Jun-2014	14:42	7	2, 3, 4, 6, 7	0.931
390263	19	29-Jul-2014	20:06	6	2, 3, 4, 5, 6	0.941
390263	20	30-Jul-2014	05:57	6	1, 2, 3, 5, 6	0.953
390263	21	30-Jul-2014	13:01	6	1, 2, 3, 5, 6	0.936
390264	02	27-Dec-1996	10:22	7	1, 2, 5, 6, 7	0.872
390264	03	08-Dec-1997	09:21	7	1, 2, 3, 5, 6	0.921
390264	04	12-Nov-1998	09:24	7	1, 2, 3, 4, 6	0.962
390264	05	20-Oct-1999	08:44	7	1, 4, 5, 6, 7	0.937
390264	06	16-Aug-2000	09:55	7	2, 3, 4, 5, 7	0.922
390264	07	04-Nov-2001	07:59	7	1, 2, 3, 6, 7	0.944
390264	08	06-Dec-2002	11:36	7	2, 3, 4, 5, 6	0.951
390264	10	04-Feb-2004	14:54	9	1, 4, 6, 7, 9	0.946
390264	11	05-May-2005	12:20	9	1, 4, 6, 8, 9	0.934
390264	17	22-May-2012	13:44	9	2, 3, 5, 7, 9	0.958
390265	02	27-Dec-1996	10:22	7	1, 2, 3, 5, 7	0.960
390265	03	08-Dec-1997	09:34	7	2, 3, 4, 5, 7	0.975
390265	04	12-Nov-1998	09:24	7	1, 2, 3, 6, 7	0.981
390265	05	20-Oct-1999	08:54	7	2, 3, 4, 5, 7	0.963
390265	06	16-Aug-2000	09:55	7	2, 3, 4, 5, 6	0.972
390265	07	04-Nov-2001	07:59	7	1, 3, 4, 5, 6	0.965
390265	08	06-Dec-2002	11:46	7	3, 4, 5, 6, 7	0.976
390265	09	29-Apr-2003	14:15	9	1, 2, 3, 4, 7	0.970
390265	10	04-Feb-2004	15:12	9	3, 4, 5, 7, 9	0.976
390265	11	05-May-2005	12:20	9	1, 5, 7, 8, 9	0.981
390265	12	08-Aug-2006	11:39	9	1, 2, 4, 6, 8	0.967
390265	13	23-Jul-2008	14:13	9	1, 2, 4, 7, 9	0.972
390265	14	21-Oct-2009	14:53	9	3, 4, 6, 7, 8	0.969
390265	15	11-Aug-2010	10:58	9	3, 5, 6, 8, 9	0.984
390265	16	18-Oct-2011	10:34	9	1, 2, 3, 5, 6	0.979
390265	17	22-May-2012	13:37	9	1, 3, 4, 5, 9	0.982
390265	18	03-Jun-2014	14:27	7	1, 2, 3, 4, 6	0.976
390265	19	29-Jul-2014	19:55	5	1, 2, 3, 4, 5	0.969
390265	20	30-Jul-2014	05:57	6	1, 2, 3, 4, 6	0.969
390265	21	30-Jul-2014	13:01	5	1, 2, 3, 4, 5	0.954
493011	01	02-Aug-1989	11:56	5	1, 2, 3, 4, 5	0.939
493011	02	01-Sep-1990	07:49	9	4, 5, 6, 7, 9	0.959
493011	03	22-Oct-1991	15:37	6	2, 3, 5, 6, 7	0.953
493011	04	12-Nov-1992	17:06	7	1, 3, 5, 6, 7	0.966
493011	05	15-Nov-1993	15:53	9	3, 5, 6, 7, 9	0.964
493011	06	13-Jan-1994	10:52	7	1, 2, 3, 4, 6	0.962
493011	07	16-Apr-1994	01:18	9	1, 2, 5, 6, 7	0.971
493011	08	14-Jul-1994	20:39	9	2, 3, 4, 5, 7	0.921
493011	09	13-Nov-1994	13:54	9	2, 3, 5, 7, 8	0.971
493011	10	15-Feb-1995	12:39	7	1, 3, 4, 5, 7	0.960
493011	11	18-May-1995	11:50	9	4, 5, 6, 7, 8	0.933
493011	12	05-Dec-1996	07:49	9	1, 2, 3, 7, 9	0.984

Section	Visit	Date	Time	Available Repeats	Selected Repeats	Composite Correlation
493011	13	05-Dec-1996	14:09	9	3, 4, 5, 8, 9	0.983
493011	14	02-Mar-1997	09:48	9	4, 6, 7, 8, 9	0.987
493011	15	02-Mar-1997	13:56	9	1, 2, 7, 8, 9	0.977
493011	16	25-Apr-1997	07:09	9	1, 4, 5, 7, 8	0.991
493011	17	25-Apr-1997	12:10	9	3, 4, 6, 8, 9	0.977
493011	18	01-Aug-1997	09:21	5	1, 2, 3, 4, 5	0.984
493011	19	01-Aug-1997	14:28	5	1, 2, 3, 4, 5	0.974
493011	20	17-Sep-1997	09:15	5	1, 2, 3, 4, 5	0.972
493011	21	17-Sep-1997	12:42	5	1, 2, 3, 4, 5	0.970
493011	22	01-Dec-1998	12:03	7	3, 4, 5, 6, 7	0.976
493011	23	13-Jul-1999	14:33	7	2, 3, 4, 6, 7	0.966
493011	24	09-Sep-2001	07:52	7	1, 3, 4, 6, 7	0.990
493011	25	26-Jan-2004	16:11	9	1, 3, 4, 7, 9	0.985
493011	26	06-Oct-2004	13:53	9	2, 4, 5, 6, 7	0.991
493011	27	20-Dec-2004	11:53	9	1, 4, 5, 6, 9	0.982
493011	28	09-Oct-2007	15:16	9	4, 5, 6, 7, 8	0.984
493011	29	26-Oct-2010	14:00	9	1, 6, 7, 8, 9	0.992
493011	30	23-Oct-2012	16:25	9	3, 4, 6, 7, 8	0.563
493011	31	20-May-2014	21:29	9	2, 3, 7, 8, 9	0.768
493011	32	18-May-2015	19:57	9	2, 5, 6, 7, 8	0.808
530201	01	18-Nov-1995	13:18	9	1, 2, 4, 5, 7	0.927
530201	02	06-Oct-1997	16:48	5	1, 2, 3, 4, 5	0.907
530201	03	15-May-1998	14:27	7	2, 3, 4, 5, 6	0.879
530201	04	07-May-1999	12:52	7	1, 3, 5, 6, 7	0.886
530201	05	29-Jun-2000	13:40	9	3, 5, 6, 7, 9	0.919
530201	06	07-Aug-2001	10:33	9	1, 2, 3, 5, 6	0.934
530201	07	05-Aug-2002	10:56	9	2, 3, 5, 6, 8	0.936
530201	08	20-Aug-2003	15:32	9	2, 3, 4, 6, 9	0.939
530201	09	23-Jul-2004	13:41	9	1, 2, 4, 5, 9	0.908
530201	10	24-Jun-2005	18:21	9	1, 2, 5, 6, 9	0.849
530201	11	07-Jun-2006	18:12	9	2, 3, 6, 7, 8	0.901
530201	12	19-Jul-2007	17:55	9	1, 2, 3, 4, 5	0.887
530201	13	12-Jun-2008	13:24	9	1, 5, 6, 8, 9	0.867
530201	14	30-Apr-2009	14:30	9	1, 3, 4, 6, 9	0.907
530201	15	29-Jul-2010	11:36	9	4, 5, 6, 7, 8	0.841
530201	16	05-Feb-2011	12:33	9	1, 2, 4, 5, 6	0.903
530201	17	14-May-2012	21:48	9	1, 5, 7, 8, 9	0.846
530201	18	17-May-2013	06:43	9	1, 2, 3, 4, 6	0.860
530201	19	17-May-2013	10:05	9	1, 2, 6, 8, 9	0.870
530201	20	17-May-2013	15:41	9	4, 5, 7, 8, 9	0.867
530201	21	16-Apr-2015	00:21	9	1, 4, 5, 6, 7	0.776
530202	01	18-Nov-1995	13:18	9	3, 4, 6, 7, 9	0.863
530202	02	06-Oct-1997	16:48	5	1, 2, 3, 4, 5	0.833
530202	03	15-May-1998	14:14	7	1, 2, 3, 4, 5	0.863
530202	04	07-May-1999	13:02	7	2, 3, 4, 6, 7	0.930
530202	05	29-Jun-2000	13:27	9	2, 4, 5, 6, 9	0.913
530202	06	07-Aug-2001	10:43	9	2, 3, 4, 5, 7	0.941
530202	07	05-Aug-2002	10:46	9	1, 2, 4, 6, 8	0.943
530202	08	20-Aug-2003	15:16	9	1, 2, 4, 6, 7	0.900
530202	09	23-Jul-2004	14:12	9	4, 5, 6, 7, 9	0.912
530202	10	24-Jun-2005	18:21	9	1, 2, 3, 8, 9	0.888

Section	Visit	Date	Time	Available Repeats	Selected Repeats	Composite Correlation
530202	11	07-Jun-2006	17:59	9	1, 3, 6, 7, 8	0.903
530202	12	19-Jul-2007	17:55	9	1, 2, 3, 4, 7	0.861
530202	13	12-Jun-2008	12:29	9	2, 5, 6, 8, 9	0.890
530202	14	30-Apr-2009	13:33	9	1, 4, 5, 7, 8	0.886
530202	15	29-Jul-2010	10:08	9	1, 2, 4, 5, 7	0.865
530202	16	05-Feb-2011	12:00	9	4, 6, 7, 8, 9	0.893
530202	17	14-May-2012	20:57	9	2, 3, 5, 7, 8	0.911
530202	18	16-May-2013	07:03	9	2, 4, 7, 8, 9	0.923
530202	19	16-May-2013	10:01	9	1, 5, 6, 7, 8	0.903
530202	20	16-May-2013	15:07	9	1, 2, 3, 6, 8	0.883
530202	21	16-Apr-2015	00:32	9	2, 3, 5, 6, 8	0.867
530203	01	18-Nov-1995	13:18	9	1, 3, 5, 6, 7	0.853
530203	02	06-Oct-1997	16:48	5	1, 2, 3, 4, 5	0.851
530203	03	15-May-1998	14:27	7	2, 4, 5, 6, 7	0.841
530203	04	07-May-1999	12:52	7	1, 2, 3, 6, 7	0.869
530203	05	29-Jun-2000	13:13	9	1, 4, 6, 7, 8	0.923
530203	06	07-Aug-2001	10:33	9	1, 2, 6, 7, 9	0.938
530203	07	05-Aug-2002	11:06	9	3, 4, 6, 8, 9	0.932
530203	08	20-Aug-2003	15:37	9	3, 4, 5, 6, 8	0.934
530203	09	23-Jul-2004	13:41	9	1, 2, 3, 6, 8	0.888
530203	10	24-Jun-2005	18:21	9	1, 3, 5, 6, 8	0.888
530203	11	07-Jun-2006	18:22	9	3, 4, 5, 7, 9	0.858
530203	12	19-Jul-2007	17:55	9	1, 2, 3, 4, 5	0.828
530203	13	12-Jun-2008	12:41	9	4, 5, 6, 8, 9	0.815
530203	14	30-Apr-2009	13:33	9	1, 2, 4, 7, 9	0.841
530203	15	29-Jul-2010	10:08	9	1, 3, 6, 8, 9	0.851
530203	16	05-Feb-2011	11:45	9	1, 2, 3, 4, 7	0.845
530203	17	14-May-2012	20:52	9	1, 3, 4, 7, 9	0.807
530203	18	16-May-2013	07:03	9	2, 4, 5, 7, 9	0.854
530203	19	16-May-2013	10:09	9	2, 3, 4, 5, 7	0.849
530203	20	16-May-2013	15:07	9	1, 2, 3, 8, 9	0.873
530203	21	16-Apr-2015	00:32	9	2, 4, 5, 8, 9	0.773
530204	01	18-Nov-1995	13:18	9	2, 5, 6, 7, 8	0.895
530204	02	06-Oct-1997	16:48	5	1, 2, 3, 4, 5	0.937
530204	03	15-May-1998	14:27	7	2, 3, 4, 5, 6	0.867
530204	04	07-May-1999	13:02	7	2, 3, 4, 6, 7	0.949
530204	05	29-Jun-2000	13:13	9	1, 2, 3, 4, 8	0.935
530204	06	07-Aug-2001	10:33	9	1, 2, 6, 7, 9	0.946
530204	07	05-Aug-2002	10:56	9	2, 3, 4, 5, 6	0.943
530204	08	20-Aug-2003	15:32	9	2, 3, 4, 6, 7	0.943
530204	09	23-Jul-2004	13:41	9	1, 2, 4, 6, 7	0.930
530204	10	24-Jun-2005	18:35	9	2, 3, 7, 8, 9	0.925
530204	11	07-Jun-2006	18:12	9	2, 5, 6, 8, 9	0.925
530204	12	19-Jul-2007	17:55	9	1, 2, 3, 4, 5	0.932
530204	13	12-Jun-2008	12:29	9	2, 3, 4, 7, 8	0.933
530204	14	30-Apr-2009	13:38	9	2, 3, 5, 7, 9	0.919
530204	15	29-Jul-2010	11:27	9	3, 4, 5, 6, 7	0.916
530204	16	05-Feb-2011	12:33	9	1, 2, 3, 4, 8	0.924
530204	17	14-May-2012	21:03	9	3, 4, 5, 6, 8	0.915
530204	18	17-May-2013	07:37	9	4, 5, 6, 7, 8	0.940
530204	19	17-May-2013	10:29	9	3, 4, 6, 7, 9	0.911

Section	Visit	Date	Time	Available Repeats	Selected Repeats	Composite Correlation
530204	20	17-May-2013	15:04	9	1, 2, 3, 5, 8	0.939
530204	21	16-Apr-2015	00:32	9	2, 4, 6, 7, 9	0.922
530205	01	18-Nov-1995	13:18	9	2, 3, 4, 5, 6	0.930
530205	02	06-Oct-1997	16:48	5	1, 2, 3, 4, 5	0.912
530205	03	15-May-1998	14:27	7	2, 4, 5, 6, 7	0.827
530205	04	07-May-1999	12:52	7	1, 3, 4, 6, 7	0.938
530205	05	29-Jun-2000	13:13	9	1, 2, 4, 6, 8	0.932
530205	06	07-Aug-2001	10:33	9	1, 2, 3, 7, 9	0.930
530205	07	05-Aug-2002	11:06	9	3, 4, 6, 7, 8	0.958
530205	08	20-Aug-2003	15:16	9	1, 2, 3, 5, 7	0.927
530205	09	23-Jul-2004	13:53	9	2, 5, 6, 7, 8	0.929
530205	10	24-Jun-2005	18:21	9	1, 2, 4, 5, 6	0.906
530205	11	07-Jun-2006	17:59	9	1, 2, 3, 4, 8	0.922
530205	12	19-Jul-2007	17:55	9	1, 2, 3, 7, 8	0.900
530205	13	12-Jun-2008	13:34	9	2, 5, 7, 8, 9	0.903
530205	14	30-Apr-2009	14:30	9	1, 2, 3, 6, 7	0.881
530205	15	29-Jul-2010	11:17	9	2, 5, 7, 8, 9	0.867
530205	16	05-Feb-2011	12:33	9	1, 2, 5, 7, 8	0.879
530205	17	14-May-2012	21:48	9	1, 2, 5, 6, 7	0.841
530205	18	17-May-2013	06:43	9	1, 3, 4, 6, 9	0.874
530205	19	17-May-2013	10:05	9	1, 3, 5, 6, 8	0.866
530205	20	17-May-2013	15:41	9	4, 5, 6, 7, 8	0.850
530205	21	16-Apr-2015	00:42	9	3, 5, 6, 8, 9	0.833
530206	01	18-Nov-1995	13:18	9	3, 4, 5, 8, 9	0.886
530206	02	06-Oct-1997	16:48	5	1, 2, 3, 4, 5	0.951
530206	03	15-May-1998	14:27	7	2, 3, 4, 5, 7	0.922
530206	04	07-May-1999	13:02	7	2, 3, 4, 5, 6	0.966
530206	05	29-Jun-2000	13:40	9	3, 4, 5, 6, 8	0.972
530206	06	07-Aug-2001	10:33	9	1, 2, 4, 5, 6	0.953
530206	07	05-Aug-2002	11:06	9	3, 4, 5, 6, 7	0.962
530206	08	20-Aug-2003	15:16	9	1, 2, 3, 6, 7	0.961
530206	09	23-Jul-2004	14:12	9	4, 6, 7, 8, 9	0.974
530206	10	24-Jun-2005	18:21	9	1, 3, 4, 5, 7	0.951
530206	11	07-Jun-2006	17:59	9	1, 4, 6, 8, 9	0.957
530206	12	19-Jul-2007	17:55	9	1, 2, 3, 4, 8	0.943
530206	13	12-Jun-2008	13:34	9	2, 4, 6, 7, 8	0.965
530206	14	30-Apr-2009	14:41	9	2, 3, 4, 5, 8	0.944
530206	15	29-Jul-2010	11:36	9	4, 5, 6, 7, 9	0.938
530206	16	05-Feb-2011	12:33	9	1, 3, 5, 7, 9	0.908
530206	17	14-May-2012	21:48	9	1, 2, 3, 7, 9	0.917
530206	18	17-May-2013	07:09	9	3, 5, 7, 8, 9	0.889
530206	19	17-May-2013	10:05	9	1, 5, 6, 7, 9	0.887
530206	20	17-May-2013	15:41	9	4, 5, 6, 8, 9	0.887
530206	21	16-Apr-2015	01:04	9	5, 6, 7, 8, 9	0.916
530207	01	18-Nov-1995	13:18	9	3, 4, 5, 6, 8	0.895
530207	02	06-Oct-1997	16:48	5	1, 2, 3, 4, 5	0.940
530207	03	15-May-1998	14:38	7	3, 4, 5, 6, 7	0.856
530207	04	07-May-1999	13:02	7	2, 4, 5, 6, 7	0.931
530207	05	29-Jun-2000	13:13	9	1, 3, 7, 8, 9	0.934
530207	06	07-Aug-2001	11:03	9	4, 5, 7, 8, 9	0.946
530207	07	05-Aug-2002	10:56	9	2, 3, 4, 8, 9	0.951

Section	Visit	Date	Time	Available Repeats	Selected Repeats	Composite Correlation
530207	08	20-Aug-2003	15:37	9	3, 4, 5, 6, 9	0.933
530207	09	23-Jul-2004	13:53	9	2, 3, 4, 7, 9	0.908
530207	10	24-Jun-2005	18:21	9	1, 2, 3, 5, 9	0.889
530207	11	07-Jun-2006	17:59	9	1, 3, 4, 5, 9	0.922
530207	12	19-Jul-2007	18:08	9	2, 5, 6, 8, 9	0.903
530207	13	12-Jun-2008	13:34	9	2, 3, 4, 5, 6	0.929
530207	14	30-Apr-2009	14:41	9	2, 3, 5, 6, 8	0.893
530207	15	29-Jul-2010	11:27	9	3, 4, 6, 8, 9	0.886
530207	16	05-Feb-2011	12:33	9	1, 3, 4, 5, 8	0.814
530207	17	14-May-2012	21:48	9	1, 3, 4, 5, 9	0.895
530207	18	17-May-2013	06:43	9	1, 2, 5, 6, 7	0.920
530207	19	17-May-2013	10:05	9	1, 2, 4, 8, 9	0.896
530207	20	17-May-2013	15:04	9	1, 2, 6, 7, 8	0.872
530207	21	16-Apr-2015	00:21	9	1, 5, 6, 7, 9	0.768
530208	01	18-Nov-1995	13:18	9	2, 4, 6, 7, 9	0.845
530208	02	06-Oct-1997	16:48	5	1, 2, 3, 4, 5	0.909
530208	03	15-May-1998	14:14	7	1, 2, 3, 4, 5	0.854
530208	04	07-May-1999	13:02	7	2, 3, 4, 5, 7	0.916
530208	05	29-Jun-2000	13:13	9	1, 4, 7, 8, 9	0.948
530208	06	07-Aug-2001	10:33	9	1, 2, 5, 8, 9	0.942
530208	07	05-Aug-2002	10:56	9	2, 3, 5, 6, 8	0.943
530208	08	20-Aug-2003	15:16	9	1, 3, 4, 5, 9	0.957
530208	09	23-Jul-2004	13:53	9	2, 3, 4, 6, 8	0.956
530208	10	24-Jun-2005	18:21	9	1, 3, 5, 6, 7	0.946
530208	11	07-Jun-2006	17:59	9	1, 2, 5, 6, 8	0.955
530208	12	19-Jul-2007	17:55	9	1, 2, 4, 5, 7	0.949
530208	13	12-Jun-2008	13:24	9	1, 2, 4, 5, 8	0.957
530208	14	30-Apr-2009	14:30	9	1, 2, 4, 8, 9	0.952
530208	15	29-Jul-2010	11:36	9	4, 5, 6, 7, 8	0.947
530208	16	05-Feb-2011	12:42	9	2, 4, 5, 6, 8	0.948
530208	17	14-May-2012	22:27	9	4, 6, 7, 8, 9	0.943
530208	18	17-May-2013	07:09	9	3, 4, 5, 6, 7	0.959
530208	19	17-May-2013	10:17	9	2, 3, 4, 8, 9	0.939
530208	20	17-May-2013	15:17	9	2, 3, 6, 7, 8	0.949
530208	21	16-Apr-2015	00:21	9	1, 2, 4, 5, 9	0.927
530209	01	18-Nov-1995	13:18	9	1, 2, 4, 6, 7	0.817
530209	02	06-Oct-1997	16:48	5	1, 2, 3, 4, 5	0.815
530209	03	15-May-1998	14:14	7	1, 2, 3, 5, 7	0.843
530209	04	07-May-1999	13:02	7	2, 3, 4, 5, 7	0.898
530209	05	29-Jun-2000	13:52	9	4, 5, 6, 8, 9	0.899
530209	06	07-Aug-2001	10:33	9	1, 4, 5, 7, 9	0.902
530209	07	05-Aug-2002	10:56	9	2, 5, 7, 8, 9	0.864
530209	08	20-Aug-2003	15:32	9	2, 3, 4, 6, 8	0.924
530209	09	23-Jul-2004	13:53	9	2, 3, 4, 5, 7	0.919
530209	10	24-Jun-2005	18:21	9	1, 2, 4, 6, 8	0.849
530209	11	07-Jun-2006	18:12	9	2, 3, 6, 7, 8	0.911
530209	12	19-Jul-2007	17:55	9	1, 2, 4, 7, 8	0.887
530209	13	12-Jun-2008	12:41	9	4, 5, 6, 7, 8	0.930
530209	14	30-Apr-2009	13:38	9	2, 4, 5, 7, 9	0.914
530209	15	29-Jul-2010	10:19	9	3, 6, 7, 8, 9	0.910
530209	16	05-Feb-2011	12:00	9	4, 5, 6, 8, 9	0.868

Section	Visit	Date	Time	Available Repeats	Selected Repeats	Composite Correlation
530209	17	14-May-2012	20:57	9	2, 5, 6, 7, 9	0.888
530209	18	16-May-2013	06:53	9	1, 2, 3, 4, 7	0.894
530209	19	16-May-2013	10:18	9	3, 4, 6, 8, 9	0.882
530209	20	16-May-2013	15:07	9	1, 3, 5, 6, 8	0.853
530209	21	16-Apr-2015	00:21	9	1, 2, 4, 5, 6	0.825
530210	01	18-Nov-1995	13:18	9	2, 3, 6, 7, 9	0.777
530210	02	06-Oct-1997	16:48	5	1, 2, 3, 4, 5	0.804
530210	03	15-May-1998	14:27	7	2, 3, 5, 6, 7	0.843
530210	04	07-May-1999	12:52	7	1, 3, 4, 5, 6	0.841
530210	05	29-Jun-2000	13:27	9	2, 3, 4, 7, 8	0.924
530210	06	07-Aug-2001	10:43	9	2, 3, 4, 7, 9	0.863
530210	07	05-Aug-2002	10:46	9	1, 2, 4, 6, 9	0.905
530210	08	20-Aug-2003	15:32	9	2, 3, 5, 7, 9	0.893
530210	09	23-Jul-2004	13:53	9	2, 3, 5, 7, 8	0.862
530210	10	24-Jun-2005	18:21	9	1, 3, 4, 5, 8	0.805
530210	11	07-Jun-2006	17:59	9	1, 3, 6, 7, 8	0.867
530210	12	19-Jul-2007	18:08	9	2, 3, 4, 5, 7	0.861
530210	13	12-Jun-2008	12:24	9	1, 2, 5, 6, 9	0.901
530210	14	30-Apr-2009	13:38	9	2, 4, 5, 6, 8	0.904
530210	15	29-Jul-2010	10:19	9	3, 4, 7, 8, 9	0.839
530210	16	05-Feb-2011	11:50	9	2, 3, 4, 6, 9	0.921
530210	17	14-May-2012	20:52	9	1, 4, 6, 8, 9	0.846
530210	18	16-May-2013	07:03	9	2, 3, 4, 5, 8	0.879
530210	19	16-May-2013	10:26	9	4, 6, 7, 8, 9	0.879
530210	20	16-May-2013	15:21	9	2, 4, 7, 8, 9	0.851
530210	21	16-Apr-2015	00:32	9	2, 3, 6, 7, 8	0.877
530211	01	18-Nov-1995	13:18	9	1, 3, 5, 8, 9	0.785
530211	02	06-Oct-1997	16:48	5	1, 2, 3, 4, 5	0.724
530211	03	15-May-1998	14:27	7	2, 4, 5, 6, 7	0.720
530211	04	07-May-1999	12:52	7	1, 2, 5, 6, 7	0.856
530211	05	29-Jun-2000	13:13	9	1, 4, 6, 7, 9	0.866
530211	06	07-Aug-2001	10:33	9	1, 2, 4, 6, 7	0.908
530211	07	05-Aug-2002	11:17	9	4, 5, 7, 8, 9	0.874
530211	08	20-Aug-2003	15:32	9	2, 3, 6, 7, 8	0.892
530211	09	23-Jul-2004	13:53	9	2, 3, 6, 7, 8	0.872
530211	10	24-Jun-2005	19:06	9	3, 5, 6, 7, 8	0.816
530211	11	07-Jun-2006	18:12	9	2, 3, 4, 7, 8	0.830
530211	12	19-Jul-2007	17:55	9	1, 3, 4, 5, 9	0.843
530211	13	12-Jun-2008	12:24	9	1, 2, 5, 7, 9	0.801
530211	14	30-Apr-2009	13:38	9	2, 4, 6, 7, 9	0.853
530211	15	29-Jul-2010	10:08	9	1, 2, 4, 5, 7	0.819
530211	16	05-Feb-2011	11:50	9	2, 3, 4, 6, 7	0.778
530211	17	14-May-2012	20:57	9	2, 3, 4, 5, 9	0.804
530211	18	16-May-2013	07:11	9	3, 5, 6, 7, 8	0.861
530211	19	16-May-2013	10:01	9	1, 3, 4, 5, 8	0.849
530211	20	16-May-2013	15:21	9	2, 3, 4, 7, 9	0.811
530211	21	16-Apr-2015	00:21	9	1, 2, 6, 7, 9	0.784
530212	01	18-Nov-1995	13:18	9	2, 5, 6, 7, 8	0.901
530212	02	06-Oct-1997	16:48	5	1, 2, 3, 4, 5	0.921
530212	03	15-May-1998	14:38	7	3, 4, 5, 6, 7	0.873
530212	04	07-May-1999	13:02	7	2, 3, 4, 6, 7	0.901

Section	Visit	Date	Time	Available Repeats	Selected Repeats	Composite Correlation
530212	05	29-Jun-2000	13:27	9	2, 3, 7, 8, 9	0.941
530212	06	07-Aug-2001	10:53	9	3, 4, 5, 6, 8	0.934
530212	07	05-Aug-2002	10:56	9	2, 4, 5, 8, 9	0.931
530212	08	20-Aug-2003	15:16	9	1, 2, 7, 8, 9	0.928
530212	09	23-Jul-2004	13:53	9	2, 3, 4, 5, 6	0.936
530212	10	24-Jun-2005	18:21	9	1, 3, 6, 7, 8	0.887
530212	11	07-Jun-2006	17:59	9	1, 2, 4, 7, 9	0.929
530212	12	19-Jul-2007	18:40	9	5, 6, 7, 8, 9	0.887
530212	13	12-Jun-2008	12:24	9	1, 4, 6, 7, 8	0.917
530212	14	30-Apr-2009	13:38	9	2, 5, 7, 8, 9	0.932
530212	15	29-Jul-2010	10:08	9	1, 2, 3, 4, 7	0.889
530212	16	05-Feb-2011	11:45	9	1, 4, 5, 8, 9	0.884
530212	17	14-May-2012	20:57	9	2, 4, 5, 7, 8	0.900
530212	18	16-May-2013	07:03	9	2, 3, 4, 5, 7	0.930
530212	19	16-May-2013	10:01	9	1, 2, 3, 6, 9	0.893
530212	20	16-May-2013	15:07	9	1, 3, 6, 7, 9	0.908
530212	21	16-Apr-2015	00:32	9	2, 3, 6, 7, 9	0.878
530259	01	18-Nov-1995	13:18	9	3, 4, 5, 6, 7	0.849
530259	02	06-Oct-1997	16:48	5	1, 2, 3, 4, 5	0.884
530259	03	15-May-1998	14:14	7	1, 2, 3, 4, 7	0.655
530259	04	07-May-1999	12:52	7	1, 2, 4, 5, 6	0.894
530259	05	29-Jun-2000	13:13	9	1, 2, 7, 8, 9	0.916
530259	06	07-Aug-2001	10:43	9	2, 3, 4, 5, 7	0.892
530259	07	05-Aug-2002	10:46	9	1, 3, 5, 8, 9	0.942
530259	08	20-Aug-2003	15:32	9	2, 3, 4, 6, 8	0.907
530259	09	23-Jul-2004	13:41	9	1, 2, 3, 5, 7	0.902
530259	10	24-Jun-2005	18:21	9	1, 2, 3, 5, 6	0.775
530259	11	07-Jun-2006	18:22	9	3, 4, 5, 7, 8	0.850
530259	12	19-Jul-2007	17:55	9	1, 2, 3, 4, 5	0.863
530259	13	12-Jun-2008	12:24	9	1, 2, 5, 7, 9	0.850
530259	14	30-Apr-2009	13:38	9	2, 4, 5, 8, 9	0.882
530259	15	29-Jul-2010	10:08	9	1, 3, 4, 6, 7	0.828
530259	16	05-Feb-2011	12:00	9	4, 5, 7, 8, 9	0.856
530259	17	14-May-2012	20:57	9	2, 4, 6, 7, 9	0.809
530259	18	16-May-2013	07:03	9	2, 5, 7, 8, 9	0.907
530259	19	16-May-2013	10:26	9	4, 5, 7, 8, 9	0.877
530259	20	16-May-2013	15:07	9	1, 3, 4, 7, 8	0.843
530259	21	16-Apr-2015	00:21	9	1, 2, 3, 5, 8	0.844

APPENDIX D. ROUGHNESS VALUES

This appendix lists the left IRI, right IRI, MRI, and HRI values for each visit of each section. In most cases, the roughness values are the average for five repeat runs. The five runs were selected from a group of as many as nine runs by automated comparison of profiles as described in appendix C. SD values are also provided for left and right IRI to reveal cases of high variability among the five measurements. However, the screening procedure used to select five runs usually helped reduce the level of scatter.

The discussion of roughness in the main report emphasizes the left and right IRI. Nevertheless, other indices provide useful additional information. MRI is the average of the left and right IRI value. HRI is calculated by converting the IRI filter into a half-car model.(94) The conversion is accomplished by collapsing the left and right profile into a single profile in which each point is the average of the corresponding left and right elevation. The IRI filter is then applied to the resulting signal. The HRI is similar to the IRI except that side-to-side deviations in profile are eliminated. The result is that the HRI value for a pair of profiles will always be lower than the corresponding MRI value. Comparing the HRI and MRI values provide a crude indication of the significance of roll (i.e., side-by-side variation in profiles) to the overall roughness. When HRI is low compared to MRI, roll is significant. This is common among asphalt pavements.(95) Certain types of pavement distress, such as longitudinal cracking, may also cause significant differences between HRI and MRI.

Figure 81 compares the HRI to MRI for profile measurements of PCC sections. The comparison includes 9,359 pairs of roughness values and excludes AC sections 040260 and 040261. The figure shows a best-fit line with a zero intercept and a line of equality. The slope of the line is 0.910, which produced a root mean square (RMS) residual of 3.41 inches/mi. A typical range for concrete pavement is 0.90 through 0.95. Note that a better linear fit was found without forcing a zero intercept. A simple linear fit produced a slope of 0.958 and an intercept of −5.03 inches/mi. This line had an RMS residual of 3.18 inches/mi.

Table 47 provides roughness values and lists the date of each measurement and age of each section. On the SPS-2 sections, the age is the time elapsed since the project was opened to traffic. On the GPS-3 sections, the age is the time elapsed since the construction date. Figure 82 through figure 166 show left and right IRI versus age for the 85 test sections and use equivalent scaling for the roughness axis. Figures for sections from the same SPS-2 project use the same age scale. The figures show annotations along the age axis for maintenance and rehabilitation.

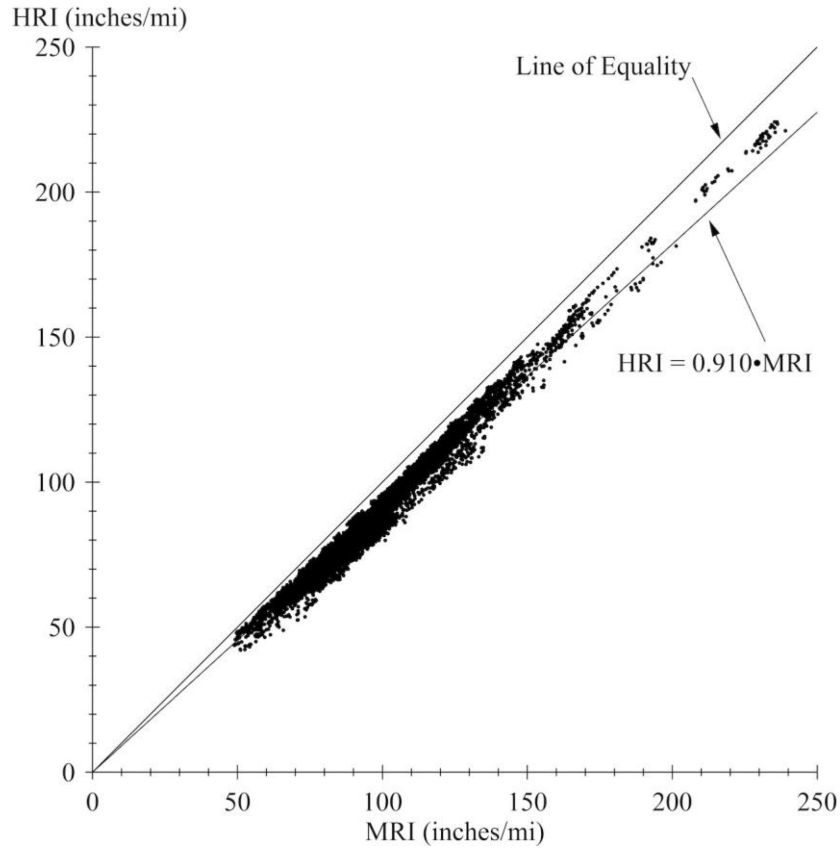

Source: FHWA.

Figure 81. Graph. Comparison of HRI and MRI.

Table 47. Roughness values.

Section	Visit	Date	Time	Age (years)	Left IRI Average (Inches/mi)	Left IRI SD (Inches/mi)	Right IRI Average (Inches/mi)	Right IRI SD (Inches/mi)	MRI (Inches/mi)	HRI (Inches/mi)
040213	01	25-Jan-1994	06:10	0.32	90.7	1.8	97.2	1.6	93.9	86.0
040213	02	05-Mar-1995	11:21	1.42	72.5	0.9	83.5	1.7	78.0	69.3
040213	03	27-Jan-1997	11:22	3.33	103.3	0.9	110.2	1.1	106.7	100.8
040213	04	04-Dec-1997	11:06	4.18	103.7	2.7	117.1	2.0	110.4	105.2
040213	05	08-Dec-1998	10:28	5.19	108.2	1.1	116.6	1.5	112.4	106.9
040213	06	15-Nov-1999	11:38	6.12	118.2	0.5	130.0	1.0	124.1	118.2
040213	07	30-Nov-2000	14:10	7.17	107.2	1.1	119.3	1.4	113.2	106.4
040213	08	08-Nov-2001	11:09	8.11	117.9	1.2	132.5	1.5	125.2	118.7
040213	09	30-Oct-2002	12:40	9.08	125.5	0.7	120.2	2.6	122.9	117.3
040213	10	04-Feb-2004	13:47	10.35	111.8	1.5	106.1	3.2	109.0	102.7
040213	11	12-Dec-2004	16:58	11.20	103.3	1.1	120.3	4.8	111.8	105.1
040213	12	11-Aug-2006	04:17	12.86	140.5	0.9	178.2	5.3	159.3	149.8
040213	13	13-Dec-2007	10:08	14.20	114.5	0.8	147.8	6.9	131.1	121.4
040213	14	20-Sep-2008	00:40	14.97	128.6	1.1	167.0	6.6	147.8	137.3
040213	15	25-Jan-2010	16:11	16.32	111.9	1.2	199.4	3.3	155.6	141.1
040213	16	08-Dec-2011	20:00	18.19	120.9	0.8	227.3	23.1	174.1	156.5
040213	17	16-Dec-2012	18:50	19.21	119.6	1.7	145.1	10.7	132.4	121.7

Section	Visit	Date	Time	Age (years)	Left IRI Average (Inches/ mi)	Left IRI SD (Inches/ mi)	Right IRI Average (Inches/ mi)	Right IRI SD (Inches/ mi)	MRI (Inches/ mi)	HRI (Inches/ mi)
040213	18	06-Feb-2014	23:57	20.35	119.5	0.9	168.2	3.4	143.8	128.0
040213	19	07-Feb-2014	09:03	20.35	119.6	0.6	171.3	4.7	145.5	129.8
040213	20	07-Feb-2014	13:10	20.35	107.2	0.4	170.9	7.0	139.1	123.0
040213	21	07-Feb-2014	16:40	20.36	99.2	1.1	154.5	10.9	126.8	112.9
040213	22	14-Nov-2014	03:22	21.12	130.2	5.1	120.6	2.0	125.4	119.6
040213	23	07-Dec-2015	18:33	22.18	107.3	1.6	239.6	44.4	173.4	154.4
040214	01	25-Jan-1994	06:10	0.32	85.7	1.9	80.4	2.0	83.0	79.7
040214	02	05-Mar-1995	11:21	1.42	55.3	0.5	59.4	1.7	57.3	50.4
040214	03	27-Jan-1997	11:38	3.33	76.2	3.2	64.1	2.6	70.2	65.0
040214	04	04-Dec-1997	11:06	4.18	69.9	2.6	68.9	2.2	69.4	64.3
040214	05	08-Dec-1998	10:28	5.19	70.1	2.8	67.5	2.4	68.8	63.5
040214	06	15-Nov-1999	11:38	6.12	81.7	2.9	73.6	2.2	77.6	71.5
040214	07	30-Nov-2000	13:37	7.17	80.7	0.8	71.2	1.2	76.0	69.6
040214	08	08-Nov-2001	11:09	8.11	78.7	2.5	79.4	0.5	79.1	73.0
040214	09	30-Oct-2002	12:40	9.08	94.9	3.5	78.6	0.9	86.7	78.3
040214	10	04-Feb-2004	13:57	10.35	101.1	3.1	87.3	1.4	94.2	85.9
040214	11	12-Dec-2004	17:14	11.20	81.1	4.0	83.9	1.0	82.5	75.5
040214	12	13-Aug-2006	03:02	12.87	81.2	1.8	83.2	0.9	82.2	75.4
040214	13	13-Dec-2007	10:35	14.20	102.1	1.2	93.6	1.7	97.8	90.1
040214	14	20-Sep-2008	00:37	14.97	94.8	3.3	86.1	1.9	90.4	83.6
040214	15	25-Jan-2010	16:08	16.32	101.5	2.3	99.8	0.5	100.6	94.6
040214	16	08-Dec-2011	19:57	18.19	102.8	2.2	94.7	1.4	98.8	92.3
040214	17	16-Dec-2012	18:47	19.21	109.6	3.6	97.4	1.4	103.5	96.1
040214	18	06-Feb-2014	21:58	20.35	112.6	2.1	108.3	0.9	110.4	102.2
040214	19	07-Feb-2014	08:39	20.35	113.4	6.7	105.9	0.8	109.7	100.6
040214	20	07-Feb-2014	12:48	20.35	117.2	5.7	107.4	3.7	112.3	104.1
040214	21	07-Feb-2014	16:21	20.36	125.4	1.6	118.5	2.2	121.9	115.0
040214	22	14-Nov-2014	00:37	21.12	107.5	1.2	100.2	0.8	103.8	96.1
040214	23	07-Dec-2015	18:33	22.18	120.2	1.8	111.9	1.2	116.0	108.3
040215	01	25-Jan-1994	06:10	0.32	89.6	0.6	91.3	1.3	90.5	80.4
040215	02	05-Mar-1995	11:21	1.42	81.8	0.8	96.8	3.3	89.3	80.1
040215	S01	05-Dec-1995	09:14	2.18	94.3	1.2	103.2	1.3	98.7	89.2
040215	S02	05-Dec-1995	14:56	2.18	87.6	0.7	96.3	2.6	91.9	82.5
040215	S03	02-May-1996	09:30	2.59	91.7	2.1	99.0	1.4	95.4	85.5
040215	S04	02-May-1996	14:58	2.59	83.8	1.6	95.4	2.8	89.6	79.4
040215	S05	12-Aug-1996	09:40	2.86	90.5	2.7	97.7	1.6	94.1	82.9
040215	S06	12-Aug-1996	14:15	2.87	84.4	2.4	93.8	2.0	89.1	78.5
040215	03	27-Jan-1997	12:11	3.33	97.5	0.7	102.5	1.4	100.0	91.5
040215	04	04-Dec-1997	11:06	4.18	100.2	3.7	104.7	2.1	102.5	94.1
040215	S07	15-Jan-1998	11:35	4.29	88.8	0.8	100.7	2.3	94.7	85.8
040215	S08	15-Jan-1998	16:43	4.29	87.2	0.7	103.0	0.9	95.1	86.7
040215	S09	13-Apr-1998	10:13	4.53	92.3	0.9	98.7	1.6	95.5	86.1
040215	S10	13-Apr-1998	15:19	4.53	91.5	1.2	98.5	1.6	95.0	84.9
040215	S11	09-Jul-1998	08:22	4.77	96.0	1.8	107.1	2.3	101.5	91.3
040215	S12	09-Jul-1998	12:10	4.77	92.6	0.7	104.8	1.9	98.7	88.5
040215	S13	30-Sep-1998	11:58	5.00	104.6	1.1	113.8	2.4	109.2	100.4
040215	S14	30-Sep-1998	14:39	5.00	99.0	2.3	111.9	1.6	105.5	96.2
040215	05	08-Dec-1998	10:28	5.19	109.4	1.2	109.7	2.1	109.6	101.1

Section	Visit	Date	Time	Age (years)	Left IRI Average (Inches/ mi)	Left IRI SD (Inches/ mi)	Right IRI Average (Inches/ mi)	Right IRI SD (Inches/ mi)	MRI (Inches/ mi)	HRI (Inches/ mi)
040215	06	15-Nov-1999	11:38	6.12	113.8	1.9	122.7	1.6	118.2	110.2
040215	07	30-Nov-2000	13:37	7.17	110.6	1.0	118.9	0.4	114.7	106.7
040215	08	08-Nov-2001	11:48	8.11	120.9	0.5	126.3	0.7	123.6	115.9
040215	S15	09-Dec-2001	09:20	8.19	125.1	0.3	128.9	0.7	127.0	119.7
040215	S16	09-Dec-2001	14:57	8.19	115.7	0.9	120.4	0.6	118.0	110.6
040215	S17	24-Jan-2002	10:16	8.32	121.9	1.2	126.7	0.9	124.3	117.0
040215	S18	24-Jan-2002	15:00	8.32	111.5	0.4	119.3	0.9	115.4	107.5
040215	S19	15-Mar-2002	09:40	8.45	130.2	1.2	133.3	1.3	131.8	124.6
040215	S20	15-Mar-2002	14:34	8.45	116.6	0.7	121.6	2.8	119.1	111.5
040215	S21	09-Oct-2002	09:00	9.02	140.9	1.4	133.6	2.9	137.3	131.2
040215	S22	09-Oct-2002	13:46	9.02	121.8	1.4	124.5	1.5	123.2	116.8
040215	09	30-Oct-2002	13:06	9.08	131.8	5.9	123.3	1.0	127.6	120.2
040215	S23	20-Dec-2002	09:05	9.22	138.8	0.8	131.8	1.2	135.3	128.8
040215	S24	20-Dec-2002	13:23	9.22	126.2	4.2	121.0	1.5	123.6	116.2
040215	S25	07-Mar-2003	09:28	9.43	125.5	1.6	119.8	2.2	122.7	116.3
040215	S26	07-Mar-2003	13:59	9.43	113.4	0.7	112.6	2.1	113.0	105.5
040215	S27	25-Jul-2003	04:24	9.81	122.0	0.3	131.4	1.3	126.7	120.2
040215	S28	25-Jul-2003	08:42	9.81	119.4	0.9	126.5	0.9	123.0	116.4
040215	S29	24-Nov-2003	09:41	10.15	124.4	1.7	127.8	1.0	126.1	119.5
040215	S30	24-Nov-2003	14:22	10.15	117.9	1.2	120.5	2.3	119.2	112.6
040215	S31	14-Dec-2003	10:32	10.20	119.9	0.7	126.5	1.1	123.2	116.4
040215	S32	14-Dec-2003	15:16	10.20	116.3	1.1	120.0	1.4	118.1	111.4
040215	10	04-Feb-2004	13:47	10.35	131.3	3.4	118.8	2.3	125.1	116.2
040215	S33	22-Apr-2004	04:58	10.56	133.6	0.4	139.8	2.1	136.7	130.6
040215	S34	22-Apr-2004	10:01	10.56	118.6	0.9	122.4	1.6	120.5	114.2
040215	S35	15-Jul-2004	04:17	10.79	132.8	1.3	142.7	1.6	137.8	132.0
040215	S36	15-Jul-2004	09:07	10.79	130.0	0.2	136.2	0.9	133.1	127.1
040215	S37	09-Sep-2004	04:01	10.94	135.4	0.1	145.6	0.6	140.5	134.6
040215	S38	09-Sep-2004	08:34	10.94	132.8	0.7	142.6	1.5	137.7	131.6
040215	11	12-Dec-2004	16:15	11.20	108.6	2.2	121.0	1.3	114.8	107.6
040215	12	13-Aug-2006	00:24	12.87	136.5	0.6	142.0	0.8	139.3	134.0
040215	13	13-Dec-2007	12:08	14.20	123.2	0.5	123.8	1.0	123.5	117.2
040215	14	20-Sep-2008	02:06	14.97	134.8	0.9	142.7	1.5	138.8	132.9
040215	15	25-Jan-2010	17:50	16.32	124.2	1.5	129.6	1.0	126.9	120.0
040215	16	08-Dec-2011	21:26	18.19	134.3	1.8	136.3	1.7	135.3	129.3
040215	17	16-Dec-2012	19:55	19.21	130.3	1.5	129.5	1.2	129.9	124.1
040215	18	06-Feb-2014	23:02	20.35	129.1	1.6	132.4	1.0	130.8	125.0
040215	19	07-Feb-2014	08:39	20.35	137.0	1.8	136.0	3.7	136.5	130.6
040215	20	07-Feb-2014	12:48	20.35	123.8	1.1	127.8	1.8	125.8	119.4
040215	21	07-Feb-2014	16:21	20.36	113.0	2.0	118.5	1.8	115.7	108.6
040215	22	14-Nov-2014	01:24	21.12	135.8	1.7	133.8	2.0	134.8	129.2
040215	23	07-Dec-2015	18:23	22.18	118.0	1.6	123.1	1.9	120.6	113.8
040216	01	25-Jan-1994	06:10	0.32	89.3	1.4	86.9	2.2	88.1	80.6
040216	02	05-Mar-1995	11:21	1.42	82.6	1.5	88.8	1.7	85.7	75.5
040216	03	27-Jan-1997	11:22	3.33	87.3	3.7	84.5	0.8	85.9	75.7
040216	04	04-Dec-1997	11:06	4.18	86.2	0.7	84.6	2.5	85.4	76.4
040216	05	08-Dec-1998	10:28	5.19	88.4	0.9	87.3	1.8	87.8	78.0
040216	06	15-Nov-1999	11:48	6.12	92.7	2.7	85.7	0.6	89.2	79.3
040216	07	30-Nov-2000	13:49	7.17	85.3	1.3	88.5	0.8	86.9	77.8

Section	Visit	Date	Time	Age (years)	Left IRI Average (Inches/ mi)	Left IRI SD (Inches/ mi)	Right IRI Average (Inches/ mi)	Right IRI SD (Inches/ mi)	MRI (Inches/ mi)	HRI (Inches/ mi)
040216	08	08-Nov-2001	11:28	8.11	84.6	1.2	90.8	1.3	87.7	78.5
040216	09	30-Oct-2002	12:40	9.08	98.3	3.7	93.1	1.2	95.7	80.5
040216	10	04-Feb-2004	13:47	10.35	99.6	3.1	100.0	1.6	99.8	84.2
040216	11	12-Dec-2004	16:15	11.20	91.1	4.6	97.8	1.6	94.4	84.4
040216	12	13-Aug-2006	00:13	12.87	89.0	1.5	99.2	1.5	94.1	85.2
040216	13	13-Dec-2007	12:08	14.20	98.3	1.7	101.6	1.4	100.0	88.5
040216	14	20-Sep-2008	02:16	14.97	100.5	2.8	98.1	0.4	99.3	85.6
040216	15	25-Jan-2010	17:37	16.32	93.7	1.0	105.9	1.8	99.8	90.4
040216	16	08-Dec-2011	21:44	18.19	101.6	1.0	100.6	0.9	101.1	85.8
040216	17	16-Dec-2012	19:46	19.21	103.6	1.4	100.5	0.9	102.0	86.0
040216	18	06-Feb-2014	23:08	20.35	103.0	1.2	100.0	1.2	101.5	86.7
040216	19	07-Feb-2014	08:39	20.35	103.9	0.8	99.6	1.7	101.7	86.2
040216	20	07-Feb-2014	12:48	20.35	96.4	1.2	102.5	2.3	99.4	89.2
040216	21	07-Feb-2014	16:21	20.36	97.4	1.4	104.5	2.1	101.0	91.1
040216	22	14-Nov-2014	01:24	21.12	104.1	1.0	99.0	1.7	101.6	84.7
040216	23	07-Dec-2015	18:43	22.18	94.6	2.4	101.9	1.0	98.3	88.6
040217	01	25-Jan-1994	06:10	0.32	93.3	0.5	81.7	1.1	87.5	79.1
040217	02	05-Mar-1995	11:21	1.42	60.8	1.4	69.6	2.3	65.2	56.0
040217	03	27-Jan-1997	11:48	3.33	83.2	0.7	77.5	1.3	80.4	70.6
040217	04	04-Dec-1997	11:40	4.18	78.6	3.7	80.2	2.7	79.4	71.8
040217	05	08-Dec-1998	10:28	5.19	81.8	3.2	78.4	2.8	80.1	71.8
040217	06	15-Nov-1999	11:38	6.12	92.8	2.2	81.4	0.9	87.1	77.4
040217	07	30-Nov-2000	14:10	7.17	84.5	1.6	74.6	0.6	79.6	69.7
040217	08	08-Nov-2001	11:09	8.11	86.8	2.2	77.1	1.7	82.0	73.6
040217	09	30-Oct-2002	12:40	9.08	87.4	1.4	74.3	0.8	80.8	70.9
040217	10	04-Feb-2004	13:47	10.35	88.8	3.2	66.8	1.7	77.8	65.3
040217	11	12-Dec-2004	16:15	11.20	84.4	4.4	74.6	1.9	79.5	69.9
040217	12	11-Aug-2006	04:17	12.86	105.7	1.7	88.8	1.9	97.3	89.5
040217	13	13-Dec-2007	10:18	14.20	80.9	2.4	74.3	1.7	77.6	66.0
040217	14	20-Sep-2008	00:40	14.97	110.4	3.5	82.0	2.0	96.2	86.6
040217	15	25-Jan-2010	16:11	16.32	81.4	1.5	75.5	2.9	78.5	68.7
040217	16	08-Dec-2011	20:25	18.19	96.8	2.5	75.3	2.8	86.1	75.0
040217	17	16-Dec-2012	18:09	19.21	90.0	2.2	72.6	2.0	81.3	71.0
040217	18	07-Feb-2014	00:04	20.35	95.7	2.4	76.2	1.9	85.9	75.2
040217	19	07-Feb-2014	09:03	20.35	94.5	1.9	76.1	1.3	85.3	75.2
040217	20	07-Feb-2014	13:10	20.35	79.4	0.9	74.5	1.5	77.0	67.6
040217	21	07-Feb-2014	16:40	20.36	75.7	1.6	67.8	1.1	71.8	60.6
040217	22	14-Nov-2014	03:22	21.12	109.4	3.2	79.0	1.8	94.2	82.2
040217	23	07-Dec-2015	18:33	22.18	78.7	1.6	73.6	1.8	76.2	64.6
040218	01	25-Jan-1994	06:10	0.32	91.9	3.8	84.6	1.9	88.3	83.0
040218	02	05-Mar-1995	11:21	1.42	65.4	1.5	58.8	1.1	62.1	53.1
040218	03	27-Jan-1997	11:22	3.33	73.6	1.5	56.1	0.4	64.8	58.5
040218	04	04-Dec-1997	11:06	4.18	72.8	1.6	60.6	2.4	66.7	59.1
040218	05	08-Dec-1998	10:28	5.19	73.8	0.9	60.3	1.2	67.1	60.2
040218	06	15-Nov-1999	11:48	6.12	79.0	1.9	65.1	0.7	72.0	65.0
040218	07	30-Nov-2000	14:00	7.17	73.6	1.1	60.6	0.7	67.1	60.6
040218	08	08-Nov-2001	11:09	8.11	70.8	1.0	62.3	0.6	66.5	58.7
040218	09	30-Oct-2002	12:55	9.08	85.8	4.7	56.0	0.9	70.9	63.8

Section	Visit	Date	Time	Age (years)	Left IRI Average (Inches/ mi)	Left IRI SD (Inches/ mi)	Right IRI Average (Inches/ mi)	Right IRI SD (Inches/ mi)	MRI (Inches/ mi)	HRI (Inches/ mi)
040218	10	04-Feb-2004	13:47	10.35	82.9	3.1	56.1	1.3	69.5	61.9
040218	11	12-Dec-2004	16:15	11.20	72.4	1.4	64.6	1.9	68.5	59.8
040218	12	13-Aug-2006	03:51	12.87	77.0	1.3	71.4	0.6	74.2	66.3
040218	13	13-Dec-2007	10:14	14.20	84.0	2.5	69.0	1.7	76.5	68.0
040218	14	20-Sep-2008	00:37	14.97	80.9	1.1	76.1	0.7	78.5	69.9
040218	15	25-Jan-2010	16:08	16.32	78.7	1.3	70.5	1.3	74.6	65.5
040218	16	08-Dec-2011	19:57	18.19	90.4	1.5	78.7	1.3	84.6	74.9
040218	17	16-Dec-2012	18:30	19.21	91.0	1.4	76.7	0.8	83.8	74.2
040218	18	06-Feb-2014	22:21	20.35	88.8	0.9	76.6	0.4	82.7	72.9
040218	19	07-Feb-2014	08:39	20.35	91.9	0.8	79.4	0.5	85.7	75.9
040218	20	07-Feb-2014	12:48	20.35	87.3	7.6	75.8	1.1	81.5	70.8
040218	21	07-Feb-2014	16:21	20.36	79.8	2.7	72.8	1.0	76.3	66.0
040218	22	14-Nov-2014	00:27	21.12	95.1	3.4	79.3	0.7	87.2	76.8
040218	23	07-Dec-2015	18:33	22.18	87.9	1.2	74.9	0.7	81.4	71.6
040219	01	25-Jan-1994	06:10	0.32	77.5	1.5	89.6	2.1	83.6	75.0
040219	02	05-Mar-1995	11:21	1.42	67.2	1.2	84.0	1.4	75.6	65.7
040219	03	27-Jan-1997	11:38	3.33	77.0	1.6	95.0	1.4	86.0	77.5
040219	04	04-Dec-1997	11:06	4.18	88.2	3.9	96.4	1.7	92.3	84.1
040219	05	08-Dec-1998	10:28	5.19	82.4	3.1	102.0	2.1	92.2	84.9
040219	06	15-Nov-1999	11:48	6.12	88.8	2.5	105.3	2.3	97.1	89.9
040219	07	30-Nov-2000	13:49	7.17	79.3	0.4	100.5	1.2	89.9	82.4
040219	08	08-Nov-2001	11:09	8.11	87.1	1.9	110.1	3.2	98.6	92.1
040219	09	30-Oct-2002	12:40	9.08	100.4	1.6	102.5	1.5	101.4	93.0
040219	10	04-Feb-2004	13:47	10.35	100.8	4.4	99.1	1.6	100.0	91.4
040219	11	12-Dec-2004	17:14	11.20	91.4	2.7	111.0	2.1	101.2	94.3
040219	12	13-Aug-2006	00:13	12.87	117.9	1.5	136.7	1.4	127.3	121.6
040219	13	13-Dec-2007	12:08	14.20	90.0	1.2	102.3	1.1	96.2	89.4
040219	14	20-Sep-2008	02:06	14.97	118.9	2.4	135.1	3.3	127.0	121.4
040219	15	25-Jan-2010	18:09	16.32	98.0	2.6	113.9	1.4	106.0	99.3
040219	16	08-Dec-2011	21:35	18.19	108.4	2.1	116.2	0.9	112.3	105.6
040219	17	16-Dec-2012	19:55	19.21	103.0	1.7	112.7	0.9	107.9	101.0
040219	18	06-Feb-2014	23:02	20.35	101.4	2.5	120.6	0.8	111.0	105.2
040219	19	07-Feb-2014	08:39	20.35	112.2	1.3	120.7	2.4	116.5	110.1
040219	20	07-Feb-2014	12:48	20.35	98.5	2.8	111.0	2.1	104.8	98.2
040219	21	07-Feb-2014	16:21	20.36	83.4	2.4	101.8	1.9	92.6	85.7
040219	22	14-Nov-2014	01:24	21.12	111.4	1.9	117.5	0.9	114.5	107.5
040219	23	07-Dec-2015	18:33	22.18	97.9	2.6	104.7	3.5	101.3	93.9
040220	01	25-Jan-1994	06:10	0.32	76.8	2.1	80.3	1.8	78.5	73.9
040220	02	05-Mar-1995	11:21	1.42	66.1	1.5	72.2	1.3	69.2	62.4
040220	03	27-Jan-1997	11:22	3.33	66.5	3.7	72.3	1.7	69.4	64.3
040220	04	04-Dec-1997	11:06	4.18	69.8	1.7	72.1	1.8	71.0	66.3
040220	05	08-Dec-1998	10:38	5.19	68.7	0.6	73.1	1.4	70.9	66.5
040220	06	15-Nov-1999	11:38	6.12	69.0	1.1	77.1	1.4	73.0	67.7
040220	07	30-Nov-2000	13:37	7.17	77.0	4.7	69.3	1.3	73.1	68.4
040220	08	08-Nov-2001	11:09	8.11	68.0	0.8	77.9	0.5	73.0	67.9
040220	09	30-Oct-2002	12:40	9.08	82.5	2.0	69.6	1.1	76.1	71.3
040220	10	04-Feb-2004	13:57	10.35	90.0	4.4	69.7	0.4	79.8	73.5
040220	11	12-Dec-2004	16:15	11.20	73.3	1.6	80.7	1.8	77.0	71.2

Section	Visit	Date	Time	Age (years)	Left IRI Average (Inches/ mi)	Left IRI SD (Inches/ mi)	Right IRI Average (Inches/ mi)	Right IRI SD (Inches/ mi)	MRI (Inches/ mi)	HRI (Inches/ mi)
040220	12	13-Aug-2006	03:46	12.87	75.4	1.6	82.7	1.0	79.0	73.7
040220	13	13-Dec-2007	10:14	14.20	86.4	2.0	85.3	1.7	85.9	80.3
040220	14	20-Sep-2008	00:47	14.97	91.8	2.2	79.6	0.8	85.7	80.1
040220	15	25-Jan-2010	16:08	16.32	80.2	2.5	84.0	1.7	82.1	76.6
040220	16	08-Dec-2011	20:13	18.19	102.2	2.1	91.7	1.2	97.0	91.1
040220	17	16-Dec-2012	18:30	19.21	99.8	3.0	89.9	1.5	94.9	89.3
040220	18	06-Feb-2014	21:58	20.35	99.4	0.8	85.5	1.4	92.5	86.4
040220	19	07-Feb-2014	08:39	20.35	100.6	5.2	89.1	1.6	94.8	89.0
040220	20	07-Feb-2014	12:48	20.35	98.2	3.6	87.0	0.9	92.6	86.7
040220	21	07-Feb-2014	16:21	20.36	84.9	5.5	83.5	3.0	84.2	78.5
040220	22	14-Nov-2014	00:37	21.12	95.8	3.7	87.3	1.4	91.6	85.4
040220	23	07-Dec-2015	18:43	22.18	89.7	4.2	86.3	0.7	88.0	82.3
040221	01	25-Jan-1994	06:10	0.32	72.6	1.9	73.2	1.7	72.9	65.3
040221	02	05-Mar-1995	11:21	1.42	56.0	0.7	60.0	1.4	58.0	47.7
040221	03	27-Jan-1997	11:22	3.33	77.8	1.6	78.2	0.4	78.0	70.8
040221	04	04-Dec-1997	11:06	4.18	82.1	3.3	83.9	2.3	83.0	77.1
040221	05	08-Dec-1998	10:28	5.19	84.8	2.7	82.5	0.9	83.6	77.5
040221	06	15-Nov-1999	11:38	6.12	84.7	1.8	87.7	1.0	86.2	79.3
040221	07	30-Nov-2000	13:37	7.17	76.4	1.2	81.9	1.6	79.2	71.2
040221	08	08-Nov-2001	11:09	8.11	84.1	2.0	85.3	0.9	84.7	78.9
040221	09	30-Oct-2002	12:40	9.08	90.6	6.6	77.9	2.5	84.3	77.2
040221	10	04-Feb-2004	13:47	10.35	76.4	1.5	74.5	3.7	75.4	68.0
040221	11	12-Dec-2004	16:44	11.20	79.5	3.0	80.3	1.3	79.9	72.8
040221	12	11-Aug-2006	04:17	12.86	100.9	1.0	99.6	1.1	100.2	94.2
040221	13	13-Dec-2007	10:08	14.20	81.3	1.3	81.6	1.5	81.5	74.4
040221	14	20-Sep-2008	00:40	14.97	96.6	1.3	94.9	1.8	95.7	88.8
040221	15	25-Jan-2010	16:19	16.32	82.5	1.5	85.0	1.5	83.7	76.7
040221	16	08-Dec-2011	20:17	18.19	93.3	2.9	85.8	2.4	89.6	83.9
040221	17	16-Dec-2012	18:57	19.21	87.1	2.8	78.5	0.5	82.8	76.7
040221	18	07-Feb-2014	00:18	20.35	90.8	1.4	82.1	2.7	86.5	80.3
040221	19	07-Feb-2014	09:03	20.35	91.4	3.6	89.0	3.3	90.2	83.4
040221	20	07-Feb-2014	13:10	20.35	79.1	0.7	81.5	3.2	80.3	73.3
040221	21	07-Feb-2014	16:40	20.36	73.7	1.2	74.5	1.5	74.1	66.1
040221	22	14-Nov-2014	03:10	21.12	89.0	1.2	77.6	1.4	83.3	76.7
040221	23	07-Dec-2015	18:23	22.18	75.8	2.3	79.9	2.5	77.9	69.9
040222	01	25-Jan-1994	06:10	0.32	72.2	1.2	71.2	1.8	71.7	64.6
040222	02	05-Mar-1995	11:21	1.42	57.4	1.4	55.5	1.0	56.4	46.8
040222	03	27-Jan-1997	11:22	3.33	72.3	0.9	55.3	0.7	63.8	55.3
040222	04	04-Dec-1997	11:06	4.18	63.4	2.9	62.5	1.9	62.9	54.7
040222	05	08-Dec-1998	10:38	5.19	66.0	0.4	62.6	1.3	64.3	55.7
040222	06	15-Nov-1999	12:00	6.12	79.6	2.4	63.4	1.1	71.5	63.8
040222	07	30-Nov-2000	13:49	7.17	77.4	1.9	60.0	0.4	68.7	61.3
040222	08	08-Nov-2001	11:28	8.11	68.0	1.6	63.6	0.8	65.8	57.2
040222	09	30-Oct-2002	12:40	9.08	88.4	4.3	57.4	0.7	72.9	63.7
040222	10	04-Feb-2004	13:47	10.35	86.3	7.3	58.2	0.8	72.3	63.8
040222	11	12-Dec-2004	16:44	11.20	68.8	3.0	65.8	1.0	67.3	58.5
040222	12	13-Aug-2006	03:46	12.87	71.8	1.0	73.1	1.6	72.4	63.1
040222	13	13-Dec-2007	10:14	14.20	91.0	2.3	69.8	0.8	80.4	73.2

Section	Visit	Date	Time	Age (years)	Left IRI Average (Inches/ mi)	Left IRI SD (Inches/ mi)	Right IRI Average (Inches/ mi)	Right IRI SD (Inches/ mi)	MRI (Inches/ mi)	HRI (Inches/ mi)
040222	14	20-Sep-2008	00:47	14.97	78.3	2.2	74.9	1.6	76.6	68.9
040222	15	25-Jan-2010	16:17	16.32	75.9	1.8	70.6	1.7	73.2	64.2
040222	16	08-Dec-2011	19:57	18.19	98.0	3.3	82.8	1.7	90.4	83.5
040222	17	16-Dec-2012	18:30	19.21	98.4	1.7	78.8	1.7	88.6	81.4
040222	18	06-Feb-2014	22:05	20.35	98.6	1.3	81.8	0.5	90.2	83.4
040222	19	07-Feb-2014	08:39	20.35	103.3	7.0	84.4	4.5	93.8	86.7
040222	20	07-Feb-2014	12:48	20.35	90.1	1.9	68.2	3.2	79.2	71.5
040222	21	07-Feb-2014	16:21	20.36	79.5	1.0	61.0	0.4	70.3	62.2
040222	22	14-Nov-2014	00:43	21.12	96.6	0.9	79.5	0.9	88.0	80.8
040222	23	07-Dec-2015	19:04	22.18	89.2	2.3	71.4	0.5	80.3	72.8
040223	01	25-Jan-1994	06:10	0.32	72.8	1.5	80.9	3.2	76.9	66.1
040223	02	05-Mar-1995	11:21	1.42	68.5	0.8	79.5	1.4	74.0	63.0
040223	03	27-Jan-1997	12:01	3.33	80.0	1.5	84.7	1.2	82.4	71.3
040223	04	04-Dec-1997	11:06	4.18	84.1	1.5	88.1	2.2	86.1	76.6
040223	05	08-Dec-1998	10:28	5.19	88.7	2.2	91.9	1.5	90.3	81.6
040223	06	15-Nov-1999	11:38	6.12	89.0	1.7	95.2	1.4	92.1	84.0
040223	07	30-Nov-2000	13:37	7.17	81.5	1.3	93.7	0.8	87.6	79.1
040223	08	08-Nov-2001	11:38	8.11	87.1	1.8	99.4	1.1	93.2	85.2
040223	09	30-Oct-2002	12:55	9.08	108.1	1.8	88.6	0.8	98.3	90.3
040223	10	04-Feb-2004	13:57	10.35	100.3	5.3	85.4	1.3	92.8	84.5
040223	11	12-Dec-2004	17:28	11.20	91.2	2.5	99.2	1.1	95.2	87.7
040223	12	13-Aug-2006	00:24	12.87	111.9	1.6	120.8	1.3	116.3	110.0
040223	13	13-Dec-2007	12:08	14.20	97.2	1.6	96.6	2.2	96.9	90.1
040223	14	20-Sep-2008	02:27	14.97	123.1	2.4	119.0	0.9	121.0	115.4
040223	15	25-Jan-2010	18:00	16.32	101.1	2.9	103.4	1.2	102.3	95.6
040223	16	08-Dec-2011	21:26	18.19	111.9	1.5	110.3	1.3	111.1	105.4
040223	17	16-Dec-2012	19:46	19.21	107.1	1.4	107.8	0.9	107.5	101.4
040223	18	06-Feb-2014	23:02	20.35	107.4	0.9	111.6	0.4	109.5	103.6
040223	19	07-Feb-2014	08:39	20.35	117.1	3.6	111.0	2.5	114.1	108.2
040223	20	07-Feb-2014	12:48	20.35	97.7	2.1	106.1	0.8	101.9	95.8
040223	21	07-Feb-2014	16:21	20.36	84.3	0.3	94.2	1.2	89.3	81.6
040223	22	14-Nov-2014	01:29	21.12	123.5	2.9	105.4	1.0	114.5	108.4
040223	23	07-Dec-2015	18:23	22.18	89.5	0.6	99.3	2.2	94.4	86.9
040224	01	25-Jan-1994	06:10	0.32	64.8	0.5	67.7	1.7	66.2	60.8
040224	02	05-Mar-1995	11:21	1.42	60.5	1.3	72.5	2.9	66.5	60.9
040224	03	27-Jan-1997	11:38	3.33	72.5	3.2	69.0	0.8	70.8	65.7
040224	04	04-Dec-1997	11:06	4.18	63.6	5.5	70.6	2.3	67.1	60.8
040224	05	08-Dec-1998	10:28	5.19	63.8	5.5	75.1	3.3	69.5	63.5
040224	06	15-Nov-1999	11:48	6.12	79.9	5.2	71.1	1.4	75.5	70.8
040224	07	30-Nov-2000	13:49	7.17	83.2	4.3	69.5	0.4	76.4	71.8
040224	08	08-Nov-2001	11:28	8.11	66.4	3.2	76.9	0.8	71.7	66.5
040224	09	30-Oct-2002	12:40	9.08	84.2	2.7	72.1	1.0	78.1	72.5
040224	10	04-Feb-2004	13:57	10.35	114.6	2.1	70.2	0.8	92.4	86.2
040224	11	12-Dec-2004	16:15	11.20	70.9	4.9	79.0	1.8	75.0	69.7
040224	12	13-Aug-2006	00:13	12.87	78.9	3.6	74.4	1.1	76.7	72.2
040224	13	13-Dec-2007	12:17	14.20	78.0	1.9	77.6	1.2	77.8	73.2
040224	14	20-Sep-2008	02:41	14.97	90.2	5.9	78.4	1.2	84.3	78.8
040224	15	25-Jan-2010	17:37	16.32	85.4	5.3	84.0	1.7	84.7	80.2

Section	Visit	Date	Time	Age (years)	Left IRI Average (Inches/ mi)	Left IRI SD (Inches/ mi)	Right IRI Average (Inches/ mi)	Right IRI SD (Inches/ mi)	MRI (Inches/ mi)	HRI (Inches/ mi)
040224	16	08-Dec-2011	21:44	18.19	112.1	1.5	94.1	1.0	103.1	98.2
040224	17	16-Dec-2012	19:46	19.21	109.8	1.6	92.2	1.0	101.0	96.4
040224	18	06-Feb-2014	23:08	20.35	110.9	1.0	91.5	0.8	101.2	96.3
040224	19	07-Feb-2014	08:39	20.35	115.1	1.8	95.5	2.4	105.3	100.7
040224	20	07-Feb-2014	12:48	20.35	104.2	4.8	85.5	1.6	94.9	89.8
040224	21	07-Feb-2014	16:21	20.36	81.4	7.7	77.0	1.4	79.2	73.9
040224	22	14-Nov-2014	01:39	21.12	121.5	1.5	87.4	1.2	104.5	99.2
040224	23	07-Dec-2015	18:43	22.18	98.5	5.2	85.7	2.2	92.1	87.0
040260	01	25-Jan-1994	06:10	0.32	56.8	0.3	69.0	1.8	62.9	49.9
040260	02	05-Mar-1995	11:21	1.42	61.2	0.8	74.8	2.8	68.0	54.1
040260	03	27-Jan-1997	11:22	3.33	64.1	0.9	70.0	2.7	67.0	51.2
040260	04	04-Dec-1997	12:13	4.18	62.4	1.5	70.2	1.3	66.3	51.5
040260	05	08-Dec-1998	10:28	5.19	61.2	1.8	68.7	1.5	65.0	50.1
040260	06	15-Nov-1999	11:48	6.12	63.1	1.4	68.0	1.4	65.6	50.9
040260	07	30-Nov-2000	13:37	7.17	62.2	0.8	67.6	0.8	64.9	50.7
040260	08	08-Nov-2001	11:28	8.11	62.0	0.6	70.1	1.4	66.1	51.4
040260	09	30-Oct-2002	12:40	9.08	65.5	1.3	61.0	1.0	63.3	48.6
040260	10	04-Feb-2004	13:47	10.35	65.8	1.5	61.5	2.2	63.6	49.0
040260	11	12-Dec-2004	16:15	11.20	80.4	19.8	70.8	2.1	75.6	58.9
040260	12	13-Aug-2006	00:17	12.87	89.0	2.9	71.9	2.4	80.5	61.3
040260	13	13-Dec-2007	11:59	14.20	106.8	6.8	68.0	2.2	87.4	69.7
040260	14	20-Sep-2008	02:10	14.97	112.1	3.9	74.1	2.0	93.1	74.2
040260	15	25-Jan-2010	17:42	16.32	121.7	3.0	79.8	1.4	100.7	79.1
040260	16	08-Dec-2011	21:28	18.19	186.7	12.7	77.1	1.4	131.9	115.1
040260	17	16-Dec-2012	19:48	19.21	144.0	4.3	103.7	61.5	123.8	104.5
040260	18	07-Feb-2014	01:16	20.35	136.8	3.6	85.3	2.4	111.1	90.8
040260	19	07-Feb-2014	09:03	20.35	140.9	1.0	80.4	2.1	110.7	90.2
040260	20	07-Feb-2014	13:10	20.35	141.4	6.6	87.0	5.7	114.2	92.8
040260	21	07-Feb-2014	16:40	20.36	137.2	3.5	89.3	6.2	113.2	92.7
040260	22	14-Nov-2014	04:06	21.12	142.1	5.0	76.4	4.8	109.2	88.8
040260	23	07-Dec-2015	18:43	22.18	143.9	1.8	85.9	4.0	114.9	94.6
040261	01	25-Jan-1994	06:10	0.32	40.2	0.4	53.2	1.5	46.7	38.6
040261	02	05-Mar-1995	11:21	1.42	38.4	0.7	60.0	1.8	49.2	39.8
040261	03	27-Jan-1997	12:11	3.33	40.3	0.5	60.0	1.4	50.1	39.9
040261	04	04-Dec-1997	11:06	4.18	41.1	0.5	58.0	2.2	49.6	39.4
040261	05	08-Dec-1998	10:48	5.19	39.1	0.9	60.0	0.9	49.6	40.1
040261	06	15-Nov-1999	11:38	6.12	38.4	1.1	58.6	1.3	48.5	39.2
040261	07	30-Nov-2000	14:00	7.17	37.9	0.4	58.6	0.7	48.2	39.5
040261	08	08-Nov-2001	11:09	8.11	40.4	0.5	60.3	1.1	50.4	40.4
040261	09	30-Oct-2002	12:40	9.08	36.7	0.5	54.8	1.8	45.7	36.5
040261	10	04-Feb-2004	13:47	10.35	37.5	0.4	54.9	1.4	46.2	36.7
040261	11	12-Dec-2004	16:15	11.20	40.7	2.5	61.3	1.0	51.0	41.2
040261	12	13-Aug-2006	03:10	12.87	42.9	1.0	66.3	1.2	54.6	43.5
040261	13	13-Dec-2007	10:14	14.20	43.5	0.5	72.9	2.3	58.2	47.5
040261	14	20-Sep-2008	00:37	14.97	46.3	1.1	82.8	3.5	64.6	52.3
040261	15	25-Jan-2010	16:08	16.32	57.1	0.7	111.4	2.6	84.2	69.2
040261	16	08-Dec-2011	20:13	18.19	68.6	0.7	144.7	5.2	106.6	89.1
040261	17	16-Dec-2012	18:30	19.21	75.6	0.9	135.1	6.7	105.3	85.4

Section	Visit	Date	Time	Age (years)	Left IRI Average (Inches/ mi)	Left IRI SD (Inches/ mi)	Right IRI Average (Inches/ mi)	Right IRI SD (Inches/ mi)	MRI (Inches/ mi)	HRI (Inches/ mi)
040261	18	06-Feb-2014	21:58	20.35	83.4	1.4	149.3	2.5	116.3	93.3
040261	19	07-Feb-2014	08:39	20.35	82.3	5.4	148.8	10.1	115.5	92.9
040261	20	07-Feb-2014	12:48	20.35	86.6	2.0	148.5	1.9	117.6	93.3
040261	21	07-Feb-2014	16:21	20.36	88.2	1.6	148.2	2.7	118.2	94.5
040261	22	14-Nov-2014	00:27	21.12	86.1	0.6	135.8	6.7	110.9	87.4
040261	23	07-Dec-2015	18:33	22.18	83.8	1.9	144.4	4.5	114.1	89.8
040262	01	25-Jan-1994	06:10	0.32	72.5	1.0	67.1	1.2	69.8	62.3
040262	02	05-Mar-1995	11:21	1.42	67.0	0.6	70.5	1.3	68.7	58.7
040262	03	27-Jan-1997	11:38	3.33	112.3	0.9	110.1	1.3	111.2	105.3
040262	04	04-Dec-1997	11:40	4.18	122.1	1.4	117.8	1.4	120.0	114.6
040262	05	08-Dec-1998	10:28	5.19	137.1	1.3	137.9	0.3	137.5	131.8
040262	06	15-Nov-1999	11:48	6.12	143.6	0.6	150.4	1.1	147.0	142.0
040262	07	30-Nov-2000	13:49	7.17	138.6	1.4	154.7	1.1	146.7	141.0
040262	08	08-Nov-2001	11:28	8.11	156.9	1.3	174.2	0.7	165.6	160.0
040262	09	30-Oct-2002	12:40	9.08	156.2	0.8	174.9	1.2	165.6	157.0
040262	10	04-Feb-2004	13:57	10.35	158.7	0.9	172.2	1.5	165.5	155.5
040262	11	12-Dec-2004	16:44	11.20	163.6	2.3	194.0	1.8	178.8	171.2
040262	12	11-Aug-2006	04:17	12.86	195.6	0.8	225.8	0.8	210.7	201.5
040262	13	13-Dec-2007	10:18	14.20	186.7	2.1	234.9	4.6	210.8	199.6
040262	14	20-Sep-2008	00:40	14.97	205.3	0.6	250.3	3.8	227.8	215.9
040262	15	25-Jan-2010	16:11	16.32	196.1	1.1	230.8	3.8	213.4	202.9
040262	16	08-Dec-2011	20:08	18.19	210.3	1.9	251.7	3.8	231.0	218.3
040262	17	16-Dec-2012	18:09	19.21	214.3	1.4	248.3	3.0	231.3	219.7
040262	18	06-Feb-2014	23:57	20.35	217.1	0.9	253.3	2.7	235.2	222.9
040262	19	07-Feb-2014	09:03	20.35	218.6	1.6	249.9	3.7	234.2	222.8
040262	20	07-Feb-2014	13:10	20.35	212.3	1.9	251.3	5.7	231.8	218.1
040262	21	07-Feb-2014	16:40	20.36	203.2	1.9	236.3	1.5	219.7	207.5
040262	22	14-Nov-2014	03:10	21.12	217.3	3.0	242.1	1.7	229.7	215.7
040262	23	07-Dec-2015	18:33	22.18	214.2	1.5	254.0	7.0	234.1	218.7
040263	01	25-Jan-1994	06:10	0.32	68.5	0.9	69.7	1.9	69.1	60.8
040263	02	05-Mar-1995	11:21	1.42	59.4	2.0	67.8	1.4	63.6	53.6
040263	03	27-Jan-1997	11:22	3.33	79.6	0.7	73.5	0.7	76.6	68.6
040263	04	04-Dec-1997	11:06	4.18	81.0	1.5	78.6	2.1	79.8	72.1
040263	05	08-Dec-1998	10:38	5.19	82.1	1.2	81.9	2.3	82.0	74.0
040263	06	15-Nov-1999	11:38	6.12	89.9	0.3	80.9	1.3	85.4	77.0
040263	07	30-Nov-2000	13:37	7.17	81.9	1.7	77.8	1.6	79.9	71.7
040263	08	08-Nov-2001	11:28	8.11	86.2	2.4	83.1	0.3	84.6	77.2
040263	09	30-Oct-2002	12:55	9.08	92.3	2.5	84.1	1.5	88.2	78.7
040263	10	04-Feb-2004	13:47	10.35	91.1	1.7	84.0	1.7	87.6	75.7
040263	11	12-Dec-2004	16:15	11.20	84.5	3.9	80.4	1.8	82.5	73.8
040263	12	11-Aug-2006	04:32	12.86	104.3	1.4	95.9	1.9	100.1	92.3
040263	13	13-Dec-2007	10:18	14.20	92.4	2.1	82.1	1.7	87.3	78.5
040263	14	20-Sep-2008	00:50	14.97	103.3	2.3	94.0	2.0	98.7	89.7
040263	15	25-Jan-2010	16:19	16.32	88.2	1.4	79.4	1.3	83.8	75.6
040263	16	08-Dec-2011	20:08	18.19	101.0	1.8	94.1	0.9	97.5	87.4
040263	17	16-Dec-2012	18:09	19.21	95.7	1.5	84.7	1.3	90.2	79.6
040263	18	07-Feb-2014	00:04	20.35	96.3	1.0	83.9	2.1	90.1	79.6
040263	19	07-Feb-2014	09:03	20.35	93.7	3.4	84.2	1.8	88.9	79.2

Section	Visit	Date	Time	Age (years)	Left IRI Average (Inches/ mi)	Left IRI SD (Inches/ mi)	Right IRI Average (Inches/ mi)	Right IRI SD (Inches/ mi)	MRI (Inches/ mi)	HRI (Inches/ mi)
040263	20	07-Feb-2014	13:10	20.35	85.0	3.6	77.2	0.8	81.1	71.4
040263	21	07-Feb-2014	16:40	20.36	86.0	2.8	73.9	3.7	80.0	69.7
040263	22	14-Nov-2014	03:10	21.12	94.5	1.8	82.2	1.5	88.3	75.4
040263	23	07-Dec-2015	18:53	22.18	86.7	3.1	72.9	0.9	79.8	69.5
040264	01	25-Jan-1994	06:10	0.32	105.3	1.9	112.9	2.4	109.1	92.7
040264	02	05-Mar-1995	11:21	1.42	93.2	1.5	117.6	2.1	105.4	89.4
040264	03	27-Jan-1997	11:22	3.33	113.3	1.4	122.4	2.5	117.9	98.4
040264	04	04-Dec-1997	11:40	4.18	114.9	2.4	126.0	1.1	120.4	102.6
040264	05	08-Dec-1998	10:38	5.19	113.5	2.0	133.3	1.7	123.4	106.1
040264	06	15-Nov-1999	11:38	6.12	121.2	1.8	130.4	2.5	125.8	107.6
040264	07	30-Nov-2000	13:37	7.17	119.3	0.7	128.5	2.7	123.9	106.6
040264	08	08-Nov-2001	11:09	8.11	118.5	1.5	140.1	3.3	129.3	113.3
040264	09	30-Oct-2002	12:40	9.08	123.1	4.8	126.5	1.2	124.8	108.6
040264	10	04-Feb-2004	14:08	10.35	121.7	5.5	125.1	3.7	123.4	107.4
040264	11	12-Dec-2004	16:15	11.20	123.3	4.6	136.4	4.3	129.8	114.6
040264	12	13-Aug-2006	00:17	12.87	140.6	1.4	142.7	0.4	141.6	126.8
040264	13	13-Dec-2007	12:11	14.20	136.1	1.7	133.9	2.8	135.0	119.5
040264	14	20-Sep-2008	02:10	14.97	150.3	1.5	149.1	1.3	149.7	135.8
040264	15	25-Jan-2010	17:42	16.32	128.7	3.6	145.2	3.1	137.0	122.5
040264	16	08-Dec-2011	21:46	18.19	140.0	1.2	147.4	1.7	143.7	129.9
040264	17	16-Dec-2012	19:48	19.21	143.4	2.0	144.1	1.0	143.8	128.8
040264	18	07-Feb-2014	01:01	20.35	146.6	2.0	143.7	2.0	145.2	131.5
040264	19	07-Feb-2014	09:03	20.35	147.1	2.1	146.0	1.5	146.5	132.5
040264	20	07-Feb-2014	13:10	20.35	132.3	3.5	142.7	1.6	137.5	122.8
040264	21	07-Feb-2014	16:40	20.36	128.6	0.6	131.1	2.1	129.8	112.2
040264	22	14-Nov-2014	04:11	21.12	150.9	2.7	140.2	2.3	145.6	129.7
040264	23	07-Dec-2015	18:23	22.18	125.6	3.0	141.4	1.6	133.5	118.8
040265	01	25-Jan-1994	06:10	0.32	83.6	2.1	88.7	2.4	86.1	72.1
040265	02	05-Mar-1995	11:21	1.42	80.7	2.1	96.3	2.1	88.5	73.0
040265	03	27-Jan-1997	11:22	3.33	96.3	1.9	105.9	0.8	101.1	87.8
040265	04	04-Dec-1997	12:13	4.18	98.5	2.5	114.8	3.2	106.7	94.3
040265	05	08-Dec-1998	10:28	5.19	106.7	2.1	123.5	2.1	115.1	103.9
040265	06	15-Nov-1999	11:38	6.12	109.0	1.4	127.5	0.9	118.3	105.8
040265	07	30-Nov-2000	13:49	7.17	107.2	0.7	133.4	0.6	120.3	108.8
040265	08	08-Nov-2001	11:28	8.11	117.7	1.6	146.4	0.5	132.0	122.0
040265	09	30-Oct-2002	12:55	9.08	114.4	2.6	141.2	0.8	127.8	114.3
040265	10	04-Feb-2004	14:08	10.35	112.6	2.3	145.8	3.9	129.2	116.8
040265	11	12-Dec-2004	16:15	11.20	115.8	2.1	159.3	4.0	137.5	127.2
040265	12	13-Aug-2006	00:27	12.87	136.0	1.5	169.3	1.3	152.7	143.2
040265	13	13-Dec-2007	12:20	14.20	123.9	0.8	169.3	1.3	146.6	134.9
040265	14	20-Sep-2008	02:10	14.97	143.9	1.7	182.8	1.5	163.3	154.3
040265	15	25-Jan-2010	17:42	16.32	133.9	1.0	181.0	0.6	157.4	146.3
040265	16	08-Dec-2011	21:28	18.19	139.9	1.5	184.9	1.8	162.4	151.9
040265	17	16-Dec-2012	19:48	19.21	141.3	1.8	186.9	1.6	164.1	153.7
040265	18	07-Feb-2014	01:01	20.35	140.4	1.0	184.2	0.8	162.3	151.5
040265	19	07-Feb-2014	09:03	20.35	143.7	1.8	185.9	3.1	164.8	154.2
040265	20	07-Feb-2014	13:10	20.35	137.9	2.3	187.9	2.8	162.9	151.2
040265	21	07-Feb-2014	16:40	20.36	130.5	0.9	183.1	1.4	156.8	143.4

Section	Visit	Date	Time	Age (years)	Left IRI Average (Inches/ mi)	Left IRI SD (Inches/ mi)	Right IRI Average (Inches/ mi)	Right IRI SD (Inches/ mi)	MRI (Inches/ mi)	HRI (Inches/ mi)
040265	22	14-Nov-2014	04:06	21.12	158.8	4.1	182.5	1.0	170.7	156.9
040265	23	07-Dec-2015	18:33	22.18	138.5	1.4	191.4	2.2	164.9	152.7
040266	01	25-Jan-1994	06:10	0.32	81.6	1.3	92.4	1.7	87.0	77.8
040266	02	05-Mar-1995	11:21	1.42	79.0	1.2	95.1	2.5	87.0	78.0
040266	03	27-Jan-1997	11:22	3.33	87.0	1.5	94.1	0.4	90.5	79.5
040266	04	04-Dec-1997	11:06	4.18	88.3	1.5	100.1	3.2	94.2	85.8
040266	05	08-Dec-1998	10:28	5.19	91.5	1.6	102.1	0.5	96.8	88.9
040266	06	15-Nov-1999	11:38	6.12	95.4	3.5	103.5	0.8	99.5	89.0
040266	07	30-Nov-2000	13:37	7.17	89.1	0.7	101.0	0.6	95.0	86.8
040266	08	08-Nov-2001	11:28	8.11	99.3	0.9	109.5	1.5	104.4	96.5
040266	09	30-Oct-2002	13:06	9.08	119.2	5.0	110.0	0.9	114.6	105.0
040266	10	04-Feb-2004	13:47	10.35	105.0	1.1	104.6	1.5	104.8	94.4
040266	11	12-Dec-2004	16:15	11.20	98.1	1.7	109.1	2.2	103.6	97.1
040266	12	13-Aug-2006	00:17	12.87	123.0	3.4	125.7	1.7	124.3	117.1
040266	13	13-Dec-2007	11:59	14.20	114.6	1.5	109.9	1.0	112.2	102.5
040266	14	20-Sep-2008	02:10	14.97	134.2	0.9	130.3	0.7	132.2	124.3
040266	15	25-Jan-2010	17:42	16.32	105.9	1.9	112.8	1.1	109.3	102.6
040266	16	08-Dec-2011	21:38	18.19	126.2	0.8	121.0	2.4	123.6	115.6
040266	17	16-Dec-2012	19:48	19.21	124.0	1.8	119.5	0.9	121.7	113.1
040266	18	07-Feb-2014	01:01	20.35	122.8	1.5	116.5	1.3	119.7	111.1
040266	19	07-Feb-2014	09:03	20.35	123.9	1.6	118.6	1.1	121.2	112.9
040266	20	07-Feb-2014	13:10	20.35	107.8	3.9	113.9	0.5	110.8	104.0
040266	21	07-Feb-2014	16:40	20.36	103.8	0.5	102.8	2.6	103.3	94.3
040266	22	14-Nov-2014	04:06	21.12	143.1	3.8	123.4	2.7	133.3	125.8
040266	23	07-Dec-2015	18:33	22.18	109.2	2.1	108.6	1.8	108.9	100.6
040267	01	25-Jan-1994	06:10	0.32	80.0	1.8	105.9	2.0	93.0	77.9
040267	02	05-Mar-1995	11:21	1.42	79.4	1.0	111.4	4.1	95.4	79.0
040267	03	27-Jan-1997	12:01	3.33	75.0	2.2	105.7	1.4	90.3	75.4
040267	04	04-Dec-1997	11:06	4.18	82.8	5.5	112.3	3.0	97.6	82.4
040267	05	08-Dec-1998	10:28	5.19	82.4	1.7	114.4	1.7	98.4	84.0
040267	06	15-Nov-1999	11:48	6.12	78.2	0.8	114.5	2.0	96.3	82.7
040267	07	30-Nov-2000	13:37	7.17	76.1	0.3	110.8	1.0	93.5	81.6
040267	08	08-Nov-2001	11:09	8.11	86.5	2.7	120.4	1.8	103.4	90.3
040267	09	30-Oct-2002	12:55	9.08	92.4	6.2	110.5	2.6	101.5	86.5
040267	10	04-Feb-2004	13:57	10.35	87.1	1.0	105.2	1.0	96.1	82.5
040267	11	12-Dec-2004	16:15	11.20	87.9	1.5	114.6	1.4	101.3	89.0
040267	12	13-Aug-2006	00:17	12.87	98.3	1.7	111.1	1.9	104.7	92.1
040267	S01	13-Aug-2006	02:01	12.87	98.9	2.9	110.0	2.2	104.5	91.4
040267	13	13-Dec-2007	11:59	14.20	81.5	1.3	84.7	1.3	83.1	71.2
040267	14	20-Sep-2008	02:10	14.97	92.2	1.5	102.1	1.6	97.2	87.7
040267	15	25-Jan-2010	17:42	16.32	77.7	2.2	92.7	1.7	85.2	74.5
040267	16	08-Dec-2011	22:03	18.19	84.0	0.8	89.6	2.3	86.8	76.6
040267	17	16-Dec-2012	19:58	19.21	81.9	1.5	87.7	2.1	84.8	74.9
040267	18	07-Feb-2014	01:01	20.35	79.1	1.6	87.1	1.1	83.1	73.4
040267	19	07-Feb-2014	09:03	20.35	80.5	0.3	95.4	9.5	88.0	77.9
040267	20	07-Feb-2014	13:10	20.35	76.8	0.7	88.4	7.9	82.6	71.8
040267	21	07-Feb-2014	16:40	20.36	72.1	0.2	92.6	5.7	82.3	72.7
040267	22	14-Nov-2014	04:06	21.12	84.0	3.2	81.3	1.7	82.6	72.1

Section	Visit	Date	Time	Age (years)	Left IRI Average (Inches/ mi)	Left IRI SD (Inches/ mi)	Right IRI Average (Inches/ mi)	Right IRI SD (Inches/ mi)	MRI (Inches/ mi)	HRI (Inches/ mi)
040267	23	07-Dec-2015	18:23	22.18	72.5	2.4	95.0	3.4	83.7	73.8
040268	01	25-Jan-1994	06:10	0.32	85.0	2.0	93.5	0.6	89.3	73.5
040268	02	05-Mar-1995	11:21	1.42	79.9	1.6	96.0	3.7	87.9	72.4
040268	03	27-Jan-1997	12:01	3.33	90.6	1.2	91.9	1.2	91.2	74.7
040268	04	04-Dec-1997	11:06	4.18	88.7	3.9	94.6	2.5	91.7	76.4
040268	05	08-Dec-1998	10:28	5.19	92.6	3.2	98.3	3.0	95.5	79.3
040268	06	15-Nov-1999	11:48	6.12	94.2	1.5	97.6	1.6	95.9	79.3
040268	07	30-Nov-2000	13:37	7.17	92.3	0.5	97.0	1.9	94.7	77.8
040268	08	08-Nov-2001	11:28	8.11	97.4	1.1	103.8	2.1	100.6	83.7
040268	09	30-Oct-2002	12:40	9.08	102.1	4.5	96.9	2.9	99.5	84.2
040268	10	04-Feb-2004	13:47	10.35	99.4	0.5	92.0	1.9	95.7	80.4
040268	11	12-Dec-2004	16:58	11.20	97.7	3.6	98.3	2.2	98.0	80.3
040268	12	13-Aug-2006	00:27	12.87	116.1	0.6	112.2	1.9	114.1	100.5
040268	13	13-Dec-2007	12:20	14.20	98.8	2.2	94.9	1.2	96.8	80.3
040268	14	20-Sep-2008	02:10	14.97	107.1	3.1	107.5	2.4	107.3	93.6
040268	15	25-Jan-2010	17:53	16.32	94.8	2.3	100.8	0.8	97.8	80.6
040268	16	08-Dec-2011	21:38	18.19	106.7	1.4	98.2	2.4	102.5	88.3
040268	17	16-Dec-2012	19:58	19.21	103.6	1.4	97.3	2.0	100.5	84.7
040268	18	07-Feb-2014	01:01	20.35	103.3	1.2	96.7	1.6	100.0	84.7
040268	19	07-Feb-2014	09:03	20.35	105.5	1.4	93.2	1.9	99.4	84.4
040268	20	07-Feb-2014	13:10	20.35	96.0	2.5	93.5	2.8	94.7	77.3
040268	21	07-Feb-2014	16:40	20.36	91.2	1.8	94.1	0.8	92.7	75.5
040268	22	14-Nov-2014	04:17	21.12	109.0	2.0	94.3	1.4	101.7	87.9
040268	23	07-Dec-2015	18:33	22.18	97.2	1.5	93.2	2.0	95.2	78.9
063021	01	01-Feb-1990	17:20	15.84	80.7	2.6	100.0	1.0	90.3	82.9
063021	02	20-Sep-1990	11:25	16.47	78.0	1.0	101.1	0.9	89.6	83.0
063021	03	12-Mar-1991	14:23	16.95	76.2	1.1	96.3	1.3	86.3	78.1
063021	04	29-Feb-1992	17:03	17.92	78.1	0.7	97.8	0.9	88.0	80.3
063021	05	02-Mar-1993	17:04	18.92	78.4	2.8	97.5	0.9	87.9	79.1
063021	06	02-Mar-1993	18:33	18.92	82.2	0.8	100.1	1.1	91.2	82.3
063021	07	10-Apr-1995	12:34	21.03	72.4	1.3	93.0	1.1	82.7	75.0
063021	08	24-Feb-1997	11:11	22.90	83.0	0.8	104.2	1.3	93.6	84.7
063021	09	16-Feb-1998	12:02	23.88	78.6	0.7	97.0	1.8	87.8	79.3
063021	10	10-Mar-1999	12:53	24.94	78.3	0.8	99.2	1.8	88.7	78.8
063021	11	15-Feb-2001	12:27	26.88	82.5	1.2	100.8	1.3	91.7	81.4
063021	12	14-Nov-2002	13:24	28.62	86.6	2.0	108.9	1.8	97.8	85.4
063021	13	04-Dec-2004	09:47	30.68	86.2	1.9	106.8	1.2	96.5	85.8
063021	14	07-Dec-2004	10:36	30.69	86.4	1.6	106.7	1.3	96.6	85.5
063021	15	29-Jan-2007	16:08	32.83	86.0	1.4	109.9	1.4	98.0	87.1
063021	16	05-Nov-2009	15:11	35.60	93.2	2.5	117.6	2.4	105.4	94.9
063021	17	08-Mar-2011	15:05	36.94	88.8	1.0	114.8	1.3	101.8	90.5
063021	18	10-Mar-2012	14:34	37.94	75.0	1.3	72.5	3.4	73.8	55.5
063021	19	23-Jan-2013	17:14	38.82	71.6	3.7	66.8	2.2	69.2	52.8
063021	20	17-Mar-2014	19:50	39.96	64.6	3.3	59.6	2.1	62.1	49.3
063021	21	15-Jan-2015	18:52	40.79	61.0	1.7	65.4	2.4	63.2	50.7
133019	01	03-Aug-1990	09:38	8.67	94.0	0.3	93.5	1.3	93.7	82.2
133019	02	20-May-1992	13:10	10.47	101.1	0.9	97.0	1.0	99.0	86.9
133019	03	27-Jul-1992	12:36	10.65	93.2	0.9	96.7	0.7	94.9	82.7

Section	Visit	Date	Time	Age (years)	Left IRI Average (Inches/ mi)	Left IRI SD (Inches/ mi)	Right IRI Average (Inches/ mi)	Right IRI SD (Inches/ mi)	MRI (Inches/ mi)	HRI (Inches/ mi)
133019	04	23-Oct-1992	09:24	10.89	95.7	0.8	99.6	1.2	97.6	85.3
133019	05	14-Jan-1993	13:57	11.12	99.2	1.0	106.2	1.4	102.7	91.0
133019	06	09-May-1994	09:25	12.44	89.6	0.6	97.3	0.9	93.4	84.3
133019	07	26-Jan-1996	06:43	14.15	97.3	1.0	116.0	1.5	106.7	94.5
133019	08	26-Jan-1996	12:12	14.15	101.5	0.5	117.7	1.2	109.6	97.2
133019	09	05-Apr-1996	07:14	14.34	99.4	2.0	129.0	2.1	114.2	102.9
133019	10	05-Apr-1996	13:02	14.35	102.7	0.8	131.8	0.6	117.3	106.1
133019	11	13-Aug-1996	10:14	14.70	97.9	1.6	106.0	1.3	101.9	90.2
133019	12	13-Aug-1996	12:53	14.70	99.2	1.3	96.9	1.0	98.0	87.1
133019	13	17-Oct-1996	07:48	14.88	97.5	0.8	93.9	0.8	95.7	84.3
133019	14	17-Oct-1996	15:40	14.88	99.8	1.0	94.7	1.4	97.2	86.1
133019	15	16-Oct-1997	09:04	15.88	101.3	0.3	95.3	1.0	98.3	87.4
133019	16	16-Oct-1997	12:16	15.88	101.4	0.8	91.3	2.2	96.4	86.2
133019	17	29-Jan-1998	07:33	16.16	104.2	0.9	89.7	1.4	97.0	86.1
133019	18	29-Jan-1998	13:12	16.16	116.0	0.5	114.8	1.4	115.4	104.7
133019	19	27-Apr-1998	08:05	16.40	107.6	1.2	107.3	2.8	107.5	95.2
133019	20	27-Apr-1998	12:06	16.40	110.6	0.9	109.1	2.0	109.8	98.0
133019	21	06-Aug-1998	10:30	16.68	108.3	0.6	136.3	2.8	122.3	108.0
133019	22	09-Dec-1998	12:00	17.02	110.6	1.3	95.5	0.7	103.1	89.9
133019	23	14-May-1999	11:18	17.45	108.6	1.0	105.9	2.2	107.2	95.5
133019	24	13-Apr-2000	09:37	18.37	104.7	1.1	110.7	0.9	107.7	95.7
133019	25	14-Aug-2000	13:55	18.70	108.2	1.0	105.1	1.3	106.6	96.2
133019	26	16-Feb-2001	10:56	19.21	113.2	0.8	118.9	1.0	116.0	104.8
133019	27	16-Feb-2001	16:55	19.21	109.4	1.2	112.6	2.4	111.0	100.5
133019	28	23-May-2001	09:16	19.48	114.8	1.4	114.0	1.9	114.4	103.7
133019	29	23-May-2001	15:26	19.48	112.1	0.9	115.3	3.5	113.7	102.9
133019	30	06-Aug-2001	07:55	19.68	107.4	0.7	102.8	1.2	105.1	94.7
133019	31	06-Aug-2001	13:23	19.68	113.0	0.7	113.3	2.1	113.2	102.1
133019	32	14-Mar-2002	08:00	20.28	108.6	0.9	115.9	0.3	112.2	101.4
133019	33	14-Mar-2002	13:01	20.28	117.1	1.2	121.6	1.5	119.4	108.2
133019	34	10-Dec-2002	10:02	21.03	107.7	1.1	115.9	1.2	111.8	100.7
133019	35	04-Aug-2004	11:55	22.68	117.1	0.6	115.9	1.4	116.5	106.1
133019	36	27-Nov-2007	16:11	25.99	115.7	0.9	111.6	3.1	113.7	103.6
133019	37	10-Feb-2010	10:45	28.20	120.8	1.7	118.2	1.7	119.5	109.6
133019	38	04-Nov-2013	14:30	31.93	55.7	1.3	48.2	1.6	52.0	42.8
133019	39	11-Oct-2014	16:43	32.86	60.6	0.6	47.5	0.9	54.1	43.8
183002	01	23-Aug-1990	10:48	14.06	124.6	3.5	102.6	1.4	113.6	107.5
183002	02	10-Sep-1991	11:00	15.11	130.7	3.0	105.7	1.6	118.2	111.8
183002	03	04-Oct-1992	15:37	16.18	122.5	0.8	100.3	2.2	111.4	105.1
183002	04	11-Jan-1994	18:41	17.45	119.6	1.5	103.2	1.0	111.4	104.6
183002	05	16-Mar-1995	08:26	18.62	126.2	2.5	99.3	0.9	112.8	105.7
183002	06	24-Oct-1995	07:48	19.23	145.1	1.0	120.6	0.8	132.8	127.2
183002	07	24-Oct-1995	11:42	19.23	139.1	1.3	114.1	1.4	126.6	121.0
183002	08	24-Oct-1995	16:01	19.23	138.0	2.0	115.3	1.3	126.6	120.6
183002	09	04-Mar-1996	07:23	19.59	134.0	2.0	105.5	3.0	119.8	112.6
183002	10	04-Mar-1996	11:36	19.59	130.3	2.8	98.2	2.5	114.2	106.4
183002	11	04-Mar-1996	15:45	19.59	133.9	4.7	113.9	13.7	123.9	114.3
183002	12	06-Sep-1996	16:39	20.10	121.7	2.4	99.3	2.0	110.5	103.5
183002	13	22-May-1997	07:44	20.81	132.8	1.2	107.2	0.3	120.0	111.3

Section	Visit	Date	Time	Age (years)	Left IRI Average (Inches/ mi)	Left IRI SD (Inches/ mi)	Right IRI Average (Inches/ mi)	Right IRI SD (Inches/ mi)	MRI (Inches/ mi)	HRI (Inches/ mi)
183002	14	05-Dec-1997	08:36	21.35	135.9	0.8	112.9	0.5	124.4	116.9
183002	15	05-Dec-1997	14:37	21.35	135.4	0.9	112.4	0.7	123.9	116.3
183002	16	05-Feb-1998	14:29	21.52	130.3	1.6	103.9	0.8	117.1	108.9
183002	17	06-Feb-1998	06:53	21.52	131.9	1.0	105.1	0.6	118.5	111.0
183002	18	26-May-1998	07:59	21.82	132.7	1.1	106.9	0.8	119.8	109.9
183002	19	26-May-1998	15:13	21.82	129.3	1.6	105.2	1.7	117.3	107.0
183002	20	16-Aug-1998	08:01	22.04	129.9	0.5	104.0	1.1	117.0	107.8
183002	21	17-Aug-1998	13:07	22.04	129.6	0.8	106.1	1.6	117.8	107.8
183002	22	29-Oct-1999	13:06	23.24	127.8	1.9	109.0	1.4	118.4	108.3
183002	23	23-Aug-2000	13:59	24.06	127.8	1.1	97.8	0.7	112.8	104.3
183002	24	11-Nov-2001	11:59	25.28	151.4	2.3	122.8	1.5	137.1	125.2
183002	25	24-Nov-2003	17:09	27.31	146.2	2.8	134.0	2.0	140.1	130.0
183002	26	26-Jul-2004	16:06	27.99	140.9	1.4	156.3	2.3	148.6	135.2
183002	27	17-Oct-2007	12:34	31.21	146.0	1.6	230.7	3.4	188.4	167.9
183002	28	20-Jul-2010	11:46	33.97	168.3	3.1	168.7	2.7	168.5	149.8
183002	29	26-Apr-2011	14:37	34.73	180.4	4.7	203.8	3.4	192.1	172.6
183002	30	24-Jul-2012	12:43	35.98	161.1	1.6	188.8	1.7	174.9	155.9
183002	31	29-Apr-2015	17:26	38.74	49.9	0.3	69.8	1.9	59.9	49.1
200201	01	14-Aug-1992	13:17	0.00	91.8	3.2	86.2	1.5	89.0	80.6
200201	02	10-Mar-1993	11:05	0.57	97.6	7.7	87.0	4.4	92.3	85.4
200201	03	15-May-1994	10:10	1.75	79.9	1.0	78.6	2.2	79.2	71.8
200201	04	18-Feb-1995	09:12	2.52	85.0	1.9	81.1	0.8	83.1	75.8
200201	05	20-Apr-1996	13:31	3.69	90.6	2.3	90.3	1.3	90.5	79.9
200201	06	03-Mar-1997	11:40	4.55	98.3	2.8	88.6	1.7	93.4	82.5
200201	07	15-May-1998	10:37	5.75	93.4	0.8	104.2	2.1	98.8	86.3
200201	08	15-Mar-1999	08:34	6.58	100.3	1.4	104.8	3.6	102.6	92.3
200201	09	01-Mar-2000	11:25	7.55	108.4	1.1	107.4	1.0	107.9	98.3
200201	10	10-May-2001	14:20	8.74	104.2	1.2	131.6	2.1	117.9	106.8
200201	11	21-Apr-2002	08:22	9.69	114.7	1.5	155.0	5.0	134.8	118.4
200201	12	20-Feb-2003	10:52	10.52	127.5	1.2	133.7	1.7	130.6	118.7
200201	13	12-Mar-2004	17:04	11.58	125.0	2.5	125.7	1.8	125.3	112.4
200201	14	05-Jun-2006	13:24	13.81	118.0	3.7	126.0	1.0	122.0	110.2
200201	15	19-Apr-2008	09:42	15.68	128.5	2.2	136.1	2.5	132.3	121.2
200201	16	07-Aug-2009	10:01	16.98	126.2	0.9	140.2	3.5	133.2	122.3
200201	17	19-Oct-2010	15:49	18.18	135.6	2.1	143.3	2.3	139.5	128.4
200201	18	21-Sep-2012	14:08	20.11	139.6	1.3	143.4	2.0	141.5	130.9
200201	19	03-Dec-2013	16:25	21.31	141.6	0.7	150.5	2.8	146.1	135.1
200201	20	05-May-2014	14:45	21.72	146.9	4.1	155.5	1.1	151.2	140.2
200201	21	06-May-2014	06:57	21.73	127.0	1.8	136.4	2.4	131.7	120.2
200201	22	06-May-2014	14:10	21.73	151.1	1.4	156.2	3.0	153.7	142.9
200201	23	06-May-2014	20:25	21.73	136.2	2.3	144.8	2.3	140.5	129.7
200201	24	09-Dec-2015	13:08	23.32	146.6	1.6	159.5	4.2	153.0	141.7
200202	01	14-Aug-1992	13:17	0.00	77.5	2.3	83.0	0.6	80.3	76.5
200202	02	10-Mar-1993	11:26	0.57	57.4	1.8	58.9	1.1	58.2	55.8
200202	03	15-May-1994	10:10	1.75	45.8	1.7	55.9	2.0	50.8	49.2
200202	04	18-Feb-1995	09:12	2.52	51.7	3.1	54.2	4.7	52.9	50.8
200202	05	20-Apr-1996	13:31	3.69	51.8	2.0	52.2	3.3	52.0	47.4
200202	06	03-Mar-1997	11:40	4.55	54.4	2.2	48.7	1.5	51.6	48.6

Section	Visit	Date	Time	Age (years)	Left IRI Average (Inches/ mi)	Left IRI SD (Inches/ mi)	Right IRI Average (Inches/ mi)	Right IRI SD (Inches/ mi)	MRI (Inches/ mi)	HRI (Inches/ mi)
200202	07	15-May-1998	10:26	5.75	53.8	1.4	68.7	1.0	61.3	58.6
200202	08	15-Mar-1999	08:34	6.58	59.1	2.7	70.0	2.9	64.5	62.1
200202	09	01-Mar-2000	11:25	7.55	53.5	0.4	63.8	0.4	58.6	56.5
200202	10	10-May-2001	14:08	8.74	50.6	0.5	64.3	2.3	57.5	54.6
200202	11	21-Apr-2002	08:01	9.69	64.2	1.2	84.4	6.4	74.3	71.4
200202	12	20-Feb-2003	10:31	10.52	59.0	0.7	69.9	1.5	64.5	61.8
200202	13	12-Mar-2004	17:15	11.58	59.8	0.6	70.4	1.5	65.1	62.3
200202	14	05-Jun-2006	12:58	13.81	60.1	1.0	69.6	1.0	64.8	61.9
200202	15	19-Apr-2008	09:52	15.68	69.0	1.0	74.6	0.5	71.8	68.9
200202	16	07-Aug-2009	09:23	16.98	68.1	1.0	76.2	0.8	72.2	69.1
200202	17	19-Oct-2010	15:59	18.18	76.5	0.5	83.6	1.0	80.1	77.1
200202	18	21-Sep-2012	13:58	20.11	84.8	0.8	83.7	0.8	84.3	81.4
200202	19	03-Dec-2013	16:25	21.31	90.1	0.7	88.8	1.1	89.4	86.8
200202	20	05-May-2014	14:35	21.72	91.6	0.3	88.7	0.7	90.2	87.7
200202	21	06-May-2014	06:57	21.73	93.1	1.1	90.1	2.8	91.6	88.9
200202	22	06-May-2014	13:53	21.73	92.7	0.1	90.0	0.7	91.3	88.7
200202	23	06-May-2014	20:25	21.73	89.6	0.4	87.3	1.0	88.5	85.9
200202	24	09-Dec-2015	13:23	23.32	99.0	0.6	94.2	0.8	96.6	93.2
200203	01	14-Aug-1992	13:17	0.00	89.1	1.7	88.4	1.6	88.8	81.9
200203	02	10-Mar-1993	11:41	0.57	105.1	3.3	99.9	1.3	102.5	93.7
200203	03	15-May-1994	10:10	1.75	96.1	2.2	82.9	0.7	89.5	82.7
200203	04	18-Feb-1995	09:12	2.52	99.5	1.1	85.0	1.8	92.2	85.1
200203	05	20-Apr-1996	13:31	3.69	98.3	3.5	91.4	0.8	94.8	87.9
200203	06	03-Mar-1997	11:52	4.55	102.2	1.6	90.9	1.4	96.5	88.6
200203	07	15-May-1998	10:37	5.75	100.8	1.3	90.4	1.5	95.6	87.0
200203	08	15-Mar-1999	08:34	6.58	100.3	1.3	89.1	3.2	94.7	87.1
200203	09	01-Mar-2000	11:25	7.55	105.4	0.9	91.7	1.1	98.6	91.0
200203	10	10-May-2001	14:08	8.74	104.5	1.4	90.7	1.2	97.6	90.8
200203	11	21-Apr-2002	08:01	9.69	99.8	1.4	95.4	6.6	97.6	89.4
200203	12	20-Feb-2003	10:31	10.52	105.5	0.9	94.5	1.2	100.0	92.9
200203	13	12-Mar-2004	17:04	11.58	106.6	1.7	94.9	2.1	100.7	93.5
200203	14	05-Jun-2006	13:14	13.81	107.9	1.9	93.6	1.4	100.7	93.4
200203	15	19-Apr-2008	10:03	15.68	106.9	1.5	97.7	1.3	102.3	95.4
200203	16	07-Aug-2009	09:34	16.98	107.6	0.5	95.0	2.1	101.3	93.5
200203	17	19-Oct-2010	15:49	18.18	108.4	2.2	100.6	1.6	104.5	96.9
200203	18	21-Sep-2012	13:58	20.11	111.6	1.3	104.2	1.1	107.9	100.7
200203	19	03-Dec-2013	16:25	21.31	111.0	0.6	103.3	1.3	107.2	100.4
200203	20	05-May-2014	14:17	21.72	111.9	1.0	106.3	1.8	109.1	102.5
200203	21	06-May-2014	06:57	21.73	103.0	2.5	94.1	3.0	98.6	91.5
200203	22	06-May-2014	14:34	21.73	112.7	0.9	107.2	1.7	110.0	103.3
200203	23	06-May-2014	20:25	21.73	109.1	0.9	102.9	3.3	106.0	99.6
200203	24	09-Dec-2015	13:08	23.32	113.5	0.7	103.0	1.0	108.2	101.1
200204	01	14-Aug-1992	13:17	0.00	98.5	1.6	80.3	1.8	89.4	84.3
200204	02	10-Mar-1993	11:05	0.57	104.1	2.7	87.7	2.0	95.9	90.3
200204	03	15-May-1994	10:10	1.75	81.0	1.4	73.1	1.2	77.0	68.3
200204	04	18-Feb-1995	09:12	2.52	87.0	1.9	74.5	1.2	80.7	73.5
200204	05	20-Apr-1996	13:31	3.69	91.4	2.0	79.9	2.9	85.6	75.2
200204	06	03-Mar-1997	11:40	4.55	85.5	2.0	76.8	0.9	81.1	68.7

Section	Visit	Date	Time	Age (years)	Left IRI Average (Inches/ mi)	Left IRI SD (Inches/ mi)	Right IRI Average (Inches/ mi)	Right IRI SD (Inches/ mi)	MRI (Inches/ mi)	HRI (Inches/ mi)
200204	07	15-May-1998	10:49	5.75	91.0	1.8	83.8	1.9	87.4	77.0
200204	08	15-Mar-1999	08:34	6.58	100.2	4.5	91.6	3.2	95.9	87.5
200204	09	01-Mar-2000	11:25	7.55	93.8	2.4	81.7	1.7	87.8	78.2
200204	10	10-May-2001	14:20	8.74	86.1	0.5	77.1	0.5	81.6	70.8
200204	11	21-Apr-2002	08:01	9.69	105.5	1.5	108.6	5.2	107.0	98.6
200204	12	20-Feb-2003	10:41	10.52	87.8	1.8	89.6	2.8	88.7	81.8
200204	13	12-Mar-2004	17:45	11.58	96.0	2.9	87.0	1.2	91.5	81.4
200204	14	05-Jun-2006	12:58	13.81	89.9	0.8	81.9	1.6	85.9	75.5
200204	15	19-Apr-2008	10:13	15.68	87.8	1.4	86.7	1.9	87.2	77.8
200204	16	07-Aug-2009	09:23	16.98	88.8	1.8	83.3	1.1	86.1	76.5
200204	17	19-Oct-2010	15:49	18.18	86.2	1.5	88.1	1.7	87.2	78.2
200204	18	21-Sep-2012	13:58	20.11	84.0	1.5	84.4	1.1	84.2	72.5
200204	19	03-Dec-2013	16:25	21.31	82.5	1.1	87.1	2.2	84.8	75.5
200204	20	05-May-2014	14:35	21.72	80.1	0.7	83.3	1.1	81.7	70.2
200204	21	06-May-2014	06:57	21.73	95.7	2.5	95.2	1.0	95.4	86.6
200204	22	06-May-2014	13:53	21.73	79.8	0.7	84.3	2.1	82.0	71.6
200204	23	06-May-2014	20:25	21.73	83.4	1.5	84.7	3.3	84.1	73.2
200204	24	09-Dec-2015	13:08	23.32	87.9	1.4	89.7	0.8	88.8	76.8
200205	01	14-Aug-1992	13:17	0.00	87.5	1.2	76.1	1.9	81.8	76.9
200205	02	10-Mar-1993	11:05	0.57	107.1	14.4	82.7	3.3	94.9	88.9
200205	03	15-May-1994	10:10	1.75	91.8	1.5	76.0	0.8	83.9	77.6
200205	04	18-Feb-1995	09:12	2.52	89.9	3.9	74.7	1.1	82.3	77.3
200205	05	20-Apr-1996	13:31	3.69	97.1	1.8	85.3	4.4	91.2	84.4
200205	06	03-Mar-1997	12:02	4.55	95.6	0.8	82.2	1.0	88.9	80.4
200205	07	15-May-1998	10:26	5.75	96.0	1.9	80.5	2.5	88.2	78.2
200205	08	15-Mar-1999	08:34	6.58	93.9	1.7	80.1	0.9	87.0	78.1
200205	09	01-Mar-2000	11:25	7.55	101.7	3.5	86.4	2.5	94.1	86.2
200205	10	10-May-2001	14:20	8.74	104.0	1.5	94.6	1.1	99.3	91.3
200205	11	21-Apr-2002	08:01	9.69	95.4	3.5	90.2	6.8	92.8	84.0
200205	12	20-Feb-2003	10:41	10.52	104.7	2.6	99.3	2.0	102.0	94.9
200205	13	12-Mar-2004	17:15	11.58	102.2	1.7	100.8	3.0	101.5	93.8
200205	14	05-Jun-2006	12:58	13.81	115.1	2.3	116.7	1.0	115.9	108.8
200205	15	19-Apr-2008	09:42	15.68	109.0	1.4	125.1	4.9	117.1	109.7
200205	16	07-Aug-2009	09:23	16.98	122.4	5.0	120.5	2.4	121.5	115.7
200205	17	19-Oct-2010	15:49	18.18	124.5	1.1	116.5	1.5	120.5	113.6
200205	18	21-Sep-2012	14:08	20.11	119.6	2.7	136.2	4.6	127.9	118.3
200205	19	03-Dec-2013	16:25	21.31	120.6	2.3	148.9	6.2	134.7	124.4
200205	20	05-May-2014	14:17	21.72	144.3	0.8	182.5	7.9	163.4	153.9
200205	21	06-May-2014	06:57	21.73	117.9	2.5	178.8	24.3	148.4	134.5
200205	22	06-May-2014	13:53	21.73	145.0	2.9	210.5	21.6	177.8	164.9
200205	23	06-May-2014	20:25	21.73	133.1	2.2	169.4	5.6	151.3	140.7
200205	24	09-Dec-2015	13:08	23.32	136.0	6.7	164.1	5.8	150.1	140.9
200206	01	14-Aug-1992	13:17	0.00	153.2	1.9	116.5	1.9	134.9	126.3
200206	02	10-Mar-1993	11:05	0.57	114.5	12.7	95.5	3.2	105.0	95.7
200206	03	15-May-1994	10:10	1.75	93.7	1.8	81.2	1.2	87.5	79.3
200206	04	18-Feb-1995	09:12	2.52	102.3	2.9	82.9	1.9	92.6	83.5
200206	05	20-Apr-1996	13:31	3.69	95.4	3.4	87.1	2.4	91.3	80.3
200206	06	03-Mar-1997	11:52	4.55	142.9	3.2	81.8	1.2	112.4	100.8

Section	Visit	Date	Time	Age (years)	Left IRI Average (Inches/ mi)	Left IRI SD (Inches/ mi)	Right IRI Average (Inches/ mi)	Right IRI SD (Inches/ mi)	MRI (Inches/ mi)	HRI (Inches/ mi)
200206	07	15-May-1998	10:26	5.75	104.5	2.7	99.8	3.0	102.2	87.6
200206	08	15-Mar-1999	08:34	6.58	112.9	4.0	97.8	3.5	105.3	93.4
200206	09	01-Mar-2000	11:25	7.55	114.2	4.3	92.3	1.4	103.3	89.9
200206	10	10-May-2001	14:20	8.74	107.4	4.5	100.0	3.6	103.7	91.2
200206	11	21-Apr-2002	08:01	9.69	111.9	2.5	102.3	7.4	107.1	93.6
200206	12	20-Feb-2003	10:31	10.52	108.1	2.1	98.7	0.6	103.4	89.9
200206	13	12-Mar-2004	17:04	11.58	124.9	5.7	96.1	2.9	110.5	96.9
200206	14	05-Jun-2006	12:58	13.81	127.6	1.6	108.5	1.4	118.0	105.1
200206	15	19-Apr-2008	09:42	15.68	129.1	1.9	109.6	2.2	119.4	107.1
200206	16	07-Aug-2009	10:01	16.98	133.2	3.1	115.9	0.4	124.5	112.6
200206	17	19-Oct-2010	15:59	18.18	135.3	1.2	113.1	1.2	124.2	111.6
200206	18	21-Sep-2012	14:08	20.11	160.9	2.4	132.1	1.3	146.5	134.7
200206	19	03-Dec-2013	16:45	21.31	150.5	3.8	129.0	1.6	139.7	128.5
200206	20	05-May-2014	14:17	21.72	173.5	2.5	152.2	1.1	162.9	152.3
200206	21	06-May-2014	06:57	21.73	152.6	7.1	124.0	2.5	138.3	126.9
200206	22	06-May-2014	13:53	21.73	176.3	1.5	154.7	1.0	165.5	155.2
200206	23	06-May-2014	20:25	21.73	170.8	9.0	140.4	2.2	155.6	145.3
200206	24	09-Dec-2015	13:08	23.32	185.4	2.8	141.4	1.4	163.4	153.9
200207	01	14-Aug-1992	13:17	0.00	101.9	2.3	97.9	0.5	99.9	93.0
200207	02	10-Mar-1993	11:05	0.57	115.7	2.5	100.1	1.1	107.9	100.6
200207	03	15-May-1994	10:10	1.75	99.6	1.3	87.9	1.5	93.7	86.2
200207	04	18-Feb-1995	09:12	2.52	108.6	1.6	90.0	1.6	99.3	90.9
200207	05	20-Apr-1996	13:31	3.69	128.6	27.2	99.4	2.6	114.0	103.9
200207	06	03-Mar-1997	11:52	4.55	115.1	3.1	99.1	2.9	107.1	95.4
200207	07	15-May-1998	10:37	5.75	108.6	0.8	101.5	1.2	105.0	93.4
200207	08	15-Mar-1999	08:34	6.58	105.1	1.9	101.6	0.7	103.3	91.8
200207	09	01-Mar-2000	11:25	7.55	109.4	1.7	102.4	1.5	105.9	96.5
200207	10	10-May-2001	14:08	8.74	118.2	1.2	109.1	1.7	113.6	103.6
200207	11	21-Apr-2002	08:01	9.69	105.7	0.7	108.8	8.2	107.3	95.1
200207	12	20-Feb-2003	10:41	10.52	114.6	1.5	111.4	2.3	113.0	102.3
200207	13	12-Mar-2004	17:04	11.58	120.7	0.8	102.7	1.8	111.7	100.6
200207	14	05-Jun-2006	12:58	13.81	124.6	1.0	124.6	1.5	124.6	116.2
200207	15	19-Apr-2008	10:03	15.68	120.4	2.2	116.3	1.4	118.3	109.8
200207	16	07-Aug-2009	09:23	16.98	136.9	2.9	130.7	2.6	133.8	125.9
200207	17	19-Oct-2010	15:49	18.18	135.1	0.4	130.7	1.0	132.9	124.6
200207	18	21-Sep-2012	13:58	20.11	146.2	1.7	136.1	1.2	141.1	133.6
200207	19	03-Dec-2013	16:25	21.31	132.5	1.5	127.7	2.9	130.1	122.2
200207	20	05-May-2014	14:17	21.72	146.4	0.6	141.3	1.6	143.8	136.6
200207	21	06-May-2014	06:57	21.73	131.1	1.3	122.1	2.2	126.6	118.3
200207	22	06-May-2014	13:53	21.73	148.9	1.5	143.1	1.8	146.0	139.1
200207	23	06-May-2014	20:25	21.73	145.8	1.7	135.6	1.5	140.7	133.0
200207	24	09-Dec-2015	13:08	23.32	144.1	1.8	129.7	0.9	136.9	128.2
200208	01	14-Aug-1992	13:17	0.00	123.8	2.3	121.8	1.4	122.8	115.1
200208	02	10-Mar-1993	11:05	0.57	133.7	3.2	132.0	7.3	132.9	125.3
200208	03	15-May-1994	11:00	1.75	117.6	0.7	112.7	1.6	115.2	107.0
200208	04	18-Feb-1995	09:12	2.52	123.2	0.7	120.6	0.6	121.9	113.7
200208	05	20-Apr-1996	13:31	3.69	134.4	16.6	123.9	3.8	129.1	119.8
200208	06	03-Mar-1997	11:40	4.55	122.5	1.1	117.8	0.8	120.1	107.2

Section	Visit	Date	Time	Age (years)	Left IRI Average (Inches/ mi)	Left IRI SD (Inches/ mi)	Right IRI Average (Inches/ mi)	Right IRI SD (Inches/ mi)	MRI (Inches/ mi)	HRI (Inches/ mi)
200208	07	15-May-1998	10:49	5.75	124.0	1.1	133.2	2.3	128.6	117.2
200208	08	15-Mar-1999	08:34	6.58	129.6	0.8	136.4	2.3	133.0	122.7
200208	09	01-Mar-2000	11:25	7.55	126.8	1.5	129.2	1.9	128.0	116.9
200208	10	10-May-2001	14:08	8.74	126.2	1.4	133.4	2.4	129.8	119.5
200208	11	21-Apr-2002	08:01	9.69	128.8	1.0	152.2	10.2	140.5	129.1
200208	12	20-Feb-2003	10:31	10.52	124.0	0.9	133.0	2.6	128.5	118.5
200208	13	12-Mar-2004	17:04	11.58	126.9	1.8	128.2	1.0	127.6	115.4
200208	14	05-Jun-2006	12:58	13.81	125.4	1.6	133.6	1.4	129.5	119.3
200208	15	19-Apr-2008	10:03	15.68	125.5	0.8	130.8	1.4	128.2	117.0
200208	16	07-Aug-2009	09:23	16.98	128.9	2.0	134.7	1.7	131.8	121.4
200208	17	19-Oct-2010	15:49	18.18	128.8	1.2	136.7	1.5	132.7	122.6
200208	18	21-Sep-2012	14:08	20.11	136.8	0.2	135.8	0.6	136.3	123.5
200208	19	03-Dec-2013	16:25	21.31	132.8	0.6	137.4	1.3	135.1	125.5
200208	20	05-May-2014	14:35	21.72	138.2	1.9	139.7	1.0	138.9	128.5
200208	21	06-May-2014	06:57	21.73	130.9	1.6	135.9	4.3	133.4	123.5
200208	22	06-May-2014	13:53	21.73	139.8	1.4	139.6	1.4	139.7	128.4
200208	23	06-May-2014	20:25	21.73	138.0	2.5	135.2	2.8	136.6	124.8
200208	24	09-Dec-2015	13:08	23.32	141.4	2.6	134.5	2.4	138.0	125.8
200209	01	14-Aug-1992	13:17	0.00	73.8	1.6	70.9	0.2	72.4	65.3
200209	02	10-Mar-1993	11:05	0.57	91.2	8.1	83.9	3.9	87.6	79.9
200209	03	15-May-1994	10:10	1.75	71.2	1.6	67.2	0.6	69.2	63.0
200209	04	18-Feb-1995	09:12	2.52	76.5	3.2	73.6	1.1	75.0	68.2
200209	05	20-Apr-1996	13:31	3.69	81.8	5.5	80.1	1.8	80.9	72.7
200209	06	03-Mar-1997	11:40	4.55	59.2	0.6	79.4	0.9	69.3	64.1
200209	07	15-May-1998	10:26	5.75	65.9	1.4	81.0	3.0	73.4	65.4
200209	08	15-Mar-1999	08:34	6.58	63.3	3.9	76.2	1.7	69.8	62.8
200209	09	01-Mar-2000	11:25	7.55	61.0	2.0	79.0	0.9	70.0	63.9
200209	10	10-May-2001	14:08	8.74	69.6	3.1	85.7	1.7	77.7	71.1
200209	11	21-Apr-2002	08:01	9.69	64.6	1.9	77.6	4.1	71.1	62.8
200209	12	20-Feb-2003	10:41	10.52	66.4	1.7	79.8	1.3	73.1	66.4
200209	13	12-Mar-2004	17:15	11.58	58.6	0.2	75.4	1.3	67.0	61.0
200209	14	05-Jun-2006	12:58	13.81	60.4	1.5	76.1	1.2	68.3	61.9
200209	15	19-Apr-2008	09:42	15.68	59.7	1.1	79.5	2.0	69.6	64.5
200209	16	07-Aug-2009	09:44	16.98	65.3	2.4	79.5	1.9	72.4	64.6
200209	17	19-Oct-2010	16:28	18.18	70.0	0.9	81.0	1.2	75.5	66.9
200209	18	21-Sep-2012	14:20	20.11	60.7	1.0	80.2	0.6	70.5	64.7
200209	19	03-Dec-2013	16:25	21.31	59.6	1.2	77.7	1.4	68.7	62.6
200209	20	05-May-2014	14:17	21.72	70.0	1.3	87.0	2.8	78.5	72.7
200209	21	06-May-2014	06:57	21.73	61.7	2.7	75.0	2.3	68.3	61.2
200209	22	06-May-2014	14:23	21.73	71.1	0.9	88.6	0.6	79.9	73.7
200209	23	06-May-2014	20:25	21.73	60.6	1.4	75.8	1.9	68.2	62.2
200209	24	09-Dec-2015	13:08	23.32	61.3	0.3	81.3	0.9	71.3	65.3
200210	01	14-Aug-1992	12:52	0.00	86.9	0.3	84.1	1.3	85.5	80.8
200210	02	10-Mar-1993	11:05	0.57	90.4	1.2	85.4	2.1	87.9	82.9
200210	03	15-May-1994	10:10	1.75	85.7	0.7	80.4	0.9	83.1	78.3
200210	04	18-Feb-1995	09:12	2.52	94.7	2.6	86.7	1.0	90.7	85.5
200210	05	20-Apr-1996	13:31	3.69	92.6	1.2	87.4	2.4	90.0	82.7
200210	06	03-Mar-1997	11:52	4.55	89.3	0.6	83.5	1.1	86.4	80.2

Section	Visit	Date	Time	Age (years)	Left IRI Average (Inches/ mi)	Left IRI SD (Inches/ mi)	Right IRI Average (Inches/ mi)	Right IRI SD (Inches/ mi)	MRI (Inches/ mi)	HRI (Inches/ mi)
200210	07	15-May-1998	10:26	5.75	92.8	1.0	98.9	3.6	95.9	88.0
200210	08	15-Mar-1999	08:34	6.58	94.7	1.5	96.3	7.6	95.5	88.6
200210	09	01-Mar-2000	11:52	7.55	93.9	1.0	85.6	1.8	89.8	82.7
200210	10	10-May-2001	14:08	8.74	91.3	1.8	99.9	1.4	95.6	87.4
200210	11	21-Apr-2002	08:01	9.69	97.4	0.9	116.7	6.7	107.1	99.1
200210	12	20-Feb-2003	10:41	10.52	92.2	1.6	95.0	5.2	93.6	86.2
200210	13	12-Mar-2004	17:24	11.58	94.7	1.4	90.1	1.6	92.4	85.8
200210	14	05-Jun-2006	12:58	13.81	95.9	0.9	91.1	1.6	93.5	86.9
200210	15	19-Apr-2008	09:52	15.68	95.5	0.9	89.2	1.9	92.4	85.3
200210	16	07-Aug-2009	09:34	16.98	95.9	1.1	92.7	2.4	94.3	87.8
200210	17	19-Oct-2010	15:59	18.18	93.9	1.1	101.3	2.4	97.6	90.4
200210	18	21-Sep-2012	14:45	20.11	93.5	1.6	86.1	1.8	89.8	83.1
200210	19	03-Dec-2013	16:25	21.31	91.3	0.9	99.1	3.9	95.2	88.2
200210	20	05-May-2014	14:45	21.72	92.7	0.6	86.2	2.5	89.4	83.0
200210	21	06-May-2014	06:57	21.73	106.1	1.0	106.2	2.8	106.1	100.3
200210	22	06-May-2014	13:53	21.73	91.8	0.8	87.6	2.7	89.7	82.7
200210	23	06-May-2014	20:25	21.73	95.1	1.0	91.4	2.0	93.3	86.7
200210	24	09-Dec-2015	13:08	23.32	92.9	0.5	86.6	1.6	89.8	83.1
200211	01	14-Aug-1992	13:17	0.00	81.8	2.9	83.2	1.5	82.5	77.3
200211	02	10-Mar-1993	11:05	0.57	85.2	6.8	86.6	1.5	85.9	79.7
200211	03	15-May-1994	10:10	1.75	68.2	1.3	75.0	1.6	71.6	65.9
200211	04	18-Feb-1995	09:12	2.52	78.1	2.8	77.7	1.0	77.9	70.8
200211	05	20-Apr-1996	13:31	3.69	87.6	5.0	89.6	1.7	88.6	81.7
200211	06	03-Mar-1997	11:40	4.55	74.7	1.8	87.3	1.4	81.0	72.6
200211	07	15-May-1998	10:26	5.75	71.7	1.6	87.6	1.6	79.6	72.2
200211	08	15-Mar-1999	08:34	6.58	69.7	1.3	84.2	2.2	76.9	69.5
200211	09	01-Mar-2000	11:25	7.55	72.9	3.5	87.6	1.4	80.2	73.0
200211	10	10-May-2001	14:20	8.74	83.6	1.1	99.1	1.3	91.4	85.2
200211	11	21-Apr-2002	08:01	9.69	70.0	2.9	89.9	4.6	80.0	71.4
200211	12	20-Feb-2003	10:31	10.52	77.9	1.2	96.3	2.9	87.1	80.8
200211	13	12-Mar-2004	17:15	11.58	73.1	2.5	89.0	1.0	81.0	72.4
200211	14	05-Jun-2006	12:58	13.81	67.3	1.7	86.2	0.8	76.7	69.1
200211	15	19-Apr-2008	09:42	15.68	66.6	1.0	86.8	1.9	76.7	68.7
200211	16	07-Aug-2009	10:01	16.98	70.6	0.6	89.8	2.0	80.2	73.3
200211	17	19-Oct-2010	16:09	18.18	69.1	1.2	88.2	1.7	78.6	71.9
200211	18	21-Sep-2012	14:08	20.11	69.6	1.6	91.6	1.2	80.6	73.1
200211	19	03-Dec-2013	16:56	21.31	66.2	1.4	85.4	0.7	75.8	67.8
200211	20	05-May-2014	14:17	21.72	76.6	0.8	95.5	1.4	86.1	79.9
200211	21	06-May-2014	06:57	21.73	64.9	1.3	78.8	1.6	71.8	63.7
200211	22	06-May-2014	14:10	21.73	81.7	2.8	98.4	1.7	90.0	84.9
200211	23	06-May-2014	20:25	21.73	69.1	2.2	85.5	2.3	77.3	69.6
200211	24	09-Dec-2015	13:08	23.32	70.1	2.6	86.5	1.0	78.3	69.8
200212	01	14-Aug-1992	13:17	0.00	110.8	1.4	117.7	3.3	114.3	108.0
200212	02	10-Mar-1993	11:05	0.57	118.3	3.5	113.6	1.6	115.9	106.7
200212	03	15-May-1994	10:10	1.75	100.2	1.1	101.7	0.7	101.0	93.0
200212	04	18-Feb-1995	09:12	2.52	106.7	2.3	104.0	1.5	105.4	97.3
200212	05	20-Apr-1996	13:31	3.69	114.7	4.9	115.7	1.2	115.2	105.8
200212	06	03-Mar-1997	12:02	4.55	114.3	3.1	107.6	1.5	110.9	97.7

Section	Visit	Date	Time	Age (years)	Left IRI Average (Inches/ mi)	Left IRI SD (Inches/ mi)	Right IRI Average (Inches/ mi)	Right IRI SD (Inches/ mi)	MRI (Inches/ mi)	HRI (Inches/ mi)
200212	07	15-May-1998	10:26	5.75	106.4	1.7	120.7	2.7	113.6	102.4
200212	08	15-Mar-1999	08:34	6.58	102.7	2.1	117.9	4.6	110.3	99.7
200212	09	01-Mar-2000	11:25	7.55	106.9	1.9	112.6	2.5	109.8	99.6
200212	10	10-May-2001	14:08	8.74	107.8	1.6	124.5	1.7	116.2	107.1
200212	11	21-Apr-2002	08:01	9.69	104.1	1.6	134.7	7.5	119.4	107.1
200212	12	20-Feb-2003	10:41	10.52	104.0	2.0	119.6	1.1	111.8	102.1
200212	13	12-Mar-2004	17:15	11.58	111.5	0.9	105.3	0.8	108.4	95.0
200212	14	05-Jun-2006	12:58	13.81	104.7	0.8	110.4	0.9	107.5	96.5
200212	15	19-Apr-2008	09:42	15.68	103.3	1.3	110.6	1.1	106.9	96.0
200212	16	07-Aug-2009	10:01	16.98	105.4	1.8	112.4	1.2	108.9	97.9
200212	17	19-Oct-2010	15:49	18.18	105.1	0.5	114.3	1.2	109.7	99.0
200212	18	21-Sep-2012	13:58	20.11	109.7	0.7	110.1	1.1	109.9	98.3
200212	19	03-Dec-2013	16:35	21.31	106.0	1.5	113.0	0.6	109.5	98.9
200212	20	05-May-2014	14:45	21.72	109.2	0.7	115.0	1.0	112.1	102.5
200212	21	06-May-2014	06:57	21.73	110.3	1.4	124.0	3.1	117.1	107.0
200212	22	06-May-2014	13:53	21.73	108.5	0.7	112.8	1.1	110.7	101.0
200212	23	06-May-2014	20:25	21.73	107.9	1.5	114.2	1.4	111.0	100.3
200212	24	09-Dec-2015	13:23	23.32	115.3	1.8	110.8	0.7	113.0	100.3
200259	02	10-Mar-1993	11:05	0.57	100.9	5.5	91.0	2.2	95.9	89.4
200259	03	15-May-1994	10:10	1.75	76.4	1.0	79.9	1.2	78.2	71.8
200259	04	18-Feb-1995	09:12	2.52	83.9	2.1	83.5	1.8	83.7	77.2
200259	05	20-Apr-1996	13:31	3.69	83.8	2.6	86.4	1.0	85.1	77.6
200259	06	03-Mar-1997	11:40	4.55	90.0	2.4	85.9	2.3	87.9	79.0
200259	07	15-May-1998	10:49	5.75	83.1	1.2	87.7	1.7	85.4	77.7
200259	08	15-Mar-1999	08:34	6.58	82.4	1.2	85.6	3.9	84.0	76.3
200259	09	01-Mar-2000	11:25	7.55	85.4	1.1	86.5	1.2	85.9	78.0
200259	10	10-May-2001	14:08	8.74	91.2	1.2	92.4	2.1	91.8	84.4
200259	11	21-Apr-2002	08:01	9.69	82.1	1.6	94.3	4.4	88.2	79.4
200259	12	20-Feb-2003	10:31	10.52	87.0	1.4	95.5	2.5	91.3	83.5
200259	13	12-Mar-2004	17:04	11.58	89.3	2.1	90.5	2.4	89.9	83.1
200259	14	05-Jun-2006	13:14	13.81	90.0	1.4	92.3	2.0	91.1	84.1
200259	15	19-Apr-2008	09:52	15.68	88.3	1.2	91.4	1.2	89.9	82.8
200259	16	07-Aug-2009	09:23	16.98	94.7	2.4	96.7	2.1	95.7	88.6
200259	17	19-Oct-2010	15:59	18.18	91.4	1.2	96.5	4.2	94.0	86.7
200259	18	21-Sep-2012	14:20	20.11	101.9	2.8	103.3	1.3	102.6	95.3
200259	19	03-Dec-2013	16:25	21.31	94.1	2.3	94.3	1.9	94.2	86.9
200259	20	05-May-2014	14:17	21.72	104.2	1.8	107.0	2.1	105.6	98.7
200259	21	06-May-2014	06:57	21.73	91.9	1.0	93.1	0.7	92.5	85.3
200259	22	06-May-2014	14:10	21.73	106.0	1.2	107.5	1.8	106.7	100.1
200259	23	06-May-2014	20:25	21.73	101.8	1.3	103.3	1.2	102.5	95.5
200259	24	09-Dec-2015	13:08	23.32	101.5	1.3	93.5	1.6	97.5	90.3
273003	01	20-Jun-1990	17:08	4.72	122.3	2.1	125.8	1.9	124.1	120.0
273003	02	10-Aug-1991	11:49	5.86	128.5	2.3	134.5	1.9	131.5	126.7
273003	03	03-Aug-1992	17:00	6.84	129.4	3.0	133.2	0.7	131.3	126.9
273003	04	23-Nov-1993	19:10	8.15	95.2	1.3	105.3	2.1	100.2	95.2
273003	05	30-Jul-1994	14:33	8.83	132.9	1.8	140.6	2.4	136.8	132.6
273003	06	01-Aug-1997	06:43	11.83	133.2	1.1	140.9	0.9	137.1	130.4
273003	07	03-Oct-1998	14:37	13.01	118.5	1.4	127.2	1.3	122.9	117.2

Section	Visit	Date	Time	Age (years)	Left IRI Average (Inches/ mi)	Left IRI SD (Inches/ mi)	Right IRI Average (Inches/ mi)	Right IRI SD (Inches/ mi)	MRI (Inches/ mi)	HRI (Inches/ mi)
273003	08	14-Jun-1999	13:24	13.70	144.4	0.7	150.4	0.8	147.4	140.6
273003	09	27-Jul-2000	09:28	14.82	138.4	1.1	147.2	2.5	142.8	136.0
273003	10	22-Aug-2001	17:00	15.89	165.4	1.2	175.2	2.1	170.3	162.3
273003	11	16-Oct-2004	12:26	19.04	169.7	3.2	166.1	0.6	167.9	159.6
273003	12	28-Jul-2009	16:53	23.82	182.8	1.5	200.0	2.7	191.4	182.5
370201	01	30-Mar-1994	10:28	−0.25	77.6	1.3	92.6	2.5	85.1	74.7
370201	S01	06-Jan-1996	04:35	1.52	86.5	0.8	87.8	1.4	87.2	76.3
370201	02	06-Jan-1996	05:46	1.52	85.0	0.9	89.1	1.4	87.0	77.0
370201	S02	28-Feb-1996	09:38	1.66	82.7	1.8	82.5	0.7	82.6	72.1
370201	03	28-Feb-1996	10:43	1.66	84.4	1.8	82.0	1.2	83.2	72.7
370201	S03	28-Feb-1996	18:26	1.66	82.1	1.5	82.2	0.9	82.1	71.4
370201	S04	23-Apr-1996	06:57	1.81	83.0	1.5	83.4	1.2	83.2	73.3
370201	S05	07-Oct-1997	07:38	3.27	85.1	2.7	88.9	1.9	87.0	74.7
370201	04	07-Oct-1997	13:36	3.27	85.2	2.2	90.2	1.5	87.7	75.4
370201	S06	17-Jan-1998	08:48	3.55	85.4	1.0	90.4	3.5	87.9	77.9
370201	S07	18-Feb-1998	07:18	3.64	86.0	2.3	87.4	2.5	86.7	75.8
370201	05	18-Feb-1998	13:23	3.64	87.1	1.2	86.2	1.1	86.6	75.6
370201	S08	19-May-1998	08:14	3.88	87.2	2.1	85.8	1.1	86.5	76.0
370201	06	19-May-1998	11:08	3.88	84.1	1.8	87.0	1.9	85.5	74.3
370201	S09	19-May-1998	14:43	3.88	86.4	1.3	85.4	0.7	85.9	74.2
370201	S10	24-Jul-1998	08:07	4.06	85.9	1.9	88.9	2.5	87.4	77.6
370201	07	24-Jul-1998	11:46	4.06	86.9	0.8	86.1	1.2	86.5	75.2
370201	08	04-Nov-1998	08:45	4.35	108.0	1.9	109.5	1.6	108.7	99.6
370201	S11	04-Nov-1998	14:03	4.35	99.0	1.0	103.2	2.3	101.1	91.8
370201	09	11-Nov-1999	00:14	5.36	91.7	0.9	95.1	3.0	93.4	83.9
370201	S12	13-Mar-2000	08:06	5.70	102.4	2.4	103.7	2.0	103.0	93.5
370201	10	13-Mar-2000	14:02	5.70	85.4	0.7	99.8	1.8	92.6	83.3
370201	S13	06-Jul-2000	12:30	6.02	84.8	2.6	96.5	3.0	90.6	81.6
370201	11	08-Nov-2000	11:28	6.36	95.2	1.0	97.0	1.0	96.1	86.3
370201	S14	23-Jan-2001	07:49	6.57	96.2	0.8	114.3	1.5	105.3	97.7
370201	S15	23-Jan-2001	14:49	6.57	88.7	1.4	101.4	0.9	95.1	86.6
370201	S16	17-May-2001	07:09	6.88	95.9	1.7	105.0	2.8	100.4	92.5
370201	S17	17-May-2001	13:28	6.88	96.1	1.0	93.2	0.7	94.7	84.6
370201	S18	14-Jul-2001	07:11	7.04	93.6	1.6	108.1	2.4	100.9	92.9
370201	12	14-Jul-2001	09:11	7.04	90.6	1.7	99.7	2.0	95.2	86.8
370201	S19	14-Jul-2001	13:31	7.04	86.0	1.2	99.5	1.5	92.7	84.3
370201	S20	11-Oct-2001	06:56	7.28	104.1	1.5	105.2	1.7	104.6	96.0
370201	13	11-Oct-2001	08:45	7.28	102.0	1.6	101.7	1.4	101.9	92.5
370201	S21	11-Oct-2001	14:03	7.28	94.3	1.3	93.0	0.7	93.6	83.5
370201	S22	10-Jan-2002	07:00	7.53	101.4	2.1	104.1	2.7	102.8	93.9
370201	S23	10-Jan-2002	13:18	7.53	96.0	0.8	92.5	0.9	94.3	84.5
370201	S24	23-May-2002	08:02	7.89	96.6	4.2	114.8	1.9	105.7	98.3
370201	14	23-May-2002	11:02	7.89	88.5	1.8	99.8	1.9	94.2	85.9
370201	S25	23-May-2002	13:43	7.89	87.7	2.1	98.0	3.6	92.8	84.1
370201	S26	16-Aug-2002	06:08	8.13	104.8	3.2	106.1	4.1	105.5	97.3
370201	S27	16-Aug-2002	13:30	8.13	93.4	1.5	100.4	2.7	96.9	88.3
370201	S28	18-Sep-2002	06:25	8.22	100.8	0.4	105.7	2.6	103.3	94.8
370201	15	19-Sep-2002	17:31	8.22	96.0	1.3	98.3	1.8	97.1	88.0
370201	S29	18-Dec-2002	06:55	8.47	101.0	3.2	97.7	1.1	99.3	89.7

Section	Visit	Date	Time	Age (years)	Left IRI Average (Inches/ mi)	Left IRI SD (Inches/ mi)	Right IRI Average (Inches/ mi)	Right IRI SD (Inches/ mi)	MRI (Inches/ mi)	HRI (Inches/ mi)
370201	S30	18-Dec-2002	12:54	8.47	95.1	2.5	101.1	3.4	98.1	89.6
370201	S31	22-Jan-2003	07:29	8.56	97.1	2.3	110.5	4.5	103.8	95.6
370201	S32	22-Jan-2003	12:51	8.56	94.1	3.6	98.4	5.2	96.2	87.9
370201	16	22-Jan-2003	15:42	8.56	92.8	0.9	105.5	2.6	99.1	90.7
370201	S33	01-Jun-2003	06:11	8.92	98.4	1.9	95.9	1.6	97.1	87.8
370201	17	01-Jun-2003	11:38	8.92	95.8	0.4	91.0	0.8	93.4	83.3
370201	S34	01-Jun-2003	13:25	8.92	92.9	1.0	90.6	1.5	91.7	82.6
370202	01	30-Mar-1994	10:28	−0.25	125.9	74.8	84.9	0.7	105.4	93.9
370202	02	06-Jan-1996	05:46	1.52	97.2	1.8	85.0	1.0	91.1	80.5
370202	03	28-Feb-1996	10:58	1.66	101.4	1.3	85.1	1.1	93.3	83.5
370202	04	07-Oct-1997	13:36	3.27	104.3	2.2	82.5	0.9	93.4	82.1
370202	05	18-Feb-1998	13:57	3.64	103.0	1.9	83.0	0.7	93.0	82.7
370202	06	19-May-1998	10:36	3.88	99.3	1.5	81.9	1.0	90.6	80.2
370202	07	24-Jul-1998	12:02	4.06	101.1	4.5	82.1	1.5	91.6	80.8
370202	08	04-Nov-1998	08:45	4.35	119.8	1.8	110.9	1.7	115.3	106.7
370202	09	10-Nov-1999	23:54	5.36	107.0	1.6	96.0	0.9	101.5	92.3
370202	10	13-Mar-2000	14:02	5.70	100.3	1.2	86.1	1.4	93.2	83.9
370202	11	08-Nov-2000	11:28	6.36	106.8	3.2	97.5	1.8	102.1	93.1
370202	12	14-Jul-2001	09:11	7.04	116.1	2.3	109.9	2.7	113.0	105.2
370202	13	11-Oct-2001	08:45	7.28	126.2	2.4	121.7	3.2	123.9	116.2
370202	14	23-May-2002	11:02	7.89	108.3	1.9	97.7	2.8	103.0	93.9
370202	15	19-Sep-2002	17:48	8.22	109.8	2.7	106.8	3.4	108.3	100.5
370202	16	22-Jan-2003	15:42	8.56	110.1	1.6	101.7	2.2	105.9	97.5
370202	17	01-Jun-2003	11:38	8.92	106.4	1.0	92.0	1.6	99.2	88.4
370203	01	30-Mar-1994	10:28	−0.25	116.0	2.2	101.0	2.8	108.5	98.8
370203	02	06-Jan-1996	05:46	1.52	115.8	1.0	103.8	0.8	109.8	101.8
370203	03	28-Feb-1996	10:58	1.66	108.7	0.7	99.2	0.6	103.9	95.3
370203	04	07-Oct-1997	13:36	3.27	116.4	1.5	104.3	0.8	110.3	101.1
370203	05	18-Feb-1998	13:40	3.64	117.1	1.6	106.4	1.1	111.8	102.5
370203	06	19-May-1998	11:23	3.88	121.0	1.2	104.8	0.9	112.9	103.3
370203	07	24-Jul-1998	11:31	4.06	119.5	1.2	105.6	0.9	112.5	103.3
370203	08	04-Nov-1998	08:45	4.35	130.8	2.0	118.2	1.8	124.5	115.6
370203	09	11-Nov-1999	00:14	5.36	122.8	0.8	113.4	0.8	118.1	108.0
370203	10	13-Mar-2000	14:24	5.70	120.7	0.7	110.8	0.4	115.7	106.7
370203	11	08-Nov-2000	11:28	6.36	121.7	0.5	107.1	1.5	114.4	106.1
370203	12	14-Jul-2001	09:19	7.04	123.0	0.6	109.1	1.4	116.0	105.8
370203	13	11-Oct-2001	08:45	7.28	131.8	1.5	117.3	2.2	124.5	116.7
370203	14	23-May-2002	10:07	7.89	123.2	1.3	108.6	2.3	115.9	106.7
370203	15	19-Sep-2002	17:31	8.22	119.2	1.1	108.3	1.6	113.8	105.7
370203	16	22-Jan-2003	15:42	8.56	121.3	1.9	109.0	1.1	115.1	106.5
370203	17	01-Jun-2003	11:28	8.92	122.1	1.0	109.5	1.1	115.8	106.7
370203	18	07-Nov-2003	09:16	9.35	126.8	1.7	117.0	2.1	121.9	112.9
370203	19	14-Nov-2004	16:09	10.38	129.2	2.7	120.1	1.8	124.6	115.9
370203	20	14-Jun-2006	16:16	11.96	124.7	0.9	114.9	2.0	119.8	110.0
370203	21	30-Nov-2006	12:41	12.42	126.7	1.1	118.0	2.7	122.4	113.1
370203	22	18-Mar-2009	15:51	14.72	119.8	1.3	109.4	1.1	114.6	106.0
370203	23	18-Apr-2010	15:03	15.80	124.3	0.9	110.9	0.7	117.6	108.9
370203	24	27-Apr-2011	19:38	16.82	127.0	1.4	112.0	2.5	119.5	110.6

Section	Visit	Date	Time	Age (years)	Left IRI Average (Inches/ mi)	Left IRI SD (Inches/ mi)	Right IRI Average (Inches/ mi)	Right IRI SD (Inches/ mi)	MRI (Inches/ mi)	HRI (Inches/ mi)
370203	25	10-Dec-2012	13:24	18.45	131.8	1.3	128.3	0.9	130.0	120.8
370203	26	24-Jun-2014	13:23	19.98	122.9	0.7	113.7	2.4	106.0	108.6
370203	27	24-Jun-2014	16:42	19.98	122.3	0.9	114.1	3.2	118.2	109.4
370203	28	24-Jun-2014	19:20	19.98	122.3	0.9	113.2	5.0	117.8	108.4
370203	29	25-Jun-2014	06:08	19.98	124.4	0.5	119.4	1.5	121.9	113.2
370203	30	09-Mar-2015	16:52	20.69	125.2	1.3	120.0	1.0	122.6	114.2
370204	01	30-Mar-1994	10:28	−0.25	86.9	1.4	72.9	1.6	79.9	68.8
370204	03	28-Feb-1996	10:53	1.66	84.4	1.0	71.2	1.3	77.8	68.1
370204	04	07-Oct-1997	13:43	3.27	86.1	2.0	74.5	0.5	80.3	70.3
370204	05	18-Feb-1998	13:45	3.64	85.3	1.1	75.6	1.2	80.5	71.1
370204	06	19-May-1998	10:41	3.88	83.7	1.7	74.4	1.0	79.1	68.7
370204	07	24-Jul-1998	11:19	4.06	82.8	0.9	73.3	0.4	78.0	68.8
370204	08	04-Nov-1998	11:47	4.35	90.7	0.6	87.0	1.0	88.8	80.5
370204	09	11-Nov-1999	04:17	5.36	90.8	2.0	86.3	0.5	88.6	79.6
370204	10	13-Mar-2000	17:46	5.70	89.2	1.3	84.6	1.4	86.9	77.7
370204	11	08-Nov-2000	12:57	6.36	88.1	1.1	83.2	0.8	85.7	76.2
370204	12	14-Jul-2001	10:39	7.04	89.7	1.9	82.3	2.1	86.0	75.8
370204	13	11-Oct-2001	08:45	7.28	101.2	2.9	101.5	1.9	101.4	93.7
370204	14	23-May-2002	11:02	7.89	89.6	2.3	82.0	3.4	85.8	76.0
370204	15	19-Sep-2002	18:15	8.22	93.1	0.8	86.8	1.7	90.0	81.0
370204	16	22-Jan-2003	16:27	8.56	94.9	1.3	91.4	2.4	93.1	84.6
370204	17	01-Jun-2003	08:03	8.92	105.1	3.0	99.3	2.3	102.2	94.3
370204	18	08-Nov-2003	13:59	9.36	100.7	1.8	96.4	1.8	98.6	89.6
370204	19	14-Nov-2004	11:02	10.37	104.3	1.5	96.8	1.3	100.5	91.9
370204	20	14-Jun-2006	16:01	11.96	99.3	1.4	93.0	1.6	96.2	87.3
370204	21	30-Nov-2006	13:01	12.42	104.2	1.2	100.4	2.0	102.3	92.9
370204	22	18-Mar-2009	16:21	14.72	98.4	0.7	96.9	0.9	97.7	88.9
370204	23	18-Apr-2010	15:03	15.80	103.5	0.7	96.1	1.0	99.8	90.9
370204	24	27-Apr-2011	19:38	16.82	112.4	0.7	113.4	1.6	112.9	103.7
370204	25	10-Dec-2012	13:30	18.45	119.7	1.3	121.1	0.8	120.4	111.6
370204	26	24-Jun-2014	13:23	19.98	109.5	1.4	109.6	1.1	98.6	100.6
370204	27	24-Jun-2014	16:42	19.98	112.8	1.8	114.1	1.4	113.4	104.5
370204	28	24-Jun-2014	19:20	19.98	113.7	3.0	117.9	3.3	115.8	107.4
370204	29	25-Jun-2014	06:08	19.98	122.8	1.7	125.6	1.2	124.2	116.1
370204	30	09-Mar-2015	16:33	20.69	119.3	1.0	123.2	1.2	121.3	114.1
370205	01	30-Mar-1994	10:28	−0.25	109.5	1.5	150.4	6.5	129.9	110.9
370205	02	06-Jan-1996	05:46	1.52	108.7	1.3	125.7	3.0	117.2	99.7
370205	03	28-Feb-1996	10:43	1.66	108.8	2.9	114.2	1.3	111.5	94.6
370205	S03	28-Feb-1996	18:16	1.66	112.8	3.5	118.7	1.9	115.8	99.3
370205	04	07-Oct-1997	13:36	3.27	115.6	3.7	131.2	5.1	123.4	105.4
370205	05	18-Feb-1998	13:23	3.64	114.3	3.7	123.7	3.0	119.0	101.9
370205	06	19-May-1998	11:08	3.88	109.3	3.9	119.8	1.1	114.6	96.1
370205	S09	19-May-1998	14:43	3.88	112.9	5.3	119.8	1.2	116.4	99.0
370205	07	24-Jul-1998	11:14	4.06	111.5	2.3	127.0	2.3	119.3	100.1
370205	08	04-Nov-1998	08:45	4.35	133.5	5.2	133.5	2.8	133.5	118.5
370205	09	10-Nov-1999	23:54	5.36	114.1	2.9	127.9	2.0	121.0	103.1
370205	10	13-Mar-2000	14:14	5.70	112.9	1.4	148.4	8.3	130.6	107.9
370205	11	08-Nov-2000	11:16	6.36	113.4	3.8	137.9	1.6	125.7	105.3

Section	Visit	Date	Time	Age (years)	Left IRI Average (Inches/ mi)	Left IRI SD (Inches/ mi)	Right IRI Average (Inches/ mi)	Right IRI SD (Inches/ mi)	MRI (Inches/ mi)	HRI (Inches/ mi)
370205	S16	17-May-2001	07:09	6.88	133.5	2.5	127.8	1.5	130.7	115.4
370205	S17	17-May-2001	13:28	6.88	127.4	2.6	123.9	1.4	125.7	109.1
370205	12	14-Jul-2001	09:11	7.04	117.4	3.3	141.7	3.1	129.6	108.7
370205	13	11-Oct-2001	08:45	7.28	132.9	4.7	128.7	2.3	130.8	114.8
370205	14	23-May-2002	10:07	7.89	119.6	4.3	145.2	5.8	132.4	110.2
370205	15	19-Sep-2002	17:31	8.22	127.9	4.7	138.9	5.6	133.4	113.4
370205	16	22-Jan-2003	15:42	8.56	120.4	1.5	138.5	3.1	129.4	109.7
370205	17	01-Jun-2003	11:38	8.92	116.5	2.4	127.6	1.3	122.1	102.1
370206	01	30-Mar-1994	10:28	−0.25	100.2	2.0	89.2	2.4	94.7	81.1
370206	02	06-Jan-1996	05:46	1.52	100.7	2.2	86.7	1.0	93.7	80.6
370206	03	28-Feb-1996	10:43	1.66	102.2	0.9	85.5	1.6	93.8	80.1
370206	04	07-Oct-1997	13:36	3.27	104.1	2.8	87.5	1.6	95.8	81.1
370206	05	18-Feb-1998	13:57	3.64	104.3	1.6	88.2	0.8	96.3	82.4
370206	06	19-May-1998	10:36	3.88	104.1	2.5	86.7	1.9	95.4	81.4
370206	07	24-Jul-1998	11:14	4.06	106.9	3.2	88.6	1.9	97.8	82.4
370206	08	04-Nov-1998	08:45	4.35	113.4	1.3	104.5	2.1	109.0	97.5
370206	09	10-Nov-1999	23:54	5.36	104.5	3.4	93.4	0.6	98.9	86.1
370206	10	13-Mar-2000	14:02	5.70	97.2	1.0	93.9	3.0	95.6	80.0
370206	11	08-Nov-2000	11:16	6.36	108.7	2.4	92.1	1.9	100.4	87.5
370206	12	14-Jul-2001	09:11	7.04	109.1	1.6	105.2	3.1	107.2	96.1
370206	13	11-Oct-2001	08:45	7.28	126.0	4.3	114.2	2.7	120.1	108.4
370206	14	23-May-2002	10:07	7.89	100.5	2.6	93.4	4.0	96.9	83.9
370206	15	19-Sep-2002	17:31	8.22	108.9	2.7	99.4	3.7	104.1	91.7
370206	16	22-Jan-2003	15:57	8.56	108.9	3.0	98.4	3.6	103.6	91.8
370206	17	01-Jun-2003	12:08	8.92	107.5	1.4	89.3	0.7	98.4	84.7
370207	01	30-Mar-1994	10:28	−0.25	120.9	1.6	110.5	1.9	115.7	102.6
370207	02	06-Jan-1996	05:46	1.52	124.7	0.6	118.7	0.5	121.7	110.9
370207	03	28-Feb-1996	10:58	1.66	116.4	1.4	110.1	0.4	113.2	103.0
370207	04	07-Oct-1997	13:55	3.27	120.7	1.4	111.9	1.1	116.3	103.7
370207	05	18-Feb-1998	13:40	3.64	121.3	1.9	112.3	1.0	116.8	104.6
370207	06	19-May-1998	11:08	3.88	119.0	2.1	110.4	0.9	114.7	102.7
370207	07	24-Jul-1998	11:46	4.06	121.4	1.2	114.2	1.4	117.8	105.7
370207	08	04-Nov-1998	08:45	4.35	122.5	0.7	126.4	1.9	124.4	114.1
370207	09	10-Nov-1999	23:54	5.36	118.1	0.8	120.7	1.7	119.4	105.4
370207	10	13-Mar-2000	14:24	5.70	121.8	2.0	116.9	1.6	119.4	105.7
370207	11	08-Nov-2000	11:28	6.36	116.2	1.4	115.7	1.3	115.9	105.6
370207	12	14-Jul-2001	09:19	7.04	119.5	1.6	122.8	1.8	121.1	109.4
370207	13	11-Oct-2001	08:45	7.28	121.7	1.4	128.8	0.8	125.2	114.4
370207	14	23-May-2002	11:02	7.89	113.9	1.3	111.6	1.4	112.8	101.4
370207	15	19-Sep-2002	18:01	8.22	120.1	0.4	120.6	2.5	120.3	109.1
370207	16	22-Jan-2003	15:42	8.56	115.3	1.9	114.5	1.1	114.9	104.3
370207	17	01-Jun-2003	11:28	8.92	119.5	1.9	115.1	0.9	117.3	105.0
370207	18	07-Nov-2003	09:16	9.35	118.2	1.2	121.1	1.5	119.6	108.5
370207	19	14-Nov-2004	16:29	10.38	119.0	1.1	125.4	1.1	122.2	110.3
370207	20	14-Jun-2006	16:16	11.96	118.2	1.6	117.5	1.6	117.8	105.5
370207	21	30-Nov-2006	12:41	12.42	118.8	0.8	121.5	1.1	120.2	107.2
370207	22	18-Mar-2009	15:51	14.72	118.8	1.8	111.6	0.7	115.2	102.8
370207	23	18-Apr-2010	15:26	15.80	118.0	1.0	117.8	1.5	117.9	105.5

Section	Visit	Date	Time	Age (years)	Left IRI Average (Inches/ mi)	Left IRI SD (Inches/ mi)	Right IRI Average (Inches/ mi)	Right IRI SD (Inches/ mi)	MRI (Inches/ mi)	HRI (Inches/ mi)
370207	24	27-Apr-2011	19:53	16.82	119.2	1.9	127.6	1.8	123.4	110.9
370207	25	10-Dec-2012	13:24	18.45	118.9	0.5	123.1	0.3	121.0	108.2
370207	26	24-Jun-2014	13:23	19.98	114.7	1.9	118.6	2.1	105.2	103.8
370207	27	24-Jun-2014	16:42	19.98	116.1	2.0	120.1	1.9	118.1	105.2
370207	28	24-Jun-2014	19:20	19.98	115.5	2.8	121.5	3.5	118.5	105.6
370207	29	25-Jun-2014	06:08	19.98	114.1	0.4	128.2	0.6	121.1	109.4
370207	30	09-Mar-2015	16:33	20.69	117.4	0.6	118.3	1.2	117.8	105.3
370208	01	30-Mar-1994	10:28	−0.25	100.7	3.0	108.8	7.8	104.7	94.3
370208	02	06-Jan-1996	05:46	1.52	103.9	0.5	122.6	1.1	113.3	103.3
370208	03	28-Feb-1996	10:43	1.66	99.8	1.7	116.1	1.4	108.0	97.5
370208	S03	28-Feb-1996	18:22	1.66	99.7	1.1	114.2	1.4	107.0	96.6
370208	04	07-Oct-1997	14:12	3.27	105.8	1.3	120.2	2.7	113.0	99.8
370208	05	18-Feb-1998	13:23	3.64	102.2	2.2	120.5	2.1	111.3	99.7
370208	06	19-May-1998	10:36	3.88	101.9	0.8	118.5	1.7	110.2	97.9
370208	07	24-Jul-1998	11:31	4.06	105.6	1.7	121.4	3.5	113.5	101.3
370208	08	04-Nov-1998	08:45	4.35	123.1	3.0	136.5	2.3	129.8	119.7
370208	09	10-Nov-1999	23:54	5.36	110.7	1.0	122.0	2.9	116.4	106.2
370208	10	13-Mar-2000	14:14	5.70	106.0	2.0	112.6	3.4	109.3	98.1
370208	11	08-Nov-2000	11:16	6.36	108.6	2.0	124.3	1.3	116.5	105.5
370208	S16	17-May-2001	08:37	6.88	132.8	1.7	142.1	2.5	137.5	128.1
370208	S17	17-May-2001	13:35	6.88	126.0	2.2	138.1	3.0	132.0	122.0
370208	12	14-Jul-2001	09:19	7.04	114.5	2.4	126.1	4.3	120.3	110.7
370208	13	11-Oct-2001	08:45	7.28	132.1	3.5	139.3	1.6	135.7	126.5
370208	14	23-May-2002	11:02	7.89	106.7	1.4	117.9	1.8	112.3	101.8
370208	15	19-Sep-2002	17:31	8.22	115.6	2.9	124.0	3.8	119.8	109.7
370208	16	22-Jan-2003	15:42	8.56	114.1	3.4	132.4	2.7	123.2	112.8
370208	17	01-Jun-2003	11:28	8.92	107.4	0.8	122.7	1.9	115.1	103.5
370208	18	07-Nov-2003	09:27	9.35	121.7	4.5	138.1	1.2	129.9	119.7
370208	19	14-Nov-2004	15:58	10.38	125.5	2.9	141.6	2.9	133.5	124.7
370208	20	14-Jun-2006	16:01	11.96	120.8	0.8	137.9	2.6	129.4	118.4
370208	21	30-Nov-2006	13:43	12.42	120.2	1.4	125.1	5.2	122.7	112.4
370208	22	18-Mar-2009	15:51	14.72	112.5	1.9	130.4	1.2	121.4	110.0
370208	23	18-Apr-2010	15:03	15.80	116.7	1.1	131.2	2.1	123.9	113.9
370208	24	27-Apr-2011	19:38	16.82	144.7	0.9	148.3	1.4	146.5	139.5
370208	25	10-Dec-2012	13:24	18.45	137.6	0.7	145.3	3.6	141.4	133.1
370208	26	24-Jun-2014	13:23	19.98	134.6	0.7	137.4	4.7	122.5	126.7
370208	27	24-Jun-2014	16:57	19.98	147.4	1.6	151.4	3.5	149.4	142.5
370208	28	24-Jun-2014	19:20	19.98	150.1	1.8	154.5	1.1	152.3	144.9
370208	29	25-Jun-2014	06:08	19.98	162.9	1.4	168.9	2.4	165.9	159.2
370208	30	09-Mar-2015	16:33	20.69	138.4	1.2	146.7	2.2	142.5	133.9
370209	01	30-Mar-1994	10:28	−0.25	73.4	3.0	81.3	2.0	77.4	68.3
370209	02	06-Jan-1996	05:46	1.52	77.2	1.4	84.9	0.6	81.0	71.8
370209	03	28-Feb-1996	10:58	1.66	74.3	0.5	86.2	1.5	80.3	71.3
370209	S03	28-Feb-1996	18:16	1.66	75.2	1.0	84.5	1.3	79.9	70.7
370209	04	07-Oct-1997	13:36	3.27	77.9	1.7	92.1	2.3	85.0	74.4
370209	05	18-Feb-1998	13:40	3.64	78.0	0.9	90.0	0.7	84.0	74.3
370209	06	19-May-1998	11:08	3.88	76.0	1.6	91.1	1.0	83.6	73.6
370209	S09	19-May-1998	14:43	3.88	76.9	1.3	92.0	1.5	84.5	74.3

Section	Visit	Date	Time	Age (years)	Left IRI Average (Inches/ mi)	Left IRI SD (Inches/ mi)	Right IRI Average (Inches/ mi)	Right IRI SD (Inches/ mi)	MRI (Inches/ mi)	HRI (Inches/ mi)
370209	07	24-Jul-1998	11:14	4.06	77.1	0.8	88.3	1.0	82.7	72.2
370209	08	04-Nov-1998	08:45	4.35	86.7	2.3	92.2	2.0	89.4	80.1
370209	09	10-Nov-1999	23:54	5.36	82.0	1.0	86.5	2.7	84.2	73.3
370209	10	13-Mar-2000	14:14	5.70	84.4	0.8	86.1	1.5	85.2	74.3
370209	11	08-Nov-2000	11:16	6.36	79.5	2.0	88.3	1.2	83.9	74.0
370209	12	14-Jul-2001	09:19	7.04	85.1	1.0	85.6	0.8	85.4	74.3
370209	13	11-Oct-2001	08:45	7.28	83.2	0.9	93.3	1.5	88.2	78.3
370209	14	23-May-2002	10:07	7.89	83.6	2.0	85.9	1.5	84.7	74.6
370209	15	19-Sep-2002	17:48	8.22	83.8	1.7	87.3	2.2	85.5	74.5
370209	16	22-Jan-2003	15:57	8.56	83.8	0.6	88.6	1.2	86.2	74.9
370209	17	01-Jun-2003	11:28	8.92	81.7	0.6	94.2	1.6	88.0	77.3
370210	01	30-Mar-1994	10:28	−0.25	85.0	2.4	74.2	4.6	79.6	69.0
370210	02	06-Jan-1996	05:46	1.52	90.1	0.4	77.9	0.7	84.0	73.4
370210	03	28-Feb-1996	11:31	1.66	109.9	2.9	86.2	2.7	98.1	88.5
370210	S03	28-Feb-1996	18:16	1.66	89.8	1.6	79.3	1.1	84.6	74.3
370210	04	07-Oct-1997	14:12	3.27	110.7	1.2	95.9	0.9	103.3	91.7
370210	05	18-Feb-1998	13:40	3.64	106.8	2.7	92.9	2.8	99.8	89.6
370210	06	19-May-1998	11:39	3.88	107.9	3.0	95.6	2.3	101.8	91.1
370210	S09	19-May-1998	14:43	3.88	106.5	2.2	91.7	1.6	99.1	88.6
370210	07	24-Jul-1998	11:14	4.06	97.1	1.9	82.8	2.7	90.0	79.0
370210	08	04-Nov-1998	08:45	4.35	88.3	1.2	78.9	2.1	83.6	72.3
370210	09	10-Nov-1999	23:54	5.36	94.9	2.1	81.4	1.4	88.2	75.9
370210	10	13-Mar-2000	14:02	5.70	101.7	1.3	96.0	4.6	98.8	88.8
370210	11	08-Nov-2000	11:28	6.36	92.6	1.3	82.9	1.1	87.8	77.2
370210	12	14-Jul-2001	09:11	7.04	86.1	1.3	87.6	2.9	86.9	76.0
370210	13	11-Oct-2001	08:45	7.28	92.4	2.6	79.3	2.2	85.9	75.2
370210	14	23-May-2002	11:02	7.89	96.5	3.2	86.8	1.2	91.7	82.2
370210	15	19-Sep-2002	17:48	8.22	88.6	1.4	89.1	3.3	88.8	78.3
370210	16	22-Jan-2003	15:42	8.56	92.7	1.7	87.0	4.1	89.9	80.2
370210	17	01-Jun-2003	11:28	8.92	106.7	1.9	94.6	1.9	100.7	90.1
370211	01	30-Mar-1994	10:28	−0.25	83.0	1.5	82.8	0.8	82.9	69.8
370211	02	06-Jan-1996	05:46	1.52	74.4	0.6	89.5	1.8	82.0	73.8
370211	03	28-Feb-1996	10:58	1.66	76.6	0.8	88.6	1.7	82.6	73.3
370211	04	07-Oct-1997	13:36	3.27	78.4	1.9	96.0	1.4	87.2	78.0
370211	05	18-Feb-1998	13:40	3.64	77.9	0.6	95.7	1.3	86.8	78.4
370211	06	19-May-1998	10:52	3.88	76.4	1.2	93.7	1.1	85.0	76.0
370211	07	24-Jul-1998	11:31	4.06	76.2	1.9	92.0	0.7	84.1	75.7
370211	08	04-Nov-1998	08:45	4.35	84.4	2.6	94.5	1.0	89.4	80.4
370211	09	10-Nov-1999	23:54	5.36	75.9	0.1	89.3	1.7	82.6	72.9
370211	10	13-Mar-2000	14:02	5.70	75.5	1.6	91.2	1.2	83.3	74.0
370211	11	08-Nov-2000	11:16	6.36	75.0	0.9	92.6	0.8	83.8	75.5
370211	12	14-Jul-2001	09:11	7.04	75.3	1.8	90.8	0.8	83.0	74.3
370211	13	11-Oct-2001	08:45	7.28	83.9	1.8	97.0	1.0	90.4	81.8
370211	14	23-May-2002	10:07	7.89	75.3	2.6	87.7	1.9	81.5	71.5
370211	15	19-Sep-2002	17:31	8.22	76.0	1.4	86.7	1.0	81.3	70.9
370211	16	22-Jan-2003	15:42	8.56	75.0	1.7	90.0	1.0	82.5	74.1
370211	17	01-Jun-2003	11:28	8.92	74.8	0.9	89.0	1.6	81.9	73.0
370211	18	07-Nov-2003	09:16	9.35	78.5	1.3	92.4	1.8	85.4	76.4

Section	Visit	Date	Time	Age (years)	Left IRI Average (Inches/ mi)	Left IRI SD (Inches/ mi)	Right IRI Average (Inches/ mi)	Right IRI SD (Inches/ mi)	MRI (Inches/ mi)	HRI (Inches/ mi)
370211	19	14-Nov-2004	15:58	10.38	77.0	0.4	89.2	0.9	83.1	72.7
370211	20	14-Jun-2006	16:16	11.96	75.5	1.1	88.5	1.3	82.0	72.4
370211	21	30-Nov-2006	12:41	12.42	77.6	4.1	88.5	2.1	83.0	71.8
370211	22	18-Mar-2009	16:21	14.72	76.5	0.6	90.2	1.2	83.4	74.6
370211	23	18-Apr-2010	15:03	15.80	75.3	0.7	88.5	0.9	81.9	72.8
370211	24	27-Apr-2011	19:38	16.82	76.0	1.5	90.4	1.0	83.2	73.2
370211	25	10-Dec-2012	13:24	18.45	76.6	1.9	87.5	1.5	82.1	72.0
370211	26	24-Jun-2014	13:23	19.98	75.5	0.7	87.7	2.0	74.0	72.0
370211	27	24-Jun-2014	16:42	19.98	77.2	1.7	88.4	1.9	82.8	71.9
370211	28	24-Jun-2014	19:20	19.98	75.4	2.1	87.3	0.7	81.3	70.9
370211	29	25-Jun-2014	06:08	19.98	77.5	3.1	90.0	1.6	83.8	72.6
370211	30	09-Mar-2015	16:33	20.69	75.0	0.5	89.1	2.2	82.1	72.9
370212	01	30-Mar-1994	10:28	−0.25	69.2	2.3	69.9	0.8	69.6	61.0
370212	02	06-Jan-1996	05:46	1.52	65.7	0.8	69.7	0.8	67.7	59.3
370212	03	28-Feb-1996	10:43	1.66	67.2	1.5	74.6	2.4	70.9	62.0
370212	04	07-Oct-1997	14:12	3.27	75.1	2.6	81.6	2.2	78.4	69.1
370212	05	18-Feb-1998	13:23	3.64	67.8	1.0	75.3	2.7	71.5	61.8
370212	06	19-May-1998	10:36	3.88	70.1	1.3	79.5	2.7	74.8	64.6
370212	07	24-Jul-1998	11:31	4.06	67.5	1.2	73.0	1.8	70.3	60.4
370212	08	04-Nov-1998	08:45	4.35	77.7	2.2	78.3	1.1	78.0	69.6
370212	09	10-Nov-1999	23:54	5.36	72.1	2.1	73.0	1.0	72.5	61.5
370212	10	13-Mar-2000	14:02	5.70	68.7	1.1	70.6	1.4	69.6	60.3
370212	11	08-Nov-2000	11:16	6.36	67.1	1.6	72.1	1.8	69.6	61.7
370212	S16	17-May-2001	08:37	6.88	83.2	1.1	81.0	1.8	82.1	74.0
370212	S17	17-May-2001	13:35	6.88	79.3	0.7	77.2	1.3	78.3	69.4
370212	12	14-Jul-2001	09:19	7.04	71.9	2.0	74.1	2.6	73.0	64.2
370212	13	11-Oct-2001	08:45	7.28	83.6	2.0	80.4	2.7	82.0	74.0
370212	14	23-May-2002	10:07	7.89	69.0	2.4	71.3	2.4	70.2	61.6
370212	15	19-Sep-2002	17:48	8.22	73.1	2.0	75.9	1.3	74.5	66.0
370212	16	22-Jan-2003	15:42	8.56	71.2	2.1	74.8	1.6	73.0	63.7
370212	17	01-Jun-2003	11:38	8.92	71.3	2.1	75.7	2.4	73.5	63.9
370212	18	07-Nov-2003	09:16	9.35	78.4	2.2	78.6	2.9	78.5	70.1
370212	19	14-Nov-2004	15:48	10.38	78.5	2.2	82.1	2.8	80.3	73.9
370212	20	14-Jun-2006	16:31	11.96	77.0	1.2	77.3	1.8	77.1	68.7
370212	21	30-Nov-2006	12:41	12.42	75.8	2.1	77.5	1.3	76.6	69.0
370212	22	18-Mar-2009	16:37	14.72	70.4	1.9	72.7	1.5	71.6	62.9
370212	23	18-Apr-2010	15:14	15.80	71.2	2.2	73.4	1.0	72.3	63.6
370212	24	27-Apr-2011	19:38	16.82	89.2	2.0	92.7	1.0	91.0	84.7
370212	25	10-Dec-2012	13:24	18.45	87.0	0.8	88.8	1.7	87.9	80.9
370212	26	24-Jun-2014	13:23	19.98	75.4	2.1	78.5	1.2	69.4	69.4
370212	27	24-Jun-2014	16:42	19.98	85.6	1.4	88.5	2.5	87.0	80.4
370212	28	24-Jun-2014	19:20	19.98	88.2	1.5	90.4	3.7	89.3	82.9
370212	29	25-Jun-2014	06:08	19.98	96.9	1.3	103.0	1.0	99.9	94.9
370212	30	09-Mar-2015	16:33	20.69	81.4	2.8	84.3	1.0	82.8	75.4
370259	01	30-Mar-1994	10:28	−0.25	82.3	1.8	95.5	2.0	88.9	77.1
370259	02	06-Jan-1996	05:46	1.52	81.0	1.1	91.0	1.2	86.0	75.6
370259	03	28-Feb-1996	10:43	1.66	80.8	1.8	88.8	0.9	84.8	75.4
370259	S03	28-Feb-1996	18:16	1.66	80.9	1.0	87.4	2.0	84.1	74.2

Section	Visit	Date	Time	Age (years)	Left IRI Average (Inches/mi)	Left IRI SD (Inches/mi)	Right IRI Average (Inches/mi)	Right IRI SD (Inches/mi)	MRI (Inches/mi)	HRI (Inches/mi)
370259	04	07-Oct-1997	13:55	3.27	81.9	0.4	94.5	1.1	88.2	78.7
370259	05	18-Feb-1998	13:23	3.64	79.8	0.9	94.2	1.3	87.0	77.8
370259	06	19-May-1998	10:36	3.88	80.7	2.9	91.7	1.7	86.2	76.7
370259	07	24-Jul-1998	11:31	4.06	79.3	0.7	91.7	0.8	85.5	75.5
370259	08	04-Nov-1998	08:45	4.35	88.4	1.3	102.1	0.7	95.3	86.4
370259	09	10-Nov-1999	23:54	5.36	78.7	0.7	93.5	1.0	86.1	76.4
370259	10	13-Mar-2000	14:24	5.70	81.4	1.7	91.9	1.1	86.6	76.9
370259	11	08-Nov-2000	11:16	6.36	80.7	2.7	93.2	1.0	86.9	77.5
370259	12	14-Jul-2001	09:19	7.04	83.0	1.2	92.5	1.3	87.8	76.8
370259	13	11-Oct-2001	08:45	7.28	87.2	1.7	99.0	1.9	93.1	84.4
370259	14	23-May-2002	10:07	7.89	82.2	1.0	93.1	1.5	87.7	78.2
370259	15	19-Sep-2002	17:31	8.22	82.4	1.5	90.5	2.5	86.4	76.1
370259	16	22-Jan-2003	15:57	8.56	79.7	2.0	92.0	1.6	85.9	76.5
370259	17	01-Jun-2003	11:28	8.92	82.5	1.3	93.8	0.8	88.1	78.2
370259	18	08-Nov-2003	12:57	9.36	82.5	0.9	93.3	1.2	87.9	77.5
370259	19	14-Nov-2004	15:46	10.38	84.8	0.9	90.1	0.8	87.4	75.8
370259	20	14-Jun-2006	16:01	11.96	80.0	0.6	93.2	0.9	86.6	77.9
370259	21	30-Nov-2006	12:41	12.42	84.5	0.7	90.9	1.1	87.7	77.1
370259	22	18-Mar-2009	15:51	14.72	87.1	1.3	93.6	0.8	90.4	80.1
370259	23	18-Apr-2010	15:14	15.80	85.5	0.7	90.9	1.8	88.2	77.9
370259	24	27-Apr-2011	19:53	16.82	86.1	0.9	87.6	0.9	86.9	74.3
370259	25	10-Dec-2012	13:20	18.45	85.6	1.2	89.5	1.0	87.6	77.4
370259	26	24-Jun-2014	13:23	19.98	85.5	1.2	86.5	2.3	77.5	73.6
370259	27	24-Jun-2014	16:42	19.98	82.2	1.2	86.6	1.3	84.4	72.1
370259	28	24-Jun-2014	19:20	19.98	83.4	2.0	87.1	1.2	85.3	72.6
370259	29	25-Jun-2014	06:08	19.98	82.4	1.5	87.5	0.9	84.9	71.6
370259	30	09-Mar-2015	16:33	20.69	83.3	1.8	90.3	0.8	86.8	77.6
370260	01	30-Mar-1994	10:28	−0.25	95.6	1.1	100.5	1.0	98.0	90.9
370260	02	06-Jan-1996	05:46	1.52	91.3	1.0	98.8	0.5	95.0	85.6
370260	03	28-Feb-1996	10:43	1.66	89.8	1.1	97.0	1.2	93.4	84.5
370260	04	07-Oct-1997	13:55	3.27	92.8	1.7	98.2	0.6	95.5	85.1
370260	05	18-Feb-1998	13:23	3.64	90.7	1.3	100.4	0.3	95.6	84.6
370260	06	19-May-1998	10:52	3.88	89.9	0.8	99.2	1.5	94.6	83.5
370260	07	24-Jul-1998	11:14	4.06	91.8	0.9	98.1	0.5	95.0	83.2
370260	08	04-Nov-1998	08:45	4.35	98.7	0.6	105.2	1.0	101.9	92.7
370260	09	11-Nov-1999	00:04	5.36	95.5	1.3	102.5	0.5	99.0	88.7
370260	10	13-Mar-2000	14:02	5.70	94.3	0.7	102.7	2.0	98.5	89.4
370260	11	08-Nov-2000	11:16	6.36	92.1	2.1	103.5	1.1	97.8	87.6
370260	12	14-Jul-2001	09:19	7.04	96.3	2.7	102.4	1.3	99.4	89.5
370260	13	11-Oct-2001	08:45	7.28	99.4	1.0	105.9	1.3	102.7	93.7
370260	14	23-May-2002	10:07	7.89	91.7	2.5	103.2	1.2	97.4	87.3
370260	15	19-Sep-2002	17:31	8.22	93.2	1.1	103.9	0.4	98.6	88.7
370260	16	22-Jan-2003	15:42	8.56	92.0	1.1	104.0	0.5	98.0	87.9
370260	17	01-Jun-2003	11:58	8.92	91.3	0.6	102.8	1.4	97.0	86.4
370260	18	07-Nov-2003	09:36	9.35	96.7	2.7	104.8	2.5	100.7	90.1
370260	19	14-Nov-2004	15:58	10.38	95.9	1.6	107.1	0.9	101.5	91.0
370260	20	14-Jun-2006	15:42	11.96	92.9	1.3	104.5	0.8	98.7	87.7
370260	21	30-Nov-2006	12:41	12.42	96.7	0.9	101.8	3.0	99.3	89.8
370260	22	18-Mar-2009	15:51	14.72	94.2	1.5	102.8	1.2	98.5	87.5

Section	Visit	Date	Time	Age (years)	Left IRI Average (Inches/ mi)	Left IRI SD (Inches/ mi)	Right IRI Average (Inches/ mi)	Right IRI SD (Inches/ mi)	MRI (Inches/ mi)	HRI (Inches/ mi)
370260	23	18-Apr-2010	15:14	15.80	94.1	2.2	103.9	1.4	99.0	88.5
370260	24	27-Apr-2011	19:38	16.82	96.5	0.7	100.6	1.3	98.6	88.9
370260	25	10-Dec-2012	13:24	18.45	99.7	0.6	102.3	2.6	101.0	91.2
370260	26	24-Jun-2014	13:23	19.98	94.4	1.3	100.4	3.1	87.9	87.8
370260	27	24-Jun-2014	16:42	19.98	96.6	1.4	101.4	2.8	99.0	88.3
370260	28	24-Jun-2014	19:20	19.98	95.5	1.3	104.6	11.8	100.1	91.0
370260	29	25-Jun-2014	06:08	19.98	97.8	2.6	106.6	2.0	102.2	91.3
370260	30	09-Mar-2015	16:33	20.69	96.8	1.0	103.6	4.4	100.2	89.3
390201	02	27-Dec-1996	10:22	0.24	87.0	0.6	81.1	1.4	84.0	78.0
390201	03	08-Dec-1997	09:21	1.19	88.7	0.8	88.3	0.9	88.5	82.3
390201	04	12-Nov-1998	09:39	2.11	93.7	0.4	91.4	0.8	92.6	87.5
390201	05	20-Oct-1999	08:44	3.05	100.9	0.9	96.2	0.4	98.6	93.1
390201	06	16-Aug-2000	09:17	3.88	92.7	0.7	92.1	1.0	92.4	87.8
390201	07	04-Nov-2001	08:30	5.09	97.7	0.7	100.0	0.4	98.8	93.2
390201	08	06-Dec-2002	11:26	6.18	103.7	0.7	101.9	1.0	102.8	98.3
390201	09	29-Apr-2003	14:15	6.58	99.2	1.2	99.1	1.1	99.2	95.0
390201	10	04-Feb-2004	15:12	7.34	106.4	0.4	102.0	1.0	104.2	99.4
390201	11	05-May-2005	12:20	8.59	109.5	1.2	107.6	0.4	108.5	104.3
390201	12	08-Aug-2006	12:10	9.85	123.1	1.6	128.4	1.3	125.7	121.1
390202	02	27-Dec-1996	10:35	0.24	76.9	0.7	71.0	0.3	73.9	68.0
390202	03	08-Dec-1997	09:21	1.19	80.8	1.0	80.7	1.1	80.8	76.1
390202	04	12-Nov-1998	09:39	2.11	86.8	0.3	85.2	0.4	86.0	81.1
390202	05	20-Oct-1999	09:04	3.05	90.9	0.5	88.4	1.1	89.6	85.1
390202	06	16-Aug-2000	09:55	3.88	91.3	0.4	87.3	0.5	89.3	84.3
390202	07	04-Nov-2001	08:18	5.09	96.7	0.9	98.7	1.2	97.7	93.7
390202	08	06-Dec-2002	11:26	6.18	100.7	0.6	102.8	0.6	101.8	97.0
390202	09	29-Apr-2003	14:19	6.58	102.2	0.7	100.4	0.9	101.3	96.2
390202	10	04-Feb-2004	14:54	7.34	108.7	0.3	106.8	0.3	107.7	102.8
390202	11	05-May-2005	12:29	8.59	113.7	0.7	114.4	0.3	114.1	109.4
390202	12	08-Aug-2006	12:10	9.85	124.7	0.7	125.6	1.1	125.2	120.3
390203	02	27-Dec-1996	10:35	0.24	72.9	1.0	60.7	1.3	66.8	58.3
390203	03	08-Dec-1997	09:21	1.19	69.8	0.6	65.2	0.4	67.5	60.2
390203	04	12-Nov-1998	09:24	2.11	72.5	1.2	69.1	1.5	70.8	64.0
390203	05	20-Oct-1999	08:44	3.05	78.1	0.4	72.9	0.8	75.5	68.8
390203	06	16-Aug-2000	09:17	3.88	69.3	0.7	63.4	1.0	66.3	59.5
390203	07	04-Nov-2001	08:18	5.09	76.1	1.6	76.6	2.6	76.3	69.2
390203	08	06-Dec-2002	11:26	6.18	76.5	0.3	72.6	1.0	74.5	67.6
390203	09	29-Apr-2003	14:15	6.58	75.9	0.8	70.1	1.0	73.0	65.2
390203	10	04-Feb-2004	15:20	7.34	75.9	1.2	72.0	0.4	73.9	65.7
390203	11	05-May-2005	12:29	8.59	75.0	0.6	68.9	1.0	72.0	64.4
390203	12	08-Aug-2006	12:21	9.85	80.8	1.4	77.2	0.8	79.0	72.0
390203	13	23-Jul-2008	14:21	11.81	82.2	1.2	81.8	1.5	82.0	75.8
390203	14	21-Oct-2009	14:32	13.06	74.6	0.9	71.0	0.4	72.8	65.8
390203	15	11-Aug-2010	10:58	13.86	79.6	0.5	72.9	0.8	76.2	68.7
390203	16	18-Oct-2011	10:41	15.05	80.4	0.5	81.0	1.2	80.7	74.8
390203	17	22-May-2012	13:37	15.64	72.4	0.5	70.3	0.4	71.4	65.5
390203	18	03-Jun-2014	14:27	17.67	79.8	0.7	70.7	1.0	75.3	67.7
390203	19	29-Jul-2014	19:55	17.83	74.1	0.4	70.7	1.7	72.4	64.1

Section	Visit	Date	Time	Age (years)	Left IRI Average (Inches/ mi)	Left IRI SD (Inches/ mi)	Right IRI Average (Inches/ mi)	Right IRI SD (Inches/ mi)	MRI (Inches/ mi)	HRI (Inches/ mi)
390203	20	30-Jul-2014	06:06	17.83	80.5	1.1	81.2	0.9	80.9	73.6
390203	21	30-Jul-2014	13:01	17.83	73.6	1.1	67.9	2.0	70.8	62.8
390204	S01	15-Aug-1996	13:15	−0.13	54.9	1.5	0.0	0.0	0.0	0.0
390204	02	27-Dec-1996	10:22	0.24	55.9	0.8	51.7	1.4	53.8	49.7
390204	03	08-Dec-1997	09:34	1.19	56.5	0.8	60.3	1.7	58.4	54.1
390204	S02	07-Mar-1998	06:12	1.43	57.9	1.1	57.0	0.9	57.4	54.2
390204	S03	07-Mar-1998	11:20	1.43	54.2	0.9	53.0	1.7	53.6	49.7
390204	S04	07-Mar-1998	15:06	1.43	57.8	0.5	54.3	0.8	56.1	52.4
390204	S05	28-May-1998	06:23	1.65	56.8	0.4	55.2	0.5	56.0	52.5
390204	S06	28-May-1998	15:06	1.66	56.5	0.7	53.6	0.7	55.0	51.1
390204	S07	13-Aug-1998	03:22	1.86	58.2	0.7	54.9	0.7	56.5	53.0
390204	S08	13-Aug-1998	07:31	1.87	58.3	0.2	55.5	0.4	56.9	53.7
390204	04	12-Nov-1998	09:24	2.11	64.7	0.8	67.9	1.3	66.3	63.3
390204	S09	12-Nov-1998	15:01	2.12	57.1	1.1	56.4	0.6	56.7	53.3
390204	S10	10-Mar-1999	06:25	2.44	63.4	0.5	64.0	2.4	63.7	60.1
390204	S11	10-Mar-1999	14:00	2.44	53.2	0.6	50.9	0.5	52.1	48.5
390204	S12	22-Jun-1999	06:14	2.72	58.0	0.7	60.0	1.3	59.0	55.2
390204	S13	22-Jun-1999	15:32	2.72	57.9	0.3	53.6	0.4	55.8	51.9
390204	05	20-Oct-1999	08:54	3.05	73.7	0.8	76.4	1.6	75.1	72.4
390204	S14	17-Jun-2000	05:23	3.71	58.5	0.7	56.3	0.4	57.4	54.3
390204	S15	17-Jun-2000	14:35	3.71	57.2	0.6	54.1	0.3	55.6	52.6
390204	06	16-Aug-2000	09:17	3.88	57.8	0.3	53.3	1.0	55.6	52.1
390204	07	04-Nov-2001	08:30	5.09	73.3	1.8	81.2	2.0	77.2	73.8
390204	08	06-Dec-2002	11:36	6.18	74.8	0.5	76.4	0.6	75.6	72.9
390204	09	29-Apr-2003	14:19	6.58	60.6	1.0	59.6	0.7	60.1	56.2
390204	10	04-Feb-2004	15:12	7.34	71.0	0.2	73.3	0.5	72.1	68.6
390204	11	05-May-2005	12:37	8.59	67.1	0.8	69.3	0.7	68.2	64.2
390204	12	08-Aug-2006	12:10	9.85	70.9	0.7	75.0	1.7	73.0	68.6
390205	02	27-Dec-1996	10:22	0.24	70.5	1.3	84.2	0.8	77.3	68.8
390205	03	08-Dec-1997	09:21	1.19	68.9	0.4	91.1	2.4	80.0	69.8
390205	04	12-Nov-1998	09:24	2.11	81.6	0.6	92.9	1.0	87.2	76.6
390205	05	20-Oct-1999	08:44	3.05	89.1	1.5	92.4	1.3	90.7	81.0
390205	06	16-Aug-2000	09:17	3.88	84.5	0.6	94.3	0.8	89.4	79.0
390205	07	04-Nov-2001	07:59	5.09	95.9	1.3	101.5	0.8	98.7	88.4
390205	08	06-Dec-2002	11:26	6.18	96.6	1.1	94.8	1.0	95.7	87.0
390205	09	29-Apr-2003	14:15	6.58	99.5	1.6	102.5	0.7	101.0	91.5
390205	10	04-Feb-2004	14:54	7.34	109.1	0.7	106.1	0.7	107.6	95.8
390205	11	05-May-2005	12:20	8.59	120.5	0.7	136.1	2.0	128.3	113.5
390205	12	08-Aug-2006	12:10	9.85	137.4	2.1	172.2	2.6	154.8	133.1
390206	02	27-Dec-1996	10:22	0.24	87.3	0.9	74.2	1.8	80.8	73.9
390206	03	08-Dec-1997	09:21	1.19	90.0	1.1	72.3	0.3	81.1	75.4
390206	04	12-Nov-1998	09:24	2.11	93.8	0.6	76.9	0.5	85.4	79.8
390206	05	20-Oct-1999	08:44	3.05	98.7	1.2	81.0	1.2	89.8	84.4
390206	06	16-Aug-2000	09:17	3.88	96.5	0.3	86.4	2.0	91.5	85.9
390206	07	04-Nov-2001	07:59	5.09	101.3	1.2	90.1	0.8	95.7	89.8
390206	08	06-Dec-2002	11:26	6.18	103.4	0.6	95.7	1.2	99.5	93.8
390206	09	29-Apr-2003	14:19	6.58	114.2	1.1	113.6	1.1	113.9	109.0
390206	10	04-Feb-2004	14:54	7.34	110.8	0.4	106.0	1.4	108.4	103.2

Section	Visit	Date	Time	Age (years)	Left IRI Average (Inches/ mi)	Left IRI SD (Inches/ mi)	Right IRI Average (Inches/ mi)	Right IRI SD (Inches/ mi)	MRI (Inches/ mi)	HRI (Inches/ mi)
390206	11	05-May-2005	12:20	8.59	117.9	1.1	117.7	5.8	117.8	110.9
390206	12	08-Aug-2006	11:39	9.85	140.7	1.5	144.5	11.5	142.6	134.5
390207	02	27-Dec-1996	10:22	0.24	93.9	1.3	81.8	1.1	87.9	78.6
390207	03	08-Dec-1997	09:21	1.19	84.2	0.6	82.7	0.9	83.4	74.6
390207	04	12-Nov-1998	09:24	2.11	81.3	1.0	79.5	1.1	80.4	69.9
390207	05	20-Oct-1999	08:44	3.05	81.3	0.8	79.5	0.7	80.4	70.0
390207	06	16-Aug-2000	09:55	3.88	92.1	0.7	95.2	0.4	93.6	85.3
390207	07	04-Nov-2001	07:59	5.09	81.5	2.1	81.2	1.1	81.4	72.5
390207	08	06-Dec-2002	11:46	6.18	85.8	1.3	85.0	0.6	85.4	75.7
390207	09	29-Apr-2003	14:15	6.58	106.0	1.1	110.8	3.2	108.4	100.4
390207	10	04-Feb-2004	14:54	7.34	93.7	1.0	82.8	1.2	88.2	78.3
390207	11	05-May-2005	12:37	8.59	102.7	1.3	105.9	2.2	104.3	96.1
390207	12	08-Aug-2006	12:10	9.85	118.3	1.1	118.6	2.2	118.5	112.7
390207	13	23-Jul-2008	14:13	11.81	106.3	0.6	103.3	2.7	104.8	98.3
390207	14	21-Oct-2009	14:32	13.06	92.9	1.6	91.8	2.6	92.3	84.1
390207	15	11-Aug-2010	10:40	13.86	95.9	0.3	88.9	0.7	92.4	83.4
390207	16	18-Oct-2011	10:48	15.05	92.2	1.0	83.7	1.2	88.0	79.0
390207	17	22-May-2012	13:37	15.64	97.6	1.6	91.9	0.6	94.8	85.9
390207	18	03-Jun-2014	14:27	17.67	118.9	1.8	119.7	1.7	119.3	111.1
390207	19	29-Jul-2014	19:55	17.83	109.8	1.6	108.4	2.6	109.1	100.0
390207	20	30-Jul-2014	05:57	17.83	112.3	2.3	107.1	1.6	109.7	100.2
390207	21	30-Jul-2014	13:01	17.83	111.1	1.7	110.8	2.1	110.9	101.8
390208	02	27-Dec-1996	10:35	0.24	98.1	1.9	91.7	0.8	94.9	87.9
390208	03	08-Dec-1997	09:34	1.19	87.3	0.9	86.5	1.2	86.9	78.0
390208	04	12-Nov-1998	09:24	2.11	84.9	1.2	82.3	1.1	83.6	74.2
390208	05	20-Oct-1999	08:44	3.05	84.6	0.9	80.8	1.2	82.7	73.4
390208	06	16-Aug-2000	09:17	3.88	98.8	1.0	90.9	1.1	94.8	86.3
390208	07	04-Nov-2001	08:30	5.09	85.2	1.7	91.9	0.9	88.6	77.8
390208	08	06-Dec-2002	11:26	6.18	86.9	0.9	83.1	0.4	85.0	76.8
390208	09	29-Apr-2003	14:19	6.58	105.3	0.6	96.0	1.7	100.6	94.1
390208	10	04-Feb-2004	15:12	7.34	87.4	0.9	81.3	0.6	84.3	77.2
390208	11	05-May-2005	12:29	8.59	100.0	0.8	94.2	1.5	97.1	89.7
390208	12	08-Aug-2006	12:10	9.85	113.0	1.7	104.2	1.1	108.6	102.1
390208	13	23-Jul-2008	14:13	11.81	105.5	2.2	115.3	2.2	110.4	100.4
390208	14	21-Oct-2009	14:46	13.06	108.2	1.6	98.4	2.5	103.3	93.4
390208	15	11-Aug-2010	10:58	13.86	109.4	0.8	106.8	1.6	108.1	97.1
390208	16	18-Oct-2011	10:34	15.05	105.5	0.5	120.5	2.3	113.0	101.6
390208	17	22-May-2012	13:37	15.64	115.8	0.9	123.7	0.9	119.7	109.4
390208	18	03-Jun-2014	14:27	17.67	172.7	2.6	152.0	2.2	162.4	148.0
390208	19	29-Jul-2014	19:55	17.83	169.8	1.4	148.3	1.6	159.1	145.3
390208	20	30-Jul-2014	05:57	17.83	171.8	2.1	153.8	3.6	162.8	149.5
390208	21	30-Jul-2014	13:01	17.83	170.1	1.7	151.4	3.2	160.8	147.0
390209	02	27-Dec-1996	10:22	0.24	66.9	1.4	60.2	0.8	63.6	56.9
390209	03	08-Dec-1997	09:21	1.19	72.3	0.5	62.0	0.3	67.2	62.5
390209	04	12-Nov-1998	09:24	2.11	77.4	0.3	67.7	1.4	72.5	67.9
390209	05	20-Oct-1999	08:44	3.05	78.3	1.1	69.6	1.5	74.0	69.3
390209	06	16-Aug-2000	09:17	3.88	74.5	0.7	65.1	0.7	69.8	65.1
390209	07	04-Nov-2001	08:30	5.09	76.4	0.4	73.2	1.0	74.8	69.3

Section	Visit	Date	Time	Age (years)	Left IRI Average (Inches/ mi)	Left IRI SD (Inches/ mi)	Right IRI Average (Inches/ mi)	Right IRI SD (Inches/ mi)	MRI (Inches/ mi)	HRI (Inches/ mi)
390209	08	06-Dec-2002	11:36	6.18	79.3	0.5	71.3	0.8	75.3	69.9
390209	09	29-Apr-2003	14:37	6.58	81.7	1.4	77.3	0.8	79.5	74.0
390209	10	04-Feb-2004	15:01	7.34	78.3	0.5	71.8	0.7	75.0	69.8
390209	11	05-May-2005	12:20	8.59	85.4	0.7	81.5	1.4	83.4	77.3
390209	12	08-Aug-2006	12:10	9.85	87.0	0.4	83.2	1.2	85.1	79.7
390209	13	23-Jul-2008	14:13	11.81	99.8	2.0	104.5	1.7	102.2	95.5
390209	14	21-Oct-2009	14:53	13.06	106.1	1.4	114.2	2.1	110.2	103.3
390209	15	11-Aug-2010	10:40	13.86	109.4	0.6	125.8	1.5	117.6	110.3
390209	16	18-Oct-2011	10:34	15.05	116.7	0.4	141.7	2.4	129.2	120.6
390209	17	22-May-2012	13:37	15.64	116.5	0.4	130.6	1.7	123.5	116.0
390210	02	27-Dec-1996	10:22	0.24	67.7	0.2	59.2	0.8	63.5	58.5
390210	03	08-Dec-1997	09:21	1.19	72.9	0.3	68.5	0.5	70.7	65.5
390210	04	12-Nov-1998	09:24	2.11	69.1	0.7	66.5	1.2	67.8	63.0
390210	05	20-Oct-1999	08:44	3.05	70.5	0.5	66.5	1.1	68.5	63.6
390210	06	16-Aug-2000	09:17	3.88	78.9	1.7	74.7	1.5	76.8	72.7
390210	07	04-Nov-2001	07:59	5.09	73.0	0.6	68.6	0.7	70.8	66.1
390210	08	06-Dec-2002	11:26	6.18	75.6	1.0	71.6	0.9	73.6	69.5
390210	09	29-Apr-2003	14:44	6.58	91.1	1.6	89.5	0.7	90.3	86.5
390210	10	04-Feb-2004	15:20	7.34	81.5	1.1	75.9	1.1	78.7	73.4
390210	11	05-May-2005	12:20	8.59	95.6	1.3	89.0	0.8	92.3	88.7
390210	12	08-Aug-2006	12:21	9.85	95.3	1.2	84.7	1.2	90.0	86.2
390211	02	27-Dec-1996	10:22	0.24	90.7	1.3	77.2	1.8	83.9	78.5
390211	03	08-Dec-1997	09:21	1.19	90.7	0.9	81.9	1.2	86.3	80.7
390211	04	12-Nov-1998	09:24	2.11	93.3	0.9	80.8	0.5	87.1	81.1
390211	05	20-Oct-1999	08:44	3.05	91.9	1.0	80.5	1.4	86.2	80.7
390211	06	16-Aug-2000	09:17	3.88	93.4	1.0	82.9	2.1	88.1	82.9
390211	07	04-Nov-2001	08:30	5.09	90.7	0.7	81.0	1.3	85.8	80.9
390211	08	06-Dec-2002	11:26	6.18	97.0	1.2	83.4	1.3	90.2	84.3
390211	09	29-Apr-2003	14:37	6.58	100.5	0.8	92.9	1.2	96.7	90.5
390211	10	04-Feb-2004	15:01	7.34	95.0	1.2	82.4	0.8	88.7	81.7
390211	11	05-May-2005	12:37	8.59	104.0	0.9	89.3	1.8	96.6	90.5
390211	12	08-Aug-2006	11:39	9.85	99.3	1.6	91.9	1.1	95.6	90.1
390211	13	23-Jul-2008	14:13	11.81	100.4	0.4	90.7	0.7	95.6	89.9
390211	14	21-Oct-2009	14:32	13.06	99.0	1.4	91.7	1.8	95.4	89.5
390211	15	11-Aug-2010	10:50	13.86	108.2	1.1	97.1	0.5	102.6	96.4
390211	16	18-Oct-2011	10:34	15.05	98.5	0.6	94.4	1.7	96.4	90.8
390211	17	22-May-2012	13:44	15.64	103.9	1.1	95.6	0.5	99.7	93.8
390211	18	03-Jun-2014	14:27	17.67	110.7	1.6	101.1	0.8	105.9	100.9
390211	19	29-Jul-2014	19:55	17.83	110.1	2.7	98.5	1.2	104.3	98.7
390211	20	30-Jul-2014	05:57	17.83	110.2	1.3	95.8	1.5	103.0	98.2
390211	21	30-Jul-2014	13:01	17.83	108.2	2.1	95.4	2.0	101.8	96.0
390212	02	27-Dec-1996	10:22	0.24	72.4	1.3	63.1	0.7	67.8	60.7
390212	03	08-Dec-1997	09:34	1.19	69.4	0.8	68.5	0.9	69.0	60.9
390212	04	12-Nov-1998	09:24	2.11	68.2	1.2	63.9	1.2	66.0	58.1
390212	05	20-Oct-1999	08:44	3.05	66.6	0.9	64.1	1.1	65.3	57.0
390212	06	16-Aug-2000	10:08	3.88	70.4	1.3	66.7	1.1	68.5	61.2
390212	07	04-Nov-2001	08:18	5.09	65.2	1.0	69.9	0.8	67.6	59.2
390212	08	06-Dec-2002	11:36	6.18	67.3	1.6	64.9	1.0	66.1	58.5

Section	Visit	Date	Time	Age (years)	Left IRI Average (Inches/ mi)	Left IRI SD (Inches/ mi)	Right IRI Average (Inches/ mi)	Right IRI SD (Inches/ mi)	MRI (Inches/ mi)	HRI (Inches/ mi)
390212	09	29-Apr-2003	14:15	6.58	84.0	0.7	77.4	1.0	80.7	74.8
390212	10	04-Feb-2004	14:54	7.34	72.7	0.6	67.5	1.5	70.1	64.0
390212	11	05-May-2005	12:29	8.59	80.5	0.6	73.7	1.2	77.1	70.8
390212	12	08-Aug-2006	12:21	9.85	75.8	1.7	74.9	0.5	75.4	68.7
390212	17	22-May-2012	13:37	15.64	76.7	0.7	86.4	0.8	81.6	73.5
390212	18	03-Jun-2014	14:27	17.67	138.8	8.9	141.9	2.6	140.4	125.6
390212	19	29-Jul-2014	19:55	17.83	140.4	3.4	142.3	4.3	141.4	125.9
390212	20	30-Jul-2014	05:57	17.83	143.9	3.7	147.6	4.2	145.7	129.2
390212	21	30-Jul-2014	13:01	17.83	141.4	3.3	140.7	2.6	141.0	125.5
390259	02	27-Dec-1996	10:35	0.24	55.8	0.6	43.9	0.6	49.8	46.2
390259	03	08-Dec-1997	09:21	1.19	55.5	0.7	46.6	0.2	51.0	48.4
390259	04	12-Nov-1998	09:24	2.11	60.8	1.1	53.8	1.0	57.3	54.9
390259	05	20-Oct-1999	09:04	3.05	66.6	1.2	63.1	1.2	64.9	62.1
390259	06	16-Aug-2000	09:55	3.88	56.1	0.9	49.3	1.1	52.7	50.1
390259	07	04-Nov-2001	08:18	5.09	61.9	2.0	60.6	2.7	61.2	58.3
390259	08	06-Dec-2002	11:46	6.18	63.8	0.6	62.7	0.5	63.3	60.0
390259	09	29-Apr-2003	14:44	6.58	61.6	0.7	53.1	0.4	57.3	54.5
390259	10	04-Feb-2004	15:12	7.34	60.7	0.4	62.8	0.7	61.8	57.9
390259	11	05-May-2005	12:37	8.59	74.2	0.9	65.3	0.9	69.7	66.0
390260	02	27-Dec-1996	10:22	0.24	80.8	0.5	58.5	1.0	69.7	61.0
390260	03	08-Dec-1997	09:21	1.19	80.1	0.9	64.1	0.8	72.1	63.5
390260	04	12-Nov-1998	09:24	2.11	80.5	0.9	65.7	1.1	73.1	64.4
390260	05	20-Oct-1999	08:44	3.05	84.2	0.8	65.5	0.4	74.8	65.6
390260	06	16-Aug-2000	09:17	3.88	84.7	1.3	63.2	0.9	73.9	66.3
390260	07	04-Nov-2001	07:59	5.09	80.8	1.1	70.9	2.3	75.8	65.9
390260	08	06-Dec-2002	11:26	6.18	83.6	1.0	66.8	0.6	75.2	66.7
390260	09	29-Apr-2003	14:15	6.58	89.8	1.3	72.8	0.9	81.3	73.4
390260	10	04-Feb-2004	15:12	7.34	87.6	0.4	69.1	1.1	78.4	70.0
390260	11	05-May-2005	12:37	8.59	93.1	0.4	74.0	0.8	83.6	76.4
390260	12	08-Aug-2006	12:21	9.85	87.5	1.2	72.8	1.7	80.2	72.4
390260	13	23-Jul-2008	14:21	11.81	89.5	0.5	72.7	0.6	81.1	72.8
390260	14	21-Oct-2009	14:32	13.06	88.3	1.4	72.8	1.6	80.5	72.4
390260	15	11-Aug-2010	10:50	13.86	87.5	1.1	74.9	1.0	81.2	72.8
390260	16	18-Oct-2011	10:41	15.05	85.1	1.1	74.6	0.6	79.9	71.4
390260	17	22-May-2012	13:37	15.64	87.0	1.0	74.6	1.1	80.8	72.2
390260	18	03-Jun-2014	14:27	17.67	90.6	0.9	75.5	1.3	83.0	76.0
390260	19	29-Jul-2014	20:06	17.83	86.5	0.8	74.2	0.2	80.3	72.5
390260	20	30-Jul-2014	05:57	17.83	85.9	1.1	77.6	0.6	81.8	73.2
390260	21	30-Jul-2014	13:01	17.83	86.7	0.4	74.3	1.5	80.5	72.8
390261	02	27-Dec-1996	10:22	0.24	77.1	0.7	67.9	1.2	72.5	64.9
390261	03	08-Dec-1997	09:34	1.19	80.0	0.9	72.6	1.0	76.3	69.0
390261	04	12-Nov-1998	09:24	2.11	80.4	1.5	72.2	1.0	76.3	68.9
390261	05	20-Oct-1999	09:04	3.05	80.8	0.9	74.0	0.9	77.4	70.4
390261	06	16-Aug-2000	09:17	3.88	77.4	1.2	71.1	0.8	74.2	67.6
390261	07	04-Nov-2001	07:59	5.09	80.6	1.0	79.0	1.0	79.8	73.5
390261	08	06-Dec-2002	11:36	6.18	81.9	1.3	71.7	0.6	76.8	70.5
390261	09	29-Apr-2003	14:15	6.58	82.4	0.9	71.5	1.1	76.9	70.3
390261	10	04-Feb-2004	14:54	7.34	86.6	0.7	72.5	0.8	79.5	72.6

Section	Visit	Date	Time	Age (years)	Left IRI Average (Inches/ mi)	Left IRI SD (Inches/ mi)	Right IRI Average (Inches/ mi)	Right IRI SD (Inches/ mi)	MRI (Inches/ mi)	HRI (Inches/ mi)
390261	11	05-May-2005	12:29	8.59	83.6	0.6	70.7	0.4	77.2	71.0
390261	12	08-Aug-2006	12:10	9.85	80.2	1.2	73.5	1.6	76.8	70.5
390261	13	23-Jul-2008	14:13	11.81	81.3	1.2	74.1	0.3	77.7	72.3
390261	14	21-Oct-2009	14:32	13.06	82.0	2.0	75.4	1.1	78.7	72.5
390261	15	11-Aug-2010	11:16	13.86	86.1	0.6	75.0	0.4	80.6	74.1
390261	16	18-Oct-2011	10:34	15.05	86.1	0.8	79.7	0.7	82.9	77.5
390261	17	22-May-2012	13:37	15.64	82.9	0.5	76.4	0.6	79.7	73.5
390261	18	03-Jun-2014	14:27	17.67	80.4	1.2	75.3	0.3	77.8	71.4
390261	19	29-Jul-2014	19:55	17.83	81.3	1.8	72.4	0.3	76.9	70.7
390261	20	30-Jul-2014	05:57	17.83	85.9	1.7	75.9	0.4	80.9	74.8
390261	21	30-Jul-2014	13:01	17.83	82.6	0.7	71.8	0.7	77.2	70.8
390262	02	27-Dec-1996	10:22	0.24	98.2	3.1	67.1	0.8	82.6	73.5
390262	03	08-Dec-1997	09:42	1.19	89.9	0.7	67.8	0.6	78.9	69.9
390262	04	12-Nov-1998	09:24	2.11	91.8	0.7	68.9	0.8	80.3	70.7
390262	05	20-Oct-1999	09:04	3.05	90.3	1.5	68.1	0.3	79.2	70.4
390262	06	16-Aug-2000	09:55	3.88	93.8	1.1	66.2	0.8	80.0	71.5
390262	07	04-Nov-2001	08:18	5.09	84.7	1.0	68.3	0.8	76.5	67.3
390262	08	06-Dec-2002	11:36	6.18	91.6	1.8	69.4	1.1	80.5	71.3
390262	10	04-Feb-2004	15:29	7.34	96.6	0.7	69.5	0.6	83.1	73.8
390262	11	05-May-2005	12:29	8.59	98.4	1.0	71.9	1.4	85.1	76.3
390262	12	08-Aug-2006	12:21	9.85	86.6	3.6	69.9	1.0	78.3	69.7
390262	13	23-Jul-2008	14:13	11.81	82.3	1.5	72.3	0.5	77.3	68.1
390262	14	21-Oct-2009	14:32	13.06	99.3	1.9	74.6	0.7	87.0	78.2
390262	15	11-Aug-2010	10:40	13.86	97.6	0.7	75.5	0.7	86.5	77.9
390262	16	18-Oct-2011	10:34	15.05	95.8	1.3	77.4	1.1	86.6	78.7
390262	17	22-May-2012	13:37	15.64	93.3	1.1	76.2	0.7	84.7	76.7
390262	18	03-Jun-2014	14:27	17.67	94.4	2.4	75.1	0.6	84.8	76.4
390262	19	29-Jul-2014	20:06	17.83	96.3	0.9	76.6	1.0	86.5	77.9
390262	20	30-Jul-2014	05:57	17.83	96.0	1.5	78.2	1.2	87.1	78.6
390262	21	30-Jul-2014	13:01	17.83	95.5	1.5	75.2	0.7	85.3	76.9
390263	02	27-Dec-1996	10:22	0.24	82.6	1.5	67.2	0.7	74.9	68.5
390263	03	08-Dec-1997	09:34	1.19	86.5	0.8	75.1	0.8	80.8	74.7
390263	04	12-Nov-1998	09:24	2.11	85.8	1.0	75.4	0.7	80.6	75.0
390263	05	20-Oct-1999	08:54	3.05	93.0	1.0	78.9	1.3	86.0	80.1
390263	06	16-Aug-2000	09:17	3.88	83.2	0.7	75.6	0.7	79.4	72.7
390263	07	04-Nov-2001	08:18	5.09	89.3	1.3	80.5	1.6	84.9	79.0
390263	08	06-Dec-2002	11:26	6.18	91.4	1.3	82.4	1.0	86.9	80.8
390263	10	04-Feb-2004	14:54	7.34	96.5	0.6	86.6	0.4	91.6	84.1
390263	11	05-May-2005	12:37	8.59	88.6	1.0	84.9	0.7	86.7	79.7
390263	12	08-Aug-2006	12:10	9.85	88.9	1.4	86.5	0.6	87.7	80.2
390263	13	23-Jul-2008	14:13	11.81	89.2	1.4	89.2	1.0	89.2	82.5
390263	14	21-Oct-2009	14:46	13.06	88.6	0.6	86.9	1.3	87.8	81.4
390263	15	11-Aug-2010	10:50	13.86	96.1	1.5	88.9	0.3	92.5	85.0
390263	16	18-Oct-2011	10:41	15.05	95.7	1.0	92.0	1.3	93.9	87.8
390263	17	22-May-2012	13:37	15.64	92.3	1.7	90.0	1.1	91.2	84.2
390263	18	03-Jun-2014	14:42	17.67	91.5	1.7	89.0	1.3	90.3	83.5
390263	19	29-Jul-2014	20:06	17.83	91.0	1.2	86.8	1.6	88.9	81.1
390263	20	30-Jul-2014	05:57	17.83	92.9	0.4	88.2	1.2	90.5	84.0

Section	Visit	Date	Time	Age (years)	Left IRI Average (Inches/ mi)	Left IRI SD (Inches/ mi)	Right IRI Average (Inches/ mi)	Right IRI SD (Inches/ mi)	MRI (Inches/ mi)	HRI (Inches/ mi)
390263	21	30-Jul-2014	13:01	17.83	90.5	1.1	86.2	1.2	88.3	79.9
390264	02	27-Dec-1996	10:22	0.24	51.0	2.4	79.0	1.4	65.0	54.6
390264	03	08-Dec-1997	09:21	1.19	64.9	1.1	95.0	3.4	80.0	71.7
390264	04	12-Nov-1998	09:24	2.11	87.6	1.8	111.0	1.0	99.3	93.3
390264	05	20-Oct-1999	08:44	3.05	97.7	4.3	126.4	1.6	112.1	107.2
390264	06	16-Aug-2000	09:55	3.88	86.5	2.5	114.8	2.4	100.7	94.4
390264	07	04-Nov-2001	07:59	5.09	117.3	6.6	144.4	2.3	130.8	122.4
390264	08	06-Dec-2002	11:36	6.18	111.3	0.9	130.3	2.7	120.8	113.9
390264	10	04-Feb-2004	14:54	7.34	93.9	1.6	119.5	0.9	106.7	99.7
390264	11	05-May-2005	12:20	8.59	90.9	4.1	107.7	1.9	99.3	90.6
390264	17	22-May-2012	13:44	15.64	103.4	1.3	91.8	0.7	97.6	91.7
390265	02	27-Dec-1996	10:22	0.24	100.7	0.8	79.2	0.9	89.9	80.4
390265	03	08-Dec-1997	09:34	1.19	104.1	0.9	87.7	0.9	95.9	86.9
390265	04	12-Nov-1998	09:24	2.11	106.4	0.7	89.1	0.3	97.7	88.8
390265	05	20-Oct-1999	08:54	3.05	108.3	0.4	91.7	1.5	100.0	91.2
390265	06	16-Aug-2000	09:55	3.88	108.5	1.3	87.5	0.4	98.0	91.0
390265	07	04-Nov-2001	07:59	5.09	106.0	1.3	97.3	0.6	101.6	93.2
390265	08	06-Dec-2002	11:46	6.18	110.5	0.7	90.5	1.0	100.5	93.3
390265	09	29-Apr-2003	14:15	6.58	113.7	1.1	92.2	1.1	103.0	96.1
390265	10	04-Feb-2004	15:12	7.34	107.0	1.2	90.0	0.6	98.5	91.1
390265	11	05-May-2005	12:20	8.59	111.6	0.8	92.6	0.5	102.1	95.6
390265	12	08-Aug-2006	11:39	9.85	108.9	0.2	92.1	0.7	100.5	93.3
390265	13	23-Jul-2008	14:13	11.81	108.4	0.8	93.6	0.6	101.0	92.9
390265	14	21-Oct-2009	14:53	13.06	111.7	0.6	94.0	1.3	102.9	95.4
390265	15	11-Aug-2010	10:58	13.86	109.9	0.5	94.6	0.4	102.3	95.1
390265	16	18-Oct-2011	10:34	15.05	110.5	0.9	100.7	0.7	105.6	98.0
390265	17	22-May-2012	13:37	15.64	112.8	0.4	97.8	1.0	105.3	97.9
390265	18	03-Jun-2014	14:27	17.67	114.7	1.2	96.9	1.3	105.8	98.9
390265	19	29-Jul-2014	19:55	17.83	110.4	1.9	97.6	1.2	104.0	96.2
390265	20	30-Jul-2014	05:57	17.83	108.5	1.0	99.4	0.4	103.9	95.9
390265	21	30-Jul-2014	13:01	17.83	110.7	2.6	96.0	1.0	103.3	95.8
493011	01	02-Aug-1989	11:56	3.26	95.2	1.9	73.9	1.4	84.6	75.5
493011	02	01-Sep-1990	07:49	4.34	108.9	1.7	92.8	1.4	100.9	93.1
493011	03	22-Oct-1991	15:37	5.48	116.2	1.8	98.2	1.1	107.2	97.3
493011	04	12-Nov-1992	17:06	6.54	122.4	1.0	109.0	0.5	115.7	107.4
493011	05	15-Nov-1993	15:53	7.54	133.9	2.5	118.0	1.0	125.9	117.6
493011	06	13-Jan-1994	10:52	7.71	130.3	1.8	118.3	9.1	124.3	115.1
493011	07	16-Apr-1994	01:18	7.96	118.3	1.4	101.3	1.1	109.8	99.4
493011	08	14-Jul-1994	20:39	8.20	117.4	3.0	104.8	1.1	111.1	102.8
493011	09	13-Nov-1994	13:54	8.54	135.9	1.7	121.4	1.2	128.6	119.5
493011	10	15-Feb-1995	12:39	8.80	120.4	1.9	104.3	1.2	112.3	103.6
493011	11	18-May-1995	11:50	9.05	117.3	2.6	104.6	2.9	110.9	102.1
493011	12	05-Dec-1996	07:49	10.60	157.3	1.3	144.9	0.8	151.1	141.6
493011	13	05-Dec-1996	14:09	10.60	150.6	1.2	135.0	1.1	142.8	134.2
493011	14	02-Mar-1997	09:48	10.84	146.0	1.2	131.0	0.3	138.5	128.6
493011	15	02-Mar-1997	13:56	10.84	141.6	0.9	126.2	2.6	133.9	124.0
493011	16	25-Apr-1997	07:09	10.99	148.1	0.3	133.7	0.5	140.9	132.7
493011	17	25-Apr-1997	12:10	10.99	130.7	0.8	122.8	0.9	126.8	118.0

Section	Visit	Date	Time	Age (years)	Left IRI Average (Inches/ mi)	Left IRI SD (Inches/ mi)	Right IRI Average (Inches/ mi)	Right IRI SD (Inches/ mi)	MRI (Inches/ mi)	HRI (Inches/ mi)
493011	18	01-Aug-1997	09:21	11.25	148.5	1.6	139.2	0.3	143.8	134.3
493011	19	01-Aug-1997	14:28	11.25	142.0	1.4	130.9	1.6	136.5	127.1
493011	20	17-Sep-1997	09:15	11.38	152.7	2.1	140.3	1.5	146.5	138.0
493011	21	17-Sep-1997	12:42	11.38	140.0	1.8	128.6	1.8	134.3	125.4
493011	22	01-Dec-1998	12:03	12.59	147.7	1.1	132.8	1.6	140.3	131.7
493011	23	13-Jul-1999	14:33	13.20	133.4	3.3	125.6	1.4	129.5	119.7
493011	24	09-Sep-2001	07:52	15.36	179.3	1.5	166.1	0.7	172.7	165.6
493011	25	26-Jan-2004	16:11	17.74	171.4	0.9	165.1	0.6	168.2	157.3
493011	26	06-Oct-2004	13:53	18.44	163.8	0.8	155.1	0.7	159.4	148.6
493011	27	20-Dec-2004	11:53	18.64	163.7	1.6	153.0	0.9	158.3	147.8
493011	28	09-Oct-2007	15:16	21.44	167.4	2.0	170.4	1.3	168.9	158.3
493011	29	26-Oct-2010	14:00	24.49	189.9	0.6	197.0	1.1	193.5	182.7
493011	30	23-Oct-2012	16:25	26.48	71.4	2.5	77.6	4.2	74.5	58.1
493011	31	20-May-2014	21:29	28.05	69.8	2.4	66.5	2.2	68.2	58.1
493011	32	18-May-2015	19:57	29.05	72.3	4.0	76.8	2.9	74.6	64.5
530201	01	18-Nov-1995	13:18	0.00	68.5	0.4	85.8	1.4	77.2	67.2
530201	02	06-Oct-1997	16:48	1.88	78.2	1.2	95.0	2.0	86.6	75.8
530201	03	15-May-1998	14:27	2.48	73.9	1.1	95.4	2.4	84.7	73.0
530201	04	07-May-1999	12:52	3.46	73.0	1.8	100.0	1.1	86.5	75.5
530201	05	29-Jun-2000	13:40	4.61	73.4	1.7	99.5	1.3	86.5	75.4
530201	06	07-Aug-2001	10:33	5.71	81.5	1.7	102.5	0.6	92.0	81.0
530201	07	05-Aug-2002	10:56	6.71	81.7	1.4	103.5	1.1	92.6	81.3
530201	08	20-Aug-2003	15:32	7.75	84.7	1.3	100.3	1.7	92.5	81.7
530201	09	23-Jul-2004	13:41	8.67	79.4	1.0	97.0	2.4	88.2	76.2
530201	10	24-Jun-2005	18:21	9.59	80.3	0.7	100.5	2.8	90.4	78.9
530201	11	07-Jun-2006	18:12	10.55	80.5	1.0	96.6	1.3	88.5	76.5
530201	12	19-Jul-2007	17:55	11.66	82.6	1.4	99.2	2.0	90.9	78.2
530201	13	12-Jun-2008	13:24	12.56	85.3	3.3	102.3	1.0	93.8	81.0
530201	14	30-Apr-2009	14:30	13.44	83.9	1.4	99.2	1.3	91.5	80.4
530201	15	29-Jul-2010	11:36	14.69	88.7	1.4	102.5	1.2	95.6	81.4
530201	16	05-Feb-2011	12:33	15.21	81.3	2.4	98.6	1.0	90.0	76.4
530201	17	14-May-2012	21:48	16.48	94.9	1.7	101.7	2.0	98.3	82.4
530201	18	17-May-2013	06:43	17.49	100.6	2.4	106.0	1.2	103.3	86.8
530201	19	17-May-2013	10:05	17.49	94.9	2.1	100.6	1.8	97.7	82.8
530201	20	17-May-2013	15:41	17.49	92.8	1.1	101.9	2.0	97.4	82.9
530201	21	16-Apr-2015	00:21	19.40	94.8	1.6	107.9	1.6	101.3	82.2
530202	01	18-Nov-1995	13:18	0.00	58.2	0.9	69.0	1.3	63.6	59.0
530202	02	06-Oct-1997	16:48	1.88	56.9	1.0	68.7	1.6	62.8	57.7
530202	03	15-May-1998	14:14	2.48	58.1	0.9	71.0	2.1	64.6	59.5
530202	04	07-May-1999	13:02	3.46	66.4	0.6	67.9	0.5	67.2	62.2
530202	05	29-Jun-2000	13:27	4.61	65.7	0.9	67.9	1.3	66.8	62.4
530202	06	07-Aug-2001	10:43	5.71	61.1	0.4	62.6	0.6	61.8	57.4
530202	07	05-Aug-2002	10:46	6.71	62.0	1.0	61.9	0.6	62.0	57.6
530202	08	20-Aug-2003	15:16	7.75	58.4	0.6	71.2	1.2	64.8	59.4
530202	09	23-Jul-2004	14:12	8.67	58.3	1.0	72.7	0.4	65.5	60.1
530202	10	24-Jun-2005	18:21	9.59	62.4	1.7	62.6	1.7	62.5	57.3
530202	11	07-Jun-2006	17:59	10.55	59.1	0.8	71.5	1.0	65.3	59.8
530202	12	19-Jul-2007	17:55	11.66	60.1	1.9	72.8	2.3	66.4	60.8

Section	Visit	Date	Time	Age (years)	Left IRI Average (Inches/ mi)	Left IRI SD (Inches/ mi)	Right IRI Average (Inches/ mi)	Right IRI SD (Inches/ mi)	MRI (Inches/ mi)	HRI (Inches/ mi)
530202	13	12-Jun-2008	12:29	12.56	63.7	2.0	73.6	1.2	68.6	63.3
530202	14	30-Apr-2009	13:33	13.44	62.2	1.8	74.9	1.9	68.6	63.1
530202	15	29-Jul-2010	10:08	14.69	62.4	1.2	67.3	2.0	64.8	59.0
530202	16	05-Feb-2011	12:00	15.21	61.4	1.0	72.8	1.0	67.1	61.6
530202	17	14-May-2012	20:57	16.48	61.5	1.2	70.5	1.2	66.0	60.7
530202	18	16-May-2013	07:03	17.48	67.6	0.9	76.0	1.0	71.8	66.8
530202	19	16-May-2013	10:01	17.49	62.0	1.7	69.5	2.1	65.8	60.6
530202	20	16-May-2013	15:07	17.49	59.8	0.8	70.7	0.7	65.3	59.9
530202	21	16-Apr-2015	00:32	19.40	64.7	1.3	63.6	1.8	64.1	59.2
530203	01	18-Nov-1995	13:18	0.00	74.7	1.5	85.9	1.6	80.3	70.6
530203	02	06-Oct-1997	16:48	1.88	74.2	2.1	86.0	2.5	80.1	68.6
530203	03	15-May-1998	14:27	2.48	72.7	2.4	86.0	2.8	79.3	67.2
530203	04	07-May-1999	12:52	3.46	78.0	3.5	87.5	3.6	82.8	68.9
530203	05	29-Jun-2000	13:13	4.61	80.2	1.6	90.2	1.7	85.2	71.6
530203	06	07-Aug-2001	10:33	5.71	81.9	1.8	93.3	2.1	87.6	75.5
530203	07	05-Aug-2002	11:06	6.71	85.8	1.4	90.5	2.5	88.1	74.1
530203	08	20-Aug-2003	15:37	7.75	84.1	0.7	95.0	1.3	89.6	79.3
530203	09	23-Jul-2004	13:41	8.67	78.7	2.8	91.7	1.7	85.2	74.0
530203	10	24-Jun-2005	18:21	9.59	86.7	1.6	88.2	1.8	87.4	72.5
530203	11	07-Jun-2006	18:22	10.55	80.8	2.1	91.7	0.4	86.2	73.9
530203	12	19-Jul-2007	17:55	11.66	83.5	0.8	93.8	0.5	88.6	76.7
530203	13	12-Jun-2008	12:41	12.56	83.9	2.0	94.4	2.8	89.1	75.0
530203	14	30-Apr-2009	13:33	13.44	79.8	2.2	91.2	3.1	85.5	72.2
530203	15	29-Jul-2010	10:08	14.69	85.3	2.7	95.1	1.1	90.2	76.7
530203	16	05-Feb-2011	11:45	15.21	80.3	2.6	92.7	1.7	86.5	73.9
530203	17	14-May-2012	20:52	16.48	88.9	2.8	98.3	1.3	93.6	79.1
530203	18	16-May-2013	07:03	17.48	95.3	1.6	103.1	0.8	99.2	84.5
530203	19	16-May-2013	10:09	17.49	97.9	2.5	101.6	1.4	99.7	83.5
530203	20	16-May-2013	15:07	17.49	89.9	3.2	96.2	0.9	93.1	79.4
530203	21	16-Apr-2015	00:32	19.40	96.5	3.0	99.6	3.0	98.1	82.1
530204	01	18-Nov-1995	13:18	0.00	75.0	1.6	74.4	1.6	74.7	68.6
530204	02	06-Oct-1997	16:48	1.88	77.9	1.6	73.7	0.9	75.8	68.7
530204	03	15-May-1998	14:27	2.48	78.7	2.2	78.7	2.9	78.7	71.4
530204	04	07-May-1999	13:02	3.46	77.4	1.3	81.4	1.7	79.4	72.0
530204	05	29-Jun-2000	13:13	4.61	77.5	1.3	82.4	1.0	79.9	72.8
530204	06	07-Aug-2001	10:33	5.71	75.1	0.7	78.5	1.3	76.8	70.8
530204	07	05-Aug-2002	10:56	6.71	80.3	0.8	77.8	1.1	79.0	72.9
530204	08	20-Aug-2003	15:32	7.75	76.7	0.8	77.0	0.7	76.9	70.1
530204	09	23-Jul-2004	13:41	8.67	75.7	1.4	77.8	1.2	76.7	70.0
530204	10	24-Jun-2005	18:35	9.59	79.9	1.6	80.2	1.3	80.1	72.8
530204	11	07-Jun-2006	18:12	10.55	78.6	1.5	81.1	1.4	79.9	72.4
530204	12	19-Jul-2007	17:55	11.66	79.2	1.1	80.0	1.3	79.6	72.3
530204	13	12-Jun-2008	12:29	12.56	78.6	1.6	78.9	0.7	78.7	71.1
530204	14	30-Apr-2009	13:38	13.44	78.7	1.3	80.9	1.9	79.8	72.1
530204	15	29-Jul-2010	11:27	14.69	76.8	1.4	80.7	1.4	78.7	71.3
530204	16	05-Feb-2011	12:33	15.21	77.6	1.0	80.7	1.0	79.2	71.9
530204	17	14-May-2012	21:03	16.48	79.6	0.7	81.2	1.1	80.4	73.6
530204	18	17-May-2013	07:37	17.49	89.2	1.6	92.9	1.1	91.1	85.3

Section	Visit	Date	Time	Age (years)	Left IRI Average (Inches/mi)	Left IRI SD (Inches/mi)	Right IRI Average (Inches/mi)	Right IRI SD (Inches/mi)	MRI (Inches/mi)	HRI (Inches/mi)
530204	19	17-May-2013	10:29	17.49	80.9	1.4	82.0	1.7	81.5	75.7
530204	20	17-May-2013	15:04	17.49	77.8	1.1	79.7	1.2	78.7	71.7
530204	21	16-Apr-2015	00:32	19.40	84.0	1.0	86.4	2.1	85.2	78.9
530205	01	18-Nov-1995	13:18	0.00	72.3	0.3	84.6	2.2	78.4	67.1
530205	02	06-Oct-1997	16:48	1.88	79.6	3.0	82.6	2.7	81.1	70.5
530205	03	15-May-1998	14:27	2.48	78.4	3.4	83.7	4.4	81.1	69.7
530205	04	07-May-1999	12:52	3.46	75.8	1.4	85.1	2.4	80.5	69.1
530205	05	29-Jun-2000	13:13	4.61	77.7	0.6	87.5	1.8	82.6	71.8
530205	06	07-Aug-2001	10:33	5.71	77.7	1.3	82.6	1.4	80.1	68.3
530205	07	05-Aug-2002	11:06	6.71	79.7	0.3	79.0	0.6	79.3	67.7
530205	08	20-Aug-2003	15:16	7.75	77.5	1.8	86.5	1.4	82.0	71.1
530205	09	23-Jul-2004	13:53	8.67	81.6	2.6	89.2	1.0	85.4	73.0
530205	10	24-Jun-2005	18:21	9.59	79.2	0.5	89.8	3.8	84.5	71.6
530205	11	07-Jun-2006	17:59	10.55	80.3	1.3	95.6	2.0	87.9	74.4
530205	12	19-Jul-2007	17:55	11.66	79.9	1.6	93.0	2.2	86.5	73.1
530205	13	12-Jun-2008	13:34	12.56	83.9	1.8	90.8	0.8	87.4	76.3
530205	14	30-Apr-2009	14:30	13.44	86.2	2.4	89.8	2.0	88.0	76.5
530205	15	29-Jul-2010	11:17	14.69	84.9	1.9	86.6	1.6	85.7	73.4
530205	16	05-Feb-2011	12:33	15.21	85.9	2.2	90.1	1.1	88.0	76.3
530205	17	14-May-2012	21:48	16.48	84.2	1.3	88.2	2.7	86.2	72.8
530205	18	17-May-2013	06:43	17.49	92.0	2.4	91.8	2.3	91.9	80.7
530205	19	17-May-2013	10:05	17.49	88.3	1.7	90.6	2.2	89.4	76.6
530205	20	17-May-2013	15:41	17.49	88.6	1.6	87.7	2.8	88.2	76.6
530205	21	16-Apr-2015	00:42	19.40	93.5	1.4	89.7	2.2	91.6	79.1
530206	01	18-Nov-1995	13:18	0.00	65.0	0.9	68.1	0.5	66.5	60.0
530206	02	06-Oct-1997	16:48	1.88	86.4	0.4	81.3	0.7	83.8	77.3
530206	03	15-May-1998	14:27	2.48	97.2	3.2	90.1	0.5	93.7	86.9
530206	04	07-May-1999	13:02	3.46	99.5	0.9	106.2	0.8	102.8	96.5
530206	05	29-Jun-2000	13:40	4.61	131.7	0.6	134.2	1.1	133.0	127.7
530206	06	07-Aug-2001	10:33	5.71	131.9	4.1	120.3	2.1	126.1	120.5
530206	07	05-Aug-2002	11:06	6.71	112.6	1.5	110.4	2.1	111.5	105.2
530206	08	20-Aug-2003	15:16	7.75	124.9	2.6	116.8	1.1	120.9	115.1
530206	09	23-Jul-2004	14:12	8.67	154.9	0.8	137.5	1.5	146.2	141.1
530206	10	24-Jun-2005	18:21	9.59	141.5	2.8	124.1	2.8	132.8	126.6
530206	11	07-Jun-2006	17:59	10.55	141.0	0.8	128.2	1.9	134.6	128.1
530206	12	19-Jul-2007	17:55	11.66	142.3	2.2	128.9	3.2	135.6	128.8
530206	13	12-Jun-2008	13:34	12.56	149.6	1.8	141.0	1.9	145.3	139.1
530206	14	30-Apr-2009	14:41	13.44	134.4	1.7	132.8	3.4	133.6	127.4
530206	15	29-Jul-2010	11:36	14.69	135.7	2.2	134.9	3.3	135.3	128.7
530206	16	05-Feb-2011	12:33	15.21	119.8	2.8	118.6	3.3	119.2	112.4
530206	17	14-May-2012	21:48	16.48	117.7	2.4	121.8	2.1	119.7	111.6
530206	18	17-May-2013	07:09	17.49	103.0	1.3	110.6	3.9	106.8	99.2
530206	19	17-May-2013	10:05	17.49	114.7	3.4	123.5	3.8	119.1	111.0
530206	20	17-May-2013	15:41	17.49	116.9	3.8	123.5	3.2	120.2	113.0
530206	21	16-Apr-2015	01:04	19.40	107.9	0.8	112.5	1.9	110.2	101.6
530207	01	18-Nov-1995	13:18	0.00	82.6	1.7	68.6	1.2	75.6	67.9
530207	02	06-Oct-1997	16:48	1.88	89.2	1.4	76.9	1.0	83.1	72.8
530207	03	15-May-1998	14:38	2.48	87.2	1.7	76.6	3.1	81.9	71.3

Section	Visit	Date	Time	Age (years)	Left IRI Average (Inches/ mi)	Left IRI SD (Inches/ mi)	Right IRI Average (Inches/ mi)	Right IRI SD (Inches/ mi)	MRI (Inches/ mi)	HRI (Inches/ mi)
530207	04	07-May-1999	13:02	3.46	90.7	1.8	79.9	1.3	85.3	73.6
530207	05	29-Jun-2000	13:13	4.61	92.4	0.5	80.5	1.1	86.4	74.7
530207	06	07-Aug-2001	11:03	5.71	93.0	0.8	80.9	0.7	86.9	73.8
530207	07	05-Aug-2002	10:56	6.71	96.8	1.1	84.6	1.3	90.7	78.6
530207	08	20-Aug-2003	15:37	7.75	92.3	1.2	80.6	1.6	86.4	74.9
530207	09	23-Jul-2004	13:53	8.67	99.7	1.3	83.2	2.0	91.5	77.3
530207	10	24-Jun-2005	18:21	9.59	102.1	2.0	84.0	1.7	93.0	78.8
530207	11	07-Jun-2006	17:59	10.55	102.8	1.3	85.4	0.8	94.1	79.4
530207	12	19-Jul-2007	18:08	11.66	97.9	1.4	88.4	1.7	93.2	79.8
530207	13	12-Jun-2008	13:34	12.56	109.1	1.6	90.1	2.2	99.6	83.3
530207	14	30-Apr-2009	14:41	13.44	109.8	1.9	88.9	1.1	99.3	82.6
530207	15	29-Jul-2010	11:27	14.69	119.5	2.2	95.2	2.4	107.4	89.8
530207	16	05-Feb-2011	12:33	15.21	104.1	4.0	88.0	1.5	96.1	80.7
530207	17	14-May-2012	21:48	16.48	127.5	2.3	91.0	1.1	109.2	92.3
530207	18	17-May-2013	06:43	17.49	108.4	1.2	91.4	0.7	99.9	81.7
530207	19	17-May-2013	10:05	17.49	118.1	4.5	93.8	2.0	106.0	86.3
530207	20	17-May-2013	15:04	17.49	119.3	3.5	93.7	2.1	106.5	87.7
530207	21	16-Apr-2015	00:21	19.40	118.7	5.3	107.4	3.2	113.1	99.5
530208	01	18-Nov-1995	13:18	0.00	72.8	2.2	68.7	1.1	70.8	65.2
530208	02	06-Oct-1997	16:48	1.88	76.4	3.6	65.0	0.8	70.7	64.6
530208	03	15-May-1998	14:14	2.48	79.0	4.2	72.9	2.4	76.0	69.7
530208	04	07-May-1999	13:02	3.46	83.3	3.0	77.3	0.8	80.3	74.2
530208	05	29-Jun-2000	13:13	4.61	97.5	2.0	96.7	1.7	97.1	91.9
530208	06	07-Aug-2001	10:33	5.71	104.1	3.7	88.7	2.6	96.4	90.9
530208	07	05-Aug-2002	10:56	6.71	87.9	1.0	86.0	1.3	87.0	81.4
530208	08	20-Aug-2003	15:16	7.75	106.7	1.0	94.3	0.4	100.5	95.2
530208	09	23-Jul-2004	13:53	8.67	120.2	1.3	113.1	1.1	116.6	111.8
530208	10	24-Jun-2005	18:21	9.59	120.3	2.3	106.2	2.0	113.2	107.8
530208	11	07-Jun-2006	17:59	10.55	129.1	1.0	108.0	2.0	118.5	112.5
530208	12	19-Jul-2007	17:55	11.66	132.4	3.0	109.8	1.6	121.1	115.6
530208	13	12-Jun-2008	13:24	12.56	131.6	1.6	117.1	0.5	124.4	119.7
530208	14	30-Apr-2009	14:30	13.44	121.6	2.7	111.6	1.7	116.6	112.0
530208	15	29-Jul-2010	11:36	14.69	132.0	1.7	116.1	2.0	124.0	119.1
530208	16	05-Feb-2011	12:42	15.21	103.1	1.5	96.3	0.9	99.7	93.9
530208	17	14-May-2012	22:27	16.48	119.1	1.4	100.5	1.9	109.8	103.7
530208	18	17-May-2013	07:09	17.49	104.7	0.9	91.1	0.7	97.9	91.4
530208	19	17-May-2013	10:17	17.49	106.0	1.9	96.8	2.5	101.4	95.7
530208	20	17-May-2013	15:17	17.49	117.7	2.4	105.4	2.2	111.5	106.5
530208	21	16-Apr-2015	00:21	19.40	100.3	1.4	97.6	2.1	98.9	92.3
530209	01	18-Nov-1995	13:18	0.00	72.8	2.9	83.4	1.6	78.1	64.4
530209	02	06-Oct-1997	16:48	1.88	81.6	2.9	85.5	1.0	83.5	67.2
530209	03	15-May-1998	14:14	2.48	84.6	1.2	89.4	0.7	87.0	70.6
530209	04	07-May-1999	13:02	3.46	74.8	1.8	99.1	1.6	87.0	70.8
530209	05	29-Jun-2000	13:52	4.61	78.3	2.0	96.8	2.6	87.6	73.2
530209	06	07-Aug-2001	10:33	5.71	73.1	2.2	99.0	2.3	86.0	69.4
530209	07	05-Aug-2002	10:56	6.71	74.6	4.1	98.4	2.7	86.5	70.1
530209	08	20-Aug-2003	15:32	7.75	84.7	1.3	90.8	1.9	87.7	72.3
530209	09	23-Jul-2004	13:53	8.67	89.5	1.8	93.4	1.3	91.5	76.1

Section	Visit	Date	Time	Age (years)	Left IRI Average (Inches/ mi)	Left IRI SD (Inches/ mi)	Right IRI Average (Inches/ mi)	Right IRI SD (Inches/ mi)	MRI (Inches/ mi)	HRI (Inches/ mi)
530209	10	24-Jun-2005	18:21	9.59	85.4	2.1	97.5	3.8	91.4	77.0
530209	11	07-Jun-2006	18:12	10.55	84.9	2.7	104.5	0.9	94.7	80.6
530209	12	19-Jul-2007	17:55	11.66	90.0	2.0	98.9	2.2	94.5	78.8
530209	13	12-Jun-2008	12:41	12.56	93.9	1.8	102.1	1.9	98.0	83.2
530209	14	30-Apr-2009	13:38	13.44	96.5	2.1	105.1	2.2	100.8	85.8
530209	15	29-Jul-2010	10:19	14.69	95.3	1.5	103.6	1.0	99.5	83.0
530209	16	05-Feb-2011	12:00	15.21	96.0	2.6	101.0	3.6	98.5	82.1
530209	17	14-May-2012	20:57	16.48	96.1	2.3	108.2	3.2	102.2	86.2
530209	18	16-May-2013	06:53	17.48	94.5	1.7	113.6	2.1	104.1	88.0
530209	19	16-May-2013	10:18	17.49	88.0	3.5	115.8	2.3	101.9	85.4
530209	20	16-May-2013	15:07	17.49	86.3	1.6	114.8	2.1	100.5	84.6
530209	21	16-Apr-2015	00:21	19.40	91.6	2.2	116.0	2.3	103.8	86.9
530210	01	18-Nov-1995	13:18	0.00	43.3	1.2	57.0	1.0	50.1	44.3
530210	02	06-Oct-1997	16:48	1.88	55.7	2.0	63.1	2.2	59.4	53.0
530210	03	15-May-1998	14:27	2.48	59.6	2.8	70.0	2.7	64.8	59.0
530210	04	07-May-1999	12:52	3.46	63.3	1.4	67.4	3.7	65.3	60.1
530210	05	29-Jun-2000	13:27	4.61	62.7	1.4	73.8	1.9	68.2	62.9
530210	06	07-Aug-2001	10:43	5.71	57.3	2.0	64.8	2.4	61.0	55.7
530210	07	05-Aug-2002	10:46	6.71	52.6	0.5	57.9	2.6	55.2	49.5
530210	08	20-Aug-2003	15:32	7.75	52.5	0.8	55.1	0.7	53.8	47.8
530210	09	23-Jul-2004	13:53	8.67	58.7	0.9	61.8	1.6	60.3	54.5
530210	10	24-Jun-2005	18:21	9.59	53.7	1.0	58.4	2.6	56.0	49.8
530210	11	07-Jun-2006	17:59	10.55	54.7	1.9	58.8	0.8	56.8	50.5
530210	12	19-Jul-2007	18:08	11.66	56.4	1.2	58.6	1.1	57.5	51.1
530210	13	12-Jun-2008	12:24	12.56	70.6	1.4	75.9	1.5	73.3	68.6
530210	14	30-Apr-2009	13:38	13.44	75.4	0.7	73.7	2.3	74.5	70.0
530210	15	29-Jul-2010	10:19	14.69	59.3	2.2	63.3	1.4	61.3	54.2
530210	16	05-Feb-2011	11:50	15.21	67.9	1.3	74.5	1.0	71.2	65.4
530210	17	14-May-2012	20:52	16.48	56.3	1.0	59.2	1.6	57.8	49.9
530210	18	16-May-2013	07:03	17.48	56.6	1.1	58.4	0.8	57.5	51.2
530210	19	16-May-2013	10:26	17.49	56.0	0.9	57.9	1.4	57.0	50.2
530210	20	16-May-2013	15:21	17.49	56.2	1.6	58.1	0.4	57.2	50.7
530210	21	16-Apr-2015	00:32	19.40	56.5	0.8	59.0	0.8	57.7	51.8
530211	01	18-Nov-1995	13:18	0.00	71.6	1.5	78.1	2.5	74.8	65.6
530211	02	06-Oct-1997	16:48	1.88	74.2	0.7	78.2	4.1	76.2	65.6
530211	03	15-May-1998	14:27	2.48	73.9	3.9	82.3	3.5	78.1	67.3
530211	04	07-May-1999	12:52	3.46	74.7	2.8	78.6	1.4	76.7	66.6
530211	05	29-Jun-2000	13:13	4.61	73.6	3.2	79.4	1.4	76.5	66.5
530211	06	07-Aug-2001	10:33	5.71	66.9	0.8	73.2	1.9	70.0	58.0
530211	07	05-Aug-2002	11:17	6.71	68.5	1.9	76.2	2.2	72.3	60.8
530211	08	20-Aug-2003	15:32	7.75	74.7	1.6	76.8	0.6	75.8	63.7
530211	09	23-Jul-2004	13:53	8.67	77.7	1.4	81.8	2.2	79.8	67.3
530211	10	24-Jun-2005	19:06	9.59	75.6	4.1	83.9	2.9	79.8	66.9
530211	11	07-Jun-2006	18:12	10.55	78.1	2.6	84.8	3.0	81.5	68.8
530211	12	19-Jul-2007	17:55	11.66	73.4	1.5	86.9	2.6	80.2	67.3
530211	13	12-Jun-2008	12:24	12.56	76.9	4.0	89.3	2.7	83.1	69.8
530211	14	30-Apr-2009	13:38	13.44	85.6	3.4	83.6	2.3	84.6	69.7
530211	15	29-Jul-2010	10:08	14.69	84.1	1.5	79.5	1.1	81.8	66.1

Section	Visit	Date	Time	Age (years)	Left IRI Average (Inches/ mi)	Left IRI SD (Inches/ mi)	Right IRI Average (Inches/ mi)	Right IRI SD (Inches/ mi)	MRI (Inches/ mi)	HRI (Inches/ mi)
530211	16	05-Feb-2011	11:50	15.21	76.1	3.1	86.4	5.4	81.2	68.8
530211	17	14-May-2012	20:57	16.48	81.6	2.3	81.4	1.6	81.5	66.3
530211	18	16-May-2013	07:11	17.48	87.3	2.2	81.5	1.9	84.4	67.9
530211	19	16-May-2013	10:01	17.49	87.6	3.3	81.4	0.7	84.5	67.7
530211	20	16-May-2013	15:21	17.49	85.0	2.6	83.8	3.1	84.4	67.6
530211	21	16-Apr-2015	00:21	19.40	87.9	1.9	81.2	3.2	84.6	66.9
530212	01	18-Nov-1995	13:18	0.00	71.3	1.6	72.6	1.4	71.9	68.0
530212	02	06-Oct-1997	16:48	1.88	75.6	1.6	69.6	1.2	72.6	67.8
530212	03	15-May-1998	14:38	2.48	79.8	2.2	79.0	4.6	79.4	74.3
530212	04	07-May-1999	13:02	3.46	74.8	2.6	83.4	2.2	79.1	74.0
530212	05	29-Jun-2000	13:27	4.61	76.4	1.1	81.6	1.5	79.0	74.4
530212	06	07-Aug-2001	10:53	5.71	67.6	1.1	78.9	1.3	73.3	68.4
530212	07	05-Aug-2002	10:56	6.71	66.6	2.3	76.1	2.1	71.3	65.9
530212	08	20-Aug-2003	15:16	7.75	69.9	0.9	68.6	0.8	69.2	64.0
530212	09	23-Jul-2004	13:53	8.67	75.1	0.9	75.5	1.3	75.3	70.5
530212	10	24-Jun-2005	18:21	9.59	69.4	2.0	68.5	2.4	69.0	63.3
530212	11	07-Jun-2006	17:59	10.55	72.8	0.9	70.0	1.2	71.4	65.8
530212	12	19-Jul-2007	18:40	11.66	69.2	2.8	68.4	1.8	68.8	62.7
530212	13	12-Jun-2008	12:24	12.56	80.6	2.0	81.8	3.5	81.2	76.0
530212	14	30-Apr-2009	13:38	13.44	79.3	1.0	78.0	1.5	78.6	73.9
530212	15	29-Jul-2010	10:08	14.69	71.3	1.9	70.0	1.0	70.6	64.8
530212	16	05-Feb-2011	11:45	15.21	73.8	2.1	71.4	1.9	72.6	66.6
530212	17	14-May-2012	20:57	16.48	69.6	1.2	68.4	0.7	69.0	62.5
530212	18	16-May-2013	07:03	17.48	61.9	1.1	63.9	0.7	62.9	57.8
530212	19	16-May-2013	10:01	17.49	63.4	1.2	65.0	1.2	64.2	58.2
530212	20	16-May-2013	15:07	17.49	67.4	1.0	66.2	0.4	66.8	60.2
530212	21	16-Apr-2015	00:32	19.40	65.3	1.9	66.6	1.7	65.9	59.5
530259	01	18-Nov-1995	13:18	0.00	70.0	2.3	62.8	2.3	66.4	57.0
530259	02	06-Oct-1997	16:48	1.88	71.6	1.9	65.3	2.2	68.4	57.6
530259	03	15-May-1998	14:14	2.48	70.0	3.7	67.5	2.5	68.7	55.7
530259	04	07-May-1999	12:52	3.46	75.7	1.1	72.8	1.5	74.2	58.4
530259	05	29-Jun-2000	13:13	4.61	75.5	1.3	75.2	2.3	75.4	58.1
530259	06	07-Aug-2001	10:43	5.71	78.9	2.8	78.1	2.4	78.5	64.6
530259	07	05-Aug-2002	10:46	6.71	75.7	1.4	81.4	1.7	78.6	63.4
530259	08	20-Aug-2003	15:32	7.75	78.6	1.6	72.2	1.6	75.4	63.5
530259	09	23-Jul-2004	13:41	8.67	77.6	0.9	70.1	1.0	73.9	62.9
530259	10	24-Jun-2005	18:21	9.59	79.5	1.4	75.3	3.4	77.4	63.8
530259	11	07-Jun-2006	18:22	10.55	78.9	2.3	71.4	1.1	75.2	63.4
530259	12	19-Jul-2007	17:55	11.66	80.8	1.4	73.6	1.3	77.2	65.0
530259	13	12-Jun-2008	12:24	12.56	81.9	1.4	73.0	1.2	77.5	64.0
530259	14	30-Apr-2009	13:38	13.44	82.2	0.8	73.7	0.8	77.9	64.2
530259	15	29-Jul-2010	10:08	14.69	83.6	1.6	76.7	2.1	80.2	65.3
530259	16	05-Feb-2011	12:00	15.21	82.6	1.6	74.1	1.4	78.4	65.5
530259	17	14-May-2012	20:57	16.48	87.0	1.4	84.1	3.1	85.6	69.1
530259	18	16-May-2013	07:03	17.48	94.9	1.7	92.7	1.6	93.8	79.3
530259	19	16-May-2013	10:26	17.49	93.6	2.4	89.2	2.3	91.4	75.4
530259	20	16-May-2013	15:07	17.49	83.2	1.9	77.2	2.6	80.2	67.0
530259	21	16-Apr-2015	00:21	19.40	91.5	2.1	90.6	1.3	91.1	74.5

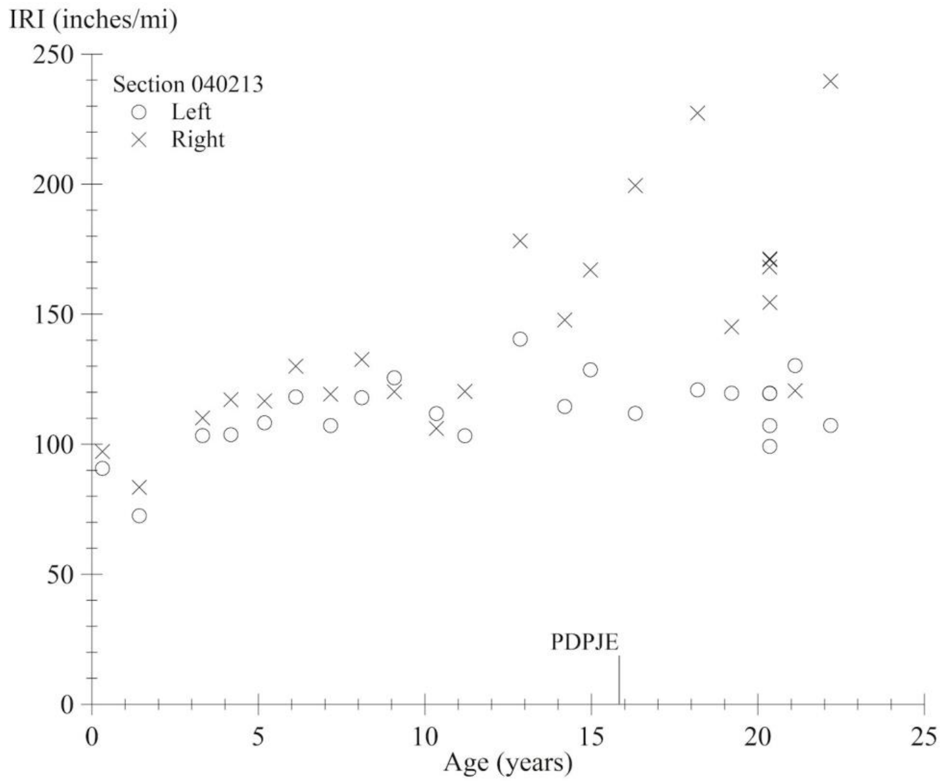

Source: FHWA.
PDPJE = partial-depth patching at joints and elsewhere.

Figure 82. Graph. IRI progression for section 040213.

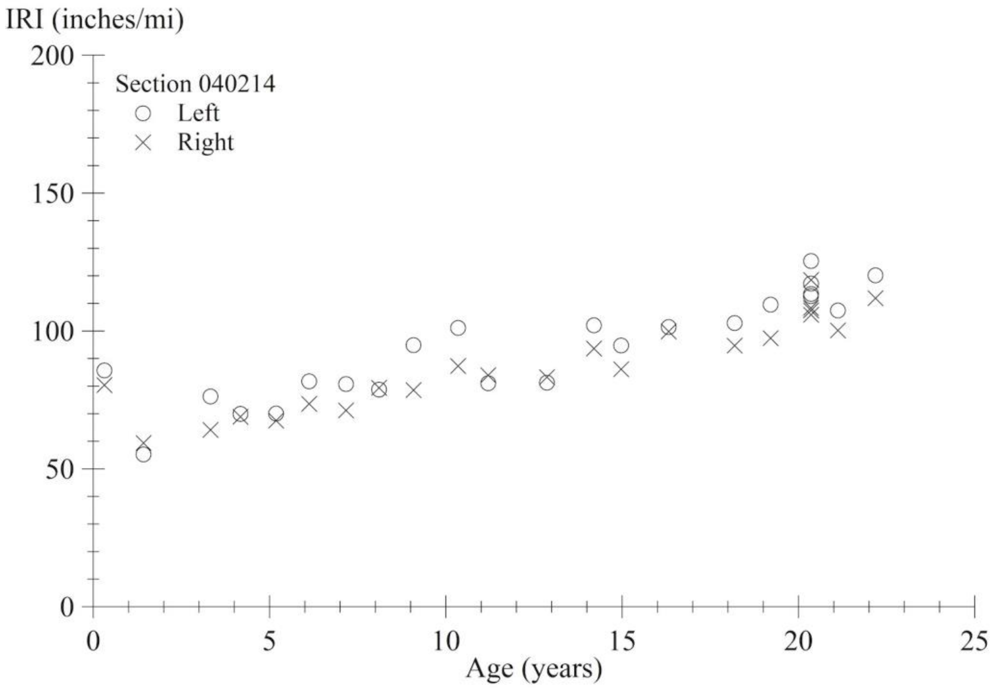

Source: FHWA.

Figure 83. Graph. IRI progression for section 040214.

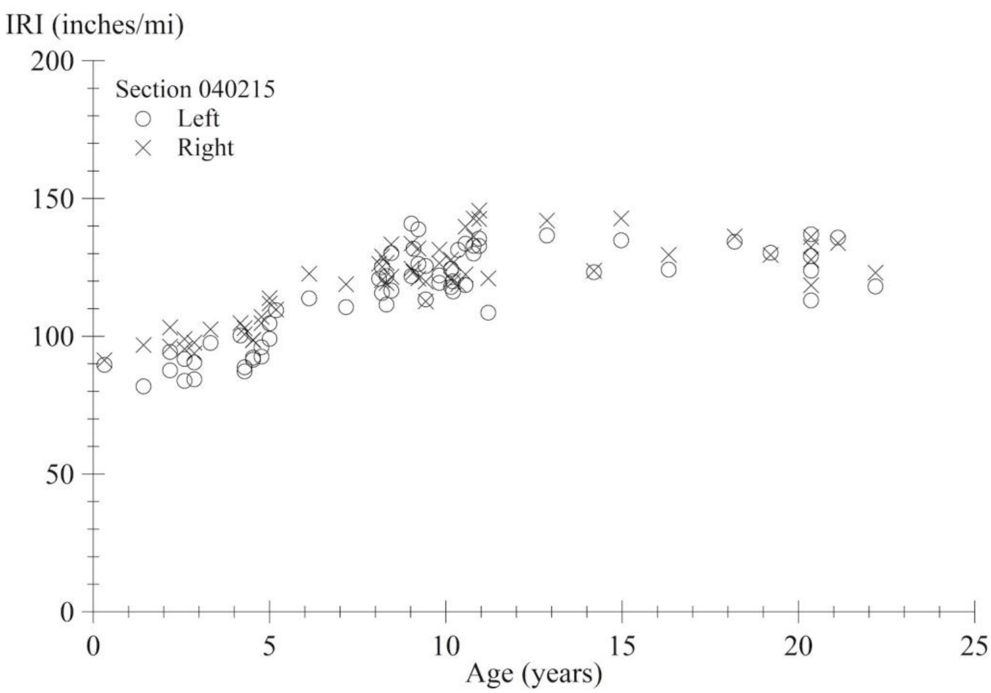

Source: FHWA.

Figure 84. Graph. IRI progression for section 040215.

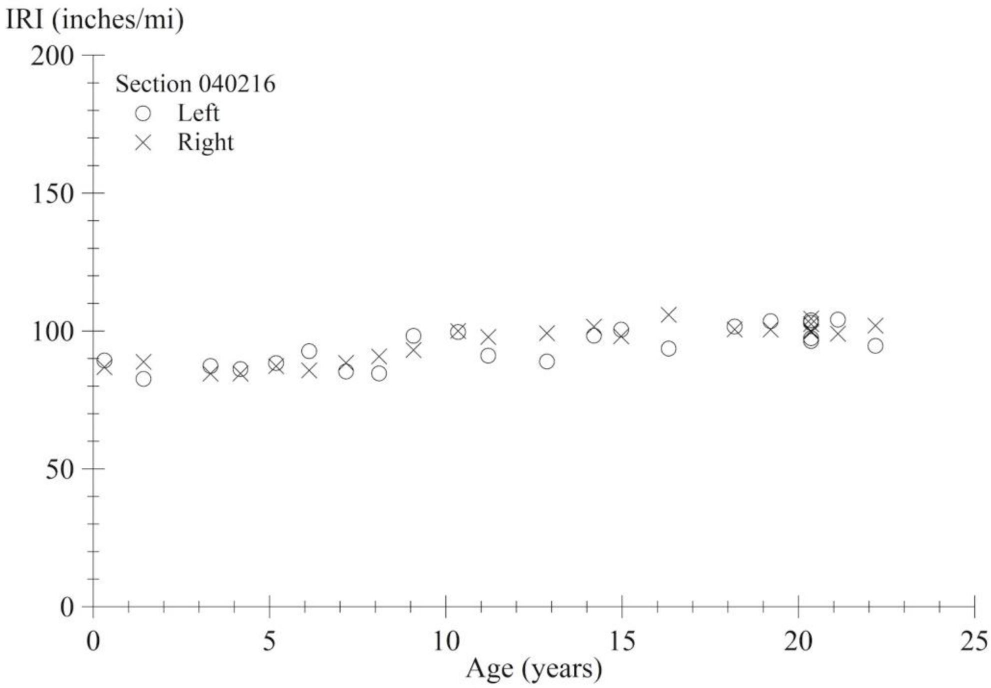

Source: FHWA.

Figure 85. Graph. IRI progression for section 040216.

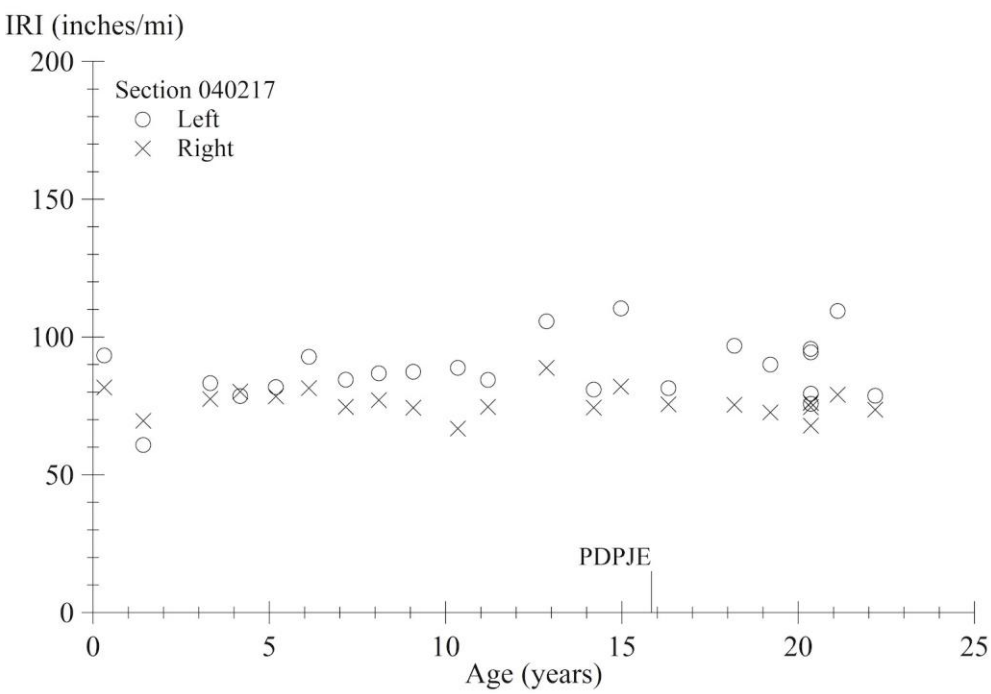

Source: FHWA.
PDPJE = partial-depth patching at joints and elsewhere.

Figure 86. Graph. IRI progression for section 040217.

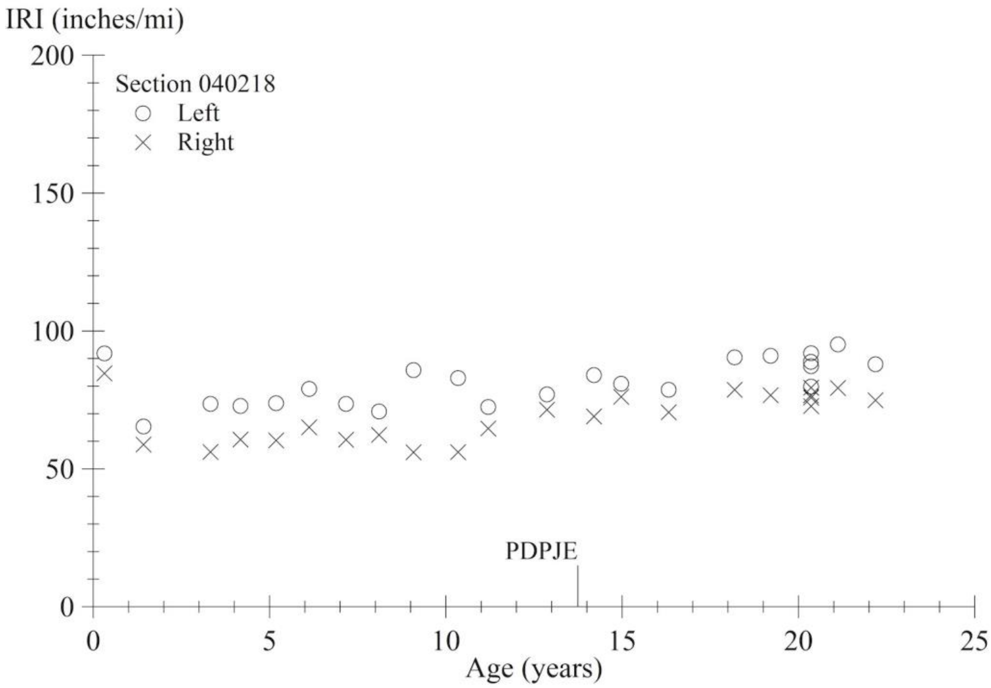

Source: FHWA.
PDPJE = partial-depth patching at joints and elsewhere.

Figure 87. Graph. IRI progression for section 040218.

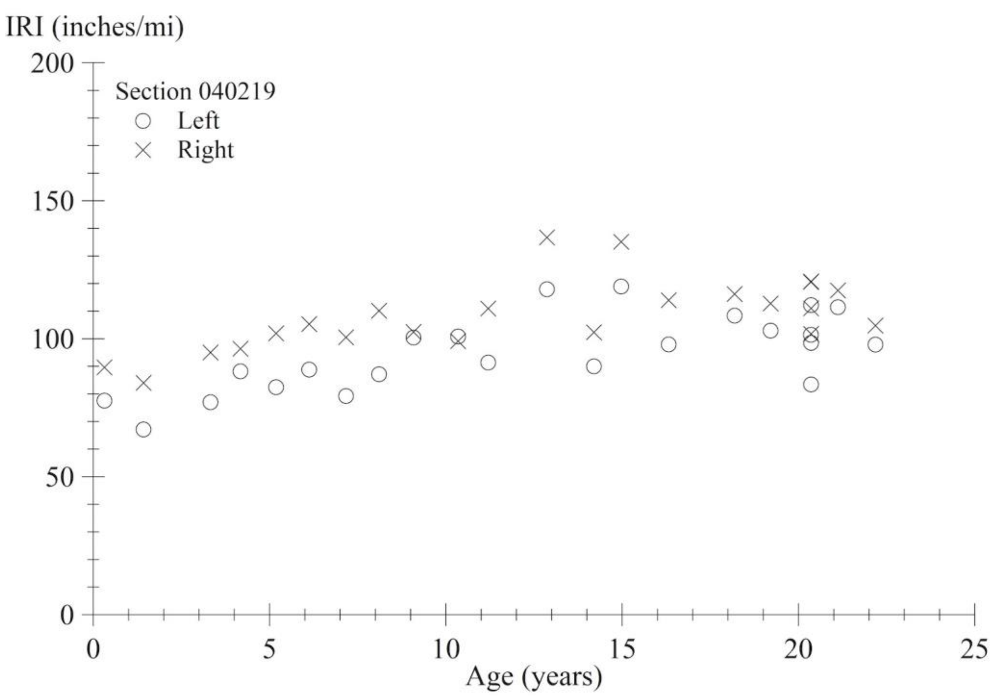

Source: FHWA.

Figure 88. Graph. IRI progression for section 040219.

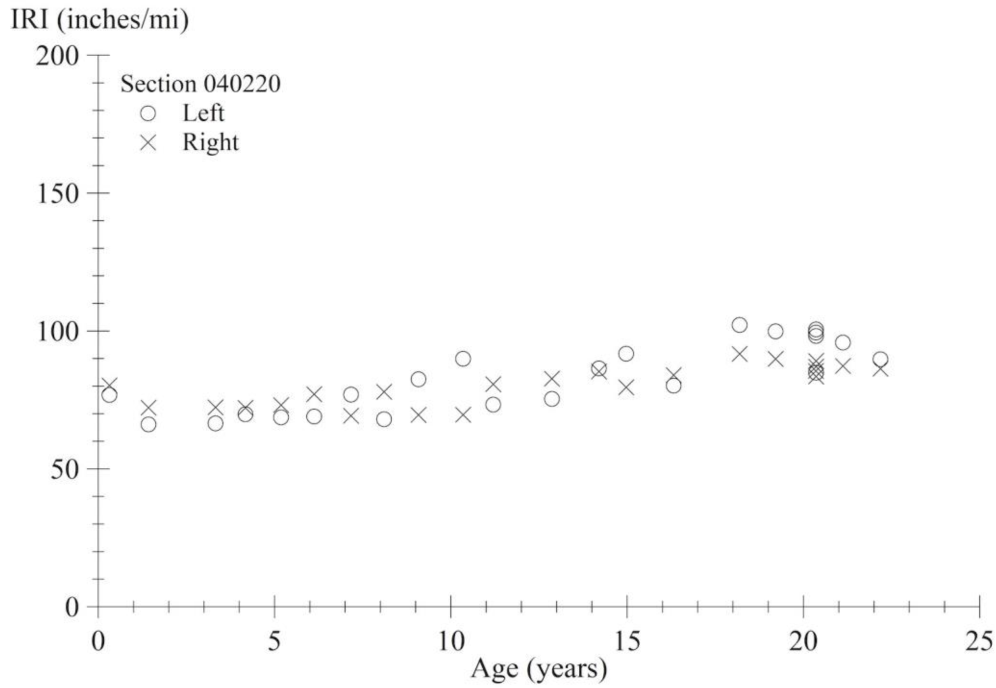

Source: FHWA.

Figure 89. Graph. IRI progression for section 040220.

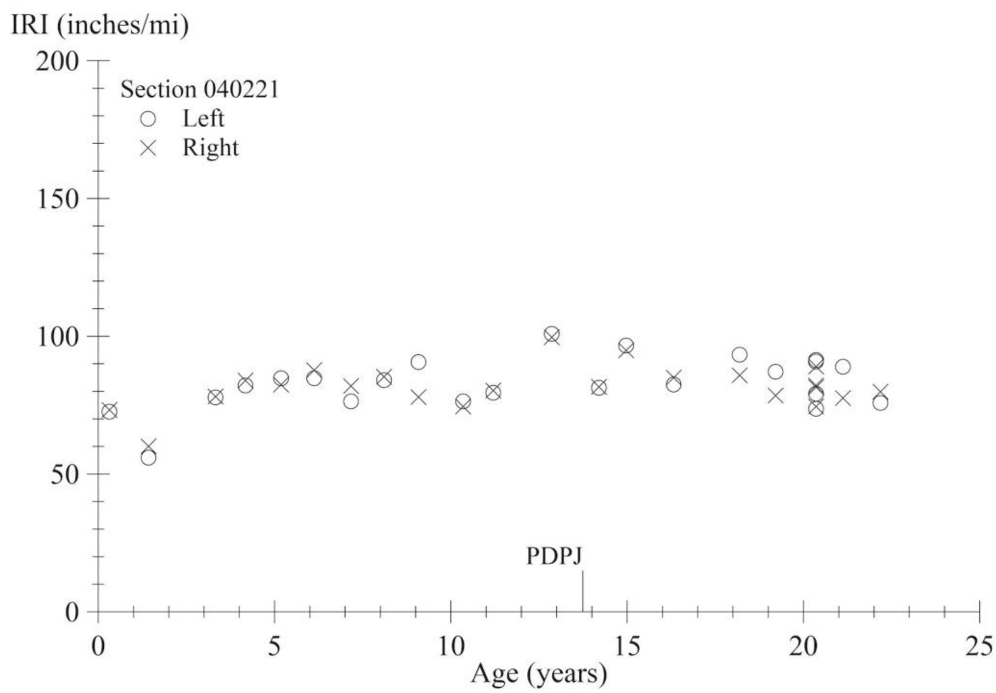

Source: FHWA.
PDPJ = partial-depth patching at joints.

Figure 90. Graph. IRI progression for section 040221.

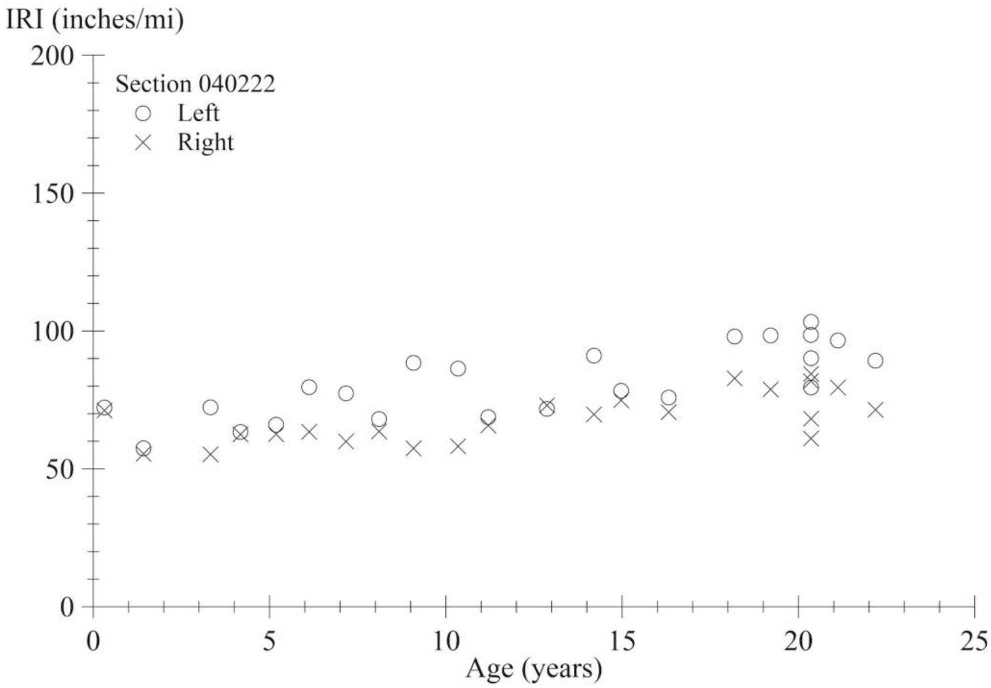

Source: FHWA.

Figure 91. Graph. IRI progression for section 040222.

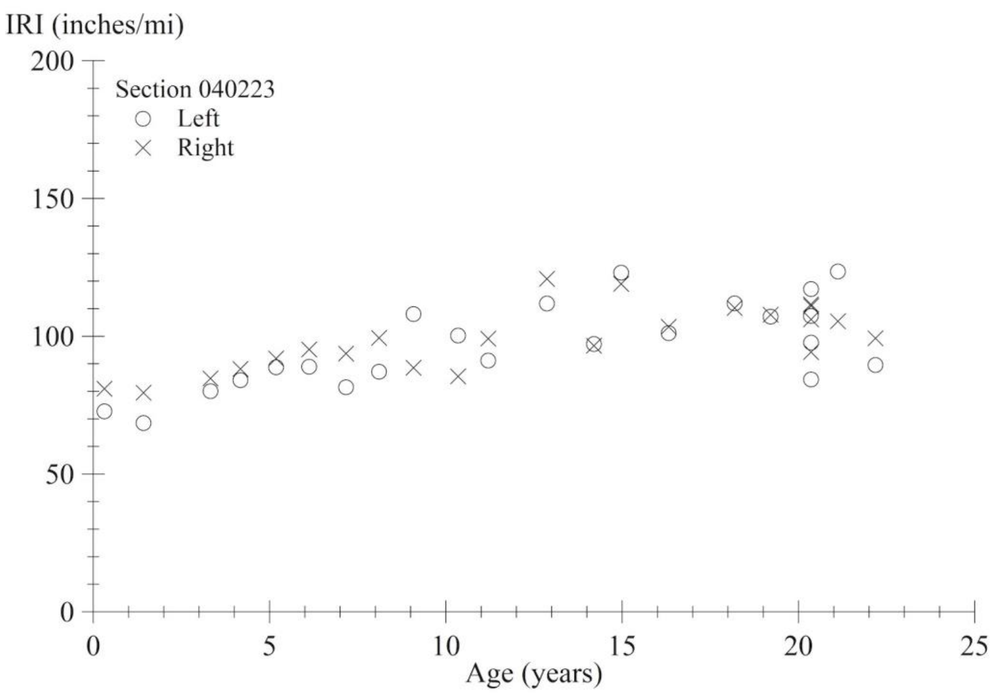

Source: FHWA.

Figure 92. Graph. IRI progression for section 040223.

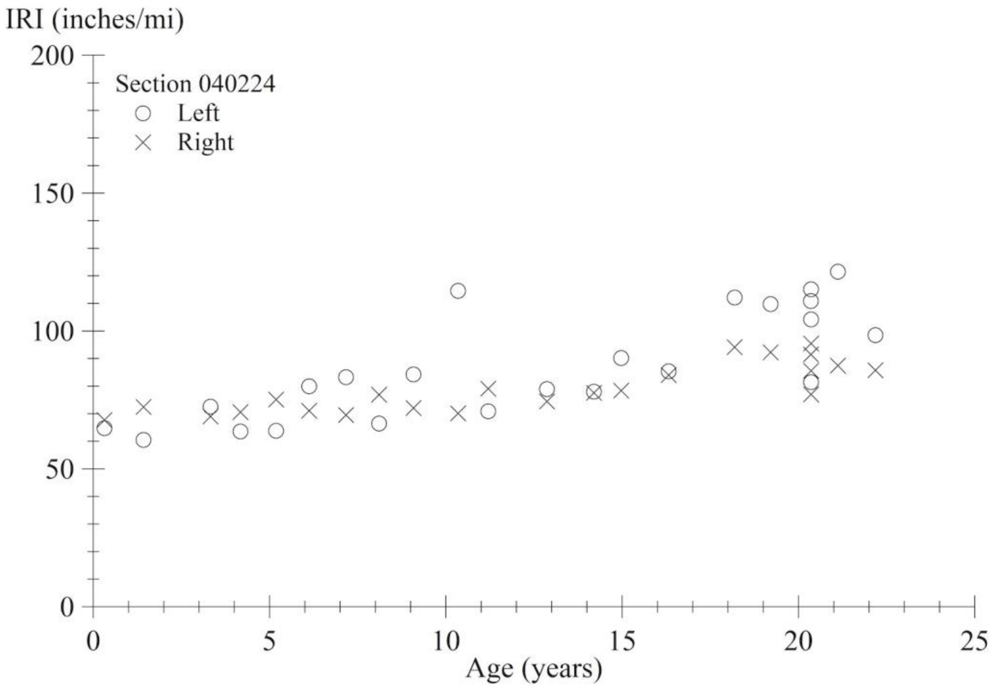

Source: FHWA.

Figure 93. Graph. IRI progression for section 040224.

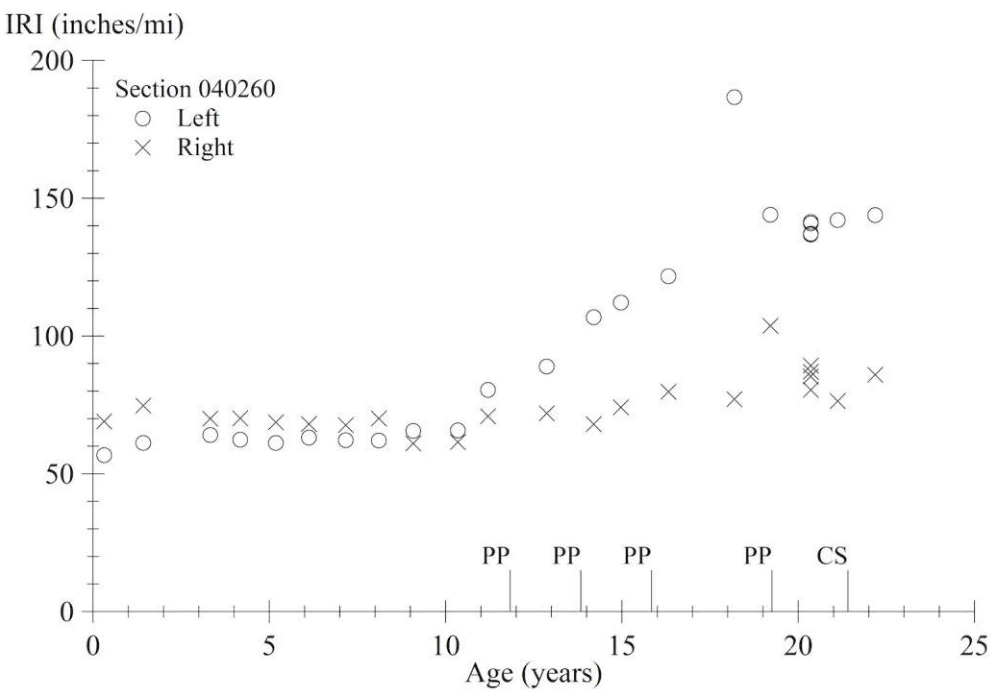

Source: FHWA.
PP = pothole patching; CS = crack sealing.

Figure 94. Graph. IRI progression for section 040260.

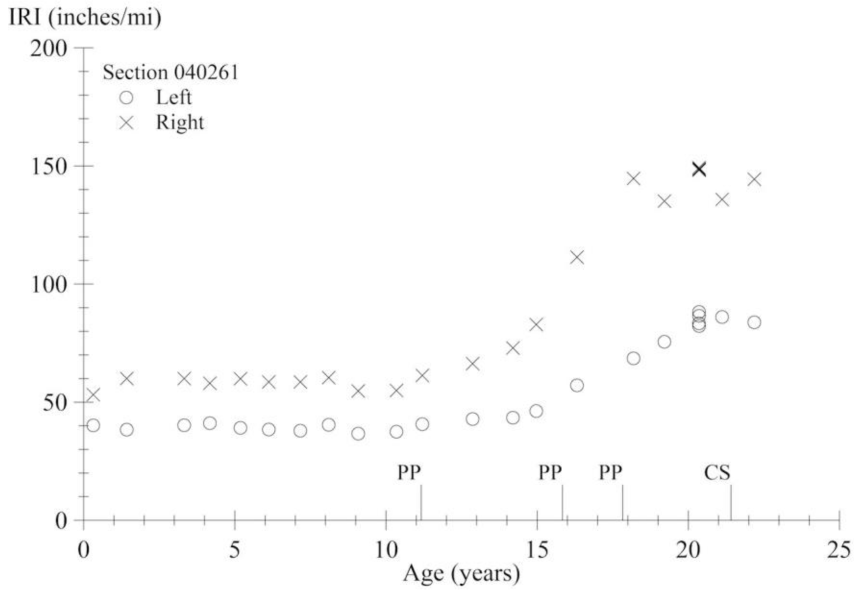

Source: FHWA.
PP = pothole patching; CS = crack sealing.

Figure 95. Graph. IRI progression for section 040261.

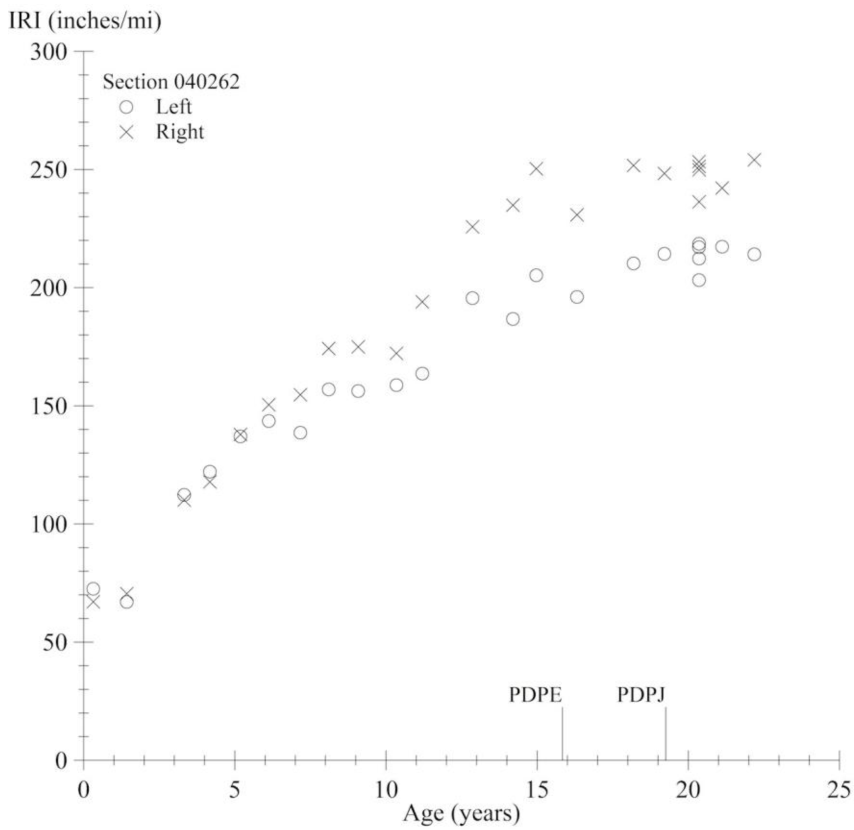

Source: FHWA.
PDPE = partial-depth patching away from joints; PDPJ = partial-depth patching at joints.

Figure 96. Graph. IRI progression for section 040262.

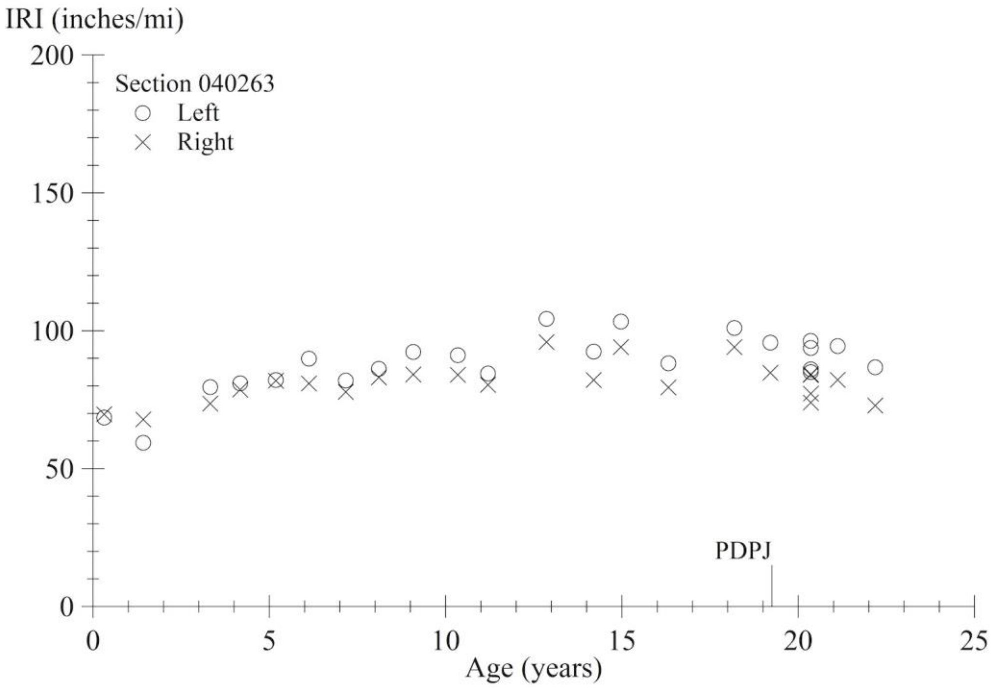

Source: FHWA.
PDPJ = partial-depth patching at joints.

Figure 97. Graph. IRI progression for section 040263.

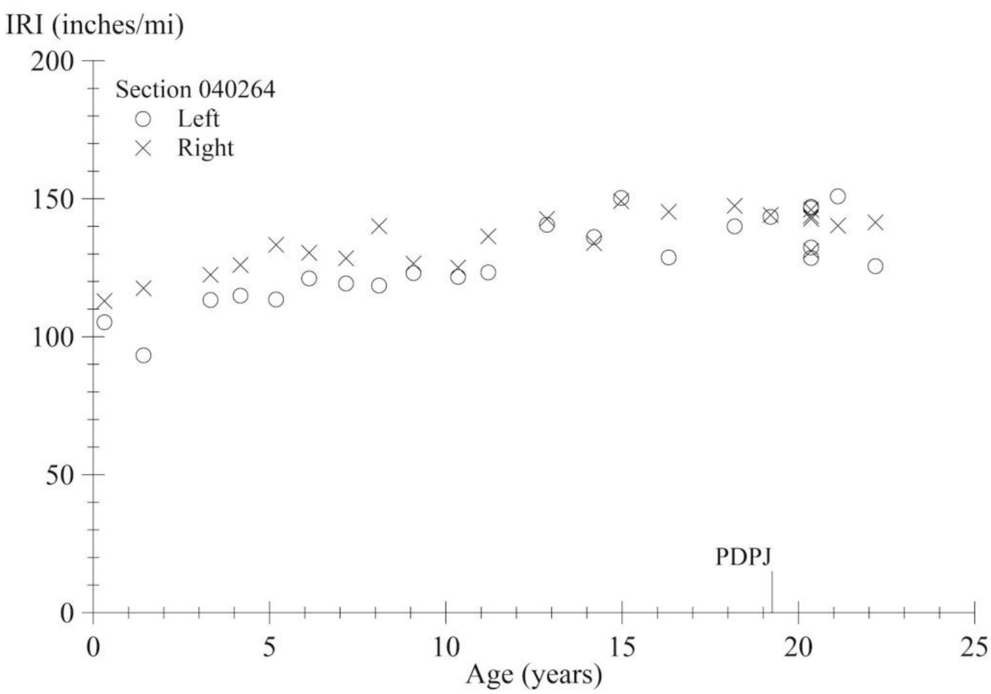

Source: FHWA.
PDPJ = partial-depth patching at joints.

Figure 98. Graph. IRI progression for section 040264.

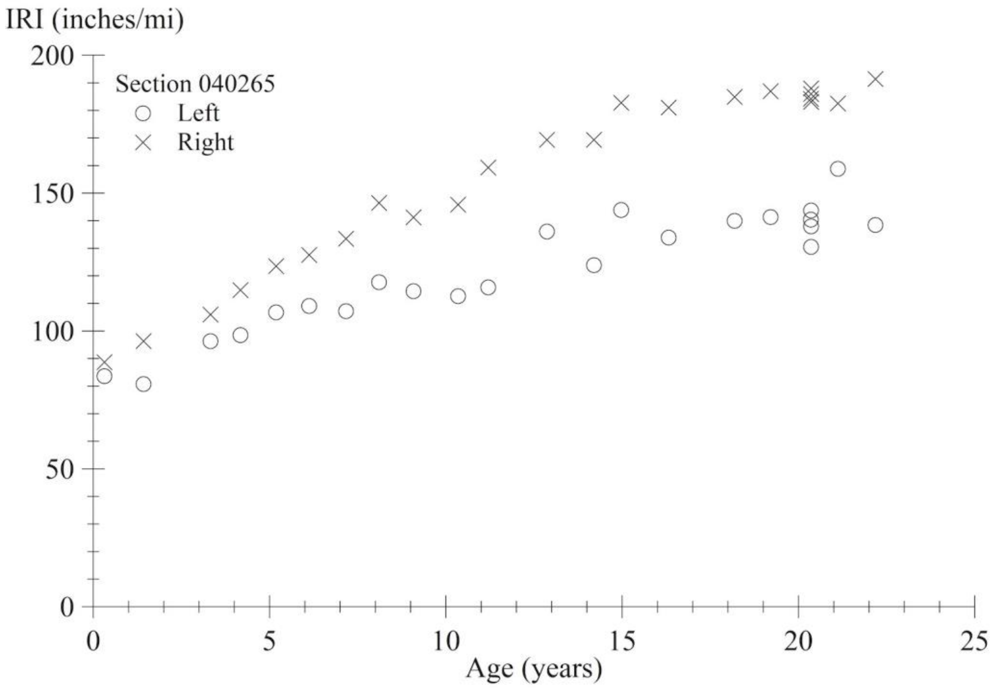

Source: FHWA.

Figure 99. Graph. IRI progression for section 040265.

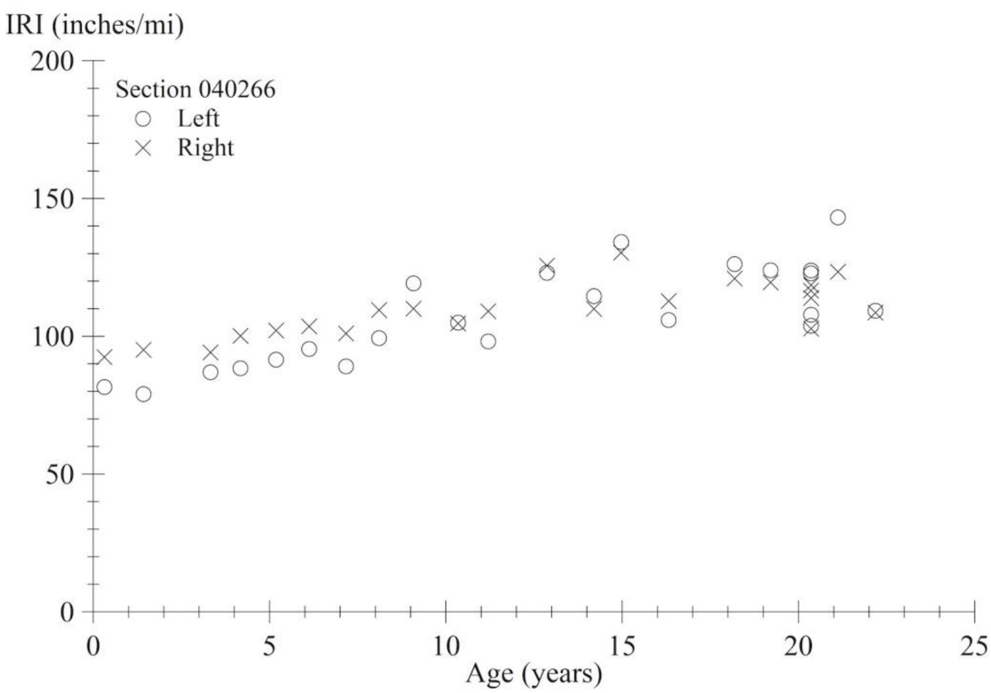

Source: FHWA.

Figure 100. Graph. IRI progression for section 040266.

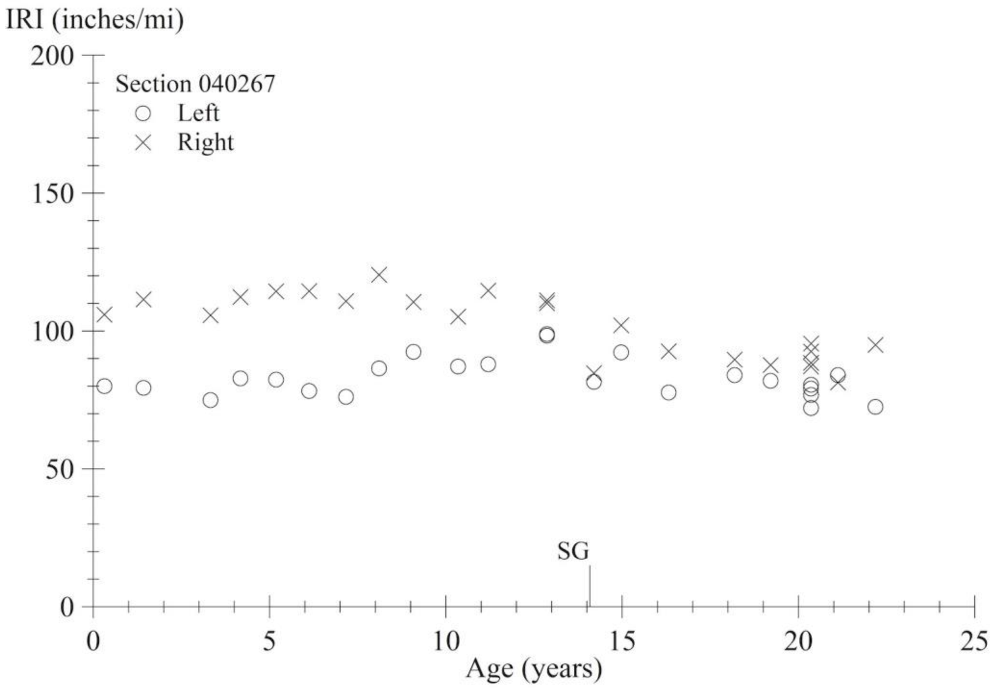

Source: FHWA.
SG = surface grinding.

Figure 101. Graph. IRI progression for section 040267.

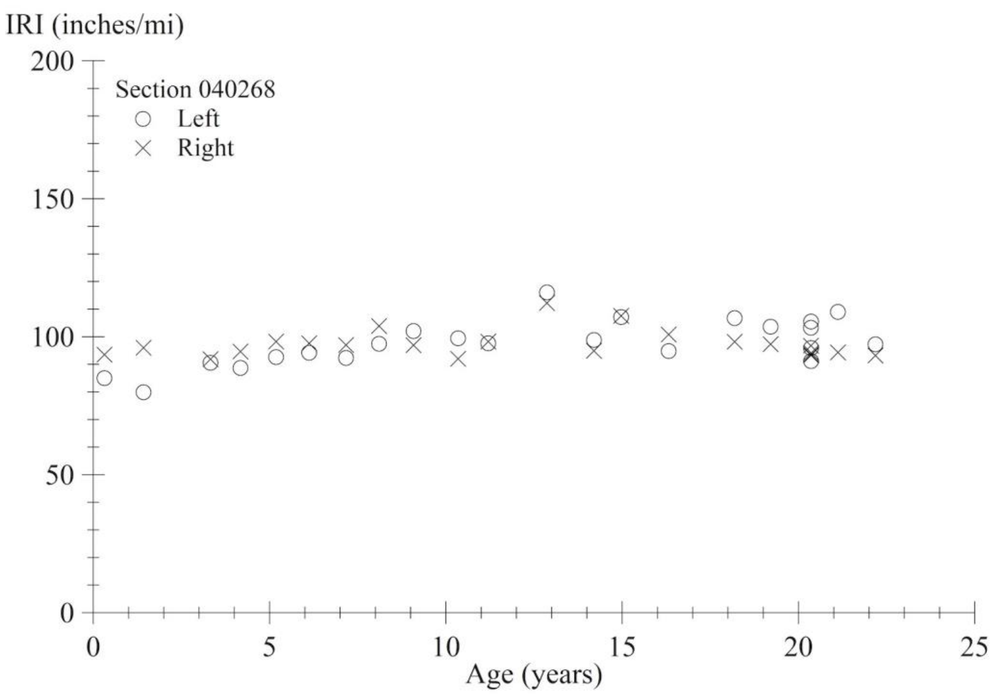

Source: FHWA.

Figure 102. Graph. IRI progression for section 040268.

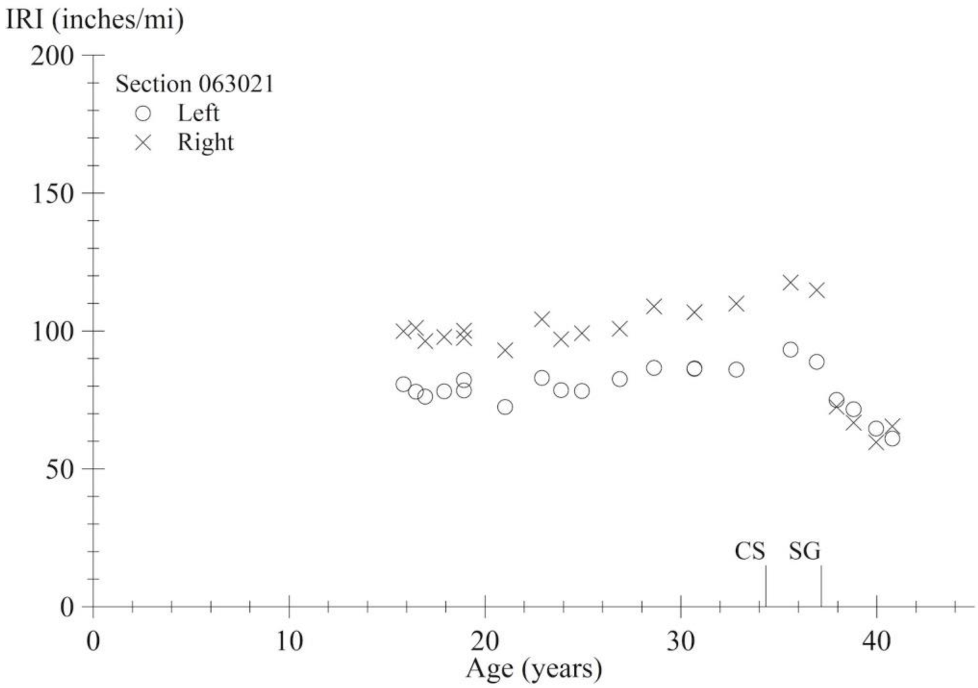

Source: FHWA.
CS = crack sealing; SG = surface grinding.

Figure 103. Graph. IRI progression for section 063021.

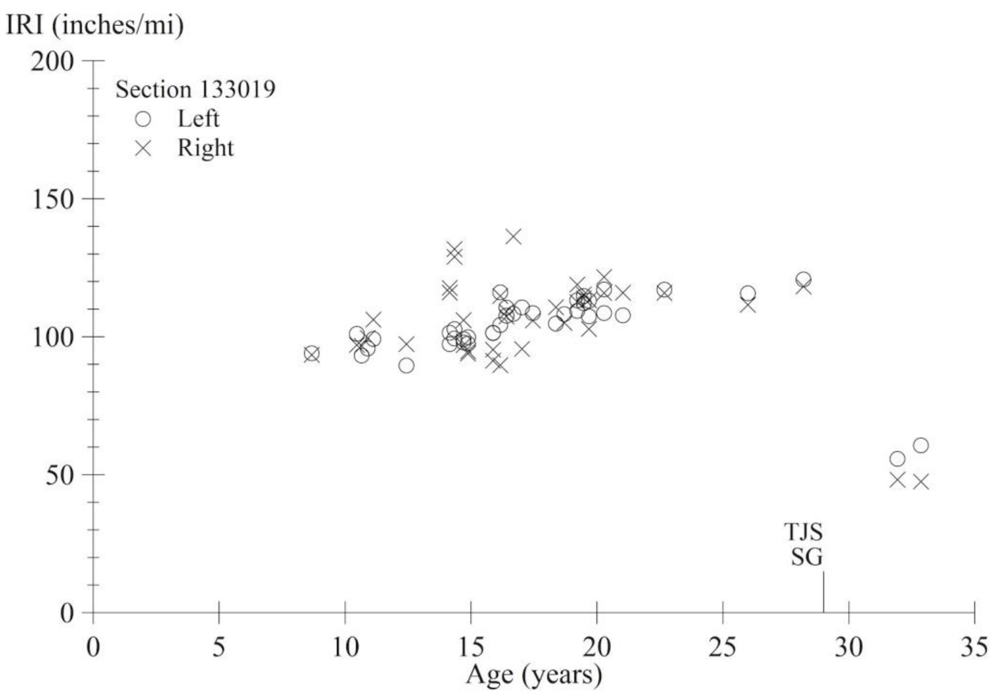

Source: FHWA.
TJS = transverse joint sealing; SG = surface grinding.

Figure 104. Graph. IRI progression for section 133019.

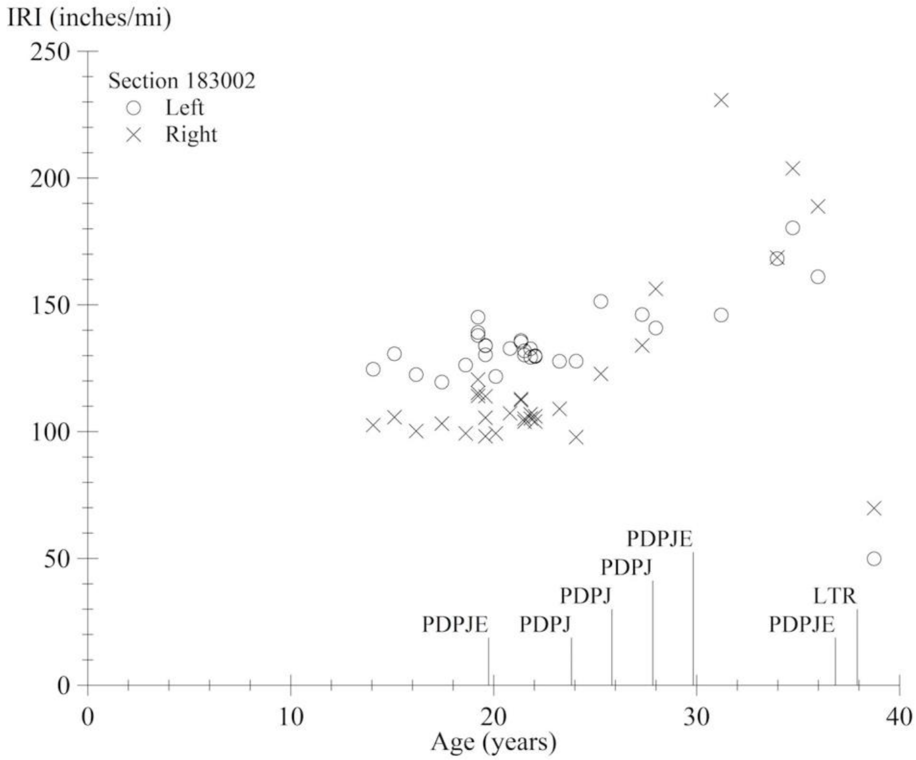

Source: FHWA.
PDPJE = partial-depth patching at joints and elsewhere; PDPJ = partial depth patching at joints; LTR = load-transfer restoration.

Figure 105. Graph. IRI progression for section 183002.

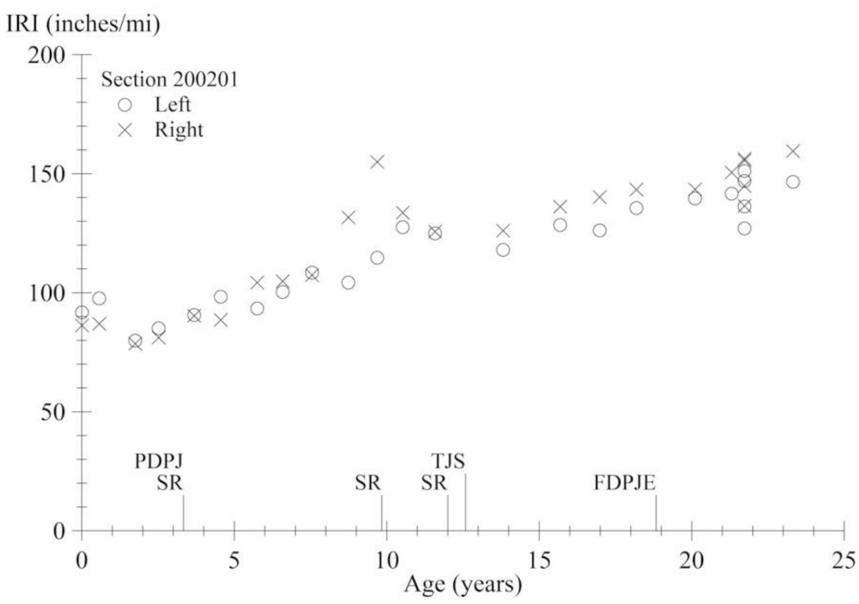

Source: FHWA.
PDPJ = partial-depth patching at joints; SR = slab replacement; TJS = transverse joint sealing; FDPJE = full-depth patching at joints and elsewhere.

Figure 106. Graph. IRI progression for section 200201.

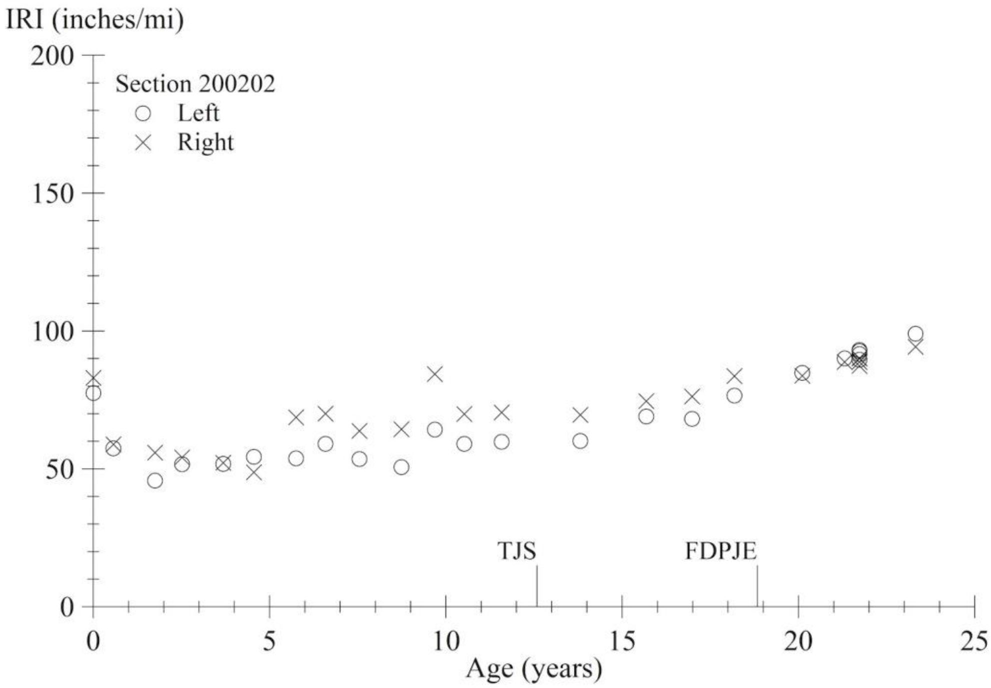

Source: FHWA.
TJS = transverse joint sealing; FDPJE = full-depth patching at joints and elsewhere.

Figure 107. Graph. IRI progression for section 200202.

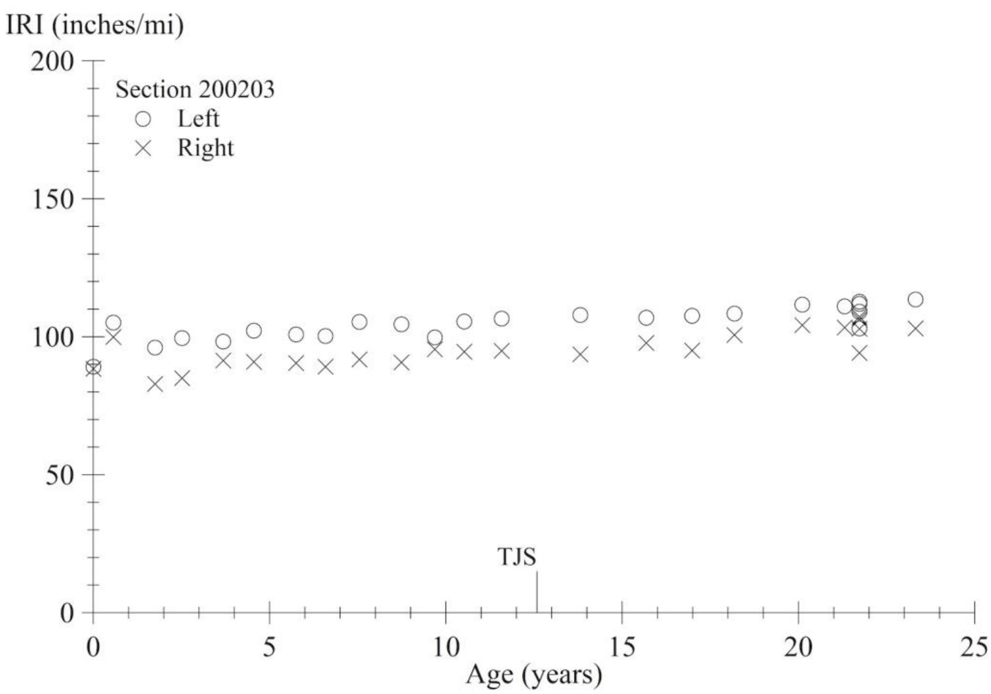

Source: FHWA.
TJS = transverse joint sealing.

Figure 108. Graph. IRI progression for section 200203.

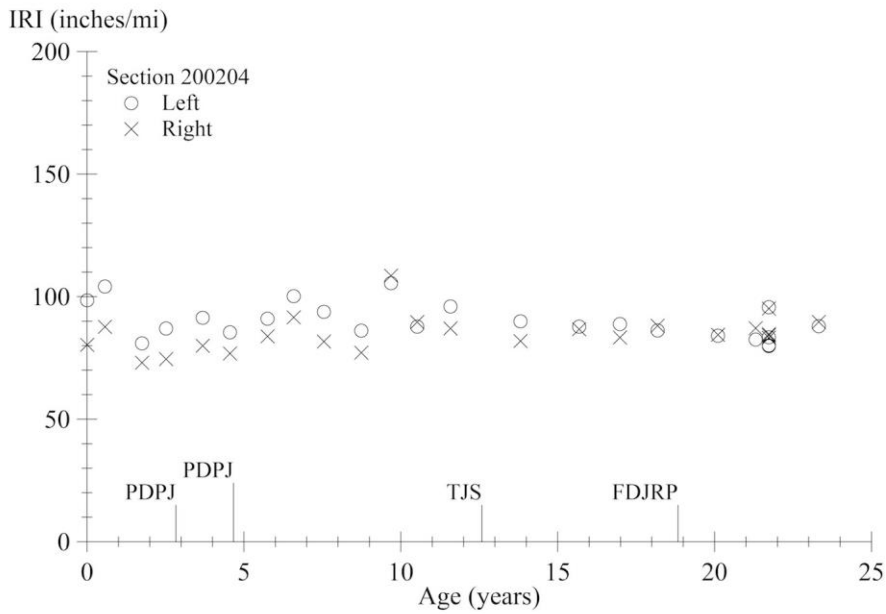

Source: FHWA.
PDPJ = partial-depth patching at joints; TJS = transverse joint sealing; FDJRP = full-depth transverse joint–repair patching.

Figure 109. Graph. IRI progression for section 200204.

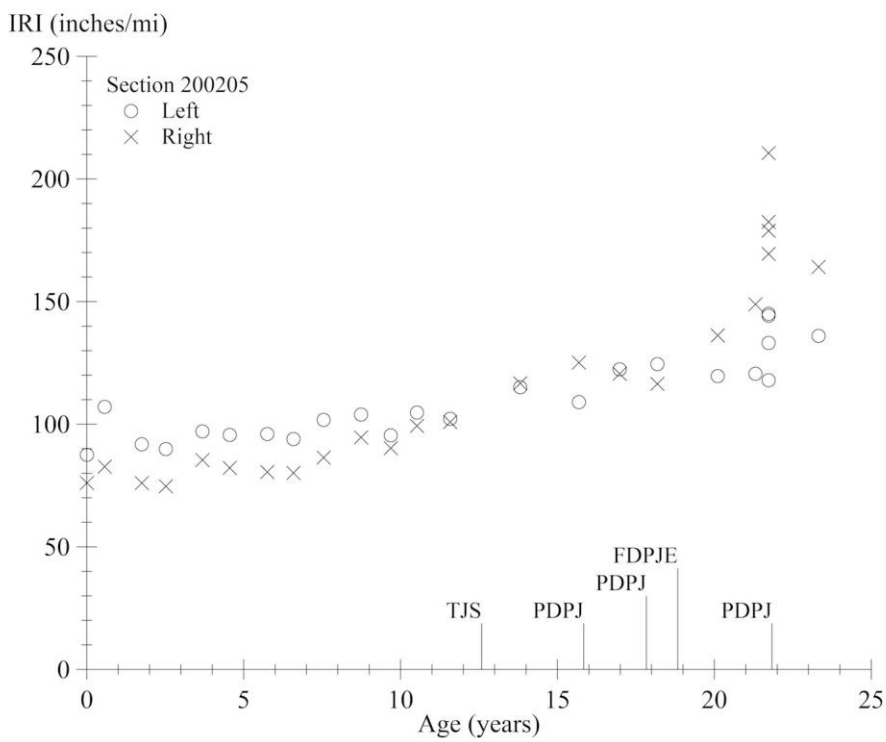

Source: FHWA.
TJS = transverse joint sealing; PDPJ = partial-depth patching at joints; FDPJE = full-depth patching at joints and elsewhere.

Figure 110. Graph. IRI progression for section 200205.

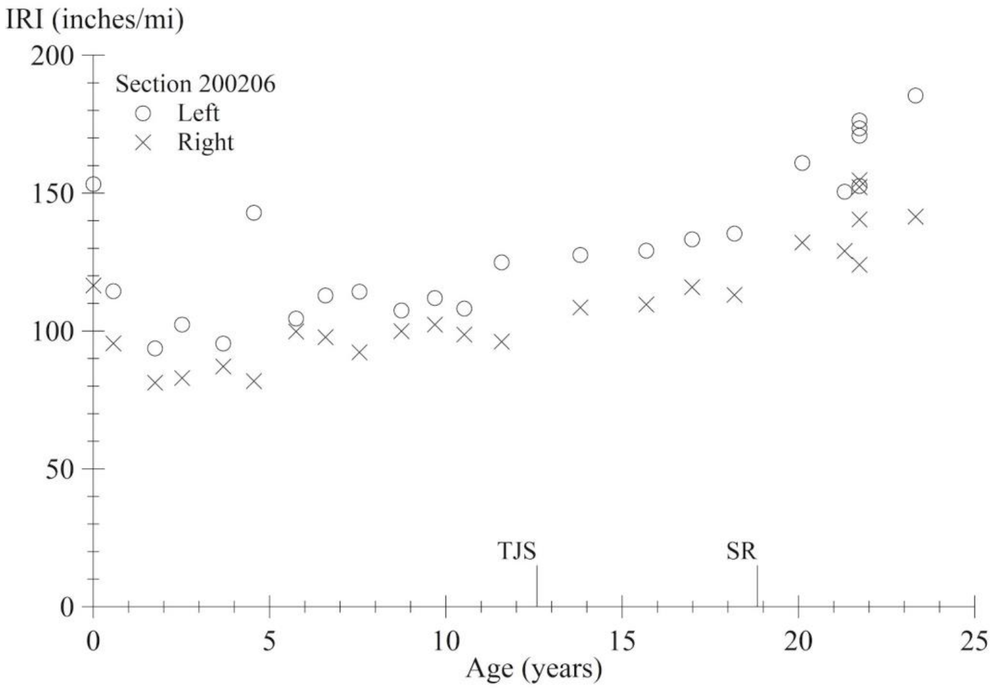

Source: FHWA.
TJS = transverse joint sealing; SR = slab replacement.

Figure 111. Graph. IRI progression for section 200206.

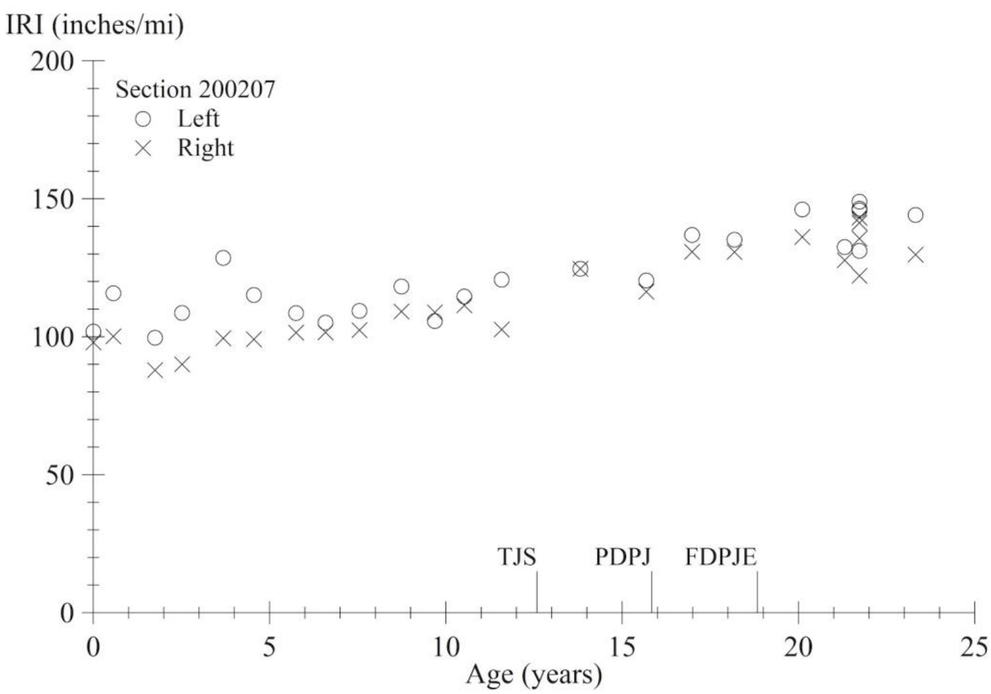

Source: FHWA.
TJS = transverse joint sealing; PDPJ = partial-depth patching at joints; FDPJE = full-depth patching at joints and elsewhere.

Figure 112. Graph. IRI progression for section 200207.

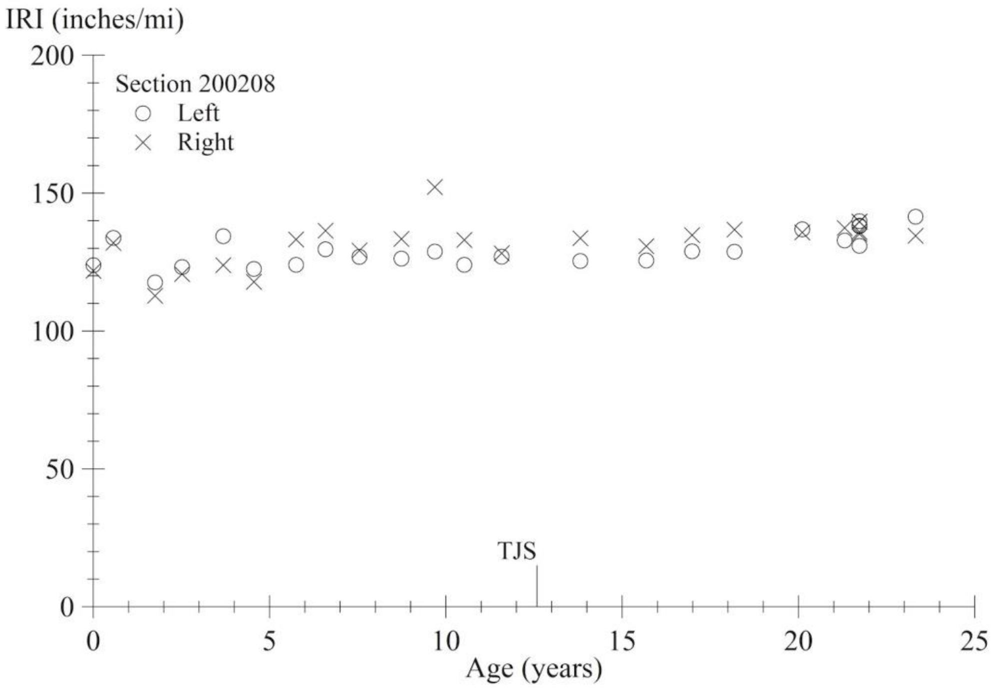

Source: FHWA.
TJS = transverse joint sealing.

Figure 113. Graph. IRI progression for section 200208.

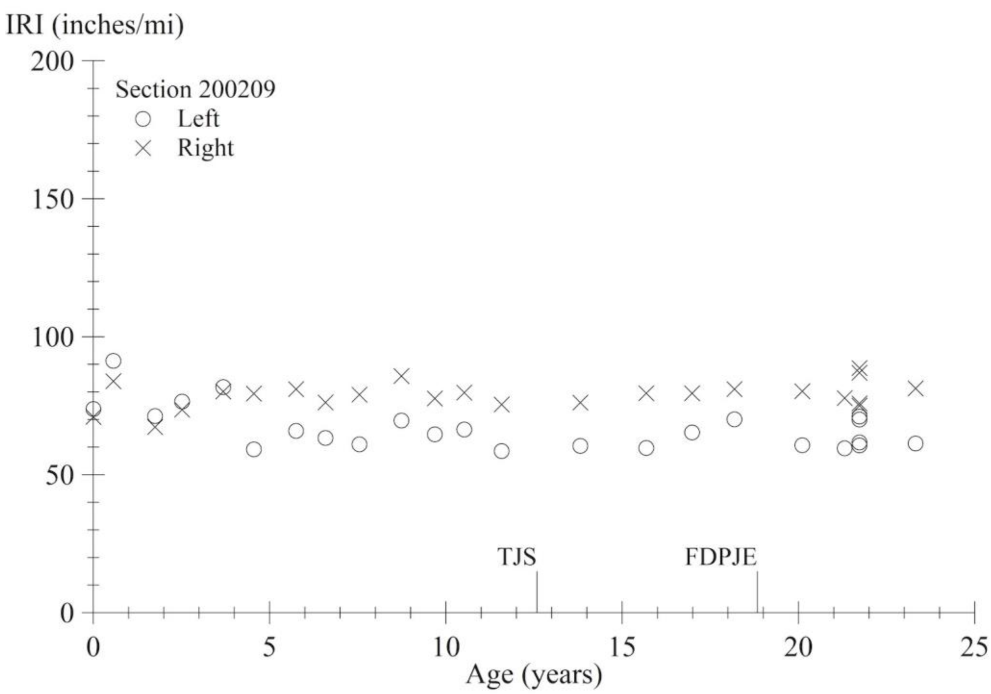

Source: FHWA.
TJS = transverse joint sealing; FDPJE = full-depth patching at joints and elsewhere.

Figure 114. Graph. IRI progression for section 200209.

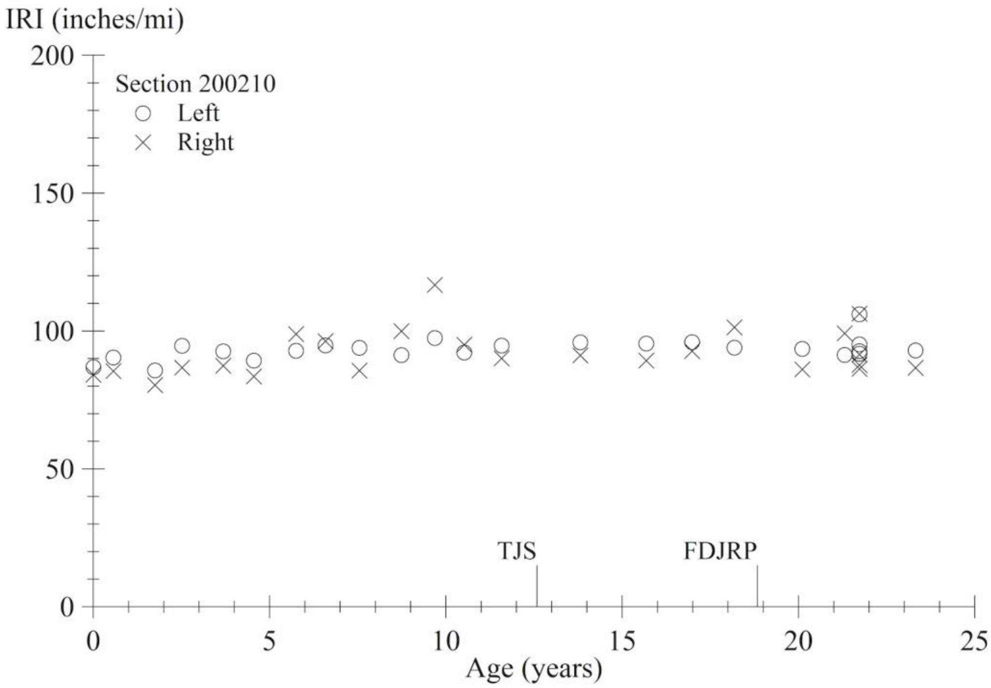

Source: FHWA.
TJS = transverse joint sealing; FDJRP = full-depth transverse-joint-repair patching.

Figure 115. Graph. IRI progression for section 200210.

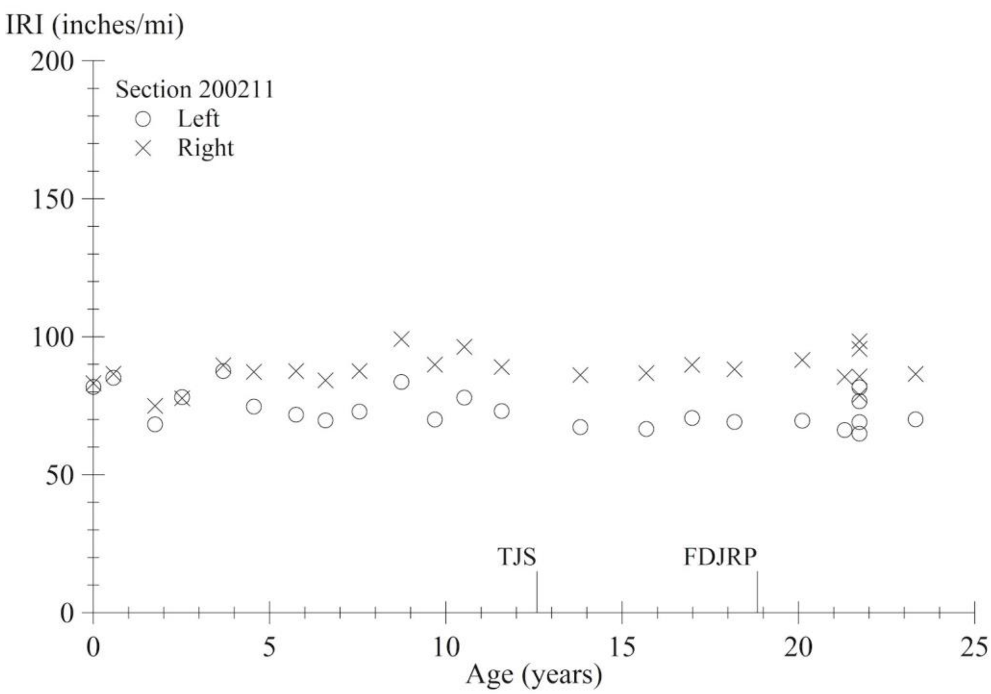

Source: FHWA.
TJS = transverse joint sealing; FDJRP = full-depth transverse-joint-repair patching.

Figure 116. Graph. IRI progression for section 200211.

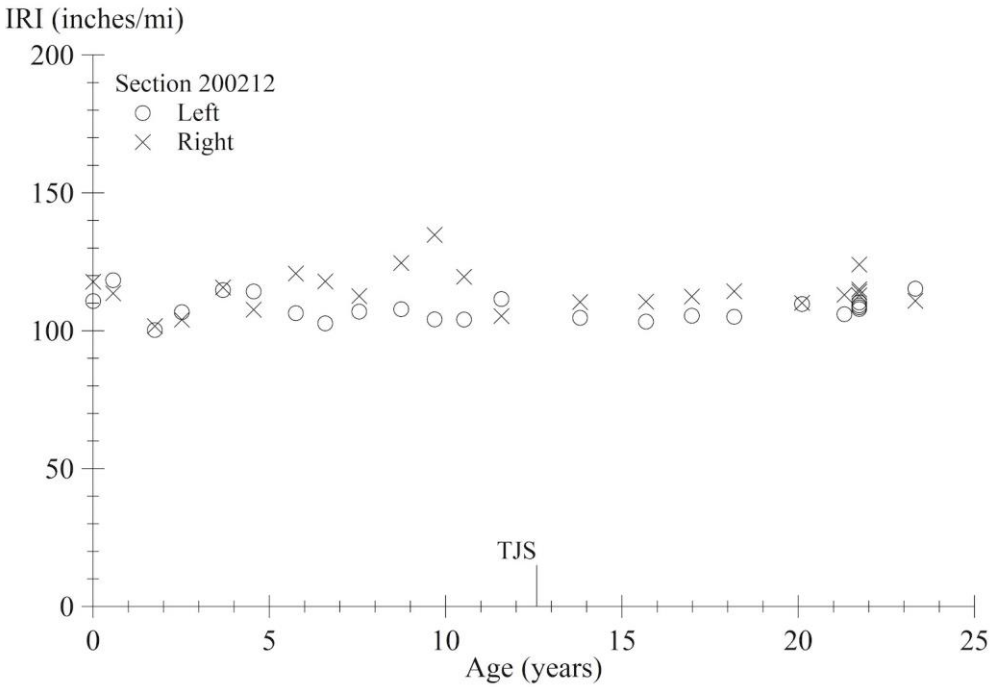

Source: FHWA.
TJS = transverse joint sealing.

Figure 117. Graph. IRI progression for section 200212.

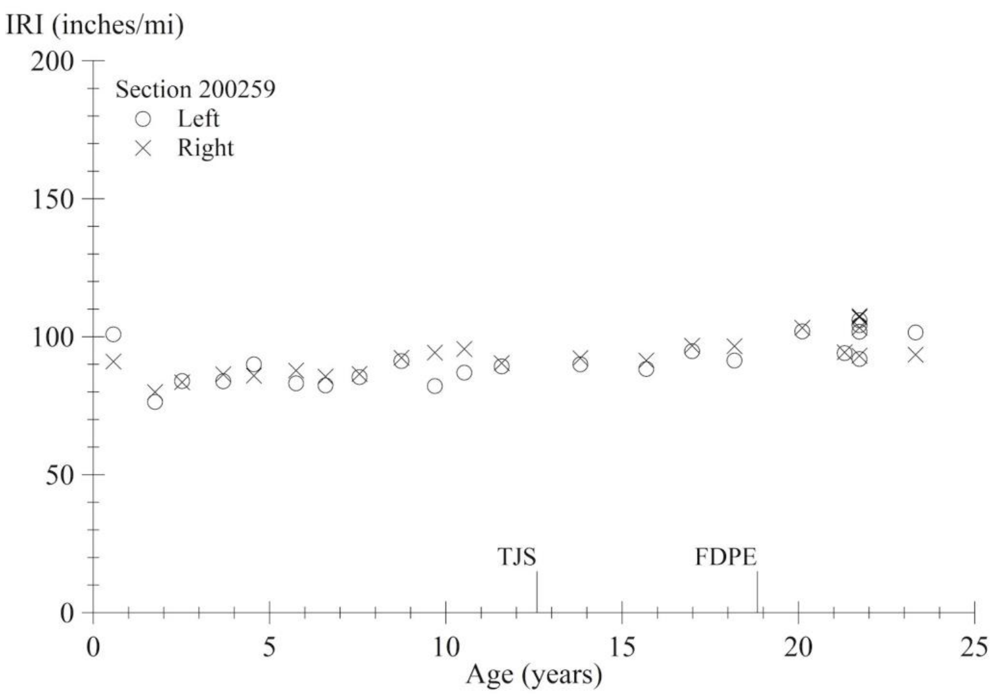

Source: FHWA.
TJS = transverse joint sealing; FDPE = full-depth patching away from joints.

Figure 118. Graph. IRI progression for section 200259.

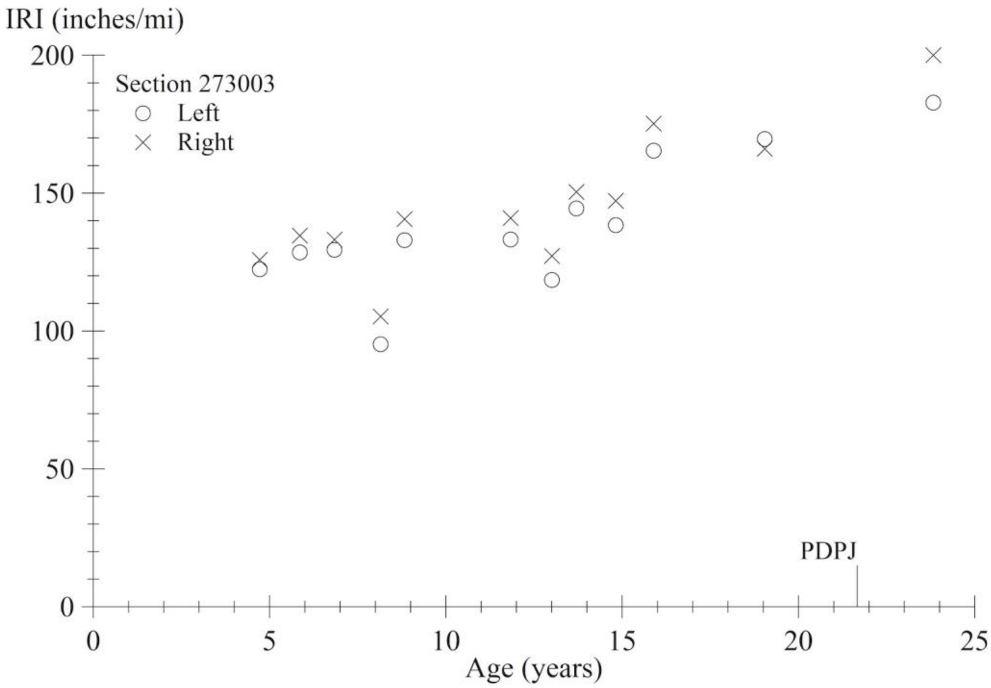

Source: FHWA.
PDPJ = partial-depth patching at joints.

Figure 119. Graph. IRI progression for section 273003.

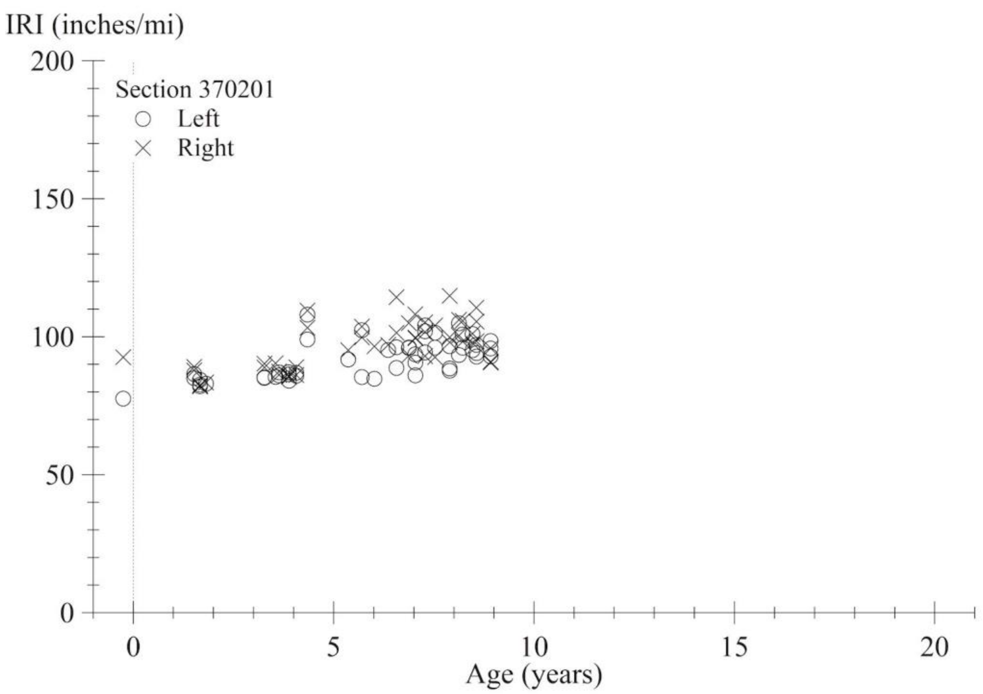

Source: FHWA.

Figure 120. Graph. IRI progression for section 370201.

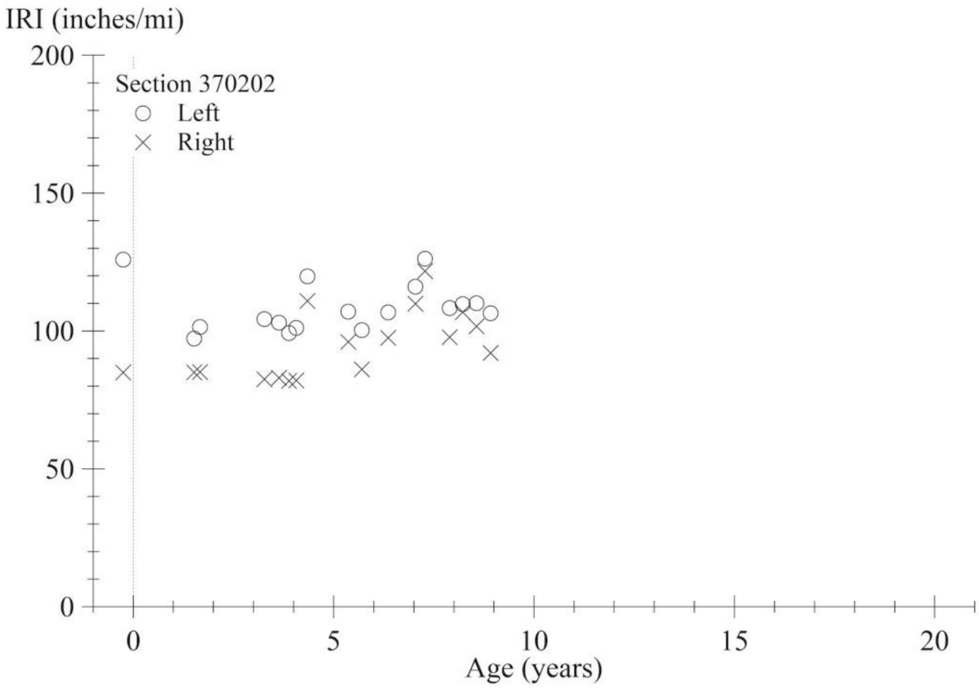

Source: FHWA.

Figure 121. Graph. IRI progression for section 370202.

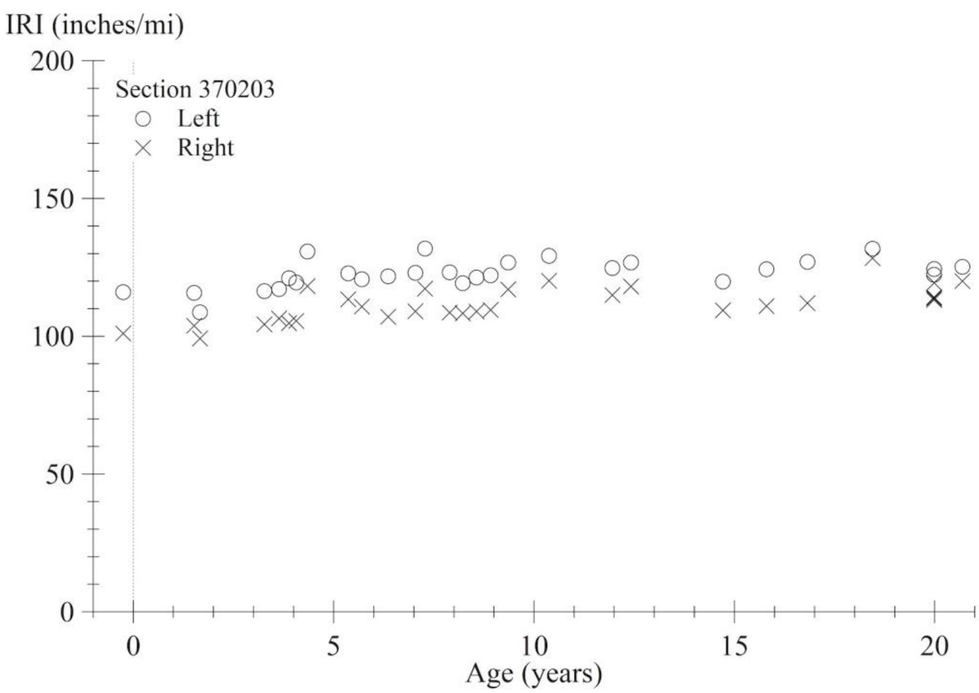

Source: FHWA.

Figure 122. Graph. IRI progression for section 370203.

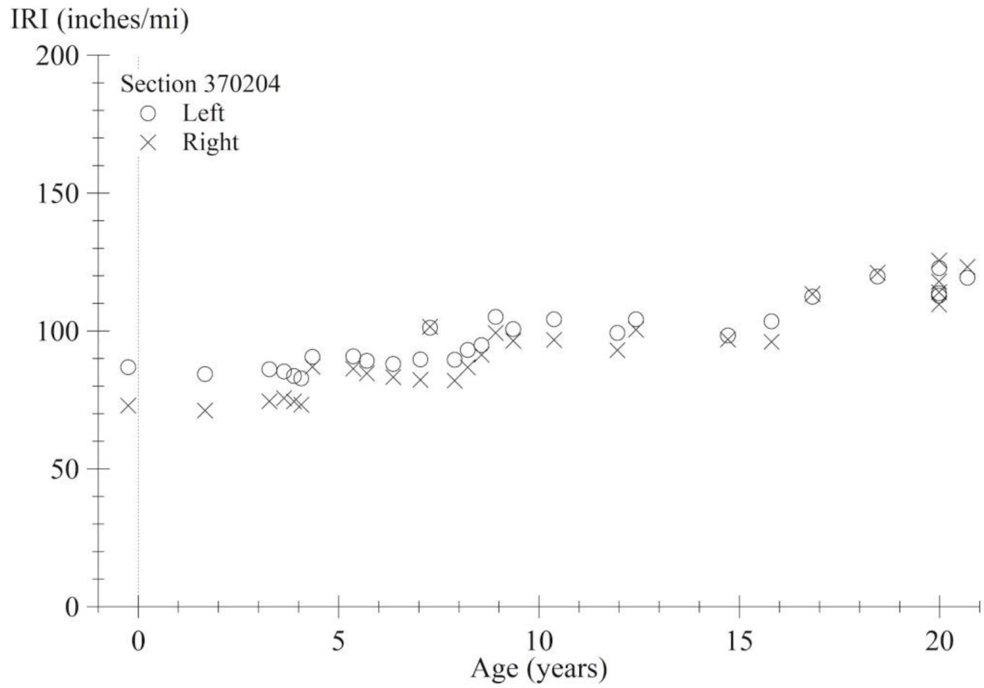

Source: FHWA.

Figure 123. Graph. IRI progression for section 370204.

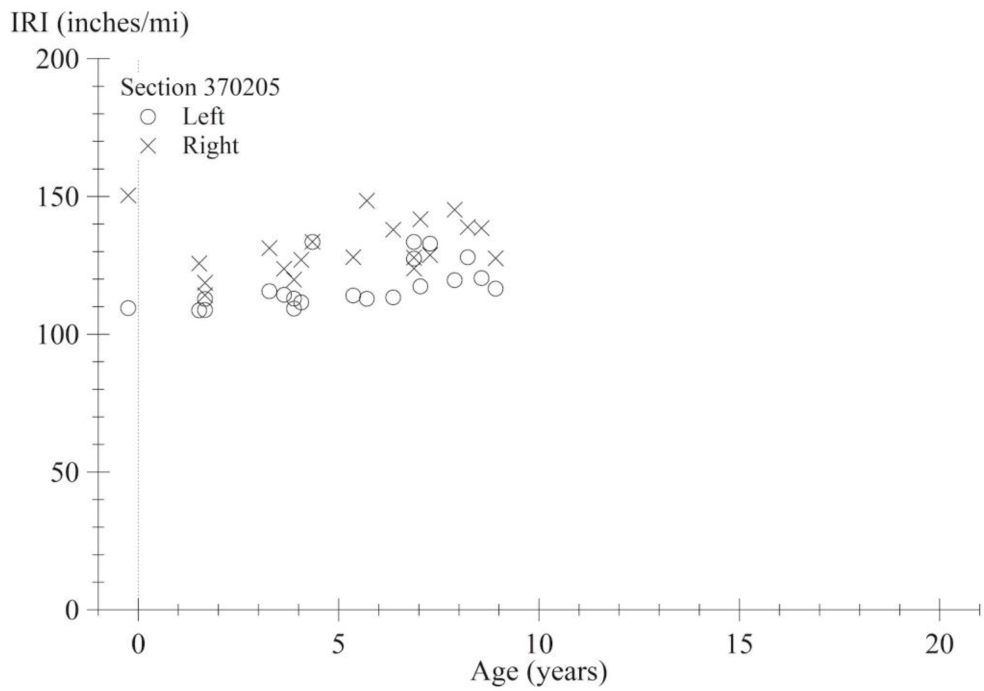

Source: FHWA.

Figure 124. Graph. IRI progression for section 370205.

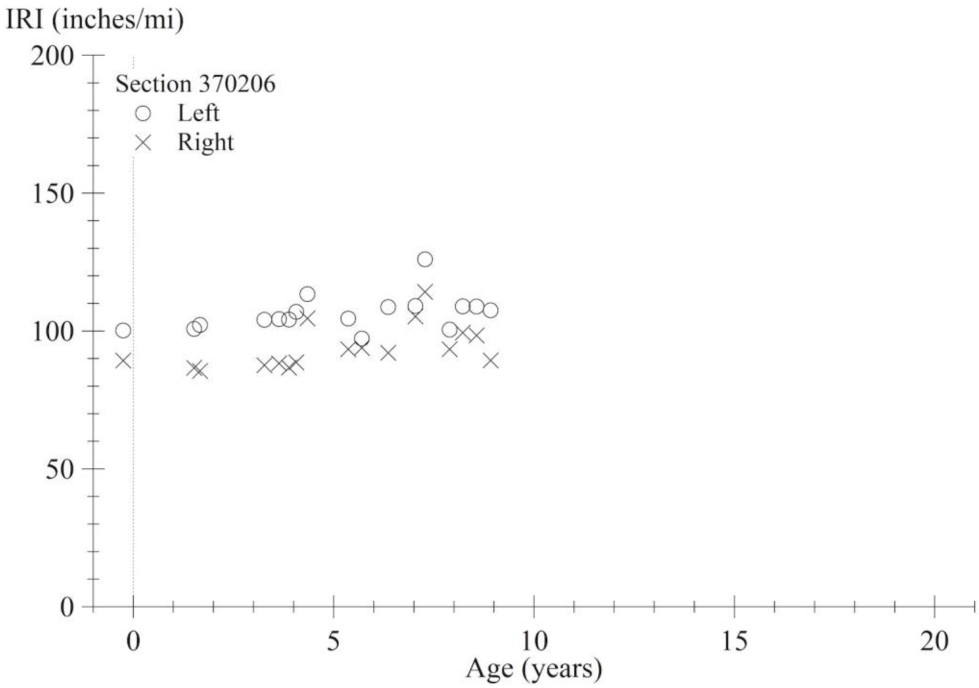

Source: FHWA.

Figure 125. Graph. IRI progression for section 370206.

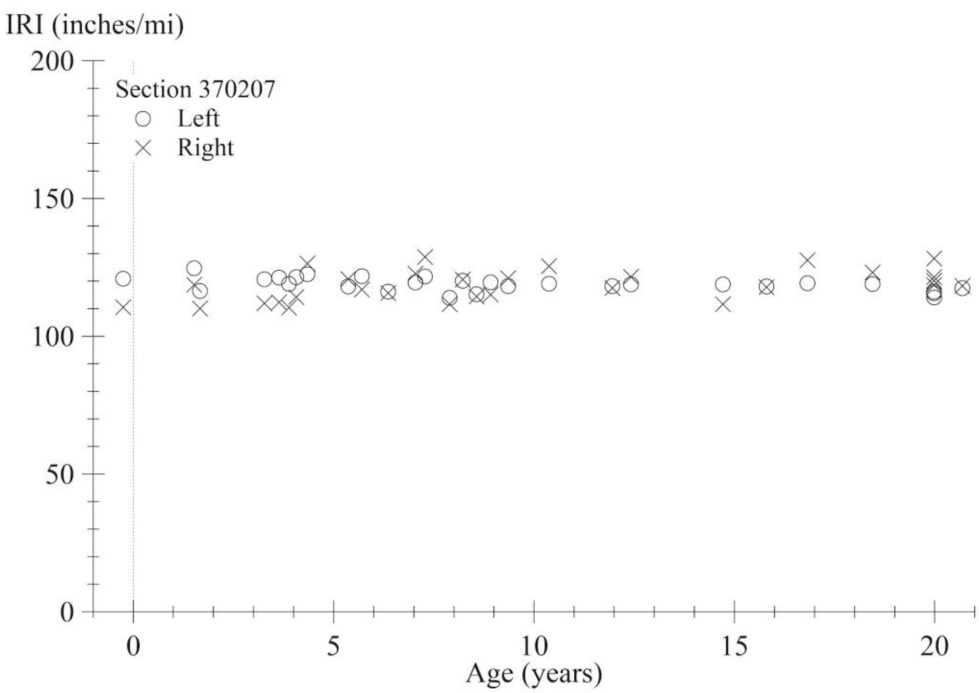

Source: FHWA.

Figure 126. Graph. IRI progression for section 370207.

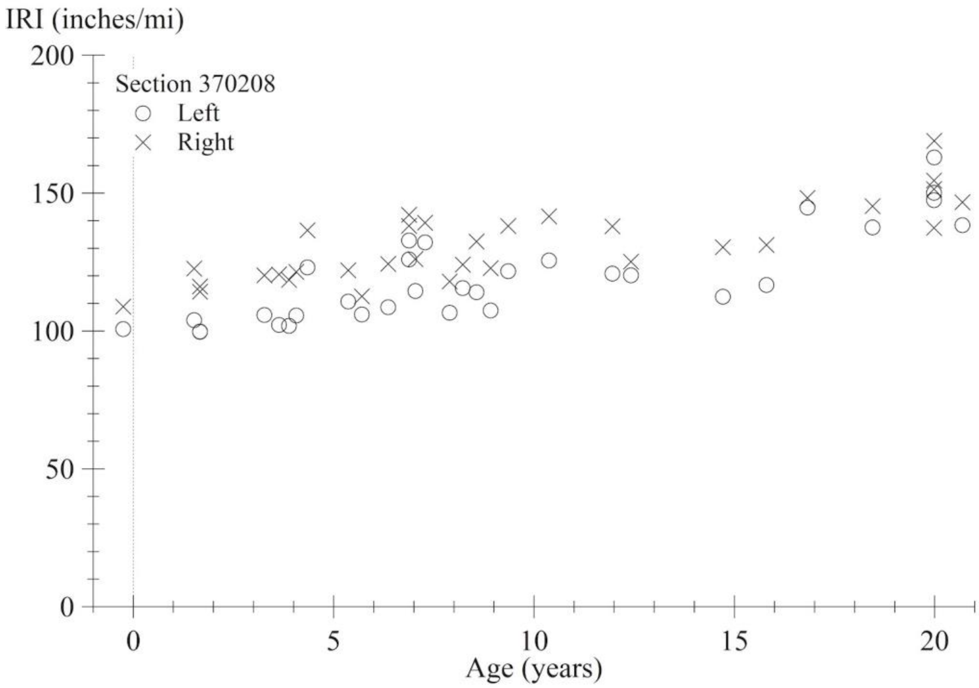

Source: FHWA.

Figure 127. Graph. IRI progression for section 370208.

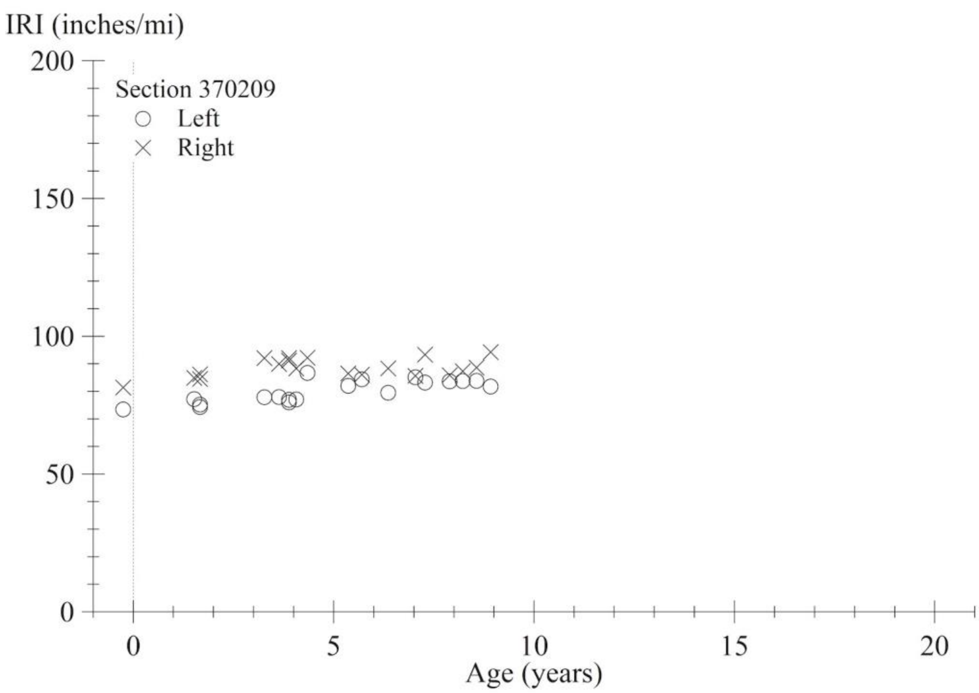

Source: FHWA.

Figure 128. Graph. IRI progression for section 370209.

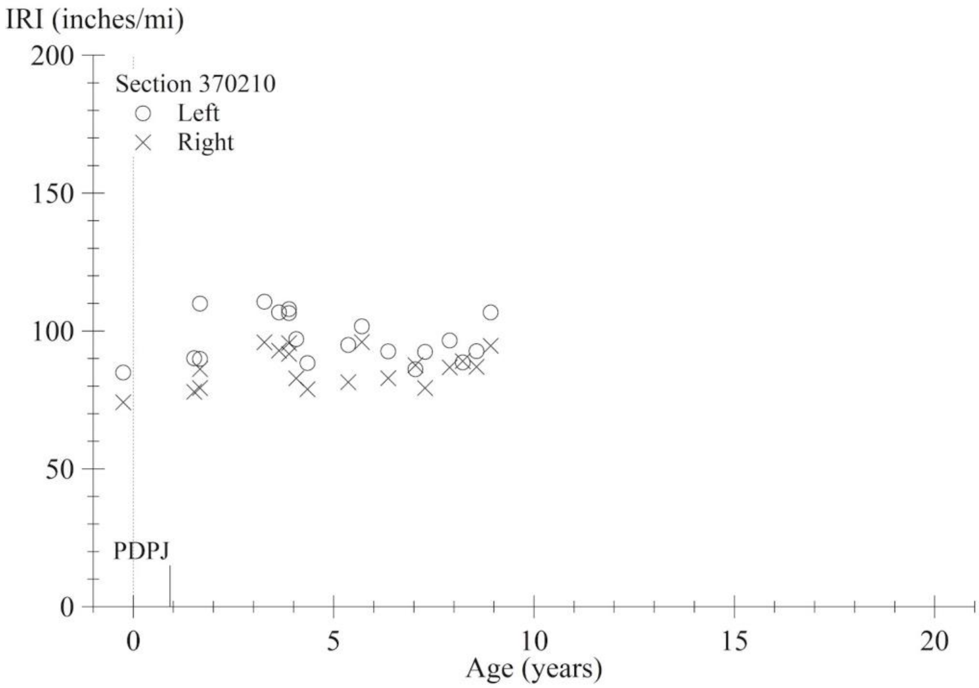

Source: FHWA.
PDPJ = partial-depth patching at joints.

Figure 129. Graph. IRI progression for section 370210.

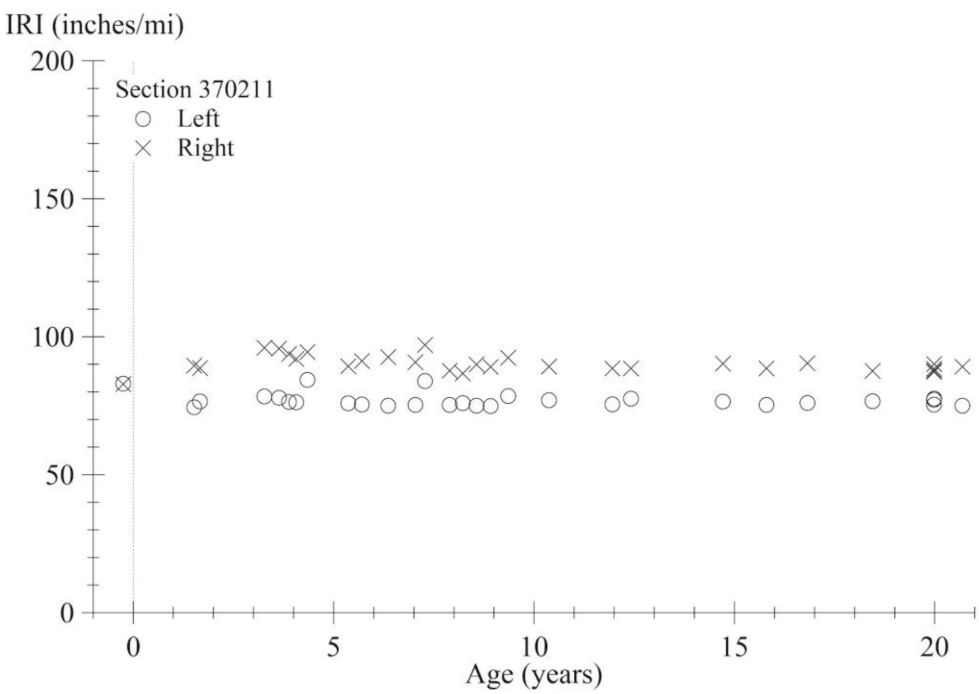

Source: FHWA.

Figure 130. Graph. IRI progression for section 370211.

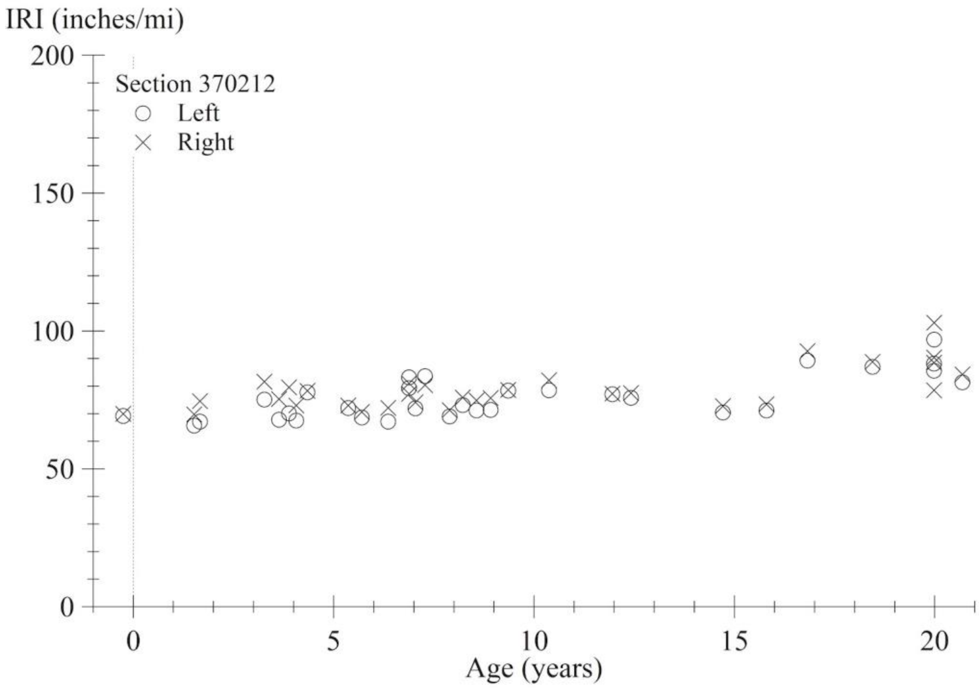

Source: FHWA.

Figure 131. Graph. IRI progression for section 370212.

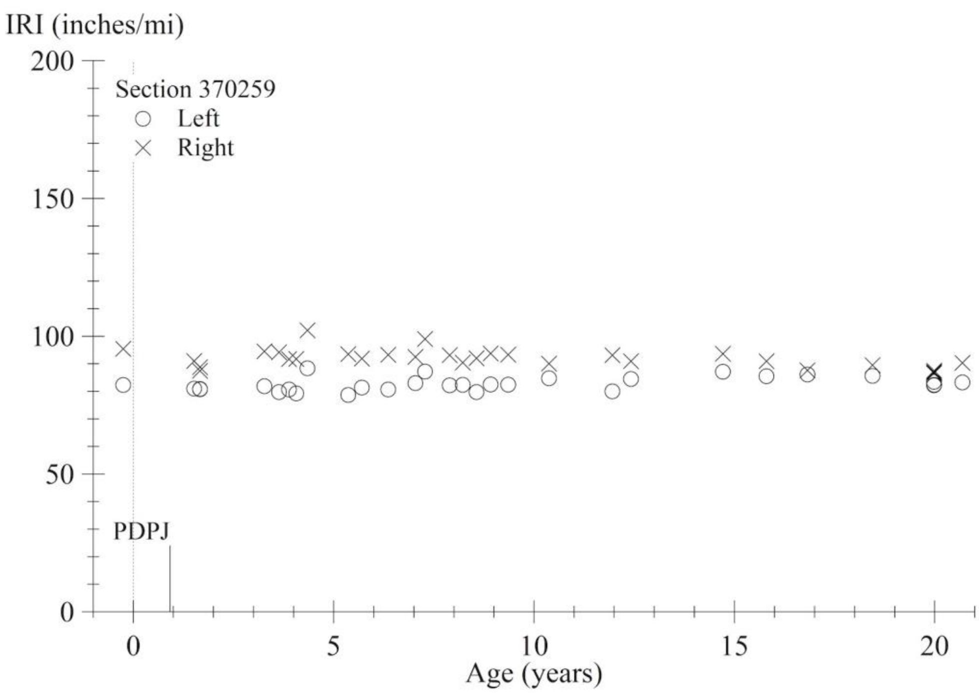

Source: FHWA.
PDPJ = partial-depth patching at joints.

Figure 132. Graph. IRI progression for section 370259.

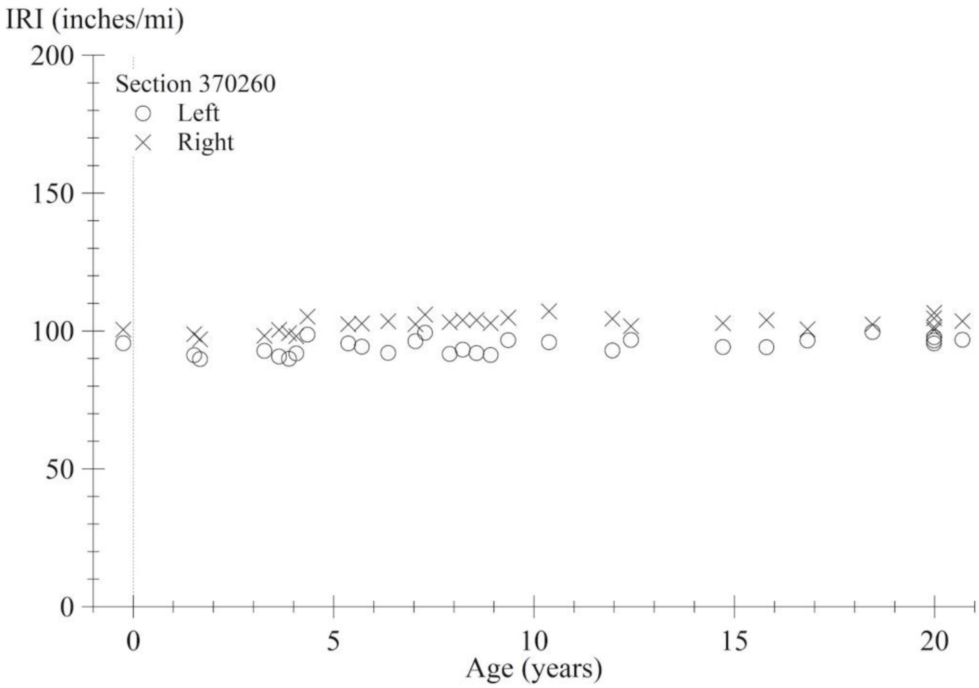

Source: FHWA.

Figure 133. Graph. IRI progression for section 370260.

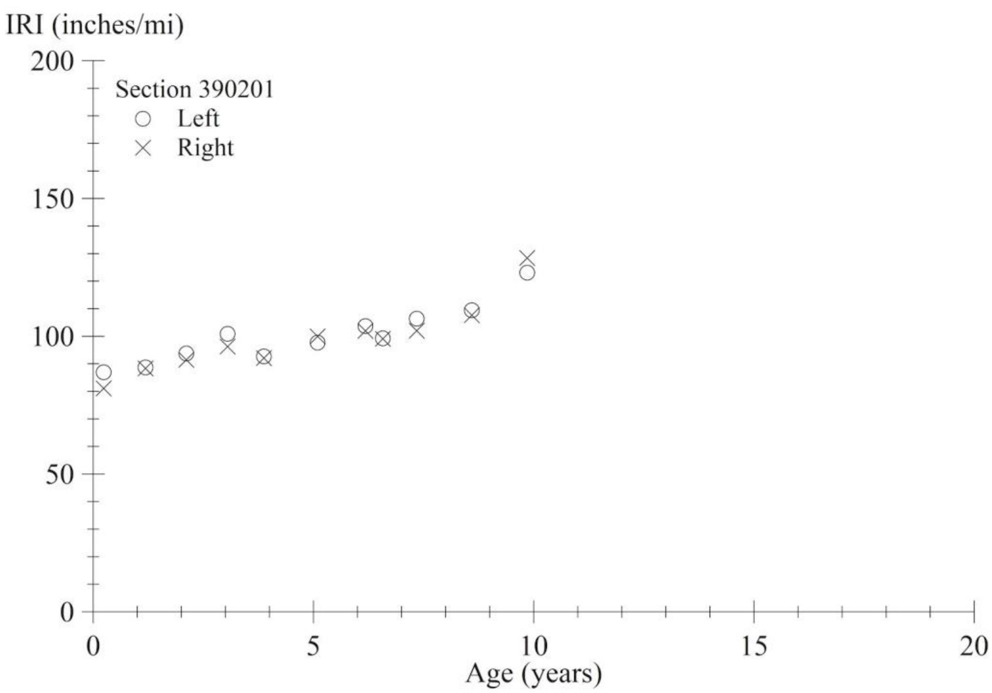

Source: FHWA.

Figure 134. Graph. IRI progression for section 390201.

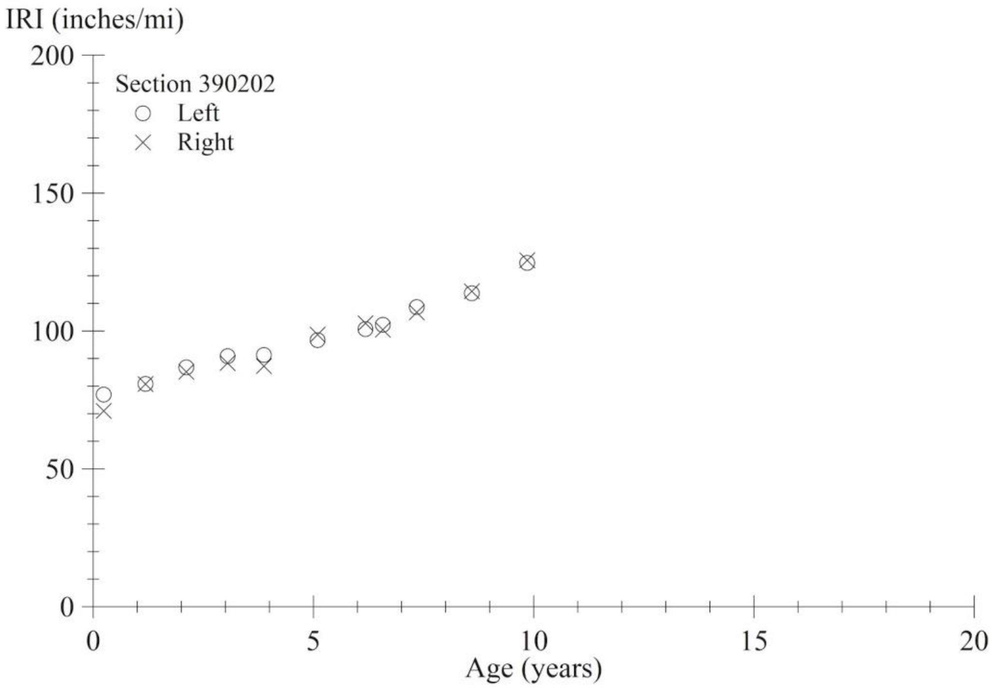

Source: FHWA.

Figure 135. Graph. IRI progression for section 390202.

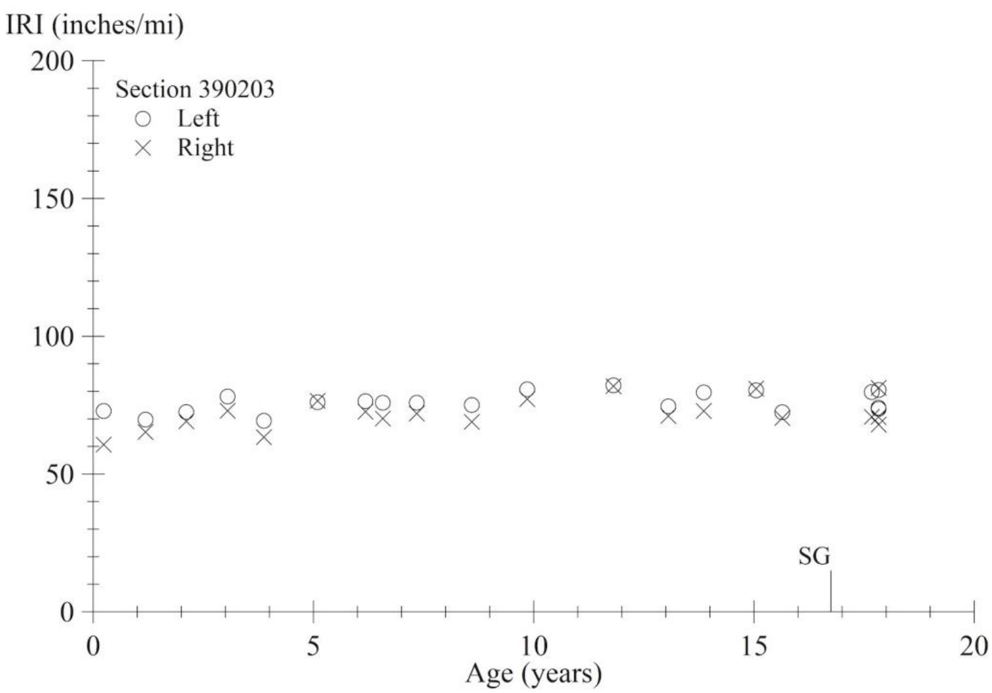

Source: FHWA.
SG = surface grinding.

Figure 136. Graph. IRI progression for section 390203.

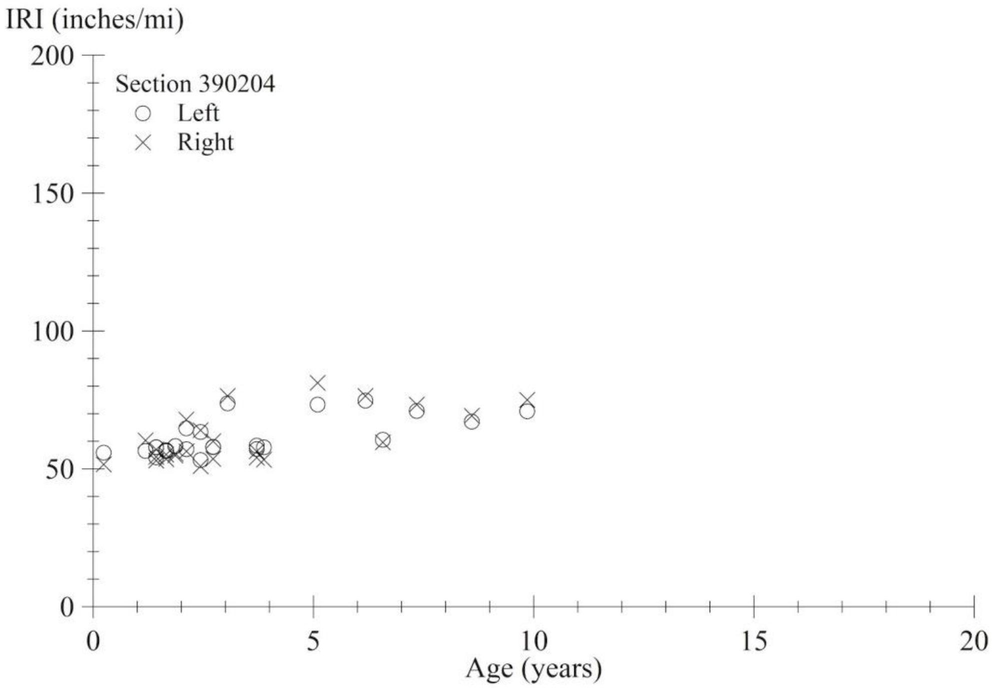

Source: FHWA.

Figure 137. Graph. IRI progression for section 390204.

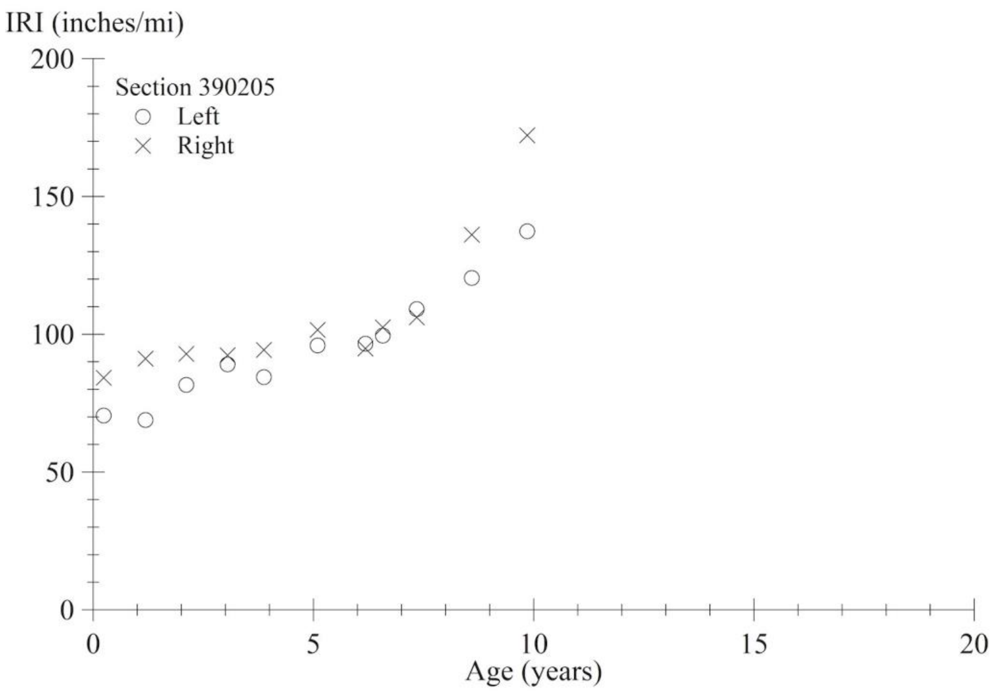

Source: FHWA.

Figure 138. Graph. IRI progression for section 390205.

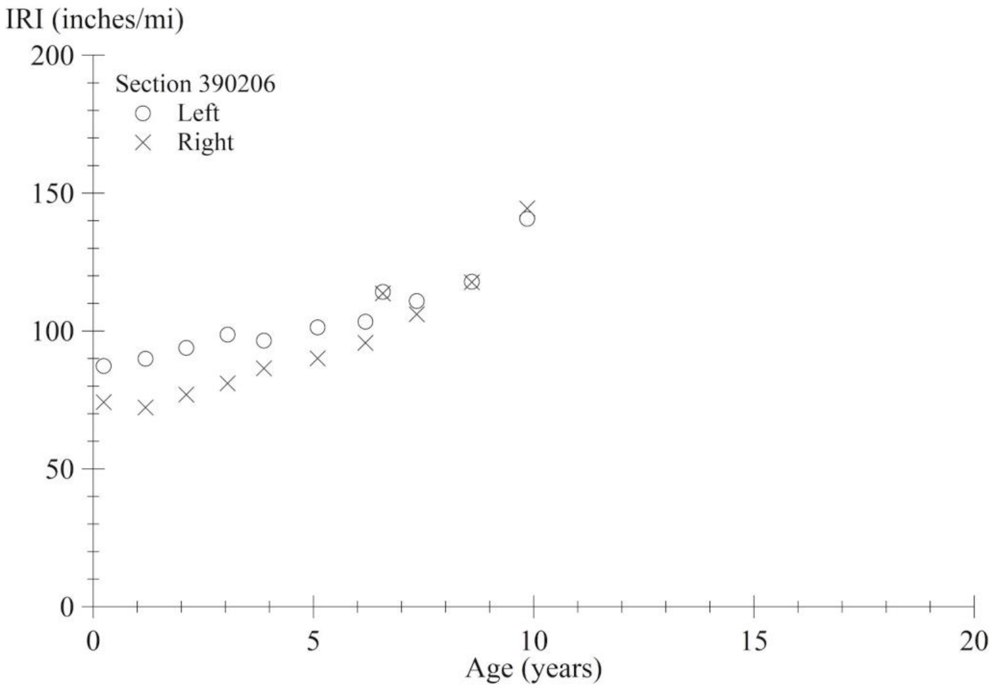

Source: FHWA.

Figure 139. Graph. IRI progression for section 390206.

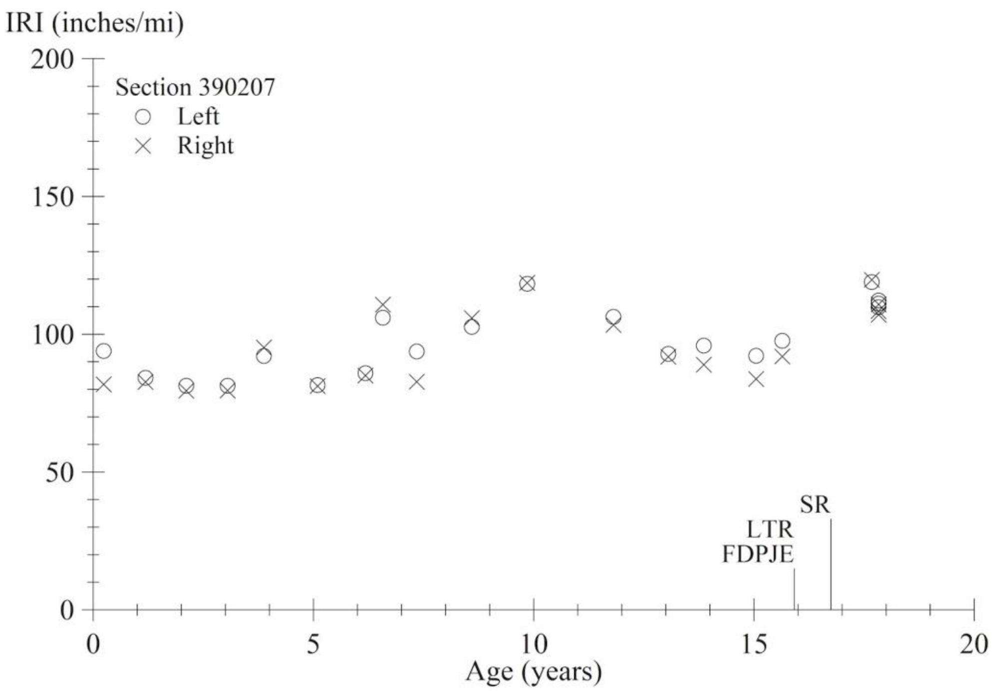

Source: FHWA.
FDPJE = full-depth patching at joints and elsewhere; LTR = load-transfer restoration; SR = slab replacement.

Figure 140. Graph. IRI progression for section 390207.

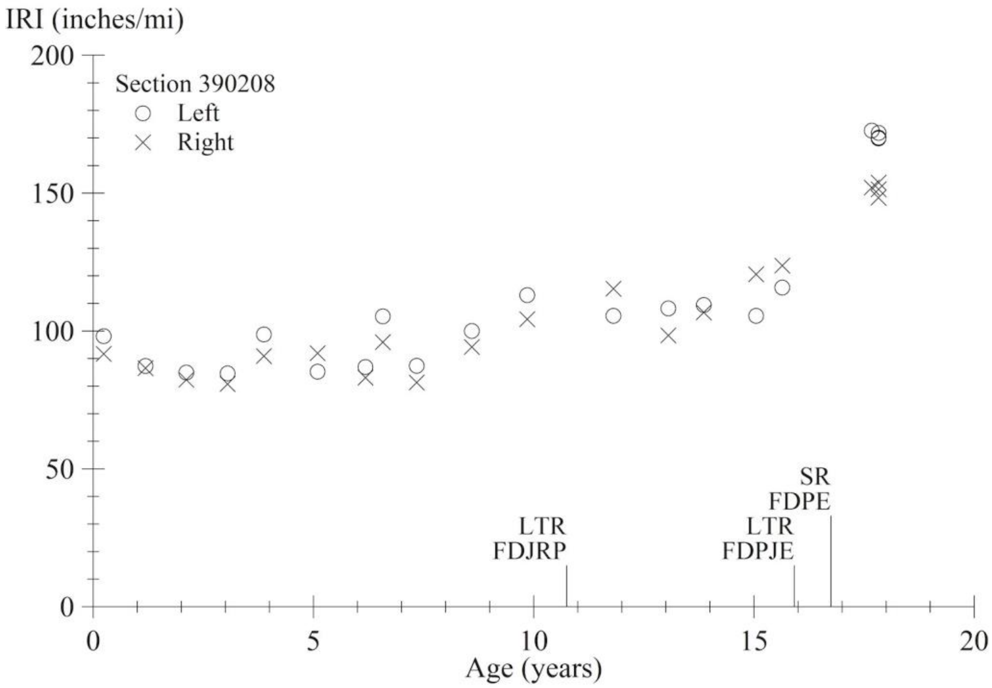

Source: FHWA.
FDJRP = full-depth transverse-joint-repair patching; LTR = load-transfer restoration; FDPJE = full-depth patching at joints and elsewhere; FDPE = full-depth patching away from joints; SR = slab replacement.

Figure 141. Graph. IRI progression for section 390208.

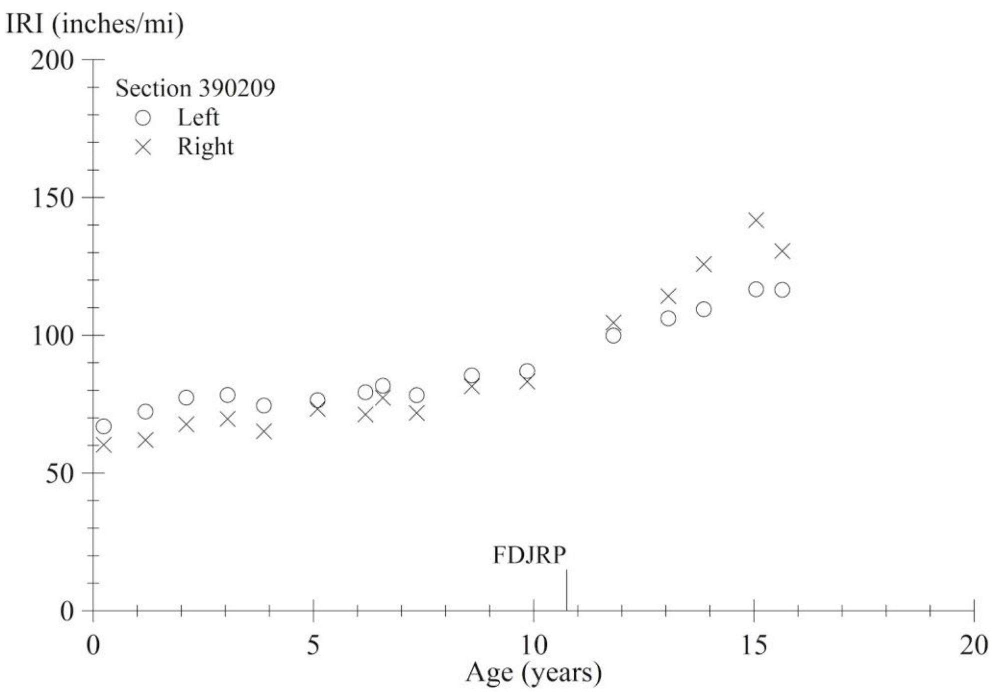

Source: FHWA.
FDJRP = full-depth transverse-joint-repair patching.

Figure 142. Graph. IRI progression for section 390209.

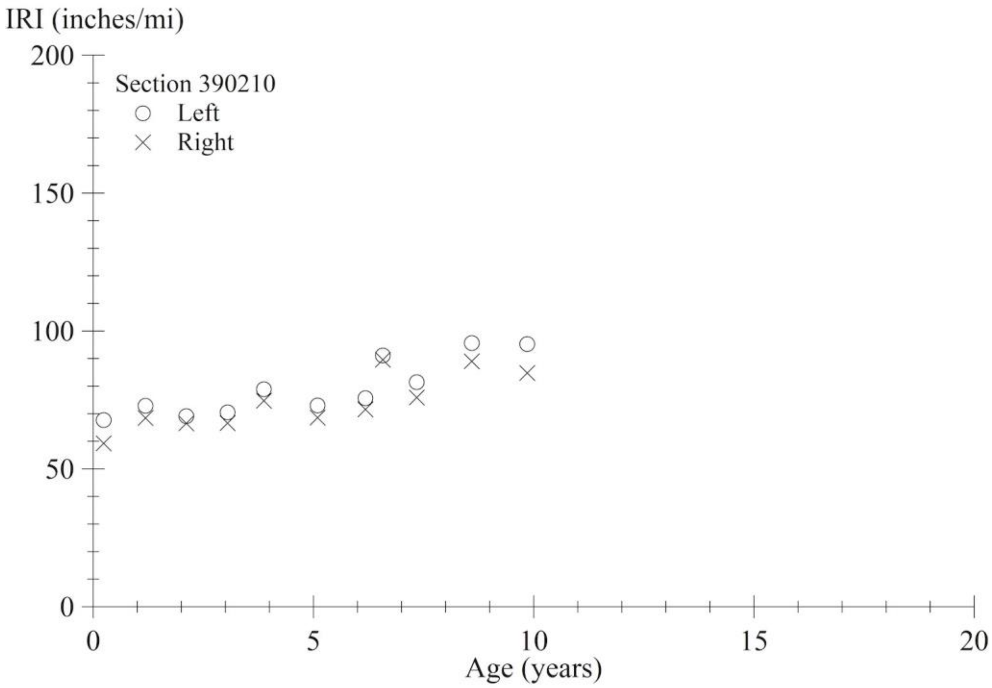

Source: FHWA.

Figure 143. Graph. IRI progression for section 390210.

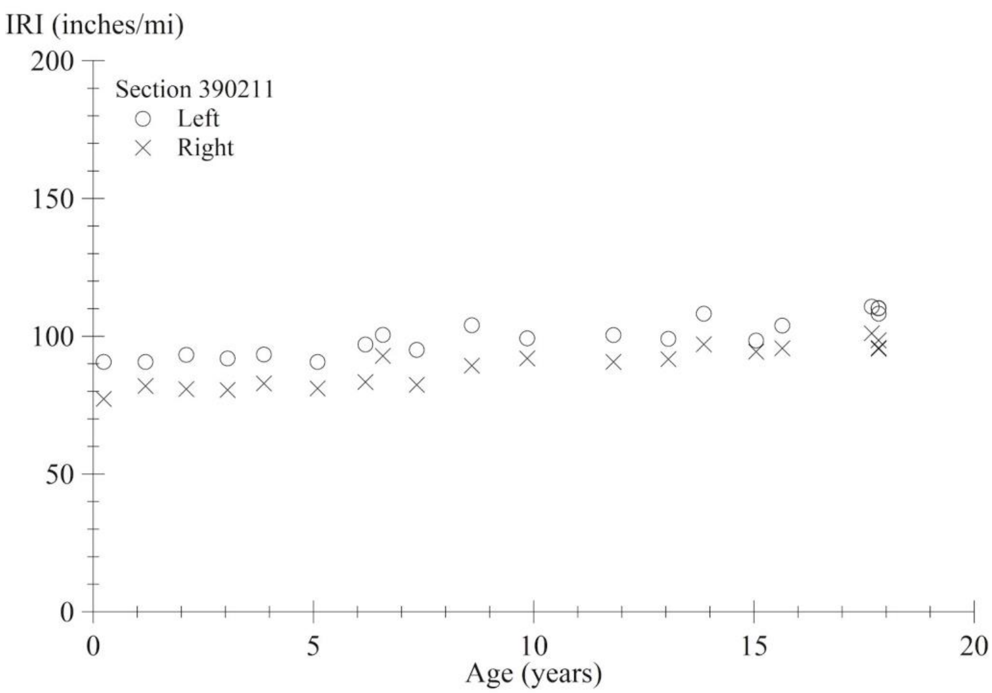

Source: FHWA.

Figure 144. Graph. IRI progression for section 390211.

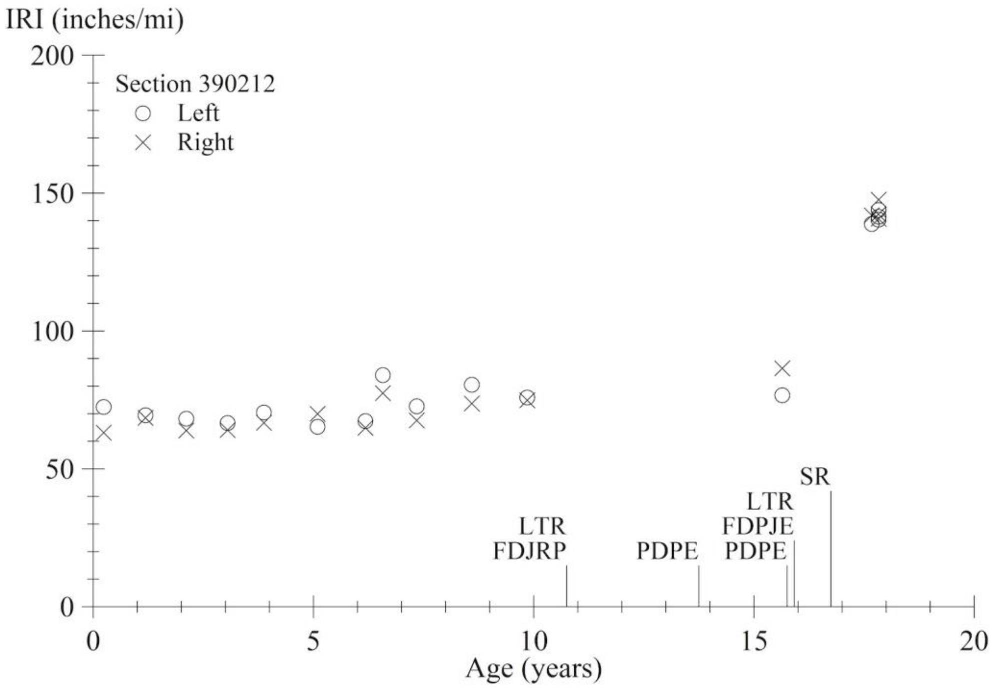

Source: FHWA.
FDJRP = full-depth transverse-joint-repair patching; LTR = load-transfer restoration; PDPE = partial-depth patching away from joints; FDPJE = full-depth patching at joints and elsewhere; SR = slab replacement.

Figure 145. Graph. IRI progression for section 390212.

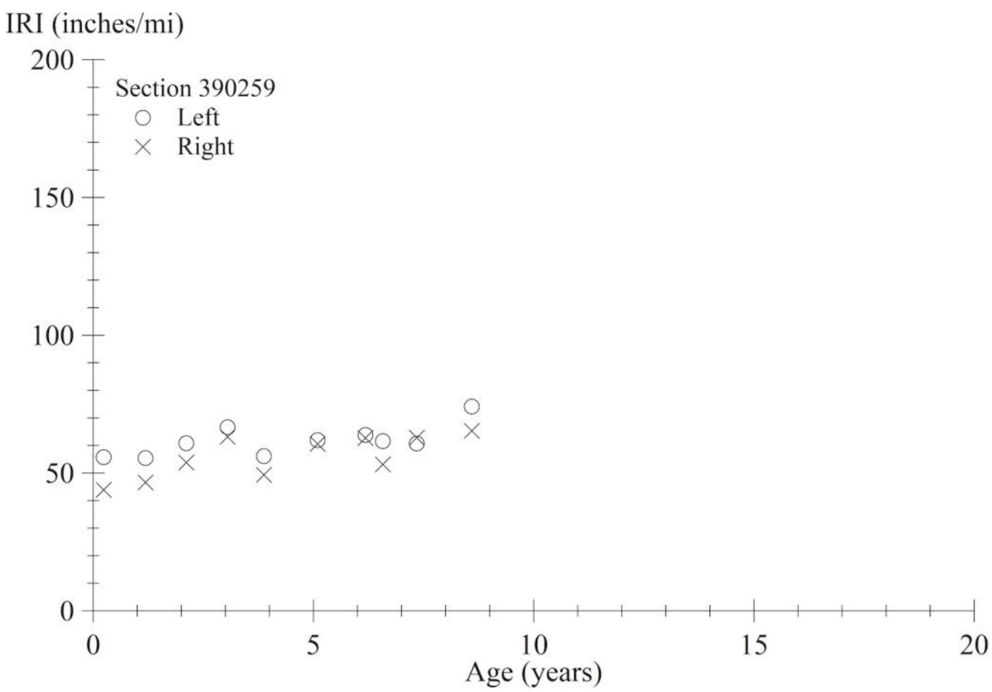

Source: FHWA.

Figure 146. Graph. IRI progression for section 390259.

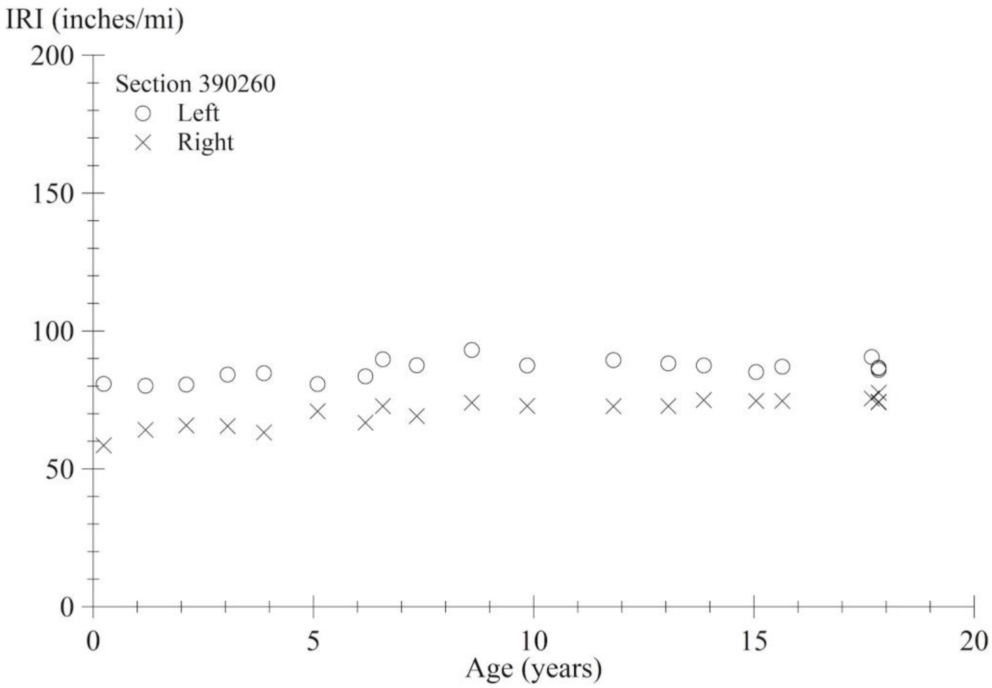

Source: FHWA.

Figure 147. Graph. IRI progression for section 390260.

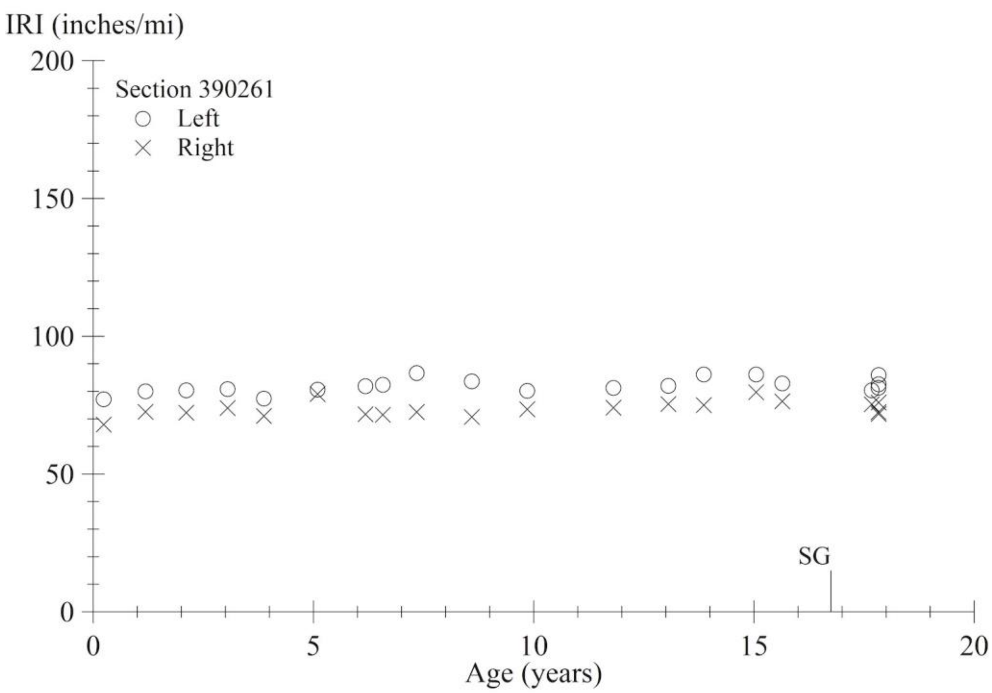

Source: FHWA.
SG = surface grinding.

Figure 148. Graph. IRI progression for section 390261.

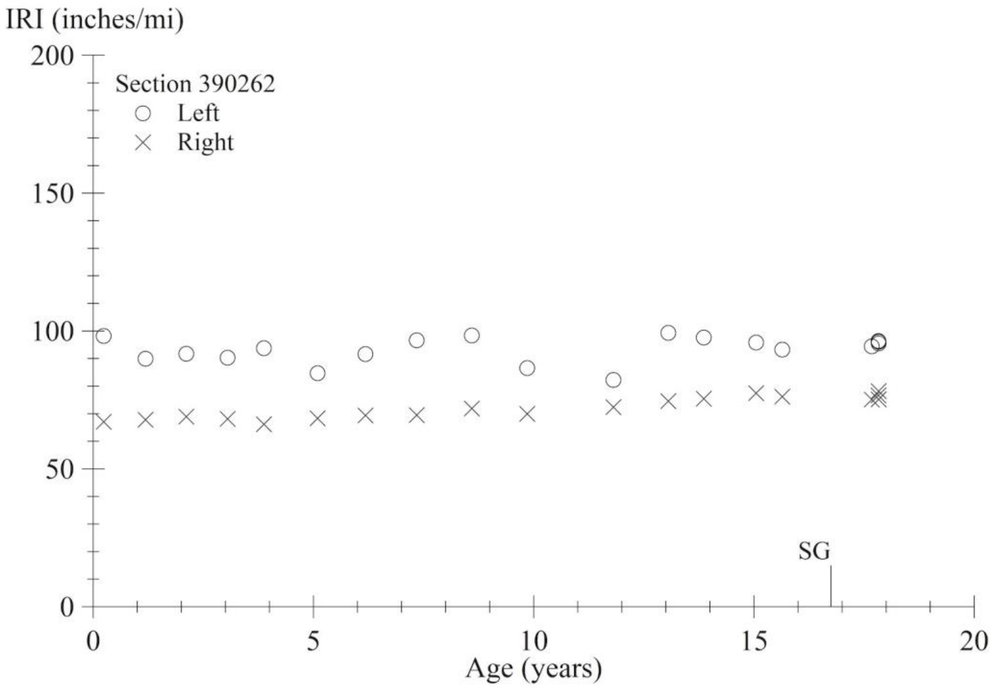

Source: FHWA.
SG = surface grinding.

Figure 149. Graph. IRI progression for section 390262.

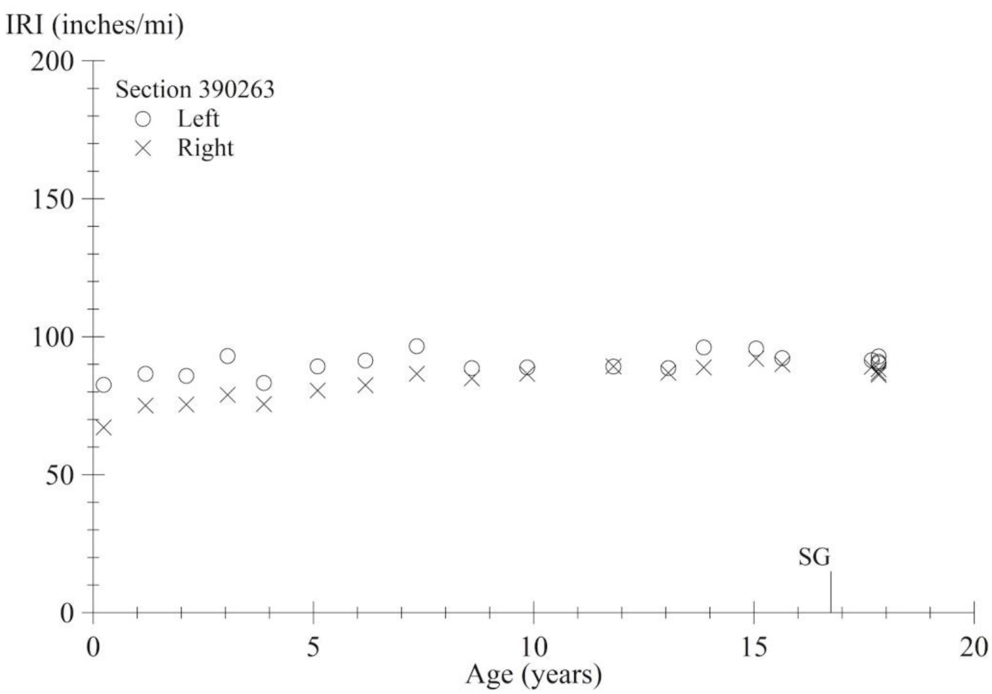

Source: FHWA.
SG = surface grinding.

Figure 150. Graph. IRI progression for section 390263.

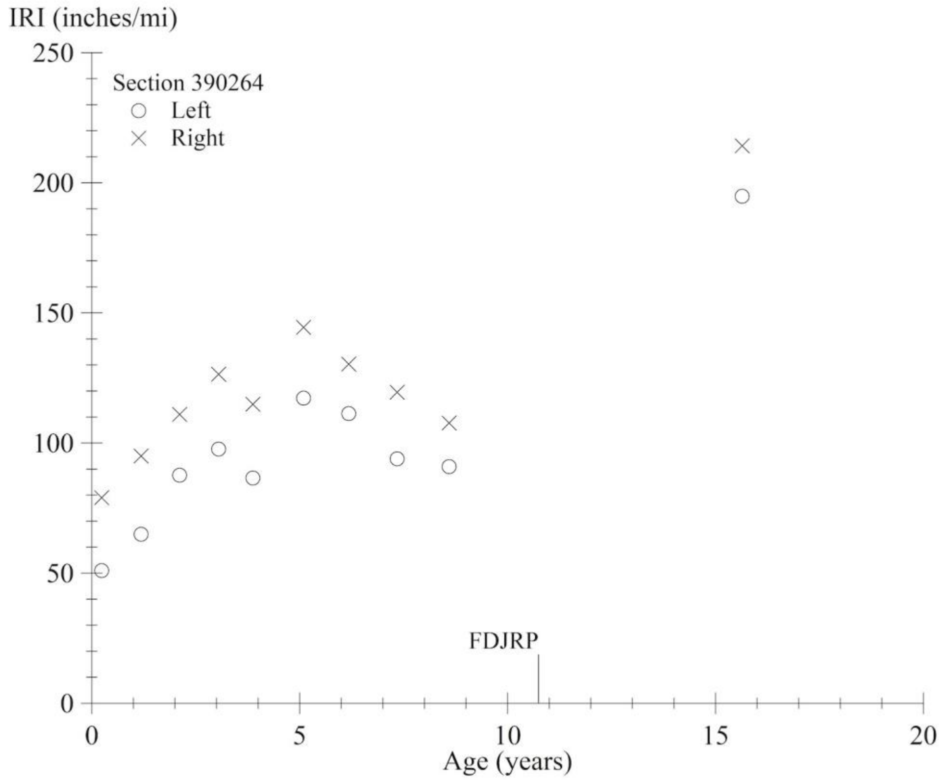

Source: FHWA.
FDJRP = full-depth transverse-joint-repair patching.

Figure 151. Graph. IRI progression for section 390264.

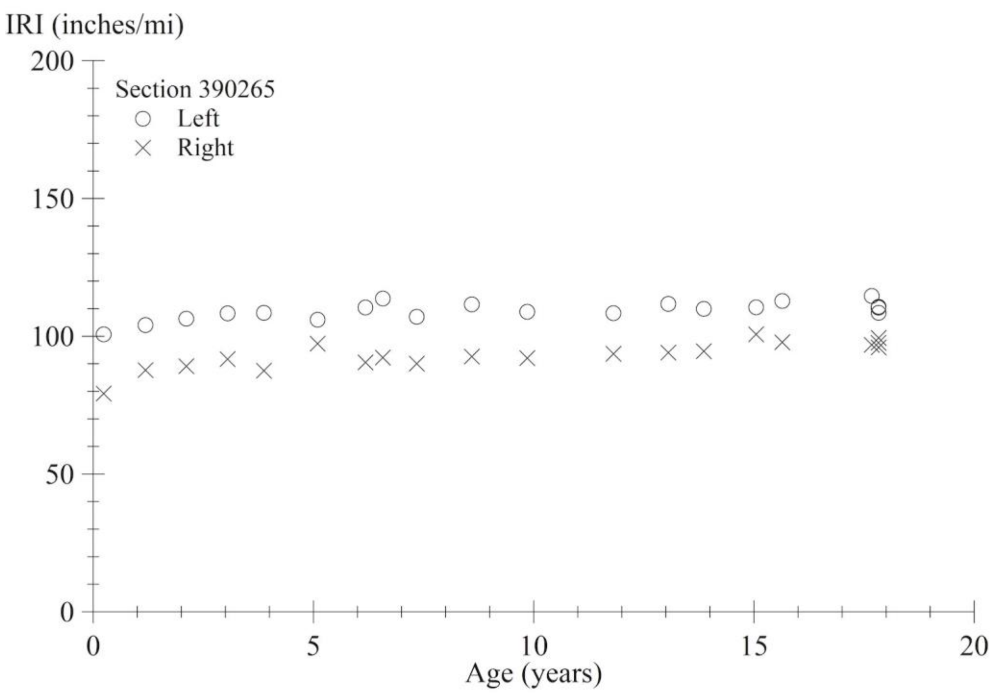

Source: FHWA.

Figure 152. Graph. IRI progression for section 390265.

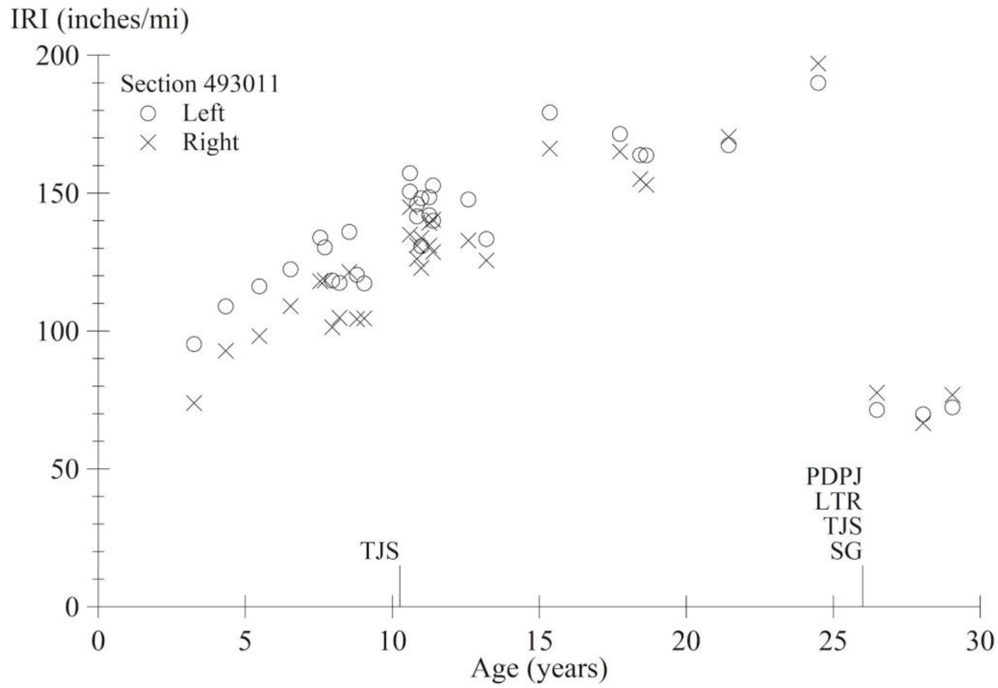

Source: FHWA.
TJS = transverse joint sealing; PDPJ = partial-depth patching at joints; LTR = load-transfer restoration; SG = surface grinding.

Figure 153. Graph. IRI progression for section 493011.

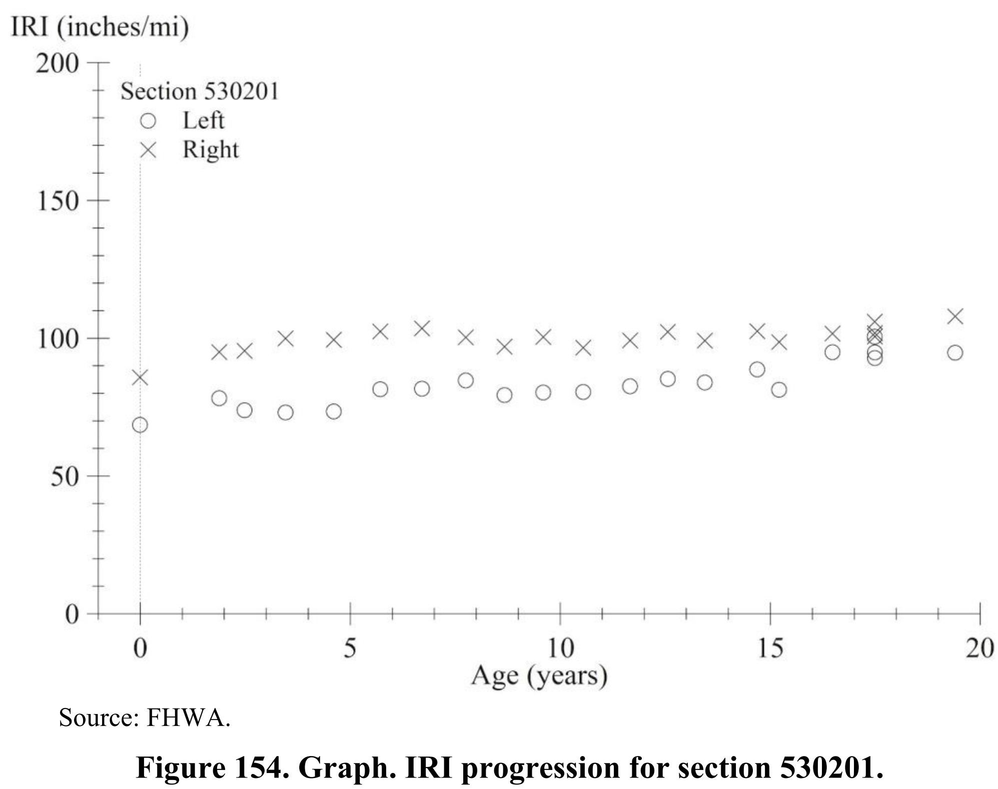

Source: FHWA.

Figure 154. Graph. IRI progression for section 530201.

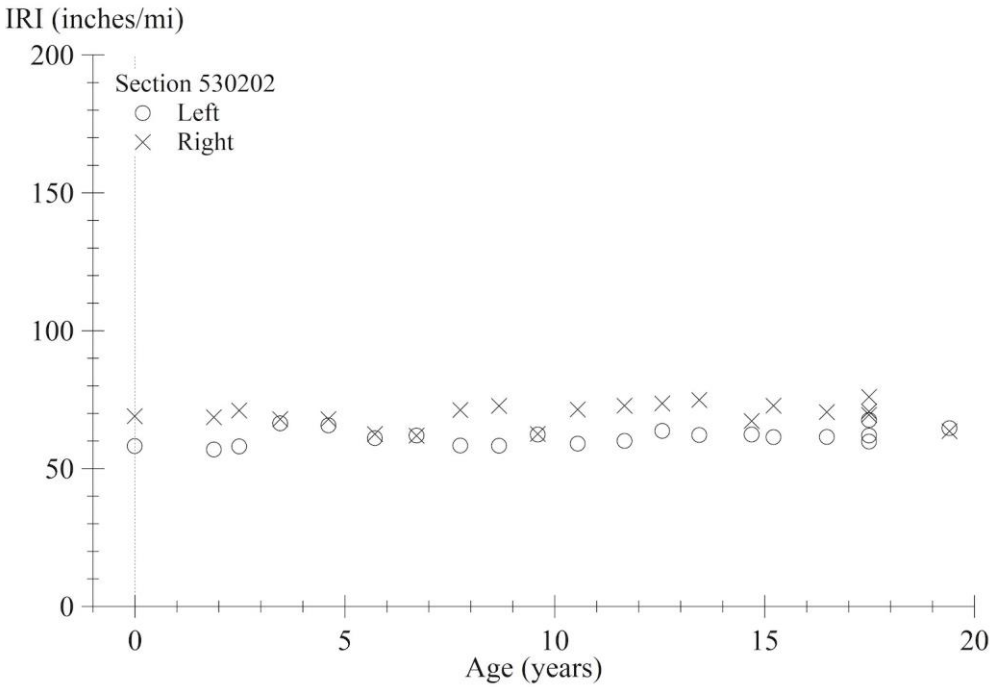

Source: FHWA.

Figure 155. Graph. IRI progression for section 530202.

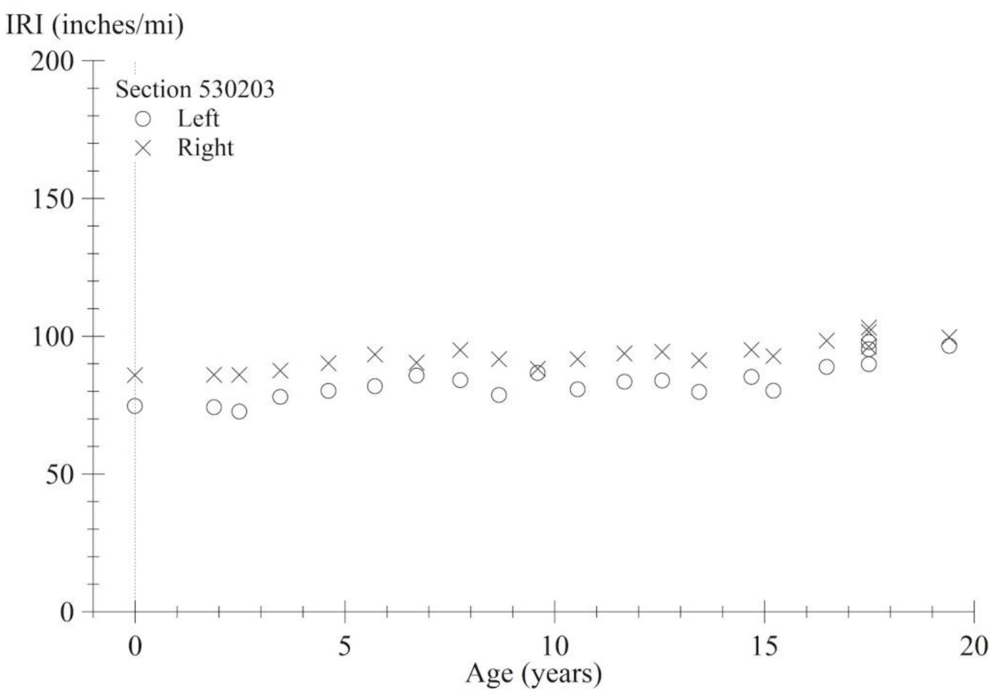

Source: FHWA.

Figure 156. Graph. IRI progression for section 530203.

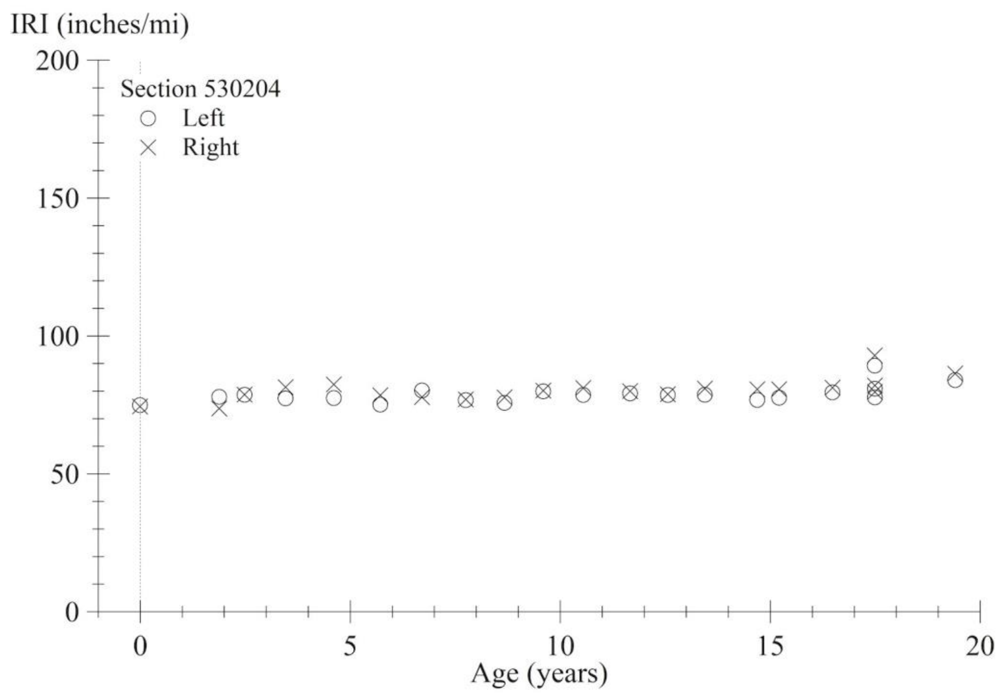

Source: FHWA.

Figure 157. Graph. IRI progression for section 530204.

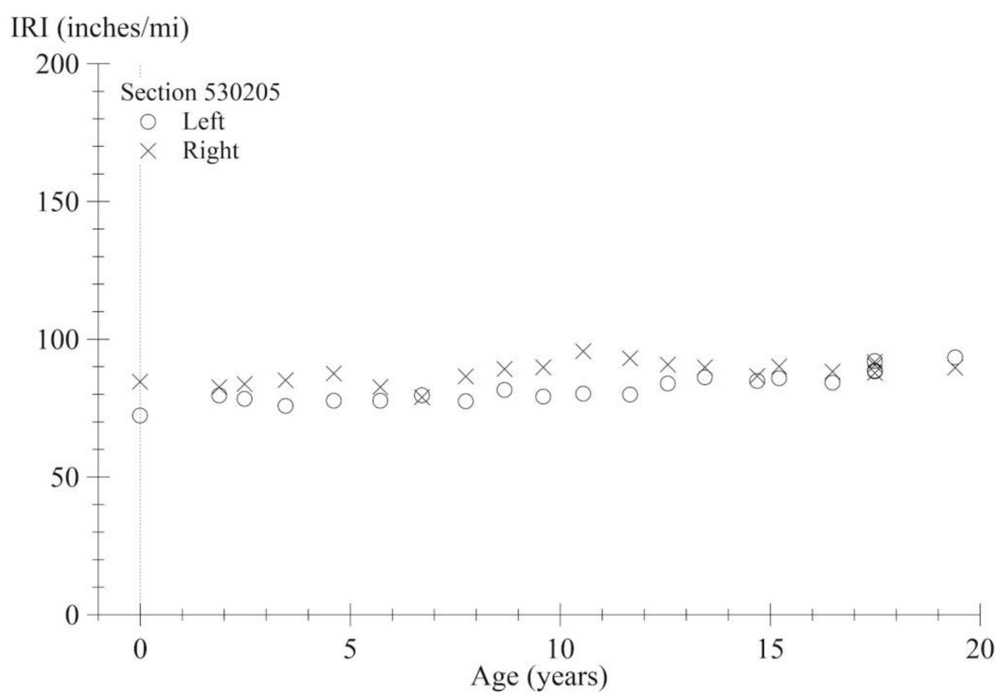

Source: FHWA.

Figure 158. Graph. IRI progression for section 530205.

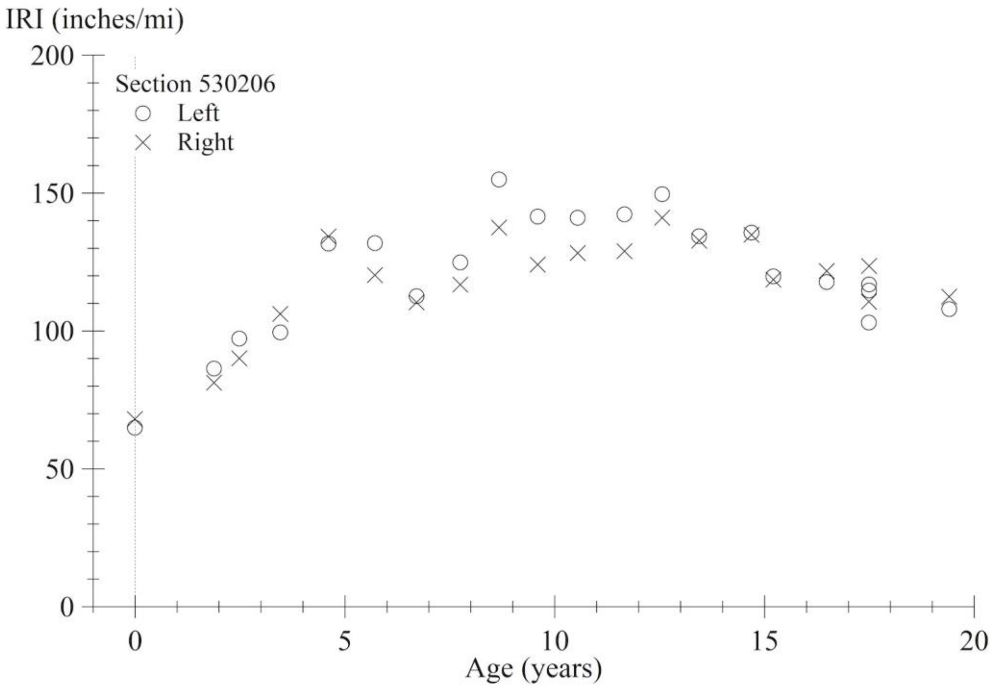

Source: FHWA.

Figure 159. Graph. IRI progression for section 530206.

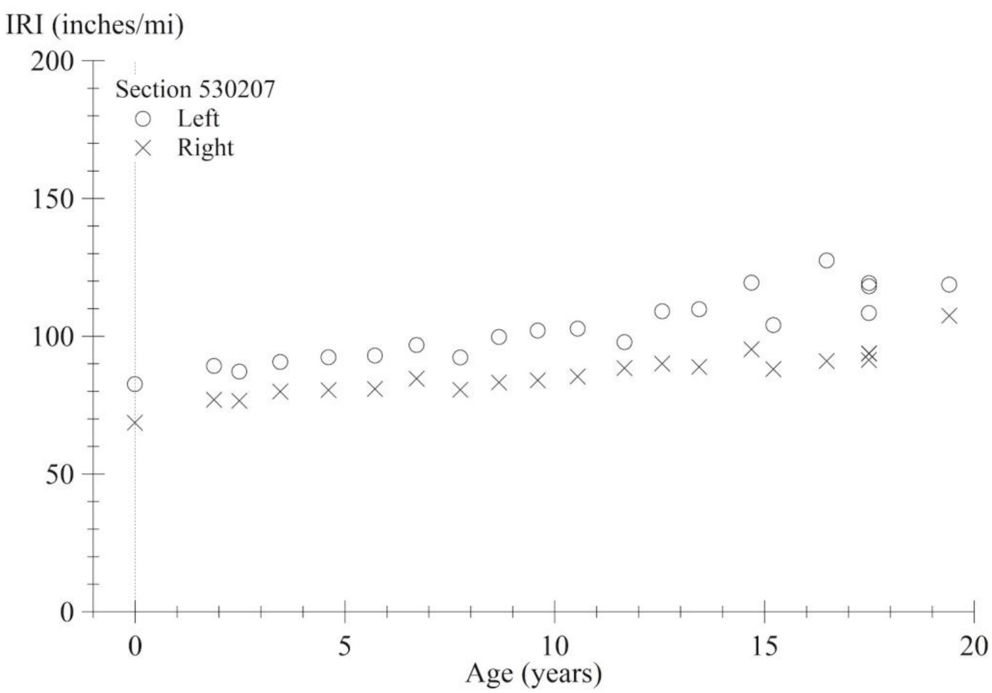

Source: FHWA.

Figure 160. Graph. IRI progression for section 530207.

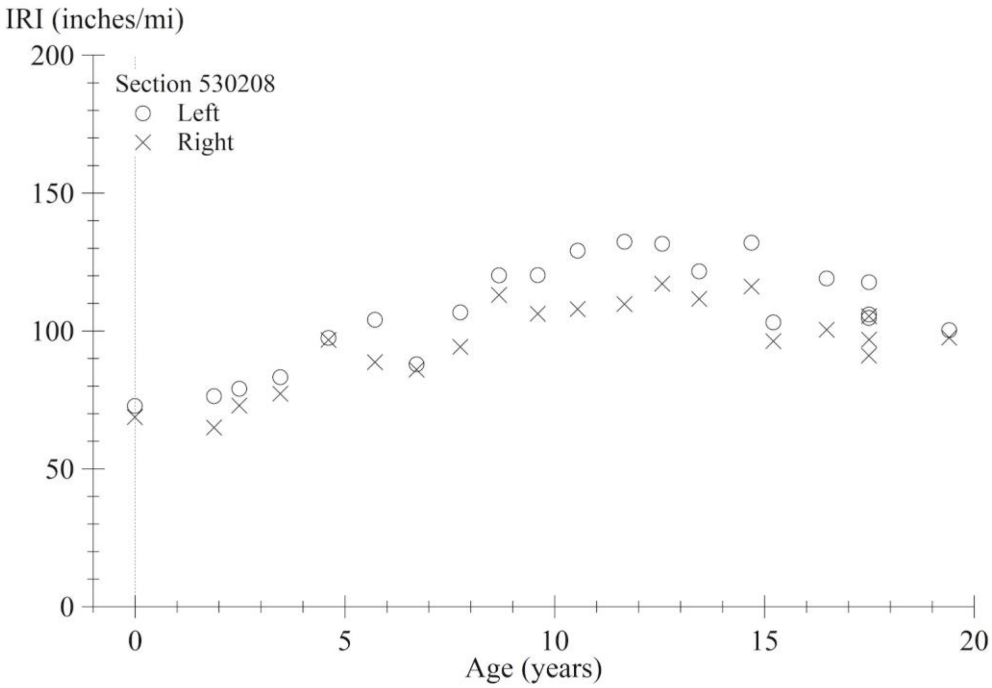

Source: FHWA.

Figure 161. Graph. IRI progression for section 530208.

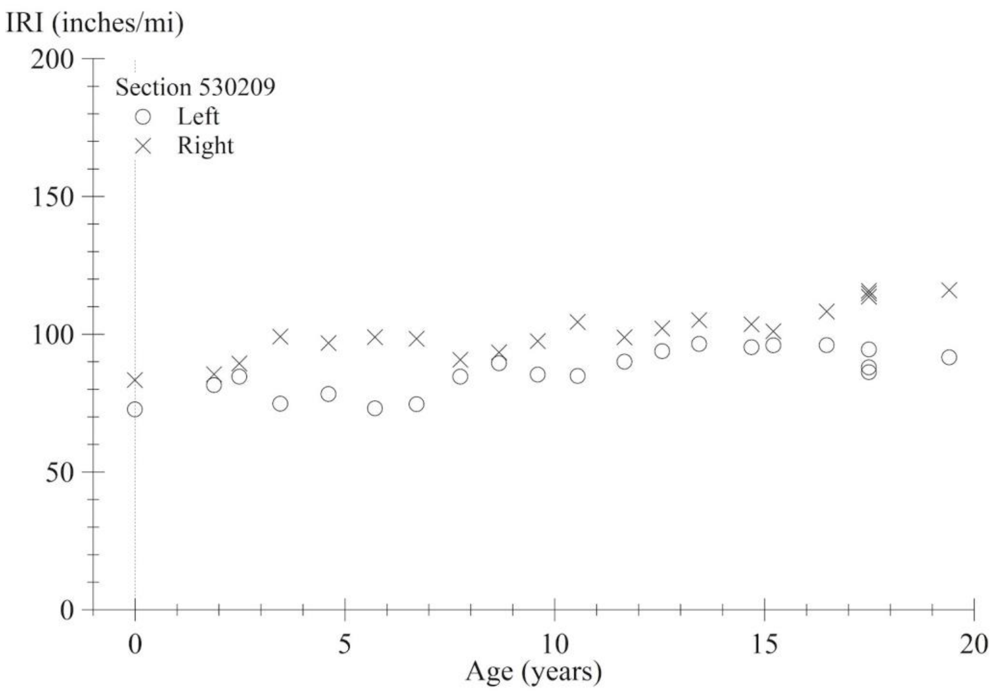

Source: FHWA.

Figure 162. Graph. IRI progression for section 530209.

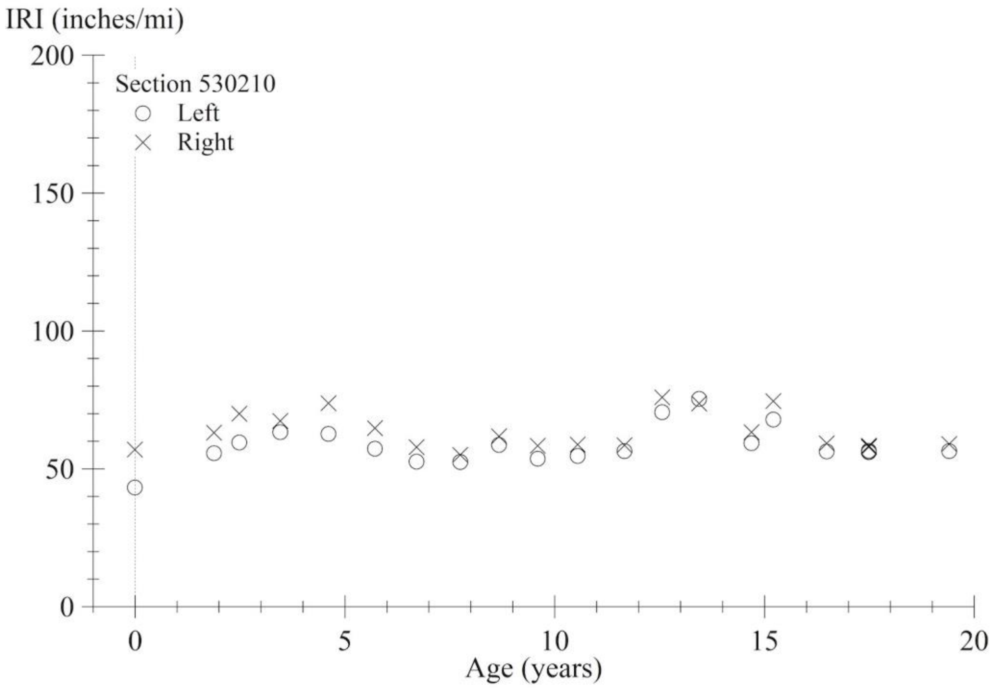

Source: FHWA.

Figure 163. Graph. IRI progression for section 530210.

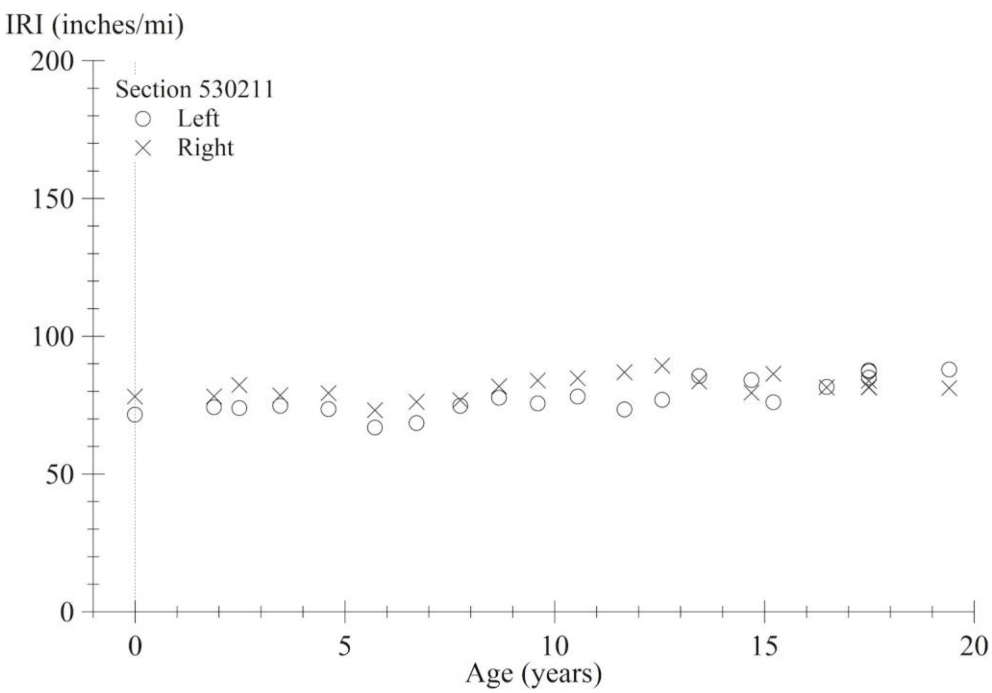

Source: FHWA.

Figure 164. Graph. IRI progression for section 530211.

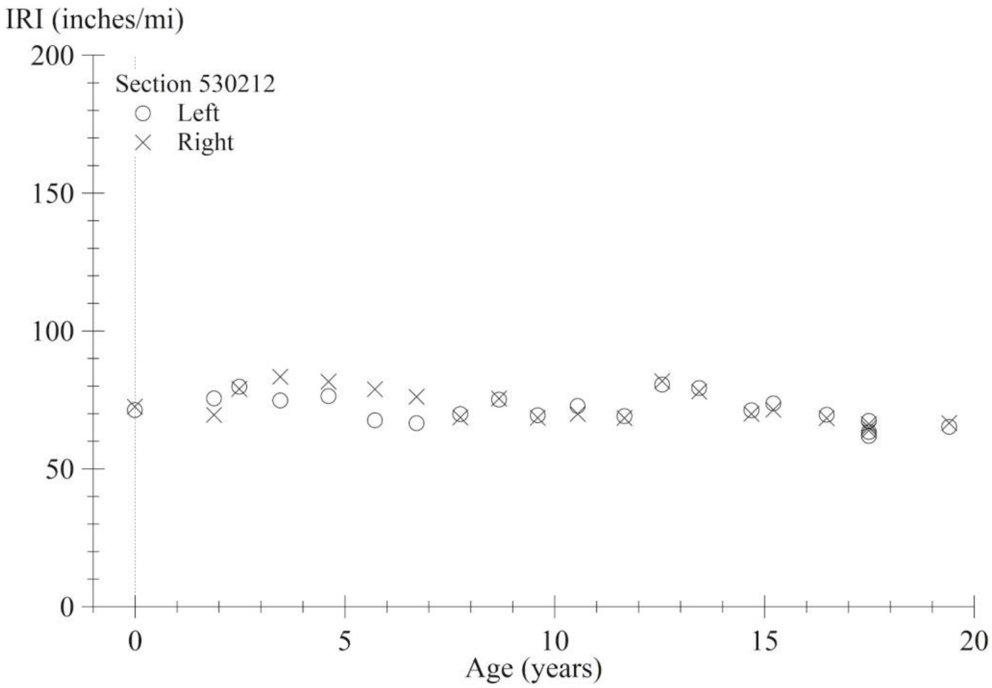

Source: FHWA.

Figure 165. Graph. IRI progression for section 530212.

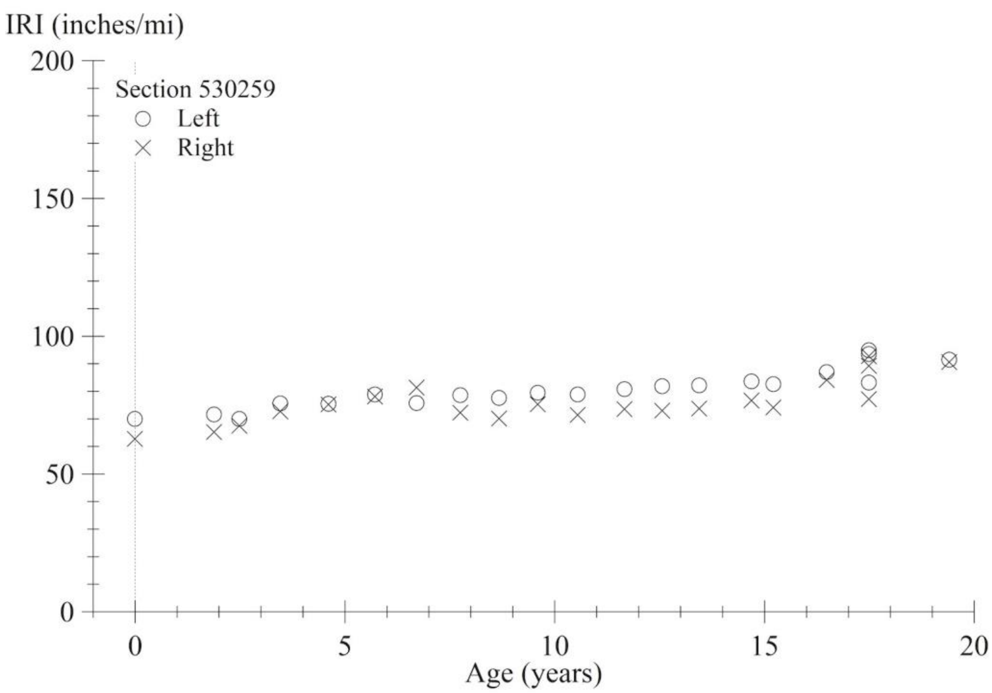

Source: FHWA.

Figure 166. Graph. IRI progression for section 530259.

APPENDIX E. IDENTIFYING JOINT LOCATIONS

This appendix describes the algorithm used to identify joint locations within measured profiles for slab-by-slab quantification of curl and warp.

BACKGROUND

Multiple algorithms have been proposed for joint identification in support of profile-based measurement of faulting for pavement management.[96,97] These algorithms search for step changes in elevation at potential faults, local minima within the profile with an adaptive threshold adjusted to seek the expected number of joints, or narrow dips that appear with an expected spacing within the profile processed with a high-pass filter.[98–100] Algorithms applied to quantify curl and warp search for joints at locations where curvature exceeds a given threshold or for narrow dips within the profile processed with a high-pass filter.[3,75]

Each algorithm is suited to specific expectations regarding the content within the profile. The most effective choice depends on aspects of pavement condition, such as the relative levels of faulting, slab curl, and joint distress within the profile; properties of the pavement surface that affect short-wavelength profile content, such as surface texture depth and type, joint width, and the status of joint sealant; and details of the measurement process, including the profiler height-sensor footprint, low-pass filtering, and recording interval.

The algorithm applied in this research was developed specifically for use on profile data collected for the LTPP program. The profiles were measured with well-documented field procedures and provisions for quality control.[8] Further, the success rate of the algorithm was improved by synchronizing the profiles for consistent longitudinal alignment throughout the monitoring history of each section and analyzing the profiles in groups.

The algorithm is based on a spike-detection procedure proposed by Chang et al. and most closely resembles an algorithm described by Karamihas and Senn.[2,6] The joint-finding strategy included the following:

- Identification of potential joint locations by seeking narrow downward spikes in each profile.
- Prioritization of locations where the spikes appeared consistently in both the left- and right-side profiles with provisions for skewed joints.
- Prioritization of locations where the spikes appeared consistently in repeated profile measurements from a given monitoring visit and among several consecutive visits.
- Recognition of locations with detected spikes that appeared throughout a test section with the expected joint spacing or joint-spacing pattern.

ANALYSIS STEPS

Step 1: Select a Group of Profiles

The joint-finding procedure was applied to several profiles simultaneously as a group. All profiles in the group covered the same test section and had consistent longitudinal alignment.

With few exceptions, profiles were grouped over all measurement visits made by the same profiler type to a specific test section. Profiles measured by different profiler types were not mixed in case different analysis settings were needed for each profiler type.

For example, the procedure was applied to a group of 60 profile measurements of section 390203 collected from 27-Dec-1996 through 04-Nov-2001. The 60 profile measurements include 5 repeat passes per visit over 6 visits and left and right profiles from each pass. The profiles were grouped together because the same profiler measured them. Likewise, a second group included 100 profiles collected from 06-Dec-2002 through 22-May-2012 by another profiler, and a third group included 40 profiles collected starting 03-Jul-2014 by another profiler.

Profiles collected for the SMP were also grouped by profiler type but were not incorporated into groups from regular monitoring visits from the same era. For example, 60 profiles measured during 6 regular visits to section 390204 by a specific profiler were analyzed as a group and 140 additional profiles from seasonal measurements by the same profiler were analyzed as a separate group. In part, the use of unique groups for seasonal visits was a matter of convenience when applying the calculation routines written for the analysis. The groups were separated because profiles from regular visits covered a range outside of the boundaries of the test section (i.e., the analysis incorporated joints just outside the test section boundaries to help establish the expected spacing pattern). Profiles from seasonal visits typically did not include pavement outside the test-section boundaries.

Step 2: Filter the Profiles

High-pass filter each profile with an antismoothing moving average filter using a base length of 0.82 ft.

Step 3: Normalize the Profiles

Normalize each filtered profile by its SD.

Step 4: Seek the Negative Spikes

Search each normalized trace and list the longitudinal position and the magnitude of any negative spike with a value below a given threshold. A default threshold value of −3 was used for most profile groups. Figure 167 shows a profile measured on section 390203 after high-pass filtering and normalization. The threshold value for negative spikes of −3 is marked on the graph.

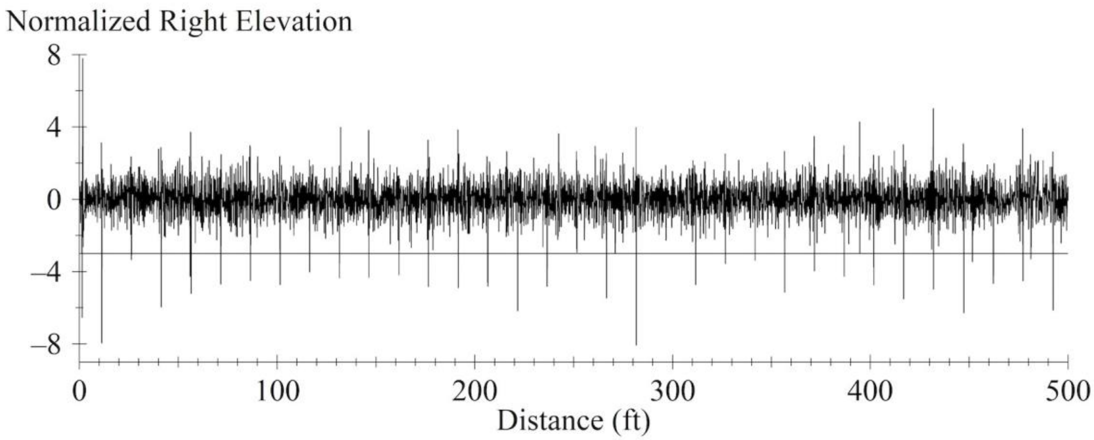

Source: FHWA.

Figure 167. Graph. Profile measured on section 390203 after high-pass filtering and normalization.

Lower threshold values were used for some groups of profiles. For example, the value was reduced to −2.5 for profiles from the SPS-2 site in Washington because the site included coarse surface texture and the downward spikes at the joints had lower magnitude relative to the content away from the joints. A lower threshold value was also used on profiles from sections 040222, 063021, 183002, 200210, 200259, 273003, 370203, 370205, and 390204. For these sections, some combination of coarse surface texture, narrow gaps at the joints, and higher joint sealant necessitated the reduction in the spike-detection threshold. In some cases, the threshold was reduced for groups of profiles collected after January 2013 because low-pass filtering reduced the magnitude of the spikes at joints.

Step 5: Remove Lesser Spikes

Eliminate any spike within a given range of a deeper spike. The default range value, which was used for most sets of profiles, was 0.2 ft. In some cases where cracking or other distress appeared near joints, other values as low as 0.1 ft and as high as 0.8 ft were used.

Step 6: Aggregate Across the Profile Group

Assemble into a single list the qualifying spike locations for the left and right profiles of all profile measurements within the group. For sections with skewed joints, offset values of longitudinal position for left-side profiles by 0.919 ft. Sections 040262–040265, 063021, and 493011 included skewed joints.

Step 7: Sort the List

Sort the list of qualifying spike locations in ascending order of longitudinal position.

Step 8: Consolidate Nearby Spikes into Clusters

Consolidate any set of closely spaced spike positions into a cluster. Merge spike positions for which no gap larger than a preset value (i.e., a gap limit) exists between consecutive values.

Set a limit for the total range covered by a single cluster of spikes (i.e., a cluster range limit). For each cluster of spikes, record the range of longitudinal position values, average longitudinal position value, and number of spikes included in the cluster. To do this, apply the following steps:

- Step 8a: Open a new spike cluster using the first item in the list.
- Step 8b: If the list of spikes is complete, close the final cluster and terminate the consolidation procedure. If not complete, promote the next item on the list to the current item.
- Step 8c: If the distance from the previous item to the current item is no greater than the gap limit and the distance from the first item in the spike cluster to the current item is no greater than the cluster range limit, add the current item to the open spike cluster and return to step 8b.
- Step 8d: If the distance from the previous item to the current item is greater than the gap limit or the distance from the first item in the spike cluster to the current item is greater than the cluster range limit, close the current spike cluster and open a new spike cluster with the current item as the first member. Return to step 8b.

The default value for gap limit was 0.1 ft; however, values as high as 0.4 ft were used and a value of 0.2 ft was used in approximately one-third of the cases. A cluster range limit of 0.82 ft was used in nearly every case.

For each group of profiles, this procedure produced a list of spike clusters that outnumbered the joints within a test section, often by a wide margin. However, spike clusters with counts approaching or equal to the number of profiles in the set typically only appeared at joints or transverse cracks.

Table 48 lists the most well-populated spike clusters from a group of 60 profile measurements of section 390203 collected from 27-Dec-1996 through 04-Nov-2001. Analysis of this profile group produced 2,291 spikes in 167 clusters, which included 96 clusters with only 1 spike, 15 clusters with 2 spikes, and 7 clusters with 3 spikes. The clusters with only three spikes are not shown in Table 48.

Table 48. Spike clusters from six visits to section 390203.

Start of Range (ft)	End of Range (ft)	Average Position (ft)	Number of Spikes	Joint-Spacing Compatibility Score
−3.76	−3.54	−3.67	65	1,638
1.32	1.56	1.41	50	61
1.83	2.24	2.03	39	49
11.21	11.42	11.32	60	1,580
26.25	26.44	26.34	51	1,638
41.29	41.42	41.36	59	1,638
56.39	56.56	56.47	57	1,635
71.41	71.52	71.47	54	1,635
82.33	82.68	82.48	27	43
86.42	86.57	86.49	52	1,635
101.35	101.54	101.44	55	1,634
116.37	116.55	116.47	55	1,635
127.95	128.02	127.98	4	Not evaluated
131.32	131.48	131.41	54	1,635
146.30	146.48	146.40	53	1,635
157.25	157.34	157.27	6	Not evaluated
161.44	161.58	161.50	54	1,635
176.35	176.51	176.43	54	1,635
191.40	191.57	191.46	52	1,635
206.37	206.53	206.44	60	1,634
221.43	221.62	221.54	53	1,637
225.87	225.97	225.90	12	Not evaluated
236.36	236.56	236.46	54	1,635
251.37	251.51	251.45	47	1,634
266.38	266.57	266.49	55	1,635
281.39	281.61	281.53	58	1,637
294.40	294.49	294.43	6	Not evaluated
296.49	296.70	296.59	48	1,743
311.49	311.63	311.55	47	1,697
323.62	323.78	323.71	4	Not evaluated
326.51	326.73	326.61	48	1,793
341.51	341.64	341.56	47	1,697
356.45	356.64	356.54	55	1,697
371.54	371.65	371.61	54	1,793
386.56	386.66	386.63	49	1,795
401.49	401.67	401.60	59	1,743
412.24	412.32	412.26	5	Not evaluated
416.58	416.69	416.64	58	1,795
431.68	431.87	431.78	59	1,836
446.97	447.13	447.05	50	540
451.32	451.45	451.41	7	Not evaluated
461.61	461.74	461.69	4	Not evaluated
461.91	462.10	461.99	60	797
476.95	477.11	477.03	46	647
480.81	481.05	480.94	7	Not evaluated
492.11	492.29	492.18	51	328
501.14	501.32	501.23	48	52
501.73	502.05	501.85	40	55
507.05	507.29	507.16	52	328

Step 9: Evaluate Each Spike Cluster in the List

Calculate a joint-spacing compatibility score for each spike cluster. To do this, seek other clusters that appear at the expected distances from the cluster under evaluation within an acceptable tolerance.

The compatibility score for a spike cluster is the sum of the spike counts from every cluster that appears at an expected distance within a given tolerance. For an expected joint spacing of 15 ft, any spike cluster that appears a multiple of 15 ft from a spike cluster contributes to the compatibility score. The distance must be within a preset tolerance, which is expressed as a percentage of the nominal joint spacing.

The distance tolerance for compatibility was set at a default value of 3 percent of the expected joint spacing, which corresponds to a tolerance of 0.45 ft for 15-ft-long slabs. A value of 6 percent was used on test sections where the joint spacing varied somewhat relative to the nominal value. In some cases, the tolerance was set as high as 12 percent. This tolerance was needed on test sections where the joint-spacing pattern did not adhere to the nominal value throughout the entire section.

For test sections with multiple slab lengths, the joint-spacing compatibility score was evaluated multiple times. Some test sections had a nominal joint-spacing pattern that repeated every fourth slab. On those sections, the compatibility score at each spike cluster was evaluated once for each possible position of a potential joint within the four-slab pattern and the highest score was reported. For multiple-slab patterns, the distance-tolerance threshold was interpreted as a percentage of the average slab length within the pattern.

Compatibility scores were typically only calculated for clusters with a spike count above a given threshold, expressed as a percentage of the number of profiles in the group. The default value was 30 percent, which was used on the majority of profile groups. For example, the group examined in Table 48 included 60 profiles and compatibility scores were only calculated for clusters that included 18 spikes or more.

In a few instances, iteration was required to determine the spike-count threshold that yielded a complete set of joint locations. For example, lower values were used in cases where downward spikes did not appear reliably at every joint in every profile measurement. In rare cases, every spike group was evaluated for compatibility.

Step 10: Designate the Most Compatible Spike Cluster as the Principal Joint

Designate the spike cluster with the highest compatibility score as a joint. If multiple clusters share the highest compatibility score, select the joint farthest upstream.

In Table 48, the highest compatibility score of 1,836 occurs at the spike cluster with an average position of 431.68 ft. Although this score is the highest, it is lower than the maximum possible score. If the spike cluster at each joint included 60 spikes, which is one per pass, then compatibility with the 35 joints within the range covered by the analysis would have produced the maximum possible score of 2,100.

Step 11: Seek Other Joints Downstream

Seek the adjacent joint location in the forward direction from the principal joint. Select the spike cluster with the highest compatibility score within the expected distance window. The distance window extends from the shortest expected joint spacing to the longest expected joint spacing in the designated pattern with an additional margin added at both ends. The margin is determined by a joint window tolerance, which is expressed as a percentage of the joint spacing. Each time a joint is found, seek the following joint using the same procedure until the end of the profile group range is reached.

The default value of joint window tolerance was 3 percent. This corresponds to a joint window of 14.55 to 15.45 ft for test sections with a constant nominal joint spacing of 15 ft. A section with a joint-spacing pattern of 13, 12, 18, and 19 ft corresponds to a joint-spacing window of 11.64 to 19.57 ft.

The default value for joint window tolerance was applied to a majority of the profile groups. A range of values from 1.5 to 15 percent was used on various test sections depending on how consistently the actual joint spacing adhered to the nominal pattern.

Step 12: Seek Other Joints Upstream

Repeat the process from step 11, starting from the principal joint and extending in the reverse direction until the end of the section is reached.

DISCUSSION

Joint Position and Joint Window

Table 49 shows the outcome of the joint-finding procedure for the profile group in Table 48. The position of each joint listed in Table 49 is the average position of the spikes in the joint cluster. Table 49 also lists the distance between adjacent joint positions. In subsequent analysis of curl and warp of each slab, such as the calculation of radius of relative stiffness, the distance between joints is used as the slab length.

Table 49 also lists the spike cluster range, which is the total distance between the first and last spike in the source cluster. The spike cluster range provides a measure of the potential variation in joint locations within the profile group. Subsequent analysis of curl and warp includes a curve fit on the profile within each slab. This analysis excludes the spike cluster range to ensure that downward spikes in profile do not affect the curve fit. The curve fit is performed on an area within the profile that extends from the end of the spike cluster range from the leading joint to the start of the spike cluster range for the trailing joint. For example, the second and third joints in Table 49 define a 15.02-ft-long slab running from 11.32 to 26.34 ft from the section start. However, as shown in Table 48, the curl-and-warp analysis will consider a 14.83-ft-long area running from 11.42 ft to 26.25 ft from the start of the section.

The average spike cluster range for joints located in profiles measured by LTPP was 0.24 ft; 95 percent of the joints had a range of 0.44 ft or less.

Table 49. Joint locations from six visits to section 390203.

Joint Position (ft)	Spike Cluster Range (ft)	Distance from Previous Joint (ft)
11.32	0.21	14.98
26.34	0.19	15.02
41.36	0.13	15.02
56.47	0.16	15.10
71.47	0.11	15.00
86.49	0.15	15.03
101.44	0.19	14.95
116.47	0.18	15.03
131.41	0.15	14.94
146.40	0.18	14.99
161.50	0.14	15.11
176.43	0.16	14.93
191.46	0.17	15.02
206.44	0.16	14.99
221.54	0.19	15.09
236.46	0.20	14.93
251.45	0.15	14.98
266.49	0.19	15.04
281.53	0.22	15.04
296.59	0.21	15.06
311.55	0.14	14.96
326.61	0.23	15.06
341.56	0.13	14.95
356.54	0.19	14.97
371.61	0.11	15.07
386.63	0.10	15.02
401.60	0.17	14.97
416.64	0.11	15.04
431.78	0.19	15.14
447.05	0.16	15.27
461.99	0.20	14.93
477.03	0.16	15.04
492.18	0.18	15.15
507.16	0.25	14.98

Termination

In some cases, the joint-finding analysis was terminated prior to the end of the monitoring period because of the following changes in the structural state of test sections:

- Analysis of section 200205 was terminated after 21-Sep-2012 because wide patches were installed at many joints.
- Analysis of section 200210 was terminated after 21-Sep-2012 because the section was diamond ground.
- Analysis of section 390208 and section 390212 was terminated after 22-May-2012 because slab replacement and patching altered some of the slabs.

- Analysis of section 183002 was terminated after 26-Apr-2011 because the section received an overlay.

- Analysis of section 493011 was terminated after 26-Oct-2010 because joint restoration included the installation of wide patches at many joints.

Extrapolation

The algorithm succeeded in locating all joints for profiles collected from December 1996 through January 2013 because those profiles were measured using narrow-footprint height sensors. Profile data collected before December 1996 were measured using a height sensor with a footprint that was 6 inches wide and 0.24 inches long and was less likely than profilers used in subsequent years to register a downward spike in a reading at a joint.[(14)] Profiles were collected using a sampling interval of 2 inches, smoothed using a moving average over a base length of 12 inches, and recorded at an interval of 6 inches. Downward spikes in elevation did not routinely appear at joints in these profiles. For profiles measured in this era, joint locations were detected from later measurements by a different profiler.

After January 2013, profile data were recorded after the application of low-pass filtering. Downward spikes at the joints did not stand out relative to other content within profile data from the Washington SPS-2 site because those test sections included coarse surface texture. Joint locations for profiles collected after January 2013 at the Washington site were assumed to be the same as in the visit in May 2012.

Joint Spacing

The joint spacing for every section included some variation around the nominal spacing pattern and some test sections included one or more joints that did not adhere to the pattern at all. Any exception to the expected joint-spacing pattern greater than 0.5 ft was verified by comparing the exception to transverse joint distance values recorded in LTPP manual distress surveys of faulting.

An additional rule for identifying joints was applied for some test sections with high levels of variation around the nominal spacing pattern. The additional rule qualifies any location as a joint if enough spikes are detected. This rule is applied in steps 11 and 12 previously noted. The criterion designates a spike cluster as a joint that includes a sufficient number of spikes as a percentage of the number of profiles in the group, regardless of whether the location is within the joint-window tolerance. The test sections using the additional rule are sections 370201–370203, 370207–370212, 370259, 200259, 200202, 063021, 390264, and 493011.

Table 50 provides details about the joint spacing within each section.

Table 50. Joint-spacing details.

Section(s)	Nominal Pattern (ft)	Notes
040213–040224	15	No notes.
040262–040265	15-12-14-13	Skewed joints.
040266–040268	15-13-14-17	No notes.
063021	12-13-19-18	Skewed joints. One 29-ft slab.
133019	20	No notes.
183002	13-12-18-19	Skewed joints.
200201–200212	15	High variation in spacing.
200210	15	One 16.8-ft-long slab.
200212	15	One slab group 11.9-13.4-19.4 ft.
200259	15	One slab group 11.5-17.9 ft.
273003	13.0-15.5-13.9-16.8	Variation from this pattern of up to 0.85 ft.
370201–370212	15	High variation in spacing.
370201	15	First full slab 13.6-ft long.
370211	15	One slab group 17.1-2.8 ft.
370259	21.6-19.2-18.7-20.6	Variation from this pattern of up to 0.58 ft. The 21.6-ft-long slab was missing in one instance of the pattern.
370260	15	No notes.
390201–390212	15	No notes.
390259–390265	15	No notes.
390264	15	One slab group 10.6-6.0-13.6 ft. One slab group 10.5-6.0-13.5 ft.
493011	17-18-13-12	Skew A wide transverse crack disrupts the pattern near the center of the section. Variation from this pattern of up to 0.5 ft.
530201–530212	15	High variation in spacing.
530259	14.1-13.1-8.8-9.9	Variation from this pattern of up to 0.7 ft.

Section 063021 included a 29-ft slab near the center of the section in place of an 18-ft slab and 12-ft slab within the pattern. A transverse crack appeared within the slab. Atypical settings for the joint-finding algorithm were required to accommodate the crack. Three sections at the Kansas SPS-2 site and two sections at the North Carolina SPS-2 site included a slab or a group of consecutive slabs that differed in length from the nominal spacing of 15 ft, as described in Table 50. At two locations within section 390264, a 6-ft patch was installed over an existing joint that disrupted the nominal joint-spacing pattern.

Joint-spacing values at the Kansas and North Carolina sites varied from the nominal value to greater extent than the Arizona, Ohio, and Washington sites. Excluding the special cases listed in Table 50, the core test sections at the Kansas site included 380 slabs that were fully within test-section boundaries. Joint-spacing values for these slabs ranged from 14.40 to 15.70 ft, with an average value of 15.00 ft and an SD of 0.21 ft. Excluding the special cases listed in Table 50, the core test sections at the North Carolina site included 384 slabs that were fully within test-section boundaries. Joint-spacing values for these slabs ranged from 14.11 to 15.94 ft, with an average value of 14.99 ft and an SD of 0.24 ft. In contrast, 385 slabs within the core sections at the Arizona site had joint-spacing values that ranged from 14.74 to 15.39 ft, with an average value of 15.00 ft and an SD of 0.06 ft. Joint-spacing values for the core sections at the Ohio and

Washington sites had variation comparable to the Arizona site, with SD values of 0.10 and 0.09 ft, respectively.

On section 273003, the nominal spacing pattern was established after inspecting the measured profiles. The values listed in Table 50 are the average joint-spacing values for each member of the pattern within the section. However, individual joint-spacing values varied from the nominal values by up to 0.85 ft.

On section 370259, the joint-finding algorithm used a constant nominal joint spacing of 20 ft with a high tolerance. The results revealed a four-slab pattern with average nominal values of 21.6, 19.2, 18.7, and 20.6 ft. However, the first slab was missing in one instance of the pattern and variation from the average values of up to 0.55 ft was observed.

On section 493011, the joint-finding algorithm used a constant nominal joint-spacing pattern of 13, 12, 17, and 18 ft. The results revealed a four-slab pattern with average nominal values of 12.8, 12.2, 16.9, and 17.9 ft. The pattern is disrupted over a 58-ft-long area near the center of the section, which included a wide transverse crack. Taking the crack into consideration, this area includes four slabs of various lengths that do not adhere to the nominal pattern. Atypical settings for the joint-finding algorithm were required to accommodate the pattern disruption.

On section 530259, the nominal spacing pattern was established after inspecting the measured profiles. The values listed in Table 50 are the average joint-spacing values for each member of the pattern within the section. However, individual joint-spacing values varied from the nominal values by up to 0.7 ft.

FHWA CURL-AND-WARP STUDY PROFILES

The joint-finding algorithm in this appendix was also applied to diurnal and seasonal profile measurements from the FHWA curl-and-warp study, *Impact of Temperature Curling and Moisture Warping on Jointed Concrete Pavement Performance*.[6] For this dataset, all profiles from a given section were analyzed as a single group. The group typically consists of 160 profiles for sections with seasonal and diurnal measurements, which includes 4 seasons, 4 times per day per season, 5 passes per time of day, and profiles from 2 sides in every pass. Sections with diurnal measurement only include 40 profiles. These profiles were measured with a high-speed profiler that used a point laser with a narrow footprint as a height sensor. The profiler was modified to provide profile at a sample interval of 0.25 inches to facilitate the joint-finding process.[85]

The joint-finding algorithm was applied to profiles with default values similar to those used on LTPP profile measurements. In several cases, a larger threshold value for spike magnitude (–4 or –5) was applied because the negative spikes at joints were deeper.

APPENDIX F. ESTIMATION OF SLAB CURL

The levels of curl and warp present within each profile were estimated using slab-by-slab analysis of local profile segments. Measured profiles of individual slabs were isolated using the joint-finding procedure described in appendix E. Deformation within each slab profile due to curl and warp was estimated using a curve fit to the Westergaard equation. The Westergaard equation predicts the deformation of a concrete slab in response to a linear strain gradient throughout its depth.

WESTERGAARD DEFORMATION MODEL

The curve-fitting procedure for measured slab profiles used an idealized shape proposed by Westergaard.[20] The idealized profile is based on the assumption of a linear strain gradient through the depth of the slab, unrestrained slab ends, and an infinite slab along the undeformed axis. Westergaard provided the solution for an infinitely long pavement of finite width. Vertical deformation (z) depends on distance from the slab center (x) as shown in the equations in figure 168.

$$z = -z_0 \frac{2\cos\lambda\cosh\lambda}{\sin 2\lambda - \sinh 2\lambda}\left[(-\tan\lambda + \tanh\lambda)\cos\frac{x}{l\sqrt{2}}\cosh\frac{x}{l\sqrt{2}} + (\tan\lambda + \tanh\lambda)\sin\frac{x}{l\sqrt{2}}\sinh\frac{x}{l\sqrt{2}}\right]$$

A. Equation. z.

$$z_0 = \frac{-(1+\mu)(\alpha\Delta T + \Delta\varepsilon_{sh})}{h} l^2$$

$\Delta\varepsilon_{sh}/h$ = moisture gradient.

$\alpha\Delta T/h$ = temperature gradient.

B. Equation. z_0.

$$\lambda = \frac{b}{l\sqrt{8}}$$

b = slab width.

C. Equation. λ.

$$l = \sqrt[4]{\frac{Eh^3}{12(1-\mu^2)k}}$$

D. Equation. l.

Figure 168. Equation. Relationship of slab elevation to position.

This study applies the solution to predict vertical deformation as a function of longitudinal distance from the center of the slab. As such, b represents slab length in this report, rather than slab width.

The curve-fitting procedure accepts b, E, μ, and k as inputs to the model and estimates the linear strain gradient by fitting the idealized slab profile to a measured profile. The estimate of linear strain gradient required to deform the slab into the measured shape is the PSG, which relates to figure 168 and is shown in Figure 169.

$$PSG = \frac{(\alpha \Delta T + \Delta \varepsilon_{sh})}{h}$$

Figure 169. Equation. PSG.

SLAB PROPERTIES

Local slab profiles were extracted from sectionwide measured profiles using the locations of the surrounding joints, as described in appendix E. The length associated with each slab profile was the distance between joint locations.

Material properties were assumed to be constant for all slabs within a given test section and throughout the monitoring history of each section. A constant value of 0.15 was used for Poisson's ratio for all test sections in this study. LTPP database table L05B provided slab thickness values, which were based on cores that were collected at the ends of each section.(8) Table 51 and Table 52 list the values of slab thickness for each test section.

Elastic modulus and modulus of subgrade reaction were derived from FWD testing using two methods of analysis: AREA and Best Fit. Khazanovich, Tayabji, and Darter describe the methods as follows:

> The Best Fit method solves for a combination of the radius of relative stiffness, *l*, and the coefficient of subgrade reaction, k, that produces the best possible agreement between the predicted and measured deflections at each sensor. The AREA method … estimates the radius of relative stiffness as a function of the AREA of the deflection basin.(101)

The Best Fit method uses least squares minimization between measured and predicted deflection, with relative weighting factors assigned to the output of each deflection sensor.(102)

Smith et al. and Hall and Mohseni describe the AREA method as it is applied to the sensor configuration used in the LTPP program.(102,103) The AREA parameter characterizes the measured deflection basin in units of distance (i.e., length). AREA is a sum that includes one term per deflection sensor. Each term is the product of the deflection measurement at a given location and the distance to an adjacent sensor. The sum approximates rectangular integration of the deflection basin in two dimensions, with an additional term for the outermost deflection measurement. The sum is normalized by the deflection measured directly under the load plate. Radius of relative stiffness is computed directly from the AREA parameter using an empirical relationship established for the specific sensor placement and loading conditions. In turn, a theoretical relationship by Westergaard provides the modulus of subgrade support, given the applied load, the load radius, the maximum deflection under the load, and the radius of relative stiffness. (20)

In both methods, elastic modulus is calculated from the derived values of radius of relative stiffness and modulus of subgrade reaction. Table 51 and Table 52 list elastic modulus, modulus of subgrade support, and radius of relative stiffness produced by the AREA and Best Fit methods, respectively.

Table 51. Test-section properties using AREA method.

Section	*h* (Inch)	*E* (ksi)	*k* (psi/Inch)	*l* (Inch)
040213	7.9	5,665	228	32.0
040214	8.3	5,515	162	35.9
040215	11.0	5,636	273	39.1
040216	11.2	4,329	239	38.4
040217	8.1	6,760	559	27.2
040218	8.3	8,211	337	33.0
040219	10.8	15,010	405	44.7
040220	11.2	5,771	307	38.7
040221	8.1	7,960	213	36.1
040222	8.6	7,928	266	35.7
040223	11.1	7,865	339	40.6
040224	10.6	6,880	220	42.2
040262	8.1	5,715	191	34.1
040263	8.2	7,807	180	37.8
040264	11.5	15,105	222	54.5
040265	10.8	7,048	225	42.8
040266	12.3	6,178	277	43.4
040267	11.3	6,470	326	39.5
040268	8.5	8,326	341	33.6
063021	8.1	5,871	190	34.4
133019	9.0	5,139	211	35.1
183002	9.6	6,284	283	36.0
200201	7.7	7,889	196	35.4
200202	7.5	5,727	144	34.6
200203	11.2	4,669	229	39.5
200204	11.3	6,918	240	43.4
200205	7.3	9,151	215	34.5
200206	7.7	8,319	180	36.6
200207	10.9	6,499	247	41.3
200208	10.9	7,143	304	40.1
200209	8.4	9,262	217	38.3
200210	8.5	7,823	197	38.0
200211	11.2	5,009	211	41.1
200212	11.1	8,015	261	43.5
200259	11.9	8,530	337	43.7
273003	7.6	5,311	150	33.9
370201	9.2	6,998	201	39.0
370202	8.9	6,278	124	41.8
370203	11.9	5,381	144	48.1
370204	11.6	7,344	137	51.7
370205	8.0	26,919	163	51.8
370206	8.4	13,633	159	45.6
370207	11.7	11,117	146	56.8
370208	11.2	21,598	202	59.8
370209	8.6	8,114	263	36.0

Section	*h* (Inch)	*E* (ksi)	*k* (psi/Inch)	*l* (Inch)
370210	9.1	7,097	144	42.2
370211	11.5	7,358	148	50.4
370212	11.2	9,266	278	44.7
370259	10.8	9,366	221	46.2
370260	11.6	13,428	210	54.0
390201	7.9	7,923	205	35.7
390202	8.3	6,192	136	38.6
390203	11.2	4,316	178	41.3
390204	11.1	7,043	319	40.1
390205	8.0	9,227	227	36.5
390206	7.9	7,972	178	37.0
390207	11.2	5,894	235	41.6
390208	11.1	7,680	242	43.9
390209	8.3	7,829	235	35.7
390210	8.0	7,308	218	34.8
390211	11.3	5,697	208	42.8
390212	10.8	8,733	306	41.8
390259	10.9	6,911	280	40.6
390260	11.6	6,576	330	40.4
390261	11.1	7,895	220	45.2
390262	11.5	10,067	303	45.6
390263	11.1	5,399	165	44.2
390264	11.5	7,793	217	46.5
390265	11.2	6,986	304	40.7
493011	10.2	8,620	281	40.8
530201	8.7	4,903	275	31.6
530202	8.3	4,344	202	32.0
530203	11.1	3,241	183	37.9
530204	11.2	5,489	326	37.7
530205	8.5	7,090	395	31.1
530206	8.6	5,495	248	33.1
530207	11.1	4,570	281	37.1
530208	11.2	4,660	406	34.2
530209	9.0	4,353	374	29.2
530210	8.3	5,794	265	32.1
530211	11.8	3,162	323	34.2
530212	11.3	5,301	354	36.8
530259	10.3	4,302	223	36.6

Table 52. Test-section properties using Best Fit method.

Section	*h* (Inch)	*E* (ksi)	*k* (psi/Inch)	*l* (Inch)
040213	7.9	6,889	198	34.8
040214	8.3	5,218	141	36.6
040215	11.0	5,354	229	40.4
040216	11.2	5,474	221	41.5
040217	8.1	7,485	651	26.9
040218	8.3	6,367	298	31.9
040219	10.8	9,261	358	40.8
040220	11.2	7,441	319	40.9
040221	8.1	9,199	236	36.5
040222	8.6	7,571	269	35.1
040223	11.1	7,489	287	41.8

Section	***h*** **(Inch)**	***E*** **(ksi)**	***k*** **(psi/Inch)**	***l*** **(Inch)**
040224	10.6	8,249	262	42.3
040262	8.1	6,991	216	34.8
040263	8.2	8,405	194	37.8
040264	11.5	9,459	203	49.6
040265	10.8	7,389	170	46.5
040266	12.3	7,689	292	45.2
040267	11.3	7,713	371	40.0
040268	8.5	9,942	346	35.0
063021	8.1	5,412	192	33.6
133019	9.0	4,789	197	35.1
183002	9.6	6,414	239	37.7
200201	7.7	6,841	184	34.7
200202	7.5	6,594	161	34.8
200203	11.2	5,951	257	40.8
200204	11.3	5,944	194	44.1
200205	7.3	9,251	199	35.2
200206	7.7	11,652	202	38.7
200207	10.9	8,626	239	44.7
200208	10.9	9,706	239	46.0
200209	8.4	8,088	188	38.4
200210	8.5	9,996	206	39.9
200211	11.2	6,478	209	43.9
200212	11.1	6,864	208	44.3
200259	11.9	8,308	260	46.3
273003	7.6	5,658	143	34.9
370201	9.2	6,622	161	40.6
370202	8.9	7,350	137	42.4
370203	11.9	7,277	147	51.6
370204	11.6	7,882	94	57.8
370205	8.0	19,556	113	52.4
370206	8.4	15,155	143	48.1
370207	11.7	12,355	131	59.9
370208	11.2	12,868	165	55.3
370209	8.6	7,707	230	36.7
370210	9.1	7,664	155	42.2
370211	11.5	7,918	137	52.3
370212	11.2	8,365	236	45.4
370259	10.8	9,843	177	49.4
370260	11.6	13,495	185	55.8
390201	7.9	7,487	167	37.1
390202	8.3	7,175	131	40.4
390203	11.2	6,029	212	43.0
390204	11.1	6,460	258	41.3
390205	8.0	6,748	196	35.0
390206	7.9	7,568	179	36.5
390207	11.2	7,025	252	42.7
390208	11.1	6,787	200	44.6
390209	8.3	7,705	212	36.5
390210	8.0	8,032	249	34.4
390211	11.3	6,912	235	43.6
390212	10.8	8,148	252	43.2
390259	10.9	6,176	232	41.4

Section	*h* (Inch)	*E* (ksi)	*k* (psi/Inch)	*l* (Inch)
390260	11.6	6,166	273	41.6
390261	11.1	10,289	239	47.3
390262	11.5	10,810	226	49.9
390263	11.1	6,366	180	45.1
390264	11.5	5,351	163	45.4
390265	11.2	6,821	247	42.6
493011	10.2	8,425	248	41.9
530201	8.7	4,738	263	31.7
530202	8.3	5,194	246	31.9
530203	11.1	4,073	210	38.8
530204	11.2	5,233	297	38.1
530205	8.5	6,523	362	31.2
530206	8.6	5,198	282	31.6
530207	11.1	5,846	305	38.7
530208	11.2	4,361	363	34.6
530209	9.0	4,227	380	28.8
530210	8.3	6,637	271	33.1
530211	11.8	3,767	362	34.7
530212	11.3	5,001	315	37.4
530259	10.3	5,296	261	37.1

SLAB-BY-SLAB ANALYSIS

Karamihas and Senn describe the method of estimating PSG for each slab profile. The analysis steps are summarized in this section.[(2)]

Step 1: Crop the Profile

Crop the profile of the slab to exclude the negative spikes at the joints, the small area near the joint where downward spikes were detected during the joint-finding procedure described in appendix E. The start-of-range and end-of-range values shown in Table 48 define the excluded areas. For example, the first two joints in section 390203 appear at 11.32 and 26.34 ft. To avoid the possibility of including a downward spike in curve fit, the slab profile is cropped to run from 11.42 through 26.25 ft.

Step 2: Shift

Move the origin of the horizontal scale to the longitudinal slab center.

Step 3: Detrend

Detrend the measured slab profile. Apply a least-squares linear fit to the profile segment and subtract the best-fit line.

Step 4: Curve Fit

Perform a nonlinear curve fit of the Westergaard model to the measured slab profile. In this study, curve fitting was performed using functions MRQMIN and MRQCOF provided in

Numerical Recipes.[104] These routines perform a nonlinear least-squares curve fit using the Levenberg–Marquardt algorithm. PSG, as defined in Figure 169, is the only fitted parameter.

APPENDIX G. PSG VERSUS TIME USING THE BEST FIT METHOD

This appendix provides plots of PSG versus age for the 83 jointed PCC test sections included in this study (figure 170 through figure 252). PSG values were derived using radius of relative stiffness values produced by the Best Fit method. PSG values are expressed in units of microstrain per inch (με/inch). PSG values for each visit are a weighted average of all slab-by-slab values from repeat passes selected for that monitoring visit. The average typically included five repeat passes. A weighting is assigned to each PSG value in proportion to the corresponding slab length. For slabs that straddle test-section boundaries, a weighting is assigned to the PSG value in proportion to the length within the test section.

On the SPS-2 sections, the age is the time elapsed since the project was opened to traffic. On the GPS-3 sections, the age is the time elapsed since the construction date. Figures for sections from the same SPS-2 project use the same age scale.

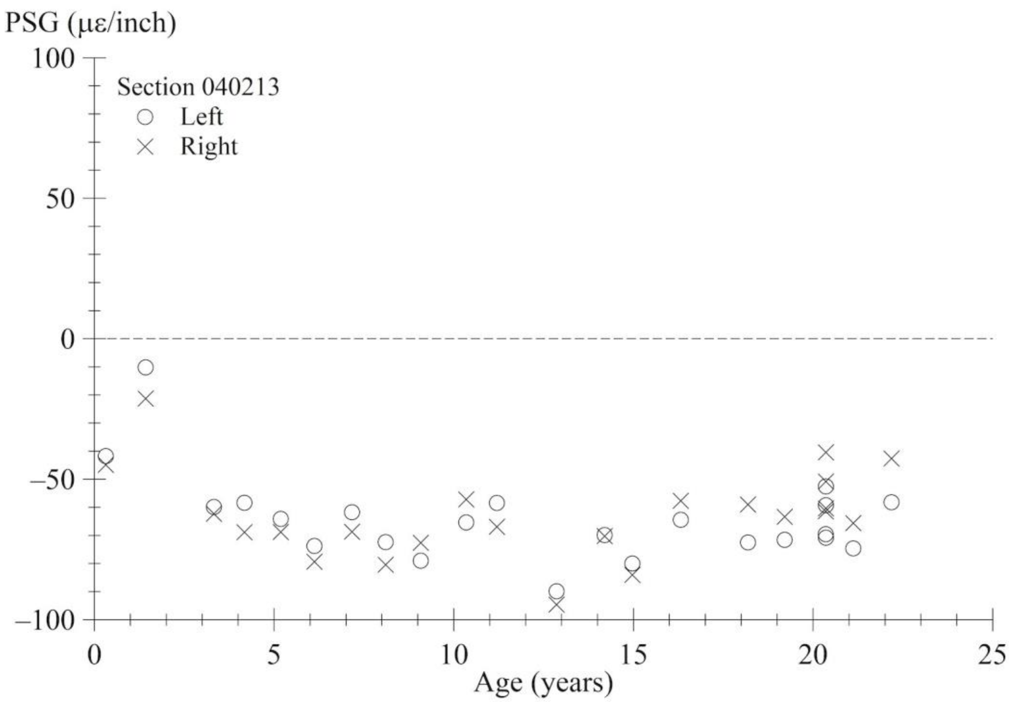

Source: FHWA.

Figure 170. Graph. PSG progression using Best Fit method for section 040213.

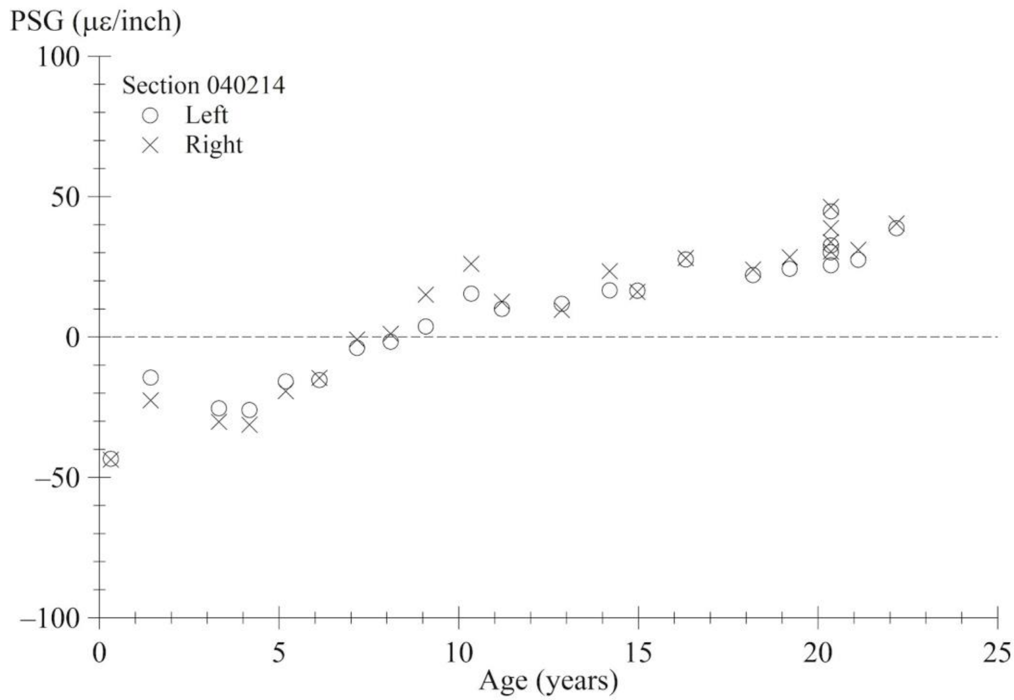

Source: FHWA.

Figure 171. Graph. PSG progression using Best Fit method for section 040214.

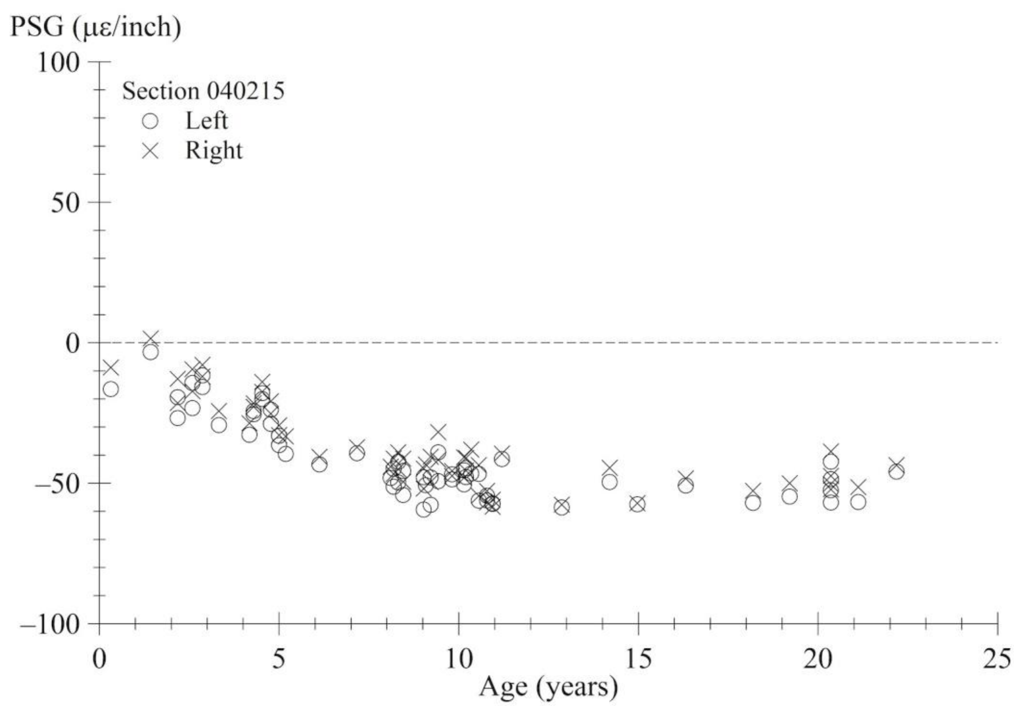

Source: FHWA.

Figure 172. Graph. PSG progression using Best Fit method for section 040215.

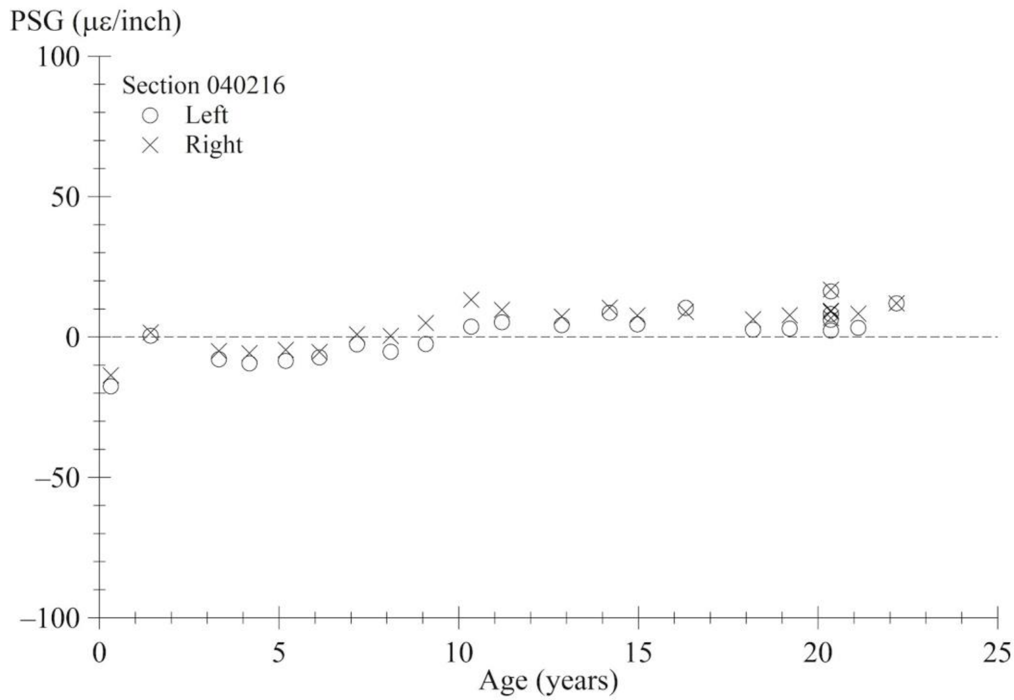

Source: FHWA.

Figure 173. Graph. PSG progression using Best Fit method for section 040216.

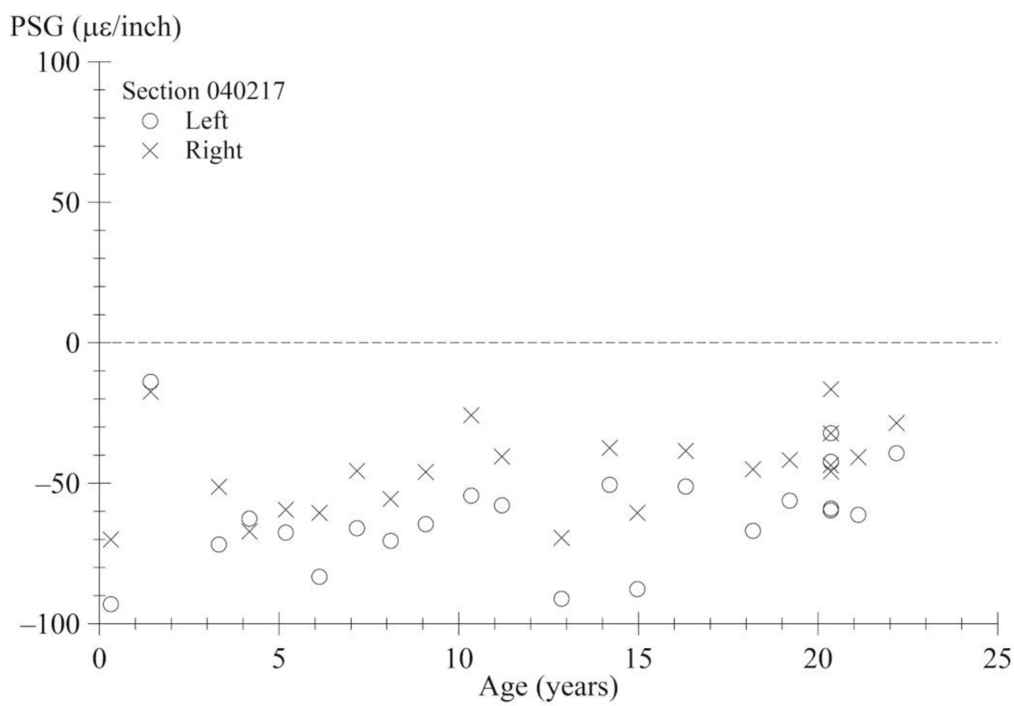

Source: FHWA.

Figure 174. Graph. PSG progression using Best Fit method for section 040217.

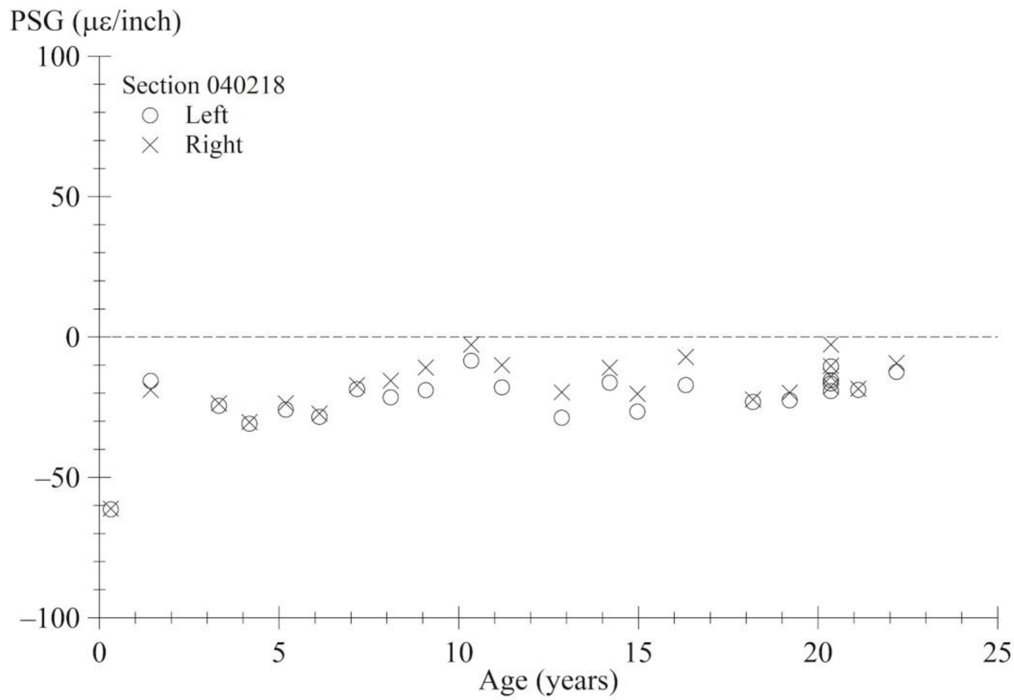

Source: FHWA.

Figure 175. Graph. PSG progression using Best Fit method for section 040218.

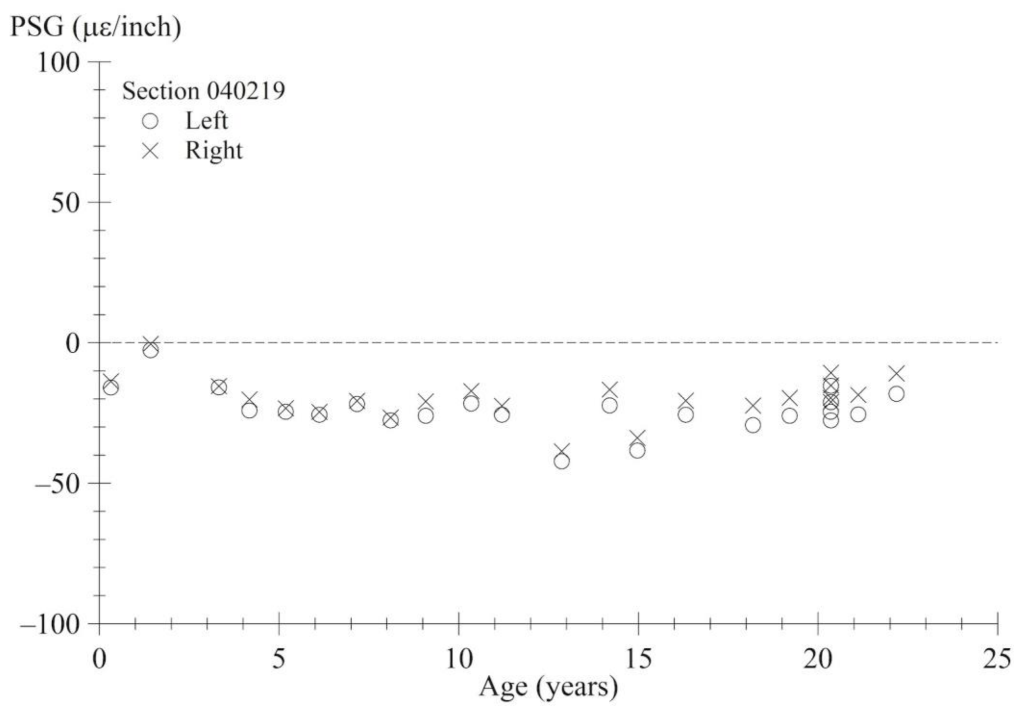

Source: FHWA.

Figure 176. Graph. PSG progression using Best Fit method for section 040219.

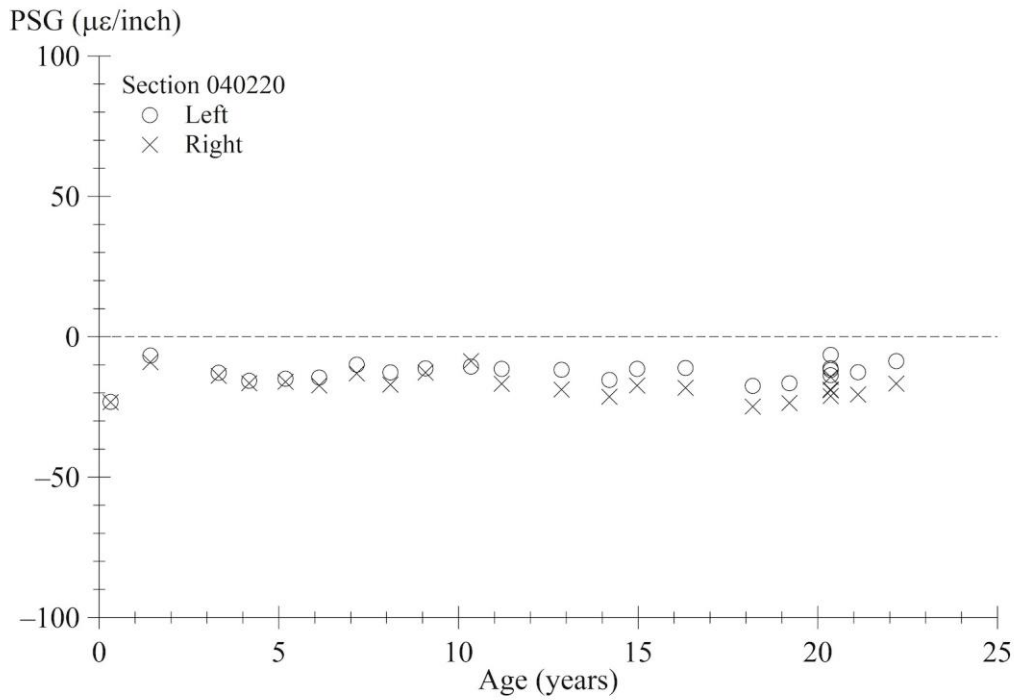

Source: FHWA.

Figure 177. Graph. PSG progression using Best Fit method for section 040220.

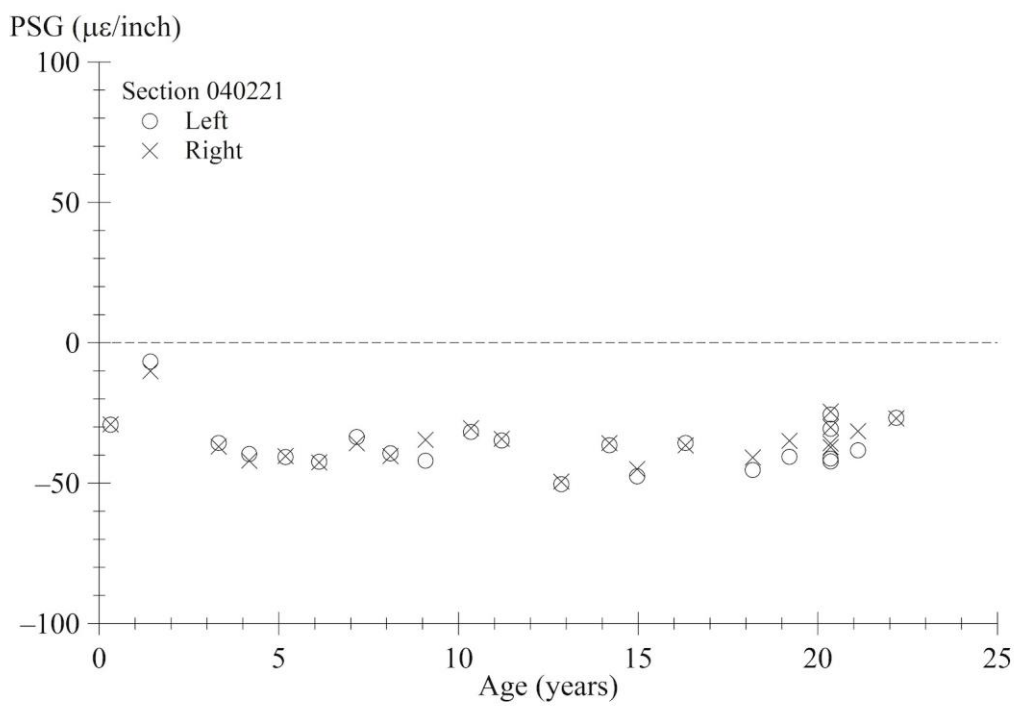

Source: FHWA.

Figure 178. Graph. PSG progression using Best Fit method for section 040221.

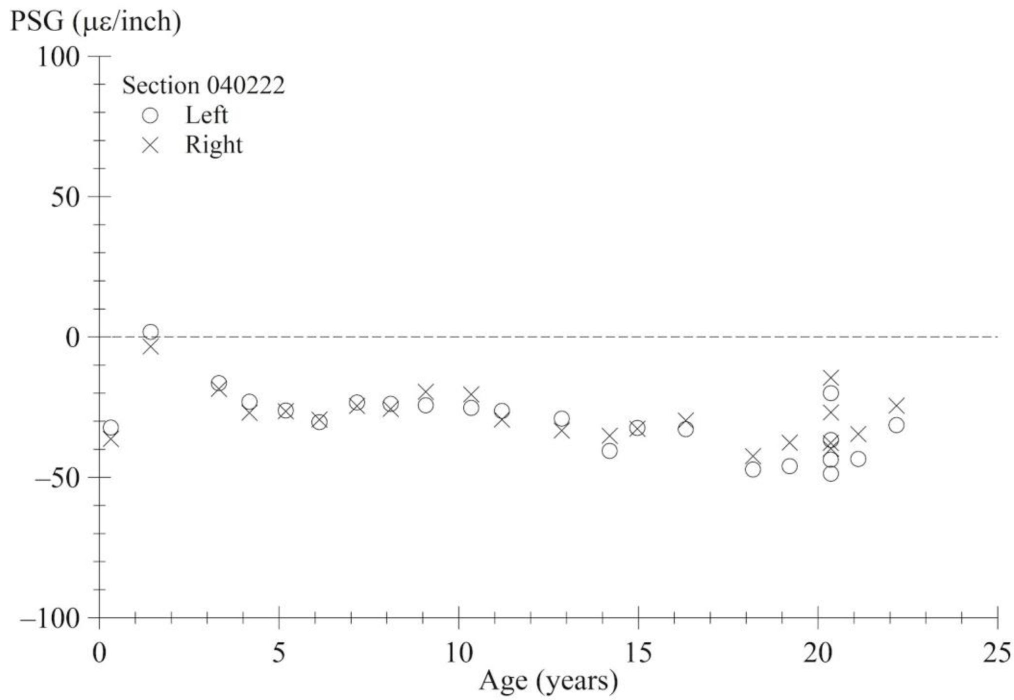

Source: FHWA.

Figure 179. Graph. PSG progression using Best Fit method for section 040222.

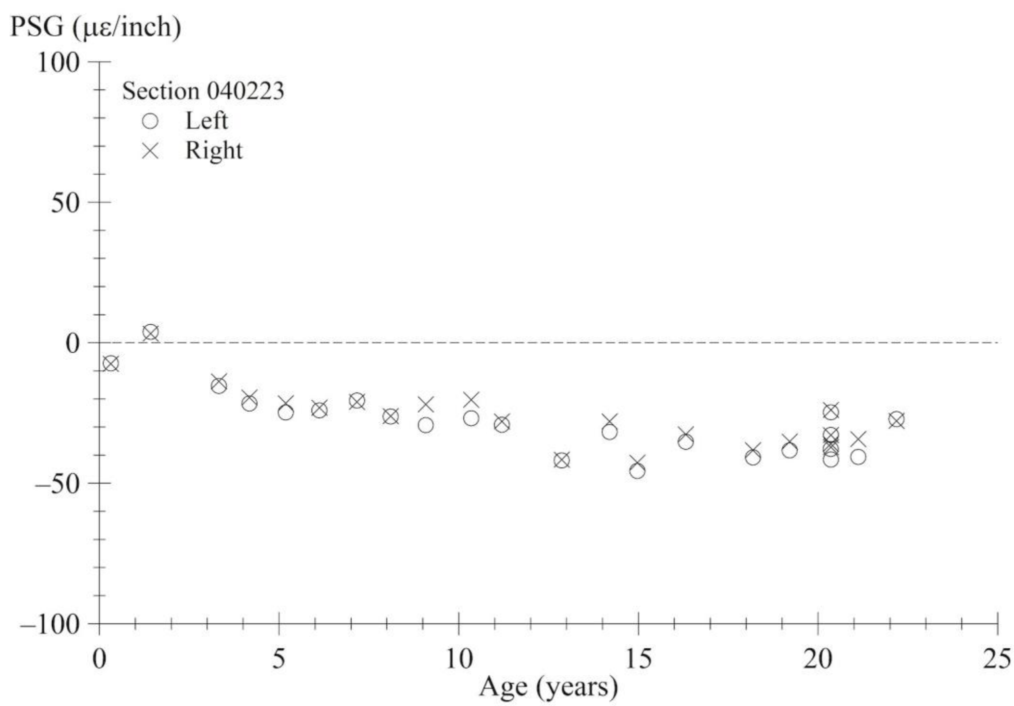

Source: FHWA.

Figure 180. Graph. PSG progression using Best Fit method for section 040223.

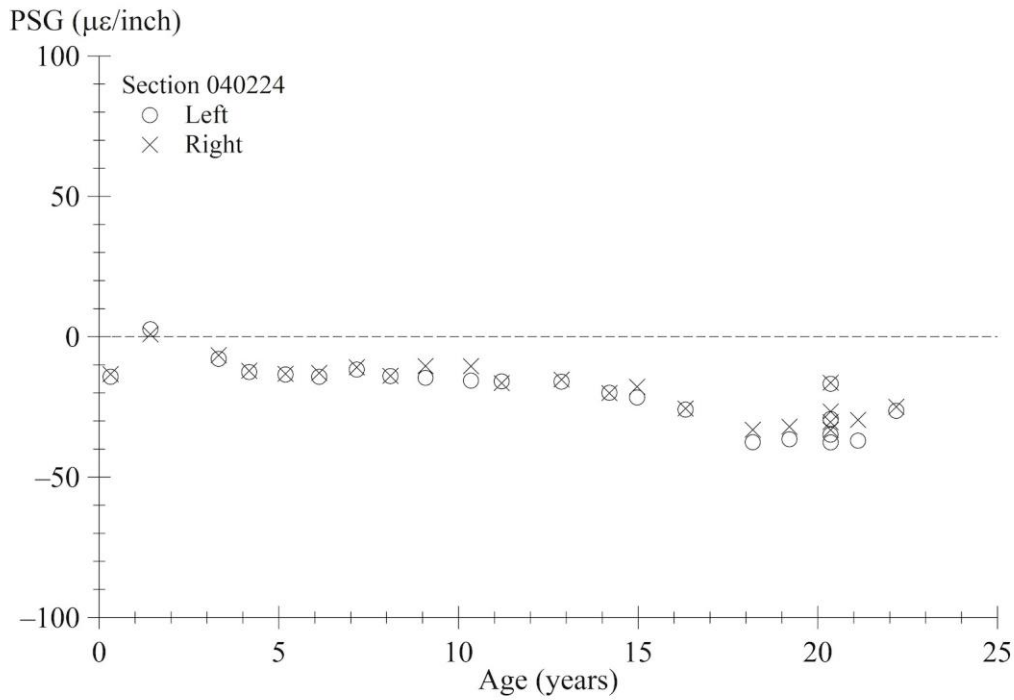

Source: FHWA.

Figure 181. Graph. PSG progression using Best Fit method for section 040224.

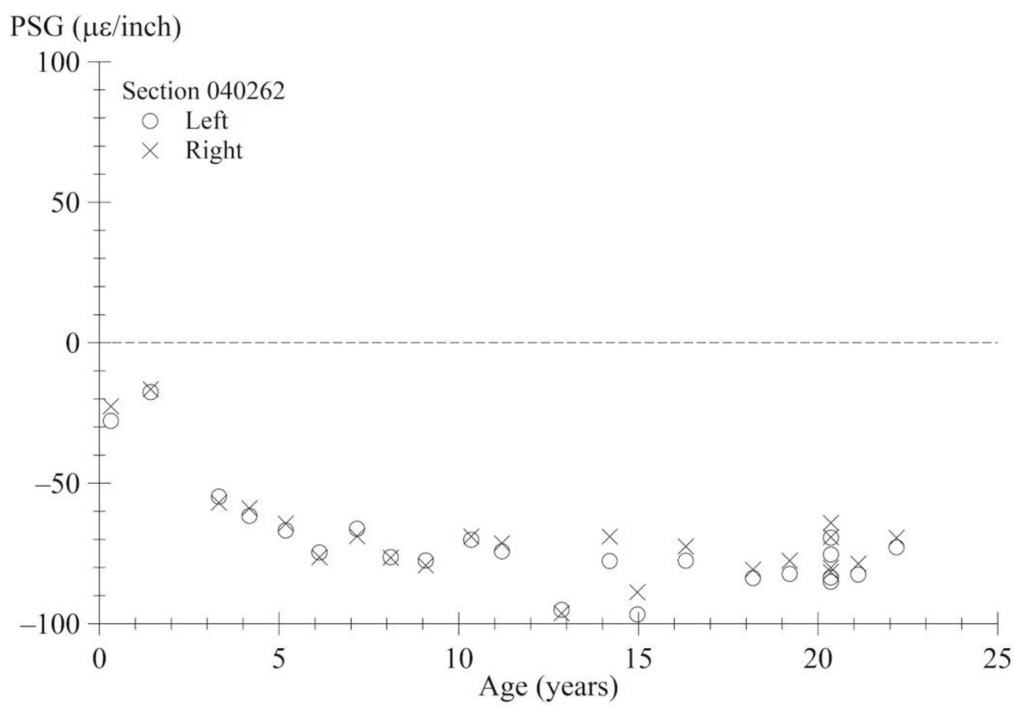

Source: FHWA.

Figure 182. Graph. PSG progression using Best Fit method for section 040262.

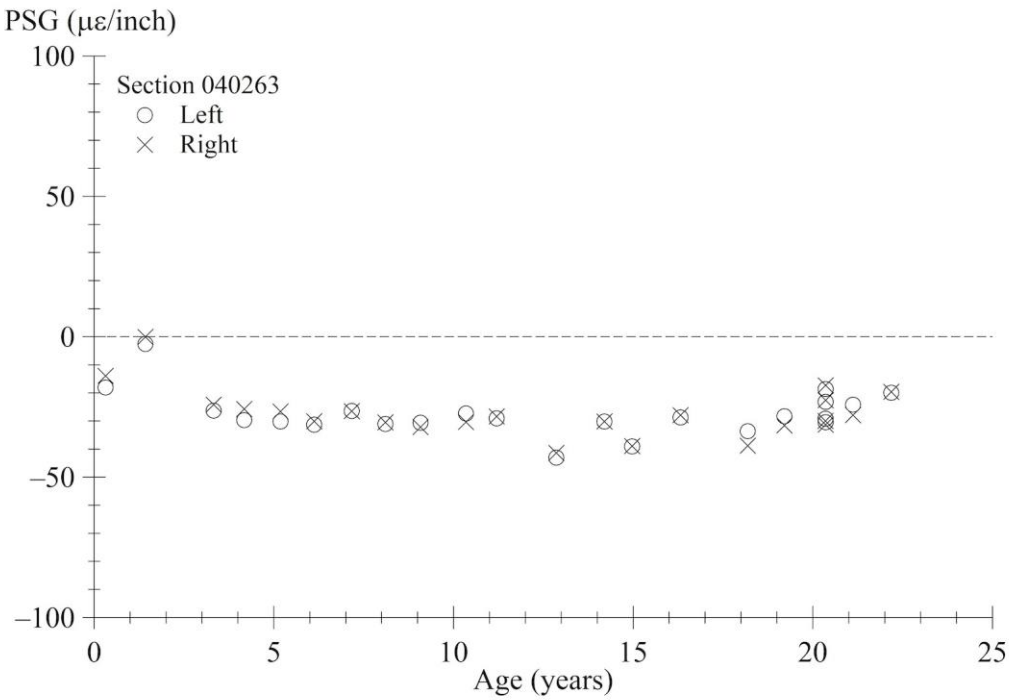

Source: FHWA.

Figure 183. Graph. PSG progression using Best Fit method for section 040263.

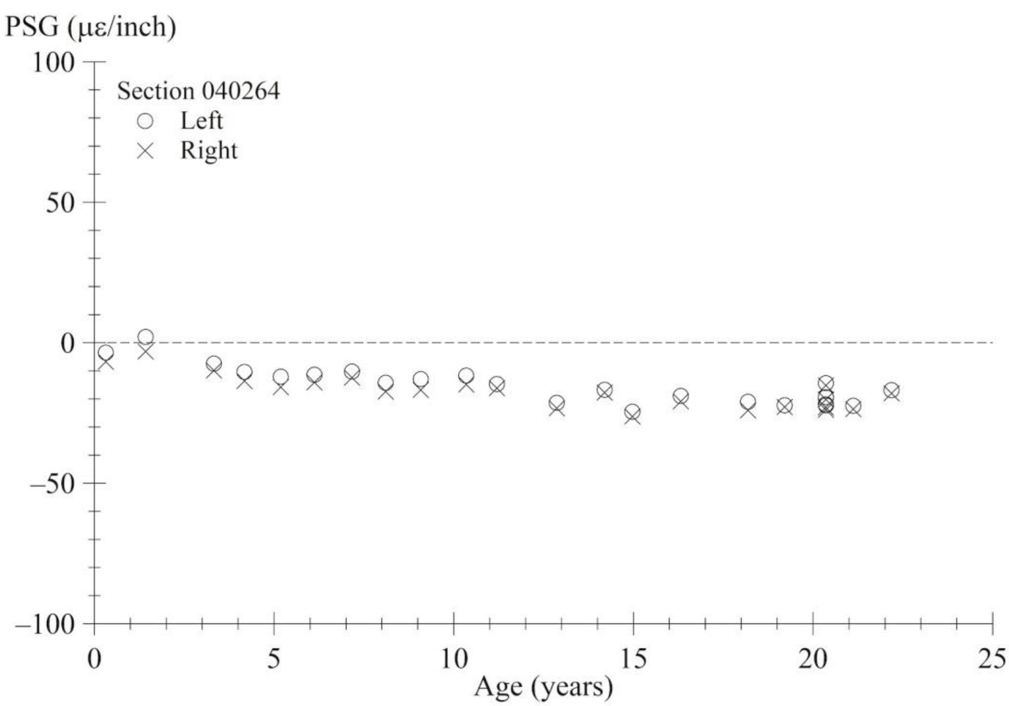

Source: FHWA.

Figure 184. Graph. PSG progression using Best Fit method for section 040264.

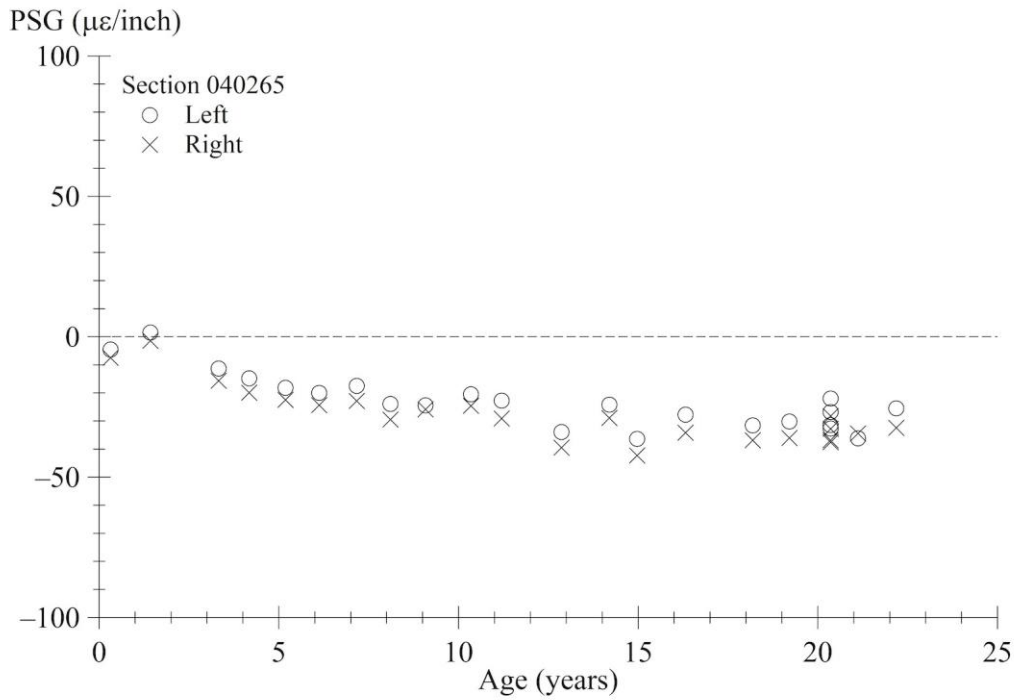

Source: FHWA.

Figure 185. Graph. PSG progression using Best Fit method for section 040265.

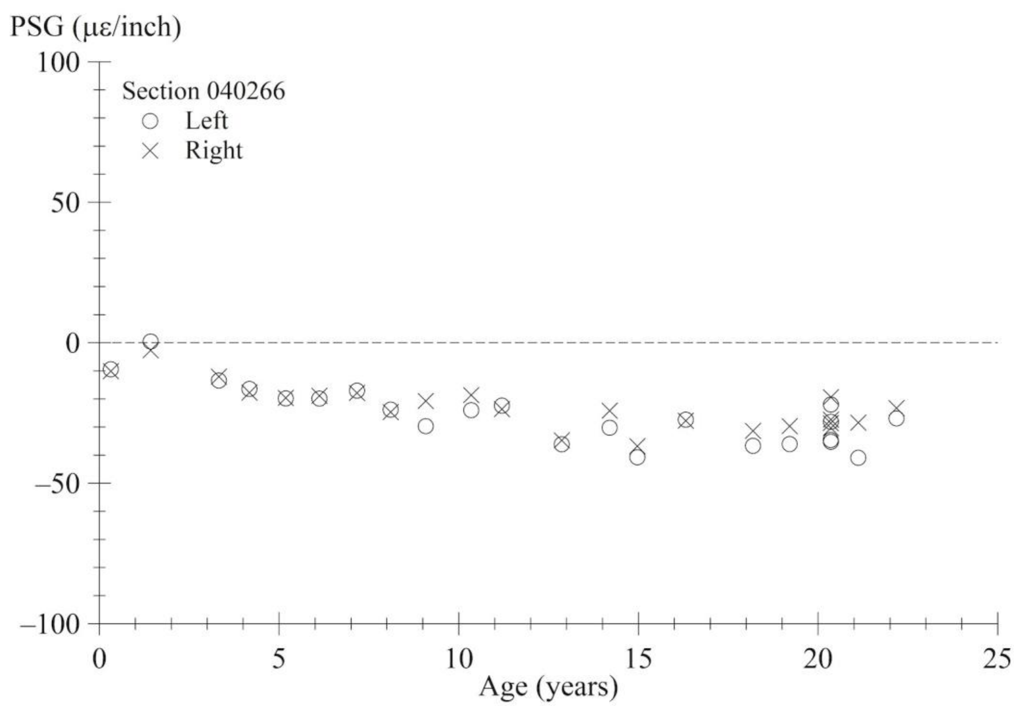

Source: FHWA.

Figure 186. Graph. PSG progression using Best Fit method for section 040266.

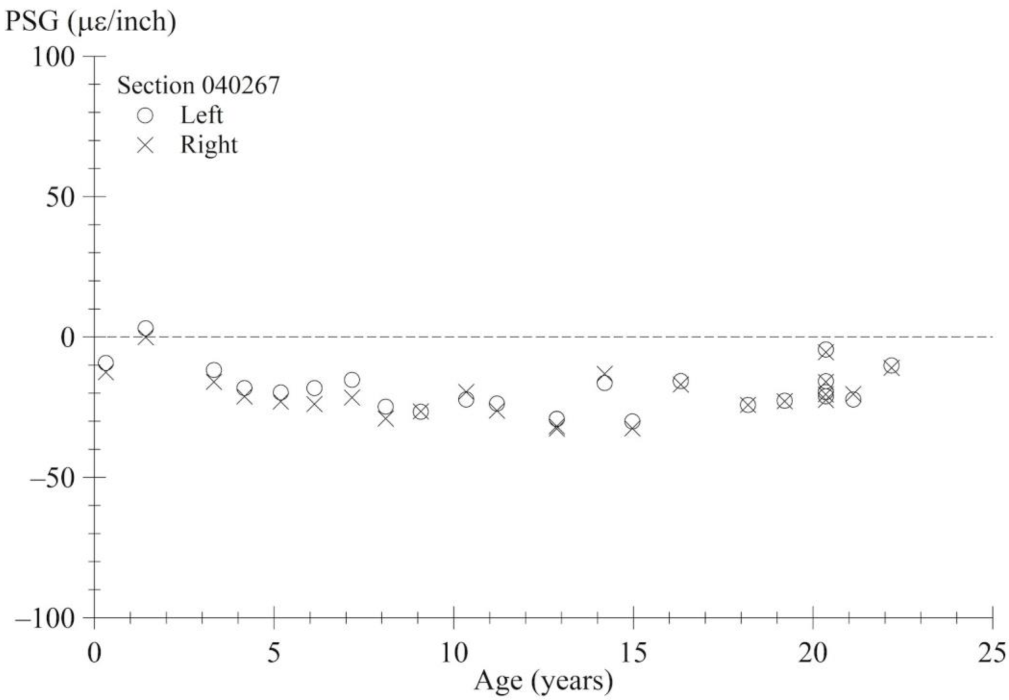

Source: FHWA.

Figure 187. Graph. PSG progression using Best Fit method for section 040267.

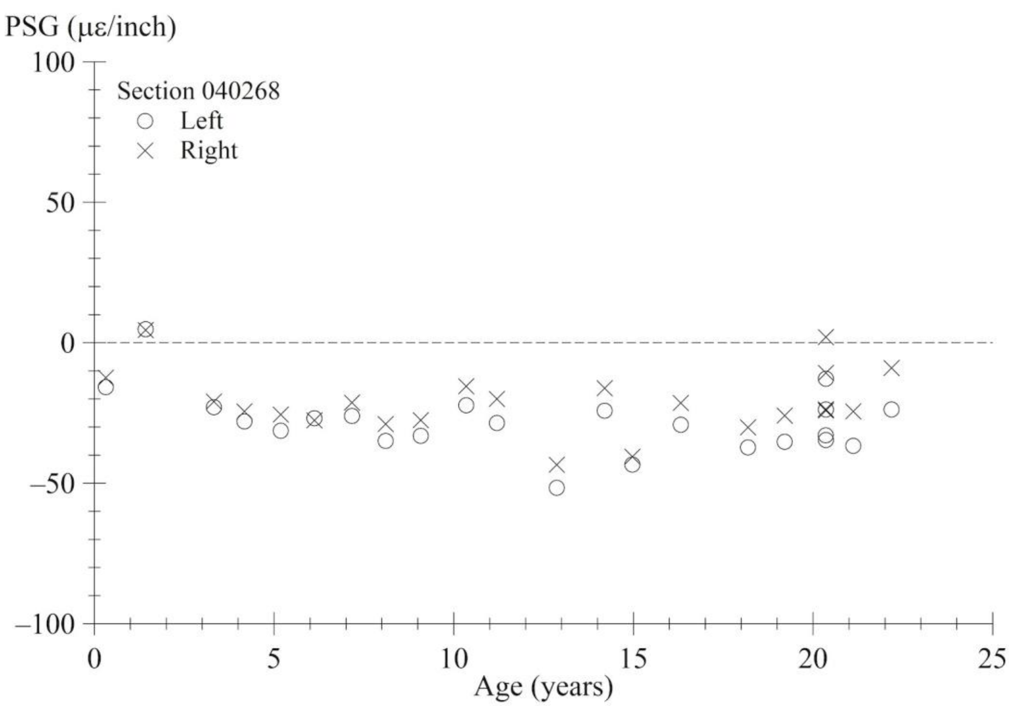

Source: FHWA.

Figure 188. Graph. PSG progression using Best Fit method for section 040268.

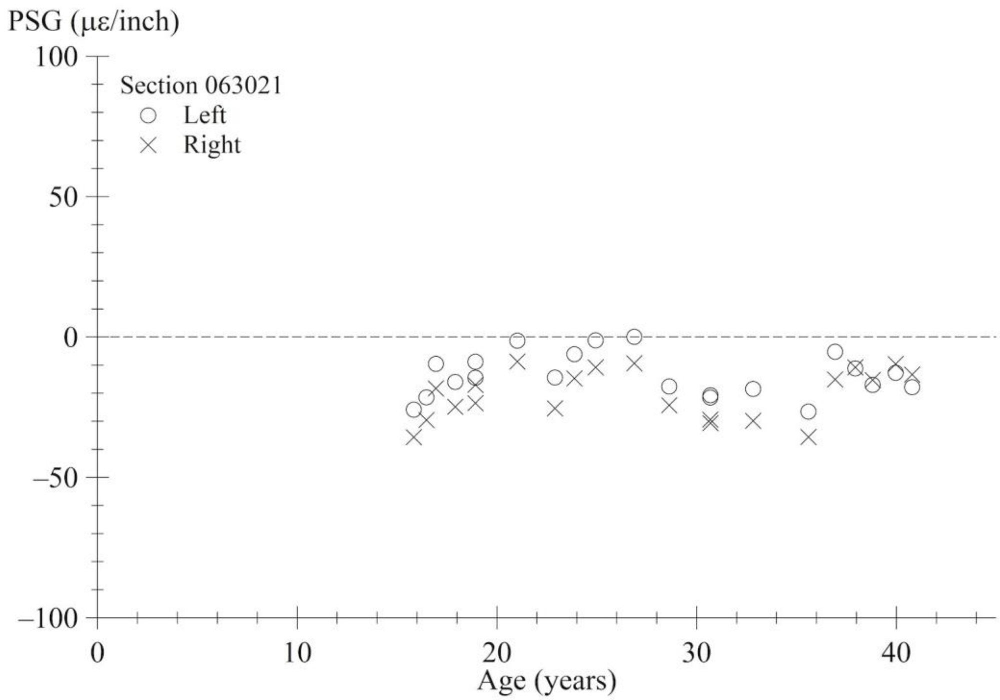

Source: FHWA.

Figure 189. Graph. PSG progression using Best Fit method for section 063021.

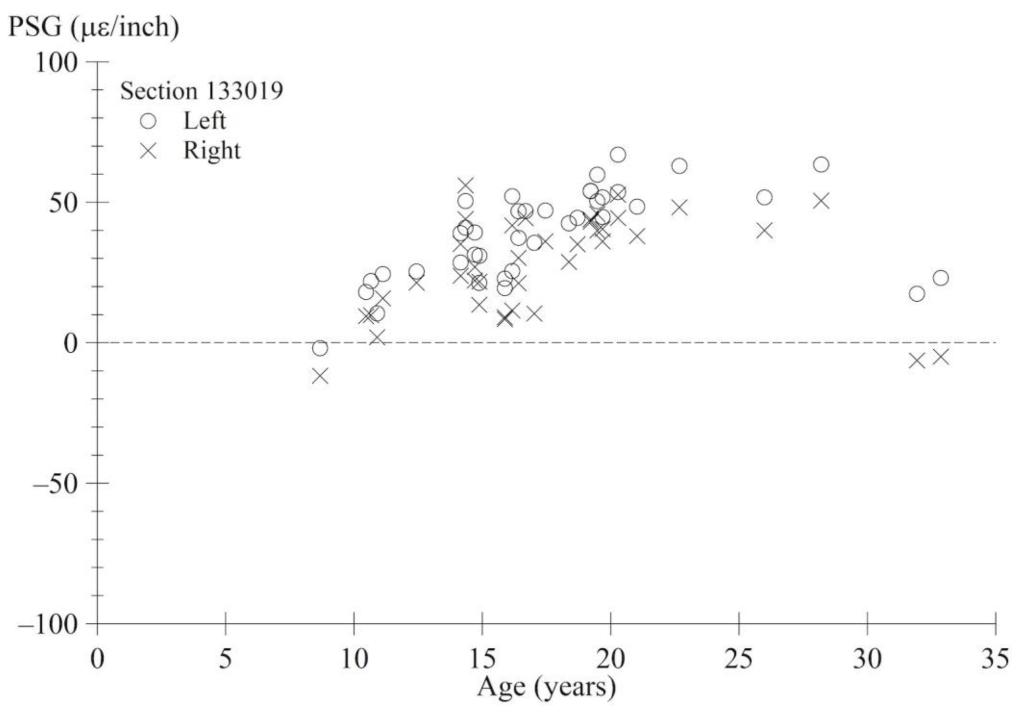

Source: FHWA.

Figure 190. Graph. PSG progression using Best Fit method for section 133019.

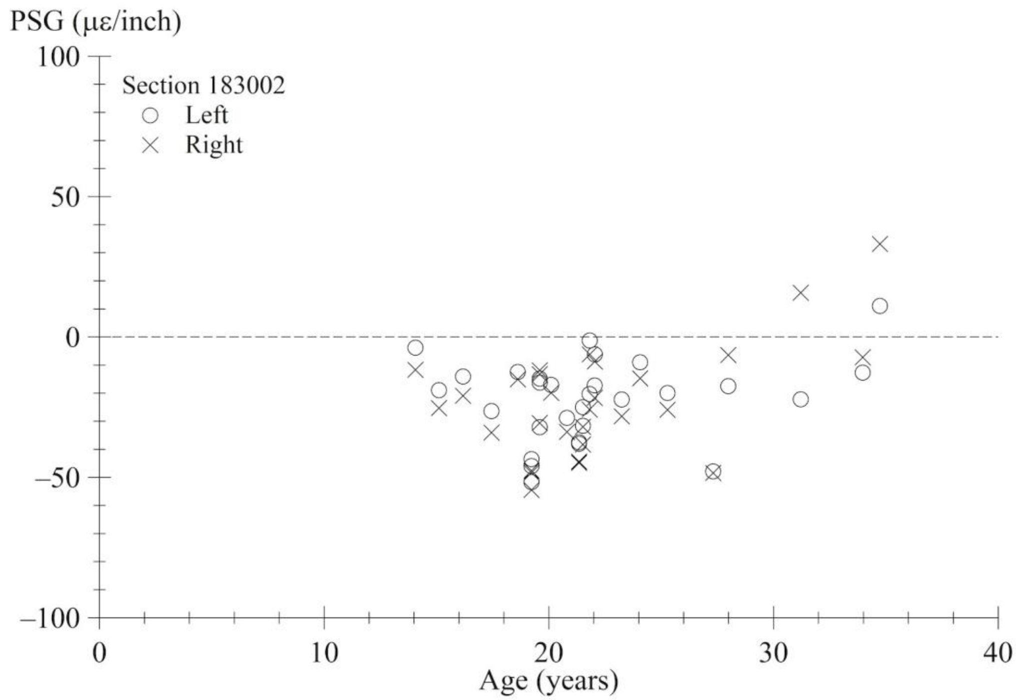

Source: FHWA.

Figure 191. Graph. PSG progression using Best Fit method for section 183002.

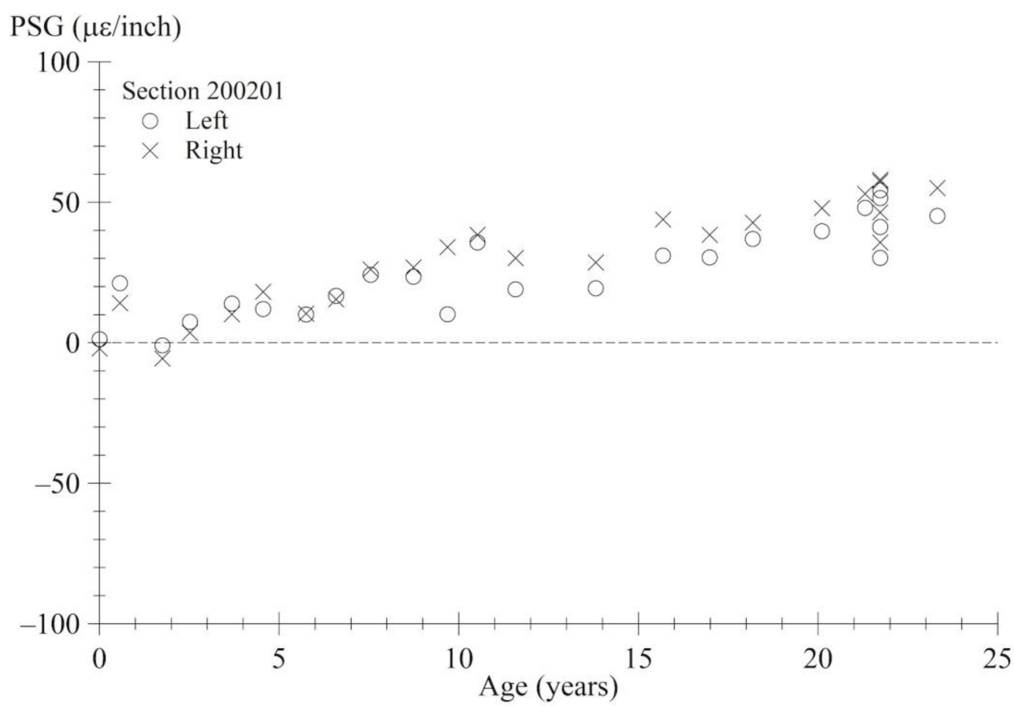

Source: FHWA.

Figure 192. Graph. PSG progression using Best Fit method for section 200201.

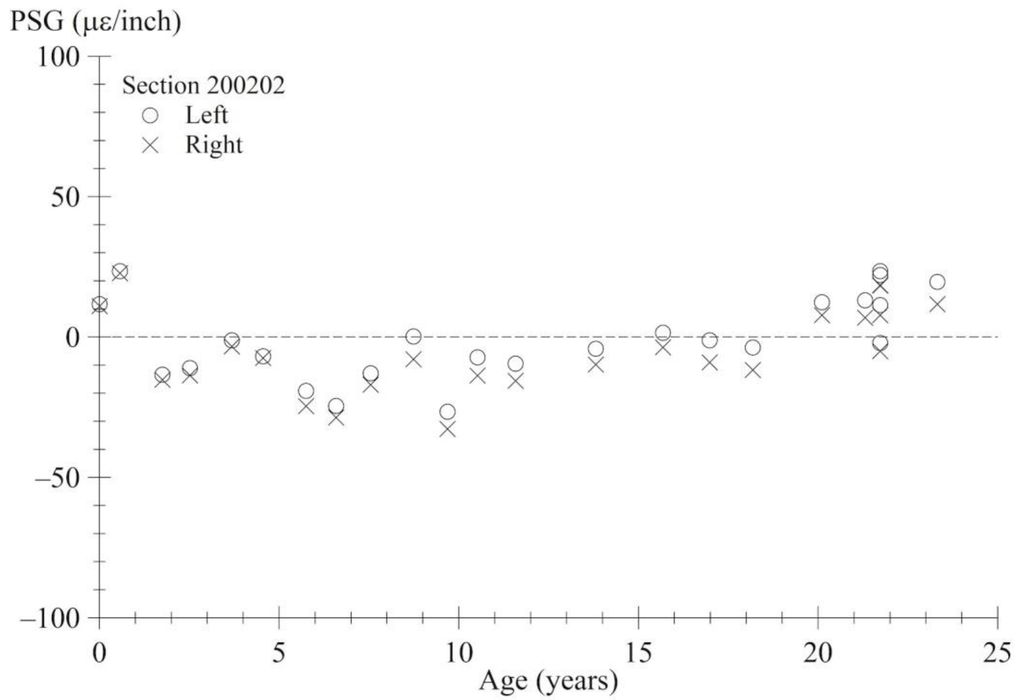

Source: FHWA.

Figure 193. Graph. PSG progression using Best Fit method for section 200202.

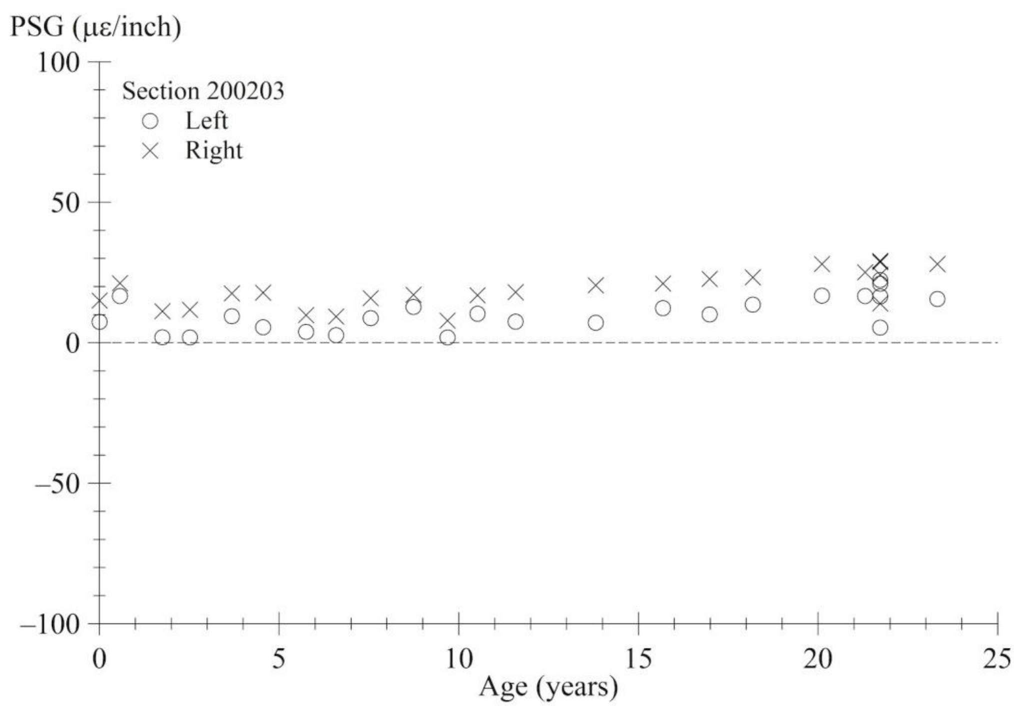

Source: FHWA.

Figure 194. Graph. PSG progression using Best Fit method for section 200203.

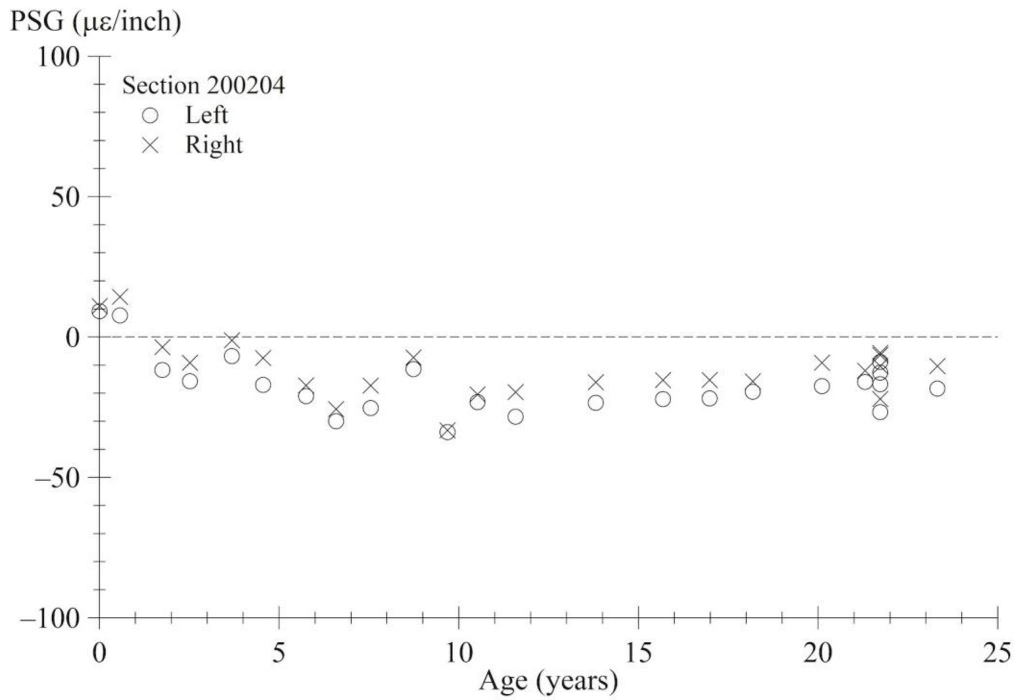

Source: FHWA.

Figure 195. Graph. PSG progression using Best Fit method for section 200204.

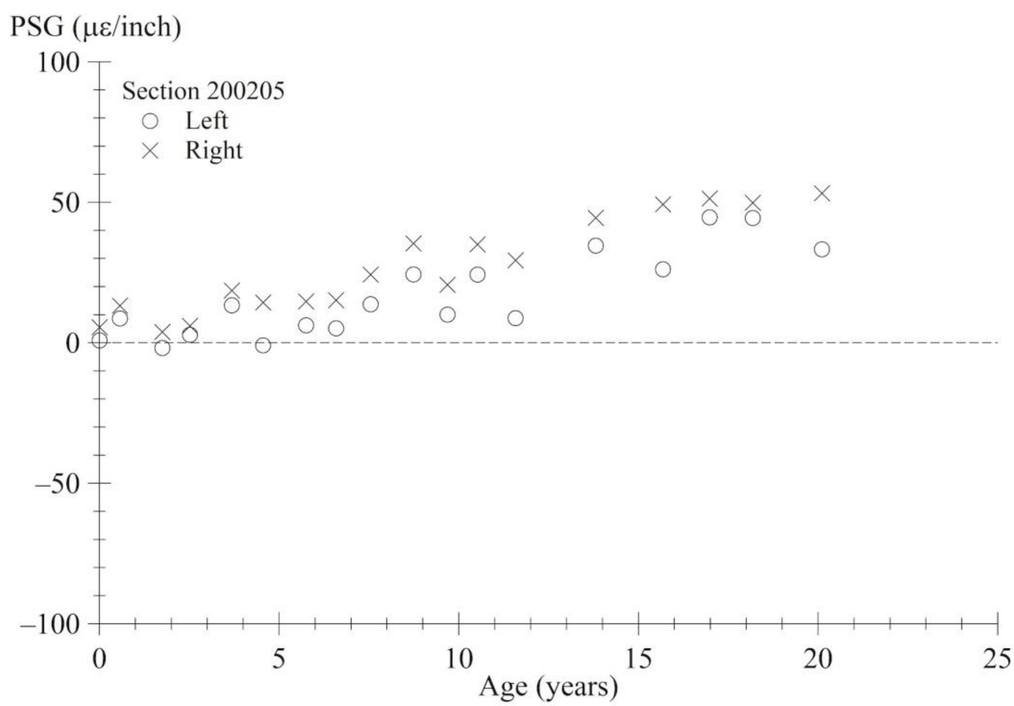

Source: FHWA.

Figure 196. Graph. PSG progression using Best Fit method for section 200205.

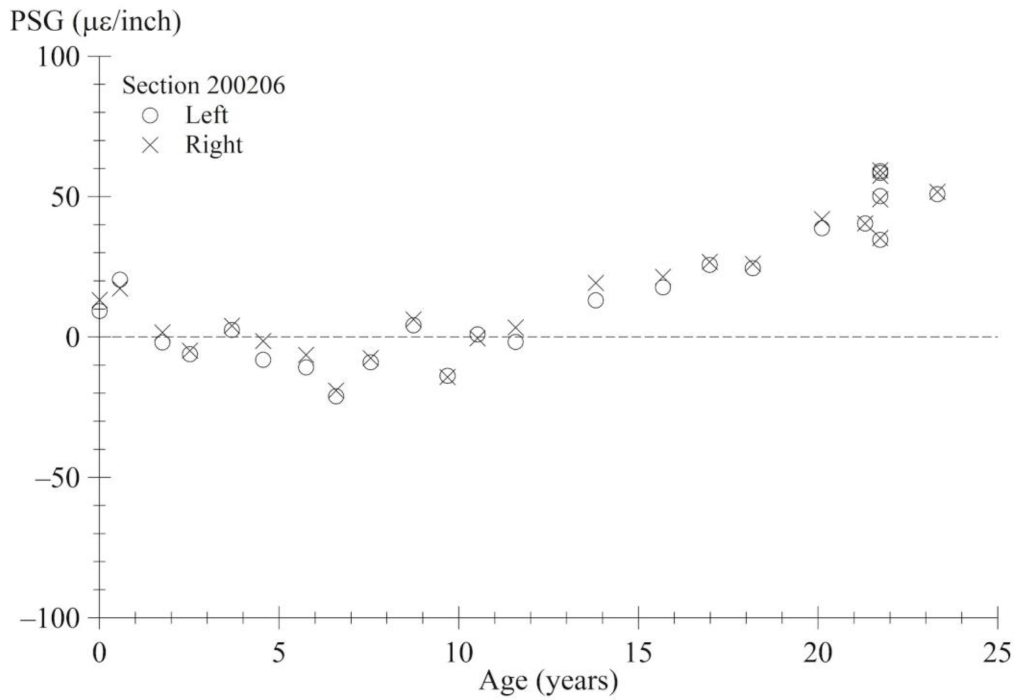

Source: FHWA.

Figure 197. Graph. PSG progression using Best Fit method for section 200206.

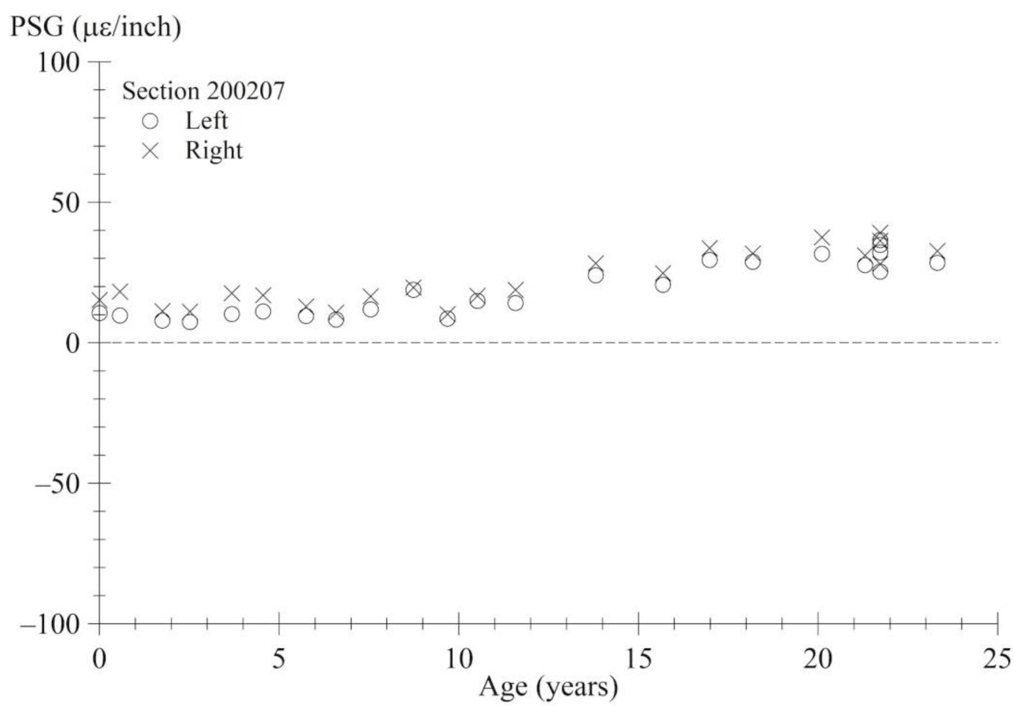

Source: FHWA.

Figure 198. Graph. PSG progression using Best Fit method for section 200207.

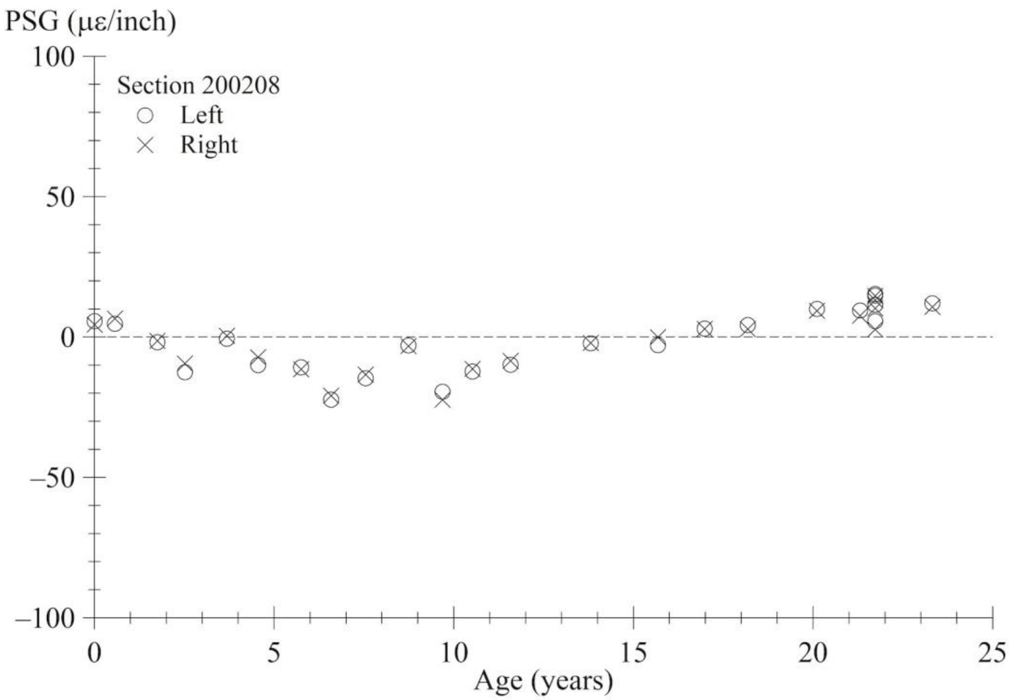

Source: FHWA.

Figure 199. Graph. PSG progression using Best Fit method for section 200208.

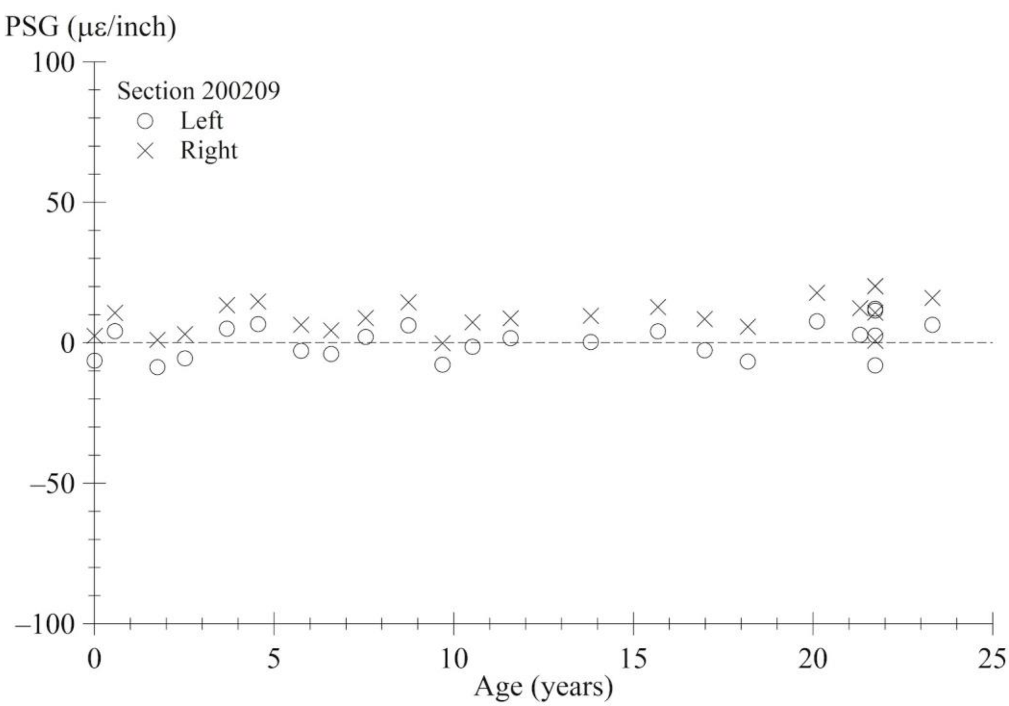

Source: FHWA.

Figure 200. Graph. PSG progression using Best Fit method for section 200209.

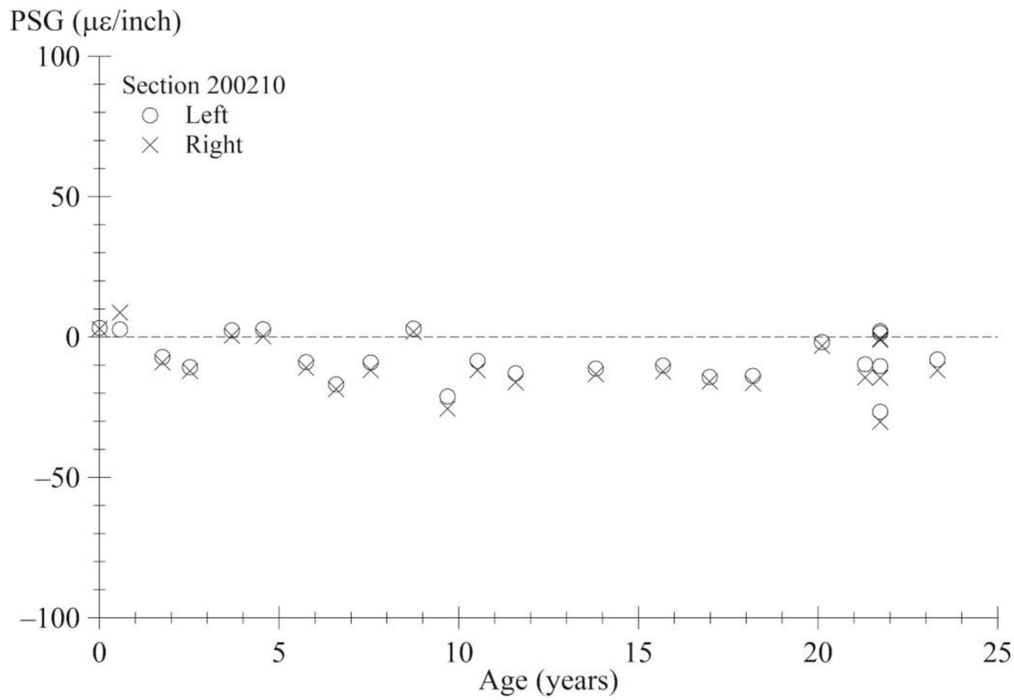

Source: FHWA.

Figure 201. Graph. PSG progression using Best Fit method for section 200210.

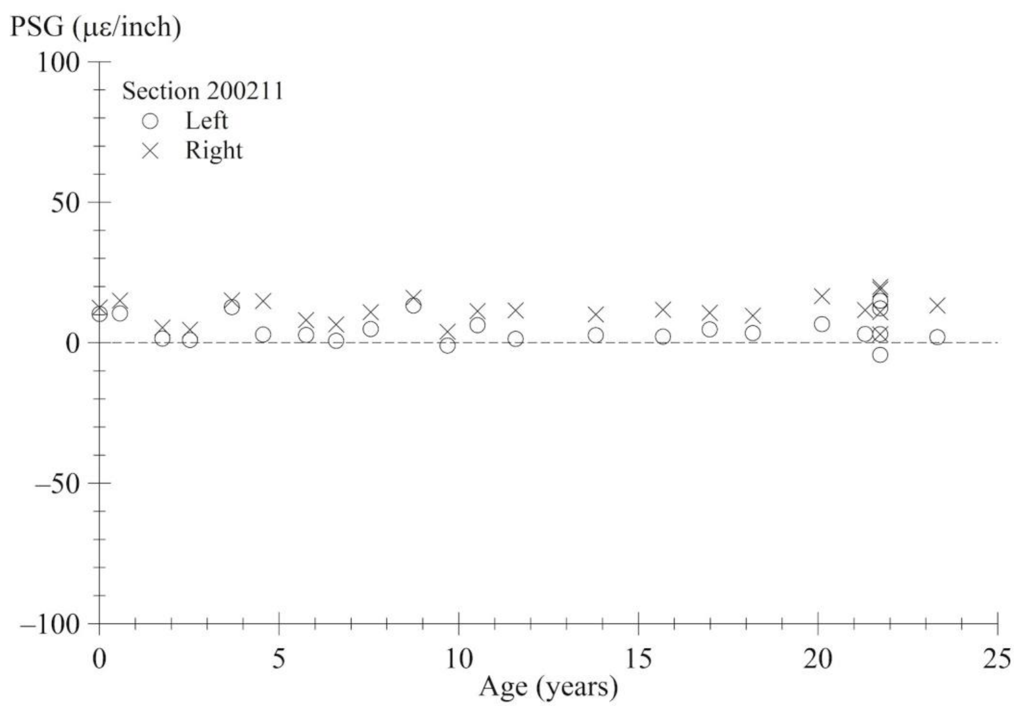

Source: FHWA.

Figure 202. Graph. PSG progression using Best Fit method for section 200211.

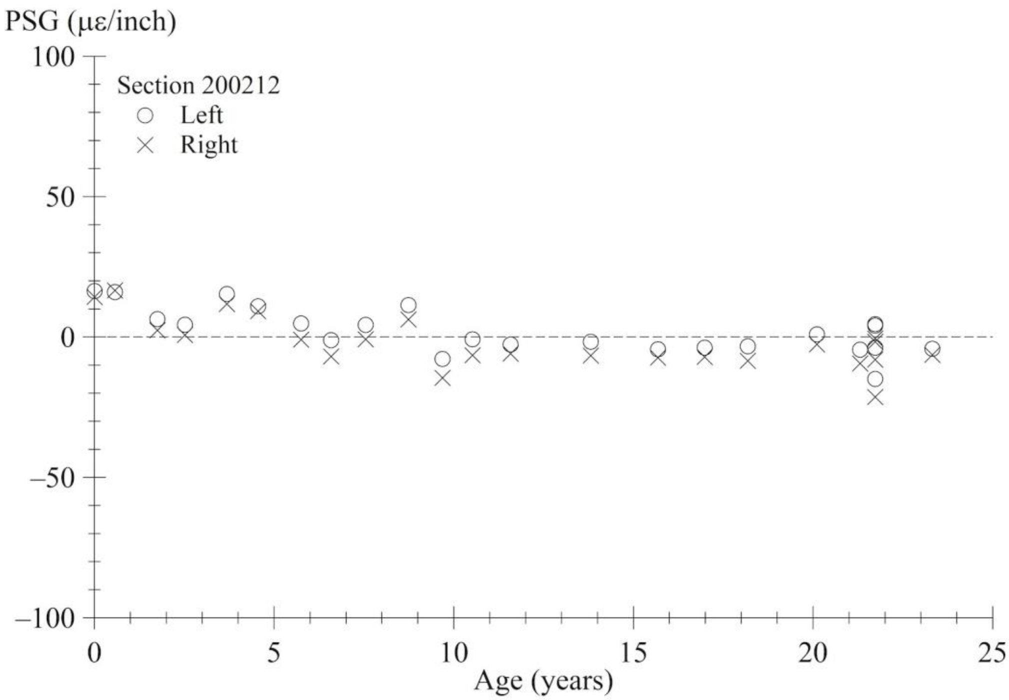

Source: FHWA.

Figure 203. Graph. PSG progression using Best Fit method for section 200212.

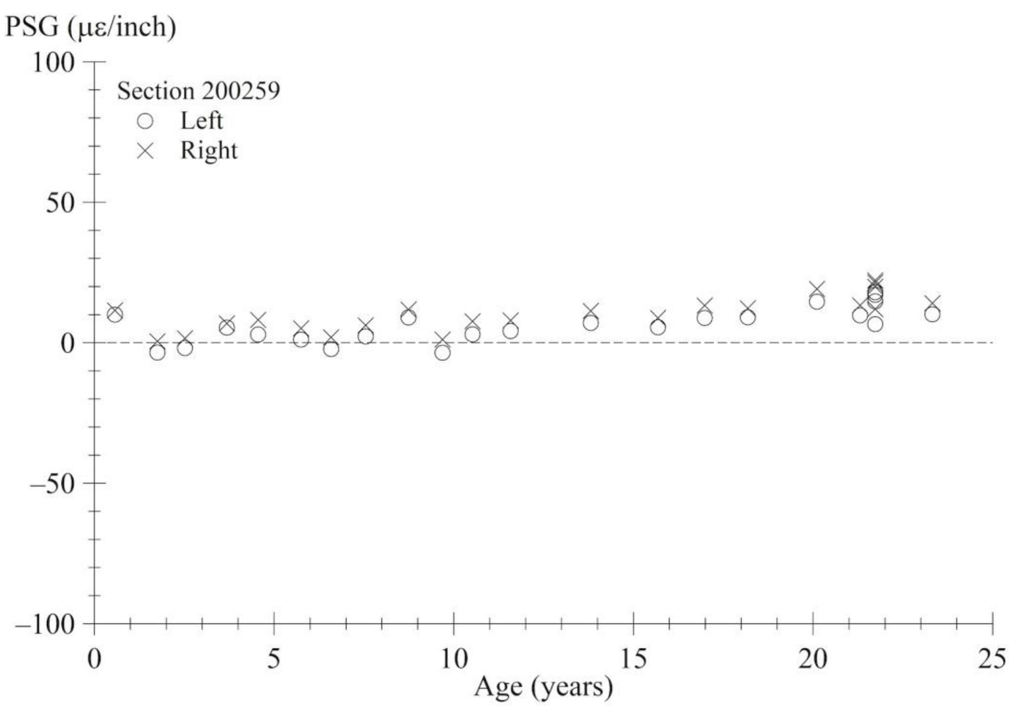

Source: FHWA.

Figure 204. Graph. PSG progression using Best Fit method for section 200259.

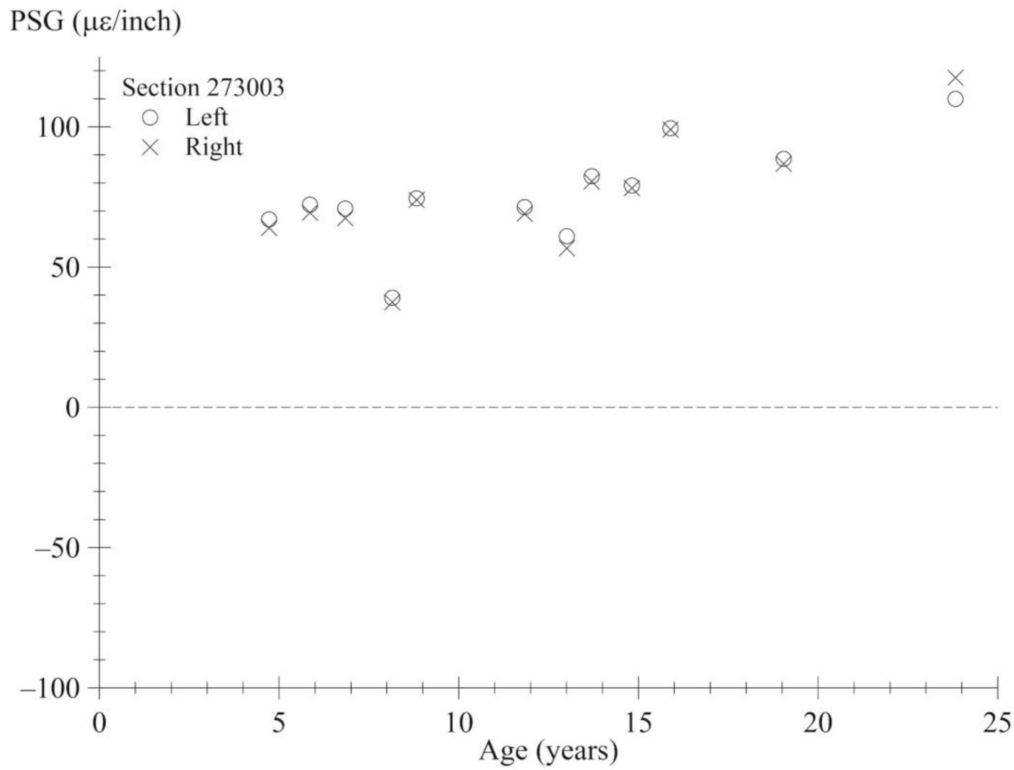

Source: FHWA.

Figure 205. Graph. PSG progression using Best Fit method for section 273003.

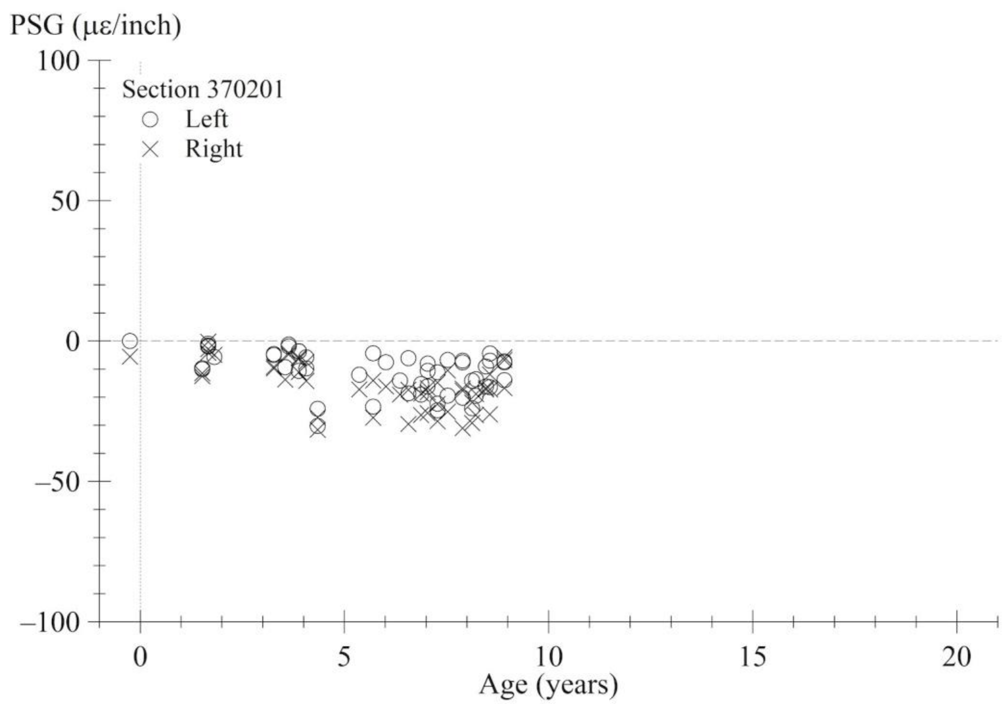

Source: FHWA.

Figure 206. Graph. PSG progression using Best Fit method for section 370201.

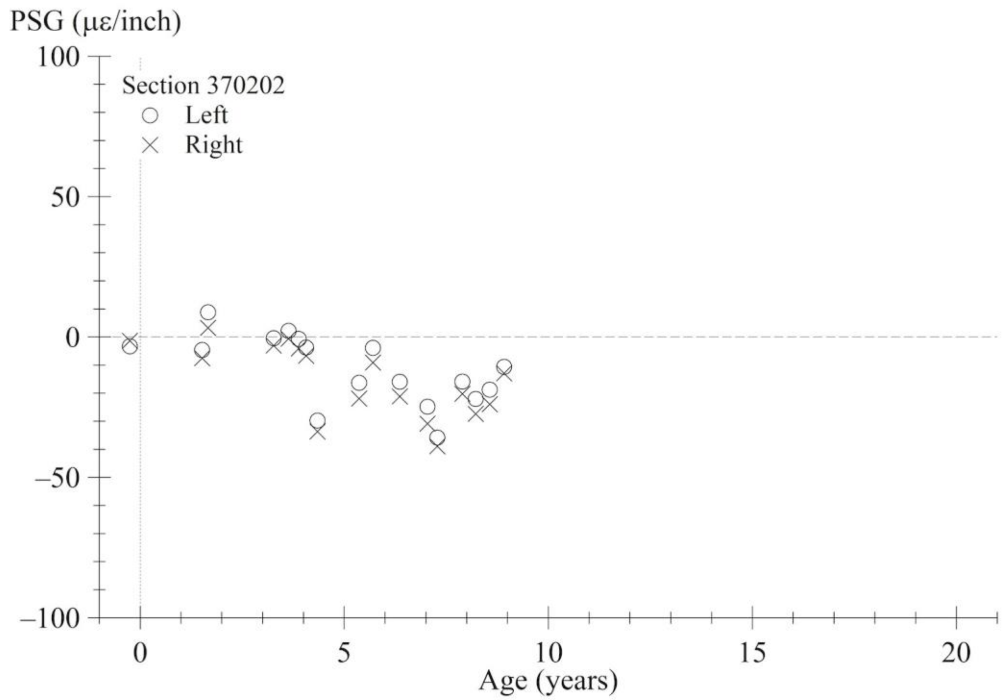

Source: FHWA.

Figure 207. Graph. PSG progression using Best Fit method for section 370202.

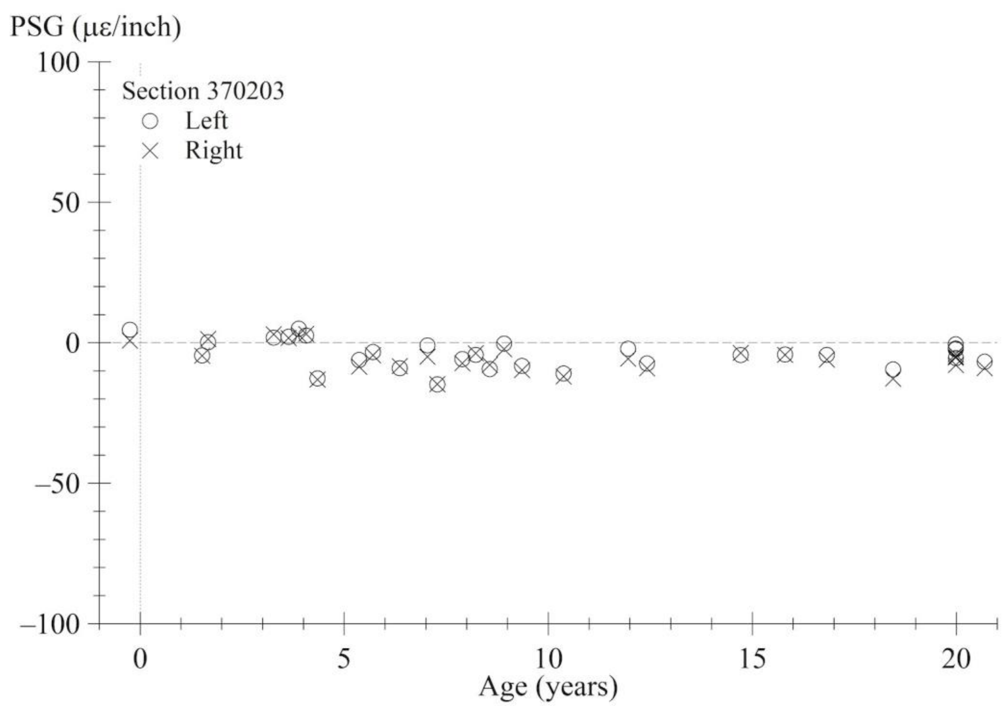

Source: FHWA.

Figure 208. Graph. PSG progression using Best Fit method for section 370203.

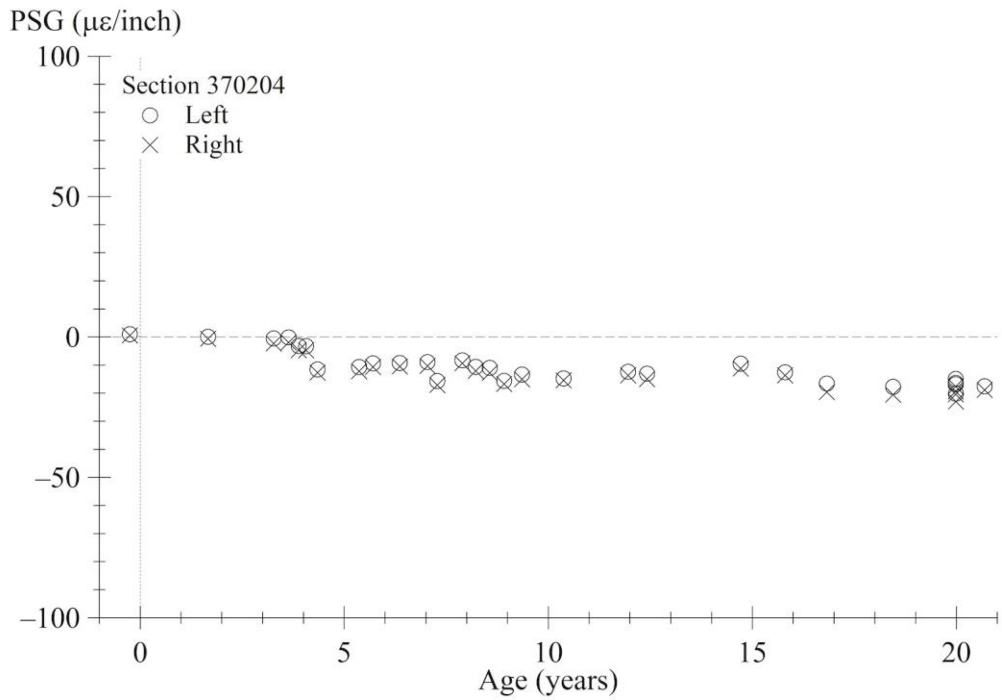

Source: FHWA.

Figure 209. Graph. PSG progression using Best Fit method for section 370204.

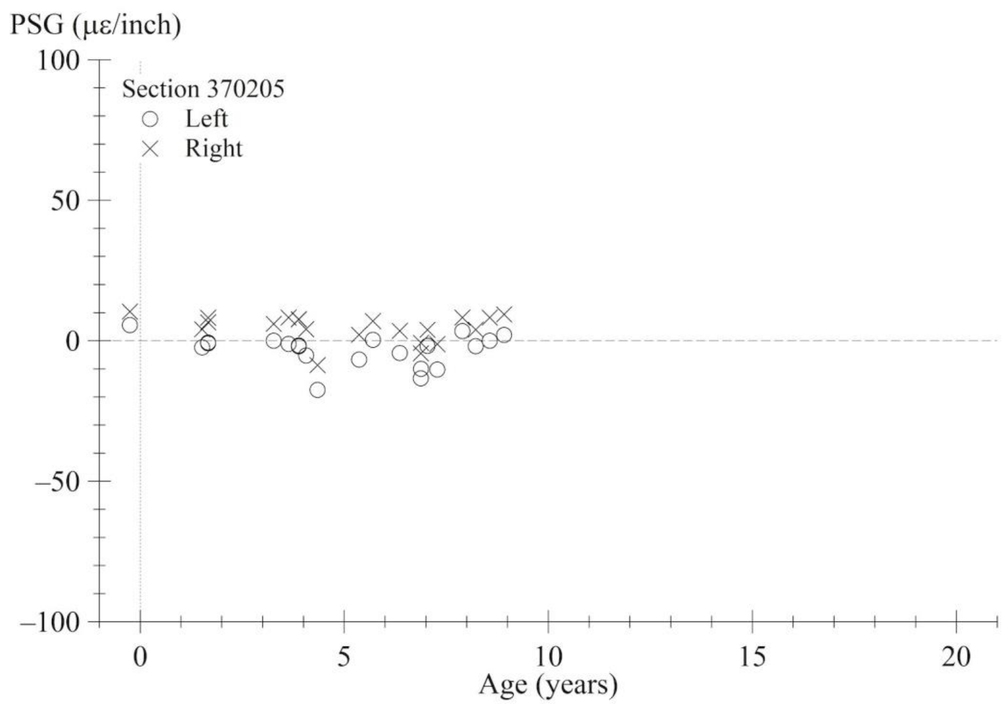

Source: FHWA.

Figure 210. Graph. PSG progression using Best Fit method for section 370205.

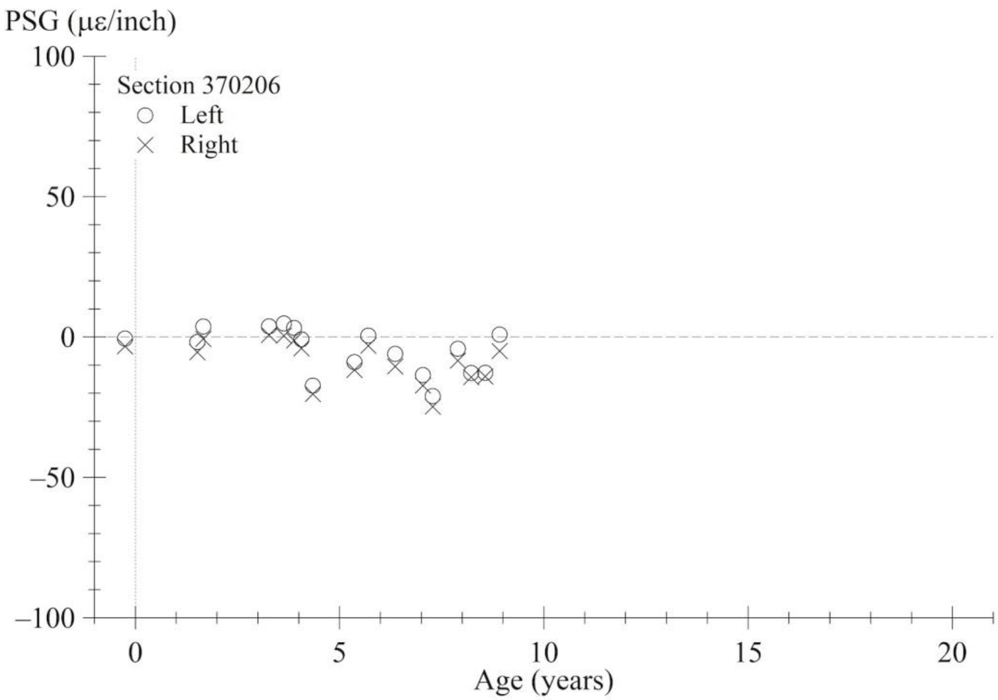

Source: FHWA.

Figure 211. Graph. PSG progression using Best Fit method for section 370206.

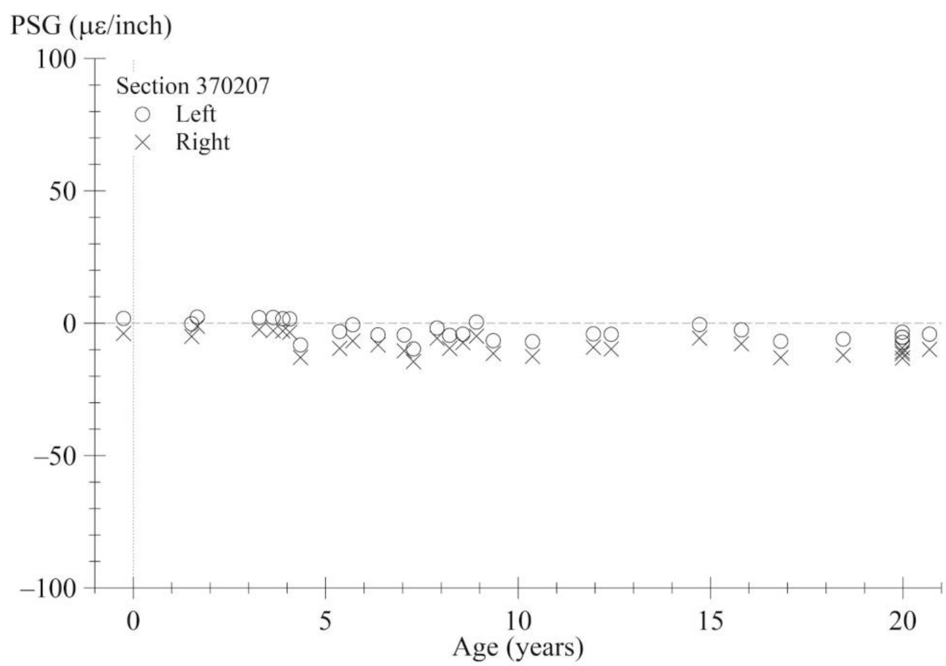

Source: FHWA.

Figure 212. Graph. PSG progression using Best Fit method for section 370207.

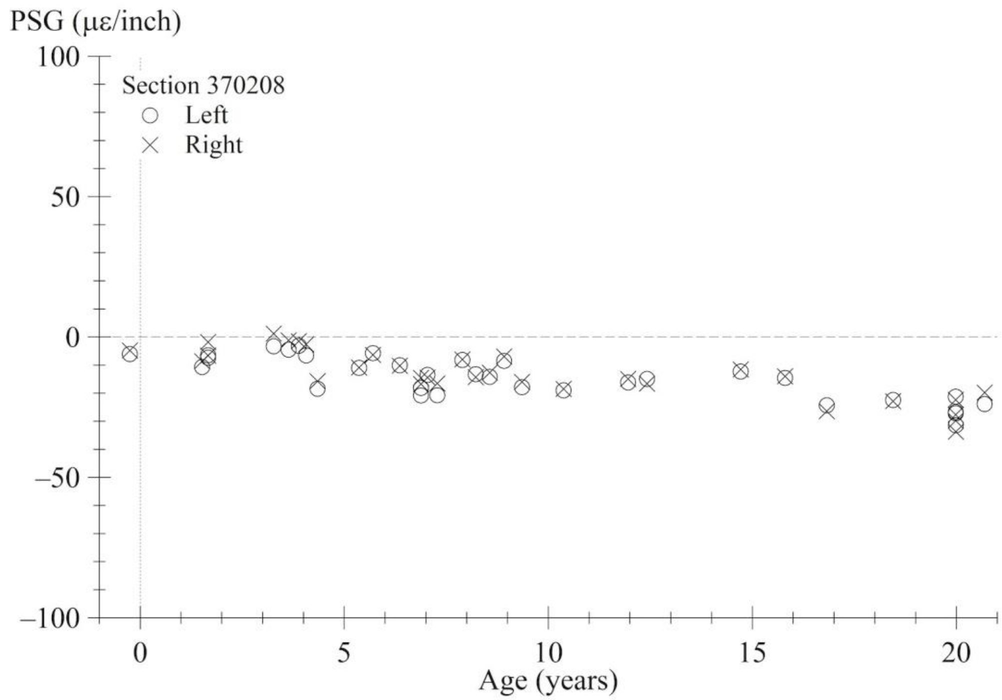

Source: FHWA.

Figure 213. Graph. PSG progression using Best Fit method for section 370208.

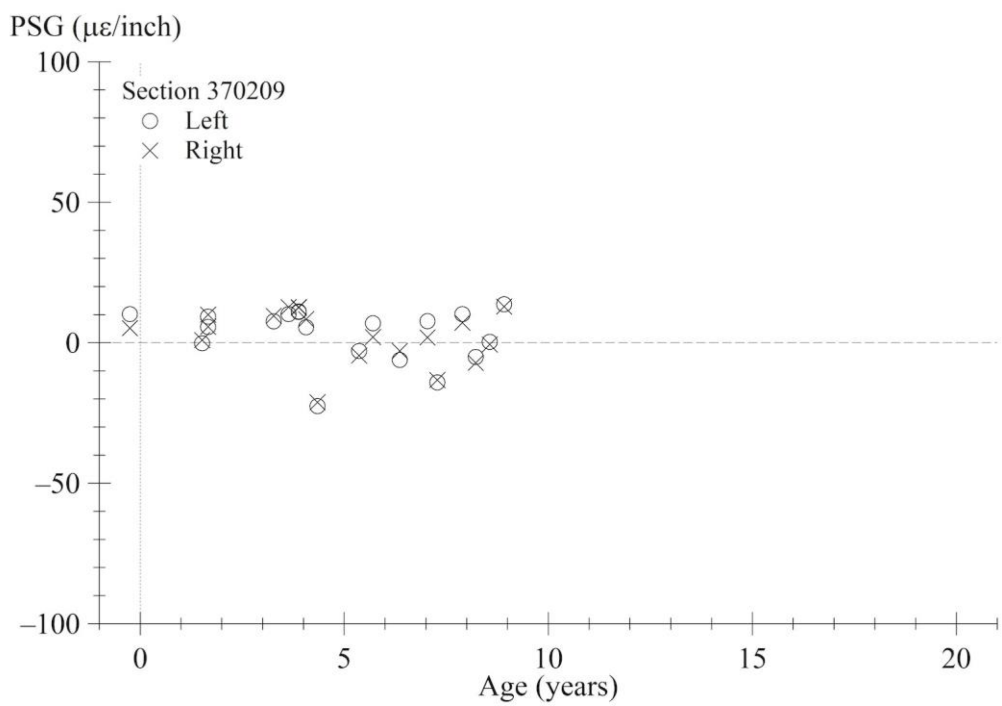

Source: FHWA.

Figure 214. Graph. PSG progression using Best Fit method for section 370209.

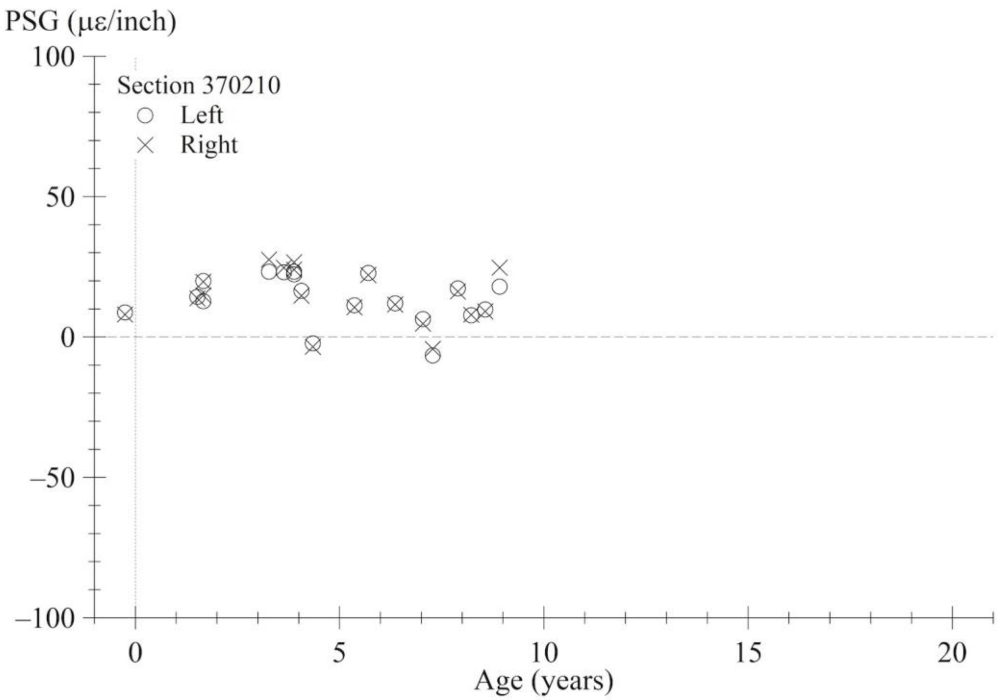

Source: FHWA.

Figure 215. Graph. PSG progression using Best Fit method for section 370210.

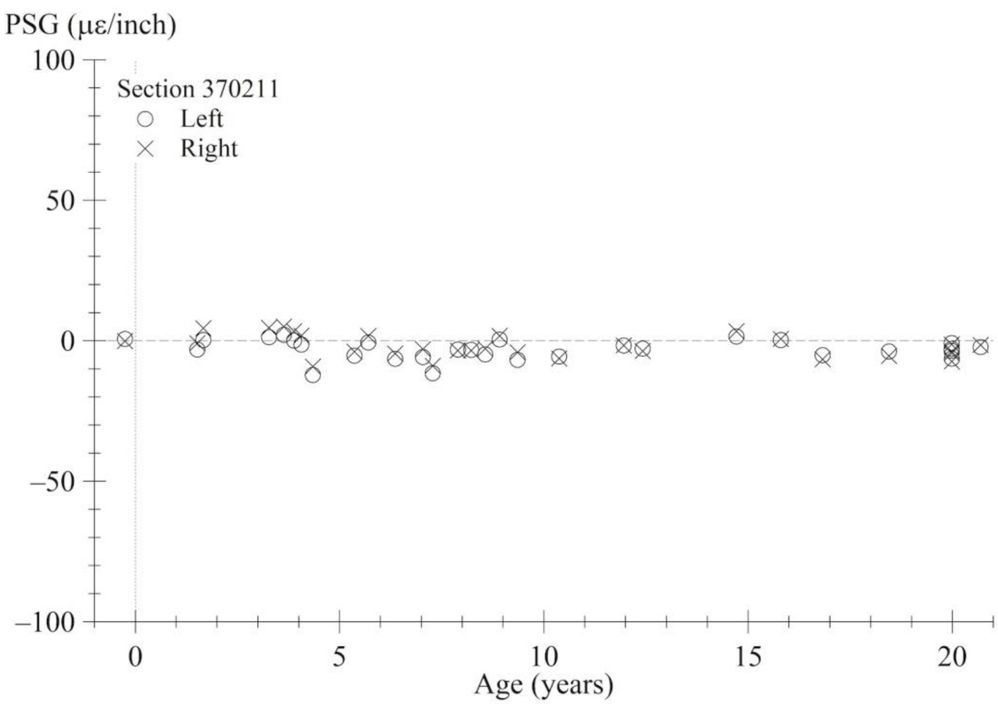

Source: FHWA.

Figure 216. Graph. PSG progression using Best Fit method for section 370211.

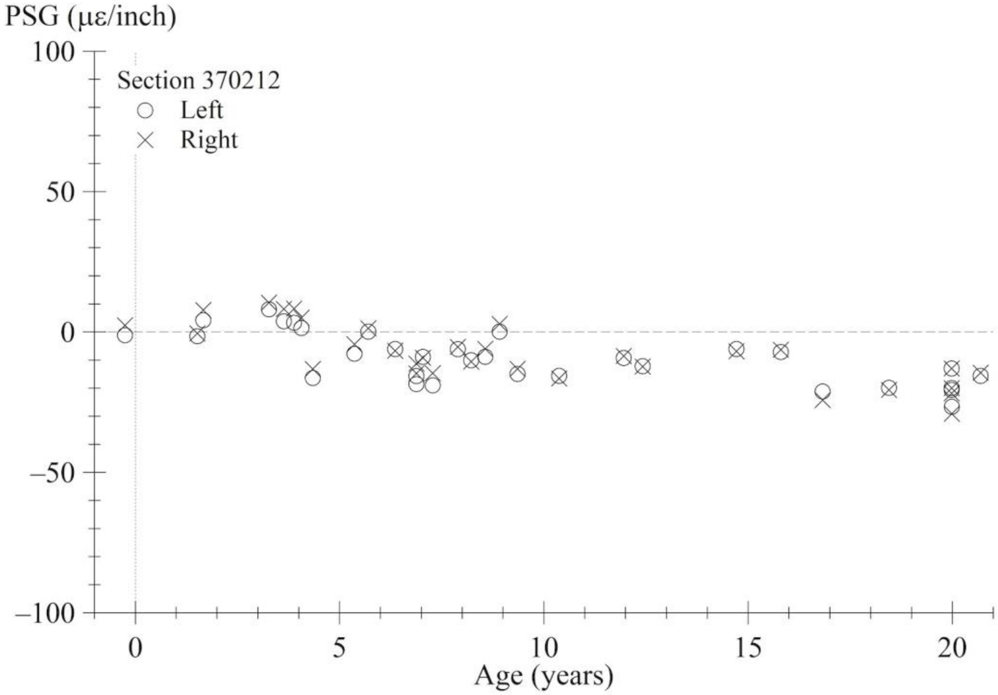

Source: FHWA.

Figure 217. Graph. PSG progression using Best Fit method for section 370212.

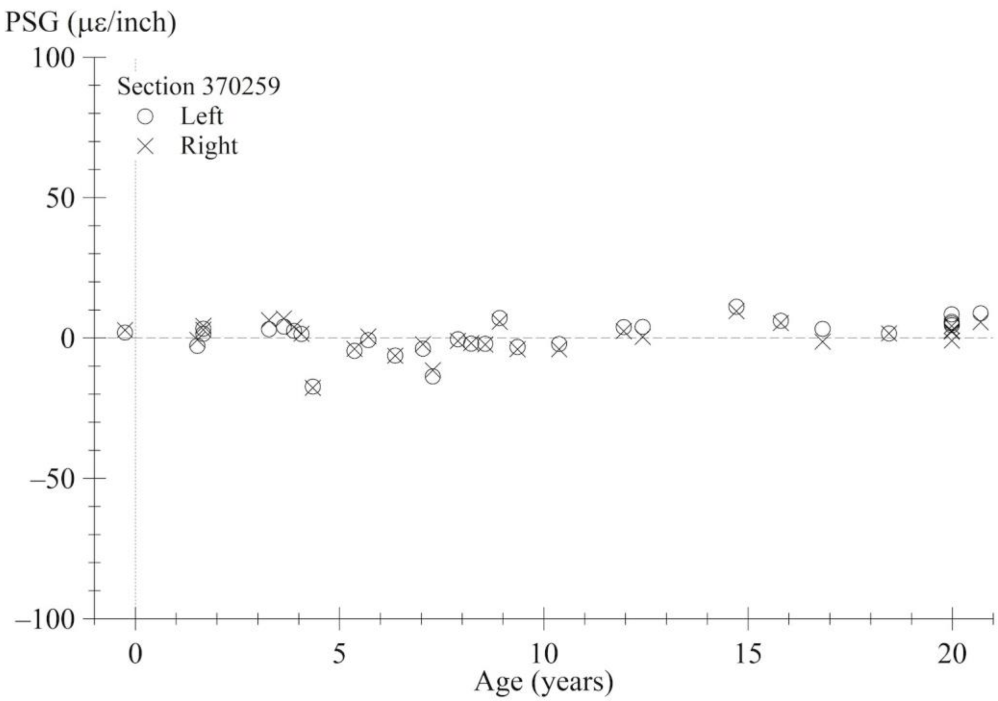

Source: FHWA.

Figure 218. Graph. PSG progression using Best Fit method for section 370259.

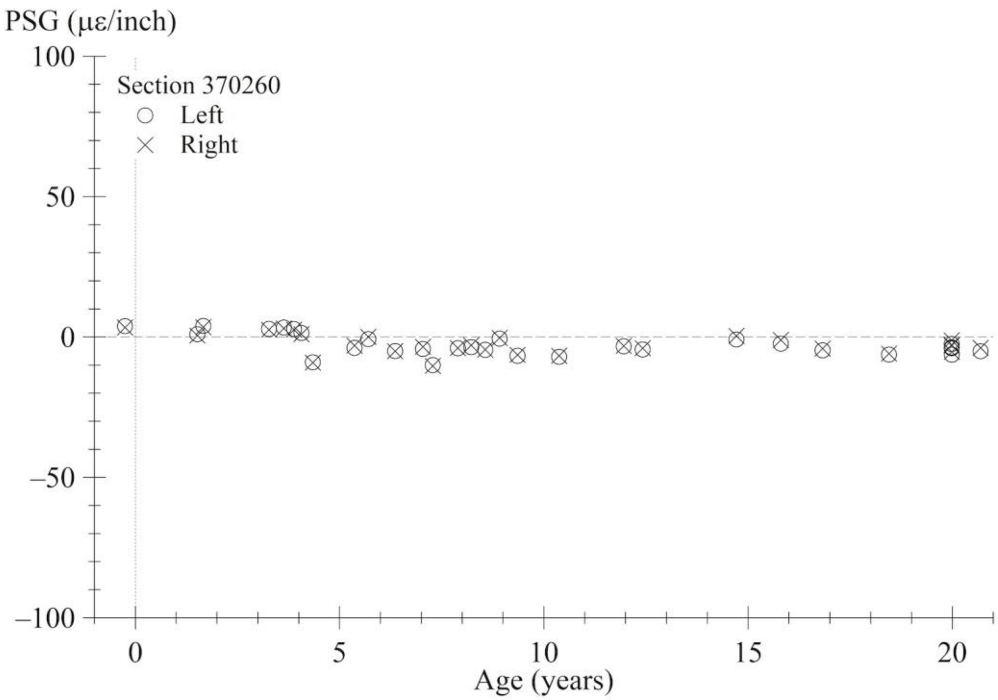

Source: FHWA.

Figure 219. Graph. PSG progression using Best Fit method for section 370260.

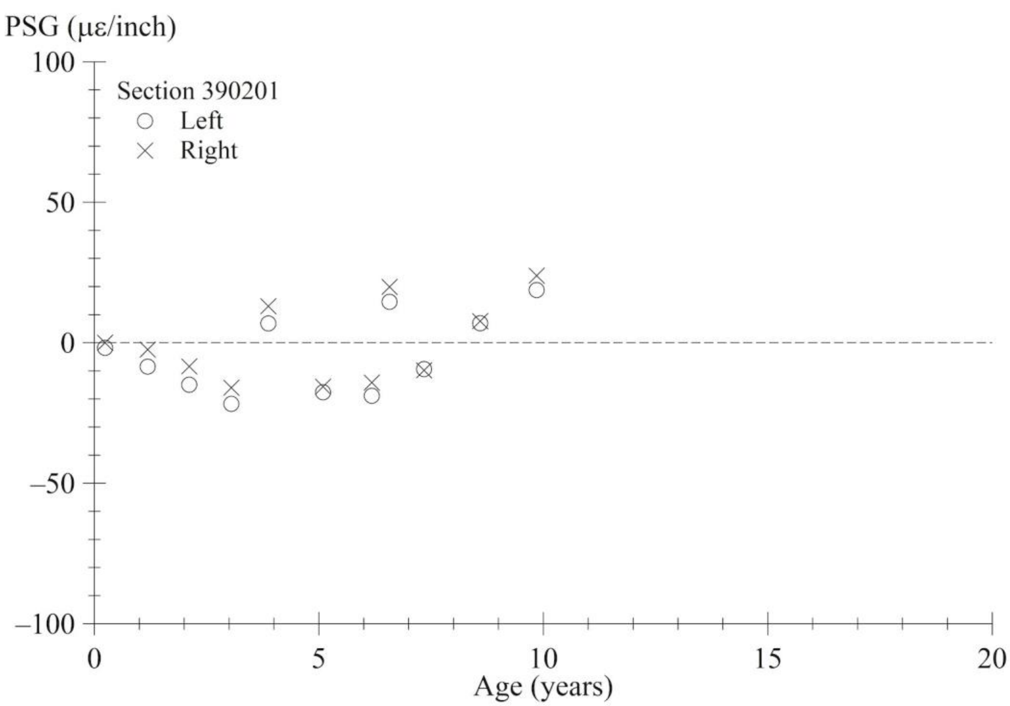

Source: FHWA.

Figure 220. Graph. PSG progression using Best Fit method for section 390201.

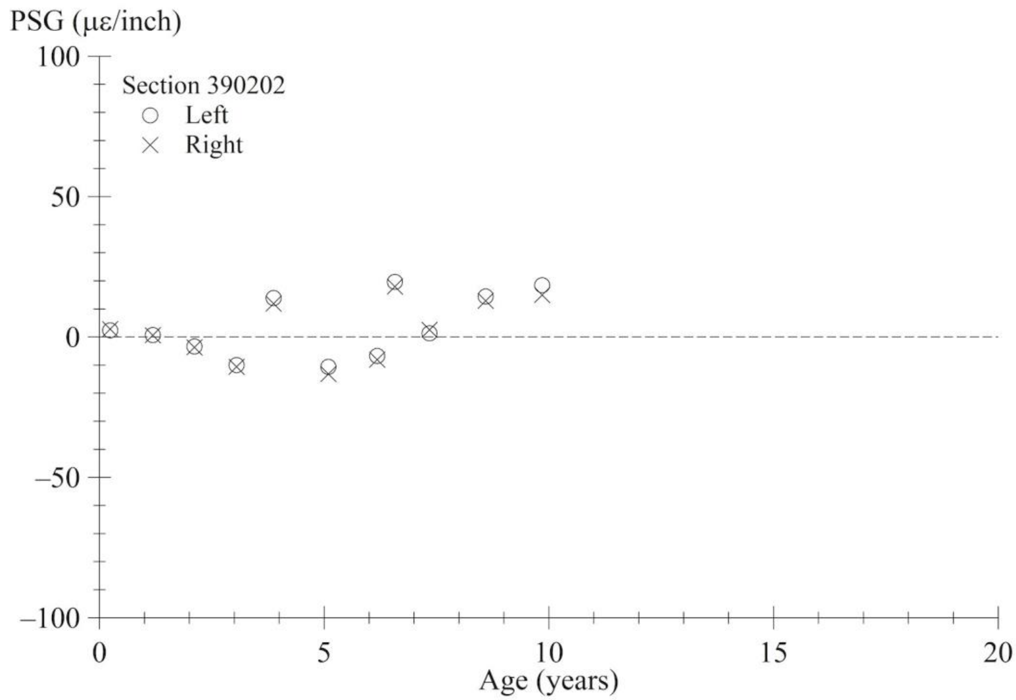

Source: FHWA.

Figure 221. Graph. PSG progression using Best Fit method for section 390202.

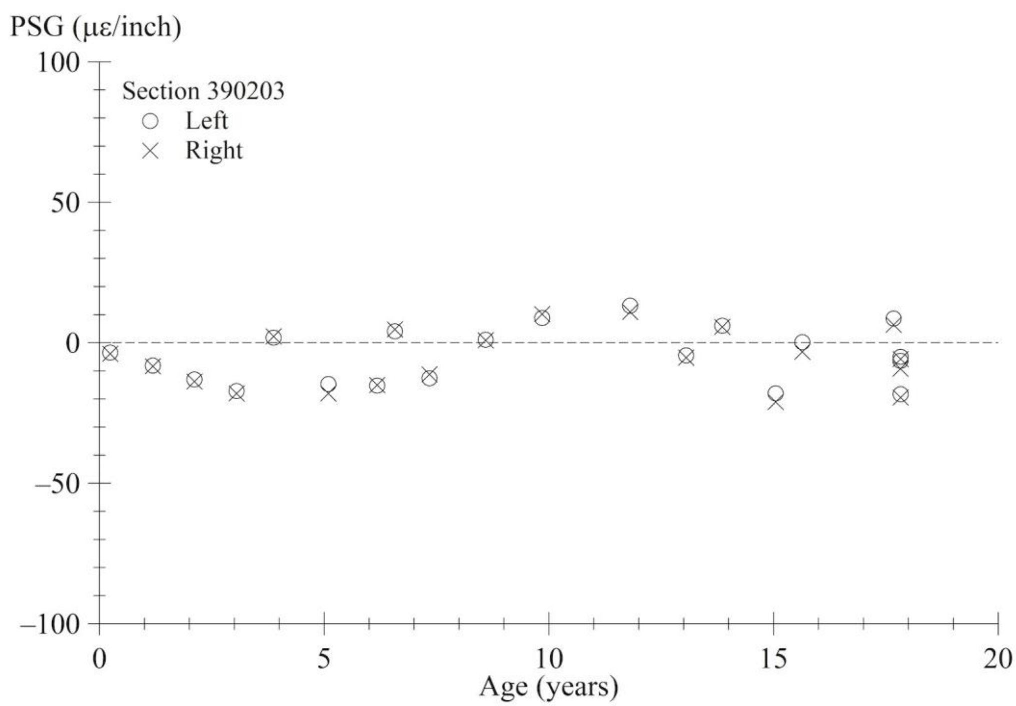

Source: FHWA.

Figure 222. Graph. PSG progression using Best Fit method for section 390203.

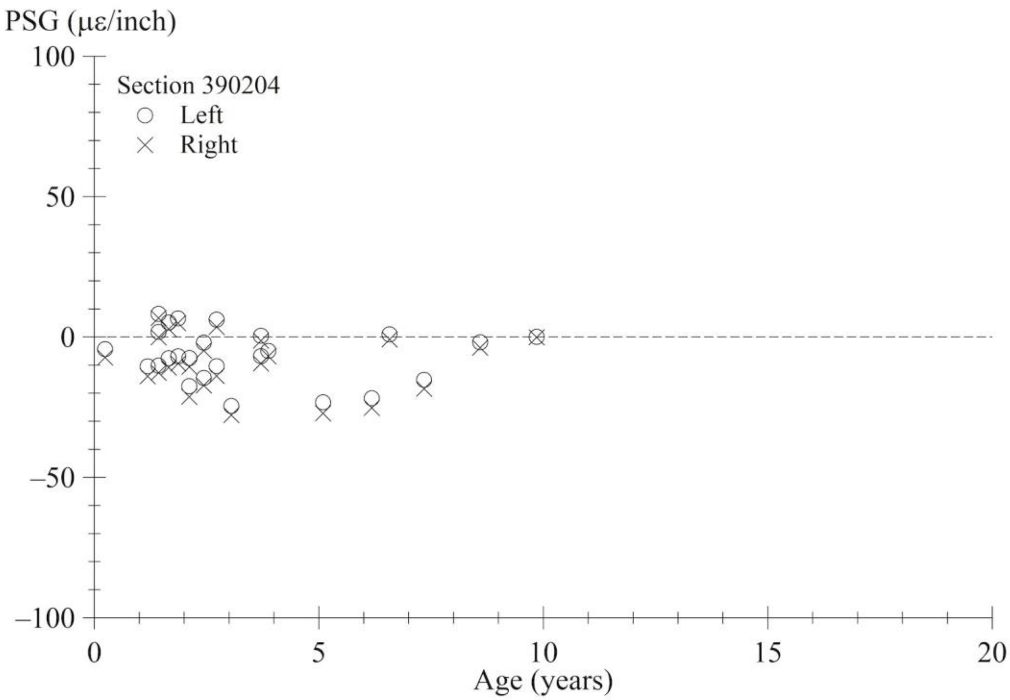

Source: FHWA.

Figure 223. Graph. PSG progression using Best Fit method for section 390204.

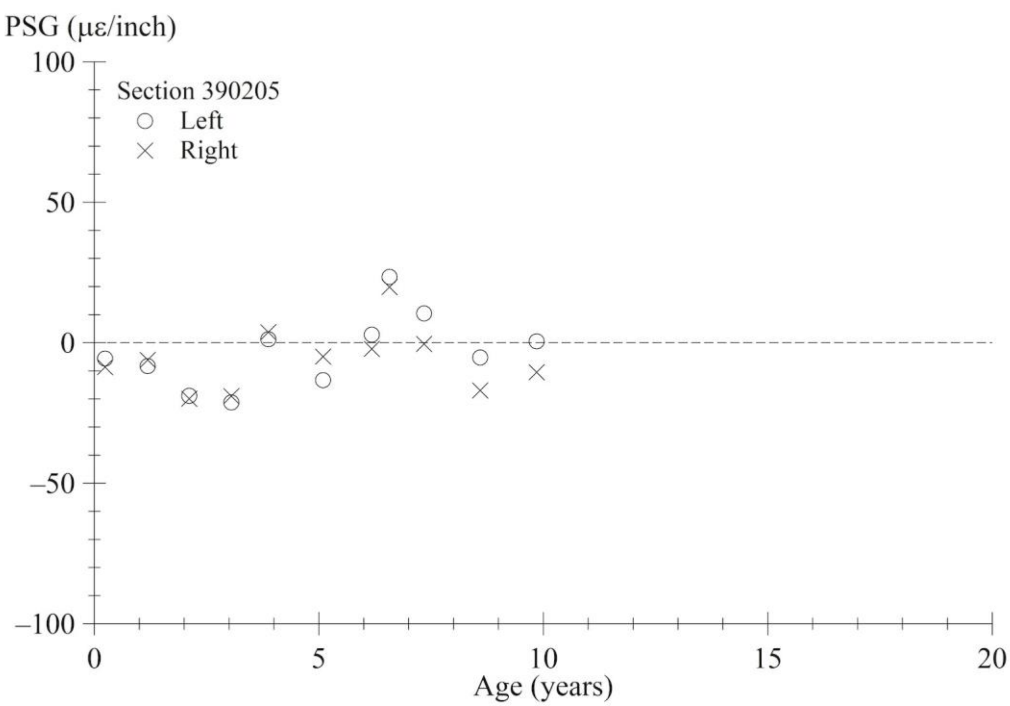

Source: FHWA.

Figure 224. Graph. PSG progression using Best Fit method for section 390205.

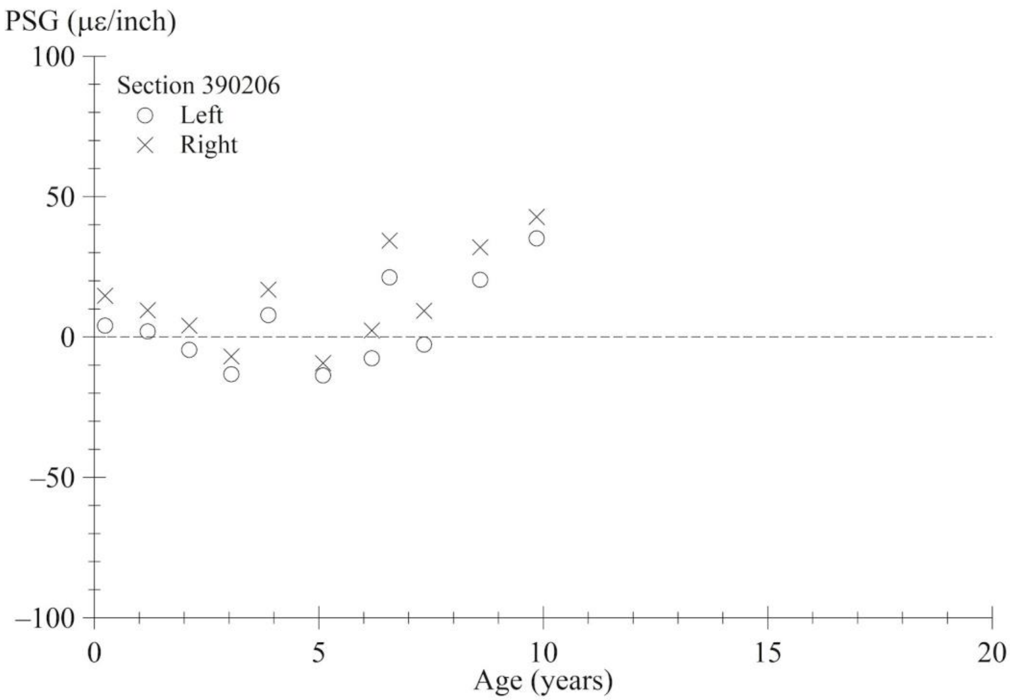

Source: FHWA.

Figure 225. Graph. PSG progression using Best Fit method for section 390206.

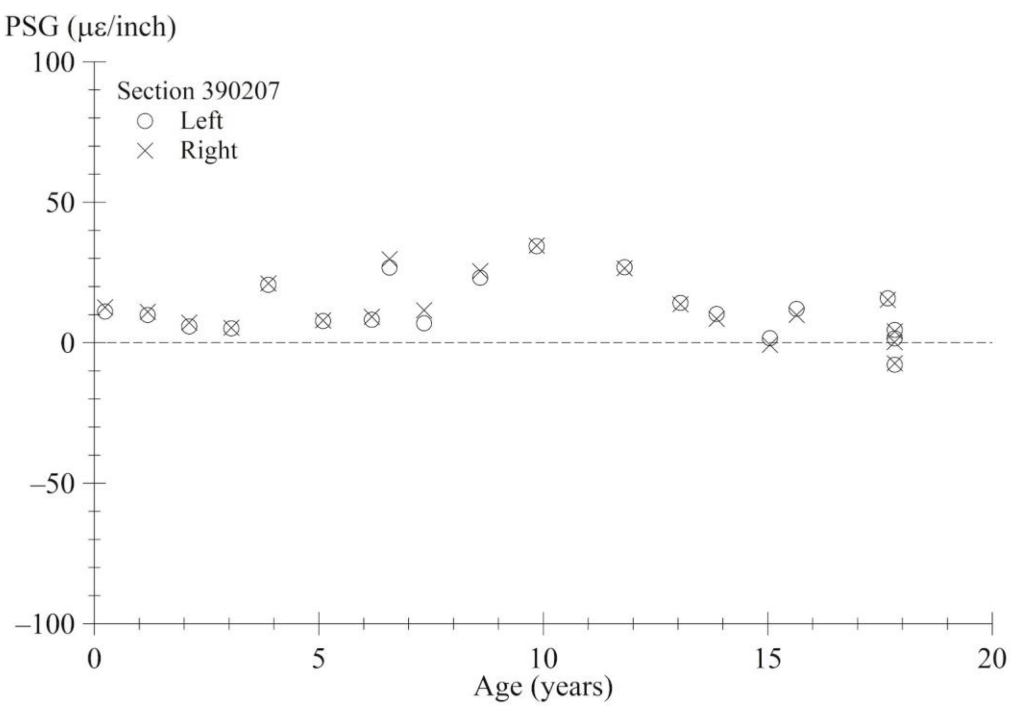

Source: FHWA.

Figure 226. Graph. PSG progression using Best Fit method for section 390207.

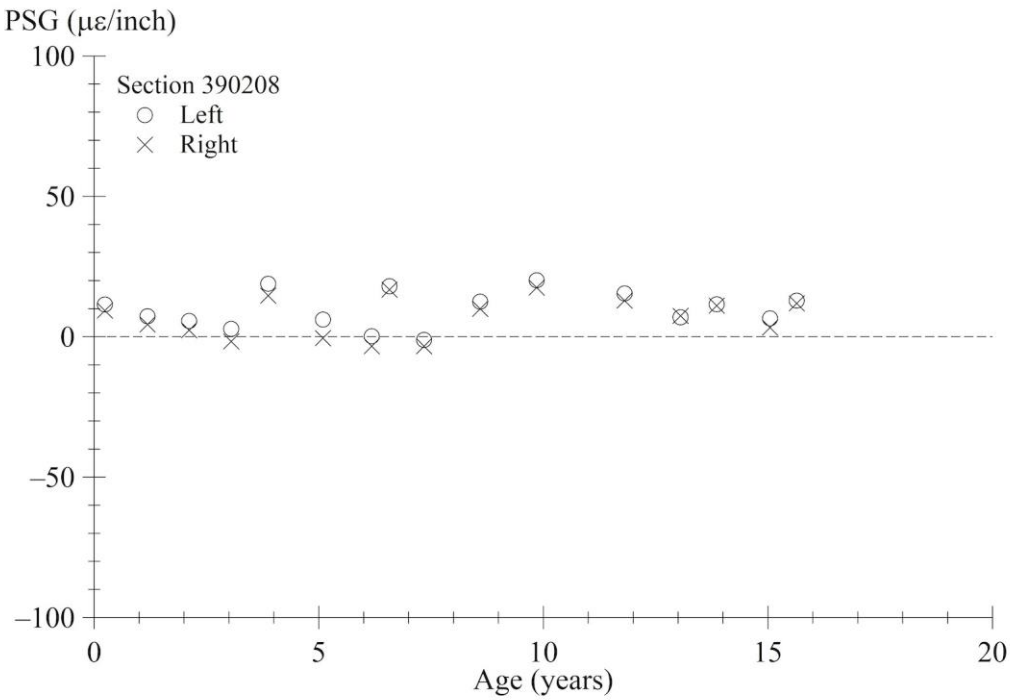

Source: FHWA.

Figure 227. Graph. PSG progression using Best Fit method for section 390208.

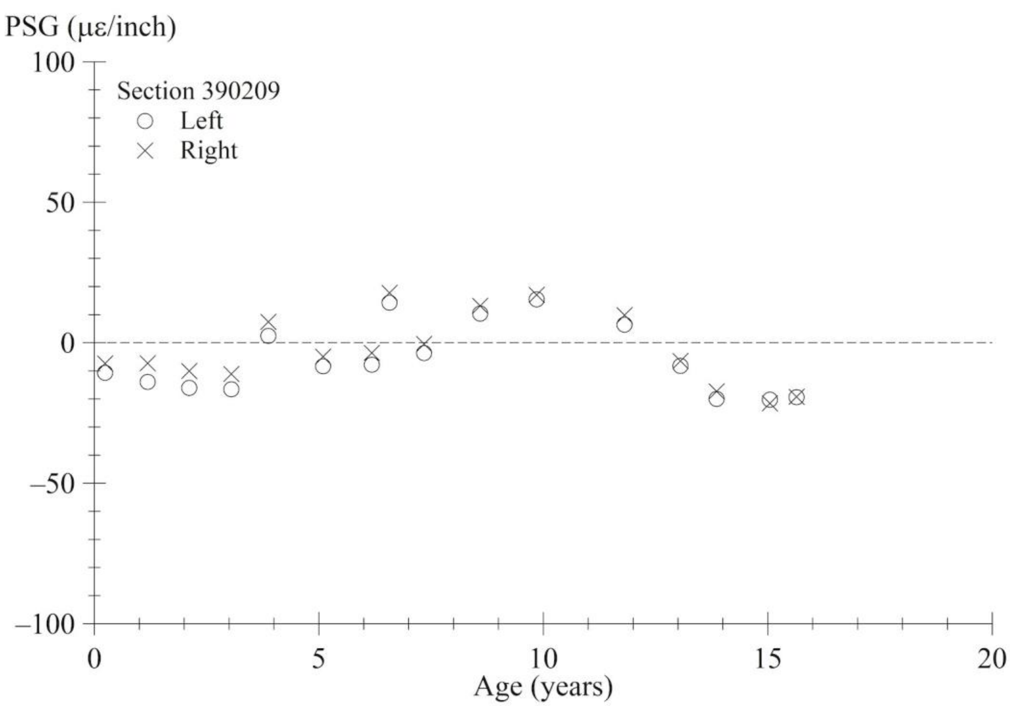

Source: FHWA.

Figure 228. Graph. PSG progression using Best Fit method for section 390209.

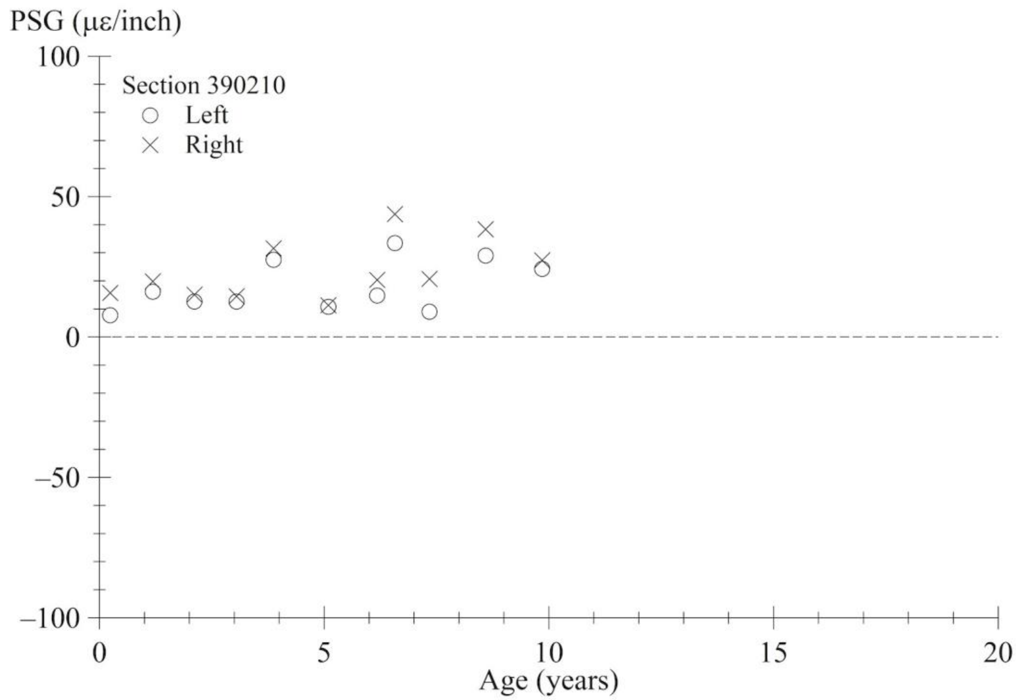

Source: FHWA.

Figure 229. Graph. PSG progression using Best Fit method for section 390210.

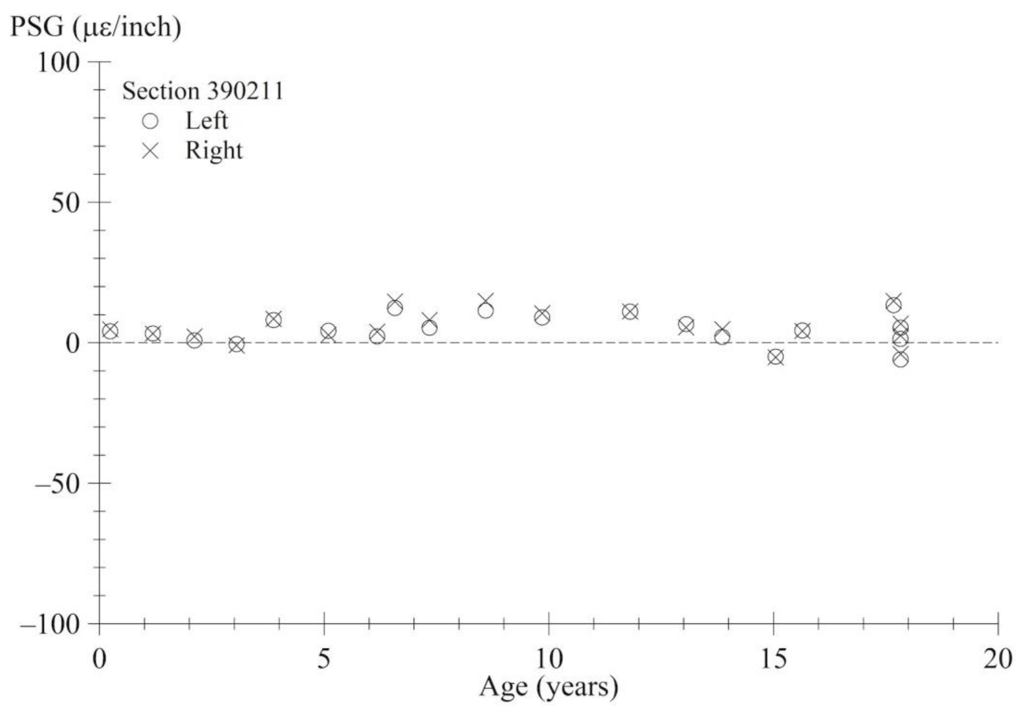

Source: FHWA.

Figure 230. Graph. PSG progression using Best Fit method for section 390211.

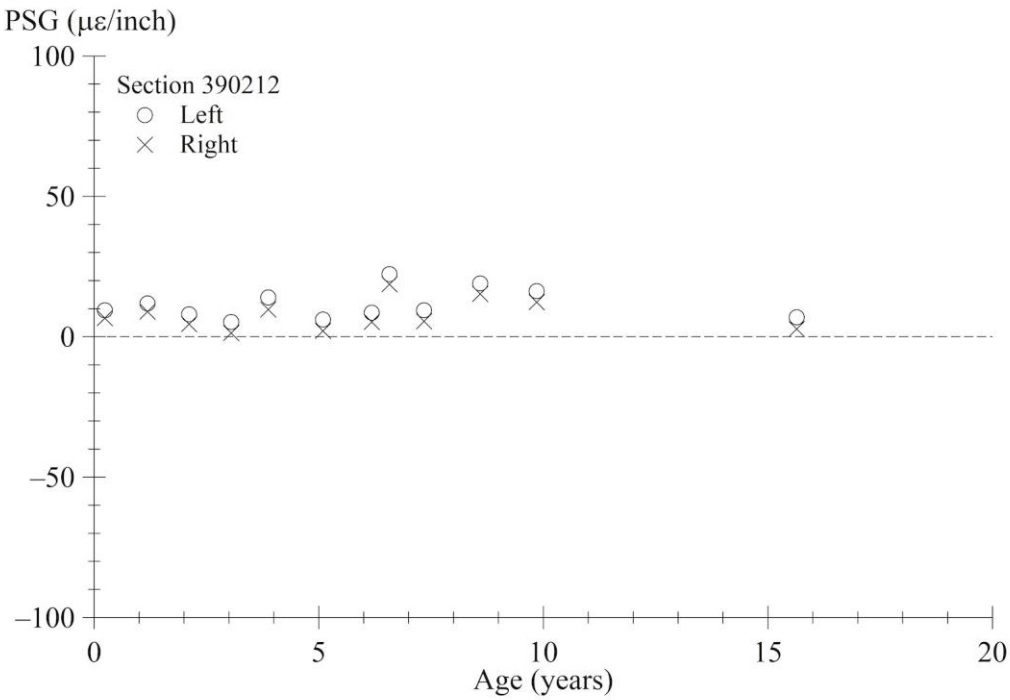

Source: FHWA.

Figure 231. Graph. PSG progression using Best Fit method for section 390212.

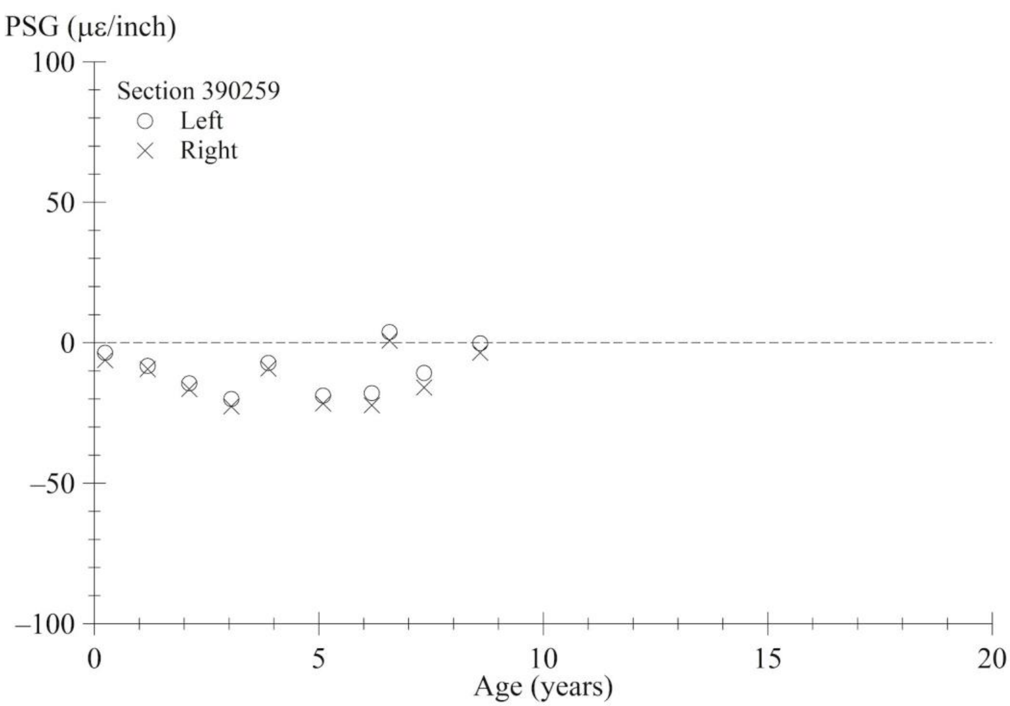

Source: FHWA.

Figure 232. Graph. PSG progression using Best Fit method for section 390259.

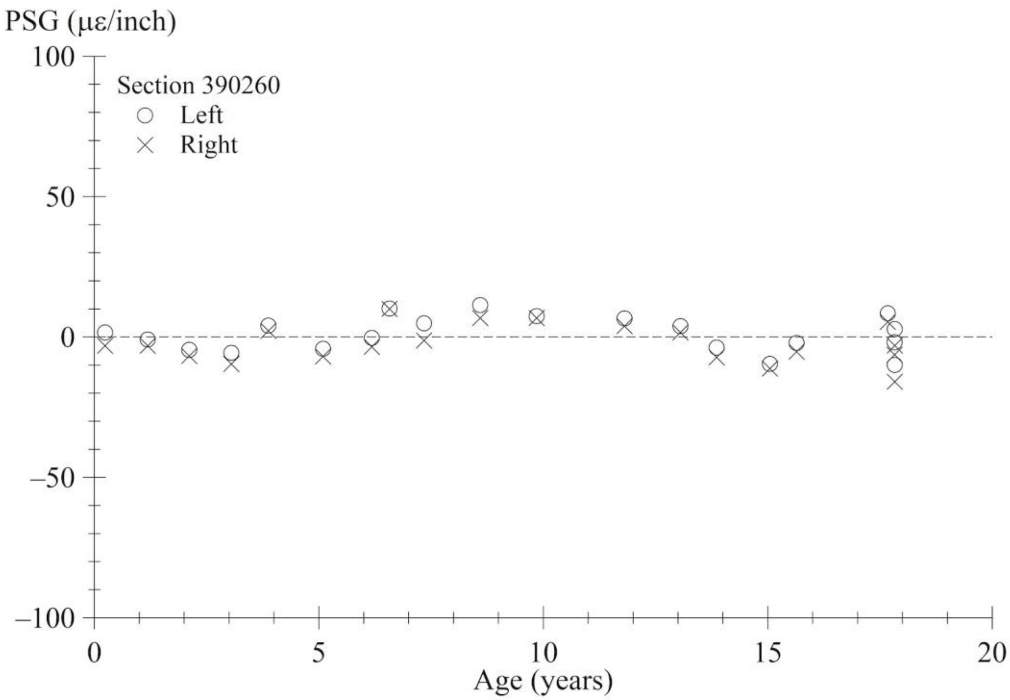

Source: FHWA.

Figure 233. Graph. PSG progression using Best Fit method for section 390260.

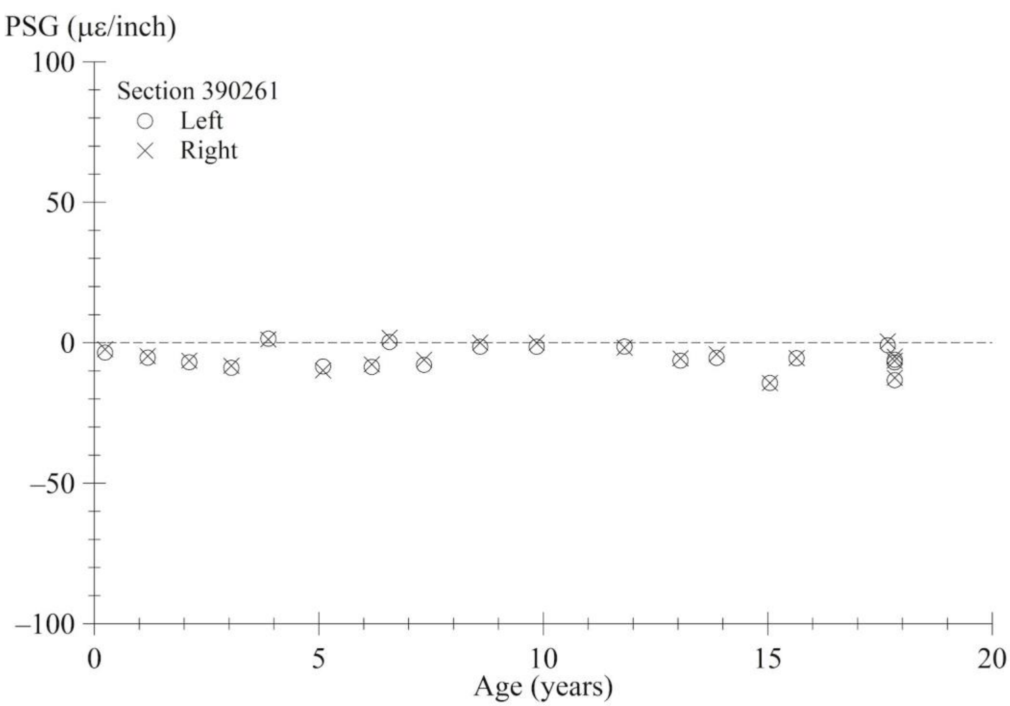

Source: FHWA.

Figure 234. Graph. PSG progression using Best Fit method for section 390261.

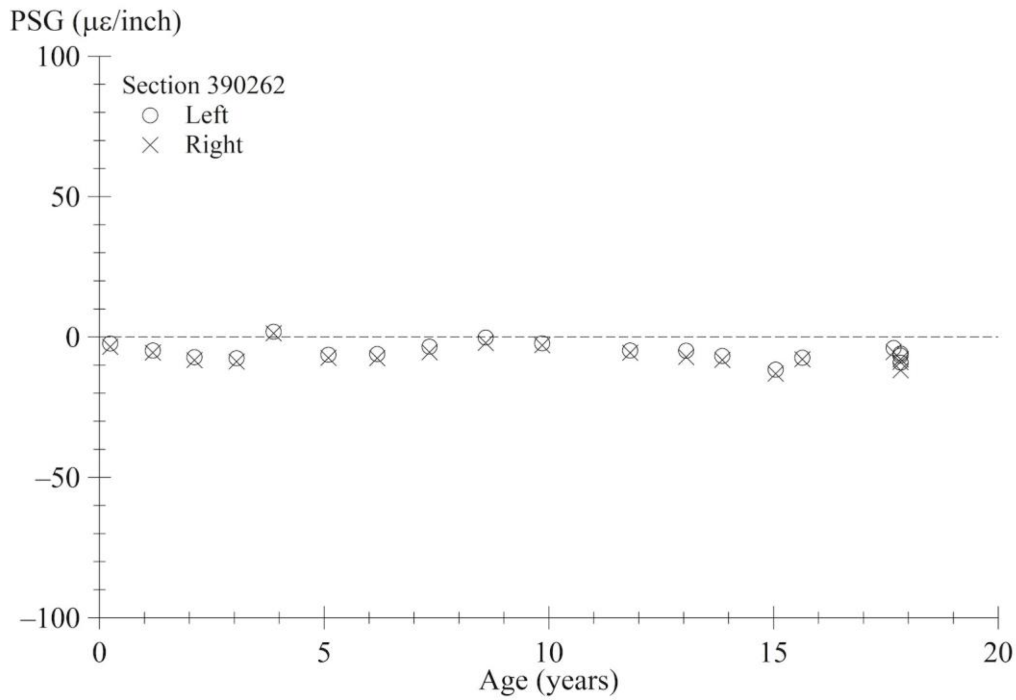

Source: FHWA.

Figure 235. Graph. PSG progression using Best Fit method for section 390262.

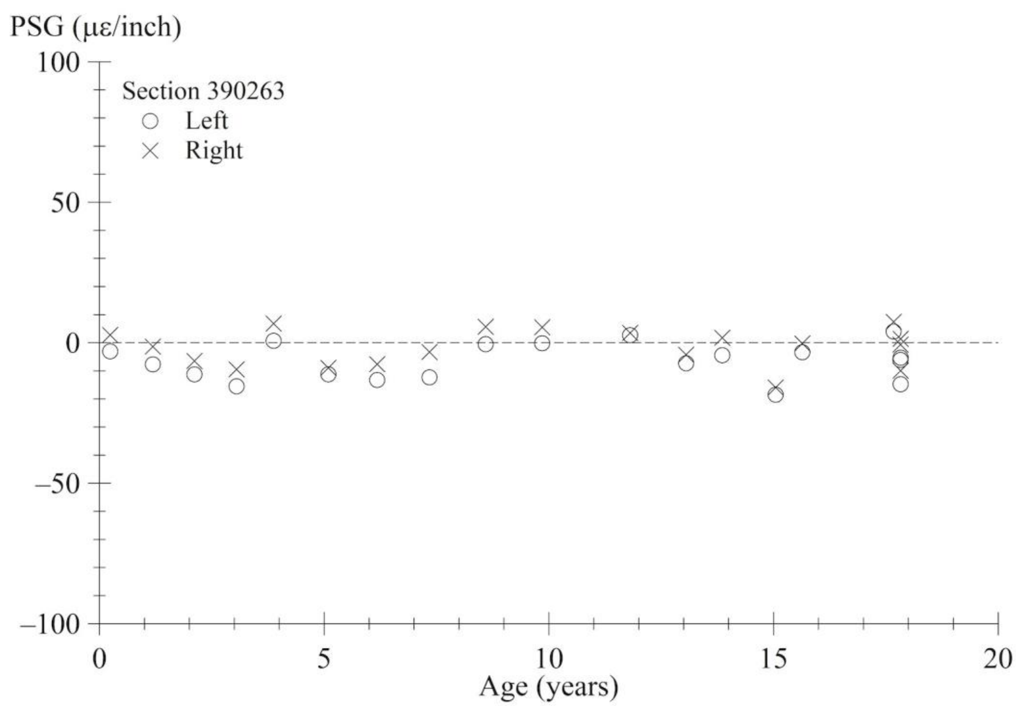

Source: FHWA.

Figure 236. Graph. PSG progression using Best Fit method for section 390263.

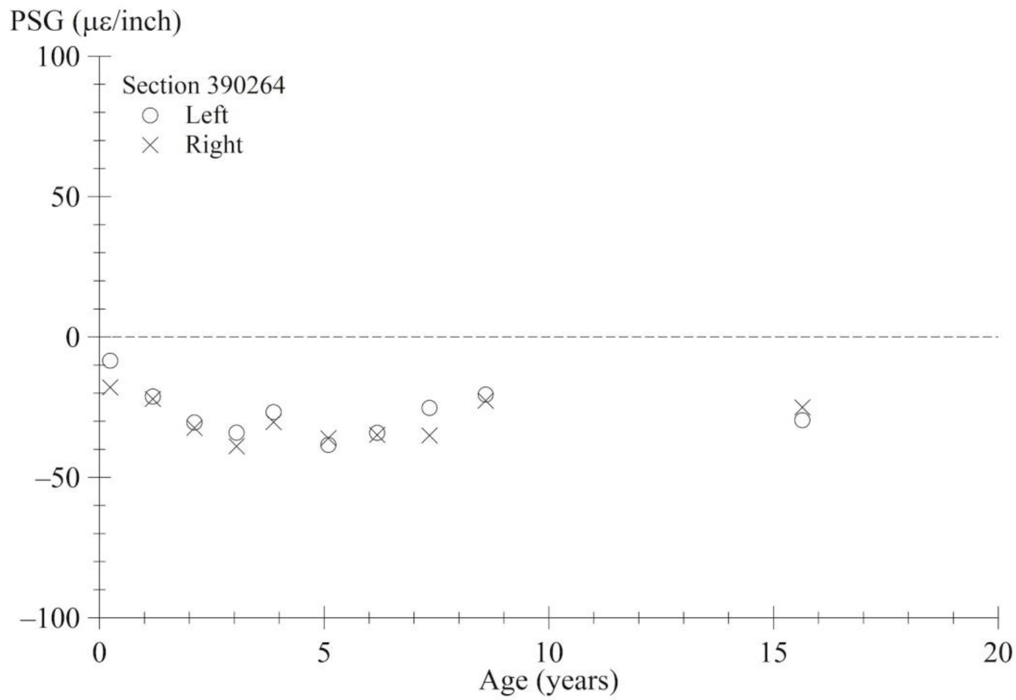

Source: FHWA.

Figure 237. Graph. PSG progression using Best Fit method for section 390264.

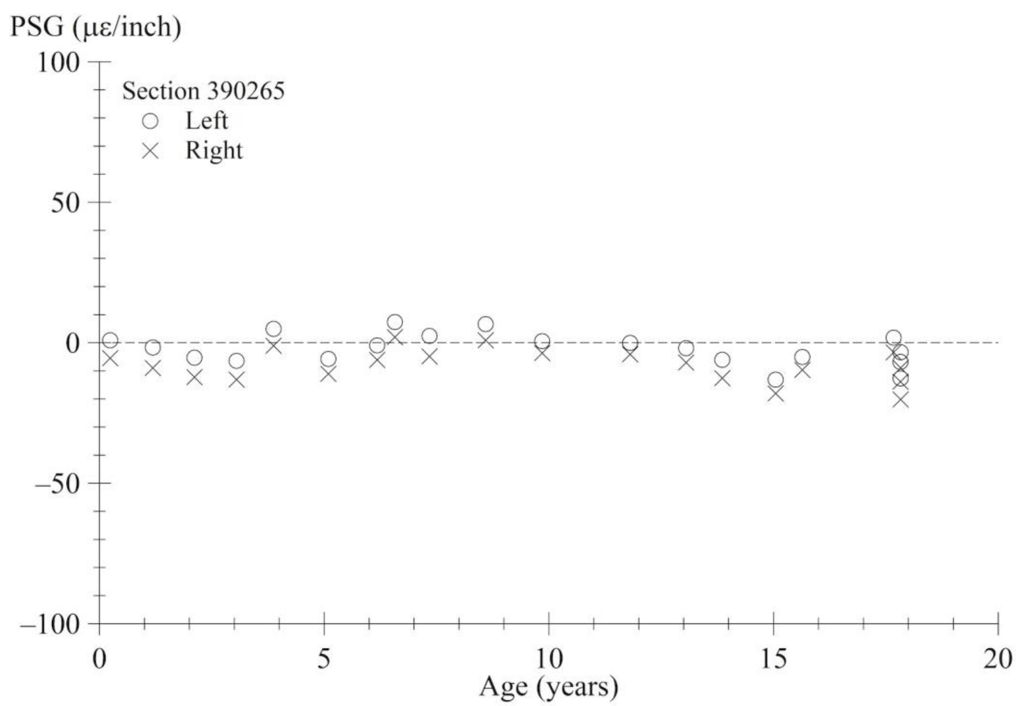

Source: FHWA.

Figure 238. Graph. PSG progression using Best Fit method for section 390265.

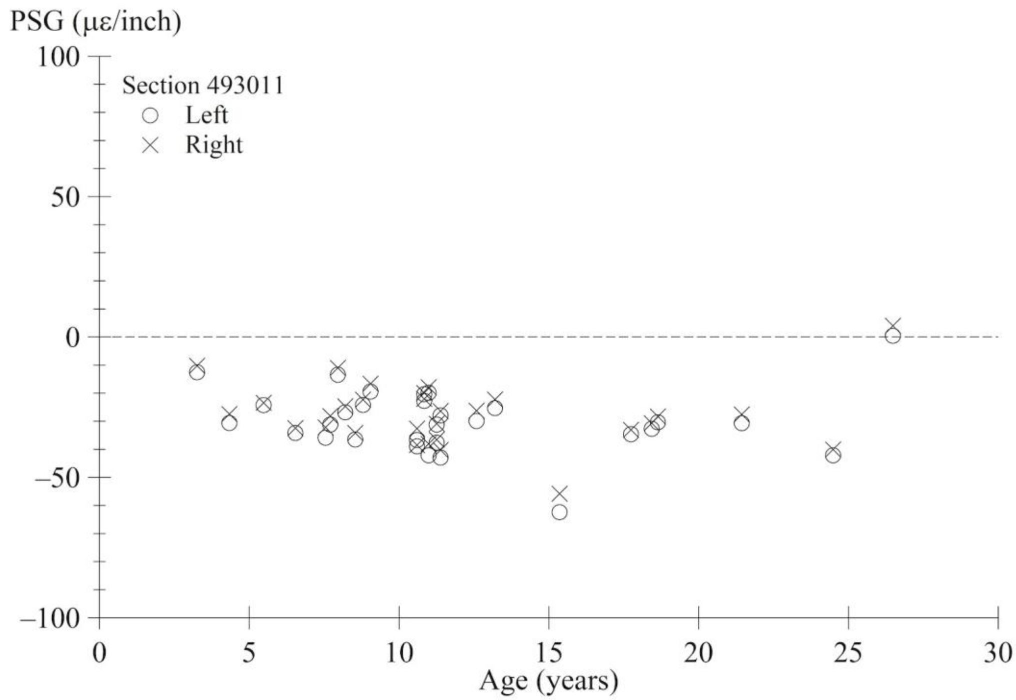

Source: FHWA.

Figure 239. Graph. PSG progression using Best Fit method for section 493011.

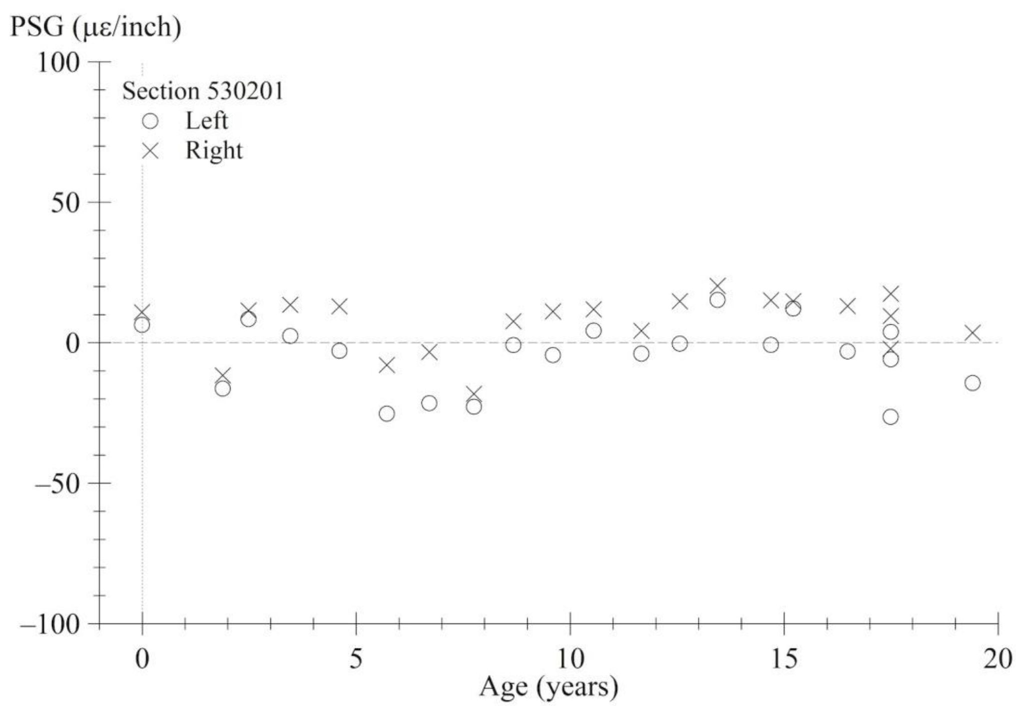

Source: FHWA.

Figure 240. Graph. PSG progression using Best Fit method for section 530201.

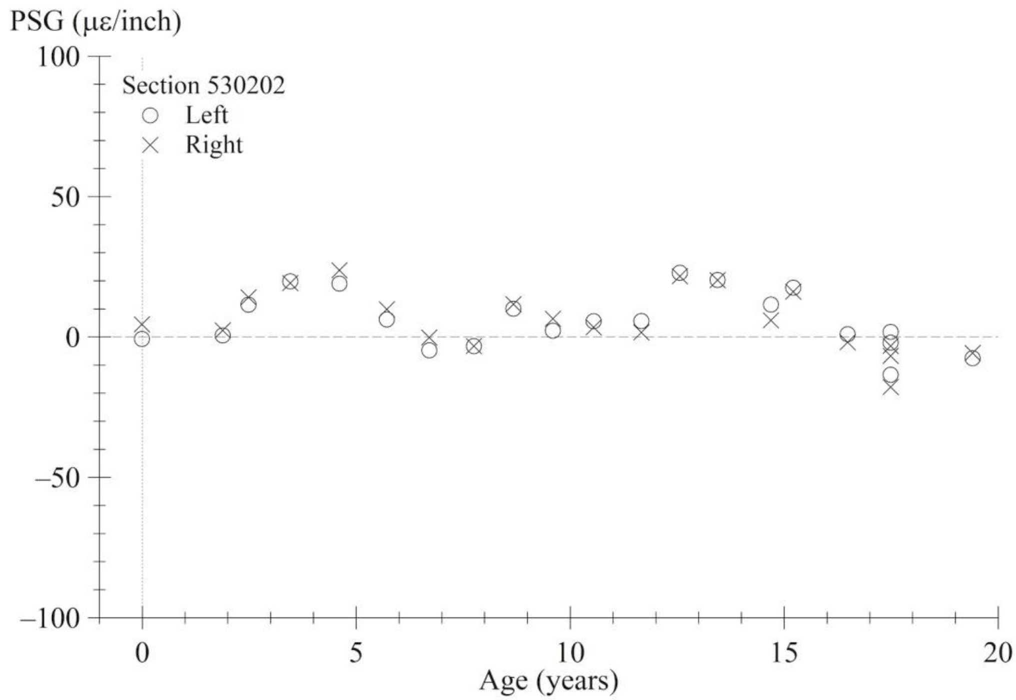

Source: FHWA.

Figure 241. Graph. PSG progression using Best Fit method for section 530202.

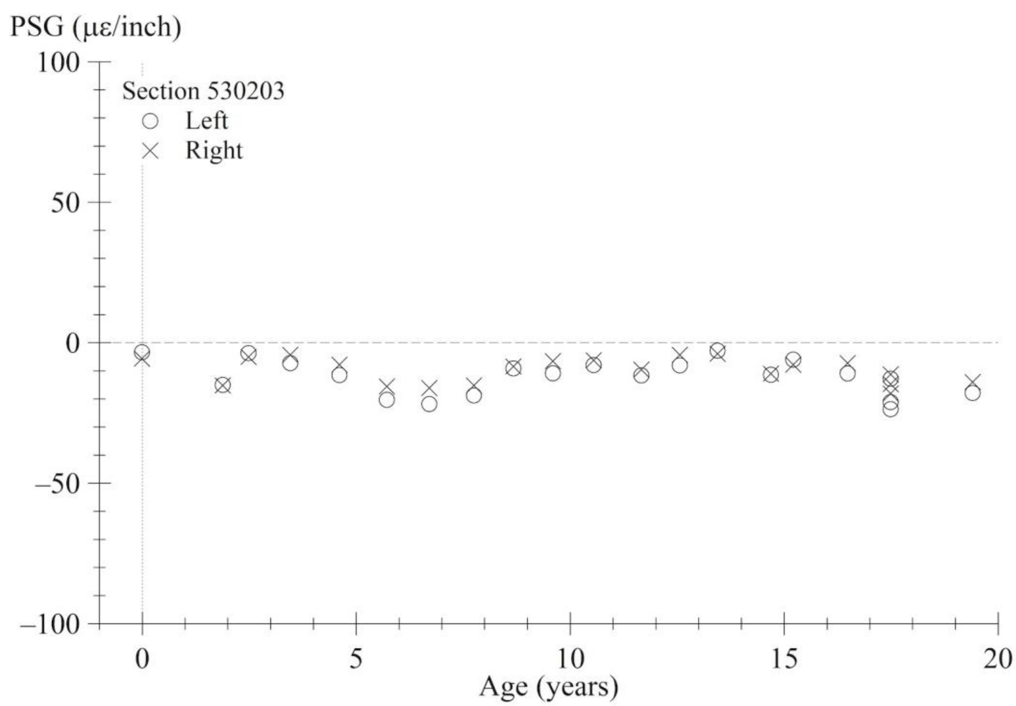

Source: FHWA.

Figure 242. Graph. PSG progression using Best Fit method for section 530203.

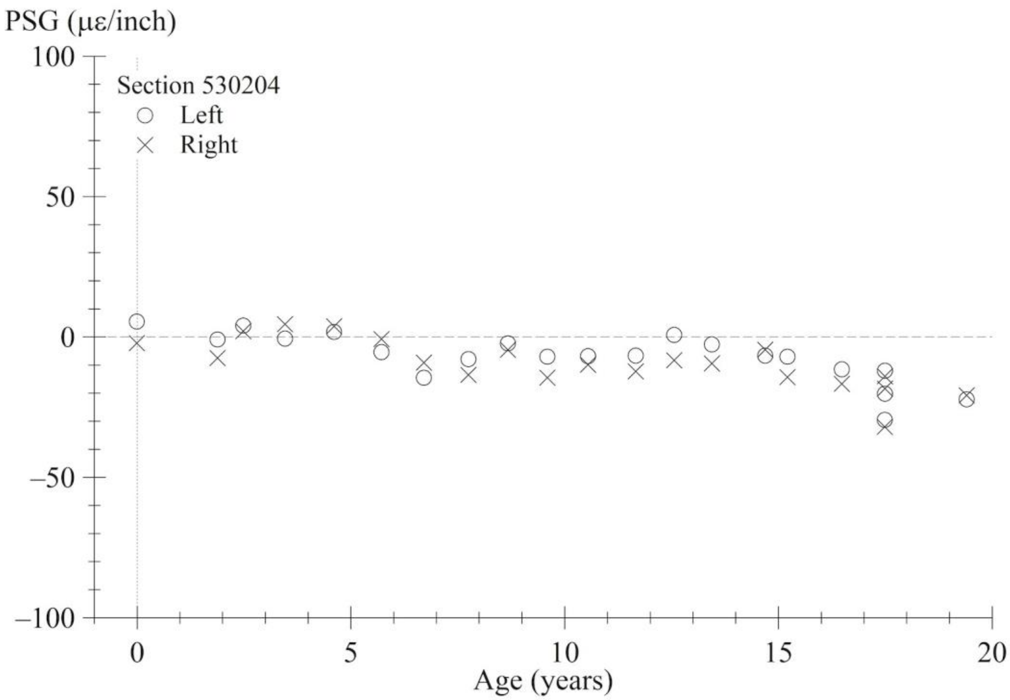

Source: FHWA.

Figure 243. Graph. PSG progression using Best Fit method for section 530204.

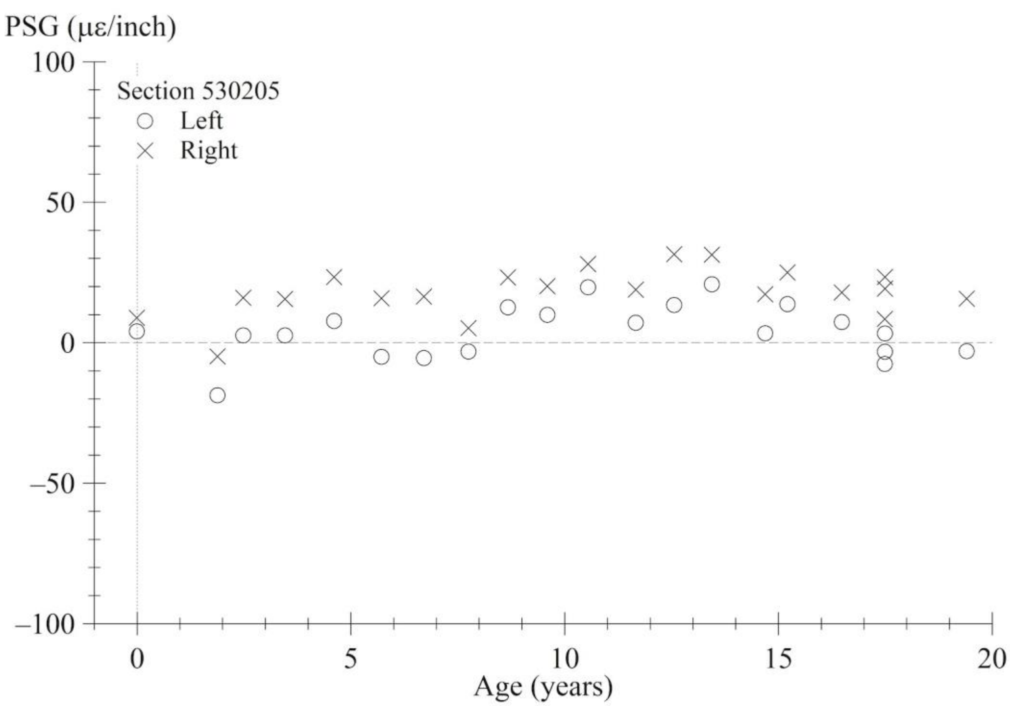

Source: FHWA.

Figure 244. Graph. PSG progression using Best Fit method for section 530205.

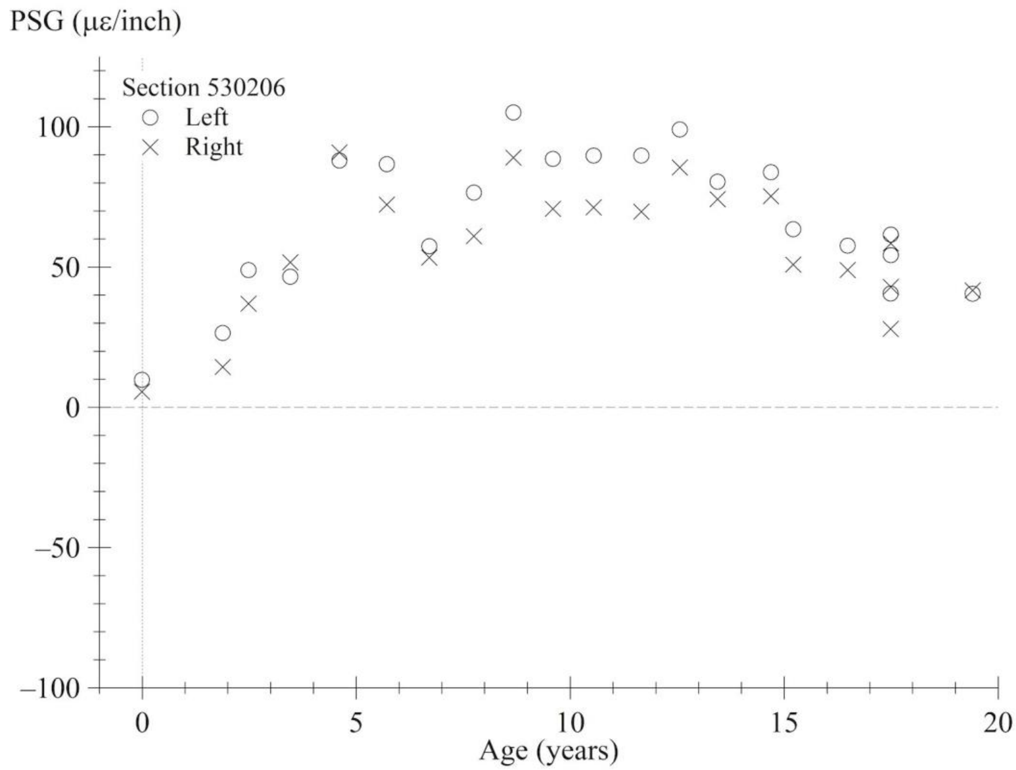

Source: FHWA.

Figure 245. Graph. PSG progression using Best Fit method for section 530206.

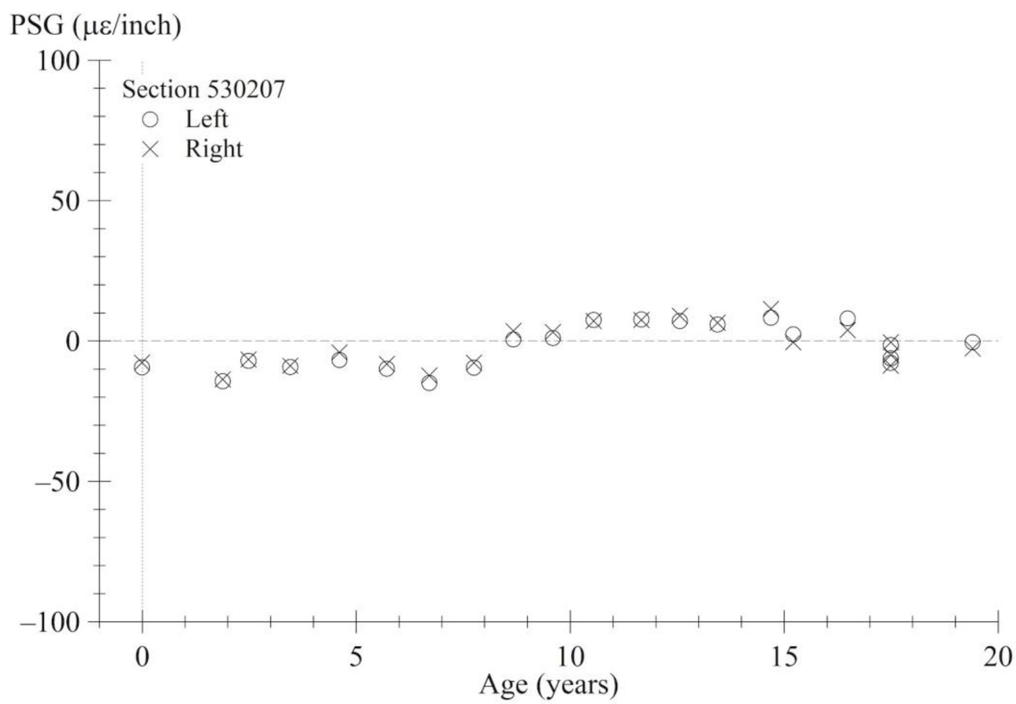

Source: FHWA.

Figure 246. Graph. PSG progression using Best Fit method for section 530207.

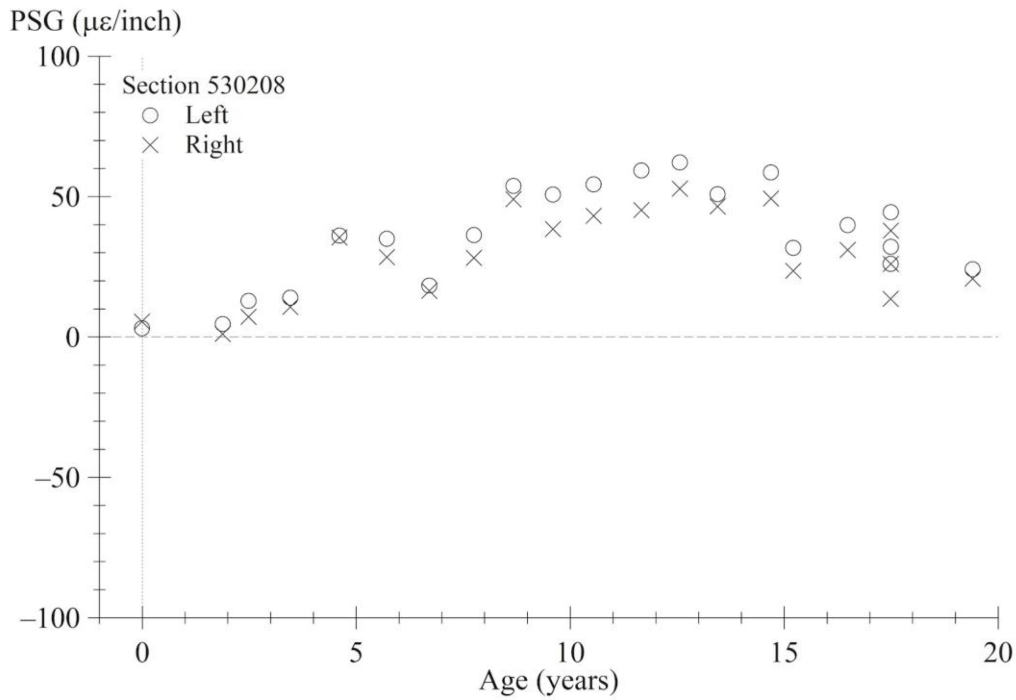

Source: FHWA.

Figure 247. Graph. PSG progression using Best Fit method for section 530208.

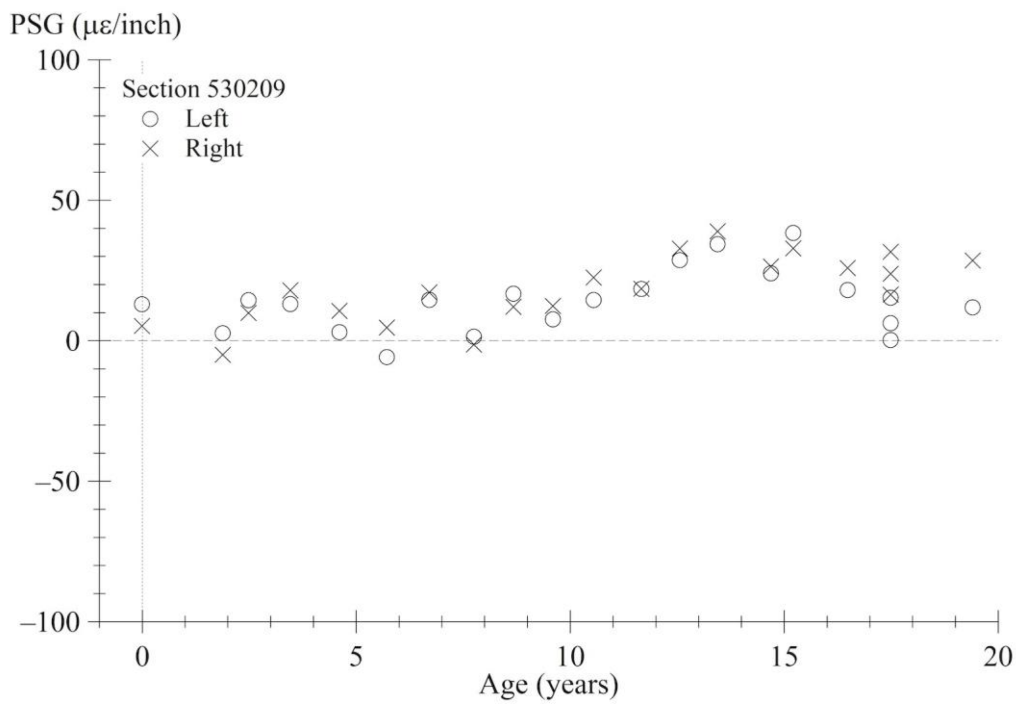

Source: FHWA.

Figure 248. Graph. PSG progression using Best Fit method for section 530209.

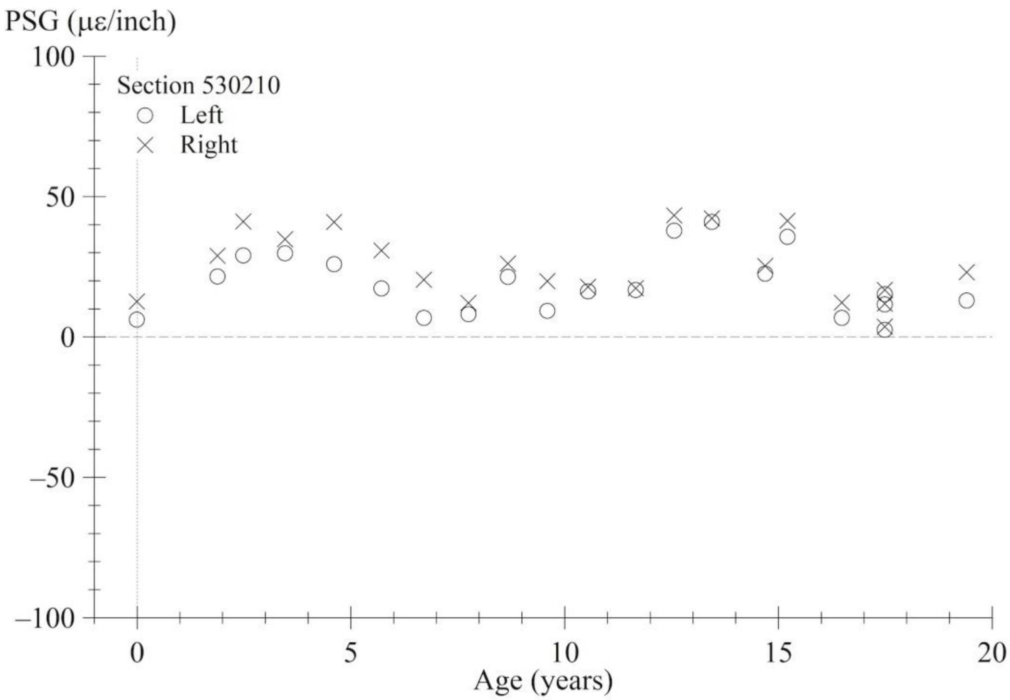

Source: FHWA.

Figure 249. Graph. PSG progression using Best Fit method for section 530210.

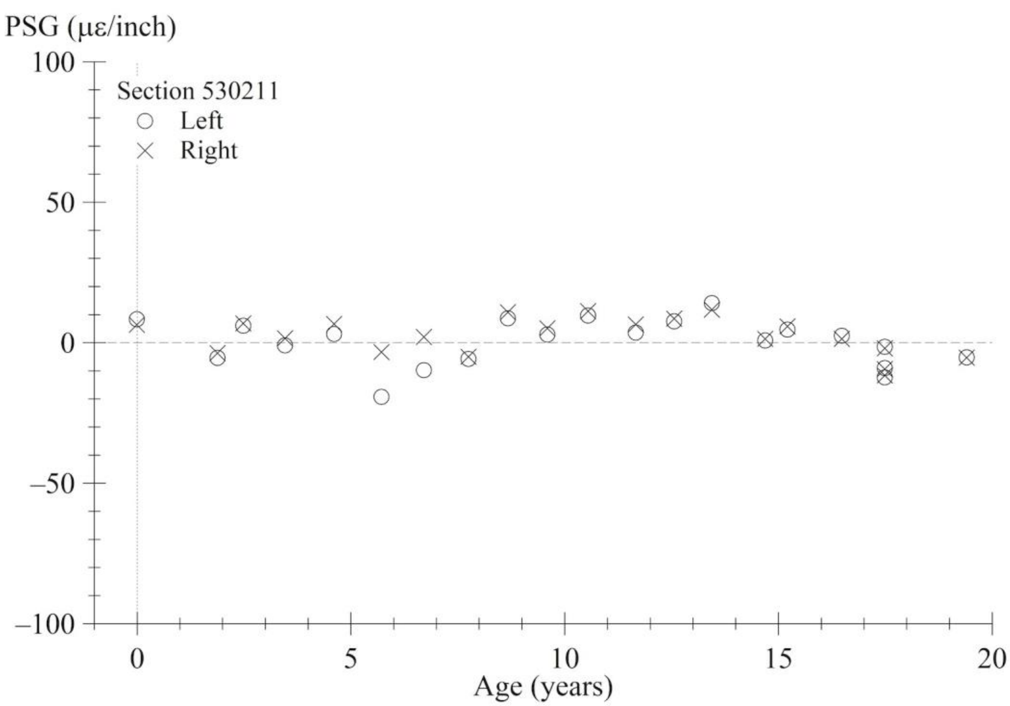

Source: FHWA.

Figure 250. Graph. PSG progression using Best Fit method for section 530211.

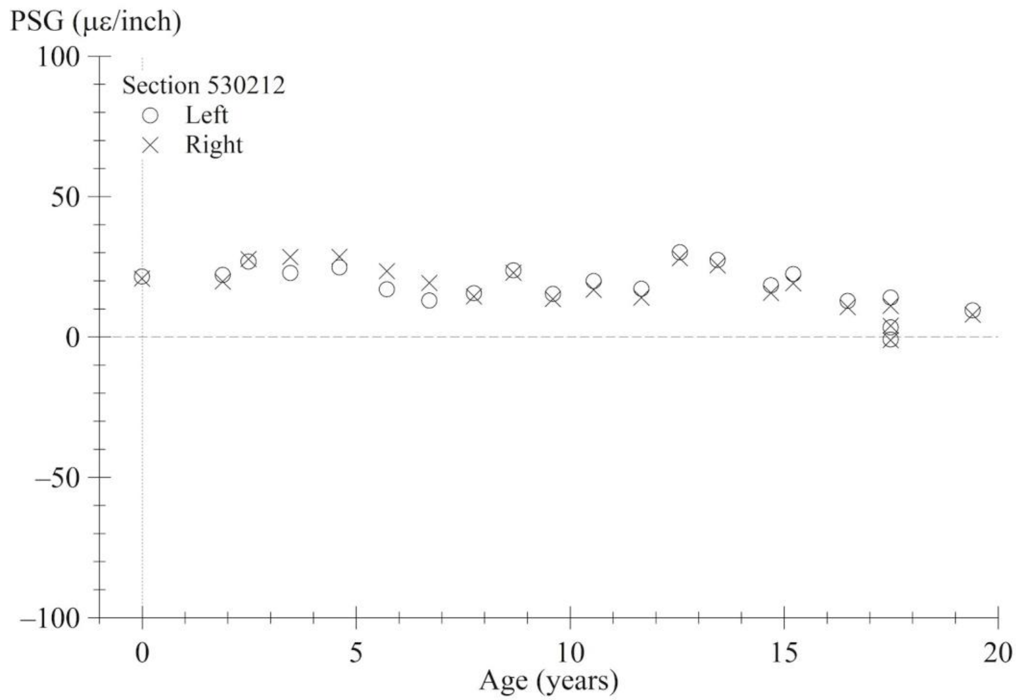

Source: FHWA.

Figure 251. Graph. PSG progression using Best Fit method for section 530212.

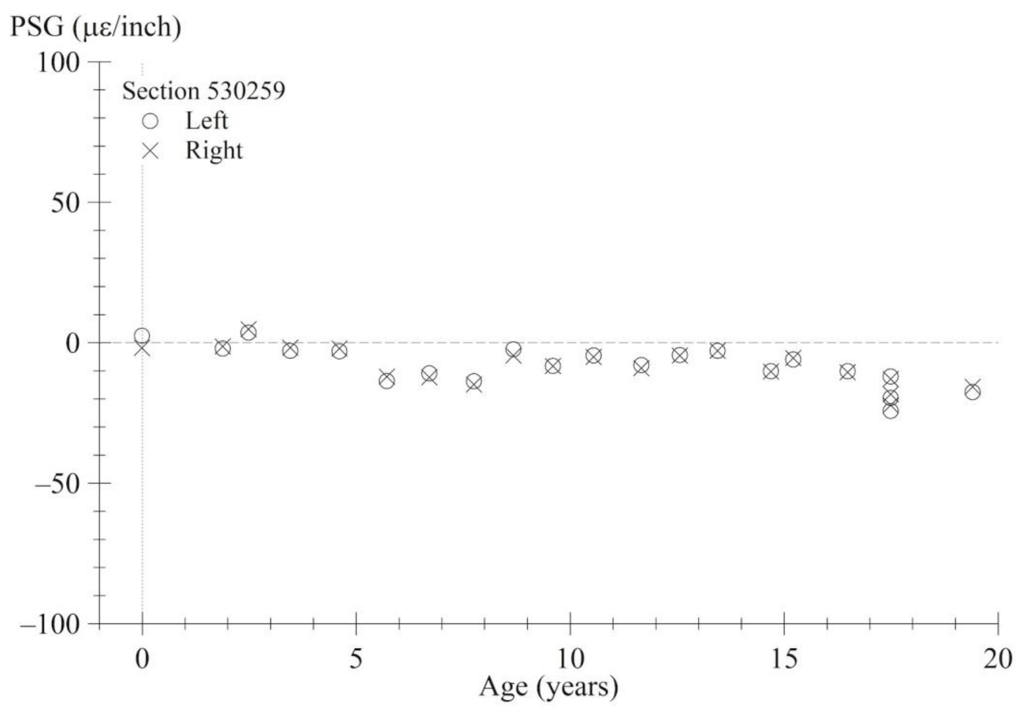

Source: FHWA.

Figure 252. Graph. PSG progression using Best Fit method for section 530259.

APPENDIX H. PSG VERSUS TIME USING AREA METHOD

This appendix provides plots of PSG versus age for the 83 jointed PCC test sections included in this study (figure 253 to Figure 335). PSG values were derived using radius of relative stiffness values produced by the AREA method. PSG values are expressed in units of microstrain per inch (με/inch). PSG values for each visit are a weighted average of all slab-by-slab values from (typically five) repeat passes selected for that monitoring visit. A weighting is assigned to each PSG value in proportion to the corresponding slab length. For slabs that straddle test sections boundaries, a weighting is assigned to the PSG value in proportion to the length that is within the test section.

On the SPS-2 sections, the age is the time elapsed since the project was opened to traffic. On the GPS-3 sections, the age is the time elapsed since the construction date. Figures for sections from the same SPS-2 project use the same age scale.

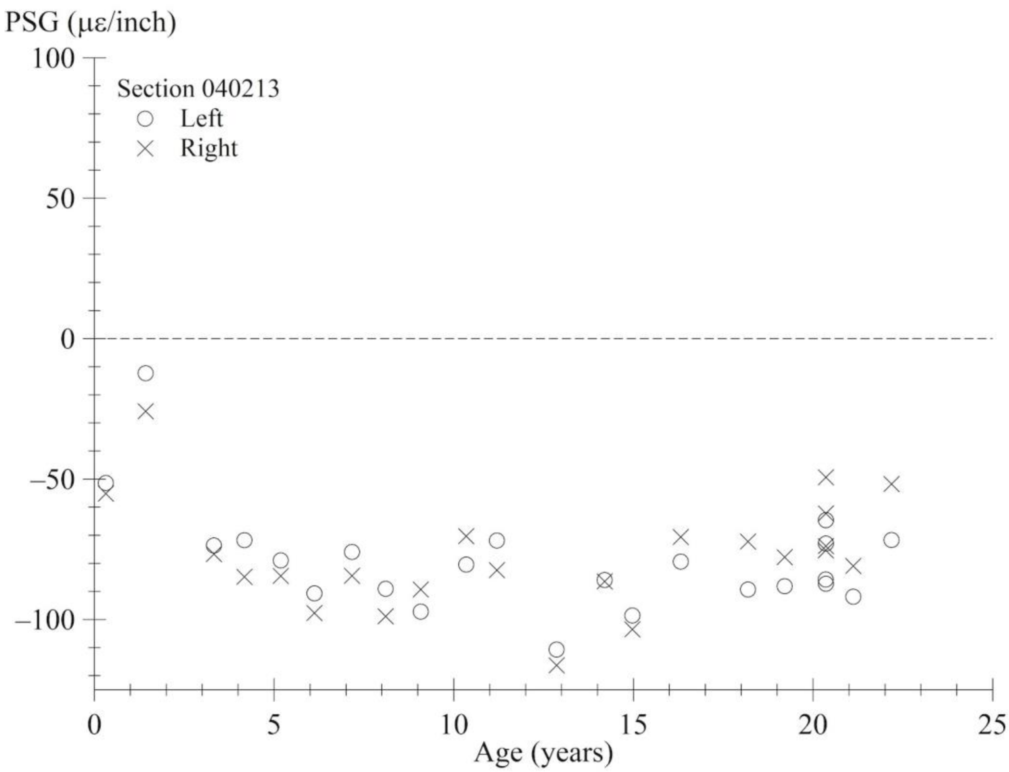

Source: FHWA.

Figure 253. Graph. PSG progression using AREA method for section 040213.

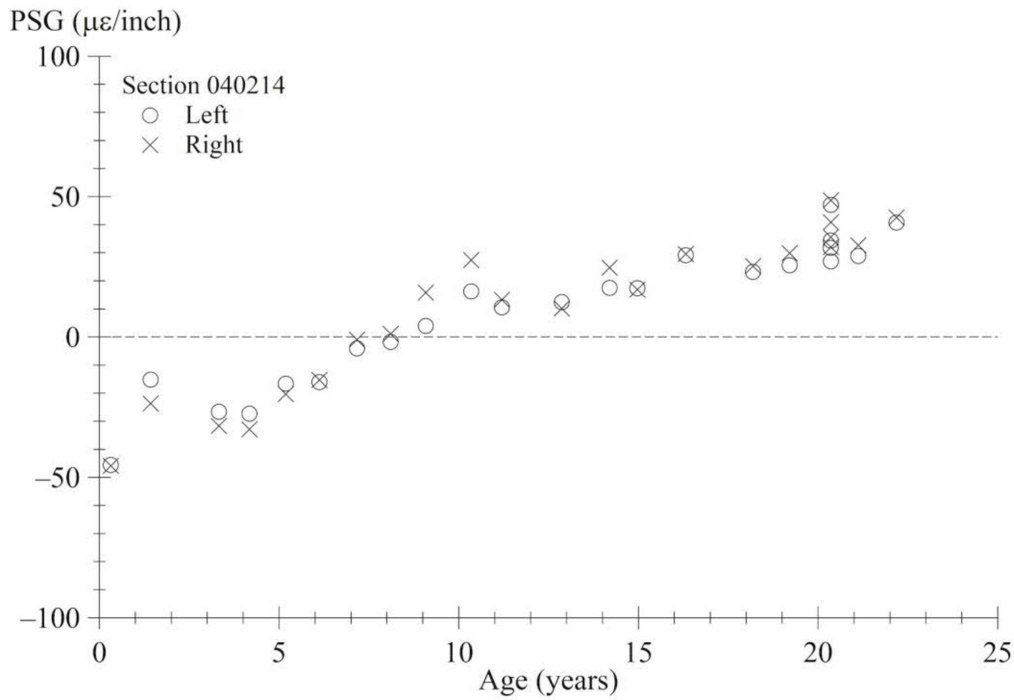

Source: FHWA.

Figure 254. Graph. PSG progression using AREA method for section 040214.

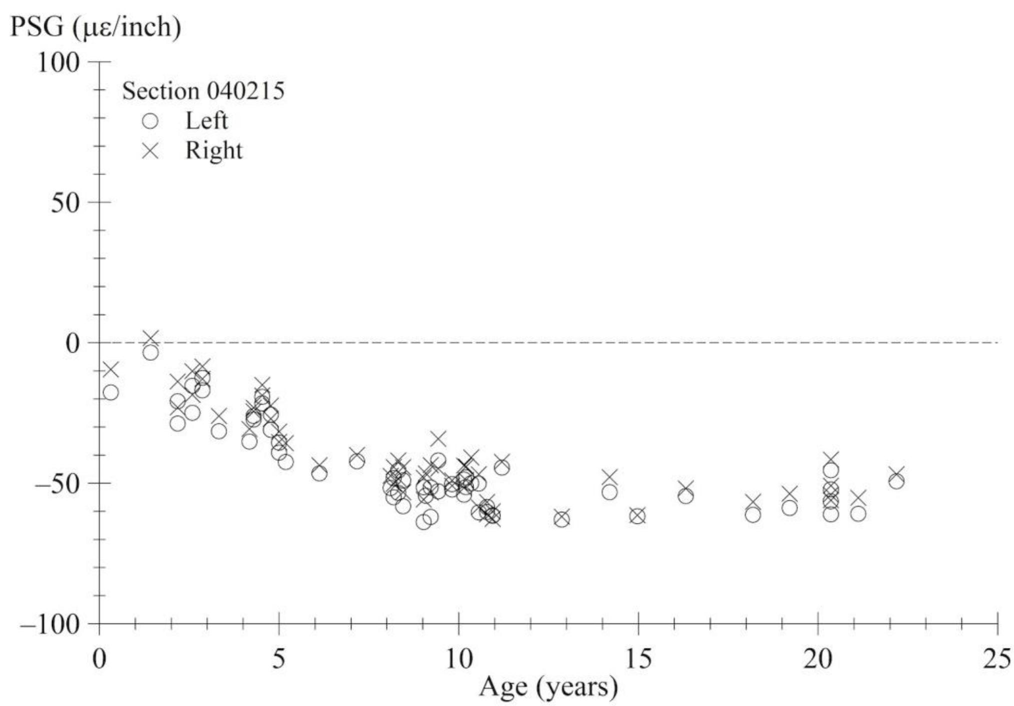

Source: FHWA.

Figure 255. Graph. PSG progression using AREA method for section 040215.

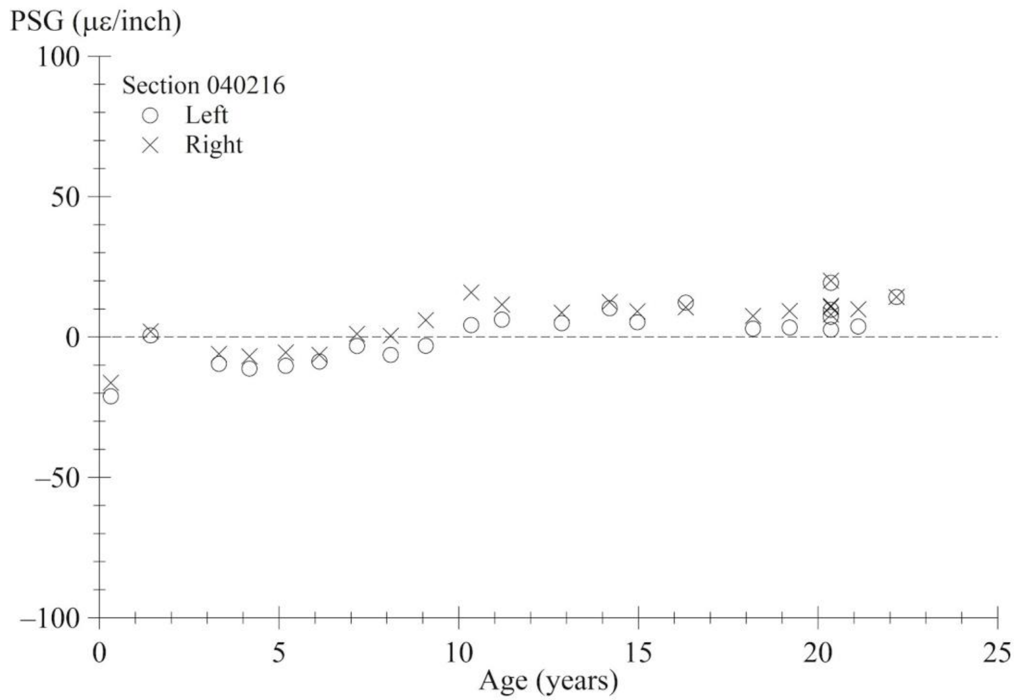

Source: FHWA.

Figure 256. Graph. PSG progression using AREA method for section 040216.

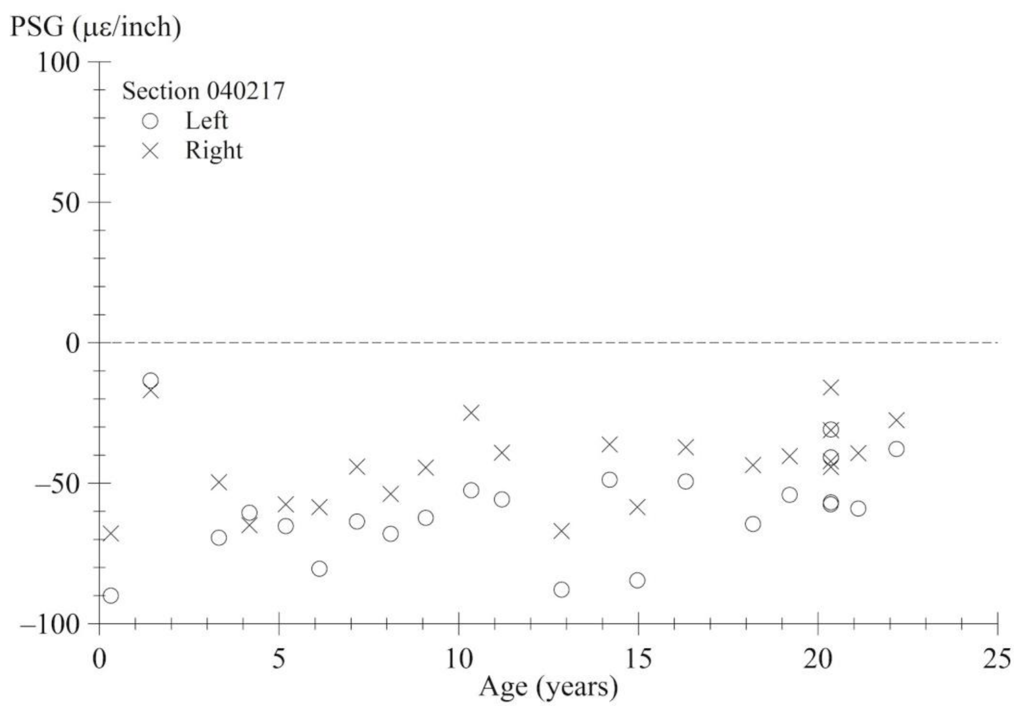

Source: FHWA.

Figure 257. Graph. PSG progression using AREA method for section 040217.

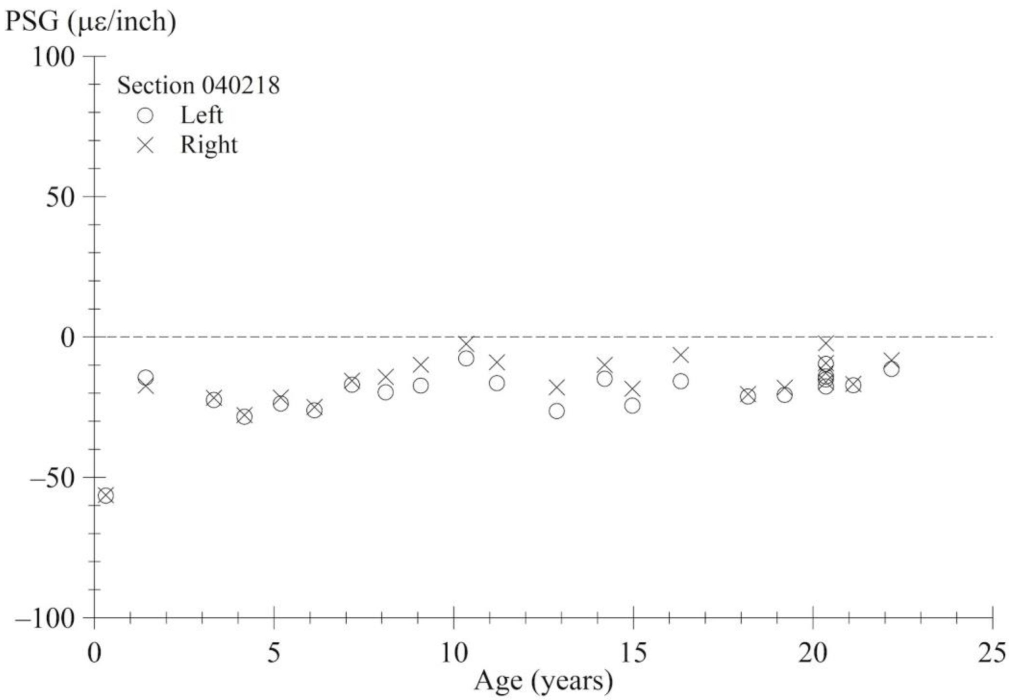

Source: FHWA.

Figure 258. Graph. PSG progression using AREA method for section 040218.

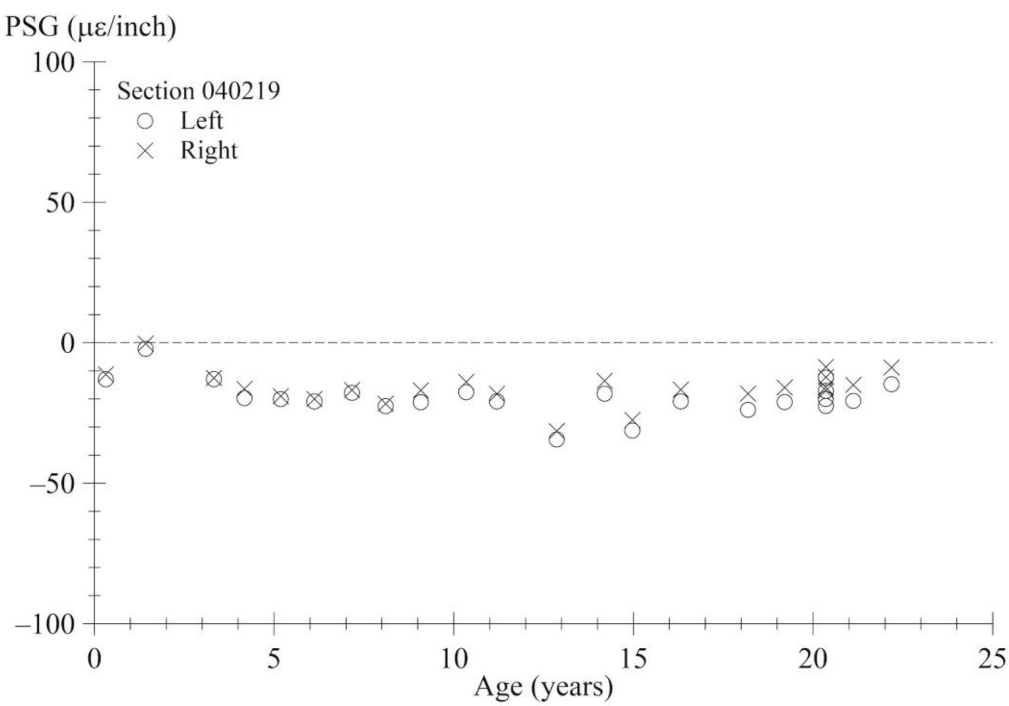

Source: FHWA.

Figure 259. Graph. PSG progression using AREA method for section 040219.

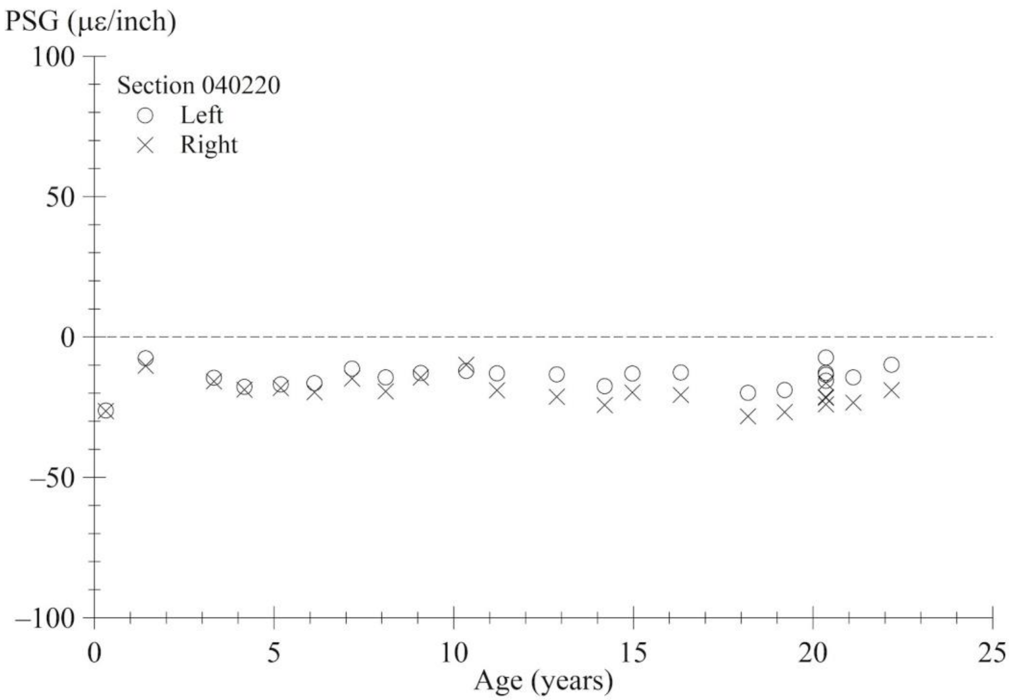

Source: FHWA.

Figure 260. Graph. PSG progression using AREA method for section 040220.

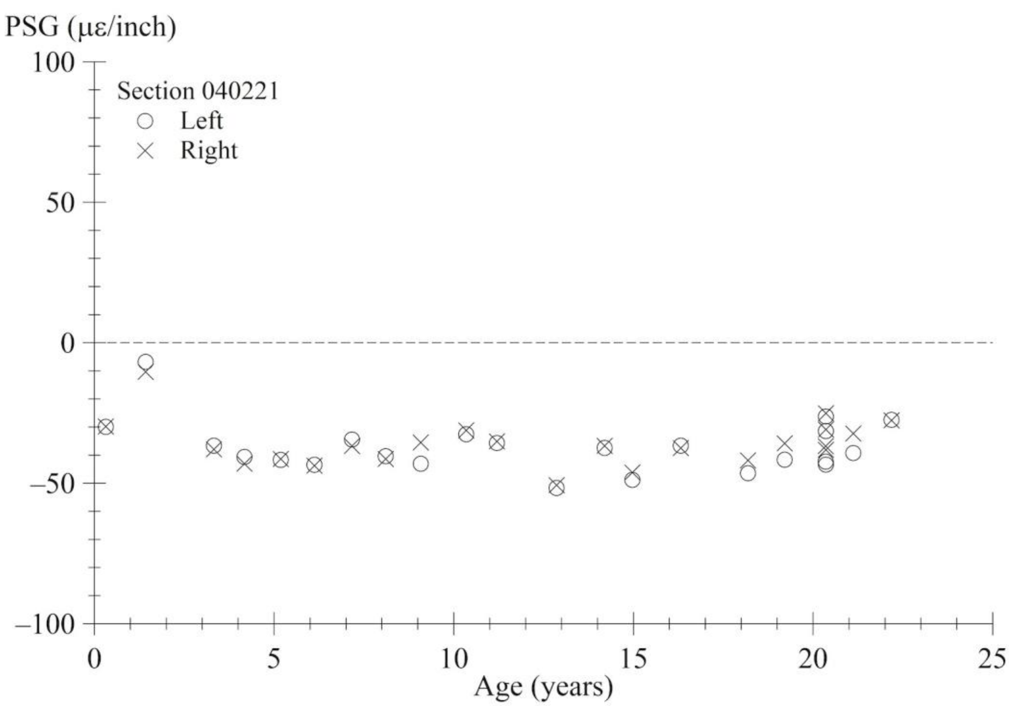

Source: FHWA.

Figure 261. Graph. PSG progression using AREA method for section 040221.

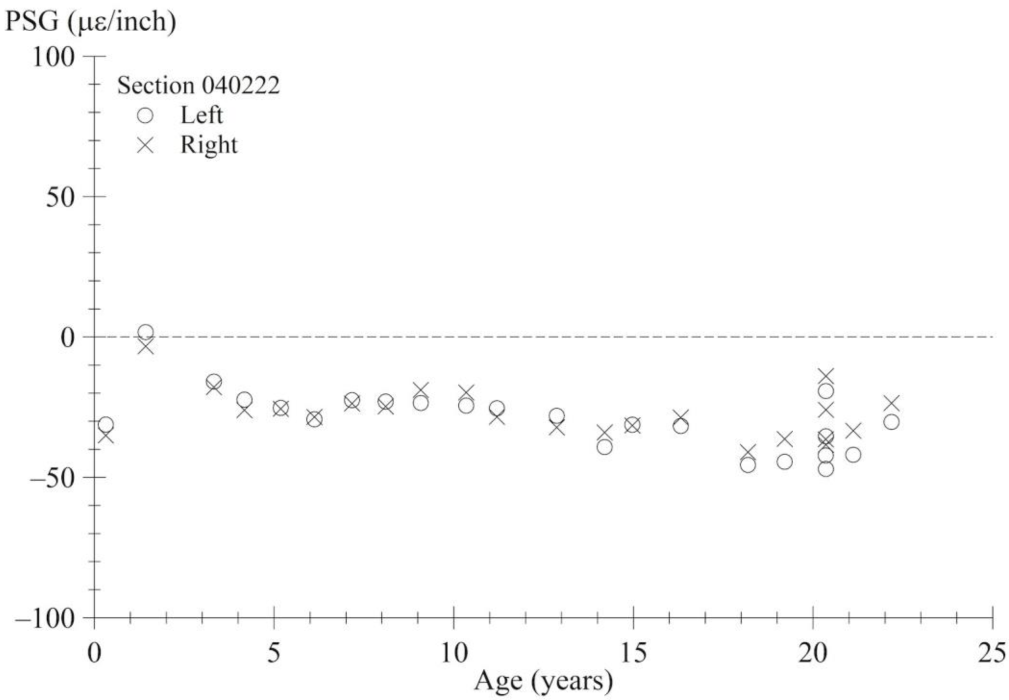

Source: FHWA.

Figure 262. Graph. PSG progression using AREA method for section 040222.

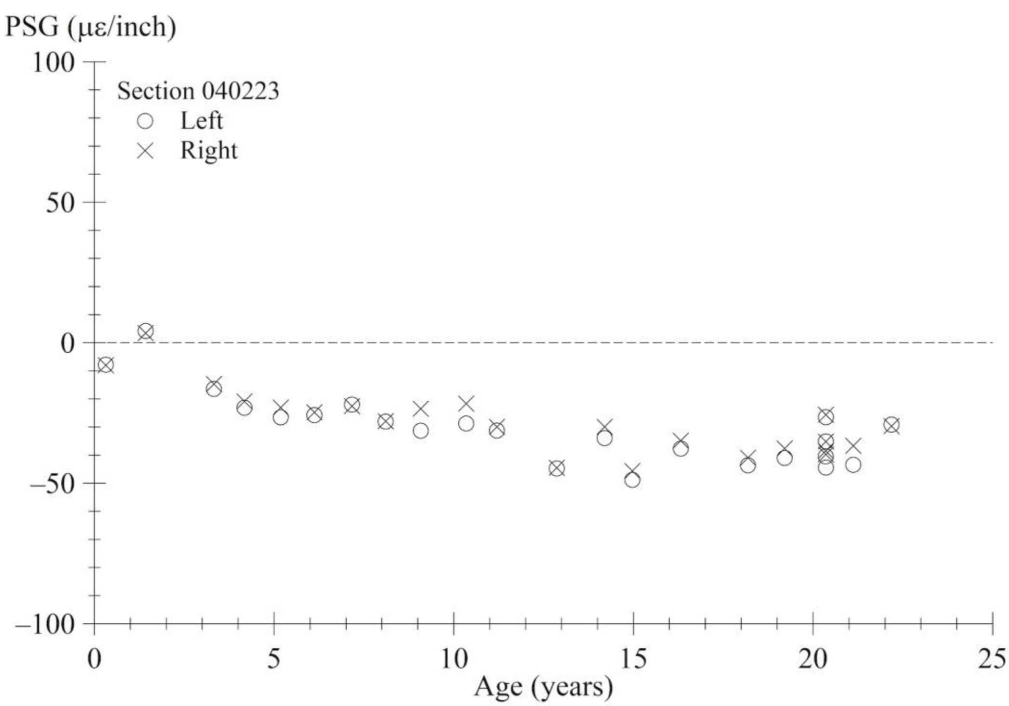

Source: FHWA.

Figure 263. Graph. PSG progression using AREA method for section 040223.

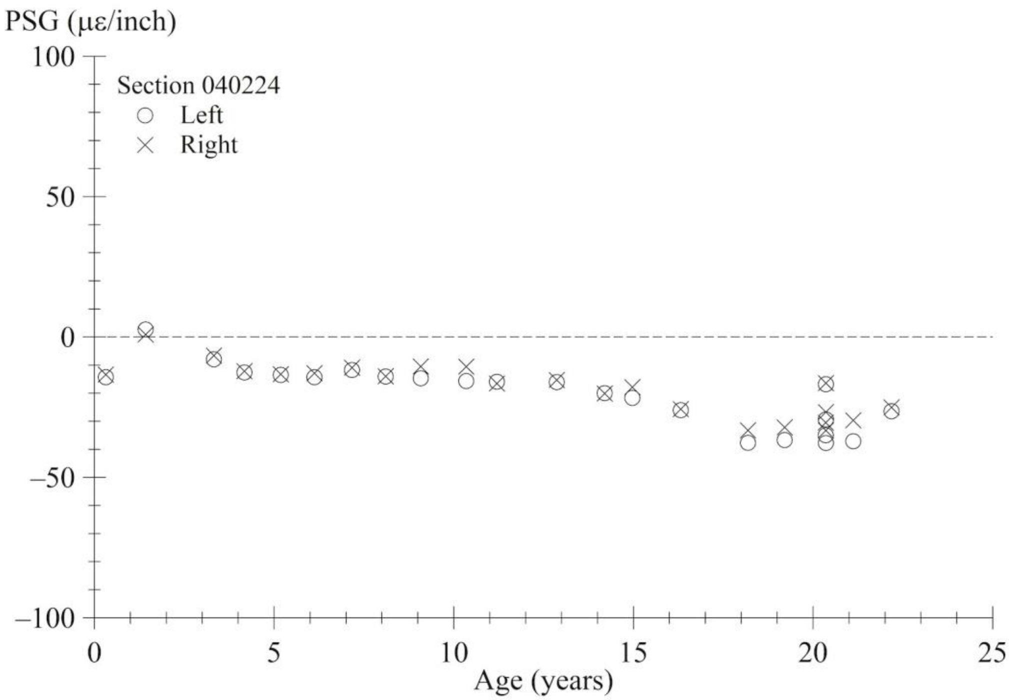

Source: FHWA.

Figure 264. Graph. PSG progression using AREA method for section 040224.

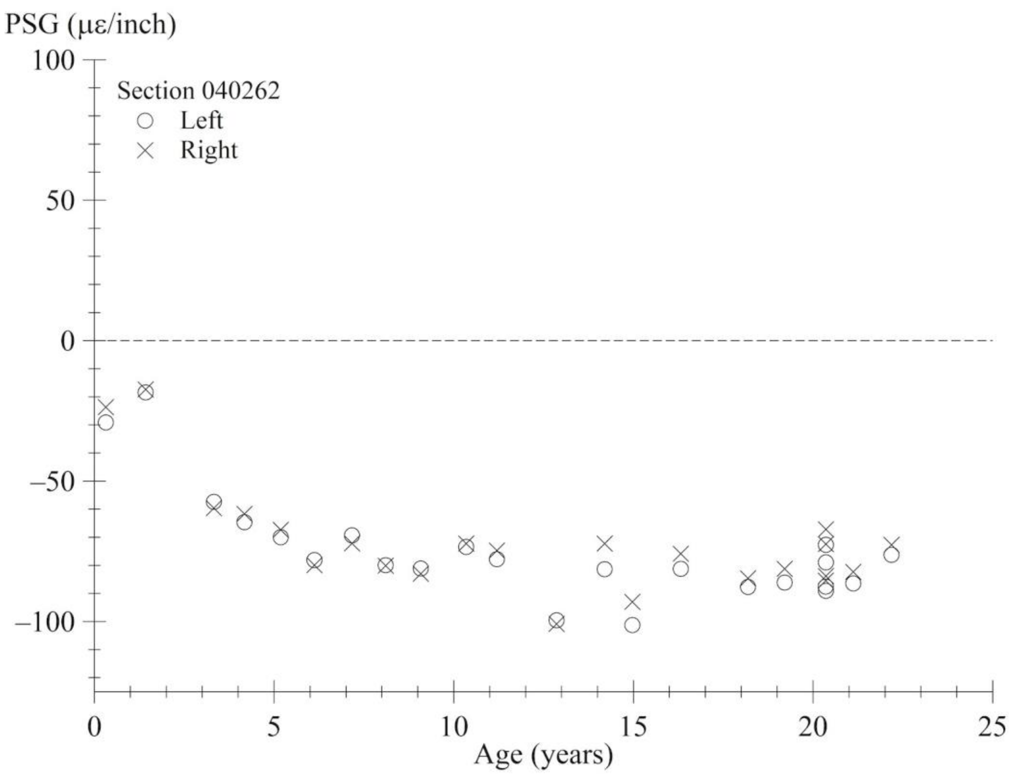

Source: FHWA.

Figure 265. Graph. PSG progression using AREA method for section 040262.

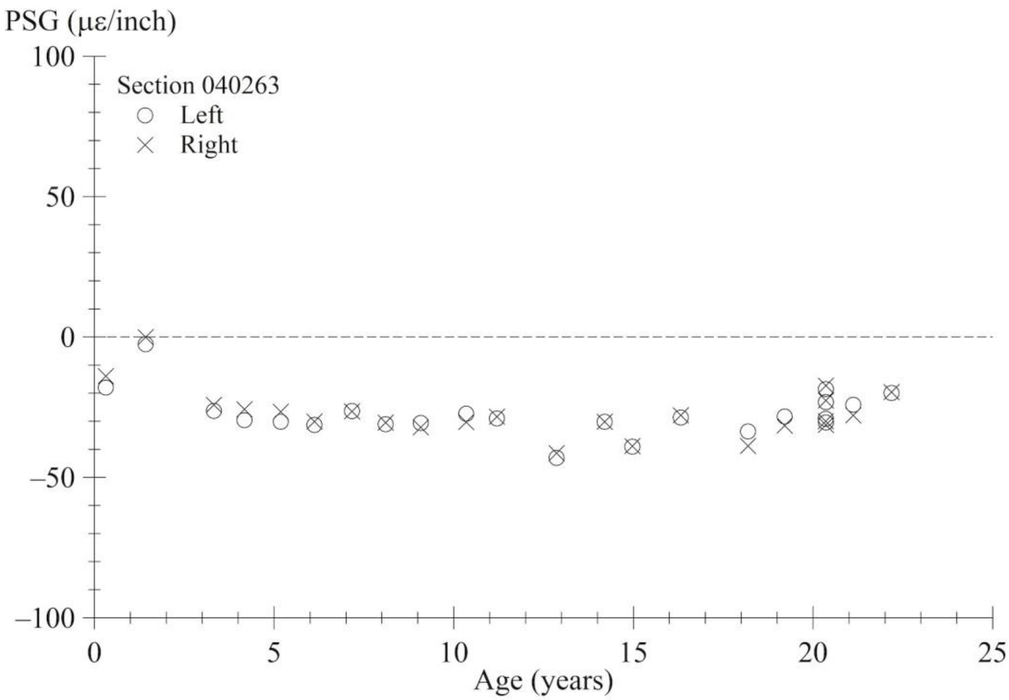

Source: FHWA.

Figure 266. Graph. PSG progression using AREA method for section 040263.

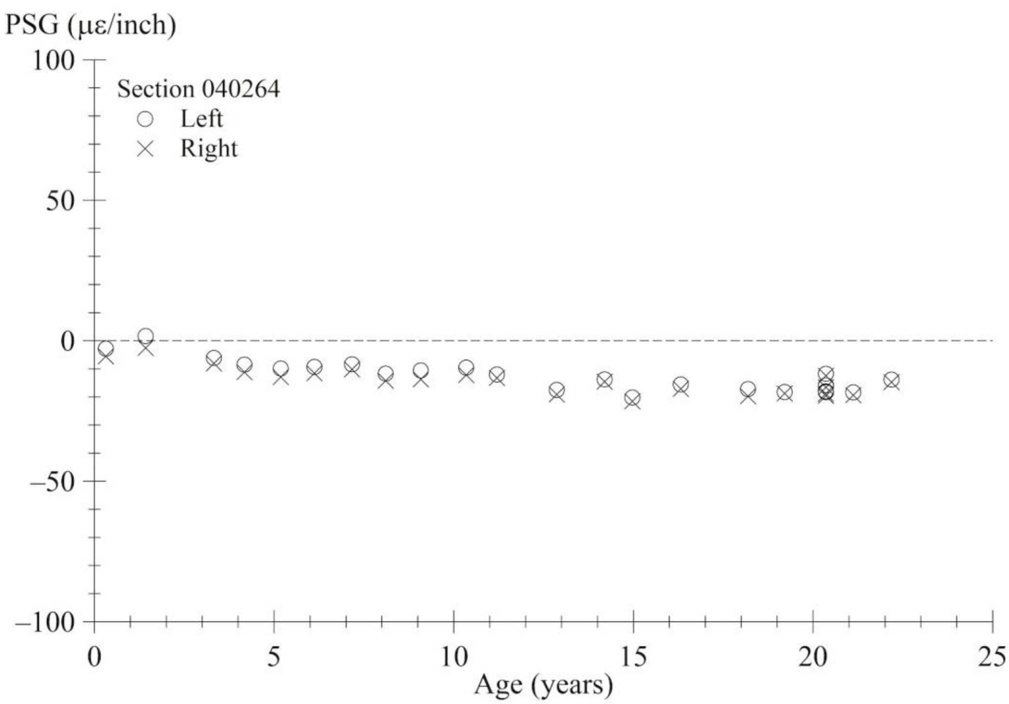

Source: FHWA.

Figure 267. Graph. PSG progression using AREA method for section 040264.

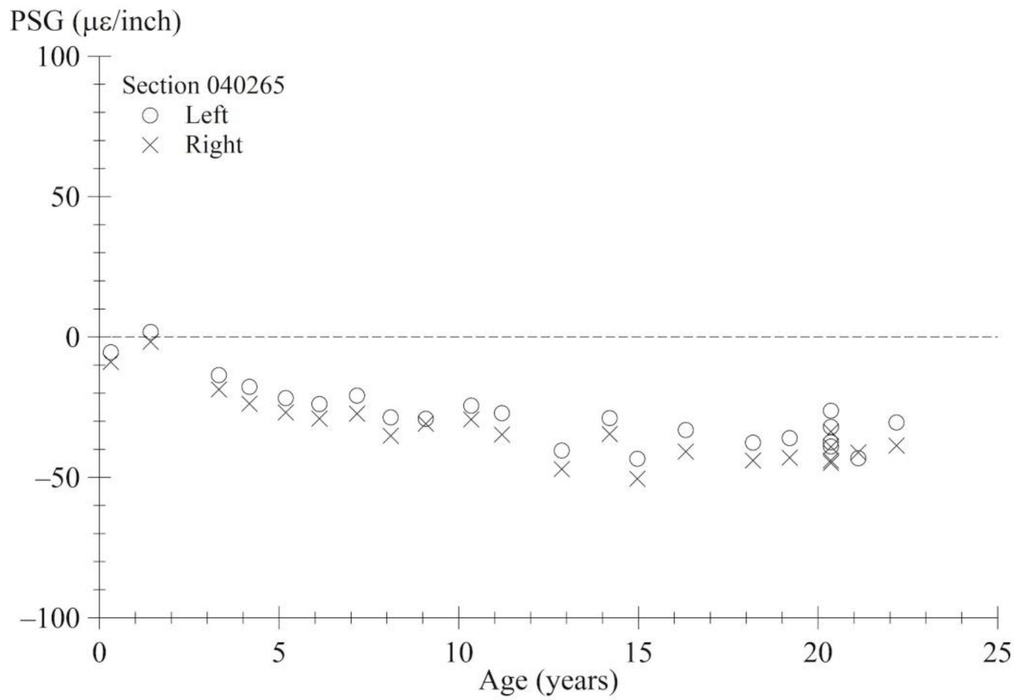

Source: FHWA.

Figure 268. Graph. PSG progression using AREA method for section 040265.

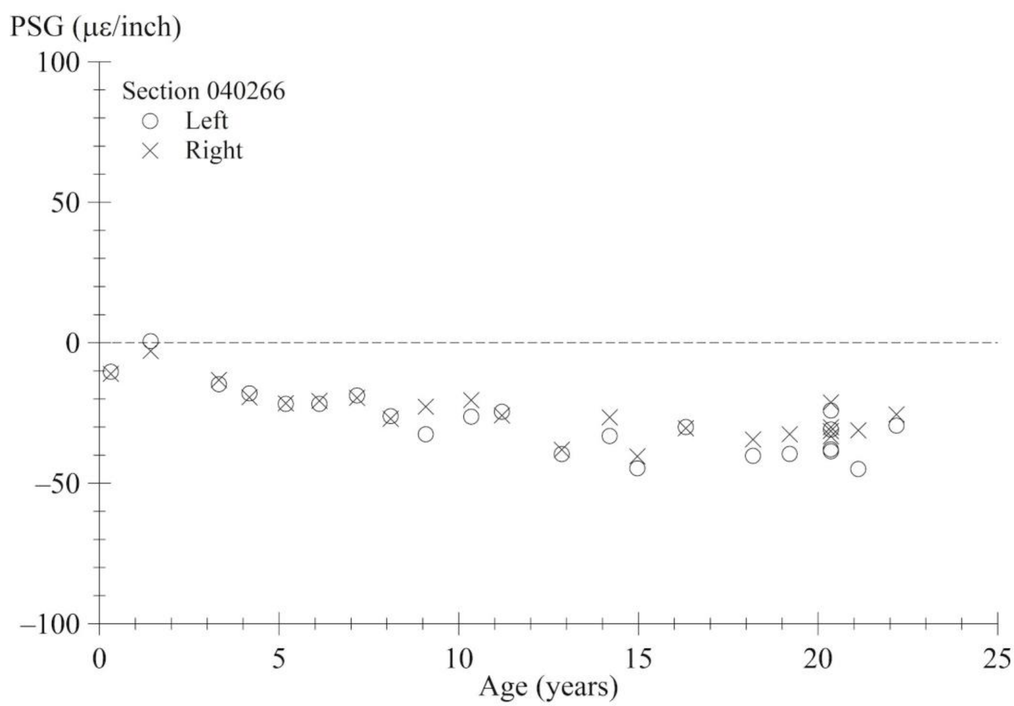

Source: FHWA.

Figure 269. Graph. PSG progression using AREA method for section 040266.

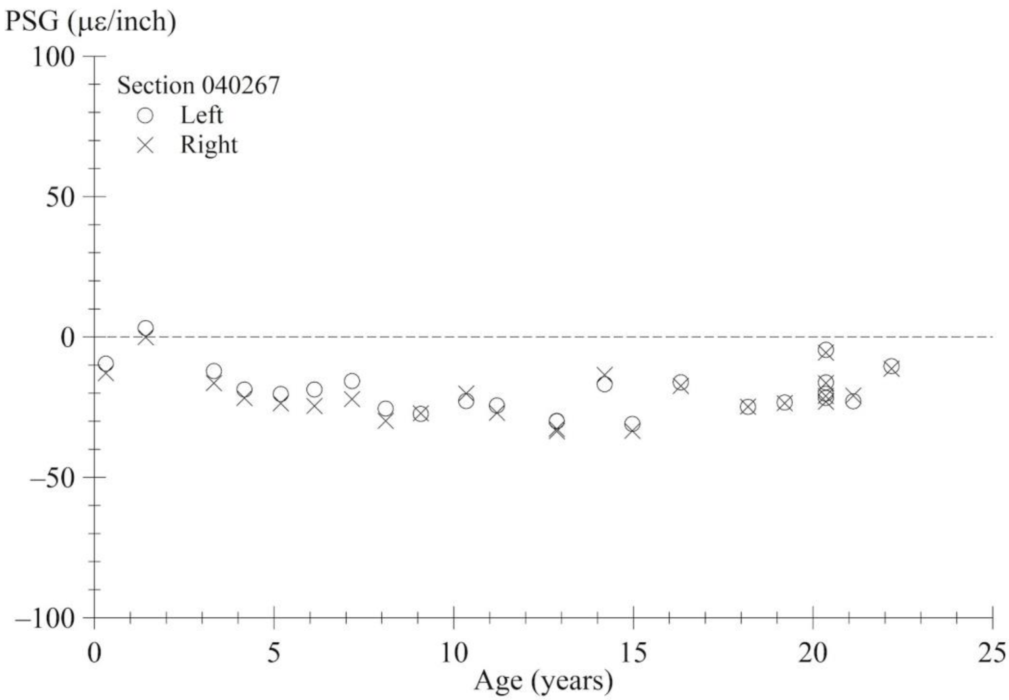

Source: FHWA.

Figure 270. Graph. PSG progression using AREA method for section 040267.

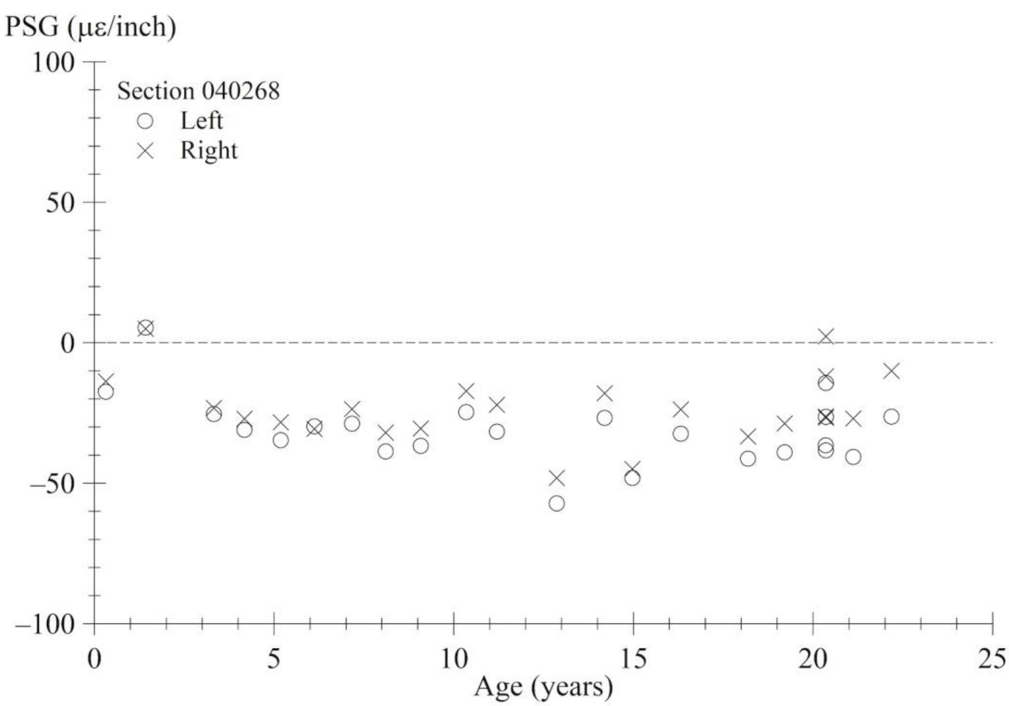

Source: FHWA.

Figure 271. Graph. PSG progression using AREA method for section 040268.

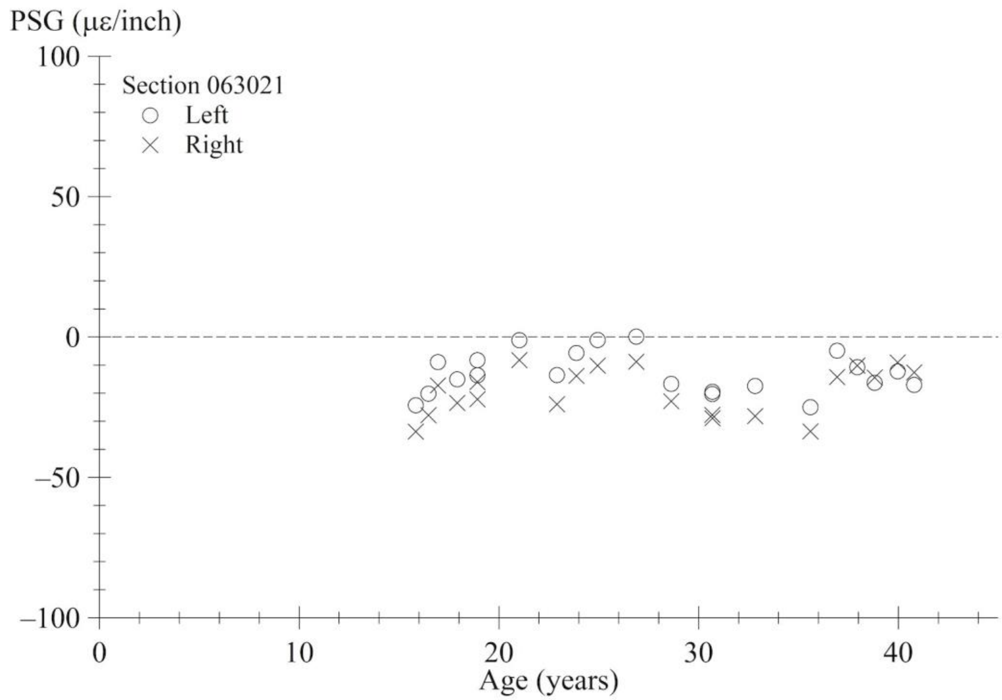

Source: FHWA.

Figure 272. Graph. PSG progression using AREA method for section 063021.

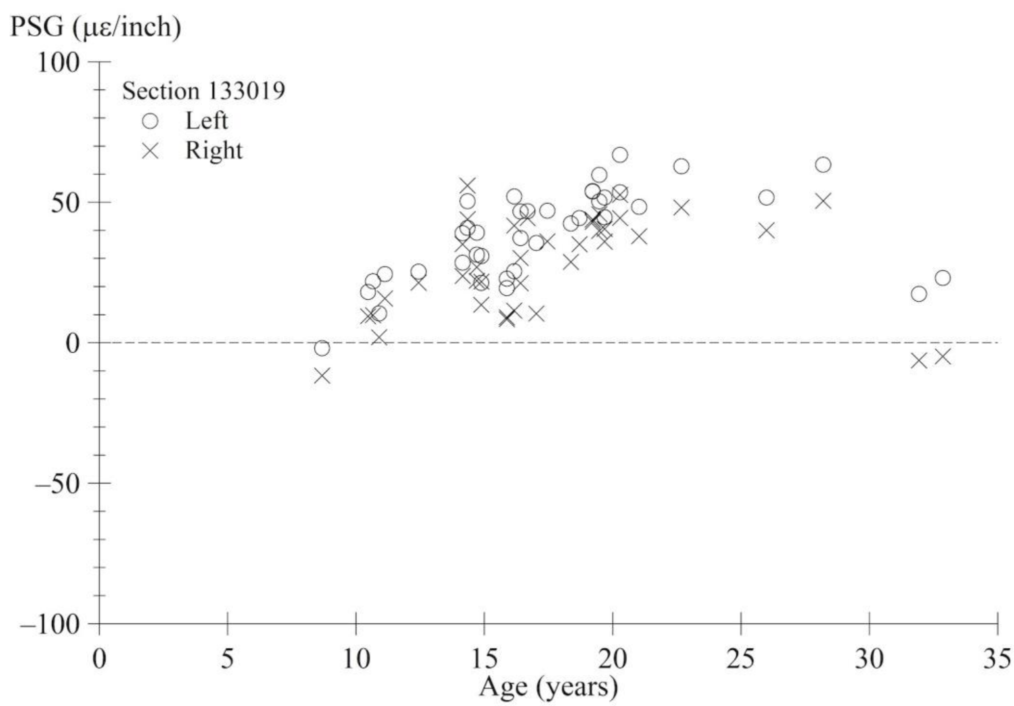

Source: FHWA.

Figure 273. Graph. PSG progression using AREA method for section 133019.

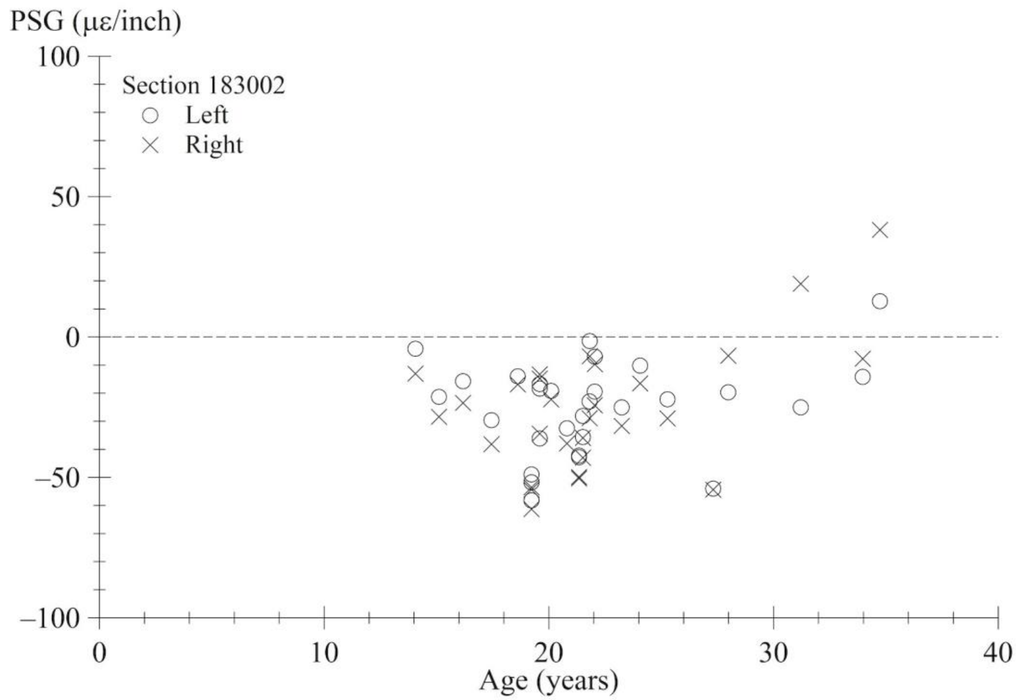

Source: FHWA.

Figure 274. Graph. PSG progression using AREA method for section 183002.

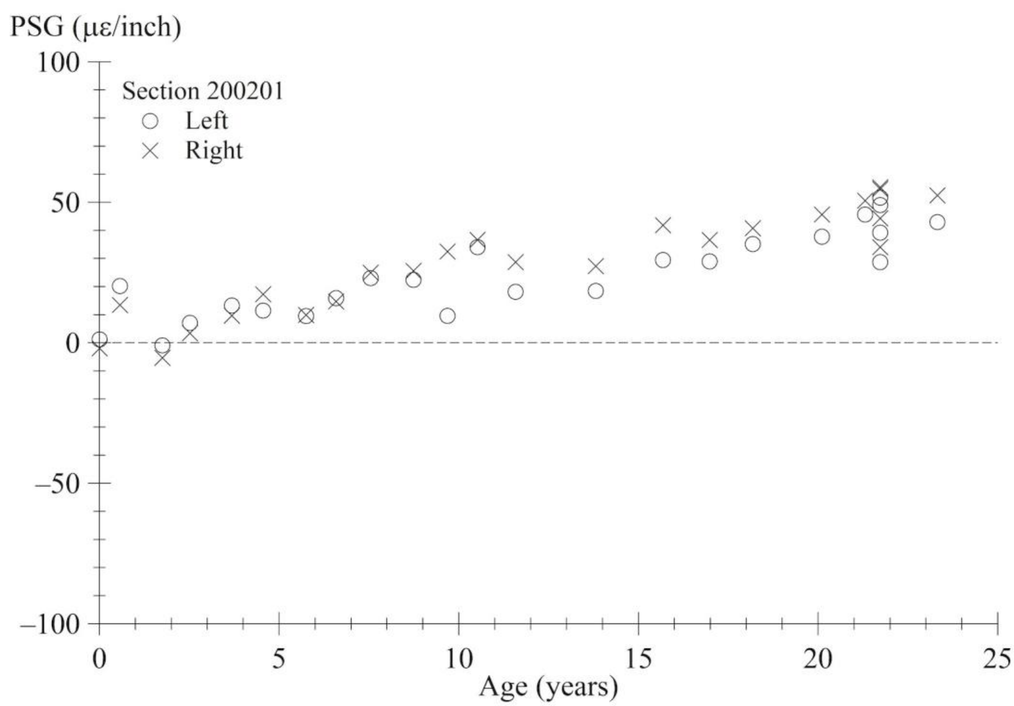

Source: FHWA.

Figure 275. Graph. PSG progression using AREA method for section 200201.

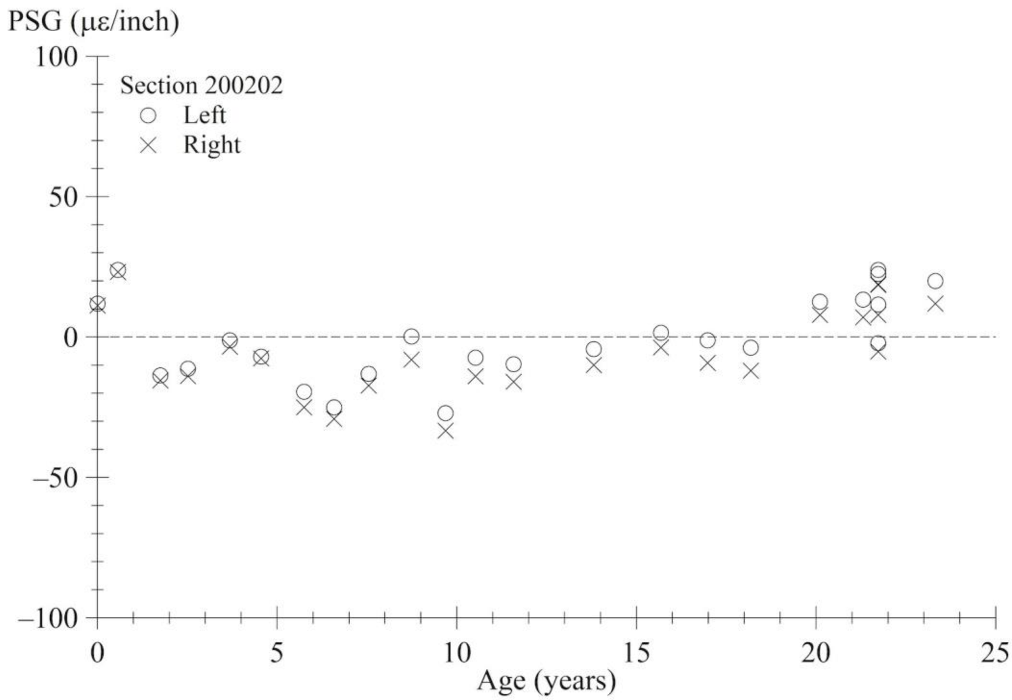

Source: FHWA.

Figure 276. Graph. PSG progression using AREA method for section 200202.

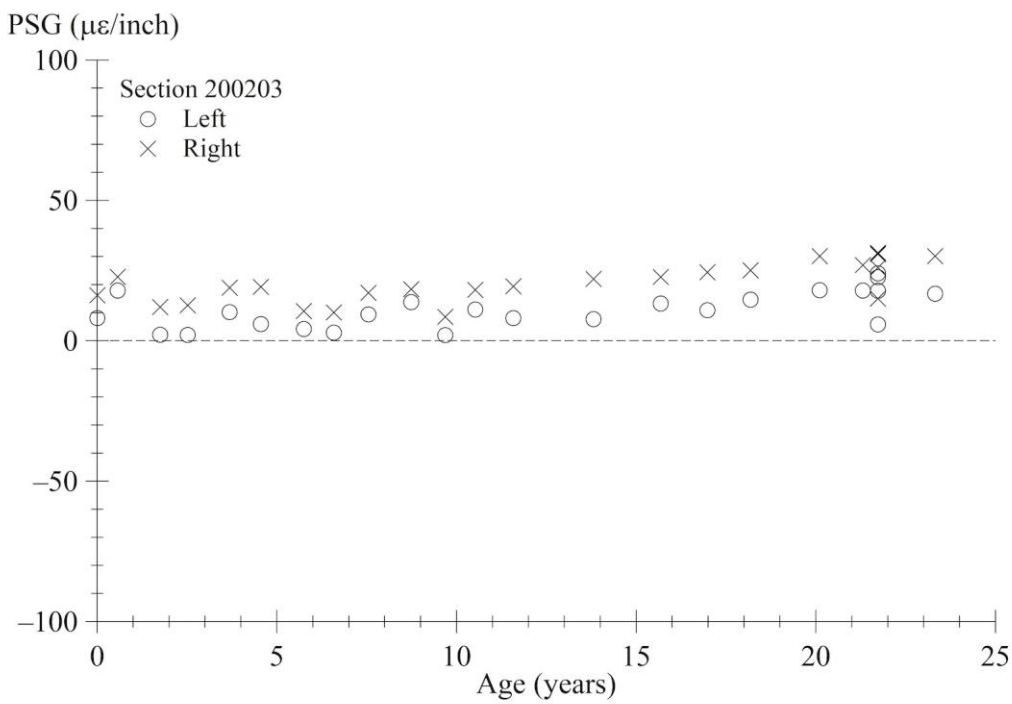

Source: FHWA.

Figure 277. Graph. PSG progression using AREA method for section 200203.

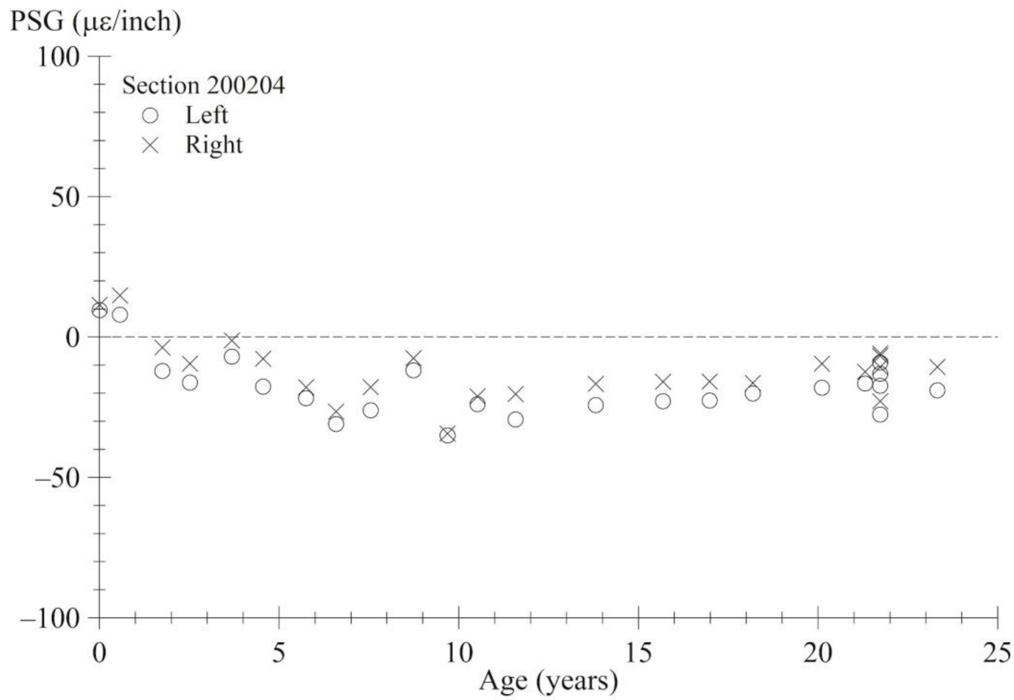

Source: FHWA.

Figure 278. Graph. PSG progression using AREA method for section 200204.

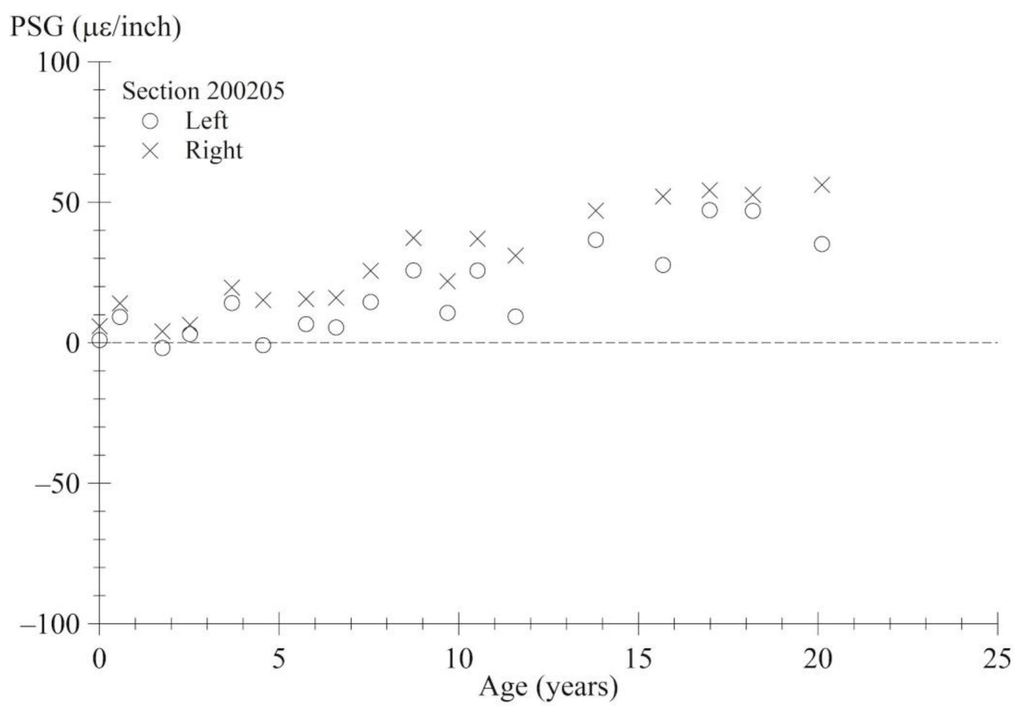

Source: FHWA.

Figure 279. Graph. PSG progression using AREA method for section 200205.

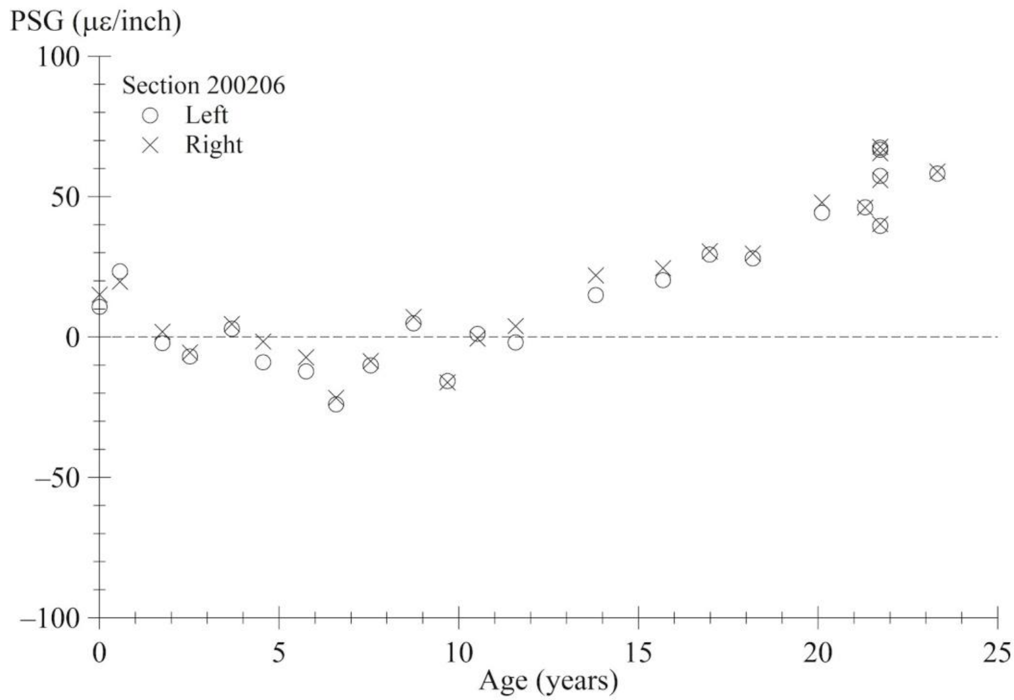

Source: FHWA.

Figure 280. Graph. PSG progression using AREA method for section 200206.

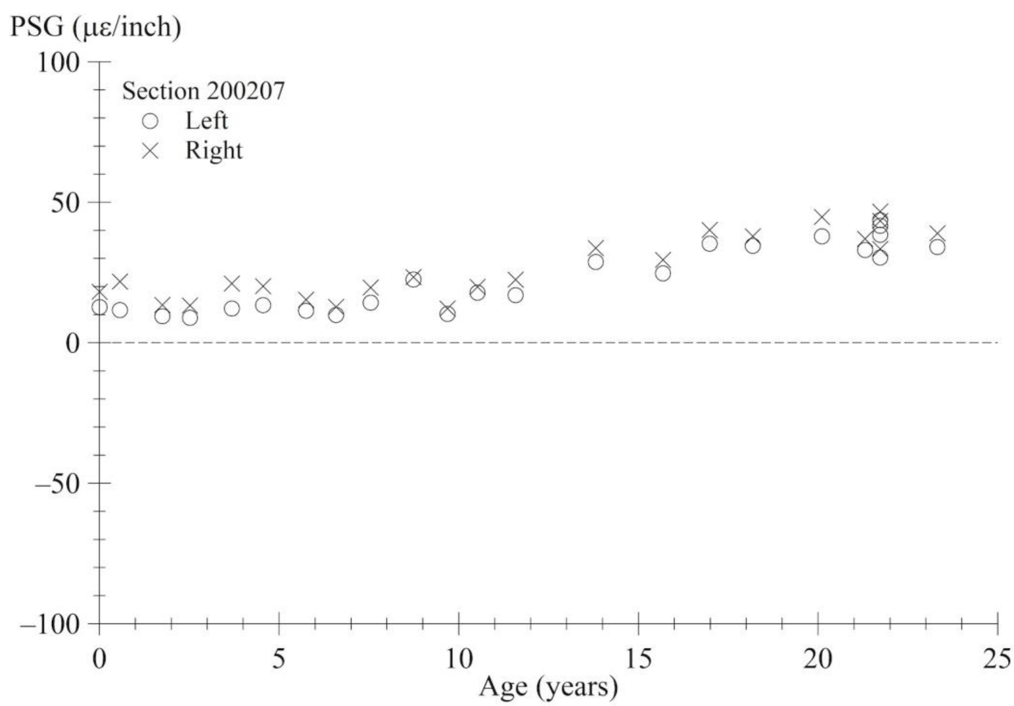

Source: FHWA.

Figure 281. Graph. PSG progression using AREA method for section 200207.

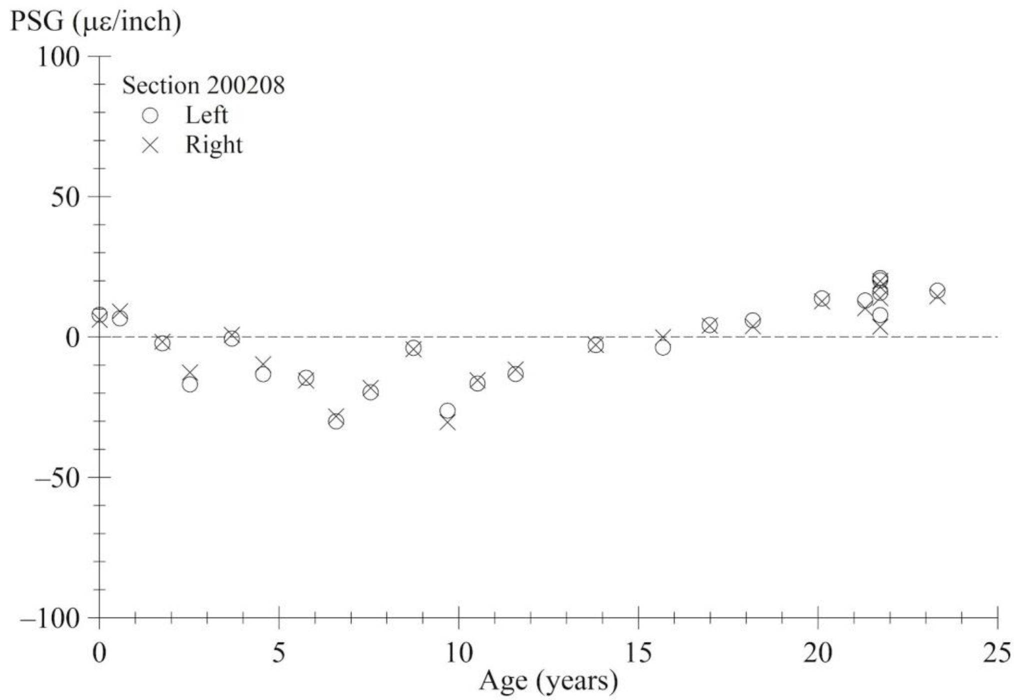

Source: FHWA.

Figure 282. Graph. PSG progression using AREA method for section 200208.

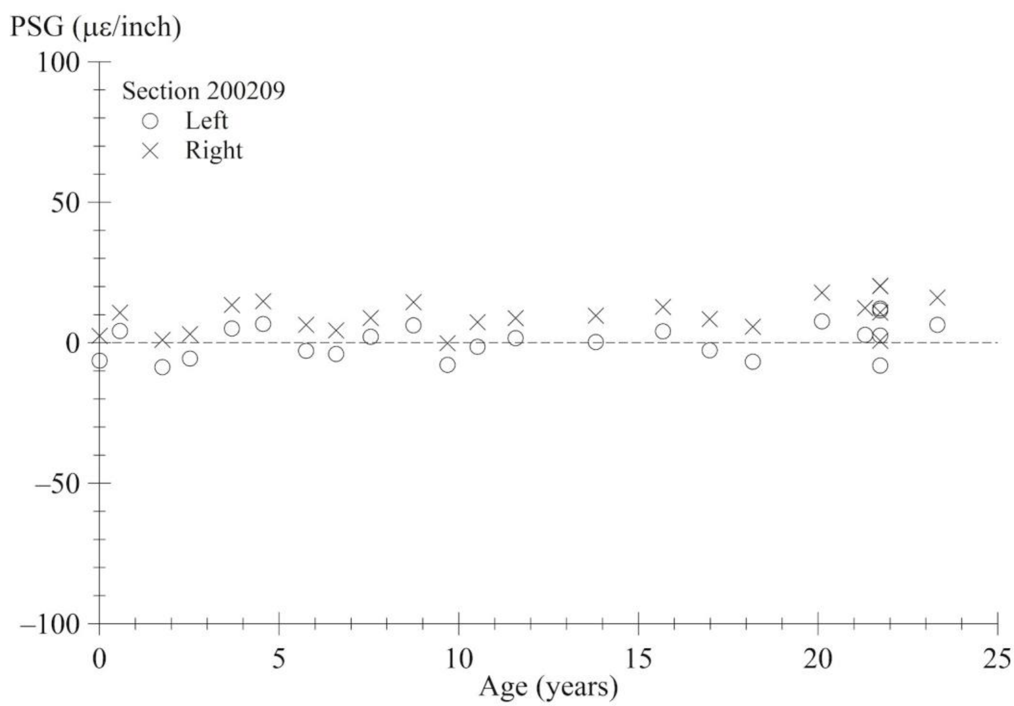

Source: FHWA.

Figure 283. Graph. PSG progression using AREA method for section 200209.

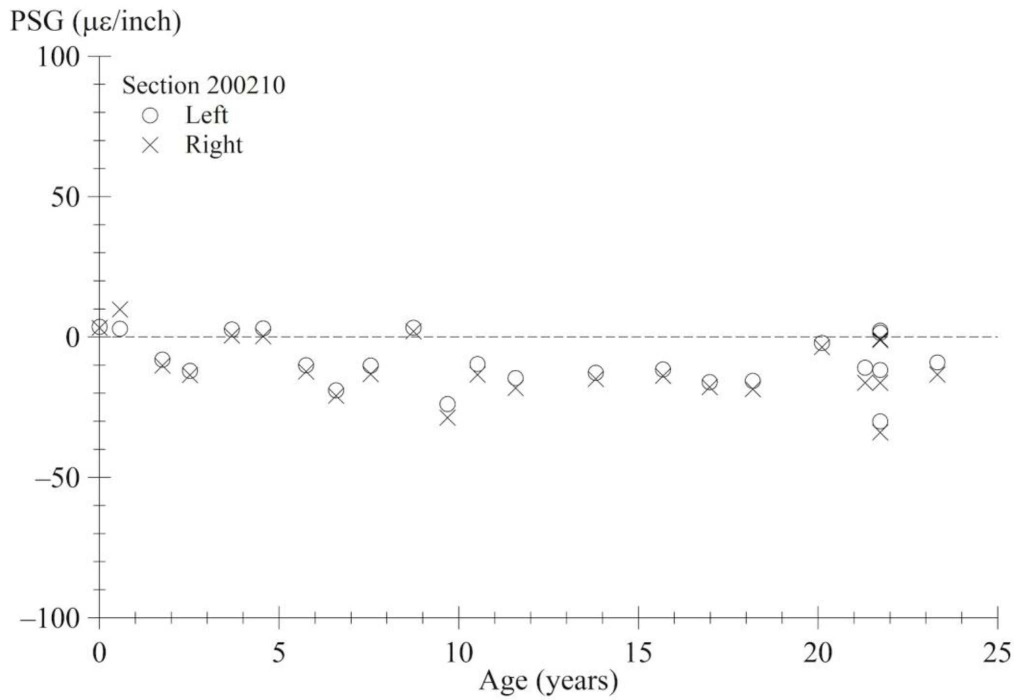

Source: FHWA.

Figure 284. Graph. PSG progression using AREA method for section 200210.

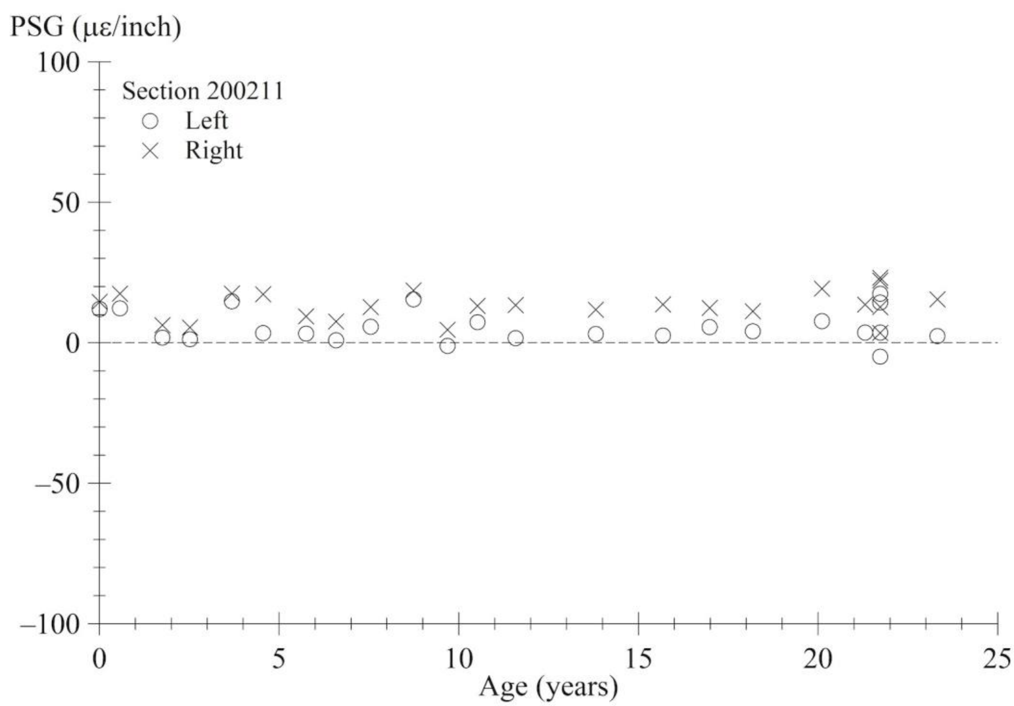

Source: FHWA.

Figure 285. Graph. PSG progression using AREA method for section 200211.

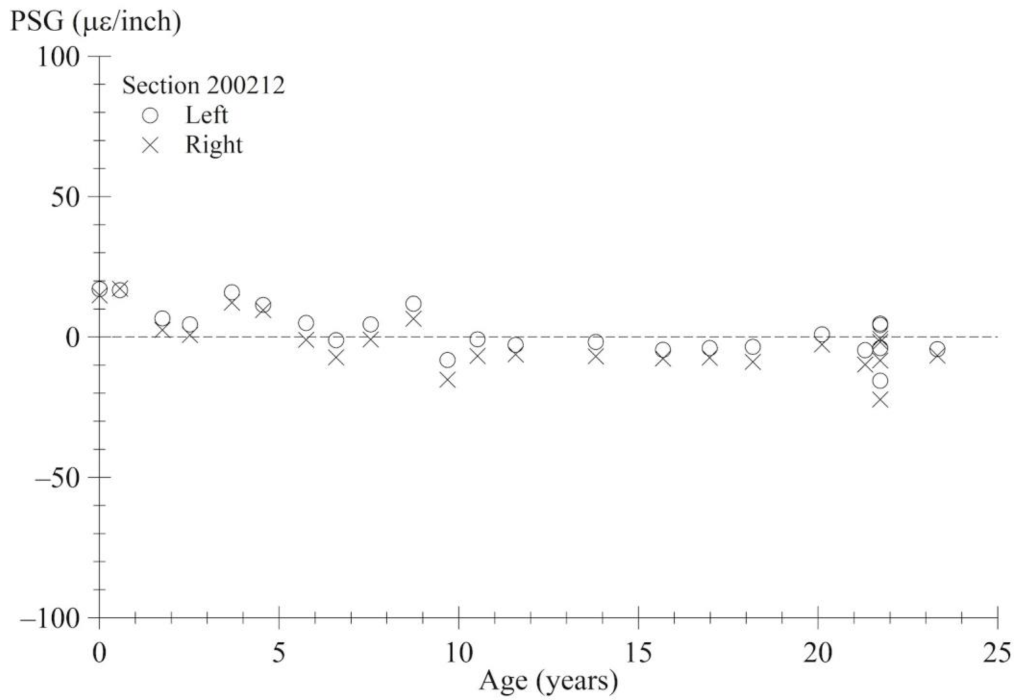

Source: FHWA.

Figure 286. Graph. PSG progression using AREA method for section 200212.

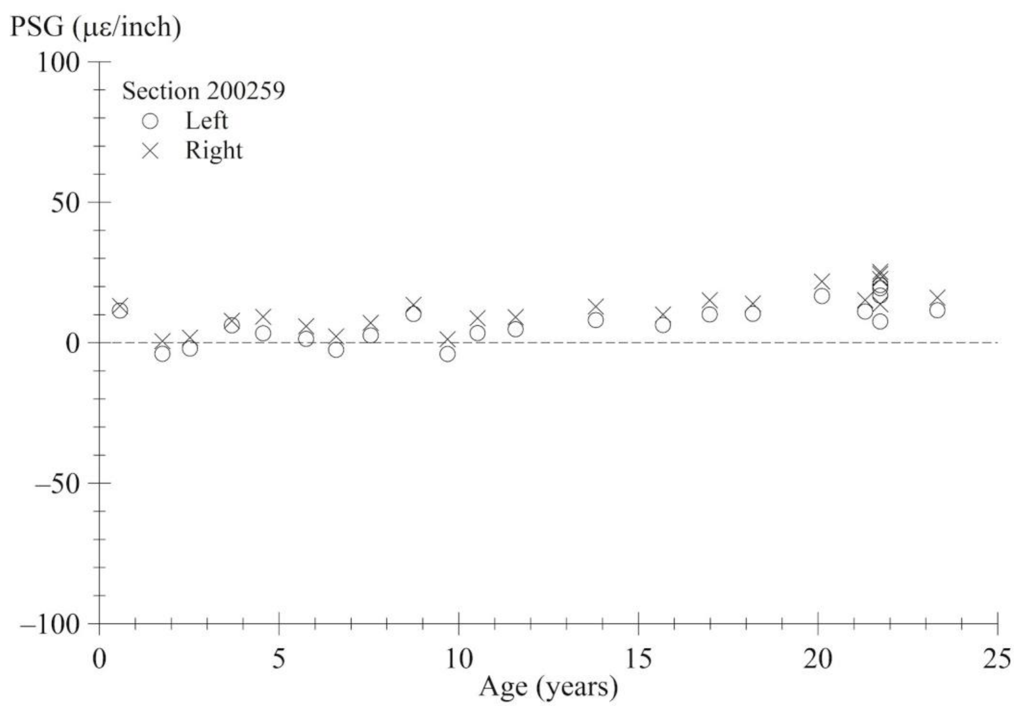

Source: FHWA.

Figure 287. Graph. PSG progression using AREA method for section 200259.

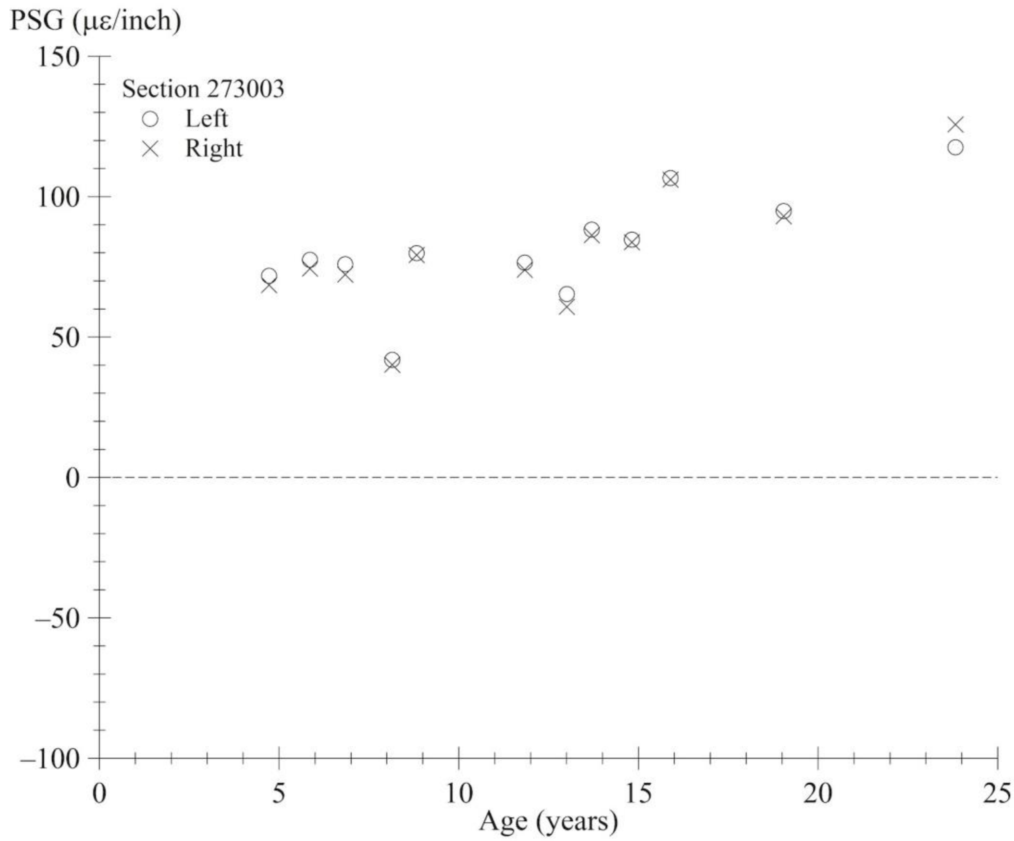

Source: FHWA.

Figure 288. Graph. PSG progression using AREA method for section 273003.

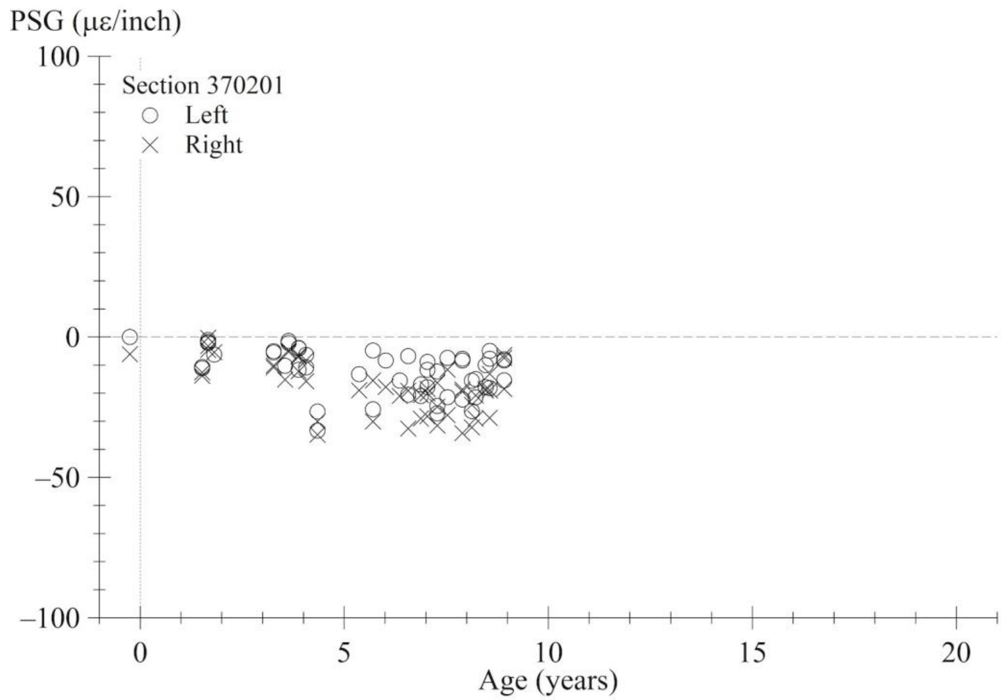

Source: FHWA.

Figure 289. Graph. PSG progression using AREA method for section 370201.

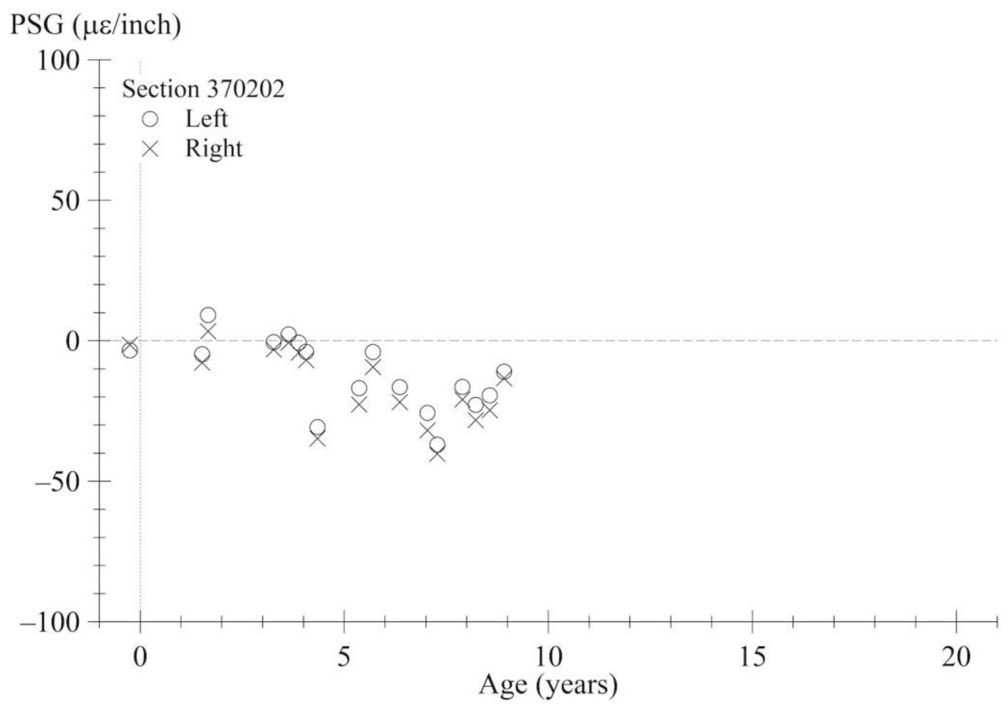

Source: FHWA.

Figure 290. Graph. PSG progression using AREA method for section 370202.

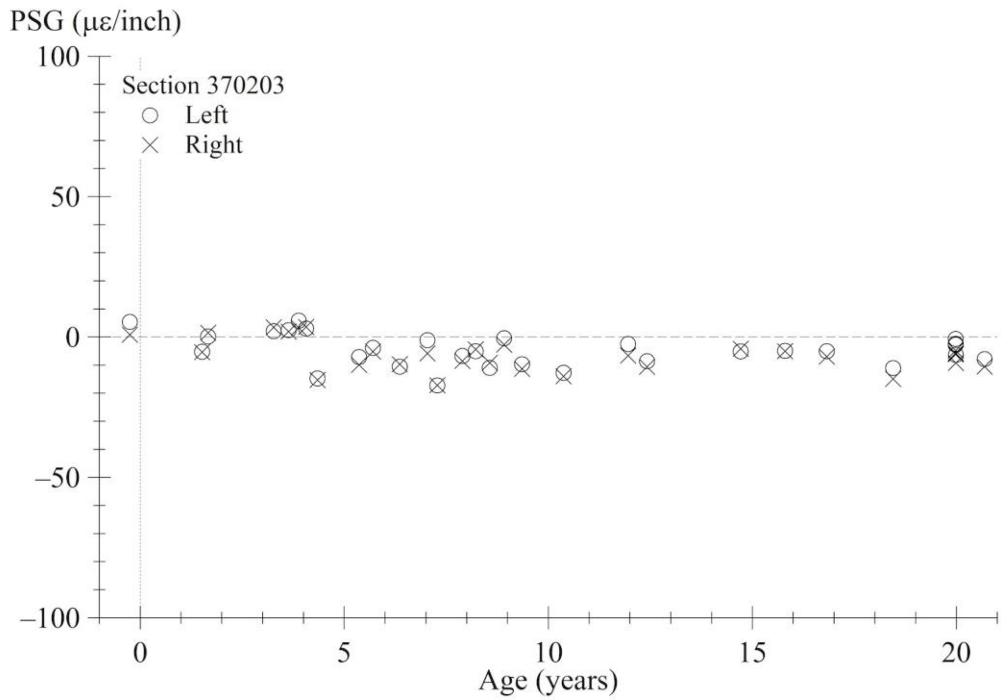

Source: FHWA.

Figure 291. Graph. PSG progression using AREA method for section 370203.

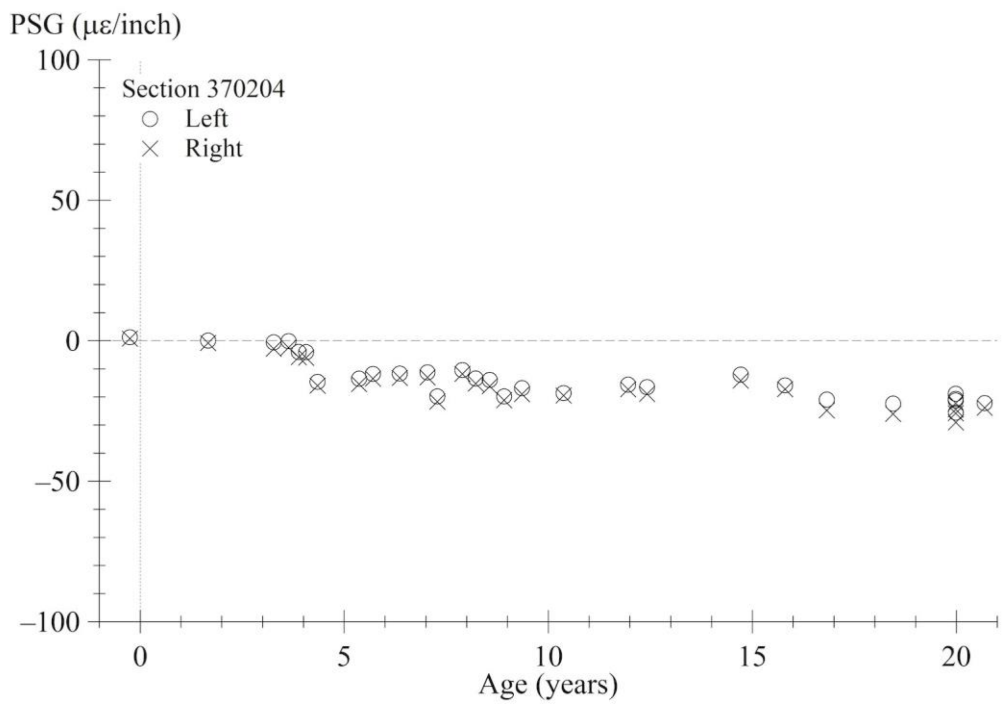

Source: FHWA.

Figure 292. Graph. PSG progression using AREA method for section 370204.

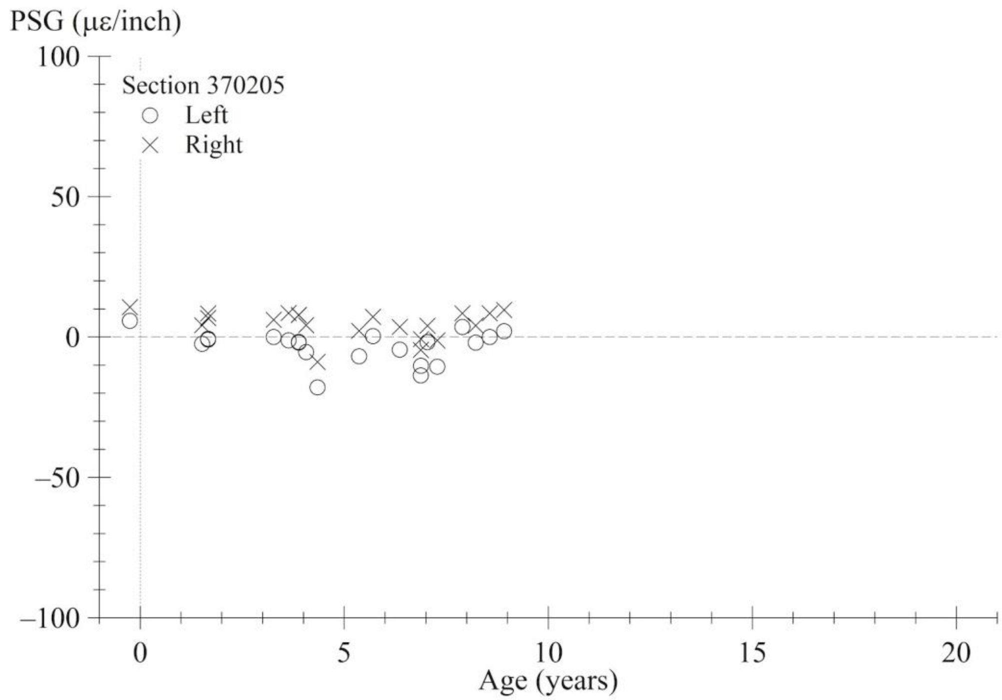

Source: FHWA.

Figure 293. Graph. PSG progression using AREA method for section 370205.

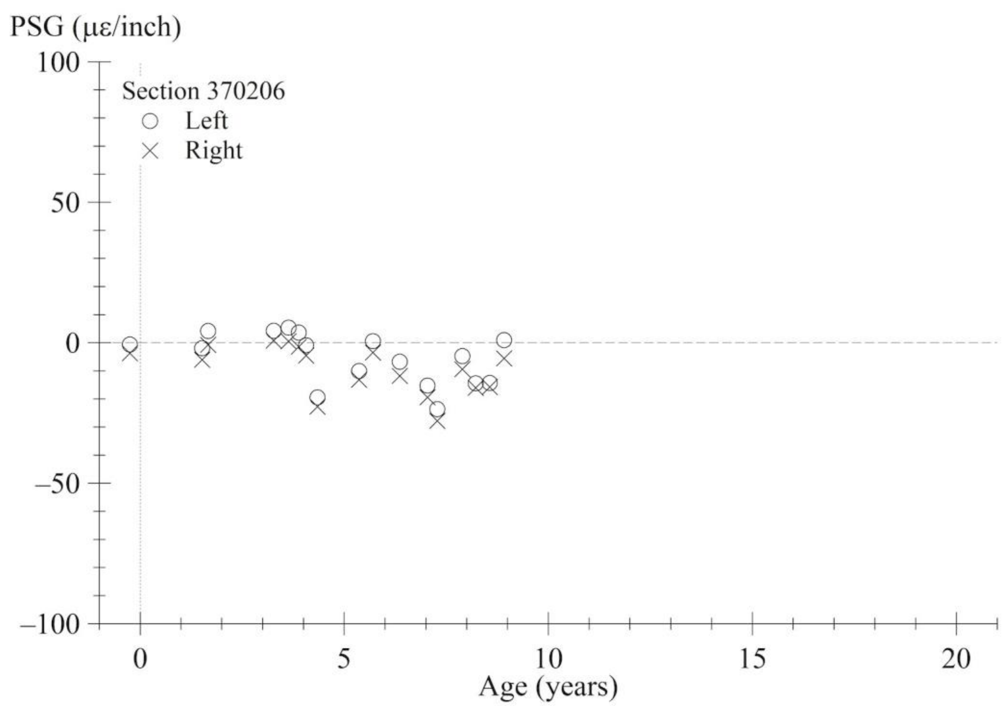

Source: FHWA.

Figure 294. Graph. PSG progression using AREA method for section 370206.

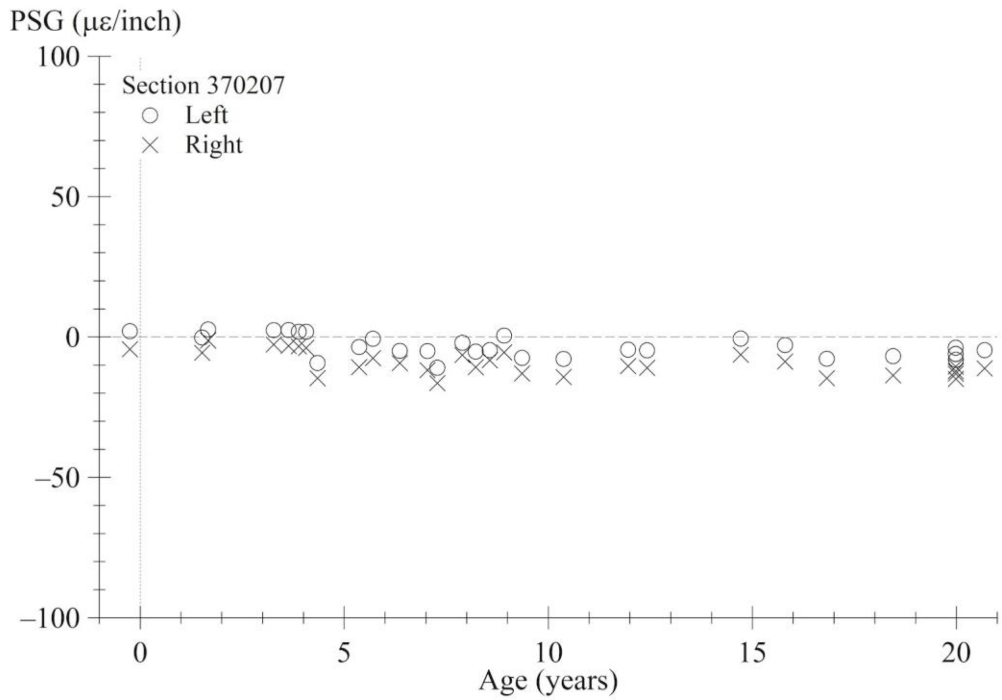

Source: FHWA.

Figure 295. Graph. PSG progression using AREA method for section 370207.

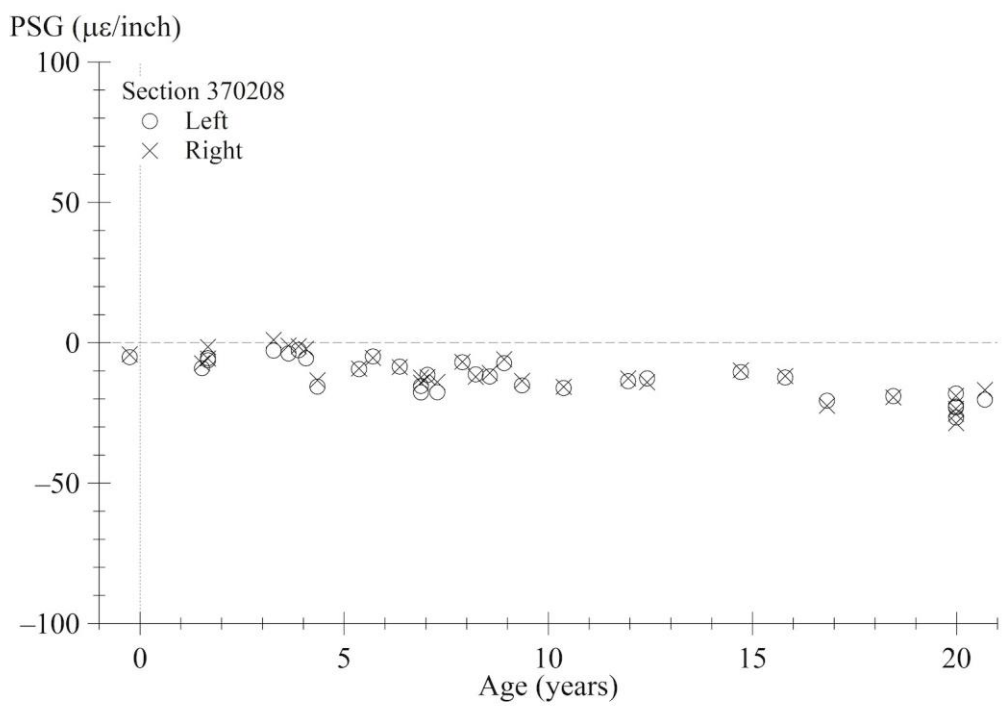

Source: FHWA.

Figure 296. Graph. PSG progression using AREA method for section 370208.

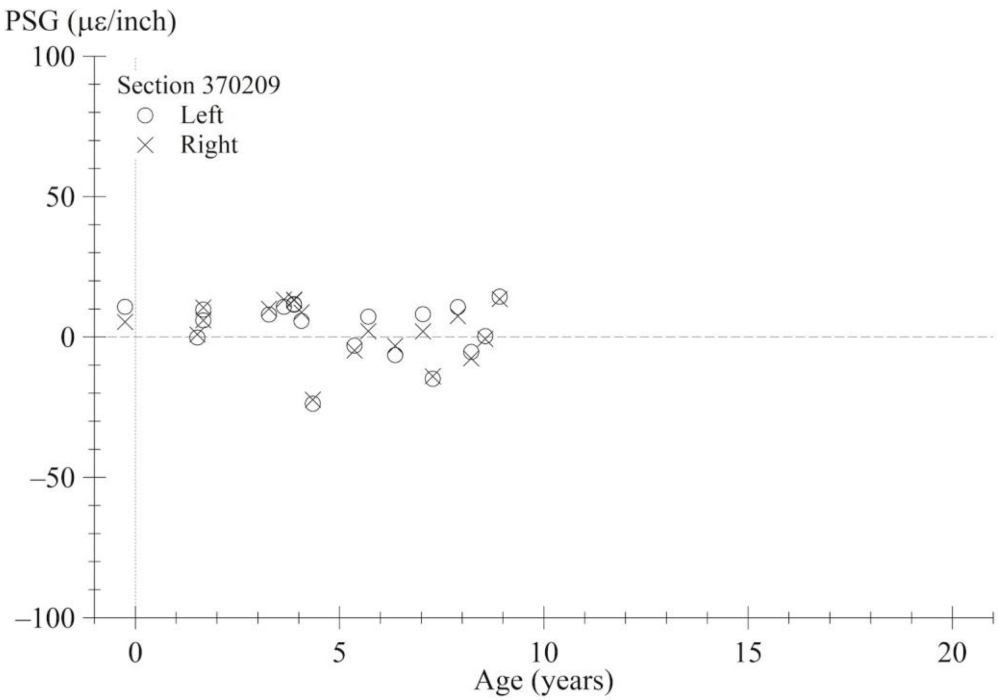

Source: FHWA.

Figure 297. Graph. PSG progression using AREA method for section 370209.

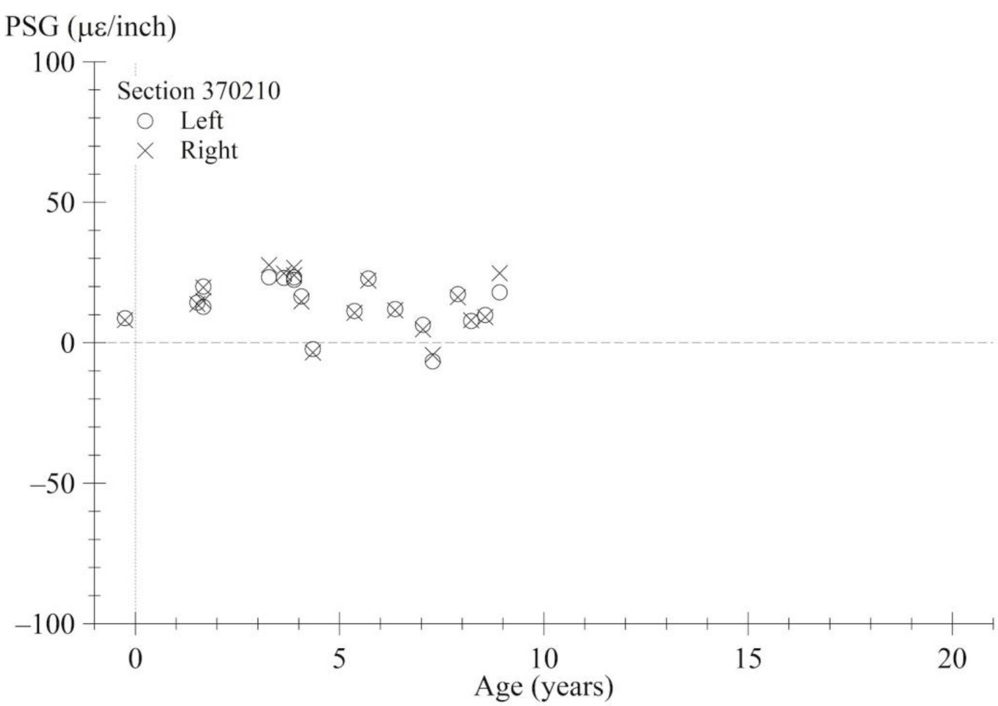

Source: FHWA.

Figure 298. Graph. PSG progression using AREA method for section 370210.

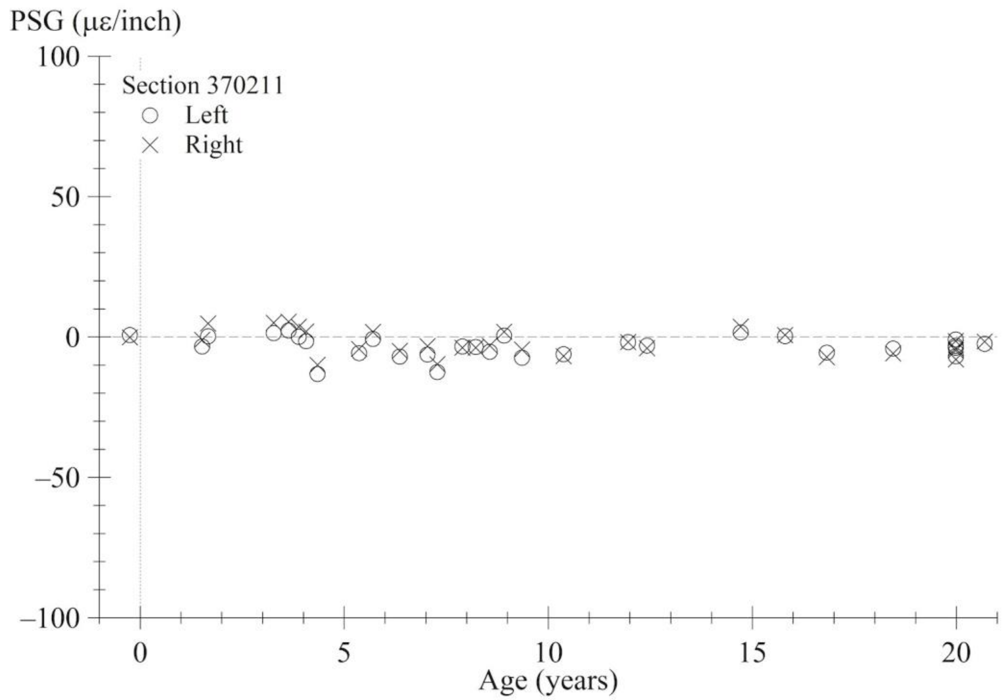

Source: FHWA.

Figure 299. Graph. PSG progression using AREA method for section 370211.

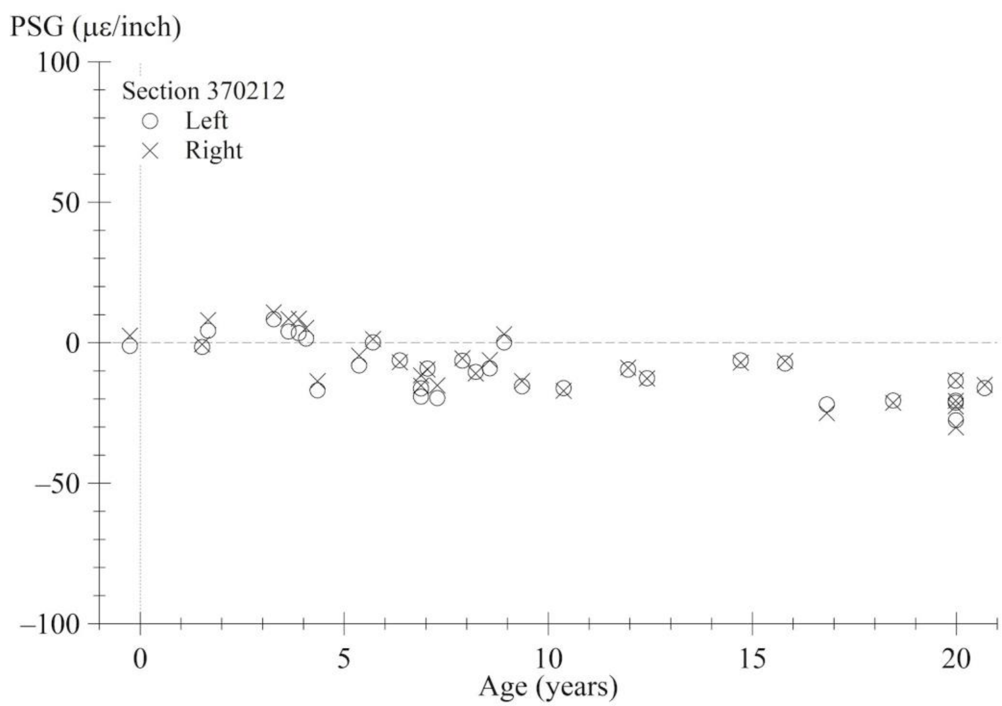

Source: FHWA.

Figure 300. Graph. PSG progression using AREA method for section 370212.

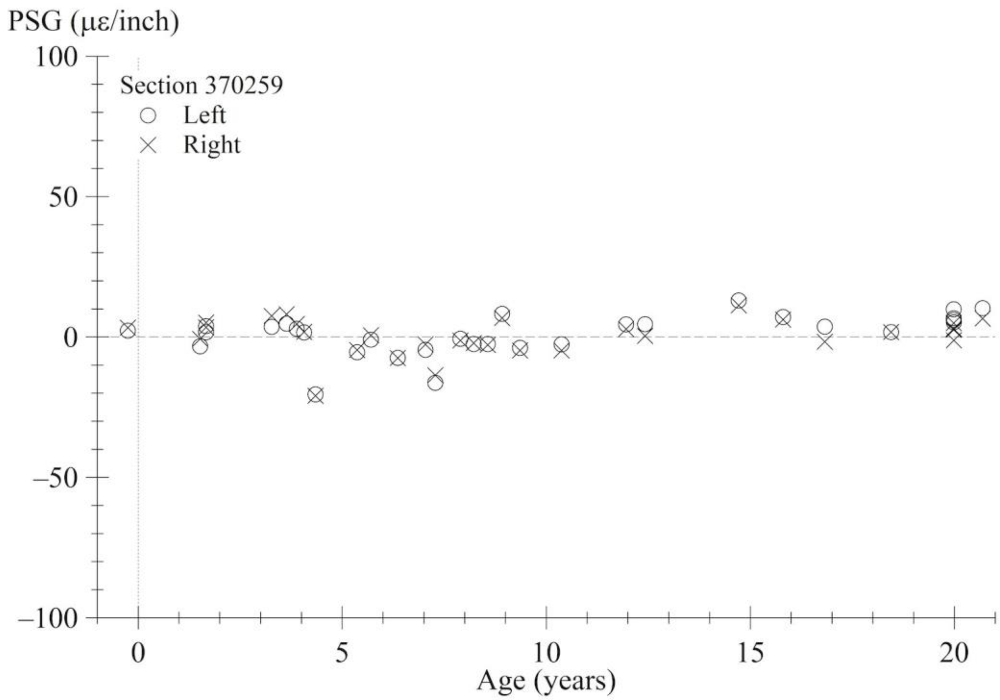

Source: FHWA.

Figure 301. Graph. PSG progression using AREA method for section 370259.

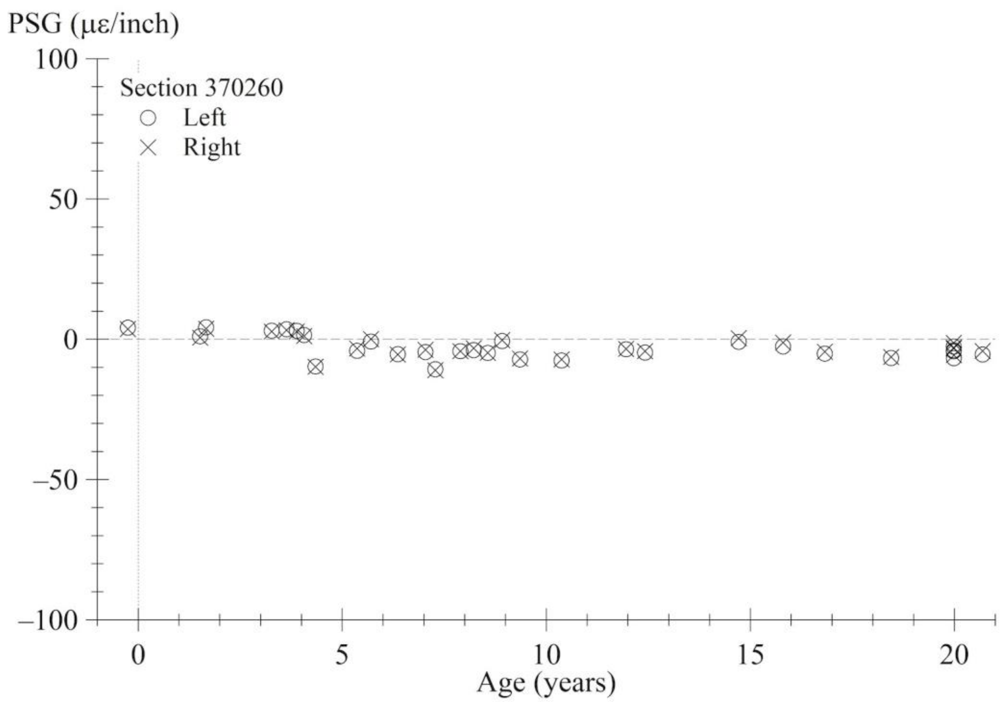

Source: FHWA.

Figure 302. Graph. PSG progression using AREA method for section 370260.

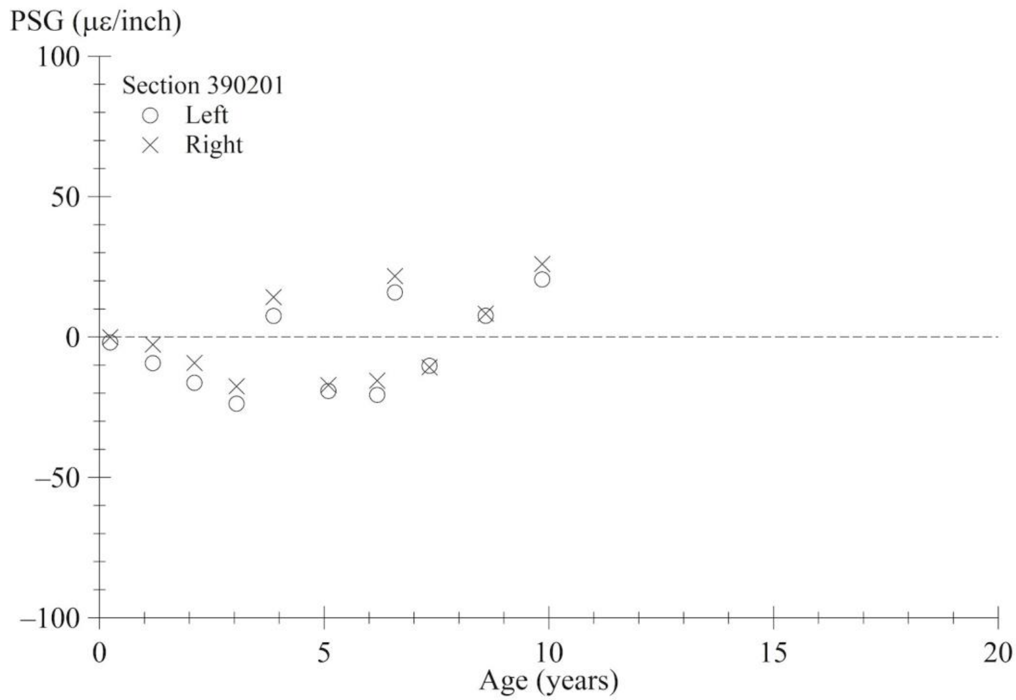

Source: FHWA.

Figure 303. Graph. PSG progression using AREA method for section 390201.

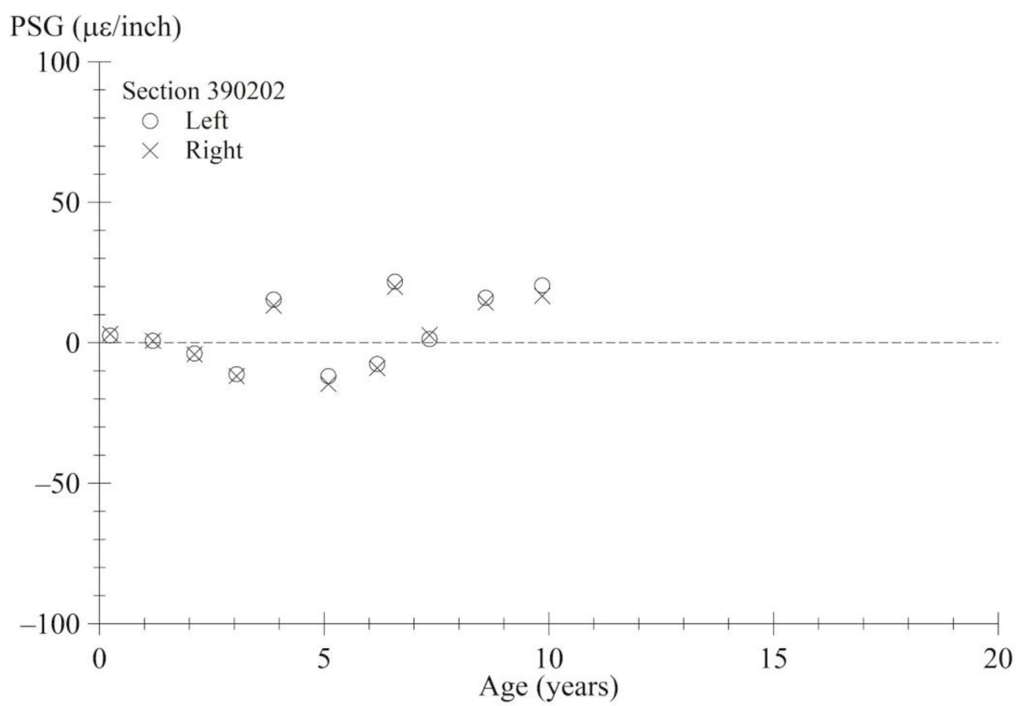

Source: FHWA.

Figure 304. Graph. PSG progression using AREA method for section 390202.

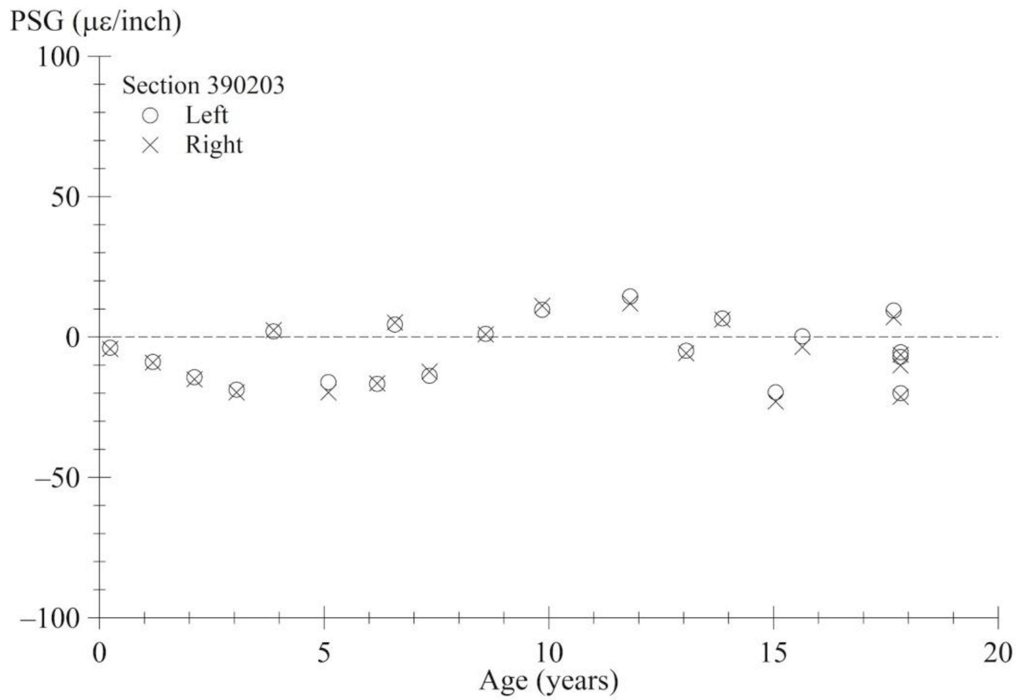

Source: FHWA.

Figure 305. Graph. PSG progression using AREA method for section 390203.

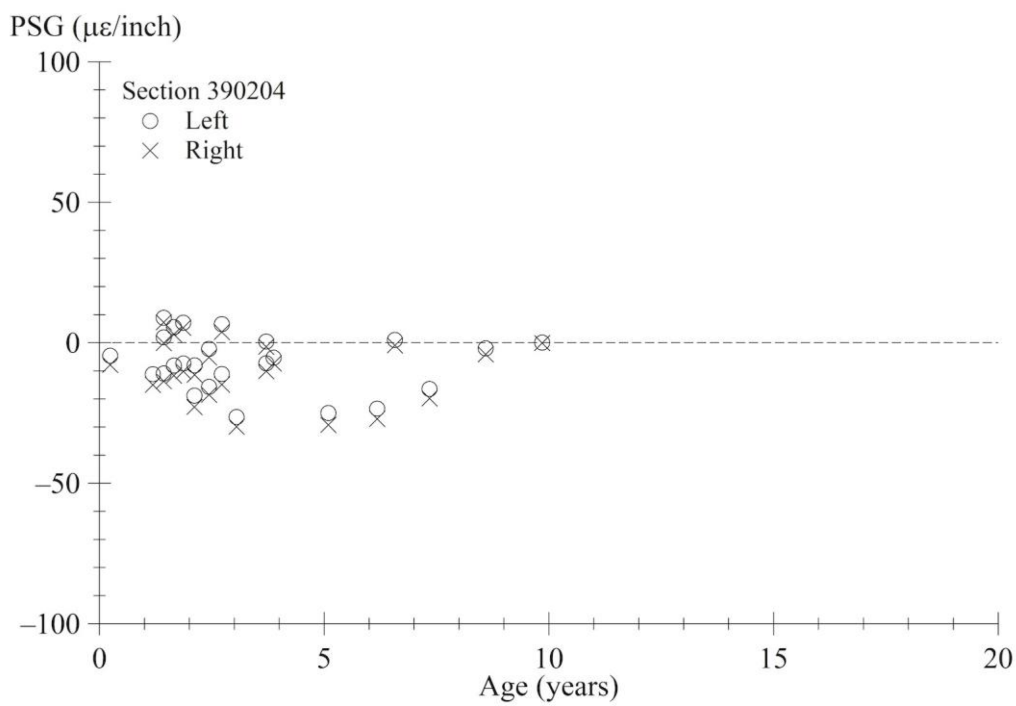

Source: FHWA.

Figure 306. Graph. PSG progression using AREA method for section 390204.

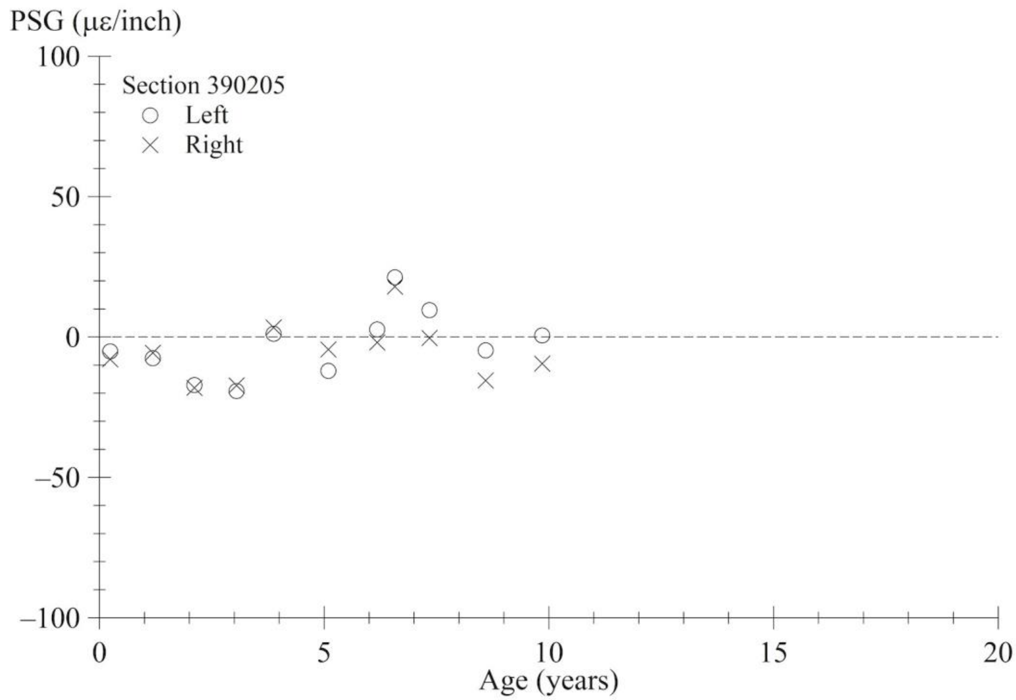

Source: FHWA.

Figure 307. Graph. PSG progression using AREA method for section 390205.

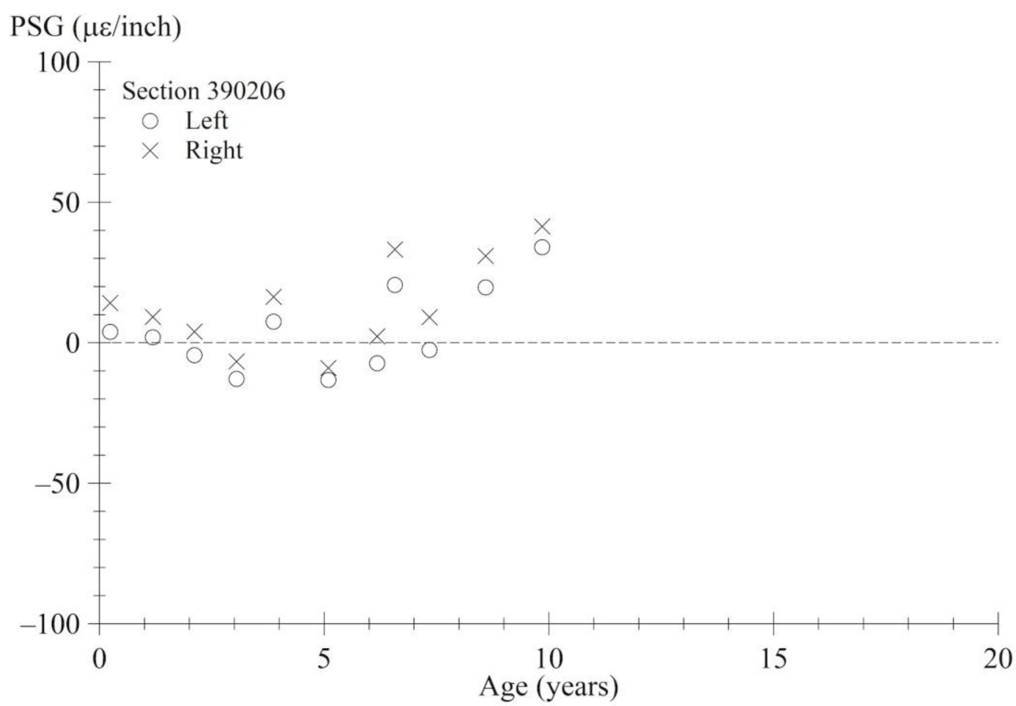

Source: FHWA.

Figure 308. Graph. PSG progression using AREA method for section 390206.

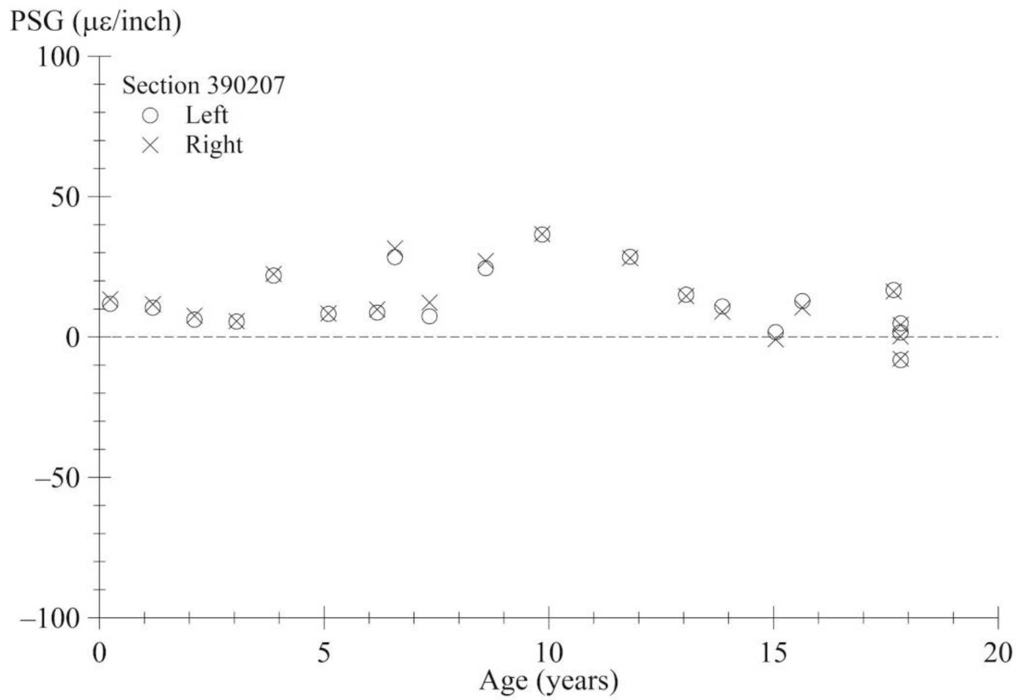

Source: FHWA.

Figure 309. Graph. PSG progression using AREA method for section 390207.

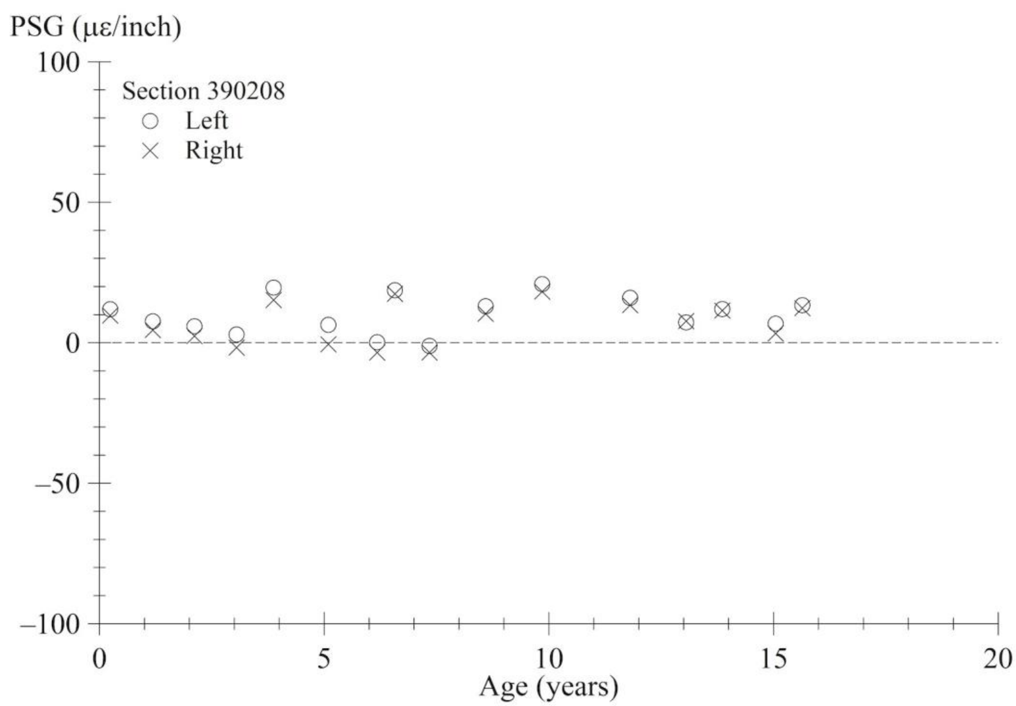

Source: FHWA.

Figure 310. Graph. PSG progression using AREA method for section 390208.

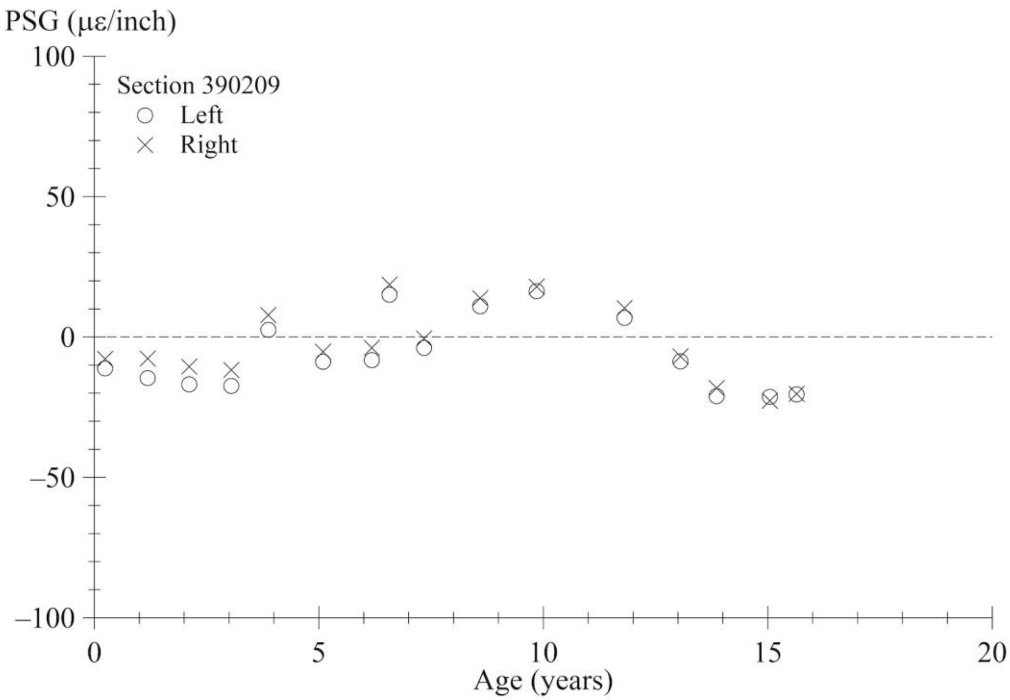

Source: FHWA.

Figure 311. Graph. PSG progression using AREA method for section 390209.

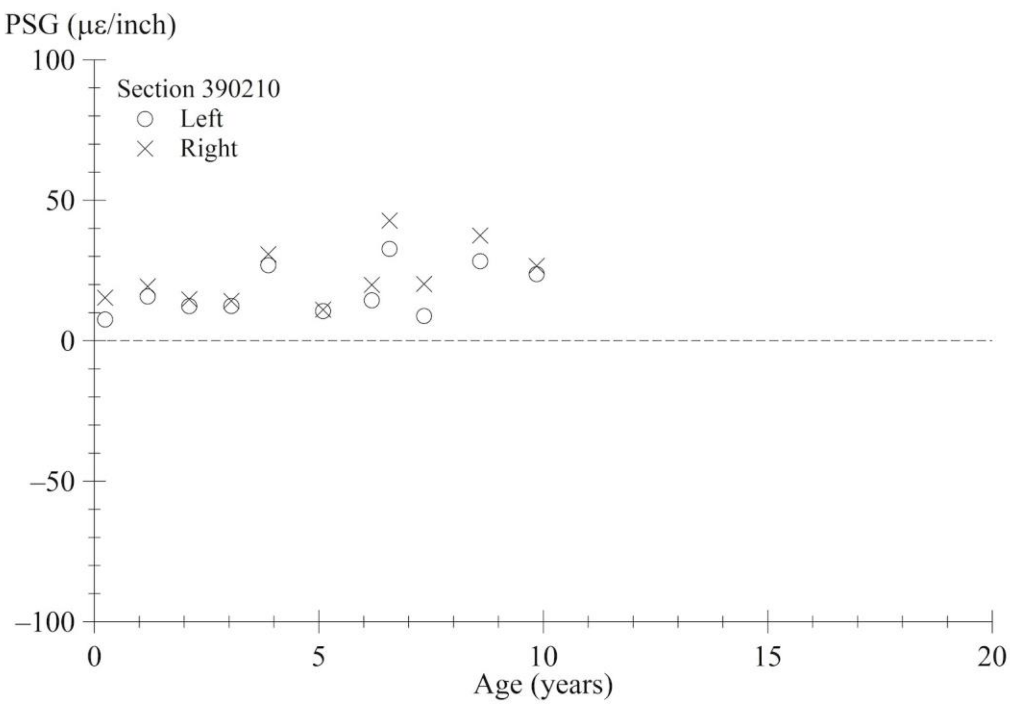

Source: FHWA.

Figure 312. Graph. PSG progression using AREA method for section 390210.

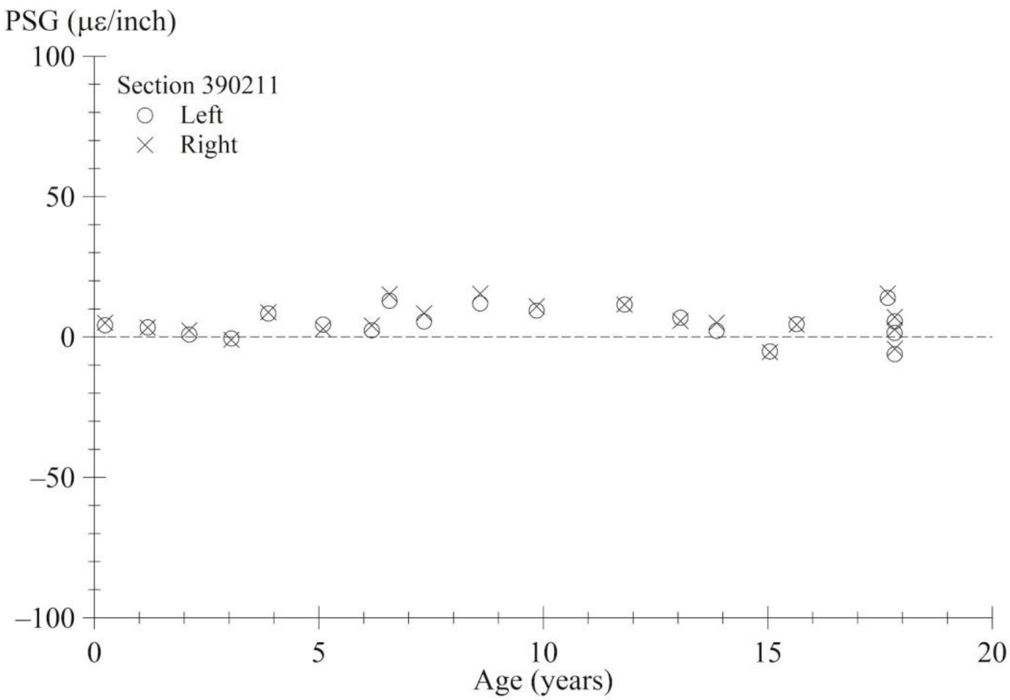

Source: FHWA.

Figure 313. Graph. PSG progression using AREA method for section 390211.

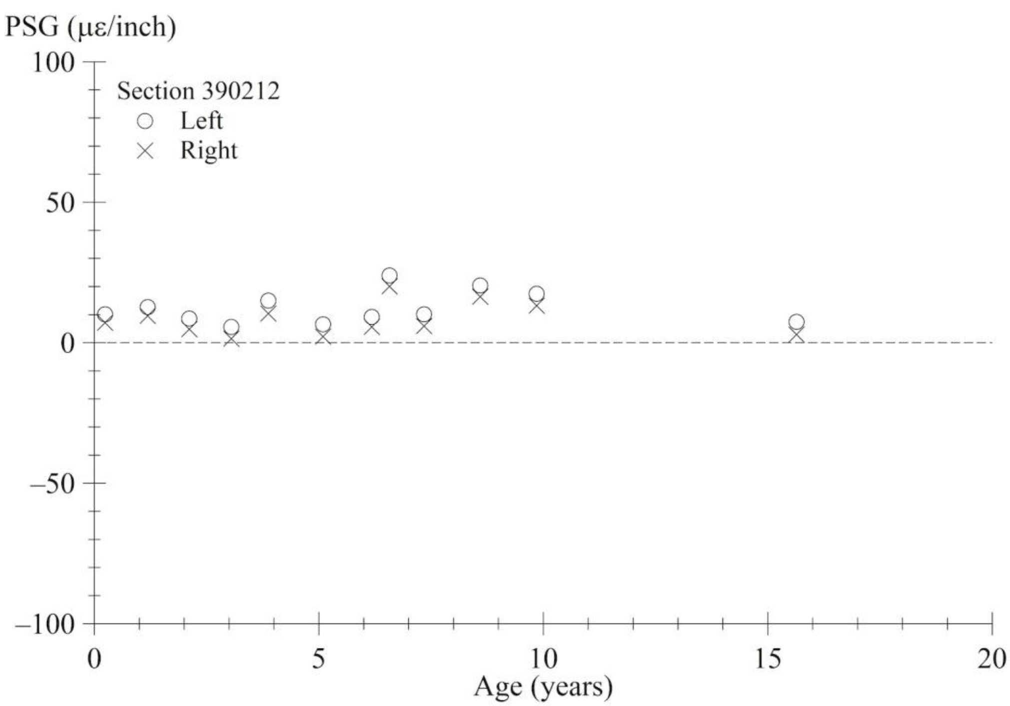

Source: FHWA.

Figure 314. Graph. PSG progression using AREA method for section 390212.

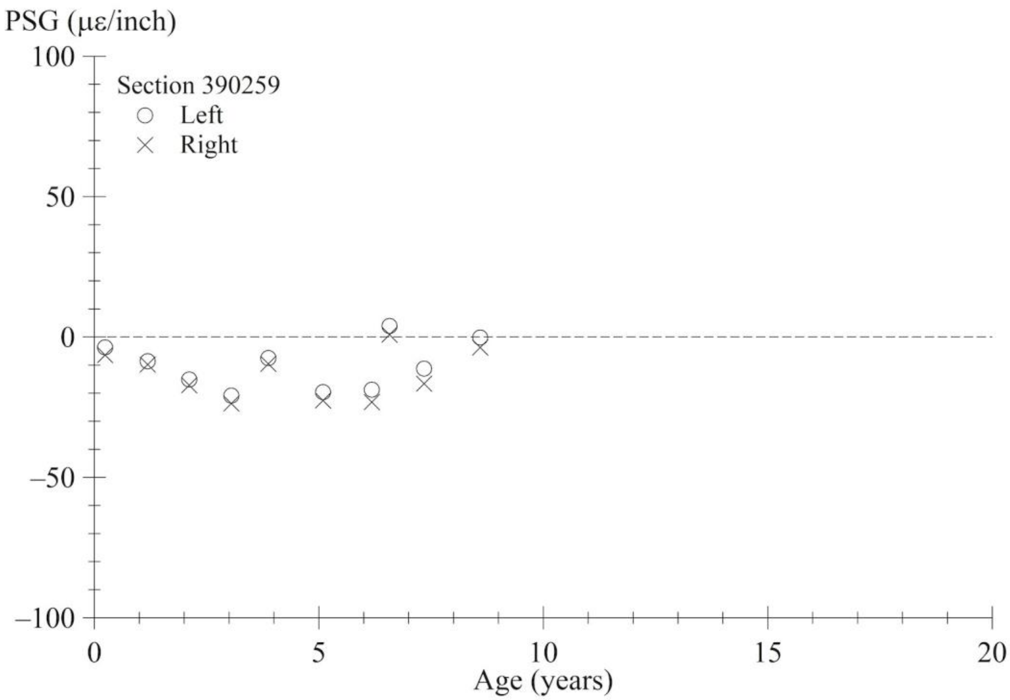

Source: FHWA.

Figure 315. Graph. PSG progression using AREA method for section 390259.

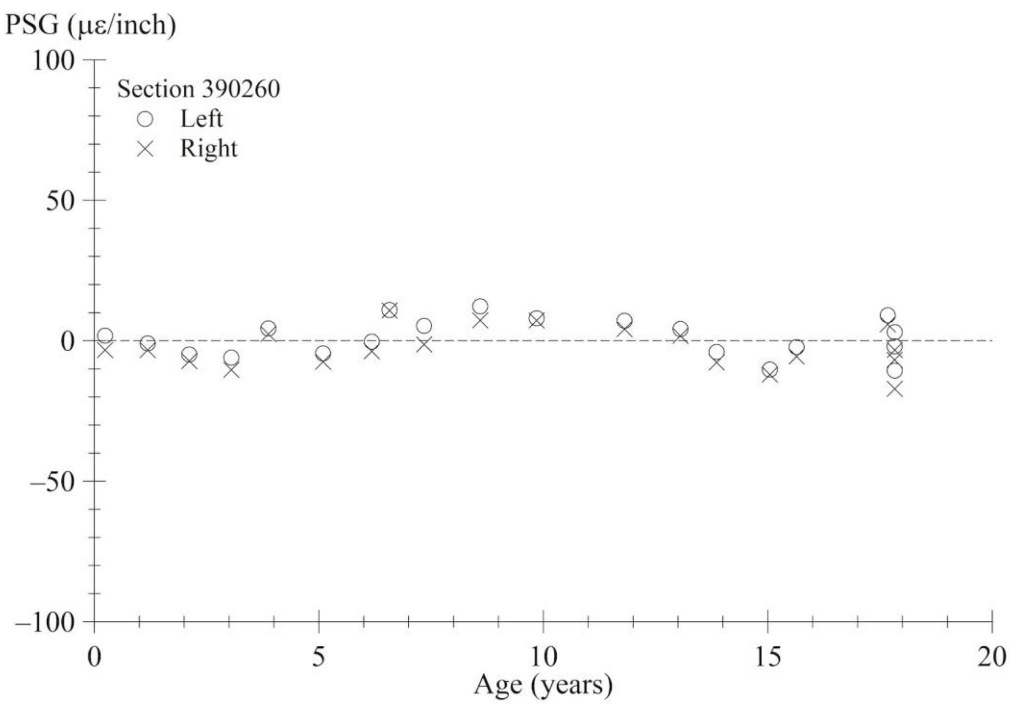

Source: FHWA.

Figure 316. Graph. PSG progression using AREA method for section 390260.

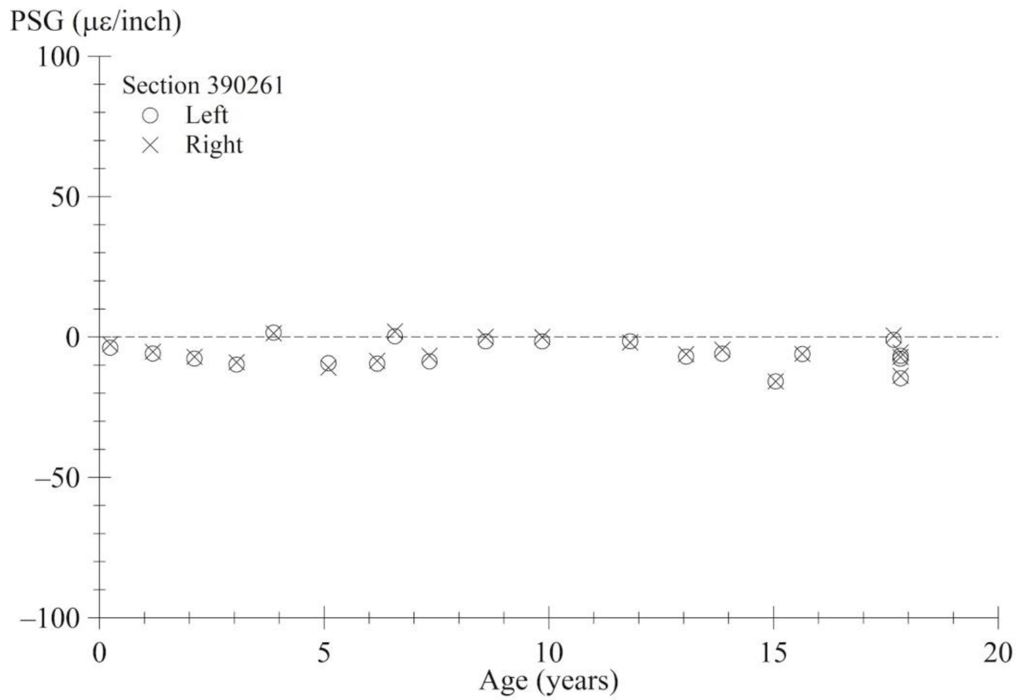

Source: FHWA.

Figure 317. Graph. PSG progression using AREA method for section 390261.

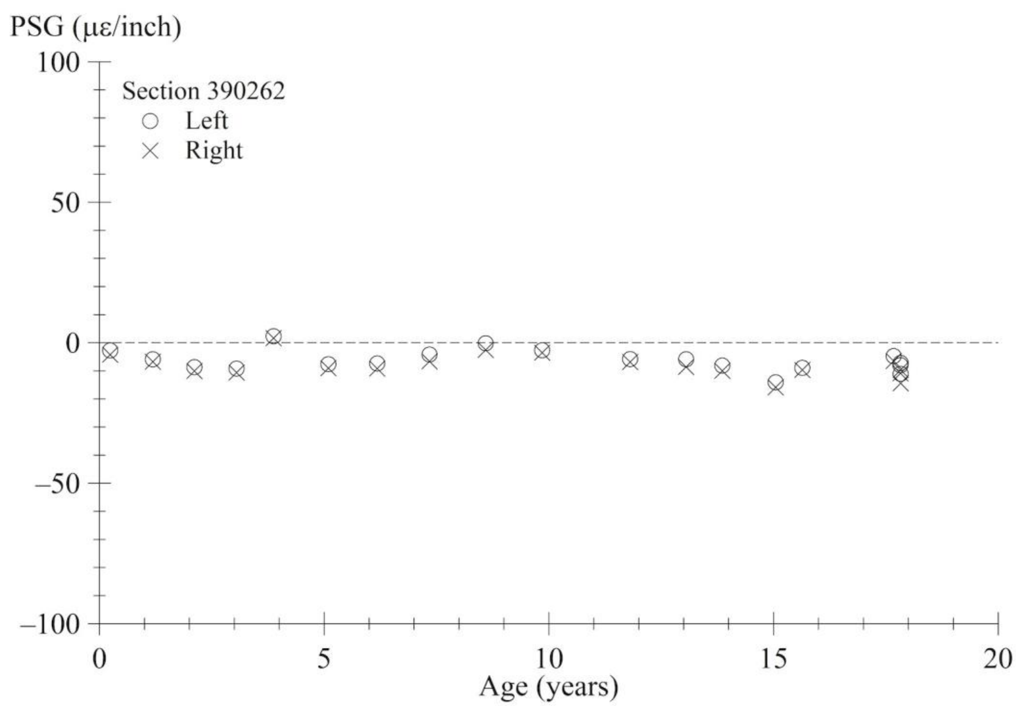

Source: FHWA.

Figure 318. Graph. PSG progression using AREA method for section 390262.

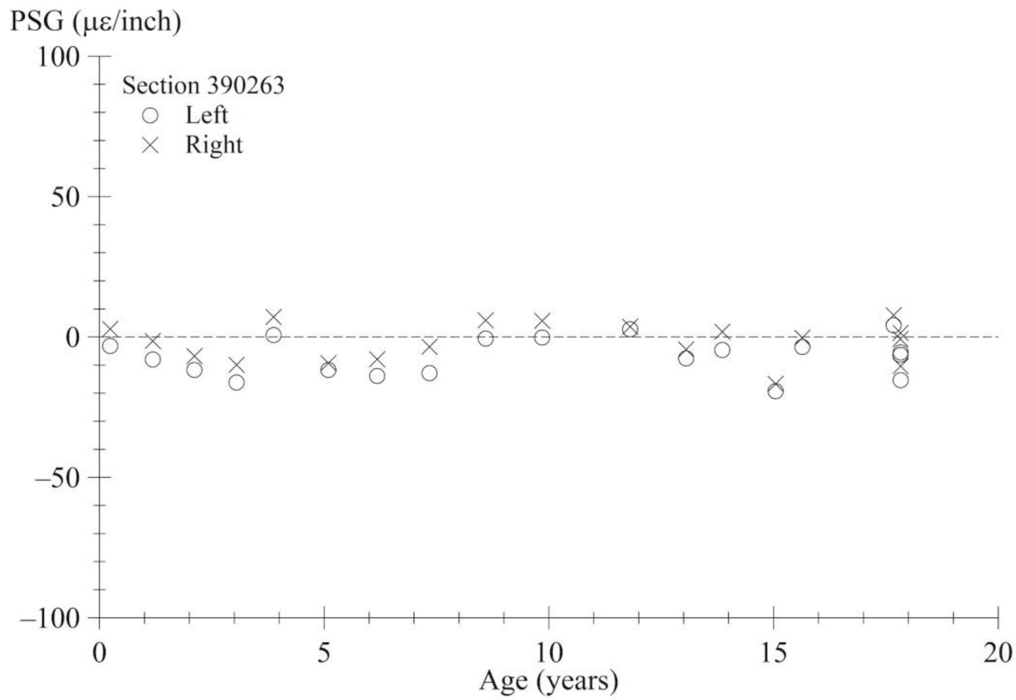

Source: FHWA.

Figure 319. Graph. PSG progression using AREA method for section 390263.

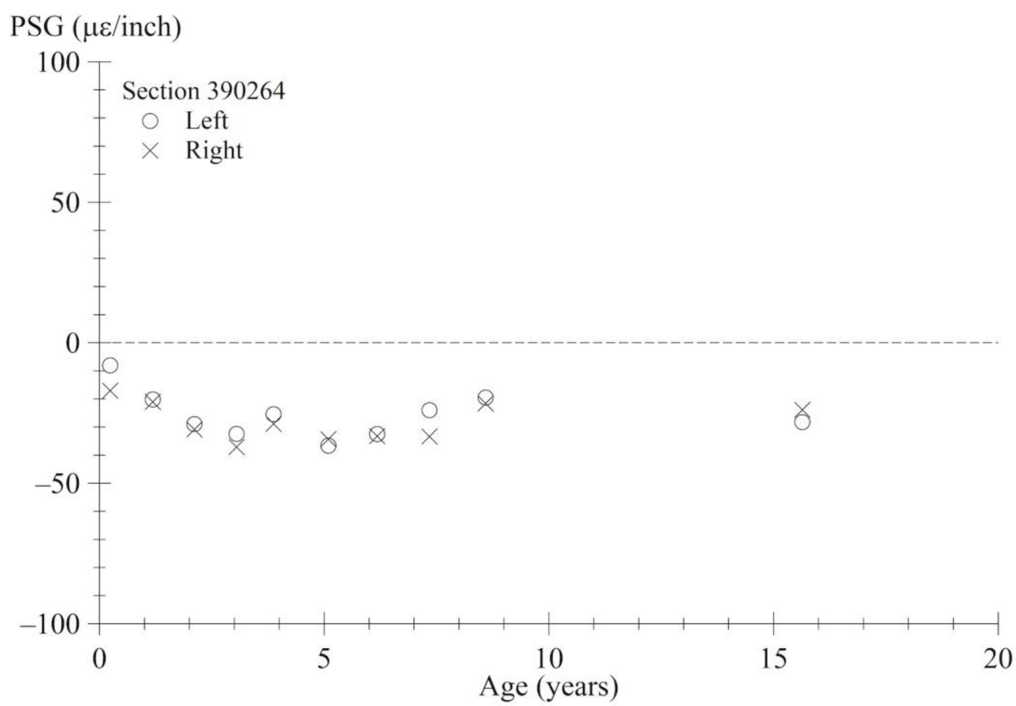

Source: FHWA.

Figure 320. Graph. PSG progression using AREA method for section 390264.

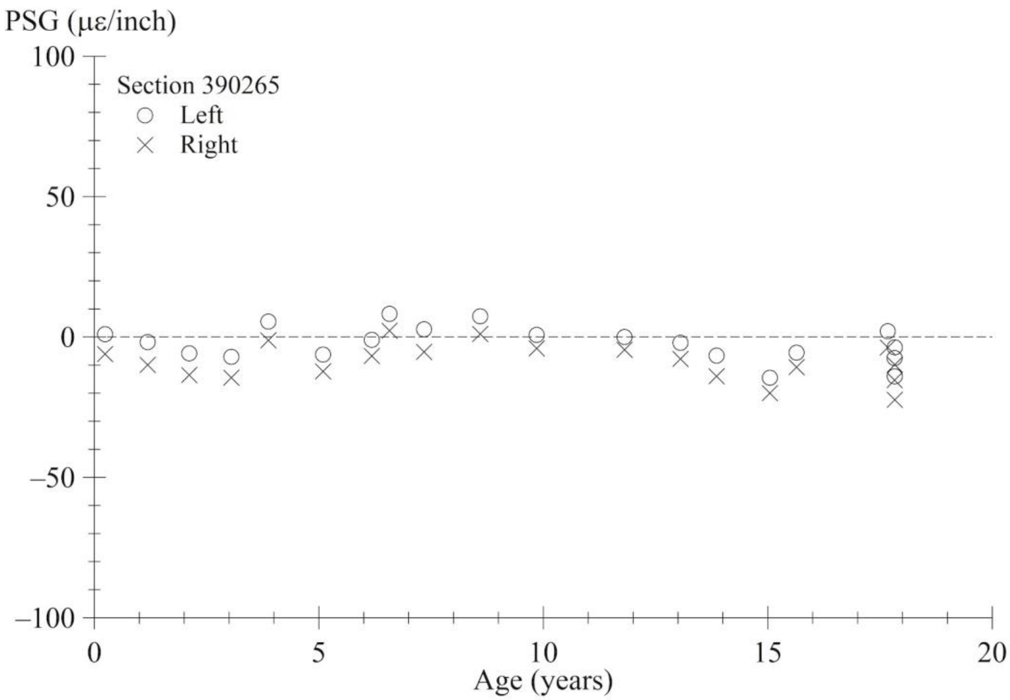

Source: FHWA.

Figure 321. Graph. PSG progression using AREA method for section 390265.

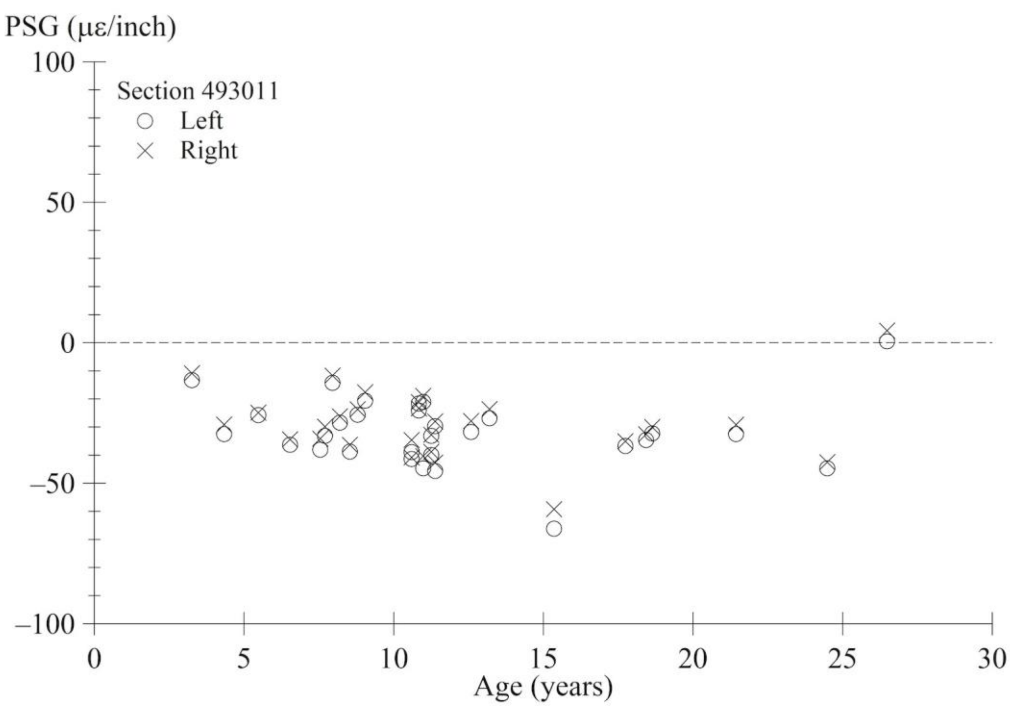

Source: FHWA.

Figure 322. Graph. PSG progression using AREA method for section 493011.

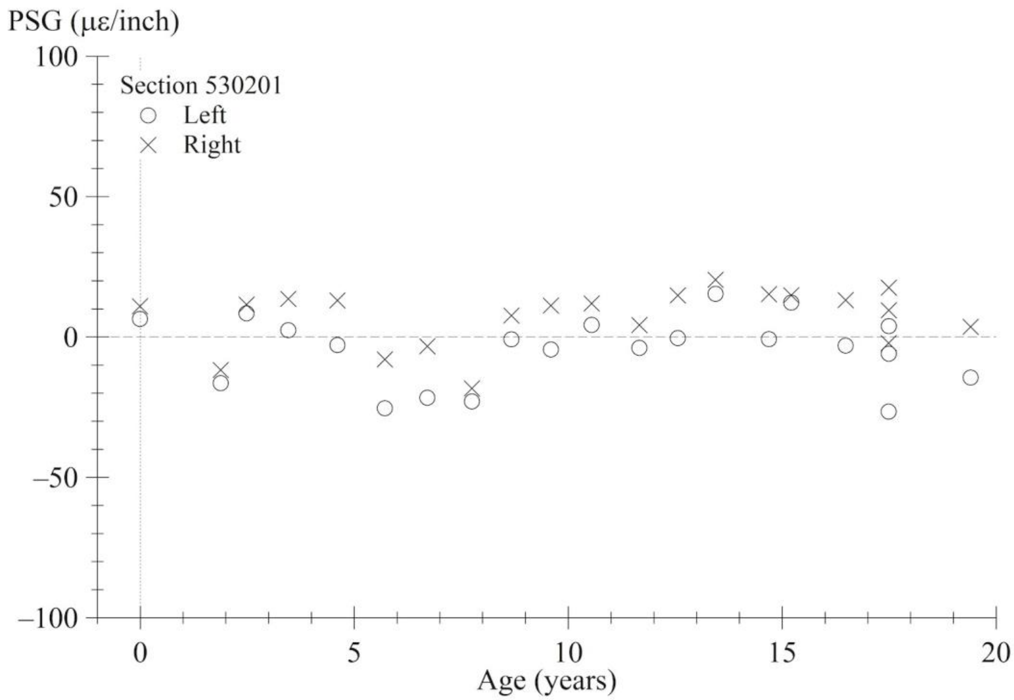

Source: FHWA.

Figure 323. Graph. PSG progression using AREA method for section 530201.

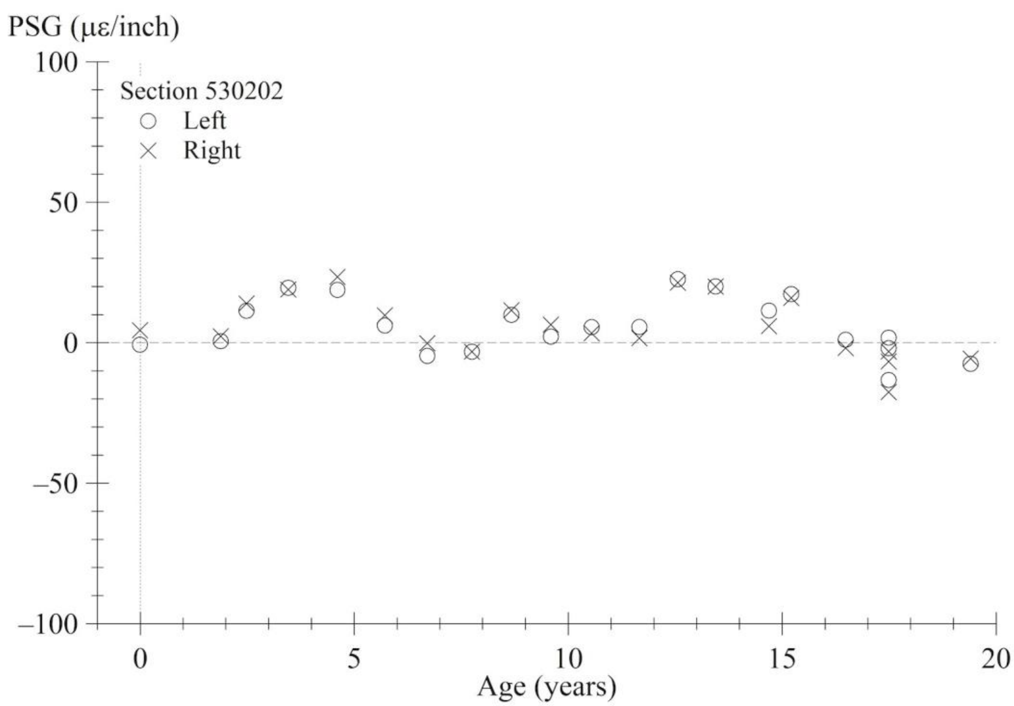

Source: FHWA.

Figure 324. Graph. PSG progression using AREA method for section 530202.

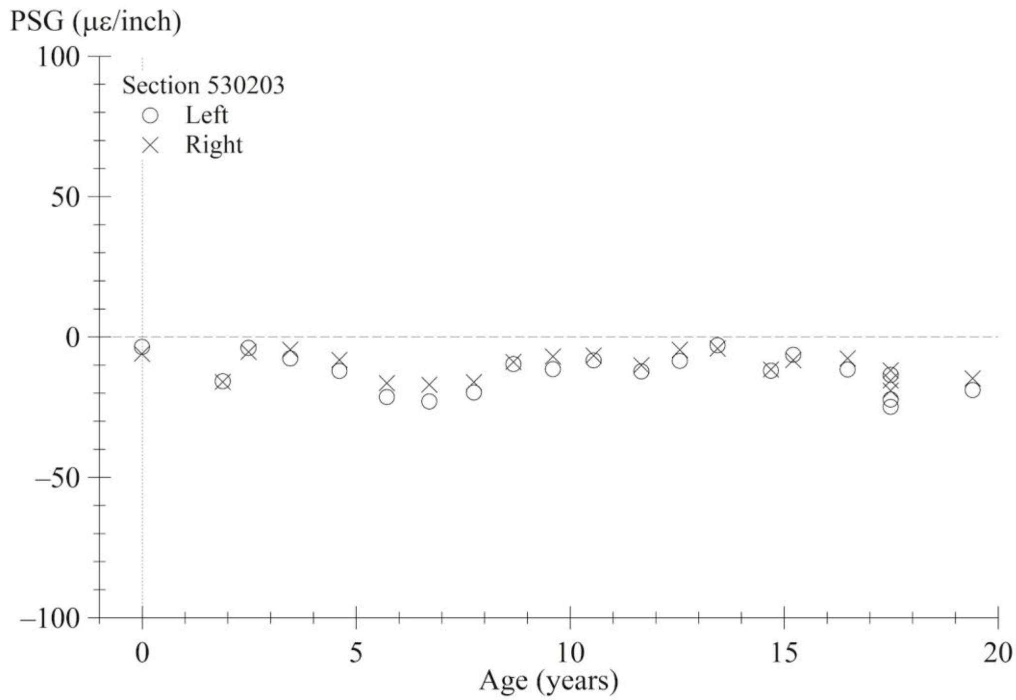

Source: FHWA.

Figure 325. Graph. PSG progression using AREA method for section 530203.

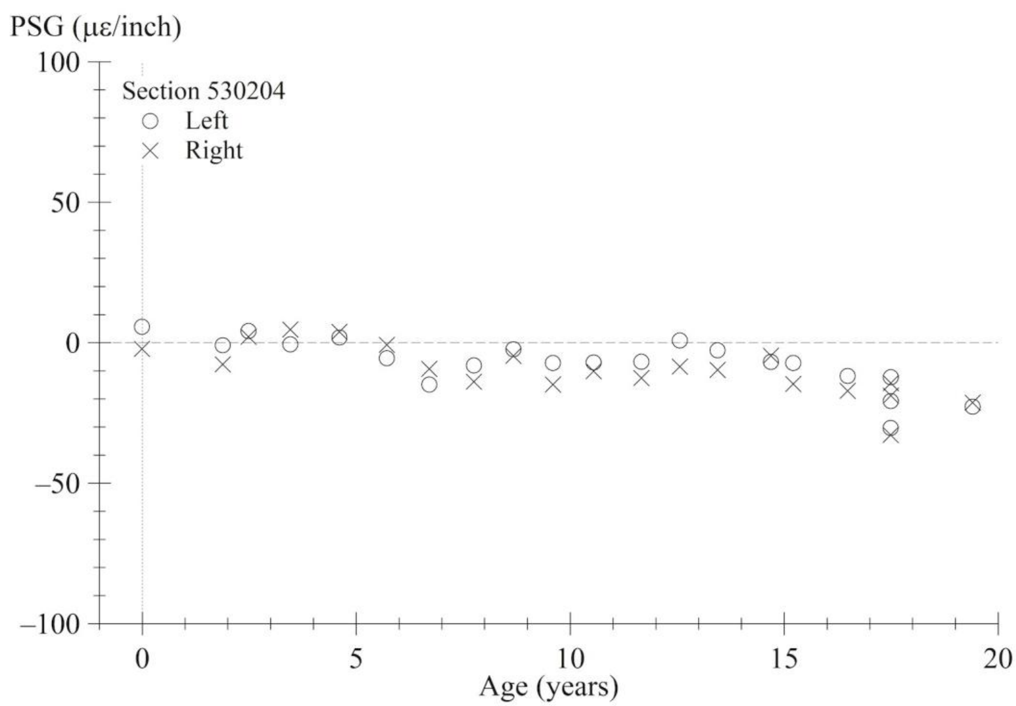

Source: FHWA.

Figure 326. Graph. PSG progression using AREA method for section 530204.

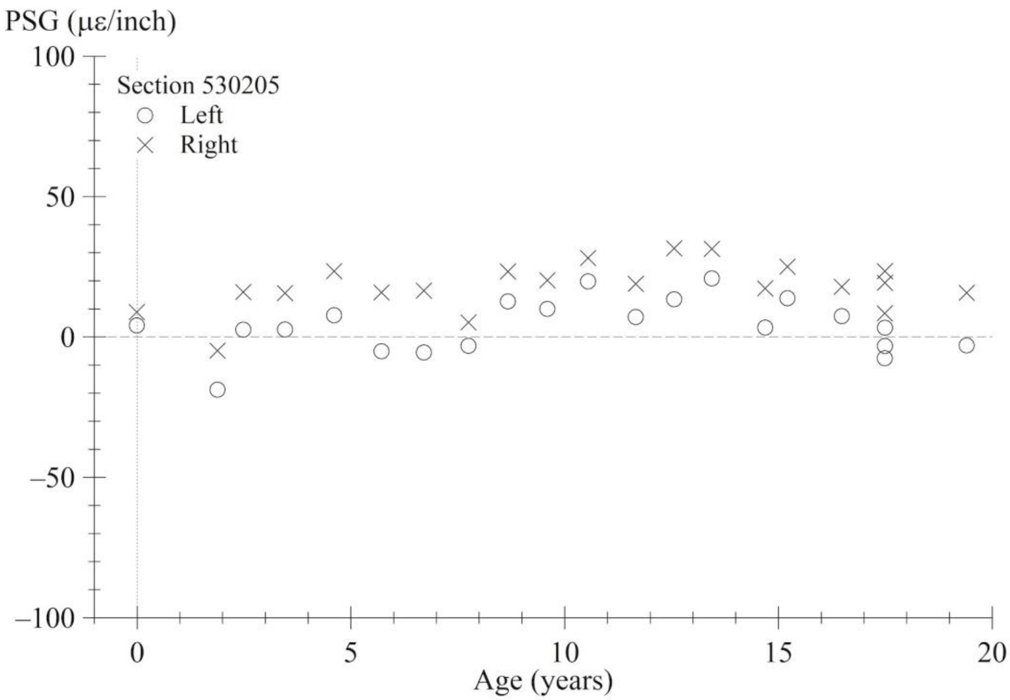

Source: FHWA.

Figure 327. Graph. PSG progression using AREA method for section 530205.

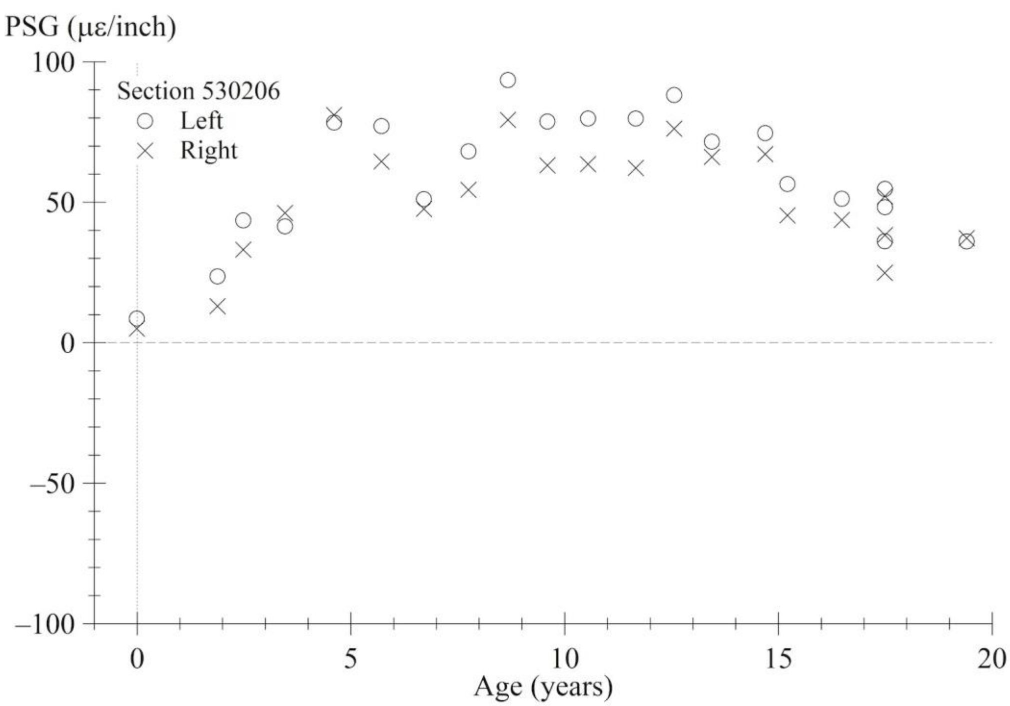

Source: FHWA.

Figure 328. Graph. PSG progression using AREA method for section 530206.

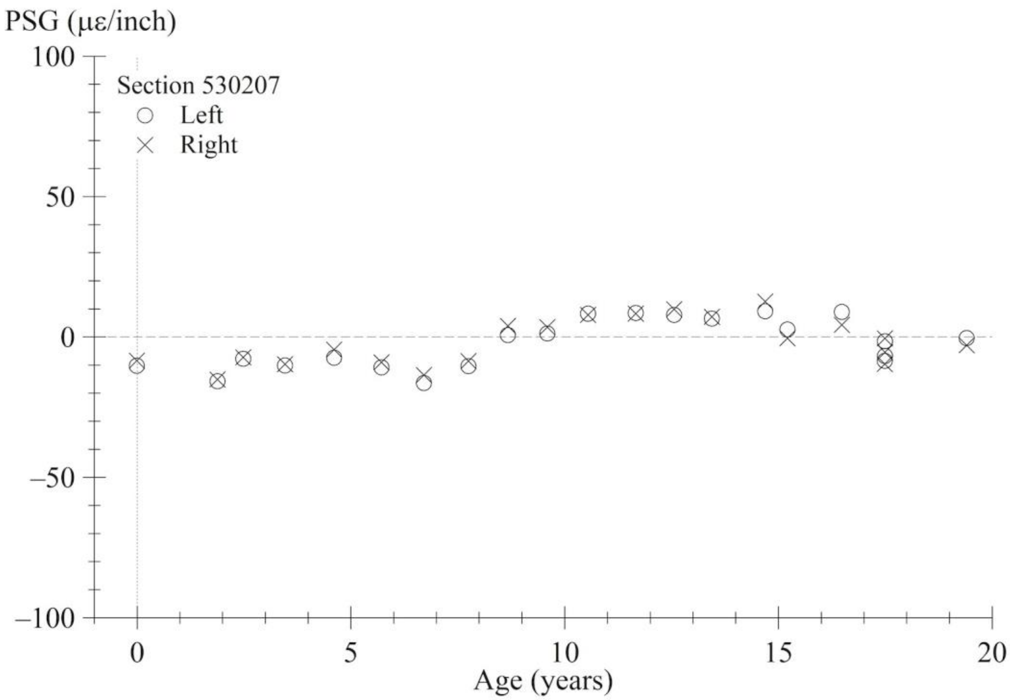

Source: FHWA.

Figure 329. Graph. PSG progression using AREA method for section 530207.

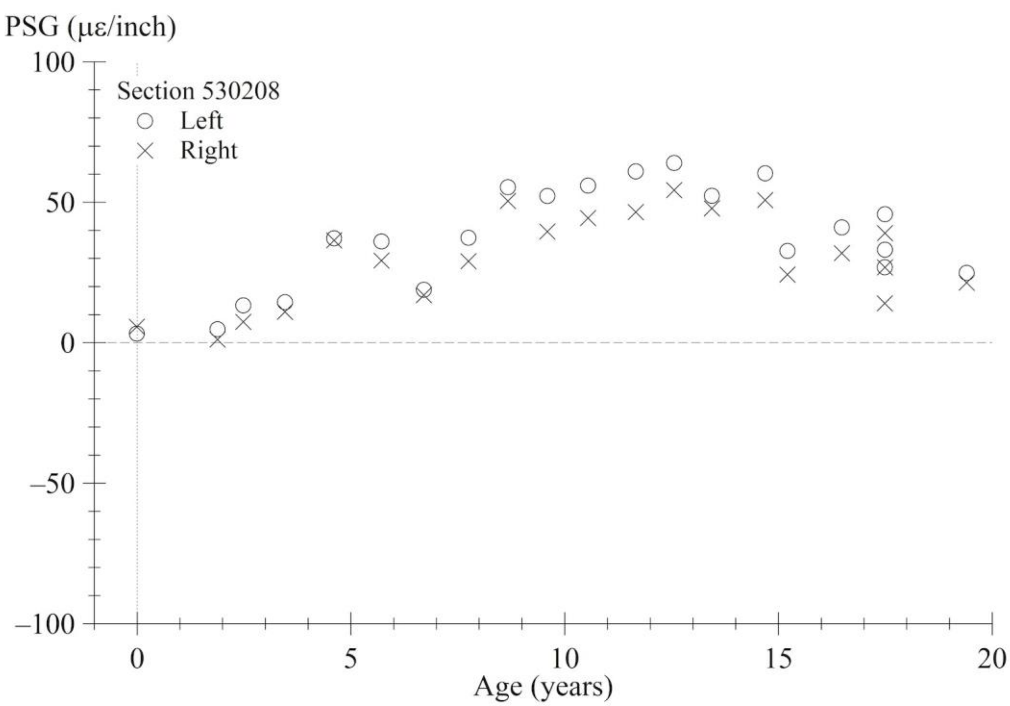

Source: FHWA.

Figure 330. Graph. PSG progression using AREA method for section 530208.

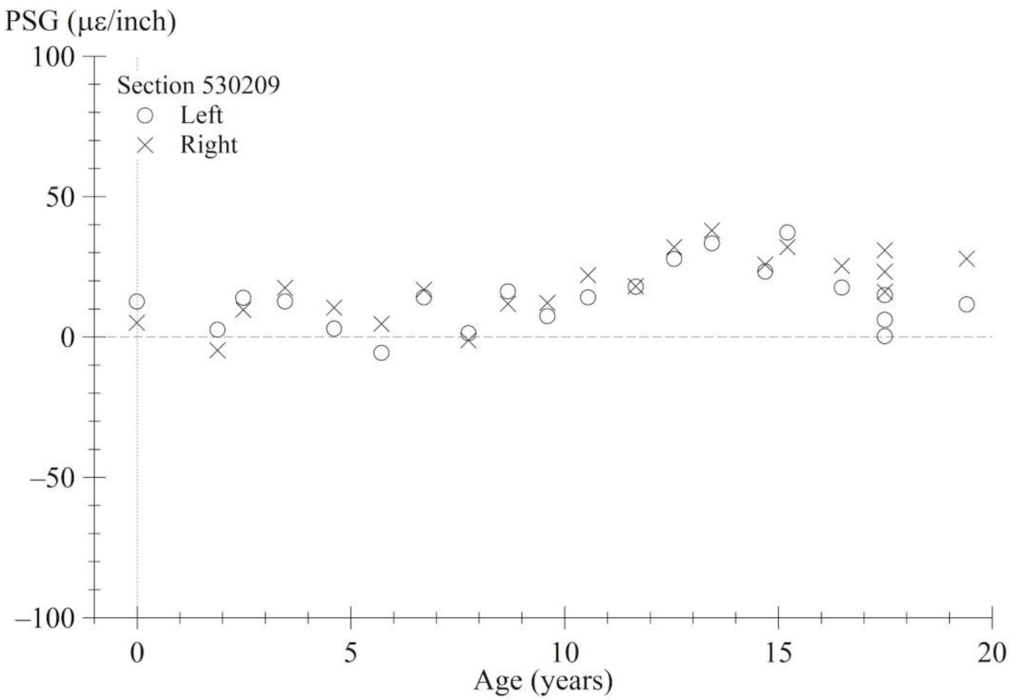

Source: FHWA.

Figure 331. Graph. PSG progression using AREA method for section 530209.

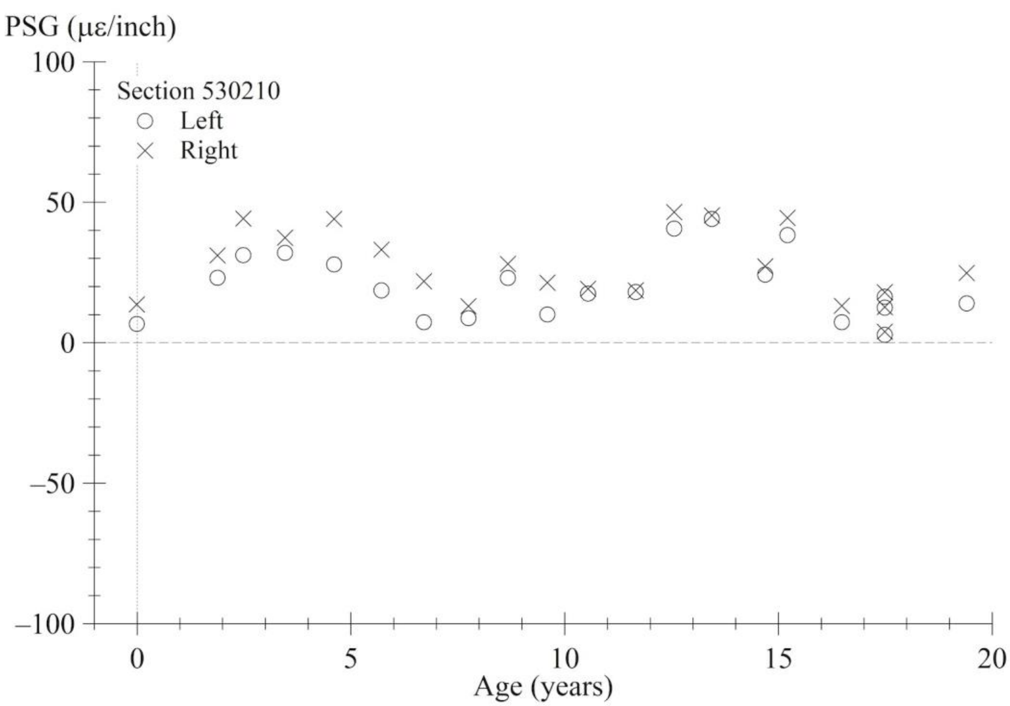

Source: FHWA.

Figure 332. Graph. PSG progression using AREA method for section 530210.

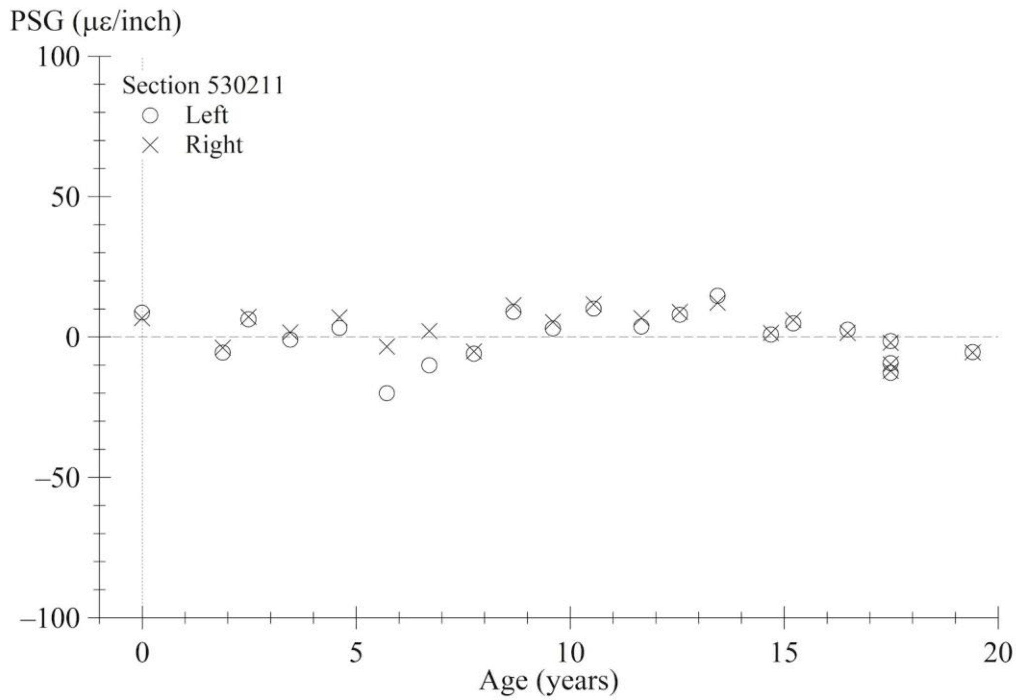

Source: FHWA.

Figure 333. Graph. PSG progression using AREA method for section 530211.

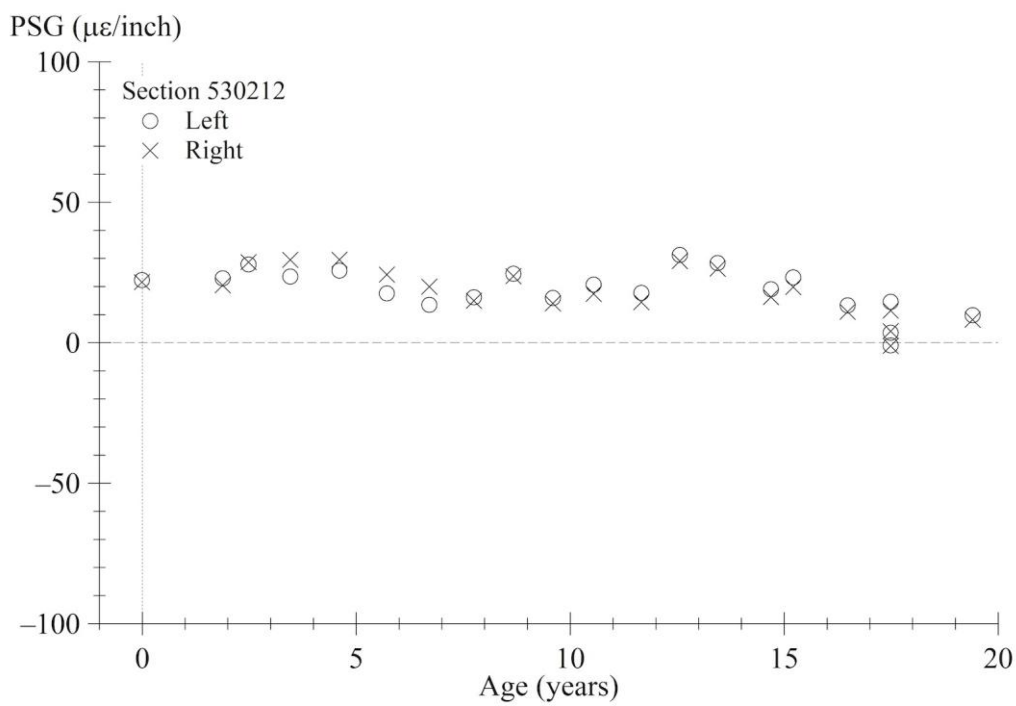

Source: FHWA.

Figure 334. Graph. PSG progression using AREA method for section 530212.

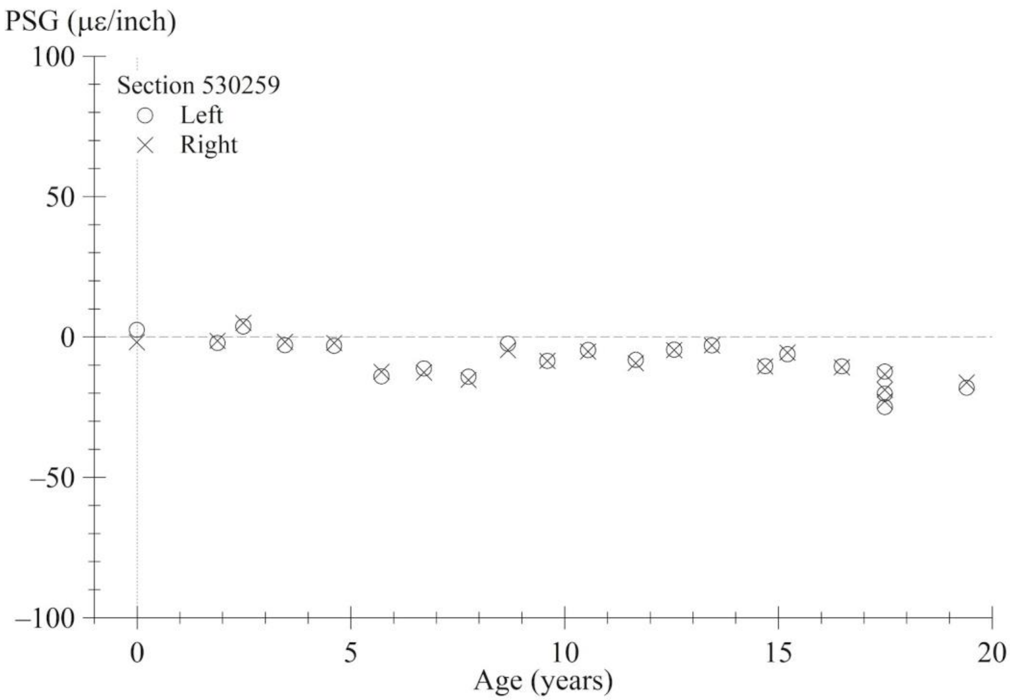

Source: FHWA.

Figure 335. Graph. PSG progression using AREA method for section 530259.

APPENDIX I. LINEAR REGRESSION STATISTICAL OUTPUTS

PSG LINEAR REGRESSION

Table 53 shows the results of the linear regression analysis performed on PSG values calculated using Best Fit and AREA methods. The results show the PSG intercept (PSG_i), the initial PSG after the pavement was constructed, the PSG slope (PSG_s), and the change in PSG per year after construction up to 10 years. The PSG_i and PSG_s values are used for analysis in chapter 8 and chapter 9.

Table 53. Linear regression slope and intercept for PSG (first 10 years).

State Code	SHRP ID	Best Fit Method Intercept (PSG)	Best Fit Method Slope (PSG/Year)	AREA Method Intercept (PSG)	AREA Method Slope (PSG/Year)
4	0217	−0.956706	−0.036938	−0.911377	−0.035152
4	0219	−0.221692	0.009808	−0.268314	0.011893
4	0218	−0.232987	0.013285	−0.256965	0.014659
4	0220	−0.003123	−0.031568	−0.003496	−0.035773
4	0264	0.174903	−0.005603	0.201377	−0.006494
4	0268	−0.136764	−0.0477	−0.116243	−0.040444
4	0266	−0.213204	0.113624	−0.207288	0.110069
4	0267	−0.482932	0.03966	−0.530763	0.043672
4	0222	−2.204418	−0.02577	−2.133728	−0.024157
4	0223	0.050124	0.046607	0.050285	0.046714
4	0221	0.46346	0.005665	0.554688	0.006642
4	0224	−0.446087	0.053605	−0.40595	0.048945
4	0263	0.754596	0.305103	0.67471	0.271467
4	0213	−0.372634	−0.078811	−0.303927	−0.064105
4	0214	−1.645933	0.122081	−1.516298	0.113185
4	0262	−0.655465	0.016985	−0.740292	0.018948
4	0215	0.33282	−0.088015	0.382195	−0.100473
4	0216	0.104927	−0.08386	0.15185	−0.114429
4	0265	0.117546	0.07137	0.126799	0.075264
20	0259	−0.00893	0.187626	−0.007985	0.193008
20	0207	0.198532	0.0804	0.210956	0.085334
20	0206	0.104747	−0.015888	0.107366	−0.016302
20	0208	0.046943	−0.059967	0.052441	−0.067335
20	0205	0.18679	0.022736	0.194073	0.023598
20	0212	0.058865	−0.051597	0.060708	−0.053079
20	0211	0.995855	−0.032251	1.031212	−0.033421
20	0209	0.048306	−0.025559	0.052394	−0.027714
20	0210	0.543103	−0.070227	0.565596	−0.073154
20	0204	0.366447	−0.012445	0.427725	−0.014488
20	0203	0.083141	0.008057	0.083666	0.008087
20	0202	0.225896	−0.072421	0.233754	−0.074927
20	0201	−0.131318	−0.05696	−0.107603	−0.046716
37	0207	1.039878	−0.032506	1.117117	−0.034911
37	0208	−0.265955	0.031323	−0.293121	0.034774
37	0205	−0.301734	−0.114236	−0.333064	−0.126678
37	0206	−0.201752	−0.088251	−0.220679	−0.096895
37	0211	0.058469	−0.063277	0.065622	−0.071278

State Code	SHRP ID	Best Fit Method Intercept (PSG)	Best Fit Method Slope (PSG/Year)	AREA Method Intercept (PSG)	AREA Method Slope (PSG/Year)
37	0212	0.069245	−0.007507	0.072709	−0.007779
37	0259	0.279894	0.008556	0.272684	0.008511
37	0210	0.044042	0.038818	0.045918	0.040393
37	0209	−0.196774	−0.098415	−0.202266	−0.101111
37	0260	−0.606559	0.112638	−0.638665	0.118654
37	0203	−0.766648	−0.025421	−0.741096	−0.024502
37	0204	0.22611	0.033665	0.242474	0.036094
37	0202	−0.225005	0.050487	−0.240918	0.054198
37	0201	0.493268	0.064587	0.482339	0.063028
39	0264	−0.134821	−0.111855	−0.144228	−0.11962
39	0262	−0.932481	−0.0854	−0.956018	−0.087643
39	0261	−0.2617	−0.031967	−0.26266	−0.03209
39	0206	−0.456176	−0.099773	−0.455888	−0.09971
39	0205	0.049782	−0.019907	0.0605	−0.024116
39	0207	0.693195	−0.028711	0.694463	−0.028765
39	0208	0.270976	−0.032055	0.284382	−0.03376
39	0265	0.146118	−0.040492	0.15643	−0.043399
39	0211	0.075296	−0.042523	0.086573	−0.049474
39	0209	0.065202	−0.070556	0.083196	−0.089274
39	0212	0.123715	−0.04327	0.1244	−0.043601
39	0260	−0.201603	0.064637	−0.225196	0.071777
39	0210	−0.211204	−0.022938	−0.227104	−0.024683
39	0202	−1.326547	−0.211243	−1.628276	−0.260362
39	0204	0.201038	−0.138866	0.208535	−0.143667
39	0203	0.132345	−0.052095	0.136455	−0.0535
39	0201	0.473821	−0.014301	0.510381	−0.015444
39	0259	0.263389	−0.131048	0.26842	−0.133495
39	0263	−1.608829	0.196032	−1.690562	0.205962
53	0207	0.105088	0.088071	0.098397	0.084107
53	0205	−0.934318	−0.270159	−0.978251	−0.283032
53	0206	−0.501058	0.050372	−0.54737	0.05507
53	0208	−0.485466	0.079957	−0.530964	0.087204
53	0259	−0.511732	0.015754	−0.534288	0.016453
53	0212	−0.202414	−0.183207	−0.216284	−0.196881
53	0210	−0.394425	0.040961	−0.47229	0.048826
53	0211	0.381256	−0.017045	0.3765	−0.016796
53	0209	−0.119553	−0.108874	−0.142636	−0.129895
53	0201	−0.29671	−0.027111	−0.312318	−0.028584
53	0204	−0.26658	0.018115	−0.278182	0.018903
53	0202	0.090858	−0.120323	0.093563	−0.124311
53	0203	−0.179065	−0.061348	−0.196881	−0.067756
53	0208	−0.485466	0.079957	−0.530964	0.087204
53	0259	−0.511732	0.015754	−0.534288	0.016453
53	0212	−0.202414	−0.183207	−0.216284	−0.196881
53	0210	−0.394425	0.040961	−0.47229	0.048826
53	0211	0.381256	−0.017045	0.3765	−0.016796
53	0209	−0.119553	−0.108874	−0.142636	−0.129895
53	0201	−0.29671	−0.027111	−0.312318	−0.028584
53	0204	−0.26658	0.018115	−0.278182	0.018903
53	0202	0.090858	−0.120323	0.093563	−0.124311
53	0203	−0.179065	−0.061348	−0.196881	−0.067756

State Code	SHRP ID	Best Fit Method Intercept (PSG)	Best Fit Method Slope (PSG/Year)	AREA Method Intercept (PSG)	AREA Method Slope (PSG/Year)
53	0208	−0.485466	0.079957	−0.530964	0.087204
53	0259	−0.511732	0.015754	−0.534288	0.016453
53	0212	−0.202414	−0.183207	−0.216284	−0.196881
53	0210	−0.394425	0.040961	−0.47229	0.048826
53	0211	0.381256	−0.017045	0.3765	−0.016796
53	0209	−0.119553	−0.108874	−0.142636	−0.129895
53	0201	−0.29671	−0.027111	−0.312318	−0.028584
53	0204	−0.26658	0.018115	−0.278182	0.018903
53	0202	0.090858	−0.120323	0.093563	−0.124311
53	0203	−0.179065	−0.061348	−0.196881	−0.067756

SHRP = Strategic Highway Research Program.

CLIMATE FACTORS

Table 54 shows the average temperature and humidity for the first month after construction. It also shows the average daily difference between maximum and minimum values of temperature and humidity of the first month after construction. These averages are based on hourly temperature and humidity from the MERRA climate database.

Table 54. MERRA climate database—first-month averages.[21]

State Code	Average Temperature (°F)	Average Humidity (%)	Average Daily Temperature Maximum Difference (°F)	Average Daily Humidity Maximum Difference (%)
4	72.8	33.3	25.5	31.6
20	76.3	73.7	18.5	40.6
37	78.2	75.0	16.0	41.5
39	63.8	72.7	20.1	49.9
53	42.3	82.3	12.9	31.3

Table 55 shows the average temperature and humidity for the first 10 years after construction. It also shows the average daily difference between maximum and minimum values of temperature and humidity of the first 10 years after construction. These averages are based on hourly temperature and humidity from the MERRA climate database.

Table 55. MERRA climate database—averages of first 10 years.[21]

State Code	Average Temperature (°F)	Average Humidity (%)	Average Daily Temperature Maximum Difference (°F)	Average Daily Humidity Maximum Difference (%)
4	72.5	26.9	32.2	32.3
20	55.0	21.1	67.2	42.4
37	58.1	20.9	73.7	43.5
39	50.4	18.7	75.6	38.4
53	50.8	20.5	62.5	44.5

Table 56 shows the average temperature and maximum humidity for the first 10 years after construction. It also shows the average total annual precipitation and the average freezing index over the first 10 years after construction. These averages are based on yearly computed parameters from LTPP virtual weather station tables.

Table 56. LTPP database—averages of first 10 years.

State Code	Average Temperature (°F)	Maximum Humidity (%)	Average Total Annual Precipitation (inches)	Average Freezing Index[1] (°F days)
4	72.7	51.8	7.6	0.0
20	54.9	81.8	32.3	536.7
37	59.4	87.9	44.6	81.5
39	51.1	85.8	39.6	651.5
53	49.3	77.3	10.9	406.4

[1]Cumulative degrees of days below freezing (32°F).

STRUCTURAL FACTORS

Table 57 shows structural properties (other than layer thickness) of the PCC slab, including average slab width, slab length, paste volume, modulus of rupture, elastic modulus, and temperature gradient. The temperature gradient is based on measurements taken during FWD testing at incremental depths from the pavement surface. The paste volume is percent of the PCC mix that is paste (i.e., water, cement, and fly ash).

Table 57. Test section structural design factors.

State Code	SHRP ID	Average Slab Width (ft)	Average Slab Length (ft)	Average Paste Volume (%)	Average PCC Modulus of Rupture (psi)	Average PCC Elastic Modulus (psi)	Average Temperature Gradient During FWD Testing (°F /Inch)
4	0213	14	4.59	21.1	630	4673414	−1.52252
4	0214	12	4.59	32.0	840	4581386	−1.44452
4	0215	12	4.59	21.1	685	4547422	−1.18079
4	0216	14	4.60	32.6	825	4871495	−0.85961
4	0217	14	4.55	21.2	623	4673414	−0.9445
4	0218	12	4.59	32.0	925	4667168	−1.0355
4	0219	12	4.57	21.2	623	4673414	−0.96483
4	0220	14	4.60	32.2	840	4815720	−0.85858
4	0221	14	4.60	21.1	623	4673414	−0.94639
4	0222	12	4.57	32.6	950	4751209	−1.50089
4	0223	12	4.57	21.1	623	4673414	−0.85394
4	0224	14	4.54	32.6	825	4763668	−0.71146
4	0262	14	4.04	20.8	670	4917092	−1.17173
4	0263	14	3.88	20.6	623	4673414	−1.39779
4	0264	12	4.03	20.6	623	4673414	−0.38661
4	0265	12	3.88	20.6	545	4673414	−0.91442
4	0266	14	4.61	21.1	623	4673414	−0.59854
4	0267	14	4.65	21.1	580	4375340	−0.50502
4	0268	14	4.57	21.1	625	4853802	−0.21911
20	0201	12	4.61	23.6	638	4137143	−1.65641
20	0202	14	4.61	34.1	911	4660000	−2.00853

State Code	SHRP ID	Average Slab Width (ft)	Average Slab Length (ft)	Average Paste Volume (%)	Average PCC Modulus of Rupture (psi)	Average PCC Elastic Modulus (psi)	Average Temperature Gradient During FWD Testing (°F /Inch)
20	0203	14	4.60	23.6	656	4320000	−0.71594
20	0204	12	4.55	34.1	849	4490000	−0.73556
20	0205	12	4.56	23.6	706	4137143	−0.83047
20	0206	14	4.55	30.0	928	4660000	−0.7026
20	0207	14	4.55	23.6	645	4000000	−0.45431
20	0208	12	4.56	34.1	1,035	4830000	−1.00285
20	0209	12	4.57	23.6	576	4137143	−0.76717
20	0210	14	4.58	34.1	839	4660000	−1.10165
20	0211	14	4.55	23.6	674	4137143	−0.79886
20	0212	12	4.54	34.1	918	4660000	−1.52806
20	0259	12	4.54	27.1	677	4402381	−1.05579
37	0201	12	4.58	25.5	673	4287000	−1.45559
37	0202	14	4.61	36.1	670	4234625	−0.78532
37	0203	14	4.51	25.5	673	4287000	−1.41008
37	0204	12	4.55	36.1	670	4234625	−1.06623
37	0205	12	4.55	25.0	673	4287000	−1.2069
37	0206	14	4.55	35.6	670	4234625	−1.38106
37	0207	14	4.62	25.0	736	4287000	−1.25587
37	0208	12	4.61	35.6	670	4234625	−1.29762
37	0209	12	4.62	25.5	673	4287000	−1.59637
37	0210	14	4.53	36.1	670	4234625	−1.3316
37	0211	14	4.57	25.5	673	4287000	−1.27676
37	0212	12	4.59	36.1	670	4234625	−1.50564
37	0259	12	6.12	27.4	616	3868000	−0.91184
37	0260	14	4.61	25.5	642	4287000	−0.67356
39	0201	12	4.56	25.3	831	2710000	−0.77725
39	0202	14	4.58	31.9	890	3540000	−3.18667
39	0203	14	4.58	25.3	702	2940000	−0.83654
39	0204	12	4.58	31.9	834	3905000	−0.89621
39	0205	12	4.58	25.3	804	2710000	−1.39466
39	0206	14	4.58	31.9	834	3905000	−0.82301
39	0207	14	4.60	25.3	804	2710000	−0.02318
39	0208	12	4.59	31.9	784	3905000	−0.77844
39	0209	12	4.57	25.3	804	2710000	−0.20902
39	0210	14	4.56	31.9	834	3905000	−1.70028
39	0211	14	4.64	25.3	880	2480000	−0.24077
39	0212	12	4.61	31.9	828	4270000	−0.34053
39	0259	12	4.60	31.9	489	3890000	−0.5938
39	0260	12	4.58	27.7	790	3520000	−0.38327
39	0261	14	4.56	25.3	661	3313333	−0.45369
39	0262	12	4.63	25.3	705	2530000	−0.23196
39	0263	14	4.53	25.3	661	3313333	−0.47291
39	0264	12	4.59	25.3	661	3313333	−1.47561
39	0265	12	4.57	25.3	661	3313333	−0.82438
53	0201	12	4.60	22.4	616	4200000	−1.30215
53	0202	14	4.57	34.4	1,041	4200000	−2.20726
53	0203	14	4.59	22.4	622	4200000	−0.97931
53	0204	12	4.60	34.4	915	4200000	−0.75028

State Code	SHRP ID	Average Slab Width (ft)	Average Slab Length (ft)	Average Paste Volume (%)	Average PCC Modulus of Rupture (psi)	Average PCC Elastic Modulus (psi)	Average Temperature Gradient During FWD Testing (°F /Inch)
53	0205	12	4.57	22.4	524	4200000	−1.71146
53	0206	14	4.60	34.2	880	4200000	−0.96714
53	0207	14	4.57	22.4	611	4200000	−1.48769
53	0208	12	4.58	34.2	945	4200000	−0.6801
53	0209	12	4.55	22.5	616	4200000	−1.28027
53	0210	14	4.60	34.4	945	4200000	−1.51709
53	0211	14	4.55	22.4	709	4200000	−0.71796
53	0212	12	4.61	34.4	945	4200000	−1.09315
53	0259	14	4.15	27.6	663	4200000	−0.90745

SHRP = Strategic Highway Research Program.

Table 58 shows the thickness of each layer in the test section by layer type. All test sections have been categorized into GB, PATB, and LCB. In the case of sections with a GB under a treated base (i.e., PATB and LCB), the GB is considered a granular subbase. Soil layers that have been chemically stabilized are classified as treated subbase.

Table 58. Thickness of test-section layers in inches by the layer type.

State Code	SHRP ID	PCC	GB	PATB	LCB	GS	TS
4	0213	7.9	5.8	0.0	0.0	0.0	0.0
4	0214	8.3	6.1	0.0	0.0	0.0	0.0
4	0215	11.0	6.3	0.0	0.0	0.0	0.0
4	0216	11.2	6.3	0.0	0.0	0.0	0.0
4	0217	8.1	0.0	0.0	6.1	0.0	0.0
4	0218	8.3	0.0	0.0	6.2	0.0	0.0
4	0219	10.8	0.0	0.0	6.2	0.0	0.0
4	0220	11.2	0.0	0.0	6.2	0.0	0.0
4	0221	8.1	0.0	4.2	0.0	4.2	0.0
4	0222	8.6	0.0	3.9	0.0	4.3	0.0
4	0223	11.1	0.0	4.1	0.0	3.5	0.0
4	0224	10.6	0.0	4.4	0.0	3.8	0.0
4	0262	8.1	6.1	0.0	0.0	0.0	0.0
4	0263	8.2	0.0	4.4	0.0	3.9	0.0
4	0264	11.5	0.0	3.8	0.0	4.4	0.0
4	0265	10.8	6.8	0.0	0.0	0.0	0.0
4	0266	12.3	0.0	3.9	0.0	0.0	0.0
4	0267	11.3	0.0	3.9	0.0	0.0	0.0
4	0268	8.5	0.0	3.8	0.0	0.0	0.0
20	0201	7.7	6.1	0.0	0.0	0.0	6.0
20	0202	7.5	6.0	0.0	0.0	0.0	6.0
20	0203	11.2	5.9	0.0	0.0	0.0	6.0
20	0204	11.3	5.8	0.0	0.0	0.0	6.0
20	0205	7.3	0.0	0.0	6.4	0.0	6.0
20	0206	7.7	0.0	0.0	6.3	0.0	6.0
20	0207	10.9	0.0	0.0	6.1	0.0	6.0
20	0208	10.9	0.0	0.0	6.4	0.0	6.0
20	0209	8.4	0.0	3.8	0.0	4.2	6.0

State Code	SHRP ID	PCC	GB	PATB	LCB	GS	TS
20	0210	8.5	0.0	3.9	0.0	4.0	6.0
20	0211	11.2	0.0	3.8	0.0	4.1	6.0
20	0212	11.1	0.0	3.7	0.0	4.1	6.0
20	0259	11.9	0.0	0.0	5.7	0.0	6.0
37	0201	9.2	9.3	0.0	0.0	0.0	8.0
37	0202	8.9	9.0	0.0	0.0	0.0	8.0
37	0203	11.9	5.6	0.0	0.0	7.0	0.0
37	0204	11.6	5.7	0.0	0.0	0.0	7.0
37	0205	8.0	0.0	0.0	6.5	0.0	8.0
37	0206	8.4	0.0	0.0	6.7	0.0	8.0
37	0207	11.7	0.0	0.0	5.7	7.7	0.0
37	0208	11.2	0.0	0.0	5.8	0.0	8.0
37	0209	8.6	0.0	5.6	0.0	5.0	5.0
37	0210	9.1	0.0	5.3	0.0	4.7	5.0
37	0211	11.5	0.0	3.6	0.0	4.1	8.0
37	0212	11.2	0.0	3.8	0.0	3.8	8.0
37	0259	10.8	0.0	4.4	0.0	0.0	8.0
37	0260	11.6	0.0	5.6	0.0	7.0	0.0
39	0201	7.9	6.2	0.0	0.0	0.0	0.0
39	0202	8.3	5.8	0.0	0.0	0.0	0.0
39	0203	11.2	6.1	0.0	0.0	0.0	0.0
39	0204	11.1	5.8	0.0	0.0	16.0	0.0
39	0205	8.0	0.0	0.0	6.2	0.0	0.0
39	0206	7.9	0.0	0.0	5.9	0.0	0.0
39	0207	11.2	0.0	0.0	6.5	0.0	0.0
39	0208	11.1	0.0	0.0	6.7	0.0	0.0
39	0209	8.3	0.0	3.9	0.0	4.1	0.0
39	0210	8.0	0.0	4.1	0.0	3.8	0.0
39	0211	11.3	0.0	3.9	0.0	4.0	0.0
39	0212	10.8	0.0	4.0	0.0	18.9	0.0
39	0259	10.9	6.3	0.0	0.0	18	0.0
39	0260	11.6	0.0	4.0	0.0	26.1	0.0
39	0261	11.1	0.0	0.0	4.2	4.3	0.0
39	0262	11.5	0.0	0.0	4.1	4.1	0.0
39	0263	11.1	7.0	0.0	0.0	0.0	0.0
39	0264	11.5	0.0	0.0	4.0	6.0	0.0
39	0265	11.2	0.0	3.8	0.0	34.0	0.0
53	0201	8.7	5.8	0.0	0.0	66.6	0.0
53	0202	8.3	6.5	0.0	0.0	36.3	0.0
53	0203	11.1	6.9	0.0	0.0	0.0	0.0
53	0204	11.2	5.9	0.0	0.0	61.3	0.0
53	0205	8.5	0.0	0.0	6.1	62.2	0.0
53	0206	8.6	0.0	0.0	6.2	55.0	0.0
53	0207	11.1	0.0	0.0	6.1	84.1	0.0
53	0208	11.2	0.0	0.0	6.5	53.4	0.0
53	0209	9.0	0.0	3.9	0.0	71.8	0.0
53	0210	8.3	0.0	3.8	0.0	53.2	0.0
53	0211	11.8	0.0	3.9	0.0	63.6	0.0
53	0212	11.3	0.0	3.5	0.0	76.3	0.0
53	0259	10.3	0.0	2.8	0.0	2.0	0.0

GS = granular subbase; SHRP = Strategic Highway Research Program; TS = treated subbase.
Note: All thickness values are expressed in inches.

DI LINEAR REGRESSION

Table 59 shows the results of linear regression analysis performed on DI values calculated from FWD testing. The results show the ΔDI intercept (ΔDI_i), the initial ΔDI after the pavement was constructed and the ΔDI slope (ΔDI_s), the change in ΔDI per year after construction up to 10 years. Intercept and slope was also computed for DI values at FWD testing locations J1 (slab center) and J2 (slab corner).

Table 59. Linear regression intercepts and slopes for DI.

State Code	SHRP ID	ΔDI_i (µm)	ΔDI_s (µm/Year)	DI_{J1i} (µm)	DI_{J1s} (µm/Year)	DI_{J2i} (µm)	DI_{J2s} (µm/Year)
4	0213	9.77721	−8.00836	14.45298	−1.99376	7.80621	5.51738
4	0214	−1.87233	2.63776	−23.23041	4.71623	2.42174	0.0132
4	0215	−67.19484	5.08486	−15.06353	0.49439	59.36949	−4.72558
4	0216	0.80371	0.10306	−1.98793	−0.5537	1.3751	−0.08392
4	0217	−62.012	−5.05898	−1.20836	−0.99863	64.65368	3.5145
4	0218	−248.1409	25.08078	−14.12212	0.93093	234.14678	−24.12628
4	0219	−117.3887	−4.6673	−1.06315	−0.48019	116.32552	4.18711
4	0265	99.88888	−27.10856	−31.82291	3.9152	−114.2345	28.8916
4	0266	−27.34335	3.03201	−18.0937	2.1549	12.19123	−1.02126
4	0267	−35.05338	4.15803	−5.95589	0.09466	24.72249	−2.93186
4	0268	−41.97217	3.93292	−15.80551	1.61856	25.95431	−2.26272
20	0201	−28.96117	−12.85242	−4.40299	0.13277	37.51604	11.5614
20	0202	−44.30824	3.03646	4.87329	−0.92135	52.4091	−3.05453
20	0203	2.32269	−0.45929	−1.58315	−0.47631	2.61257	0.31093
20	0204	−19.08814	−14.0511	−2.14428	0.5472	16.2702	16.20037
20	0205	−11.84433	−6.13923	2.23327	−1.76782	19.39008	3.87877
20	0206	−8.69877	−2.2923	0.10839	−1.97463	10.73385	0.67534
20	0207	−2.77959	0.39016	−1.89324	−0.54852	6.82269	−0.84642
20	0208	−6.38999	−0.69893	2.34907	−0.78162	10.75263	1.08046
20	0209	−6.68363	−4.24846	−4.19563	−0.70384	9.04091	3.12849
20	0210	−0.50814	−1.17265	5.58598	−1.60102	6.92251	−0.02961
20	0211	−7.3436	0.30189	1.92858	−0.84804	9.94492	−0.37623
20	0212	10.57708	−4.46903	2.04832	−0.44651	−1.2643	3.95268
20	0259	−2.74149	0.38223	5.31363	−1.27539	7.91506	−1.07408
37	0201	−39.00285	1.97924	−11.88901	0.63397	34.06512	−1.30413
37	0202	−12.8224	−1.68007	−14.58125	0.30413	7.93203	1.26325
37	0203	−7.64595	1.18434	−2.89195	−0.64702	5.57076	−0.35682
37	0204	−29.24517	−8.45494	0.73098	−0.08225	32.56694	8.15765
37	0205	−46.47105	−31.54105	−5.65109	−1.25812	44.38733	29.78818
37	0206	−15.44943	−5.73375	−10.61193	−0.60805	8.70294	4.87699
37	0207	−12.45737	−0.84787	−0.08088	−1.62416	12.43218	0.31403
37	0208	−46.87125	−6.22616	1.20704	−1.58258	49.21064	4.4938
37	0209	−11.05789	1.59922	−15.29166	1.05956	5.85798	−0.43684
37	0210	−2.10828	−1.17717	−11.93228	−0.35486	−1.67312	1.51138
37	0211	0.94378	0.44027	−12.60587	0.92183	0.26767	0.22959
37	0212	−9.85218	−4.61581	−1.989	−0.03469	10.95699	4.98705
37	0259	−27.1948	−1.92252	−4.28709	0.13033	36.02714	0.80262
37	0260	3.55152	−0.91947	1.99509	−0.2665	−0.07531	0.77898
39	0201	−130.8292	27.09795	1.77562	−1.89362	127.67067	−20.31706
39	0202	25.08761	1.13311	11.94844	−0.50127	0.0000	0.0000
39	0203	4.71424	0.1877	0.33702	−0.6492	0.68281	0.00891

State Code	SHRP ID	ΔDI_i (µm)	ΔDI_s (µm/Year)	DI_{J1i} (µm)	DI_{J1s} (µm/Year)	DI_{J2i} (µm)	DI_{J2s} (µm/Year)
39	0204	−8.9159	−1.60665	−27.02649	5.7286	14.79469	1.54437
39	0205	−19.59697	1.01967	−3.30676	−1.6375	19.00177	−1.11336
39	0206	5.83167	−1.26409	−1.29863	−1.61858	2.62272	−0.13915
39	0207	0.95004	−0.56317	−1.15584	–0.9566	0.77414	−0.08128
39	0208	−3.4797	1.99096	−2.35703	−0.16448	2.88848	−0.26537
39	0209	−98.24292	20.08562	−3.40907	−1.25041	94.61768	−15.19586
39	0210	10.53933	1.24109	−3.22534	−1.30934	0.0000	0.0000
39	0211	4.18845	1.04671	3.29149	−1.35497	0.84022	−0.11434
39	0212	26.07621	−2.69808	−9.51981	1.05203	−4.31088	1.04939
39	0259	−11.03534	4.65194	0.53678	−0.61407	14.55548	−2.11945
39	0260	7.04494	0.16398	−1.65047	−0.9893	0.85168	−0.04359
39	0261	5.59426	−0.47238	−1.04846	−0.358	−0.42296	0.24925
39	0262	−20.89482	4.04499	1.79234	−0.13925	21.18275	−2.92414
39	0263	−37.17806	6.08792	5.62706	−1.02846	42.5989	−6.44014
39	0264	−183.6636	26.65113	−26.5101	3.27117	56.11313	−6.96193
39	0265	10.51183	−1.10648	−1.10638	0.07804	−3.84273	1.79962
53	0201	−89.03458	−21.82868	−15.524	−0.04947	94.4682	19.14319
53	0202	−25.0659	−0.20562	−16.69861	2.70685	20.14697	1.91485
53	0203	−3.35399	−2.29797	−12.95982	−0.43977	5.58983	0.70601
53	0204	8.17289	−2.44699	−12.2868	−0.46208	−0.2204	0.46252
53	0205	−37.26479	−10.76946	−16.34432	0.97348	36.0088	10.0839
53	0206	−27.54665	2.81222	−11.25338	0.52018	18.39723	−2.05976
53	0207	−10.15828	0.48042	−11.21543	0.36266	4.91182	−0.32728
53	0208	−4.99143	−3.31321	−10.42091	−0.01295	−1.03804	3.00812
53	0209	10.18756	−2.95386	−19.51314	0.61512	−0.24257	0.1931
53	0210	9.53061	−0.33472	−13.18451	0.37017	0.0000	0.0000
53	0211	1.97305	−0.26545	−12.50254	−0.23022	0.0000	0.0000
53	0212	17.56149	−0.90396	−12.96738	−0.3594	0.0000	0.0000
53	0259	12.02413	−8.14247	−8.24847	−0.56498	−12.39629	7.02923

SHRP = Strategic Highway Research Program.

LTE LINEAR REGRESSION

Table 60 shows the results of linear regression analysis performed on LTE values calculated from FWD testing. The results show the LTE intercept (LTE_i), the initial LTE after the pavement was constructed and the LTE slope (LTE_s), and the change in LTE per year after construction up to 10 years.

Table 60. Linear regression intercepts and slopes for LTE.

State Code	SHRP ID	LTE_i (%)	LTE_s (%/Year)
4	0213	87.75626	−1.04305
4	0214	75.09169	1.78057
4	0215	74.82586	0.10451
4	0216	82.15781	0.37596
4	0217	68.68687	−2.43131
4	0218	70.05301	−2.68807
4	0219	59.09027	−2.03114
4	0220	87.32719	−3.20712
4	0221	76.90138	−2.20398
4	0222	81.35223	−2.08318

State Code	SHRP ID	LTE_i (%)	LTE_s (%/Year)
4	0223	74.79376	−0.69149
4	0224	76.46068	−0.06196
4	0262	65.38007	1.88253
4	0264	84.65164	−3.71659
4	0265	70.31366	−3.34187
4	0266	85.02242	−3.2514
4	0267	84.18136	−3.50943
4	0268	80.42020	−2.20100
20	0201	85.68363	0.00614
20	0202	83.80981	0.39147
20	0203	83.46154	0.66505
20	0204	73.80806	0.46924
20	0205	84.21396	0.10090
20	0206	82.43118	0.65801
20	0207	84.53725	0.27973
20	0208	83.09841	0.85724
20	0209	88.83743	0.25871
20	0210	86.94369	0.37823
20	0211	84.91629	0.27876
20	0212	89.72478	0.34090
20	0259	75.90885	2.05721
37	0201	85.35618	−0.76934
37	0202	95.12165	−3.00668
37	0203	90.50659	−0.34865
37	0204	95.88537	−2.34916
37	0205	87.80315	−3.68891
37	0206	83.02451	−2.30517
37	0207	93.45814	−3.72251
37	0208	76.33617	−1.09567
37	0209	88.15671	−4.10285
37	0210	92.59077	−3.89767
37	0211	83.82185	−2.12187
37	0212	69.64235	−2.12445
37	0259	91.75010	−4.78589
37	0260	93.65586	−1.33180
39	0201	94.02691	−0.17719
39	0202	92.19937	0.56367
39	0203	92.95048	0.22193
39	0204	92.06758	−0.39566
39	0205	90.18279	−1.31599
39	0206	96.48185	−1.33481
39	0207	97.16824	−1.0995
39	0208	93.13998	0.37759
39	0209	94.56928	0.42706
39	0210	91.62462	−0.3143
39	0211	89.25426	1.12104
39	0212	93.81589	−0.02315
39	0259	90.87774	0.31139
39	0260	89.71525	0.39901
39	0261	90.22279	0.90011
39	0262	92.03791	0.54369
39	0263	89.00686	0.88947

State Code	SHRP ID	LTE_i (%)	LTE_s (%/Year)
39	0264	100.30948	−0.55419
39	0265	89.83071	1.00477
53	0201	87.36863	0.20767
53	0202	74.75473	1.10670
53	0203	87.81424	0.41400
53	0204	79.09059	0.62517
53	0205	77.74092	0.54087
53	0206	78.39233	1.04454
53	0207	77.70140	1.06520
53	0208	75.73421	1.32042
53	0209	80.44788	−0.54839
53	0210	85.27003	−0.19789
53	0211	82.33166	−0.64076
53	0212	82.46389	0.33022
53	0259	85.88441	−3.80067

SHRP = Strategic Highway Research Program.

RSTUDIO® RESULTS FROM LINEAR REGRESSION ANALYSIS OF CLIMATIC AND STRUCTURAL FACTORS TO PSG VALUES

Linear regression analysis computations were completed using RStudio, a free and open-source integrated development environment using the R programming language.[22] The following linear model summaries (Figure 336 through Figure 341) are the results of using climatic and structural factors to predict the intercept and slope of PSG values (PSG_i and PSG_s). The interpretation of these models and the significance of their parameters are analyzed further in chapter 8 of this report. These modeling results are supplemental to that analysis.

Dependent variables included the following:

- PSG_i = psg_i_bfit
- PSG_s = psg_s_bfit

Independent variables included the following:

- T_0 = temp_0
- Δ_{T0} = temp_0_dif
- H_0 = hum_0
- Δ_{H0} = hum_0_dif
- W_{slab} = slab_width
- L_{slab} = slab_length
- h_{PC} = pc_thk
- h_{GB} = gb_thk
- h_{PATB} = patb_thk
- h_{LCB} = lcb_thk
- h_{GS} = gs_thk
- h_{TS} = ts_thk
- PV = paste_vol

- F = mod_rupt
- E = mod_elast
- ΔT = temp_grad

```
Call:
lm(formula = psg_i_bfit ~ temp_0 + temp_0_dif + hum_0 +
    hum_0_dif + slab_width + slab_length + pc_thk +
    gb_thk + patb_thk + lcb_thk + gs_thk + ts_thk +
    paste_vol + mod_rupt + mod_elast + temp_grad,
    data = R_CLM_GB)

Residuals:
     Min       1Q   Median       3Q      Max
-0.50573 -0.15106  0.00033  0.12414  0.43981

Coefficients: (2 not defined because of singularities)
                 Estimate Std. Error t value Pr(>|t|)
(Intercept)     -8.722e+00  6.241e+00  -1.398   0.1957
temp_0           2.344e-02  2.522e-02   0.929   0.3770
temp_0_dif       2.759e-01  1.812e-01   1.523   0.1620
hum_0            8.845e-02  5.314e-02   1.664   0.1304
hum_0_dif       -9.592e-02  7.312e-02  -1.312   0.2221
slab_width       6.088e-02  8.933e-02   0.682   0.5127
slab_length     -7.825e-01  5.137e-01  -1.523   0.1620
pc_thk           1.960e-01  7.630e-02   2.568   0.0303 *
gb_thk           1.259e-01  1.400e-01   0.899   0.3920
patb_thk                NA         NA      NA       NA
lcb_thk                 NA         NA      NA       NA
gs_thk           1.405e-02  8.232e-03   1.706   0.1222
ts_thk           4.430e-02  8.405e-02   0.527   0.6109
paste_vol       -4.540e-03  2.768e-02  -0.164   0.8733
mod_rupt         4.533e-04  1.039e-03   0.436   0.6728
mod_elast       -2.708e-07  4.081e-07  -0.664   0.5236
temp_grad       -2.986e-01  2.018e-01  -1.479   0.1731
---
Signif. codes:  0 ‘***’ 0.001 ‘**’ 0.01 ‘*’ 0.05 ‘.’ 0.1 ‘ ’ 1

Residual standard error: 0.355 on 9 degrees of freedom
Multiple R-squared:  0.805,     Adjusted R-squared:  0.5017
F-statistic: 2.654 on 14 and 9 DF,  p-value: 0.07243
```


Figure 336. Illustration. Software output from climate analysis and PSG intercept for GB pavements.[(22)]

```
Call:
lm(formula = psg_s_bfit ~ meera_avg_temp + meera_temp_var +
    meera_avg_hum + meera_hum_var + slab_width + slab_length +
    pc_thk + gb_thk + patb_thk + lcb_thk + gs_thk +
    ts_thk + paste_vol + mod_rupt + mod_elast +
    temp_grad, data = R_CLM_GB)

Residuals:
      Min        1Q    Median        3Q       Max
-0.152126 -0.033421 -0.000402  0.037580  0.142512

Coefficients: (2 not defined because of singularities)
                  Estimate Std. Error t value Pr(>|t|)
(Intercept)     -9.055e+00  6.815e+00  -1.329    0.217
meera_avg_temp  -1.263e-01  9.102e-02  -1.388    0.199
meera_temp_var   6.536e-01  4.779e-01   1.368    0.205
meera_avg_hum    5.891e-02  4.690e-02   1.256    0.241
meera_hum_var   -3.412e-02  3.573e-02  -0.955    0.365
slab_width      -2.896e-02  2.751e-02  -1.053    0.320
slab_length      1.433e-01  1.582e-01   0.906    0.389
pc_thk           4.817e-03  2.350e-02   0.205    0.842
gb_thk           4.353e-02  4.313e-02   1.009    0.339
patb_thk                NA         NA      NA       NA
lcb_thk                 NA         NA      NA       NA
gs_thk          -9.524e-04  2.535e-03  -0.376    0.716
ts_thk          -3.683e-02  2.589e-02  -1.423    0.189
paste_vol        1.373e-02  8.524e-03   1.610    0.142
mod_rupt        -3.263e-04  3.198e-04  -1.020    0.334
mod_elast       -2.119e-07  1.257e-07  -1.686    0.126
temp_grad       -5.627e-02  6.216e-02  -0.905    0.389

Residual standard error: 0.1093 on 9 degrees of freedom
Multiple R-squared:  0.5764,    Adjusted R-squared:  -0.08256
F-statistic: 0.8747 on 14 and 9 DF,  p-value: 0.6033
```


Figure 337. Illustration. Software output from climate analysis and PSG slope for GB pavements.[(22)]

```
Call:
lm(formula = psg_i_bfit ~ temp_0 + temp_0_dif + hum_0 +
    hum_0_dif + slab_width + slab_length + pc_thk +
    gb_thk + patb_thk + lcb_thk + gs_thk + ts_thk +
    paste_vol + mod_rupt + mod_elast + temp_grad,
    data = R_CLM_AT)

Residuals:
     Min       1Q   Median       3Q      Max
-0.49313 -0.19835  0.02118  0.18342  0.43602

Coefficients: (2 not defined because of singularities)
                  Estimate Std. Error t value Pr(>|t|)
(Intercept)     -6.047e+00  4.567e+00  -1.324    0.205
temp_0          -1.709e-02  3.282e-02  -0.521    0.610
temp_0_dif       1.314e-01  1.489e-01   0.882    0.392
hum_0            4.063e-02  3.780e-02   1.075    0.299
hum_0_dif       -3.494e-02  4.683e-02  -0.746    0.467
slab_width       4.125e-02  7.615e-02   0.542    0.596
slab_length     -5.206e-02  2.521e-01  -0.206    0.839
pc_thk           8.286e-02  6.085e-02   1.362    0.193
gb_thk                  NA         NA      NA       NA
patb_thk         2.809e-01  2.846e-01   0.987    0.339
lcb_thk                 NA         NA      NA       NA
gs_thk           5.537e-04  6.953e-03   0.080    0.938
ts_thk           4.419e-02  9.121e-02   0.484    0.635
paste_vol        2.761e-02  2.672e-02   1.033    0.318
mod_rupt        -2.032e-04  1.120e-03  -0.181    0.858
mod_elast        9.288e-08  2.580e-07   0.360    0.724
temp_grad       -1.034e-01  2.399e-01  -0.431    0.673

Residual standard error: 0.3588 on 15 degrees of freedom
Multiple R-squared:  0.673,     Adjusted R-squared:  0.3679
F-statistic: 2.205 on 14 and 15 DF,  p-value: 0.07032
```


Figure 338. Illustration. Software output from climate analysis and PSG intercept for PATB pavements.[22]

```
Call:
lm(formula = psg_s_bfit ~ meera_avg_temp + meera_temp_var +
    meera_avg_hum + meera_hum_var + slab_width + slab_length +
    pc_thk + gb_thk + patb_thk + lcb_thk + gs_thk +
    ts_thk + paste_vol + mod_rupt + mod_elast +
    temp_grad, data = R_CLM_AT)

Residuals:
      Min        1Q    Median        3Q       Max
-0.038108 -0.018997 -0.002164  0.022036  0.047742

Coefficients: (2 not defined because of singularities)
                  Estimate Std. Error t value Pr(>|t|)
(Intercept)      1.314e+00  1.953e+00   0.673    0.511
meera_avg_temp   4.998e-03  1.990e-02   0.251    0.805
meera_temp_var  -5.076e-02  1.176e-01  -0.432    0.672
meera_avg_hum   -4.385e-03  1.343e-02  -0.326    0.749
meera_hum_var   -2.928e-03  8.766e-03  -0.334    0.743
slab_width      -5.074e-03  7.079e-03  -0.717    0.485
slab_length     -1.573e-04  2.344e-02  -0.007    0.995
pc_thk          -5.466e-03  5.657e-03  -0.966    0.349
gb_thk                  NA         NA      NA       NA
patb_thk         1.382e-02  2.646e-02   0.522    0.609
lcb_thk                 NA         NA      NA       NA
gs_thk           1.147e-04  6.464e-04   0.177    0.862
ts_thk           2.970e-03  8.480e-03   0.350    0.731
paste_vol       -8.084e-04  2.484e-03  -0.325    0.749
mod_rupt         6.176e-05  1.041e-04   0.593    0.562
mod_elast       -2.142e-08  2.398e-08  -0.893    0.386
temp_grad        1.183e-02  2.230e-02   0.531    0.603

Residual standard error: 0.03336 on 15 degrees of freedom
Multiple R-squared:  0.8099,    Adjusted R-squared:  0.6324
F-statistic: 4.563 on 14 and 15 DF,  p-value: 0.003002
```


Figure 339. Illustration. Software output from climate analysis and PSG slope for PATB pavements.[(22)]

```
Call:
lm(formula = psg_i_bfit ~ temp_0 + temp_0_dif + hum_0 + 
    hum_0_dif + slab_width + slab_length + pc_thk + 
    gb_thk + patb_thk + lcb_thk + gs_thk + ts_thk + 
    paste_vol + mod_rupt + mod_elast + temp_grad, 
    data = R_CLM_CT)

Residuals:
     Min       1Q   Median       3Q      Max 
-0.92027 -0.07521 -0.00436  0.15115  0.70841 

Coefficients: (2 not defined because of singularities)
                  Estimate Std. Error t value Pr(>|t|)
(Intercept)     -4.766e+01  4.113e+01  -1.159    0.276
temp_0          -5.899e-02  6.457e-02  -0.914    0.385
temp_0_dif       9.638e-02  2.197e-01   0.439    0.671
hum_0            7.194e-02  6.115e-02   1.176    0.270
hum_0_dif       -6.759e-02  8.087e-02  -0.836    0.425
slab_width       1.106e-01  1.581e-01   0.699    0.502
slab_length      9.587e+00  8.713e+00   1.100    0.300
pc_thk           8.880e-02  9.414e-02   0.943    0.370
gb_thk                  NA         NA      NA       NA
patb_thk                NA         NA      NA       NA
lcb_thk          2.459e-01  1.861e-01   1.321    0.219
gs_thk          -4.156e-02  3.139e-02  -1.324    0.218
ts_thk           7.129e-02  1.387e-01   0.514    0.620
paste_vol       -2.999e-02  6.288e-02  -0.477    0.645
mod_rupt        -4.672e-04  1.832e-03  -0.255    0.804
mod_elast        3.459e-07  4.592e-07   0.753    0.471
temp_grad        1.489e-01  4.807e-01   0.310    0.764

Residual standard error: 0.4858 on 9 degrees of freedom
Multiple R-squared:  0.7795,    Adjusted R-squared:  0.4365 
F-statistic: 2.273 on 14 and 9 DF,  p-value: 0.109
```


Figure 340. Illustration. Software output from climate analysis and PSG intercept for LCB pavements.[(22)]

```
Call:
lm(formula = psg_s_bfit ~ meera_avg_temp + meera_temp_var +
    meera_avg_hum + meera_hum_var + slab_width + slab_length +
    pc_thk + gb_thk + patb_thk + lcb_thk + gs_thk +
    ts_thk + paste_vol + mod_rupt + mod_elast +
    temp_grad, data = R_CLM_CT)

Residuals:
      Min        1Q    Median        3Q       Max
-0.100817 -0.027396  0.002338  0.033652  0.072458

Coefficients: (2 not defined because of singularities)
                 Estimate Std. Error t value Pr(>|t|)
(Intercept)      1.623e+00  7.001e+00   0.232    0.822
meera_avg_temp   8.846e-03  8.073e-02   0.110    0.915
meera_temp_var  -7.783e-02  4.908e-01  -0.159    0.878
meera_avg_hum   -1.624e-02  5.828e-02  -0.279    0.787
meera_hum_var    3.277e-02  5.356e-02   0.612    0.556
slab_width      -6.427e-03  2.360e-02  -0.272    0.791
slab_length     -5.811e-02  1.300e+00  -0.045    0.965
pc_thk          -2.028e-02  1.405e-02  -1.443    0.183
gb_thk                  NA         NA      NA       NA
patb_thk                NA         NA      NA       NA
lcb_thk          5.206e-03  2.777e-02   0.187    0.855
gs_thk          -1.646e-03  4.684e-03  -0.351    0.733
ts_thk          -2.011e-02  2.070e-02  -0.971    0.357
paste_vol        9.411e-03  9.383e-03   1.003    0.342
mod_rupt        -1.122e-04  2.734e-04  -0.411    0.691
mod_elast       -6.196e-08  6.853e-08  -0.904    0.389
temp_grad        6.397e-02  7.173e-02   0.892    0.396

Residual standard error: 0.07249 on 9 degrees of freedom
Multiple R-squared:  0.7509,    Adjusted R-squared:  0.3634
F-statistic: 1.938 on 14 and 9 DF,  p-value: 0.1602
```


Figure 341. Illustration. Software output from climate analysis and PSG slope for LCB pavements.[(22)]

RSTUDIO RESULTS FROM LINEAR REGRESSION ANALYSIS OF DI AND STRUCTURAL FACTORS TO PSG VALUES

Linear regression analysis computations were completed using RStudio.[(22)] The following linear model summaries (figure 342 through figure 347) are the results of using climatic and structural factors to predict PSG_i and PSG_s values. The interpretation of these models and the significance of their parameters are analyzed further in chapter 9 of this report. These modeling results are a supplement to that analysis.

Dependent variables included the following:

- PSG_i = psg_i_bfit
- PSG_s = psg_s_bfit

Independent variables included the following:

- ΔDI_i = di_j1_j2_intercept
- ΔDI_s = di_j1_j2_regr
- $(D_{J1})_i$ = di_j1_intercept
- $(D_{J1})_s$ = di_j1_regr

- $(D_{J2})_i$ = di_j2_intercept
- $(D_{J2})_s$ = di_j2_regr
- W_{slab} = slab_width
- L_{slab} = slab_length
- h_{PC} = pc_thk
- h_{GB} = gb_thk
- h_{PATB} = patb_thk
- h_{LCB} = lcb_thk
- h_{GS} = gs_thk
- h_{TS} = ts_thk
- PV = paste_vol
- F = mod_rupt
- E = mod_elast
- ΔT = temp_grad

```
Call:
lm(formula = psg_i_bfit ~ di_j1_j2_intercept + di_j1_j2_regr +
    di_j1_intercept + di_j1_regr + di_j2_intercept + di_j2_regr +
    slab_width + slab_length + pc_thk + gb_thk +
    patb_thk + lcb_thk + gs_thk + ts_thk + paste_vol +
    mod_rupt + mod_elast + temp_grad, data = R_DI_GB)

Residuals:
     Min       1Q   Median       3Q      Max
-0.49879 -0.12961  0.00466  0.19269  0.33359

Coefficients: (2 not defined because of singularities)
                     Estimate Std. Error t value Pr(>|t|)
(Intercept)        -2.772e+00  4.509e+00  -0.615   0.5582
di_j1_j2_intercept  1.913e-03  3.624e-02   0.053   0.9594
di_j1_j2_regr       6.160e-02  1.151e-01   0.535   0.6091
di_j1_intercept    -2.672e-02  3.014e-02  -0.887   0.4048
di_j1_regr         -1.247e-01  1.313e-01  -0.950   0.3738
di_j2_intercept     3.549e-03  3.921e-02   0.091   0.9304
di_j2_regr          7.384e-02  1.235e-01   0.598   0.5689
slab_width          1.855e-01  1.489e-01   1.246   0.2529
slab_length        -3.346e-01  8.630e-01  -0.388   0.7097
pc_thk              2.049e-01  1.075e-01   1.906   0.0983 .
gb_thk             -9.189e-02  1.702e-01  -0.540   0.6060
patb_thk                   NA         NA      NA       NA
lcb_thk                    NA         NA      NA       NA
gs_thk              1.223e-02  8.893e-03   1.375   0.2115
ts_thk              1.415e-01  4.904e-02   2.885   0.0235 *
paste_vol          -1.253e-02  2.935e-02  -0.427   0.6824
mod_rupt            7.779e-04  1.137e-03   0.684   0.5159
mod_elast          -2.394e-07  2.661e-07  -0.900   0.3983
temp_grad          -3.271e-01  2.340e-01  -1.398   0.2048
---
Signif. codes:  0 ‘***’ 0.001 ‘**’ 0.01 ‘*’ 0.05 ‘.’ 0.1 ‘ ’ 1

Residual standard error: 0.4106 on 7 degrees of freedom
Multiple R-squared:  0.797,     Adjusted R-squared:  0.3331
F-statistic: 1.718 on 16 and 7 DF,  p-value: 0.2392
```


Figure 342. Illustration. Software output from DI analysis and PSG intercept for GB pavements.[22]

```
Call:
lm(formula = psg_s_bfit ~ di_j1_j2_intercept + di_j1_j2_regr +
    di_j1_intercept + di_j1_regr + di_j2_intercept + di_j2_regr +
    slab_width + slab_length + pc_thk + gb_thk +
    patb_thk + lcb_thk + gs_thk + ts_thk + paste_vol +
    mod_rupt + mod_elast + temp_grad, data = R_DI_GB)

Residuals:
     Min       1Q   Median       3Q      Max
-0.11110 -0.02794  0.00040  0.02361  0.12416

Coefficients: (2 not defined because of singularities)
                    Estimate Std. Error t value Pr(>|t|)
(Intercept)        -1.133e+00  1.271e+00  -0.891    0.402
di_j1_j2_intercept  6.087e-03  1.022e-02   0.596    0.570
di_j1_j2_regr       2.905e-02  3.244e-02   0.895    0.400
di_j1_intercept    -6.447e-03  8.496e-03  -0.759    0.473
di_j1_regr         -7.694e-03  3.700e-02  -0.208    0.841
di_j2_intercept     5.584e-03  1.105e-02   0.505    0.629
di_j2_regr          2.999e-02  3.482e-02   0.861    0.418
slab_width          1.181e-02  4.197e-02   0.281    0.786
slab_length         3.053e-01  2.432e-01   1.255    0.250
pc_thk             -7.708e-03  3.030e-02  -0.254    0.806
gb_thk             -1.485e-02  4.797e-02  -0.310    0.766
patb_thk                   NA         NA      NA       NA
lcb_thk                    NA         NA      NA       NA
gs_thk             -5.543e-04  2.507e-03  -0.221    0.831
ts_thk             -1.502e-03  1.382e-02  -0.109    0.917
paste_vol           4.687e-04  8.272e-03   0.057    0.956
mod_rupt           -1.108e-04  3.205e-04  -0.346    0.740
mod_elast          -5.924e-08  7.500e-08  -0.790    0.456
temp_grad           6.327e-03  6.595e-02   0.096    0.926

Residual standard error: 0.1157 on 7 degrees of freedom
Multiple R-squared:  0.6307,    Adjusted R-squared:  -0.2134
F-statistic: 0.7471 on 16 and 7 DF,  p-value: 0.7043
```


Figure 343. Illustration. Software output from DI analysis and PSG slope for GB pavements.[22]

```
Call:
lm(formula = psg_i_bfit ~ di_j1_j2_intercept + di_j1_j2_regr +
    di_j1_intercept + di_j1_regr + di_j2_intercept + di_j2_regr +
    slab_width + slab_length + pc_thk + gb_thk +
    patb_thk + lcb_thk + gs_thk + ts_thk + paste_vol +
    mod_rupt + mod_elast + temp_grad, data = R_DI_AT)

Residuals:
     Min       1Q   Median       3Q      Max
-0.49550 -0.15270 -0.02566  0.22799  0.38019

Coefficients: (2 not defined because of singularities)
                     Estimate Std. Error t value Pr(>|t|)
(Intercept)        -3.159e+00  2.415e+00  -1.308    0.215
di_j1_j2_intercept  1.628e-02  1.641e-02   0.993    0.341
di_j1_j2_regr       2.978e-03  1.694e-01   0.018    0.986
di_j1_intercept    -2.144e-02  2.266e-02  -0.946    0.363
di_j1_regr          5.418e-02  1.832e-01   0.296    0.773
di_j2_intercept     2.319e-02  2.248e-02   1.031    0.323
di_j2_regr          2.949e-02  2.115e-01   0.139    0.891
slab_width          1.742e-01  1.203e-01   1.447    0.173
slab_length        -2.423e-01  3.746e-01  -0.647    0.530
pc_thk              5.361e-02  7.469e-02   0.718    0.487
gb_thk                     NA         NA      NA       NA
patb_thk            1.442e-01  1.707e-01   0.845    0.415
lcb_thk                    NA         NA      NA       NA
gs_thk              6.437e-03  6.917e-03   0.931    0.370
ts_thk              4.943e-02  3.964e-02   1.247    0.236
paste_vol           2.873e-02  2.621e-02   1.096    0.294
mod_rupt            3.039e-04  1.263e-03   0.241    0.814
mod_elast          -1.563e-07  2.578e-07  -0.606    0.556
temp_grad          -1.545e-01  3.139e-01  -0.492    0.632

Residual standard error: 0.3855 on 12 degrees of freedom
Multiple R-squared:  0.6845,    Adjusted R-squared:  0.2638
F-statistic: 1.627 on 16 and 12 DF,  p-value: 0.199
```


Figure 344. Illustration. Software output from DI analysis, PSG intercept for PATB pavements.[22]

```
Call:
lm(formula = psg_s_bfit ~ di_j1_j2_intercept + di_j1_j2_regr +
    di_j1_intercept + di_j1_regr + di_j2_intercept + di_j2_regr +
    slab_width + slab_length + pc_thk + gb_thk +
    patb_thk + lcb_thk + gs_thk + ts_thk + paste_vol +
    mod_rupt + mod_elast + temp_grad, data = R_DI_AT)

Residuals:
      Min        1Q    Median        3Q       Max
-0.046863 -0.014501  0.001339  0.015675  0.038511

Coefficients: (2 not defined because of singularities)
                     Estimate Std. Error t value Pr(>|t|)
(Intercept)         4.358e-01  2.077e-01   2.098   0.0577 .
di_j1_j2_intercept  1.232e-03  1.411e-03   0.873   0.3999
di_j1_j2_regr       1.974e-03  1.458e-02   0.135   0.8945
di_j1_intercept    -1.923e-03  1.949e-03  -0.987   0.3433
di_j1_regr         -2.322e-02  1.576e-02  -1.473   0.1665
di_j2_intercept    -7.790e-04  1.934e-03  -0.403   0.6942
di_j2_regr         -9.947e-03  1.819e-02  -0.547   0.5945
slab_width         -1.912e-02  1.035e-02  -1.847   0.0895 .
slab_length         2.289e-02  3.222e-02   0.710   0.4910
pc_thk             -3.904e-03  6.425e-03  -0.608   0.5548
gb_thk                     NA         NA      NA       NA
patb_thk           -9.838e-03  1.468e-02  -0.670   0.5156
lcb_thk                    NA         NA      NA       NA
gs_thk             -6.330e-04  5.950e-04  -1.064   0.3084
ts_thk             -1.856e-03  3.410e-03  -0.544   0.5963
paste_vol           6.303e-04  2.254e-03   0.280   0.7846
mod_rupt           -6.565e-05  1.086e-04  -0.604   0.5568
mod_elast          -4.763e-08  2.218e-08  -2.148   0.0529 .
temp_grad          -1.075e-02  2.700e-02  -0.398   0.6976
---
Signif. codes:  0 ‘***’ 0.001 ‘**’ 0.01 ‘*’ 0.05 ‘.’ 0.1 ‘ ’ 1

Residual standard error: 0.03316 on 12 degrees of freedom
Multiple R-squared:  0.8401,    Adjusted R-squared:  0.6269
F-statistic: 3.941 on 16 and 12 DF,  p-value: 0.01033
```


Figure 345. Illustration. Software output from DI analysis, PSG slope for PATB pavements.[22]

```
Call:
lm(formula = psg_i_bfit ~ di_j1_j2_intercept + di_j1_j2_regr +
    di_j1_intercept + di_j1_regr + di_j2_intercept + di_j2_regr +
    slab_width + slab_length + pc_thk + gb_thk +
    patb_thk + lcb_thk + gs_thk + ts_thk + paste_vol +
    mod_rupt + mod_elast + temp_grad, data = R_DI_CT)

Residuals:
    Min      1Q  Median      3Q     Max
-0.9727 -0.1553 -0.0128  0.2167  0.7645

Coefficients: (2 not defined because of singularities)
                     Estimate Std. Error t value Pr(>|t|)
(Intercept)        -3.521e+01  4.472e+01  -0.787    0.457
di_j1_j2_intercept  6.997e-02  6.562e-02   1.066    0.322
di_j1_j2_regr       4.351e-01  4.641e-01   0.937    0.380
di_j1_intercept    -9.576e-02  1.266e-01  -0.756    0.474
di_j1_regr         -4.803e-01  8.185e-01  -0.587    0.576
di_j2_intercept     6.678e-02  6.998e-02   0.954    0.372
di_j2_regr          4.426e-01  4.768e-01   0.928    0.384
slab_width         -6.267e-02  2.420e-01  -0.259    0.803
slab_length         7.586e+00  9.886e+00   0.767    0.468
pc_thk              3.056e-02  1.413e-01   0.216    0.835
gb_thk                     NA         NA      NA       NA
patb_thk                   NA         NA      NA       NA
lcb_thk             8.421e-02  3.269e-01   0.258    0.804
gs_thk              9.356e-03  1.608e-02   0.582    0.579
ts_thk              1.398e-01  7.829e-02   1.785    0.117
paste_vol          -5.009e-03  6.487e-02  -0.077    0.941
mod_rupt           -1.754e-04  2.526e-03  -0.069    0.947
mod_elast           1.093e-07  5.035e-07   0.217    0.834
temp_grad           6.994e-01  8.326e-01   0.840    0.429

Residual standard error: 0.6719 on 7 degrees of freedom
Multiple R-squared:  0.6719,    Adjusted R-squared:  -0.07795
F-statistic: 0.8961 on 16 and 7 DF,  p-value: 0.5999
```


Figure 346. Illustration. Software output from DI analysis and PSG intercept for LCB pavements.[(22)]

```
Call:
lm(formula = psg_s_bfit ~ di_j1_j2_intercept + di_j1_j2_regr +
    di_j1_intercept + di_j1_regr + di_j2_intercept + di_j2_regr +
    slab_width + slab_length + pc_thk + gb_thk +
    patb_thk + lcb_thk + gs_thk + ts_thk + paste_vol +
    mod_rupt + mod_elast + temp_grad, data = R_DI_CT)

Residuals:
     Min       1Q   Median       3Q      Max
-0.11184 -0.03181  0.00130  0.03521  0.09708

Coefficients: (2 not defined because of singularities)
                     Estimate Std. Error t value Pr(>|t|)
(Intercept)         5.934e-01  5.863e+00   0.101    0.922
di_j1_j2_intercept -3.804e-03  8.603e-03  -0.442    0.672
di_j1_j2_regr      -2.029e-02  6.085e-02  -0.333    0.749
di_j1_intercept     5.906e-03  1.660e-02   0.356    0.733
di_j1_regr          2.023e-02  1.073e-01   0.189    0.856
di_j2_intercept    -3.769e-03  9.176e-03  -0.411    0.694
di_j2_regr         -2.152e-02  6.252e-02  -0.344    0.741
slab_width         -9.838e-03  3.173e-02  -0.310    0.766
slab_length        -6.043e-02  1.296e+00  -0.047    0.964
pc_thk             -2.362e-02  1.853e-02  -1.274    0.243
gb_thk                     NA         NA      NA       NA
patb_thk                   NA         NA      NA       NA
lcb_thk             2.185e-02  4.286e-02   0.510    0.626
gs_thk              2.420e-03  2.108e-03   1.148    0.289
ts_thk             -1.033e-02  1.027e-02  -1.006    0.348
paste_vol           8.473e-03  8.505e-03   0.996    0.352
mod_rupt           -6.934e-05  3.312e-04  -0.209    0.840
mod_elast          -3.622e-08  6.602e-08  -0.549    0.600
temp_grad           8.179e-02  1.092e-01   0.749    0.478

Residual standard error: 0.08809 on 7 degrees of freedom
Multiple R-squared:  0.7138,    Adjusted R-squared:  0.05974
F-statistic: 1.091 on 16 and 7 DF,  p-value: 0.4809
```


Figure 347. Illustration. Software output from DI analysis and PSG slope for LCB pavements.[(22)]

RSTUDIO RESULTS FROM LINEAR REGRESSION ANALYSIS OF LTE AND STRUCTURAL FACTORS TO PSG VALUES

Linear regression analysis computations were complete using RStudio.[(22)] The following linear model summaries (figure 348 through figure 353) are the results of using climatic and structural factors to predict PSG_i and PSG_s values. The interpretation of these models and the significance of their parameters are analyzed further in chapter 9 of this report. These modeling results are a supplement that analysis.

Dependent variables included the following:

- PSG_i = psg_i_bfit
- PSG_s = psg_s_bfit

Independent variables included the following:

- LTE_i = lte_intercept
- LTE_s = lte_regr

- W_{slab} = slab_width
- L_{slab} = slab_length
- h_{PC} = pc_thk
- h_{GB} = gb_thk
- h_{PATB} = patb_thk
- h_{LCB} = lcb_thk
- h_{GS} = gs_thk
- h_{TS} = ts_thk
- PV = paste_vol
- F = mod_rupt
- E = mod_elast
- ΔT = temp_grad

```
Call:
lm(formula = psg_i_bfit ~ lte_intercept + lte_regr + slab_width +
    slab_length + pc_thk + gb_thk + patb_thk +
    lcb_thk + gs_thk + ts_thk + paste_vol + mod_rupt +
    mod_elast + temp_grad, data = R_LTE_GB)

Residuals:
     Min       1Q   Median       3Q      Max
-0.49756 -0.17006  0.07233  0.19055  0.32080

Coefficients: (2 not defined because of singularities)
                 Estimate Std. Error t value Pr(>|t|)
(Intercept)    -6.312e-01  2.964e+00  -0.213  0.83524
lte_intercept  -1.794e-02  2.759e-02  -0.650  0.52894
lte_regr       -1.018e-01  1.121e-01  -0.908  0.38332
slab_width      1.411e-01  9.823e-02   1.437  0.17862
slab_length    -9.829e-02  8.976e-01  -0.109  0.91478
pc_thk          1.855e-01  6.729e-02   2.756  0.01868 *
gb_thk         -7.182e-02  1.063e-01  -0.676  0.51303
patb_thk               NA         NA      NA       NA
lcb_thk                NA         NA      NA       NA
gs_thk          1.619e-02  4.728e-03   3.424  0.00569 **
ts_thk          1.424e-01  3.485e-02   4.086  0.00180 **
paste_vol      -2.074e-02  2.389e-02  -0.868  0.40389
mod_rupt        8.004e-04  1.205e-03   0.664  0.52021
mod_elast      -3.755e-07  2.677e-07  -1.403  0.18834
temp_grad      -2.530e-01  1.818e-01  -1.392  0.19149
---
Signif. codes:  0 ‘***’ 0.001 ‘**’ 0.01 ‘*’ 0.05 ‘.’ 0.1 ‘ ’ 1

Residual standard error: 0.3663 on 11 degrees of freedom
Multiple R-squared:  0.7462,    Adjusted R-squared:  0.4694
F-statistic: 2.695 on 12 and 11 DF,  p-value: 0.05558
```


Figure 348. Illustration. Software output from LTE analysis and PSG intercept for GB pavements.[(22)]

```
Call:
lm(formula = psg_s_bfit ~ lte_intercept + lte_regr + slab_width +
    slab_length + pc_thk + gb_thk + patb_thk +
    lcb_thk + gs_thk + ts_thk + paste_vol + mod_rupt +
    mod_elast + temp_grad, data = R_LTE_GB)

Residuals:
      Min        1Q    Median        3Q       Max
-0.135801 -0.048396 -0.009624  0.024071  0.155564

Coefficients: (2 not defined because of singularities)
                  Estimate Std. Error t value Pr(>|t|)
(Intercept)     -5.562e-02  8.753e-01  -0.064    0.950
lte_intercept    2.019e-03  8.148e-03   0.248    0.809
lte_regr         2.778e-02  3.312e-02   0.839    0.419
slab_width      -3.243e-02  2.901e-02  -1.118    0.287
slab_length      7.359e-02  2.651e-01   0.278    0.786
pc_thk           2.312e-03  1.987e-02   0.116    0.909
gb_thk           1.224e-02  3.138e-02   0.390    0.704
patb_thk                NA         NA      NA       NA
lcb_thk                 NA         NA      NA       NA
gs_thk          -1.131e-03  1.396e-03  -0.810    0.435
ts_thk          -8.287e-03  1.029e-02  -0.805    0.438
paste_vol        5.240e-03  7.057e-03   0.742    0.473
mod_rupt        -8.368e-05  3.559e-04  -0.235    0.818
mod_elast       -6.258e-08  7.908e-08  -0.791    0.445
temp_grad       -2.909e-02  5.370e-02  -0.542    0.599

Residual standard error: 0.1082 on 11 degrees of freedom
Multiple R-squared:  0.493,     Adjusted R-squared:  -0.06016
F-statistic: 0.8912 on 12 and 11 DF,  p-value: 0.5791
```


Figure 349. Illustration. Software output from LTE analysis and PSG slope for GB pavements.[(22)]

```
Call:
lm(formula = psg_i_bfit ~ lte_intercept + lte_regr + slab_width +
    slab_length + pc_thk + gb_thk + patb_thk +
    lcb_thk + gs_thk + ts_thk + paste_vol + mod_rupt +
    mod_elast + temp_grad, data = R_LTE_AT)

Residuals:
     Min       1Q   Median       3Q      Max
-0.56754 -0.18922  0.03416  0.17424  0.44659

Coefficients: (2 not defined because of singularities)
                 Estimate Std. Error t value Pr(>|t|)
(Intercept)     -4.129e+00  2.234e+00  -1.849   0.0831 .
lte_intercept    2.487e-02  1.411e-02   1.762   0.0971 .
lte_regr        -2.640e-03  5.619e-02  -0.047   0.9631
slab_width       8.649e-02  6.918e-02   1.250   0.2292
slab_length     -1.896e-01  2.557e-01  -0.741   0.4692
pc_thk           5.797e-02  5.339e-02   1.086   0.2936
gb_thk                  NA         NA      NA       NA
patb_thk         1.190e-02  1.363e-01   0.087   0.9315
lcb_thk                 NA         NA      NA       NA
gs_thk           1.092e-02  3.879e-03   2.815   0.0124 *
ts_thk           4.285e-02  3.489e-02   1.228   0.2372
paste_vol        3.026e-02  2.350e-02   1.288   0.2161
mod_rupt        -3.912e-04  1.107e-03  -0.353   0.7285
mod_elast        4.644e-08  1.567e-07   0.296   0.7707
temp_grad       -2.012e-01  2.427e-01  -0.829   0.4194
---
Signif. codes:  0 ‘***’ 0.001 ‘**’ 0.01 ‘*’ 0.05 ‘.’ 0.1 ‘ ’ 1

Residual standard error: 0.3552 on 16 degrees of freedom
Multiple R-squared:  0.6428,    Adjusted R-squared:  0.375
F-statistic:   2.4 on 12 and 16 DF,  p-value: 0.05195
```


Figure 350. Illustration. Software output from LTE analysis and PSG intercept for PATB pavements.[22]

```
Call:
lm(formula = psg_s_bfit ~ lte_intercept + lte_regr + slab_width +
    slab_length + pc_thk + gb_thk + patb_thk +
    lcb_thk + gs_thk + ts_thk + paste_vol + mod_rupt +
    mod_elast + temp_grad, data = R_LTE_AT)

Residuals:
      Min        1Q    Median        3Q       Max
-0.041124 -0.025612 -0.001526  0.019067  0.049812

Coefficients: (2 not defined because of singularities)
                 Estimate Std. Error t value Pr(>|t|)
(Intercept)     1.498e-01  2.118e-01   0.707  0.48956
lte_intercept   2.651e-03  1.338e-03   1.981  0.06502 .
lte_regr        5.444e-03  5.326e-03   1.022  0.32192
slab_width     -6.950e-03  6.558e-03  -1.060  0.30501
slab_length    -8.880e-03  2.424e-02  -0.366  0.71896
pc_thk         -5.500e-03  5.061e-03  -1.087  0.29324
gb_thk                 NA         NA      NA       NA
patb_thk        7.667e-04  1.292e-02   0.059  0.95342
lcb_thk                NA         NA      NA       NA
gs_thk          2.200e-04  3.677e-04   0.598  0.55797
ts_thk         -8.380e-04  3.308e-03  -0.253  0.80321
paste_vol       7.143e-04  2.227e-03   0.321  0.75261
mod_rupt       -1.235e-05  1.050e-04  -0.118  0.90780
mod_elast      -5.434e-08  1.485e-08  -3.659  0.00212 **
temp_grad      -5.039e-03  2.301e-02  -0.219  0.82942
---
Signif. codes:  0 ‘***’ 0.001 ‘**’ 0.01 ‘*’ 0.05 ‘.’ 0.1 ‘ ’ 1

Residual standard error: 0.03367 on 16 degrees of freedom
Multiple R-squared:  0.7802,    Adjusted R-squared:  0.6153
F-statistic: 4.733 on 12 and 16 DF,  p-value: 0.002383
```


Figure 351. Illustration. Software output from LTE analysis and PSG slope for PATB pavements.[22]

```
Call:
lm(formula = psg_i_bfit ~ lte_intercept + lte_regr + slab_width +
    slab_length + pc_thk + gb_thk + patb_thk +
    lcb_thk + gs_thk + ts_thk + paste_vol + mod_rupt +
    mod_elast + temp_grad, data = R_LTE_CT)

Residuals:
     Min       1Q   Median       3Q      Max
-0.95299 -0.19022 -0.01636  0.17518  0.87010

Coefficients: (2 not defined because of singularities)
                  Estimate Std. Error t value Pr(>|t|)
(Intercept)     -4.127e+01  4.049e+01  -1.019   0.3300
lte_intercept    2.608e-02  1.912e-02   1.364   0.1999
lte_regr         1.777e-01  1.308e-01   1.359   0.2014
slab_width       2.965e-02  1.601e-01   0.185   0.8564
slab_length      7.981e+00  8.712e+00   0.916   0.3793
pc_thk           2.944e-02  9.191e-02   0.320   0.7548
gb_thk                  NA         NA      NA       NA
patb_thk                NA         NA      NA       NA
lcb_thk          3.692e-01  2.284e-01   1.617   0.1343
gs_thk           4.813e-03  9.293e-03   0.518   0.6148
ts_thk           1.045e-01  5.512e-02   1.896   0.0845 .
paste_vol       -4.006e-03  4.078e-02  -0.098   0.9235
mod_rupt        -5.590e-04  1.670e-03  -0.335   0.7442
mod_elast        1.865e-08  3.333e-07   0.056   0.9564
temp_grad        2.441e-01  4.923e-01   0.496   0.6297
---
Signif. codes:  0 ‘***’ 0.001 ‘**’ 0.01 ‘*’ 0.05 ‘.’ 0.1 ‘ ’ 1

Residual standard error: 0.5665 on 11 degrees of freedom
Multiple R-squared:  0.6334,    Adjusted R-squared:  0.2336
F-statistic: 1.584 on 12 and 11 DF,  p-value: 0.2272
```


Figure 352. Illustration. Software output from LTE analysis and PSG intercept for LCB pavements.[(22)]

```
Call:
lm(formula = psg_s_bfit ~ lte_intercept + lte_regr + slab_width +
    slab_length + pc_thk + gb_thk + patb_thk +
    lcb_thk + gs_thk + ts_thk + paste_vol + mod_rupt +
    mod_elast + temp_grad, data = R_LTE_CT)

Residuals:
      Min        1Q    Median        3Q       Max
-0.104851 -0.036500  0.000033  0.018897  0.109452

Coefficients: (2 not defined because of singularities)
                  Estimate Std. Error t value Pr(>|t|)
(Intercept)      3.874e-01  5.203e+00   0.074   0.9420
lte_intercept    2.617e-04  2.457e-03   0.107   0.9171
lte_regr        -3.868e-03  1.681e-02  -0.230   0.8222
slab_width      -1.409e-02  2.057e-02  -0.685   0.5075
slab_length     -1.116e-02  1.120e+00  -0.010   0.9922
pc_thk          -2.189e-02  1.181e-02  -1.854   0.0908 .
gb_thk                  NA         NA      NA       NA
patb_thk                NA         NA      NA       NA
lcb_thk          6.982e-03  2.935e-02   0.238   0.8163
gs_thk           2.331e-03  1.194e-03   1.953   0.0768 .
ts_thk          -9.440e-03  7.082e-03  -1.333   0.2095
paste_vol        7.837e-03  5.240e-03   1.496   0.1629
mod_rupt        -4.472e-05  2.147e-04  -0.208   0.8388
mod_elast       -1.825e-08  4.283e-08  -0.426   0.6783
temp_grad        9.846e-02  6.326e-02   1.556   0.1479
---
Signif. codes:  0 '***' 0.001 '**' 0.01 '*' 0.05 '.' 0.1 ' ' 1

Residual standard error: 0.0728 on 11 degrees of freedom
Multiple R-squared:  0.6929,    Adjusted R-squared:  0.3579
F-statistic: 2.068 on 12 and 11 DF,  p-value: 0.1195
```


Figure 353. Illustration. Software output from LTE analysis and PSG slope for LCB pavements.[22]

APPENDIX J. AREAS OF LOCALIZED ROUGHNESS

INTRODUCTION

Typical studies of pavement roughness and roughness progression address the average IRI over the road segments of interest. In most cases, studies do not examine the contributions of localized roughness to overall IRI. Many States that specify smoothness using the IRI include requirements on the average IRI over a standard length (e.g., 528 ft) and on localized roughness. Per AASHTO R54-14, ALRs are defined as any region where the IRI averaged over a 25-ft base length is greater than a specified threshold.(24) Negative pay adjustments and requirements for corrective action are often based on the area of pavement out of compliance and the peak roughness value within the ALR. Typically, IRI and ALR are based on a single pass over the specified road segment.

The literature offers broad information about changes to average IRI values over time and statistical repeatability of IRI measurements produced by multiple passes over the same pavement section. However, little information is available regarding changes over time, seasonal, and diurnal changes in ALR of jointed PCC pavement or agreement in ALR between repeated profile measurements. This appendix presents examples of long- and short-term changes in ALR on jointed PCC test sections within the LTPP program and examines the repeatability of extent, severity, and placement of ALR.

The profile measurements discussed in this report offer a research-quality dataset for quantifying potential short- and long-term changes in ALR on five LTPP SPS-2 projects and five LTPP GPS-3 test sections. Long-term changes are examined using profile measurements by the LTPP program. These changes include annual visits (with few exceptions) to the GPS-3 sections starting in 1990 and to SPS-2 sites starting from the year each site was opened to traffic. Many of these sites and sections have been monitored over more than 20 years. Three of the GPS-3 sections and three of the SPS-2 sites also include sets of seasonal or diurnal measurements collected under the LTPP SMP. (Appendix B describes the monitoring history of each site and section in detail.)

Short-term changes are examined using profile measurements of the same SPS-2 sites and GPS-3 sections using profile measurements from an FHWA study of jointed PCC curl and warp conducted from 2003 to 2004.(85) The study collected profile measurements over diurnal and seasonal cycles. Diurnal monitoring typically included profile-measurement visits before sunrise, after sunrise, in the midafternoon, and after sunset. Seasonal monitoring typically included four visits throughout a 12-month period that approximated one visit per season. Of the 83 jointed PCC test sections included within the LTPP dataset, the FHWA study included seasonal and diurnal monitoring of 44 test sections and diurnal monitoring of another 20 test sections. The FHWA study did not include the remaining 19 test sections

Postprocessing of raw profile measurements from both sources removed minor inconsistencies in longitudinal offset and in the output of distance-measurement instruments (DMIs) among all measurements from each section. Researchers removed longitudinal offset between profile measurements by using cross-correlation of filtered profiles; a process called automated synchronization.[2,11] The DMI adjustment procedure ensured consistent longitudinal scaling among all passes over a given section. This process is equivalent to optimal DMI adjustment described by Perera and Karamihas.[105]

Each series from the FHWA curl-and-warp study included at least 7 and as many as 11 passes by the profiler. Seven or nine passes were common for the LTPP program. Researchers performed data-quality screening to select five repeat profile measurements per section from each series. Among the group of available runs, five measurements that exhibited the best agreement with each other were selected for further analysis. Agreement between two profiles was judged by cross-correlating the profiles after applying the IRI filter.[2,11] Chapter 4 of this report describes the synchronization and quality-screening procedures in detail.

The quality-screening process sought five passes from each visit with the highest repeatability. The resulting repeatability in ALR represents the best case (i.e., research-quality field-measurement procedures followed by rigorous synchronization and quality screening). The aligned profile data provided an opportunity to compare the extent and severity of ALR without variation caused by inconsistent longitudinal placement of profile features. Changes in ALR among repeat passes from the same visit are attributed to variations in lateral tracking of the profiler and limitations with height sensors and accelerometers. Additional changes in ALR between measurement visits are attributed to changes in the actual profile of the pavement.

BACKGROUND

ALRs are derived from roughness profiles. Sayers originally proposed roughness profiles as a way to show the distribution of roughness in detail over the length of a road.[106] Sayers recommended using roughness profiles for specifying "the quality of pavements after construction or repair, and the accuracy of profiling equipment."[107] A roughness profile displays a continuous report of roughness averaged over a specified length as a function of distance along a particular road section. In contrast to discrete interval reporting of roughness, which provides a listing of roughness values for consecutive segments, a roughness profile provides the roughness of all possible segments of a given length.[107]

A roughness profile is calculated from an elevation profile. The calculation is detailed in the following three steps:

Step 1: Filter the elevation profile using the IRI algorithm. The IRI algorithm includes smoothing the profile by applying the moving average with a 9.84-inch base length and filtering the profile using the Golden Car Model.[108] The Golden Car Model is a quarter-car simulation with standard parameter values, and the predicted output used for the IRI is spatial velocity across the suspension. For engineering purposes, the IRI algorithm can be considered a filter that, when applied to an elevation profile, produces a trace in units of slope (e.g., inches/mi) and emphasizes content that causes vibration in passing vehicles.

Step 2: Rectify the filtered trace by taking the absolute value of each point.

Step 3: Apply a moving average to the rectified trace. The base length of the moving average corresponds to the desired segment length used for averaging.

Figure 354 through Figure 357 demonstrate the process on a profile of section 390204 measured 9.9 years after it was opened to traffic. Figure 354 shows the left elevation profile. The profile is high-pass filtered with a cutoff wavelength of 100 ft to make features that affect the IRI more visible. This is a jointed PCC section with a nominal joint spacing of 15 ft. The profile includes downward spikes at many joints.

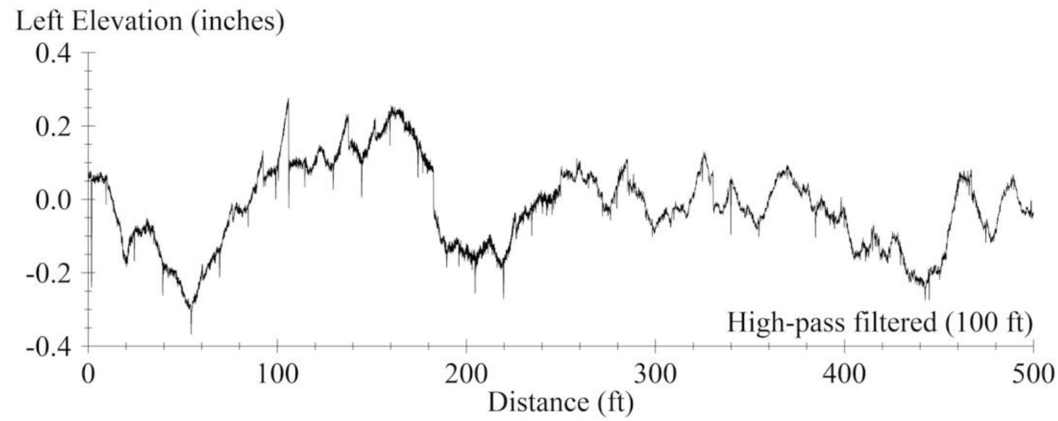

Source: FHWA.

Figure 354. Graph. Left elevation profile of section 390204 at 9.9 years.

Figure 355 shows the outcome of step 1. The graph is the raw output of the IRI algorithm in units of inches/mi. The total range of values extends from −544 to 290 inches/mi. The most severe value occurs 106 ft from the start of the section, which is the location of a downward step in the elevation profile.

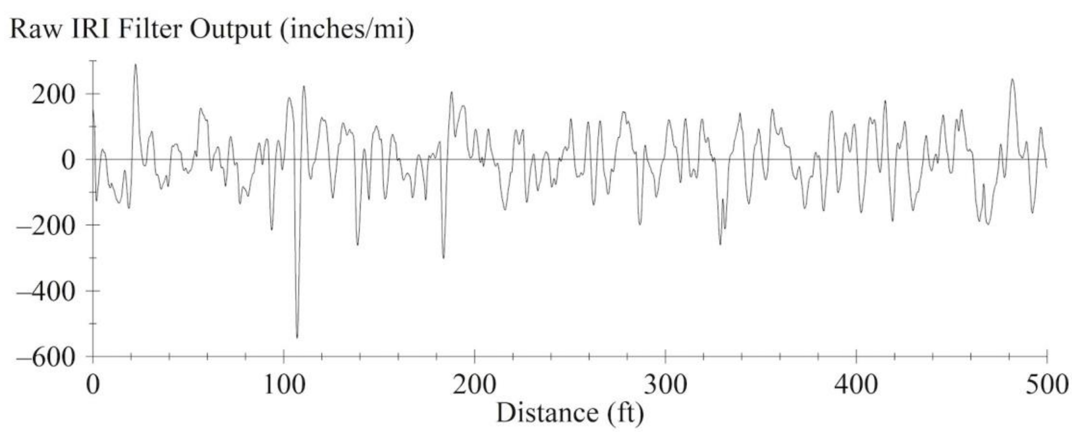

Source: FHWA.

Figure 355. Graph. Raw IRI filter output of section 390204 at 9.9 years.

Figure 356 shows the outcome of step 2, which is obtained by taking the absolute value of each point in the trace from Figure 355. The overall IRI for the entire 500-ft section is 71.8 inches/mi and is the average value of every point in this trace. For shorter segments within the section, the IRI is calculated by averaging the values within the desired range.

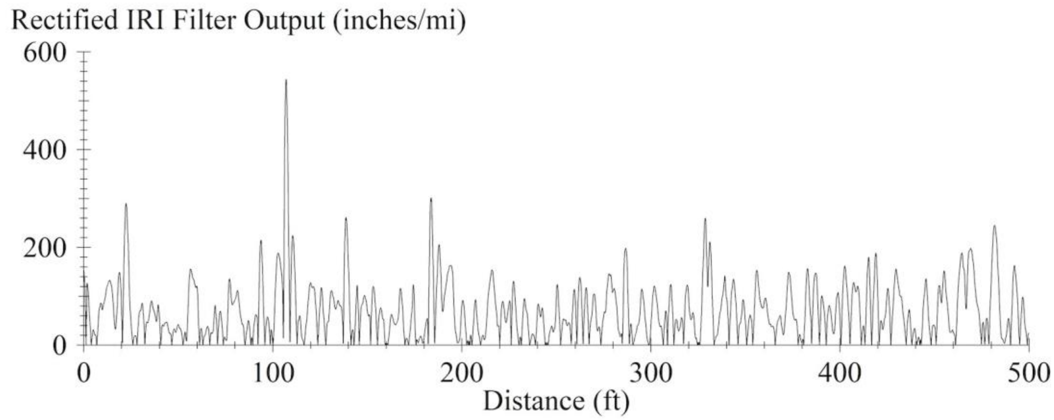

Source: FHWA.

Figure 356. Graph. Rectified IRI filter output for section 390204 at 9.9 years.

Figure 357 shows the outcome of step 3, which is the roughness profile for a base length of 25 ft. Each point in Figure 357 represents the IRI of a 25-ft-long segment that begins 12.5 ft upstream and ends 12.5 ft downstream. Note that features of the profile outside the section boundaries affect the roughness values in the first and last 12.5 ft of the trace.

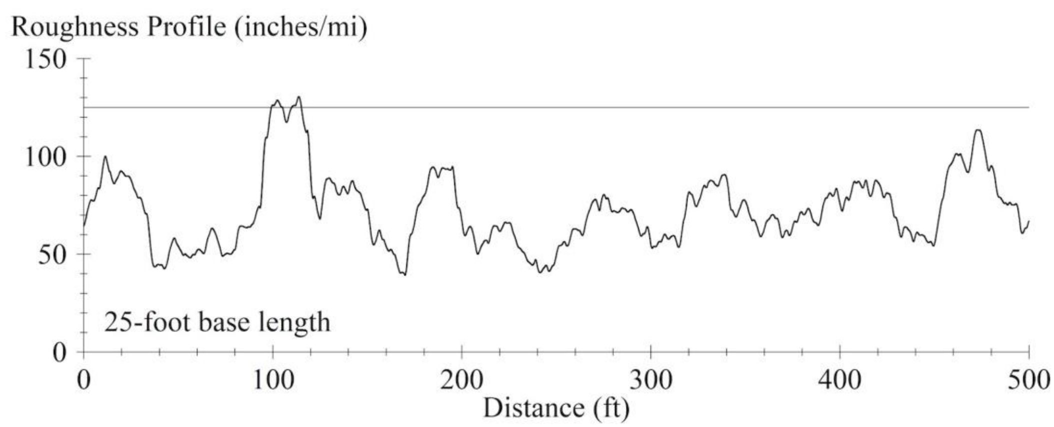

Source: FHWA.

Figure 357. Graph. Left roughness profile for section 390204 at 9.9 years.

The short-interval roughness profile shows how roughness is distributed along the section and whether any areas exist that contribute disproportionately to overall roughness. Any area in which the trace is greater than a designated threshold is considered an ALR. A threshold of 125 inches/mi is marked in Figure 357. Two areas violate this threshold. The first ranges from 99.2 to 105.1 ft with a peak value of 128.7 inches/mi and the second ranges from 110.0 to 115.1 ft with a peak value of 130.5 inches/mi.

One tilted slab causes both ALRs that appear in Figure 357. Figure 358 shows a closeup view of the left elevation profile. Downward spikes are visible at three joints, including those at 99.1 and 114.5 ft from the start of the section. The slab between these joints is cracked, and the leading portion of the slab is tilted upward. The primary cause of the localized roughness is the 0.18-inch fault at the midslab crack, which is 106.0 ft from the start of the section. The roughness profile fluctuates between 99 and 115 ft because each point includes additional influence from other roughness within the 25-ft averaging range. This example demonstrates the importance of inspecting the elevation profile to determine a cause once ALRs are identified.

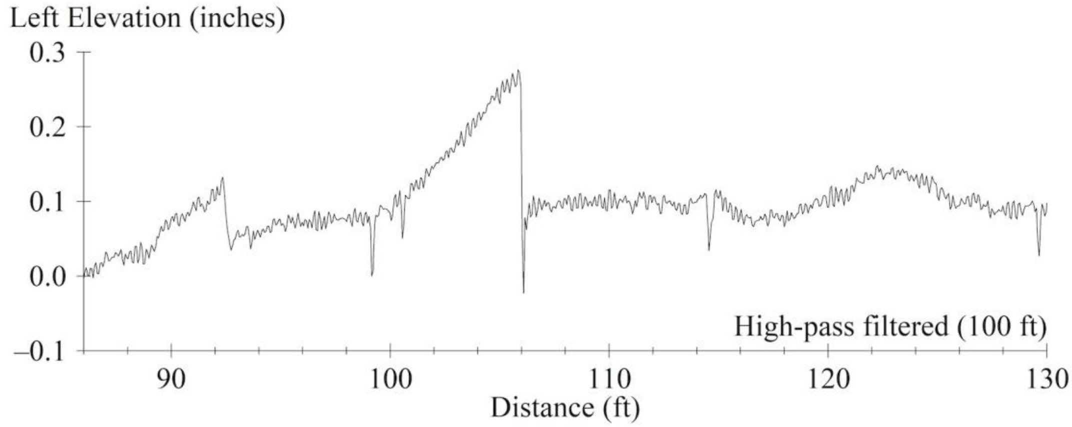

Source: FHWA.

Figure 358. Graph. Closeup view of left elevation profile for section 390204 at 9.9 years.

ALR SETTINGS

This study reports statistics that describe short- and long-term changes and repeatability of ALR using IRI from each wheel path, a base length of 25 ft, and threshold values of 125 inches/mi and 160 inches/mi. ALRs are primarily quantified in terms of total area. This section demonstrates the influence of alternative index options, base lengths, and methods of quantifying the extent and severity of ALRs.

Base Length

The ALR detected from a profile is sensitive to base length. The maximum roughness observed in a roughness profile is expected to increase as base length decreases, and short base lengths reveal highly localized roughness averaged using longer base lengths.(106) Figure 359 and Figure 360 provide an example from section 040213 measured 14.2 years after it was opened to traffic. Figure 359 shows the right elevation profile. The profile is high-pass filtered with a cutoff wavelength of 100 ft to make features that affect the IRI more visible. Section 040213 is jointed PCC with a nominal joint spacing of 15 ft. The profile includes evidence of upwardly curled slabs, which contribute to roughness throughout the test section. Deep narrow spikes appear in areas where the profiler passed over wandering longitudinal cracks, which make localized contributions to roughness.

Figure 360 compares the roughness profile corresponding to Figure 359 for base-length values of 10, 25, 50, and 100 ft. The figures show that the range of values for the roughness profiles grows more extreme as base length decreases. At a base length of 100 ft, the highest values in the roughness profiles appear in areas that include the narrow dips at the longitudinal cracks. However, the influence of the dips is averaged by lower roughness in the surrounding area. As base length decreases, peak values in the roughness profiles increase, and the trace identifies the location of the localized roughness more closely.

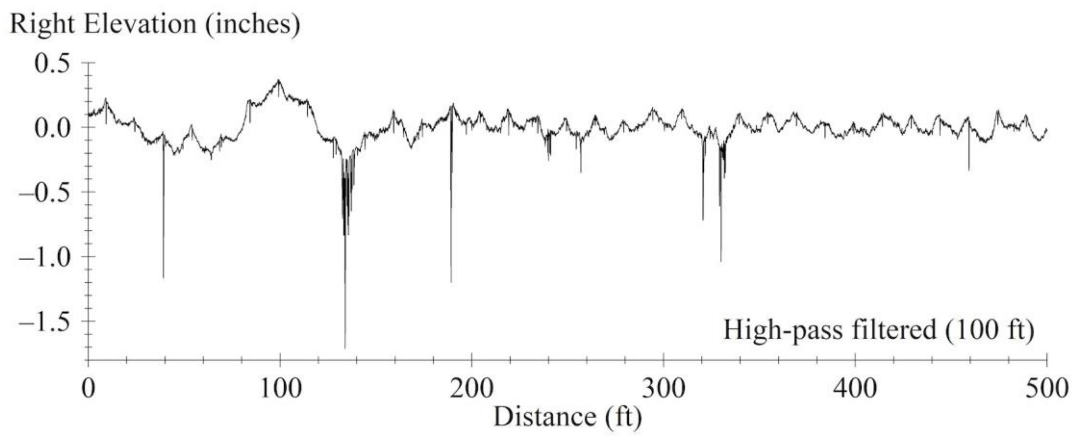

Source: FHWA.

Figure 359. Graph. Right elevation profile of section 040213 at 14.2 years.

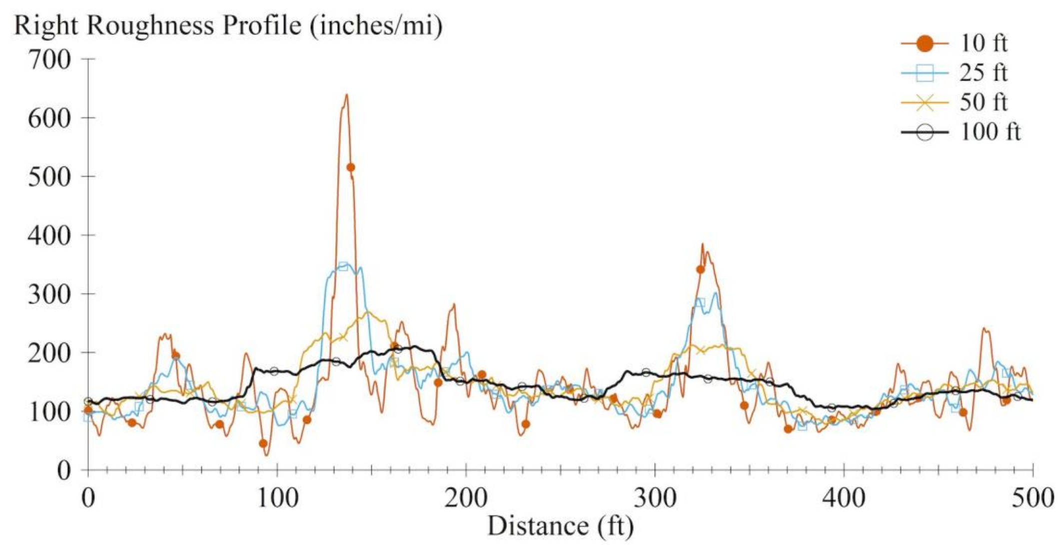

Source: FHWA.

Figure 360. Graph. Right roughness profiles of section 040213 at 14.2 years.

The average value of each trace in Figure 360 approximates the average IRI for the section of 145.0 inches/mi to within 1 inch/mi because, except for end effects, the average value is independent of base length. "End effects" refers to roughness profiles including some influence from profile outside section boundaries within half of the base length at either end. Each trace has a slightly different average value because the range changes with base length. When the length of the section increases relative to the base length, the average value of the roughness profile more closely approaches the average IRI for the section.

Figure 361 provides an additional demonstration of the influence of base length on variations that appear in a roughness profile. The figure shows the cumulative probability distribution of roughness from each trace in Figure 360. The distribution is shown in length rather than percentage. The total range of roughness values increases as base length decreases. For example, the values range from 104.0 inches/mi to 210.8 inches/mi at a base length of 100 ft and from 24.6 inches/mi to 640.1 inches/mi at a base length of 10 ft.

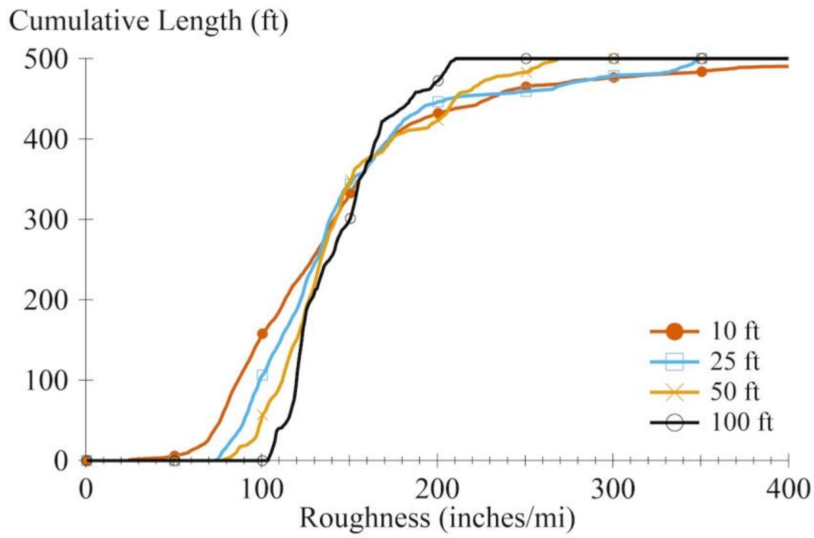

Source: FHWA.

Figure 361. Graph. Cumulative roughness of section 040213 at 14.2 years.

Figure 361 presents a potential summary of the localized roughness that exists within a long pavement section. For a given base length and roughness threshold, the cumulative distribution provides the total extent of ALR, which can be presented in length, as shown, or percentage.

For the highly localized narrow dips shown in Figure 359, base lengths of 10 and 25 ft pinpointed the roughness source more closely. A short base length is often desirable to detect localized rough features and quantify their severity. Karamihas et al. recommended a minimum base length of 25 ft and warned that for very short base lengths, such as 10 ft, height-sensor dropouts and other sensor errors were more likely to register as ALR. Additionally, peak roughness in an ALR was likely to vary between profiler types depending of the details of the sample procedures and height-sensor footprint.(109) Sayers recommended using a 20-ft base length for detecting localized roughness, but that the base length should be shorter than the minimum distance between rough features.(106)

Figure 362 through Figure 364 demonstrate the need to consider the source of roughness when selecting an appropriate base length for detecting ALR. Figure 362 shows the left elevation profile for an area of section 133019 measured approximately 22.7 years after it was constructed. The profile is high-pass filtered with a cutoff wavelength of 100 ft to make features that affect the IRI more visible. Section 133019 is jointed PCC with a nominal joint spacing of 20 ft. Each slab shown has a net downward curvature, and the most severe roughness appears as dips at the joints.

Figure 363 shows the roughness profile for a base length of 10 ft over the same range of section 133019 shown in Figure 362. The arrows indicate the joint locations. Localized roughness is registered at each joint. The center of each area in the roughness profile with the highest magnitude is shifted slightly from the joint locations. The shift occurs because the IRI algorithm reacts to the roughness starting at each rough feature and over a short distance past the joint locations.

Figure 364 shows the roughness profile for a base length of 25 ft with arrows at each joint location. Using this base length, the peak values in the roughness profiles appear between the joints and some of the lower roughness values appear at the joints because the base length is greater than the spacing between the positions of localized rough features. At the center of each slab, the 25-ft range used to calculate roughness values includes two of the joints. The roughness within 7.5 ft of each joint includes the influence of only one joint.

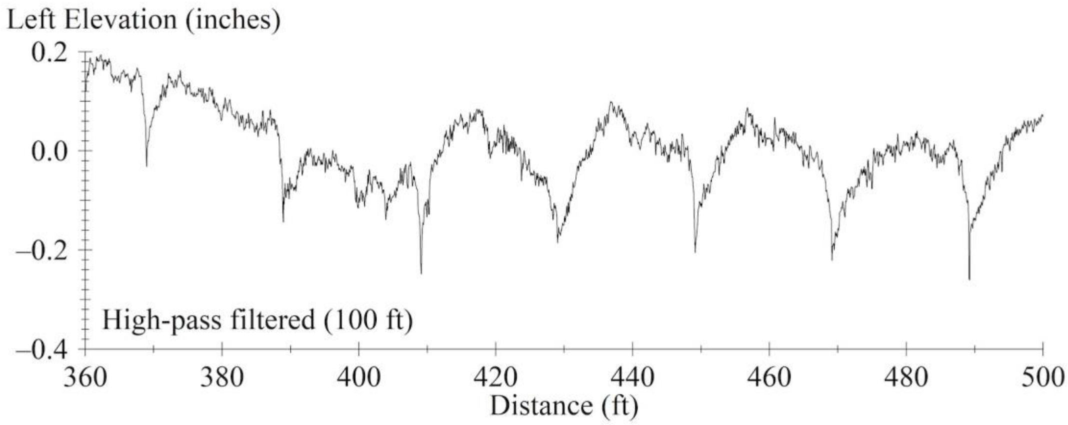

Source: FHWA.

Figure 362. Graph. Left elevation profile of section 133019 at 22.7 years.

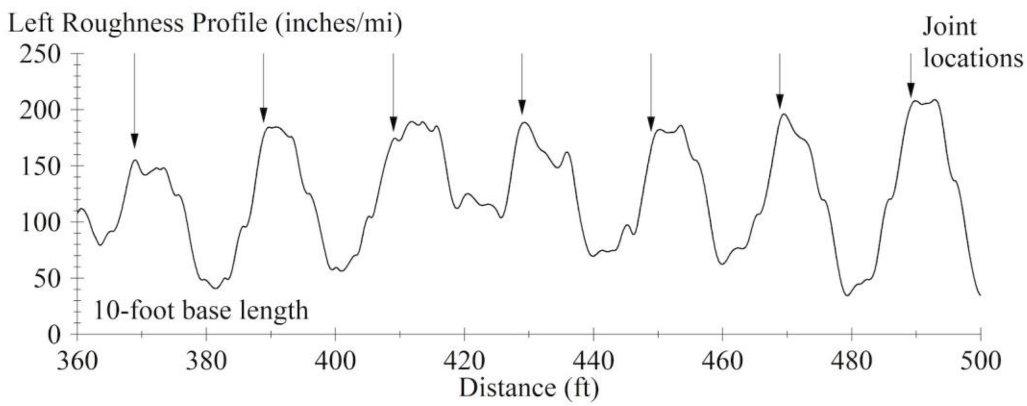

Source: FHWA.

Figure 363. Graph. Left roughness profile of 10-ft base length for section 133019 at 22.7 years.

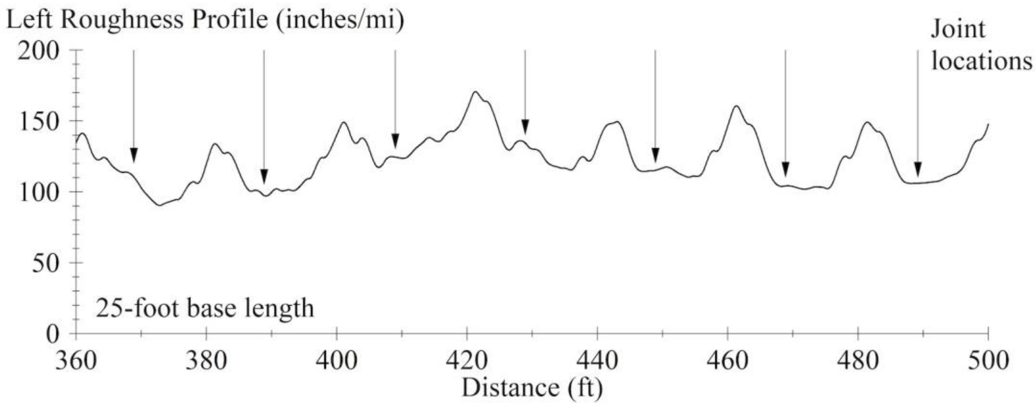

Source: FHWA.

Figure 364. Graph. Left roughness profile of 25-ft base length for section 133019 at 22.7 years.

A longer base length may be useful for identifying rough areas in a long section of roadway. When evaluating miles of pavement, a roughness profile with a base length of 528 ft provides a way to identify areas that need attention. For example, the format of the pay adjustment schedule recommended by AASHTO R54-14 is based on roughness profiles calculated using a base length of 528 ft.(24) Swan and Karamihas demonstrated the use of roughness profiles with a base length of 264 ft for general pavement acceptance and 25 ft for investigation of roughness within areas that do not meet the specification.(107)

This research examines 500-ft-long sections. The 500-ft length imposes a limit on base length. Figure 365 provides an example of using a relatively long base length on a short section to quantify the functional aspects of pavement behavior. Figure 365 shows the right roughness profile from section 040214 measured 10.4 years after it was opened to traffic. The roughness profile was calculated using a base length of 100 ft. The average IRI for this profile is 89.1 inches/mi. This section is roughest over the first 100 ft with a peak value of 164.2 inches/mi. The roughness decreases over the next 200 ft and is lowest over the last 200 ft with values of 70.7 inches/mi or less and a minimum value of 48.8 inches/mi.

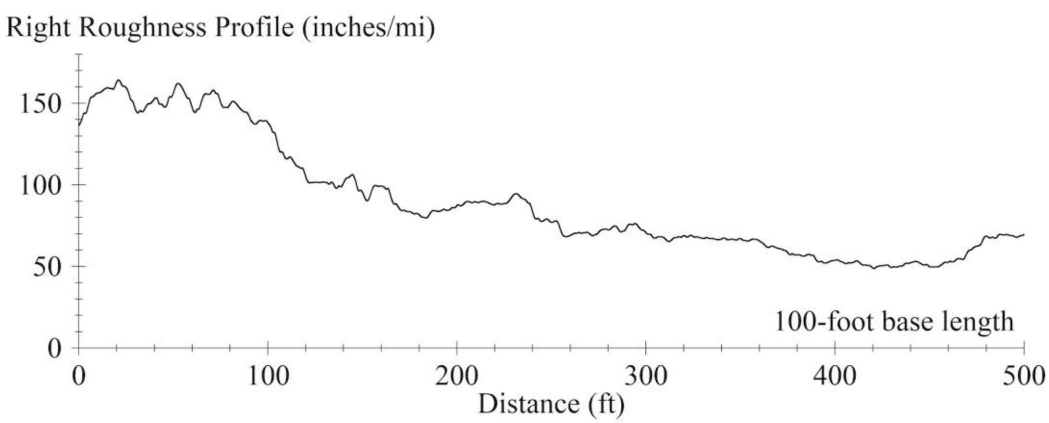

Source: FHWA.

Figure 365. Graph. Right roughness profile of section 040214 at 10.4 years.

A change in slab curl and warp throughout the section causes the change in roughness shown in Figure 365. Section 040214 is jointed PCC with a nominal joint spacing of 15 ft. The slabs have downward curvature in the first 300 ft of the section, and the magnitude of the curvature decreases along the section. In the last 200 ft of the section, the slabs are relatively flat. (The Spatial Trends section in chapter 5 provides more information.)

Index Options

The preceding examples present roughness profiles and ALR derived from IRI in either the left or right profile. Two other options for identifying ALR include the following:

- MRI**:** The average of the IRI from the left and right wheel paths. An MRI-based roughness profile is calculated using a point-by-point average of the roughness profile from the left and right wheel path.

- HRI: The profiles are combined using point-by-point averages of the elevation values from the two sides. An HRI-based roughness profile is calculated after passing the combined profile through the IRI algorithm.

MRI or HRI moderate localized roughness that appears on only one side of the lane or is much rougher on one side than the other. HRI is always less than or equal to MRI because averaging the elevation profiles eliminates aspects of fluctuations in elevation that are not consistent on both sides. HRI preserves the bounce component of roughness but eliminates the roll component.

Figure 366 through Figure 368 demonstrate the potential contrast to the IRI from individual wheel paths of HRI and MRI. Figure 366 shows the left elevation profile for section 040213 measured 14.2 years after it was opened to traffic. The profile is high-pass filtered with a cutoff wavelength of 100 ft to make features that affect the IRI more visible. This profile was measured in the same pass as the right elevation profile shown in Figure 359, and Figure 359 and Figure 366 have compatible vertical scaling. Profiles from both sides include upwardly curled slabs, which introduced roughness with features similar in each wheel path. Profiles from both sides also include a long wavelength disturbance in the first 150 ft for the test section. However, open longitudinal cracks do not appear in the left side of the lane, and the left elevation profiles do not include the patches of downward spikes that appear in Figure 359.

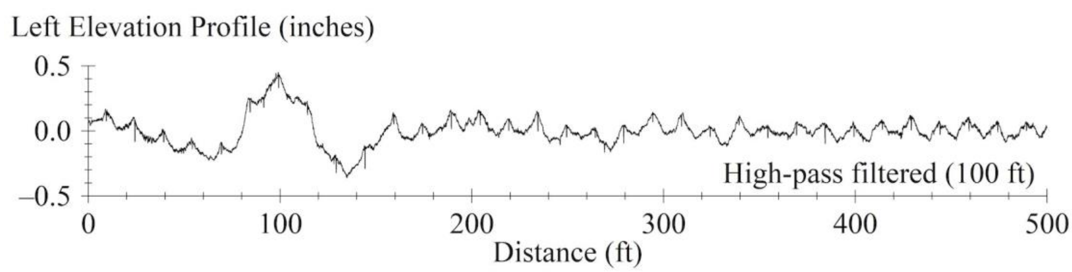

Source: FHWA.

Figure 366. Graph. Left elevation profile of section 040213 at 14.2 years.

Figure 367 shows the roughness profiles for both wheel paths using a base length of 25 ft. Figure 367 identifies a threshold of 150 inches/mi. With this threshold, the left profile includes eight

ALRs with a total length of 157.9 ft, and the right profile includes seven ALRs with a total length of 41.9 ft.

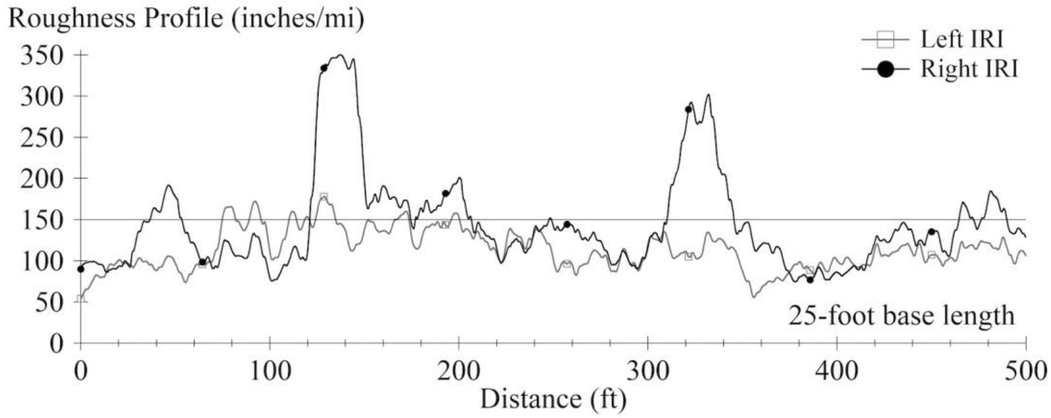

Source: FHWA.

Figure 367. Graph. Left and right roughness profiles for section 040213 at 14.2 years.

Table 61 lists the boundaries, length, and peak roughness for each ALR. The table also lists excess roughness (ER), which is discussed in the following section. The most severe localized roughness appears in areas of the right wheel path in which narrow dips were measured over the opened longitudinal cracks. The left wheel path registers several ALRs with relatively lower peak roughness, which do not correspond to individual surface defects. Upwardly curled slabs contribute to roughness but not sufficiently in the first 70 ft or the last 300 ft of the test section. ALRs only appear where the distributed contribution of the long-wavelength disturbance shown in Figure 366 exacerbates the roughness.

Figure 368 shows the MRI- and HRI-based roughness profiles using a base length of 25 ft and a marked threshold value of 150 inches/mi. These roughness profiles were derived from the same elevation profiles as Figure 367 and are displayed with vertical scaling compatible with Figure 368. Figure 368 shows that averaging across both wheel paths moderates the effects of the severe roughness that appear on the right side. Averaging greatly reduces the values of peak roughness values and eliminates the ALR from the first 55 ft of the section. The ALR in the last 50 ft of the right roughness profiles are eliminated in the HRI profile and are nearly eliminated in the MRI profile.

Table 61. ALR in left and right profiles for section 040213 at 14.2 years.

Side	ALR Start (ft)	ALR End (ft)	ALR Range (ft)	Peak Roughness (Inches/mi)	ER (Inches/mi)
Left	74.8	82.0	7.2	165.7	0.16
Left	89.1	95.4	6.4	172.4	0.17
Left	110.1	114.1	4.0	160.0	0.05
Left	118.5	120.7	2.3	153.7	0.01
Left	124.2	134.8	10.7	178.2	0.37
Left	166.1	166.6	0.6	150.4	<0.01
Left	167.2	173.7	6.5	160.1	0.07
Left	196.0	200.3	4.3	157.9	0.05
Right	36.5	53.3	16.8	191.6	0.67
Right	121.0	174.4	53.4	350.2	9.84
Right	176.8	206.5	29.7	201.0	1.23
Right	247.6	248.8	1.2	152.0	<0.01
Right	310.0	345.4	35.4	301.9	5.85
Right	464.4	472.1	7.7	171.1	0.15
Right	476.2	489.8	13.6	184.7	0.45

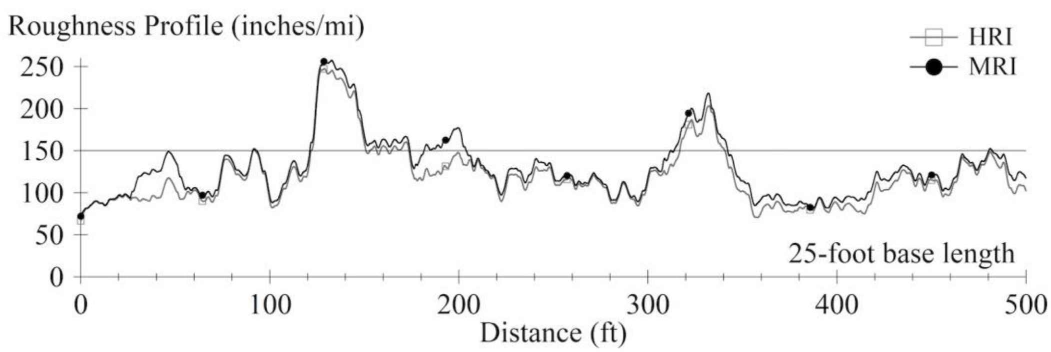

Source: FHWA.

Figure 368. Graph. MRI- and HRI-based roughness profiles for section 040213 at 14.2 years.

The ALR for MRI and HRI are listed in Table 62. With a threshold of 150 inches/mi, the MRI profile included six ALRs with a total length of 107.9 ft. The HRI profile showed lower values than the MRI profile throughout the section. The HRI profile included six ALR due to the area of roughness that straddles the threshold line in the range from 150 to 175 ft. Using HRI, the total length is reduced to 70.7 ft, the peak roughness values are reduced, and the ALR from 180 to 205 ft is eliminated.

Table 62. ALR derived from MRI and HRI profiles for section 040213 at 14.2 years.

Index	ALR Start (ft)	ALR End (ft)	ALR Range (ft)	Peak Roughness (Inches/mi)	ER (Inches/mi)
MRI	91.0	93.0	2.0	152.4	<0.01
MRI	121.2	174.1	52.9	247.7	4.68
MRI	181.6	203.9	22.4	177.2	0.47
MRI	312.0	312.5	0.5	150.3	<0.01
MRI	313.8	342.2	28.4	218.2	1.82
MRI	480.2	482.0	1.7	152.5	<0.01
HRI	91.1	92.4	1.3	151.5	<0.01
HRI	121.8	150.8	29.0	247.5	3.68
HRI	152.9	156.5	3.5	155.4	0.02
HRI	158.5	162.3	3.8	155.6	0.03
HRI	164.4	173.6	9.2	160.4	0.08
HRI	316.8	340.7	23.9	203.3	1.17

Using MRI or HRI offers an advantage because it reduces the amount of data to assimilate by half. Each index captures the most severe localized roughness. However, neither index offers information about whether the source of roughness exists on one side of the lane or both. In contrast, analyzing roughness profiles from both wheel paths helps identify the sources of roughness. A higher threshold is needed for ALRs based on MRI than for IRI from individual wheel paths for capturing the features that cause the same reduction in functional quality. The HRI is not as sensitive as IRI to features that are not the same on each side of the lane (e.g., a bump on one side and a dip of the same layout and shape on the other side). As a result, HRI-based roughness profiles will underestimate the reduction in functional quality caused by some features, requiring an even higher threshold for capturing the features that cause the same reduction in functional quality.

OPTIONS FOR QUANTIFYING LOCALIZED ROUGHNESS SEVERITY

Table 61 and Table 62 demonstrate three possible methods for quantifying the severity of localized roughness: number of ALRs, total length of ALRs, and peak roughness values. Practical application of roughness profiles for project-level pavement assessment typically requires using all three.

Table 61 shows that the number of ALRs does not characterize the severity of localized roughness. The left and right wheel paths included the same number of ALR, although the overall length and severity of ALR was much greater for the right wheel path. However, the number of ALRs may be of interest if corrective action is required for ALRs. The number and layout of ALRs may also be of interest if corrective action is permitted to reduce negative pay adjustment or if ALRs are used to plan surface rehabilitation.

For planning corrective action or rehabilitation, further viewing and analysis of the elevation profiles is needed to identify the sources of roughness and apply options for reducing roughness cost effectively. For example, Figure 357 and Figure 358 demonstrated a case in which more than one ALR corresponded to the same surface defect. Figure 366 and Figure 367 showed a case in which two sources of background roughness distributed over a length greater than the base length caused several ALRs. A corrective strategy based on addressing the eight ALRs individually is likely to be less effective than a corrective strategy based on mitigating the long-wavelength disturbance or roughness at the joints associated with upward curl.

The total length of ALR provides a suitable summary of the status of a pavement section in some cases but not others. Normalized by section length, the total length of ALR defines the proportion of the section out of specification, which offers a simple way to compare the status of pavement sections. However, the total length of ALR does not capture potential variations in the severity of roughness. For example, based on total length, the eight ALRs listed for the left wheel path in Table 61 incorrectly implies a greater reduction in the health of the pavement than the area listed for the right wheel path from 310.0 to 345.4 ft. The eight ALRs for the left wheel path have a total length of 41.9 ft, and the highest peak value is 178.2 inches/mi. The ALR from 310.0 to 345.4 ft in the right wheel path has a smaller length but a much higher peak roughness value of 301.9 inches/mi.

In contrast to the number and length of ALR, peak roughness values provide a measure of the severity of localized roughness but no measure of the extent. The use of peak roughness requires the analyst to consider a potentially large number of values. Weighting the length of ALRs by their severity provides an alternative that may help prioritize investment in corrective action or assign negative pay adjustments based on degradation in functional quality. The following example is similar to the provisions for calculating negative pay adjustments for localized roughness in AASHTO R54-14.[(24)]

Figure 369 shows the distribution of roughness for left and right roughness profiles of section 040213, measured 14.2 years after it was opened to traffic. The distribution is weighted by length. These plots show the distribution of roughness that appears in each trace from Figure 367. This distribution sorts roughness into discrete bins with an increment of 5 inches/mi. The horizontal line marks an example roughness threshold of 150 inches/mi. For each wheel path, the sum of the length for bins above 150 inches/mi is equal to the total length of ALR for each wheel path. (The total length of ALR is proportional to the area left of the curve and above the threshold line.)

Table 63 shows the estimated ALR weighted by severity. The table lists six nonzero bins with roughness above 150 inches/mi for the left wheel path (Figure 369). Each value of roughness above the threshold is the center of the corresponding range, which is the value at the center of the bin within the distribution minus the roughness threshold. Roughness-weighted length for each range is the product roughness above the threshold and length. The total value of 468.4 ft×inches/mi is calculated from the probability distribution, but it is also the total roughness-weighted length for all ALRs within the test section. The roughness-weighted length is an estimate of the area above and below the threshold line by the left roughness profile in Figure 367.

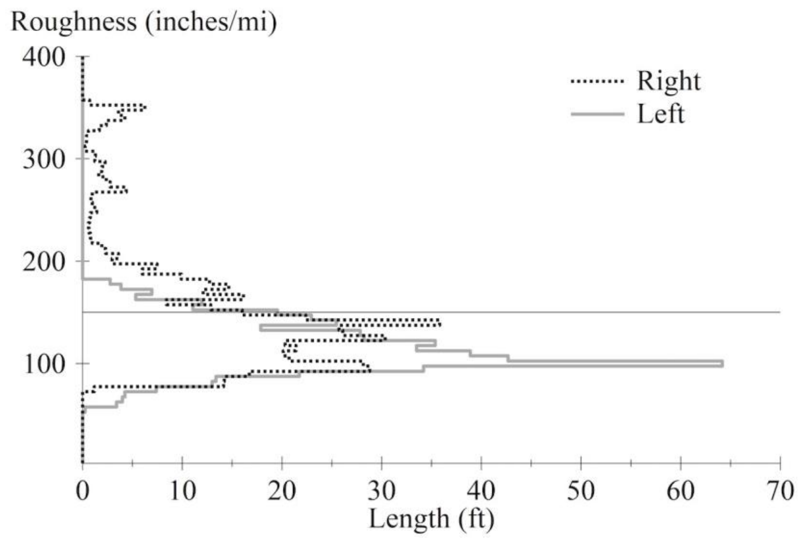

Source: FHWA.

Figure 369. Graph. Roughness distribution of section 040213 at 14.2 years.

Table 63. ALR severity for section 040213 at 14.2 years for the left wheel path.

Roughness Range (Inches/mi)	Length (ft)	Roughness Above Threshold (Inches/mi)	Roughness-Weighted Length (ft×Inches/mi)	ER (Inches/mi)
150–155	11.06	2.5	27.6	0.055
155–160	11.96	7.5	89.7	0.179
160–165	5.34	12.5	66.7	0.133
165–170	6.94	17.5	121.5	0.243
170–175	3.86	22.5	86.8	0.174
175–180	2.76	27.5	76.0	0.152
>150	41.91	—	468.4	0.937

—No data.

Roughness-weighted length summarizes the severity of ALRs for a test section in a way that incorporates length and peak roughness. However, the units of ft×inches/mi are not intuitive, and the value grows in proportion to section length for the same density of localized roughness. The excess roughness (ER) column in Table 63 lists the contribution from each roughness range. The ER is the roughness-weighted length normalized by the section length, which is 500 ft. (This could have been calculated directly if fFigure 369 and the Length column of Table 63 were expressed in terms of probability rather than length.) The total excess roughness (TER) is 0.937 inches/mi for the left wheel path, which is the total roughness-weighted length normalized by the section length and quantifies the contribution of ER to the average roughness of the section. Reducing the roughness within all ALR to the threshold value would reduce the overall IRI by 0.937 inches/mi.

Calculation of roughness-weighted length for the right wheel path includes contributions from 41 bins (from 150 to 355 inches/mi), and produces a total of 9,614.2 ft×inches/mi. This produces an estimate of TER of 19.228 inches/mi. As such, localized roughness greater than the threshold accounts for an increase in the sectionwide IRI of 0.94 inches/mi for the left wheel path and 19.23 inches/mi for the right wheel path. This TER estimate is less than the total contribution of the corresponding features of the elevation profile to roughness. It only accounts for the portion of the roughness above 150 inches/mi in the roughness profile.

An equivalent calculation of TER is possible using the roughness profile directly. The TER is the sum of the ER at every point in the profile ($R_{E,i}$) times the profile recording interval (Δx) and normalized by the section length (L_S), as shown in figure 370.

$$TER = \frac{1}{L_S} \sum_{i=1}^{N} \Delta x \bullet R_{E,i}$$

Figure 370. Equation. TER.

In the equation in figure 370, N is the number of points in the roughness profile and i is the point index. ER at a given point is calculated as shown in figure 371.

$$R_{E,i} = \max(0.0, R_i - R_T)$$

Figure 371. Equation. ER at a point.

In the equation in figure 371, R_i is the value of the roughness profile at point i, R_T is the roughness threshold, and the max function returns the more positive value among its inputs. Note that only those points in the roughness profile greater than the threshold roughness contribute to the sum in the equation in figure 370. The profile recording interval is constant and the $L=N\times\Delta$ calculation of TER is simplified by the equation shown in figure 372.

$$TER = \frac{1}{N} \sum_{i=1}^{N} \max(0.0, R_i - R_T)$$

Figure 372. Equation. Simplified TER.

For the roughness profiles shown in Figure 367 and summarized in Figure 369, TER calculation includes 7,777 points. The sum includes 652 nonzero points for the left roughness profile, which corresponds to a total ALR length of 41.9 ft, and 2,456 nonzero points for the right roughness profile, which corresponds to a total ALR length of 157.9 ft. TER values for the left and right are 0.927 and 19.22 inches/mi, respectively. These values are more precise than the values calculated from the roughness distribution because those values sorted roughness values into discrete bins.

With minor modification, the expression in figure 372 quantifies the relative severity of each ALR on a standard scale. ER for an individual area is calculated as shown in figure 373.

$$ER = \frac{\Delta x}{L_S} \sum_{i=N_S}^{N_E} \left(R_i - R_T \right)$$

Figure 373. Equation. ER for an ALR.

In the equation in figure 371, Δx is the recording interval, R_i is the value of the roughness profile at point i and R_T is the roughness threshold, N_S is the index of the first value above the threshold for the ALR, N_E is the index of the last value above the threshold for the ALR, and L is a standard section length of 528 ft.

ER is normalized by 528 ft to cast ALR severity onto a constant scale. ALR of equal roughness density will produce the same ER value regardless of actual section length. ER quantifies the roughness above the threshold of an ALR in terms of its contribution to the overall IRI of a 528-ft long section. Table 61 and Table 62 list the ER for each ALR. Using ER distinguishes ALR based on both area and peak roughness level and helps identify the ALR that most affects overall roughness and functional quality.

SHORT-TERM CHANGES

This section presents short-term changes in ALR for 59 LTPP SPS-2 test sections and 5 LTPP GPS-3 test sections. Data were collected in 2003 and 2004 to support an FHWA study of jointed concrete curl and warp.(85)

The FHWA study included diurnal measurements of 19 test sections and diurnal and seasonal measurements of 19 additional test sections distributed throughout the United States.(85) The analysis was performed on a subset of measurements collected on LTPP test sections, which include GPS-3 test sections 063021, 133019, 183002, 273003, and 493011, and SPS-2 test sections 040217, 040219, 200205, 200207, 370201, 390209, 390211, 530206, and 530207. Raw profile measurements at the five SPS-2 sites often included coverage of 50 additional test sections incorporated into this study.

Profile data included measurements over a diurnal cycle in every visit to the SPS-2 sites and GPS-3 sections. Diurnal profile measurements included four series of passes over a 24-hour cycle: before sunrise, after sunrise, midafternoon, and after sunset. The diurnal cycle did not always begin before sunrise. For example, the earliest visit to section 063021 began with a series of measurements after sunset, which was followed by the other three visits the next day. Profile data include seasonal measurements of three of the SPS-2 sites and four of the GPS-3 sections. Seasonal measurements occurred in four visits over a 1-year cycle, and each seasonal measurement visit included measurements over a diurnal cycle.

Table 64 and Table 65 list the SPS-2 sites and GPS-3 sections, respectively. The tables list the measurement dates and timing of the first pass in each of the diurnal series. A typical series of passes occurred over 50–80 minutes at SPS-2 sites, although some took up to 2 hours. A typical series of passes occurred over an hour or less at GPS-3 sections. Each series included at least seven repeat profile passes. Five passes from each series were selected for analysis based on agreement in profile, as described in the Quality Screening section of chapter 4.

Table 64. Measurement dates and times for SPS-2 sites.

Site	Date	BD	AD	MA	AS
Arizona	17-Aug-2003	04:16	08:55	12:00	19:20††
Arizona	13-Dec-2003	05:26	09:45	14:05	18:26
Arizona	08-Mar-2004	05:19†	10:35	14:00	20:42
Arizona	02-Jun-2004	03:14†	07:10	12:18	20:05
Kansas	05-Sep-2003	04:30	08:27	13:26††	19:00††
Kansas	19-Nov-2003	04:03†	09:10	12:08	18:02
Kansas	17-Mar-2004	04:10†	08:15	12:02	18:40
Kansas	19-Apr-2004	04:00†	08:06	12:00	19:30
North Carolina	16-May-2003	05:34	08:01	15:59††	—
Ohio	20-Sep-2003	05:09	09:49	13:10††	21:14††
Ohio	27-Oct-2003	04:53	08:06	12:18	18:51
Ohio	25-Jan-2004	04:05	07:46	12:11††	18:32††
Ohio	16-Jun-2004	04:06	08:07	12:39	18:23
Washington	22-Aug-2003	04:44	08:02	12:32	17:04

—No data.
† = measured the following morning.
†† = measured the previous afternoon/evening.
BD = before dawn; AD = after dawn; MA = midafternoon; AS = after sunset.

Table 65. Measurement dates and times for GPS-3 sections.

Section	Date	BD	AD	MA	AS
063021	18-Aug-2003	4:49	8:13	12:31	18:53††
063021	12-Dec-2003	4:42	9:05	13:03	17:18
063021	10-Mar-2004	5:57†	10:20†	14:14	20:17
063021	03-Jun-2004	4:06†	7:29†	12:13	20:06
133019	10-Jul-2003	4:35	8:23	12:41	19:13††
133019	21-Oct-2003	7:04	9:01	14:07††	20:34††
133019	10-Jan-2004	4:28	8:03	12:58††	18:34††
133019	19-May-2004	4:44	8:08	12:01	20:34
183002	30-Oct-2003	5:52†	10:45	14:10	18:47
273003	16-Sep-2003	5:17	8:48	12:38	21:31
273003	11-Nov-2003	5:01†	9:11	13:36	19:31
273003	24-Feb-2004	4:06	7:17	12:26††	18:14††
273003	27-Apr-2004	4:09	8:06	12:06	19:34††
493011	27-Aug-2003	5:09†	8:22	13:21	19:44
493011	04-Dec-2003	5:07	10:17	13:21††	19:14††
493011	15-Mar-2004	4:15	7:56	12:02	18:01
493011	08-Jun-2004	4:21	7:17	12:17	22:17††

† = measured the following morning.
†† = measured the previous afternoon/evening.
BD = before dawn; AD = after dawn; MA = midafternoon; AS = after sunset.

Table 66 lists the average roughness in the right wheel path for the five repeat passes selected from each diurnal and seasonal series. The table lists the age of each section on the date of the earliest visit. For the SPS-2 sites, the age is the time in years since the open to traffic date. For the GPS-3 sections, the age is the time in years since the date of construction. The seasonal test sections were not actually visited once per season; rather, they were visited once in each of four consecutive time slots ranging from July to September 2003, October to December 2003, January to March 2004, and April to June 2004. Table 66 shows raw measurements lacked the range to include section 040262, 200203, 200204, 390203, 390207, 390208, 390262, 390263, and 390265 in one of the four seasonal visits. Data were not collected after sunset at the North Carolina SPS-2 site.

As shown in Table 66, the overall IRI of many test sections changes over seasonal and diurnal cycles. Most of the cyclic change in roughness is attributed to cyclic changes in curl and warp. Cyclic changes in the extent and severity of ALR are likewise linked to changes in curl and warp. Changes in curl and warp are attributed to changes in environment, which induce changes in the temperature and moisture gradient throughout the depth of PCC slabs.

Note that the same profiler collected all measurements. Data collection included an effort to capture diverse environmental conditions. However, the specific dates of the measurements were influenced by the need to complete a data-collection cycle by the profiler and its crew that covered these and many other sections in a cost-effective circuit. As such, the conditions throughout the diurnal visits do not necessarily represent the maximum potential for cyclic changes in roughness. The changes observed on these 64 test sections represent examples of the changes that may occur.

Diurnal changes in IRI from the right wheel path of 25 inches/mi or greater were observed on sections 040222, 040262, 200205, 273003, 493011, and the odd-numbered sections from the Arizona SPS-2 site. Odd-numbered SPS-2 sections have lower flexural strength than even-numbered sections. Sections 200205 and 273003 have slabs with downward curl. Their roughness is lowest before dawn and after sunset. The other sections have upward curl, and their roughness is highest before dawn and after sunset.

The 11 sections with large diurnal changes in roughness also exhibited large seasonal changes. Sections 390202, 390204, 390204, and 390207 also showed a seasonal change. The slabs within these sections shifted toward downward curl in the final (i.e., summer) seasonal visit. The change in curl was either a reduction in upward curl, a reverse in the direction of curl, or an increase in downward curl.

Table 66. Average IRI by visit for the right wheel path.

Section	Age (years)	S1, BD	S1, AD	S1, MA	S2, BD	S2, AD	S2, MA	S2, AS	S3, BD	S3, AD	S3, MA	S3, AS	S4, BD	S4, AD	S4, MA	S4, AS	S5, BD	S5, AD	S5, MA	S5, AS
040213	9.9	—	—	—	152	140	125	139	141	122	117	133	130	118	111	127	145	150	122	135
040214	9.9	—	—	—	78	77	79	77	83	83	85	82	83	90	83	82	82	84	82	81
040215	9.9	—	—	—	134	128	115	123	136	128	120	130	131	119	109	120	136	136	122	126
040216	9.9	—	—	—	95	92	94	92	95	95	94	95	95	96	97	95	95	97	99	96
040217	9.9	—	—	—	91	76	69	88	81	74	72	76	83	69	67	82	105	90	75	92
040218	9.9	—	—	—	74	65	62	64	78	68	64	73	72	59	61	69	79	75	66	72
040219	9.9	—	—	—	131	112	101	122	124	114	104	118	123	101	96	115	147	140	106	129
040220	9.9	—	—	—	75	71	68	71	89	84	74	82	82	73	70	74	82	82	75	76
040221	9.9	—	—	—	104	83	73	94	94	85	76	91	94	74	73	91	116	106	81	105
040222	9.9	—	—	—	75	58	55	63	85	72	63	79	78	59	55	75	93	92	61	70
040223	9.9	—	—	—	116	106	88	106	111	104	95	104	112	92	87	102	125	123	93	107
040224	9.9	—	—	—	74	71	72	72	84	79	74	79	82	72	70	76	78	81	71	73
040262	9.9	—	—	—	202	189	172	198	199	194	187	194	195	176	170	189	—	—	—	—
063021	29.4	—	—	—	105	109	111	108	111	108	109	109	111	111	109	107	112	107	108	105
133019	21.6	—	—	—	118	113	116	119	114	127	121	114	114	112	116	117	109	117	118	108
183002	27.2	—	—	—	—	—	—	—	132	132	123	130	—	—	—	—	—	—	—	—
200201	11.1	—	—	—	123	130	135	128	120	121	131	123	119	117	135	122	116	121	131	120
200202	11.1	—	—	—	70	63	52	54	77	64	60	72	69	63	59	60	78	71	57	61
200203	11.1	—	—	—	—	—	—	—	91	92	97	94	90	93	104	95	90	90	99	94
200204	11.1	—	—	—	—	—	—	—	100	92	86	92	99	93	84	89	94	99	82	85
200205	11.1	—	—	—	86	88	101	90	91	99	104	93	93	97	115	99	89	96	114	96
200206	11.1	—	—	—	89	87	93	91	95	97	96	89	88	90	99	92	98	91	96	93
200207	11.1	—	—	—	100	102	116	106	98	101	109	103	101	100	114	106	101	101	111	109
200208	11.1	—	—	—	130	127	123	127	133	127	132	132	133	129	126	129	132	131	125	127
200211	11.1	—	—	—	80	82	93	83	—	—	—	—	84	86	100	87	82	85	96	85
200212	11.1	—	—	—	108	106	105	105	113	108	105	106	108	106	108	106	113	110	110	107
273003	18.0	—	—	—	147	155	184	159	153	159	177	156	166	168	175	172	154	160	180	169
370201	8.9	94	94	94	—	—	—	—	—	—	—	—	—	—	—	—	—	—	—	—
370202	8.9	121	121	112	—	—	—	—	—	—	—	—	—	—	—	—	—	—	—	—
370203	8.9	110	113	107	—	—	—	—	—	—	—	—	—	—	—	—	—	—	—	—
370205	8.9	126	130	128	—	—	—	—	—	—	—	—	—	—	—	—	—	—	—	—

370206	8.9	112	110	102	—	—	—	—	—	—	—	—	—	—	—	—	—	—	—	—
370209	8.9	90	93	92	—	—	—	—	—	—	—	—	—	—	—	—	—	—	—	—
370210	8.9	84	80	83	—	—	—	—	—	—	—	—	—	—	—	—	—	—	—	—
370259	8.9	89	94	93	—	—	—	—	—	—	—	—	—	—	—	—	—	—	—	—
390201	7.0	—	—	—	103	99	97	97	111	109	100	108	112	111	106	109	102	102	101	103
390202	7.0	—	—	—	102	99	100	97	112	110	101	108	120	120	112	118	105	104	104	106
390203	7.1	—	—	—	—	—	—	—	83	83	72	80	89	90	78	85	69	70	69	70
390204	7.0	—	—	—	73	69	60	63	85	85	75	81	92	92	80	86	65	64	65	65
390205	7.0	—	—	—	110	104	101	110	121	117	108	117	116	121	113	116	113	109	109	112
390206	7.0	—	—	—	104	105	116	106	106	108	104	107	115	111	104	110	107	121	107	118
390207	7.1	—	—	—	—	—	—	—	80	81	89	82	78	81	85	80	100	98	101	106
390208	7.1	—	—	—	—	—	—	—	88	85	86	83	93	90	86	88	90	93	91	93
390209	7.0	—	—	—	83	76	77	76	84	82	75	81	80	78	75	79	76	76	77	77
390210	7.0	—	—	—	64	70	79	67	73	70	74	70	68	70	73	71	72	74	72	78
390211	7.0	—	—	—	83	83	86	84	86	86	86	85	83	84	83	82	87	89	87	90
390212	7.0	—	—	—	67	66	72	65	70	70	69	69	69	71	66	67	68	67	68	71
390260	7.0	—	—	—	72	69	68	67	74	73	68	70	71	75	66	69	68	67	67	68
390261	7.0	—	—	—	74	73	74	74	80	79	74	77	85	83	76	80	74	75	73	74
390262	7.1	—	—	—	—	—	—	—	71	71	67	69	75	73	68	71	68	68	68	70
390263	7.1	—	—	—	—	—	—	—	89	89	83	88	96	93	84	89	81	81	81	81
390265	7.1	—	—	—	—	—	—	—	96	96	95	95	94	94	92	92	91	92	92	93
493011	17.3	—	—	—	176	164	145	154	165	161	157	164	165	161	149	156	168	167	145	156
530201	7.8	—	—	—	121	121	122	119	—	—	—	—	—	—	—	—	—	—	—	—
530202	7.8	—	—	—	86	86	89	89	—	—	—	—	—	—	—	—	—	—	—	—
530204	7.8	—	—	—	94	92	97	95	—	—	—	—	—	—	—	—	—	—	—	—
530205	7.8	—	—	—	95	94	96	97	—	—	—	—	—	—	—	—	—	—	—	—
530206	7.8	—	—	—	107	105	106	104	—	—	—	—	—	—	—	—	—	—	—	—
530207	7.8	—	—	—	89	89	88	91	—	—	—	—	—	—	—	—	—	—	—	—
530208	7.8	—	—	—	85	85	84	86	—	—	—	—	—	—	—	—	—	—	—	—
530209	7.8	—	—	—	103	106	101	103	—	—	—	—	—	—	—	—	—	—	—	—
530210	7.8	—	—	—	67	62	64	61	—	—	—	—	—	—	—	—	—	—	—	—
530211	7.8	—	—	—	89	87	89	85	—	—	—	—	—	—	—	—	—	—	—	—
530212	7.8	—	—	—	68	69	66	67	—	—	—	—	—	—	—	—	—	—	—	—

—No data.
† = measured the following morning.
†† = measured the previous afternoon/evening.
BD = before dawn; AD = after dawn; MA = midafternoon; AS = after sunset.

Table 67 through Table 69 quantify sectionwide ALR for the right wheel path in several ways. Similar to overall roughness, the extent and severity of ALR is heavily influenced by curl and warp. However, the values in Table 67 through Table 69 do not directly correlate to the overall roughness values provided in Table 66 because the roughness threshold determines which features affect the extent, severity, and presence of ALR. In many cases, ALRs appear at a small number of rough features. As such, interactions with changes in curl and warp only depend on the behavior of a few slabs.

Table 67 lists the total ALR length (in feet) for each visit for a base length of 25 ft and a roughness threshold of 125 inches/mi. These values are the average sectionwide ALR length for five visits from each series. Several test sections have no ALR when the threshold value is set at 125 inches/mi and the corresponding table entry is zero. In most cases, these are the sections with the lowest overall IRI values. For example, no visit with average IRI less than 64.7 inches/mi produced any ALR. Every visit with average IRI greater than 80.2 inches/mi produced at least one ALR.

Any series with an average overall IRI above roughness threshold has a commensurately high total ALR length. The lowest total ALR length for a series with an average IRI of 125 inches/mi or above is 123 ft.

Table 68 lists the total ALR length (in feet) for each visit for a base length of 25 ft and a roughness threshold of 160 inches/mi. Results are provided for a higher threshold to show the change in ALR as threshold rises. For some sections with a longer service history, a threshold of 160 inches/mi may be more appropriate. Other sections simply have high roughness. Of the 736 series of runs quantified in Table 67 and Table 68, 152 had at least one ALR for a threshold of 125 inches/mi but none for a threshold of 160 inches/mi.

Table 67. Total ALR length of the right wheel path at 125-inch/mi threshold.

Section	Age (years)	S1, BD	S1, AD	S1, MA	S2, BD	S2, AD	S2, MA	S2, AS	S3, BD	S3, AD	S3, MA	S3, AS	S4, BD	S4, AD	S4, MA	S4, AS	S5, BD	S5, AD	S5, MA	S5, AS
040213	9.9	—	—	—	415	334	251	339	323	212	184	293	294	163	139	252	380	400	208	284
040214	9.9	—	—	—	26	45	47	29	36	54	66	53	61	103	84	55	34	46	67	42
040215	9.9	—	—	—	329	280	161	244	334	271	219	299	310	199	123	219	341	335	221	279
040216	9.9	—	—	—	47	49	48	49	62	61	53	61	55	60	63	54	59	58	61	54
040217	9.9	—	—	—	35	10	0	16	17	18	0	4	19	2	0	13	93	31	17	35
040218	9.9	—	—	—	0	0	0	0	1	0	0	0	0	0	0	0	5	1	0	0
040219	9.9	—	—	—	300	165	90	232	246	159	97	190	242	91	55	168	384	352	113	277
040220	9.9	—	—	—	0	0	0	0	6	2	0	0	1	0	0	0	2	2	0	0
040221	9.9	—	—	—	94	51	29	60	57	33	32	52	56	37	39	48	136	93	27	90
040222	9.9	—	—	—	1	0	0	0	16	0	0	0	0	0	0	1	64	44	0	1
040223	9.9	—	—	—	181	75	6	85	116	65	22	71	121	15	6	65	270	242	14	87
040224	9.9	—	—	—	1	0	0	0	4	3	0	3	6	0	0	1	1	1	1	0
040262	9.9	—	—	—	500	498	484	499	499	500	494	498	498	489	483	496	—	—	—	—
063021	29.4	—	—	—	114	120	140	108	144	130	139	138	142	133	129	123	145	119	137	112
133019	21.6	—	—	—	173	158	164	184	163	223	202	165	163	161	181	186	142	183	192	112
183002	27.2	—	—	—	—	—	—	—	211	228	203	205	—	—	—	—	—	—	—	—
200201	11.1	—	—	—	119	126	123	130	135	132	145	142	135	129	159	133	131	131	148	133
200202	11.1	—	—	—	0	0	0	0	10	0	0	1	0	0	0	0	15	2	0	0
200203	11.1	—	—	—	—	—	—	—	43	45	59	53	39	53	91	45	41	34	63	41
200204	11.1	—	—	—	—	—	—	—	92	55	18	52	76	53	8	16	65	84	7	10
200205	11.1	—	—	—	16	14	63	24	31	58	96	37	46	60	154	66	19	48	117	57
200206	11.1	—	—	—	74	69	78	87	87	88	110	81	72	91	115	100	92	88	107	94
200207	11.1	—	—	—	60	65	150	102	58	67	95	77	62	60	126	92	73	65	114	115
200208	11.1	—	—	—	280	267	240	258	311	292	296	302	305	310	262	298	304	305	263	283
200211	11.1	—	—	—	22	20	30	20	—	—	—	—	21	22	66	22	22	21	49	21
200212	11.1	—	—	—	118	113	115	114	126	115	109	121	121	116	120	111	127	119	134	117
273003	18.0	—	—	—	343	385	465	397	379	402	452	392	433	435	450	442	377	397	467	423
370201	8.9	54	53	53	—	—	—	—	—	—	—	—	—	—	—	—	—	—	—	—
370202	8.9	194	187	122	—	—	—	—	—	—	—	—	—	—	—	—	—	—	—	—
370203	8.9	141	168	141	—	—	—	—	—	—	—	—	—	—	—	—	—	—	—	—
370205	8.9	263	278	274	—	—	—	—	—	—	—	—	—	—	—	—	—	—	—	—

370206	8.9	138	132	77	—	—	—	—	—	—	—	—	—	—	—	—	—	—	—	—
370209	8.9	42	38	58	—	—	—	—	—	—	—	—	—	—	—	—	—	—	—	—
370210	8.9	18	15	42	—	—	—	—	—	—	—	—	—	—	—	—	—	—	—	—
370259	8.9	55	68	57	—	—	—	—	—	—	—	—	—	—	—	—	—	—	—	—
390201	7.0	—	—	—	65	61	56	57	103	85	63	85	126	120	101	113	73	74	71	75
390202	7.0	—	—	—	111	103	94	95	146	137	109	128	183	182	153	174	122	120	118	120
390203	7.1	—	—	—	—	—	—	—	1	4	0	0	18	14	0	1	0	0	0	0
390204	7.0	—	—	—	2	1	0	0	26	25	7	19	47	47	23	29	0	0	0	0
390205	7.0	—	—	—	140	121	115	144	200	175	133	165	161	187	142	169	172	170	161	157
390206	7.0	—	—	—	133	133	170	136	129	139	127	132	164	145	121	135	141	161	136	189
390207	7.1	—	—	—	—	—	—	—	65	62	86	63	49	56	81	60	101	100	105	113
390208	7.1	—	—	—	—	—	—	—	55	40	36	38	62	47	53	47	61	60	58	71
390209	7.0	—	—	—	40	39	32	37	38	36	25	37	38	32	36	37	38	40	46	33
390210	7.0	—	—	—	0	0	0	0	0	0	0	0	0	0	0	1	0	0	0	0
390211	7.0	—	—	—	31	32	27	36	38	37	37	36	35	37	33	36	36	45	42	44
390212	7.0	—	—	—	6	6	7	5	6	7	7	7	0	2	0	0	7	7	6	7
390260	7.0	—	—	—	0	0	0	0	0	0	0	0	0	0	0	0	0	0	0	0
390261	7.0	—	—	—	16	25	20	21	33	25	22	28	46	42	19	30	27	25	24	23
390262	7.1	—	—	—	—	—	—	—	0	0	0	0	0	0	0	0	0	0	0	0
390263	7.1	—	—	—	—	—	—	—	34	41	34	42	51	41	27	36	34	35	30	29
390265	7.1	—	—	—	—	—	—	—	90	86	76	89	77	78	69	75	59	66	60	63
493011	17.3	—	—	—	477	445	344	396	459	429	412	451	447	432	394	420	456	456	344	406
530201	7.8	—	—	—	230	214	233	207	—	—	—	—	—	—	—	—	—	—	—	—
530202	7.8	—	—	—	8	9	11	7	—	—	—	—	—	—	—	—	—	—	—	—
530204	7.8	—	—	—	28	25	45	23	—	—	—	—	—	—	—	—	—	—	—	—
530205	7.8	—	—	—	61	61	65	73	—	—	—	—	—	—	—	—	—	—	—	—
530206	7.8	—	—	—	63	67	62	63	—	—	—	—	—	—	—	—	—	—	—	—
530207	7.8	—	—	—	28	27	30	31	—	—	—	—	—	—	—	—	—	—	—	—
530208	7.8	—	—	—	23	17	13	27	—	—	—	—	—	—	—	—	—	—	—	—
530209	7.8	—	—	—	127	145	108	129	—	—	—	—	—	—	—	—	—	—	—	—
530210	7.8	—	—	—	0	0	0	0	—	—	—	—	—	—	—	—	—	—	—	—
530211	7.8	—	—	—	30	28	27	24	—	—	—	—	—	—	—	—	—	—	—	—
530212	7.8	—	—	—	0	0	0	0	—	—	—	—	—	—	—	—	—	—	—	—

—No data.

BD = before dawn; AD = after dawn; MA = midafternoon; AS = after sunset.

S1 = May 2003; S2 = Jul–Sep 2003; S3 = Oct–Dec 2003; S4 = Jan–Mar 2004; S5 = Apr–Jun 2004.

Table 68. Total ALR length of the right wheel path at 160-inch/mi threshold.

Section	Age (years)	S1, BD	S1, AD	S1, MA	S2, BD	S2, AD	S2, MA	S2, AS	S3, BD	S3, AD	S3, MA	S3, AS	S4, BD	S4, AD	S4, MA	S4, AS	S5, BD	S5, AD	S5, MA	S5, AS
040213	9.9	—	—	—	178	103	33	96	94	35	17	80	57	47	26	59	151	159	42	85
040214	9.9	—	—	—	2	13	20	3	10	20	23	14	16	32	19	11	0	15	10	1
040215	9.9	—	—	—	66	43	22	35	91	59	27	52	60	33	10	23	89	92	50	46
040216	9.9	—	—	—	4	1	5	3	0	0	3	6	7	7	8	4	1	1	5	1
040217	9.9	—	—	—	0	0	0	0	1	2	0	0	0	0	0	0	0	2	1	0
040218	9.9	—	—	—	0	0	0	0	0	0	0	0	0	0	0	0	0	0	0	0
040219	9.9	—	—	—	68	31	10	42	52	36	15	47	44	17	2	28	160	111	16	70
040220	9.9	—	—	—	0	0	0	0	0	0	0	0	0	0	0	0	0	0	0	0
040221	9.9	—	—	—	30	29	6	24	17	13	9	30	32	17	18	20	45	22	6	43
040222	9.9	—	—	—	0	0	0	0	0	0	0	0	0	0	0	0	0	0	0	0
040223	9.9	—	—	—	2	0	0	0	0	0	0	0	1	0	0	0	18	10	0	1
040224	9.9	—	—	—	0	0	0	0	0	0	0	0	0	0	0	0	0	0	0	0
040262	9.9	—	—	—	472	428	349	467	462	456	416	449	448	362	324	423	—	—	—	—
063021	29.4	—	—	—	20	42	39	40	35	20	26	27	37	20	26	23	32	20	38	25
133019	21.6	—	—	—	73	43	63	72	62	110	75	54	49	37	63	65	26	71	60	9
183002	27.2	—	—	—	—	—	—	—	145	151	126	140	—	—	—	—	—	—	—	—
200201	11.1	—	—	—	78	82	78	87	101	89	101	102	96	85	103	91	93	90	108	97
200202	11.1	—	—	—	0	0	0	0	0	0	0	0	0	0	0	0	0	0	0	0
200203	11.1	—	—	—	—	—	—	—	0	0	0	0	0	0	2	0	0	0	0	0
200204	11.1	—	—	—	—	—	—	—	2	0	0	0	0	0	0	0	0	0	0	0
200205	11.1	—	—	—	0	0	3	1	0	3	8	1	17	21	38	24	0	22	37	1
200206	11.1	—	—	—	41	35	43	46	43	48	51	37	36	43	53	49	44	40	54	47
200207	11.1	—	—	—	26	26	28	26	26	26	27	27	26	26	28	26	26	26	26	26
200208	11.1	—	—	—	80	74	73	80	97	76	90	101	94	82	75	85	92	86	73	79
200211	11.1	—	—	—	16	17	18	17	—	—	—	—	17	17	18	18	16	17	18	16
200212	11.1	—	—	—	71	66	55	63	84	72	60	68	70	67	58	61	79	80	66	62
273003	18.0	—	—	—	155	208	372	230	191	226	327	215	263	276	317	289	189	223	344	282
370201	8.9	0	0	0	—	—	—	—	—	—	—	—	—	—	—	—	—	—	—	—
370202	8.9	19	15	10	—	—	—	—	—	—	—	—	—	—	—	—	—	—	—	—
370203	8.9	32	47	33	—	—	—	—	—	—	—	—	—	—	—	—	—	—	—	—
370205	8.9	61	85	75	—	—	—	—	—	—	—	—	—	—	—	—	—	—	—	—

370206	8.9	27	30	16	—	—	—	—	—	—	—	—	—	—	—	—	—	—	—	—
370209	8.9	0	0	0	—	—	—	—	—	—	—	—	—	—	—	—	—	—	—	—
370210	8.9	0	0	0	—	—	—	—	—	—	—	—	—	—	—	—	—	—	—	—
370259	8.9	5	10	4	—	—	—	—	—	—	—	—	—	—	—	—	—	—	—	—
390201	7.0	—	—	—	47	48	48	47	49	50	50	48	48	48	48	48	49	49	49	50
390202	7.0	—	—	—	48	43	43	39	65	61	51	56	97	93	75	94	61	58	58	56
390203	7.1	—	—	—	—	—	—	—	0	0	0	0	0	0	0	0	0	0	0	0
390204	7.0	—	—	—	0	0	0	0	0	0	0	0	3	7	0	0	0	0	0	0
390205	7.0	—	—	—	55	41	42	65	75	63	47	67	66	75	61	65	72	59	56	65
390206	7.0	—	—	—	5	11	22	16	9	23	22	21	32	13	10	24	20	49	20	52
390207	7.1	—	—	—	—	—	—	—	20	20	24	21	7	8	16	9	34	34	36	47
390208	7.1	—	—	—	—	—	—	—	4	5	10	4	6	6	2	4	13	15	10	15
390209	7.0	—	—	—	0	0	0	0	0	0	0	0	0	0	0	0	0	0	0	0
390210	7.0	—	—	—	0	0	0	0	0	0	0	0	0	0	0	0	0	0	0	0
390211	7.0	—	—	—	5	1	0	4	7	5	0	2	7	5	2	7	1	0	0	1
390212	7.0	—	—	—	0	0	0	0	0	0	0	0	0	0	0	0	0	0	0	0
390260	7.0	—	—	—	0	0	0	0	0	0	0	0	0	0	0	0	0	0	0	0
390261	7.0	—	—	—	5	5	3	4	5	5	3	4	9	9	6	7	6	5	6	5
390262	7.1	—	—	—	—	—	—	—	0	0	0	0	0	0	0	0	0	0	0	0
390263	7.1	—	—	—	—	—	—	—	0	10	3	8	5	2	1	2	2	1	0	0
390265	7.1	—	—	—	—	—	—	—	28	26	24	28	21	22	14	17	6	7	9	6
493011	17.3	—	—	—	319	246	147	199	282	227	207	262	265	253	164	220	271	263	137	206
530201	7.8	—	—	—	29	31	36	27	—	—	—	—	—	—	—	—	—	—	—	—
530202	7.8	—	—	—	0	0	0	0	—	—	—	—	—	—	—	—	—	—	—	—
530204	7.8	—	—	—	0	0	0	0	—	—	—	—	—	—	—	—	—	—	—	—
530205	7.8	—	—	—	12	3	15	15	—	—	—	—	—	—	—	—	—	—	—	—
530206	7.8	—	—	—	13	11	8	10	—	—	—	—	—	—	—	—	—	—	—	—
530207	7.8	—	—	—	0	0	0	0	—	—	—	—	—	—	—	—	—	—	—	—
530208	7.8	—	—	—	0	0	0	0	—	—	—	—	—	—	—	—	—	—	—	—
530209	7.8	—	—	—	11	39	6	29	—	—	—	—	—	—	—	—	—	—	—	—
530210	7.8	—	—	—	0	0	0	0	—	—	—	—	—	—	—	—	—	—	—	—
530211	7.8	—	—	—	1	0	0	0	—	—	—	—	—	—	—	—	—	—	—	—
530212	7.8	—	—	—	0	0	0	0	—	—	—	—	—	—	—	—	—	—	—	—

—No data.

BD = before dawn; AD = after dawn; MA = midafternoon; AS = after sunset.

S1 = May 2003; S2 = Jul–Sep 2003; S3 = Oct–Dec 2003; S4 = Jan–Mar 2004; S5 = Apr–Jun 2004.

Table 69. Average ER of right wheel path at 125-inch/mi threshold.

Section	Age (years)	S1, BD	S1, AD	S1, MA	S2, BD	S2, AD	S2, MA	S2, AS	S3, BD	S3, AD	S3, MA	S3, AS	S4, BD	S4, AD	S4, MA	S4, AS	S5, BD	S5, AD	S5, MA	S5, AS
040213	9.9	—	—	—	29.1	20.4	10.1	18.4	22.0	8.4	6.8	16.3	12.9	10.1	6.0	14.2	22.8	27.7	9.1	18.9
040214	9.9	—	—	—	1.2	2.2	2.6	1.0	1.8	2.8	3.4	2.4	2.6	5.7	3.4	2.2	1.1	2.2	2.5	1.2
040215	9.9	—	—	—	15.3	11.2	5.3	9.0	17.3	11.8	7.5	12.7	13.8	7.1	3.5	7.4	17.7	17.2	9.3	10.9
040216	9.9	—	—	—	1.3	1.3	1.5	1.3	1.1	1.0	1.5	1.8	1.8	1.8	2.2	1.5	1.5	1.3	1.5	1.2
040217	9.9	—	—	—	0.5	0.1	0.0	0.2	0.4	0.6	0.0	0.0	0.4	0.0	0.0	0.2	2.3	0.8	0.6	0.7
040218	9.9	—	—	—	0.0	0.0	0.0	0.0	0.0	0.0	0.0	0.0	0.0	0.0	0.0	0.0	0.0	0.0	0.0	0.0
040219	9.9	—	—	—	14.6	6.3	2.7	9.4	10.9	6.9	3.1	8.7	9.9	3.4	1.8	6.4	26.3	19.7	4.1	13.7
040220	9.9	—	—	—	0.0	0.0	0.0	0.0	0.0	0.0	0.0	0.0	0.0	0.0	0.0	0.0	0.0	0.0	0.0	0.0
040221	9.9	—	—	—	5.6	4.2	1.3	3.8	3.4	1.8	1.9	4.6	5.3	2.7	2.6	3.3	8.9	4.8	1.1	7.9
040222	9.9	—	—	—	0.0	0.0	0.0	0.0	0.2	0.0	0.0	0.0	0.0	0.0	0.0	0.0	1.3	0.7	0.0	0.0
040223	9.9	—	—	—	4.3	1.5	0.0	1.6	2.6	1.2	0.3	1.6	2.9	0.1	0.0	1.2	8.5	7.2	0.1	1.8
040224	9.9	—	—	—	0.0	0.0	0.0	0.0	0.0	0.0	0.0	0.0	0.1	0.0	0.0	0.0	0.0	0.0	0.0	0.0
040262	9.9	—	—	—	76.9	63.6	46.7	72.3	73.5	68.4	61.7	69.1	70.1	50.7	44.9	63.3	—	—	—	—
063021	29.4	—	—	—	4.9	7.0	7.2	6.3	6.7	5.3	5.8	5.6	6.9	5.2	5.9	5.0	6.5	4.6	6.9	5.1
133019	21.6	—	—	—	11.2	8.1	10.0	11.5	9.6	16.3	12.2	9.3	8.5	7.7	10.0	10.4	6.1	11.0	10.5	4.1
183002	27.2	—	—	—	—	—	—	—	27.6	26.4	21.8	27.5	—	—	—	—	—	—	—	—
200201	11.1	—	—	—	45.0	45.3	48.0	40.6	32.1	31.1	34.4	32.1	33.8	31.9	35.5	33.8	31.2	31.4	33.6	31.5
200202	11.1	—	—	—	0.0	0.0	0.0	0.0	0.1	0.0	0.0	0.0	0.0	0.0	0.0	0.0	0.2	0.0	0.0	0.0
200203	11.1	—	—	—	—	—	—	—	0.8	1.0	1.5	1.3	0.8	1.2	2.4	1.0	0.8	0.6	1.5	0.9
200204	11.1	—	—	—	—	—	—	—	2.1	0.9	0.1	0.7	1.5	0.7	0.1	0.1	1.4	1.7	0.0	0.1
200205	11.1	—	—	—	0.5	0.3	1.7	0.6	0.7	1.5	3.1	0.8	2.3	3.0	7.5	3.4	0.5	3.5	9.8	1.1
200206	11.1	—	—	—	5.1	4.6	5.7	5.7	6.3	6.7	8.3	5.4	4.8	6.1	8.7	6.9	6.8	6.2	7.9	6.4
200207	11.1	—	—	—	5.4	5.7	9.4	6.7	5.6	5.7	7.4	6.6	5.7	5.7	8.0	6.4	5.9	5.7	7.3	7.0
200208	11.1	—	—	—	13.9	12.6	12.7	13.9	16.8	13.9	16.4	16.8	16.0	14.7	13.5	14.8	16.4	15.5	13.4	13.5
200211	11.1	—	—	—	1.9	2.0	2.8	2.2	—	—	—	—	2.2	2.5	3.6	2.6	2.2	2.4	3.2	2.4
200212	11.1	—	—	—	15.2	14.3	12.1	13.3	16.9	14.9	13.7	14.6	15.8	14.4	13.3	14.0	16.3	15.9	14.8	14.3
273003	18.0	—	—	—	29.3	34.8	60.3	38.1	33.0	37.8	53.5	35.2	43.4	44.8	50.8	48.1	33.9	38.4	55.8	47.1
370201	8.9	1.1	1.2	1.3	—	—	—	—	—	—	—	—	—	—	—	—	—	—	—	—
370202	8.9	5.9	6.1	3.7	—	—	—	—	—	—	—	—	—	—	—	—	—	—	—	—
370203	8.9	6.3	7.8	5.9	—	—	—	—	—	—	—	—	—	—	—	—	—	—	—	—
370205	8.9	13.0	16.1	15.4	—	—	—	—	—	—	—	—	—	—	—	—	—	—	—	—

370206	8.9	5.3	5.8	3.3	—	—	—	—	—	—	—	—	—	—	—	—	—	—	—	—
370209	8.9	0.8	0.5	1.0	—	—	—	—	—	—	—	—	—	—	—	—	—	—	—	—
370210	8.9	0.3	0.2	0.8	—	—	—	—	—	—	—	—	—	—	—	—	—	—	—	—
370259	8.9	1.7	2.6	1.7	—	—	—	—	—	—	—	—	—	—	—	—	—	—	—	—
390201	7.0	—	—	—	8.8	9.1	9.8	9.2	9.5	9.4	9.5	9.3	10.0	9.5	9.4	9.6	10.6	10.9	10.7	11.2
390202	7.0	—	—	—	7.3	6.8	6.1	6.0	10.2	9.2	7.5	8.3	13.8	13.9	10.9	13.7	8.8	8.3	8.3	8.4
390203	7.1	—	—	—	—	—	—	—	0.0	0.0	0.0	0.0	0.4	0.1	0.0	0.0	0.0	0.0	0.0	0.0
390204	7.0	—	—	—	0.0	0.0	0.0	0.0	0.5	0.5	0.1	0.3	1.4	1.9	0.4	0.8	0.0	0.0	0.0	0.0
390205	7.0	—	—	—	8.6	7.1	7.2	10.0	13.8	11.6	9.4	11.7	10.6	12.9	10.4	11.1	11.4	9.7	9.8	10.3
390206	7.0	—	—	—	4.0	5.5	10.9	7.5	5.4	6.3	6.5	7.8	8.9	5.2	4.2	6.9	5.8	17.5	5.2	10.2
390207	7.1	—	—	—	—	—	—	—	2.8	2.9	4.4	3.1	1.8	2.1	3.2	2.4	5.9	5.9	6.3	7.8
390208	7.1	—	—	—	—	—	—	—	1.8	1.4	2.1	1.4	2.1	1.7	1.7	1.6	2.4	2.4	2.2	2.8
390209	7.0	—	—	—	1.1	0.8	0.6	0.7	0.7	0.7	0.4	0.8	0.9	0.6	0.9	0.9	0.8	0.9	1.1	0.7
390210	7.0	—	—	—	0.0	0.0	0.0	0.0	0.0	0.0	0.0	0.0	0.0	0.0	0.0	0.0	0.0	0.0	0.0	0.0
390211	7.0	—	—	—	1.1	1.0	0.5	1.3	1.6	1.5	1.0	1.2	1.6	1.6	1.1	1.5	0.8	1.3	1.2	1.2
390212	7.0	—	—	—	0.1	0.1	0.1	0.1	0.1	0.1	0.1	0.1	0.0	0.0	0.0	0.0	0.2	0.2	0.1	0.2
390260	7.0	—	—	—	0.0	0.0	0.0	0.0	0.0	0.0	0.0	0.0	0.0	0.0	0.0	0.0	0.0	0.0	0.0	0.0
390261	7.0	—	—	—	0.7	1.0	0.7	0.8	1.1	0.9	0.9	0.9	1.4	1.4	0.8	1.1	0.9	0.9	0.9	0.8
390262	7.1	—	—	—	—	—	—	—	0.0	0.0	0.0	0.0	0.0	0.0	0.0	0.0	0.0	0.0	0.0	0.0
390263	7.1	—	—	—	—	—	—	—	0.9	2.0	1.1	1.7	1.6	1.0	0.6	1.0	1.0	0.9	0.7	0.4
390265	7.1	—	—	—	—	—	—	—	4.7	4.5	4.0	4.7	3.9	4.1	3.2	3.7	2.4	2.5	2.6	2.5
493011	17.3	—	—	—	50.4	39.3	23.9	31.5	39.9	36.9	34.2	39.2	39.9	36.9	27.2	32.5	43.6	41.6	23.6	32.6
530201	7.8	—	—	—	8.6	8.4	9.5	7.7	—	—	—	—	—	—	—	—	—	—	—	—
530202	7.8	—	—	—	0.1	0.1	0.1	0.1	—	—	—	—	—	—	—	—	—	—	—	—
530204	7.8	—	—	—	0.4	0.3	0.8	0.3	—	—	—	—	—	—	—	—	—	—	—	—
530205	7.8	—	—	—	2.6	1.3	3.0	3.1	—	—	—	—	—	—	—	—	—	—	—	—
530206	7.8	—	—	—	2.8	2.6	2.2	2.4	—	—	—	—	—	—	—	—	—	—	—	—
530207	7.8	—	—	—	0.7	0.6	0.8	0.8	—	—	—	—	—	—	—	—	—	—	—	—
530208	7.8	—	—	—	0.3	0.2	0.1	0.5	—	—	—	—	—	—	—	—	—	—	—	—
530209	7.8	—	—	—	3.9	7.4	2.7	5.9	—	—	—	—	—	—	—	—	—	—	—	—
530210	7.8	—	—	—	0.0	0.0	0.0	0.0	—	—	—	—	—	—	—	—	—	—	—	—
530211	7.8	—	—	—	0.7	0.4	0.3	0.3	—	—	—	—	—	—	—	—	—	—	—	—
530212	7.8	—	—	—	0.0	0.0	0.0	0.0	—	—	—	—	—	—	—	—	—	—	—	—

—No data.

BD = before dawn; AD = after dawn; MA = midafternoon; AS = after sunset.

S1 = May 2003; S2 = Jul–Sep 2003; S3 = Oct–Dec 2003; S4 = Jan–Mar 2004; S5 = Apr–Jun 2004.

Figure 374 through Figure 379 provide graphical examples of short-term changes in total ALR length. Figure 374 shows the total ALR length for the right wheel path in each visit to section 040223 using a base length of 25 ft and a roughness threshold of 125 inches/mi. The measurements included a diurnal cycle within each seasonal set of visits. ALR length was largest in the predawn visit and lowest for the midafternoon visit in each season. The highest total ALR length for a midafternoon visit was 22 ft, and the lowest ALR length for a predawn visit was 116 ft.

The slabs within section 040223 were curled upward. Slab curl was typically the most severe at night and less severe at midday. Changes in slab curl account for the large range on overall IRI values of 87–125 inches/mi and the large range in overall ALR length of 6–270 ft for a roughness threshold of 125 inches/mi. Table 67 and Table 68 show several sections that exhibited similar behavior because of diurnal changes in upward curl.

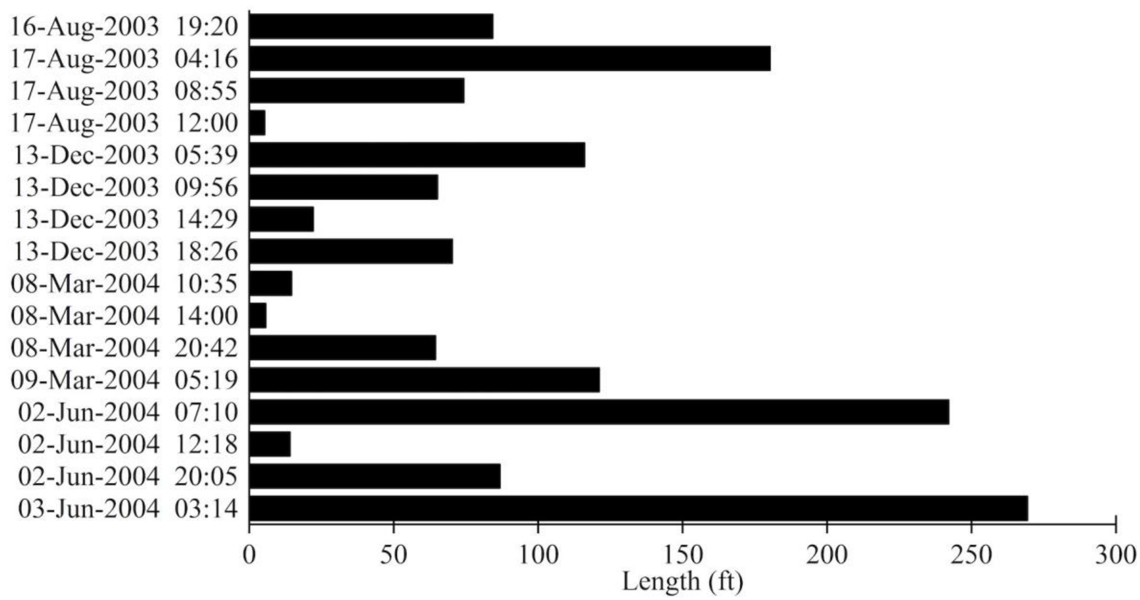

Source: FHWA.

Figure 374. Graph. Total ALR length of section 040223 for the right wheel path.

Figure 375 compares ALR behavior of the midafternoon visit on 02-Jun-2004 to the predawn visit on the following day. The figure shows the total ALR length from the right wheel path versus roughness threshold for one pass from each visit using a base length of 25 ft. Both traces have the same shape but are offset from each other by approximately 30 inches/mi. On section 040223, the increase in upward curl at night increased the roughness by about 30 inches/mi throughout its length. The increase in upward curl did not introduce localized roughness; rather, it exacerbated the existing localized roughness within the section.

Figure 376 shows the total ALR length for the right wheel path in each visit to section 200202 using a base length of 25 ft and a roughness threshold of 100 inches/mi. Similar to section 040223, section 200202 exhibited diurnal changes in roughness due to changes in the severity of upward curl. The overall IRI for the right wheel path had a minimum value of 52 inches/mi for the midday visit on 04-Sep-2003. The IRI for the right wheel path for the predawn visit on

20-Apr-2004 was 78 inches/mi, a 50-percent increase. A noteworthy feature of the data in Figure 376 is the contrast between more than 80 ft of total ALR length for two of the visits and the absence or near absence of ALR in four others.

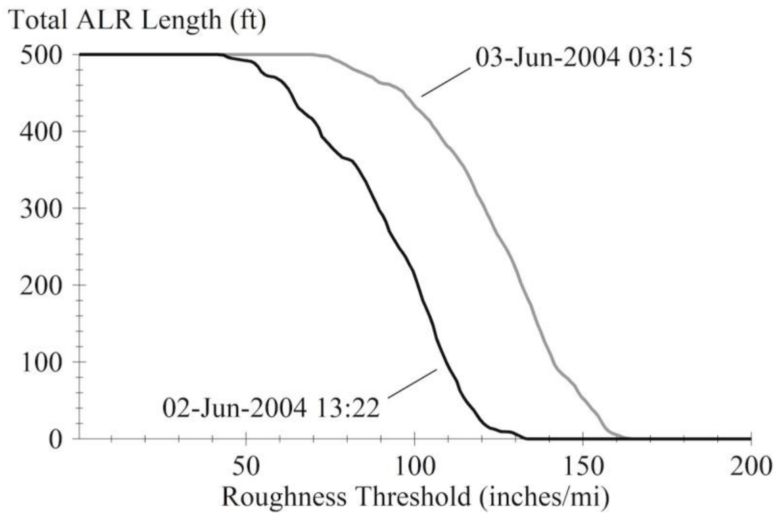

Source: FHWA.

Figure 375. Graph. Cumulative ALR length of section 040223 for the right wheel path.

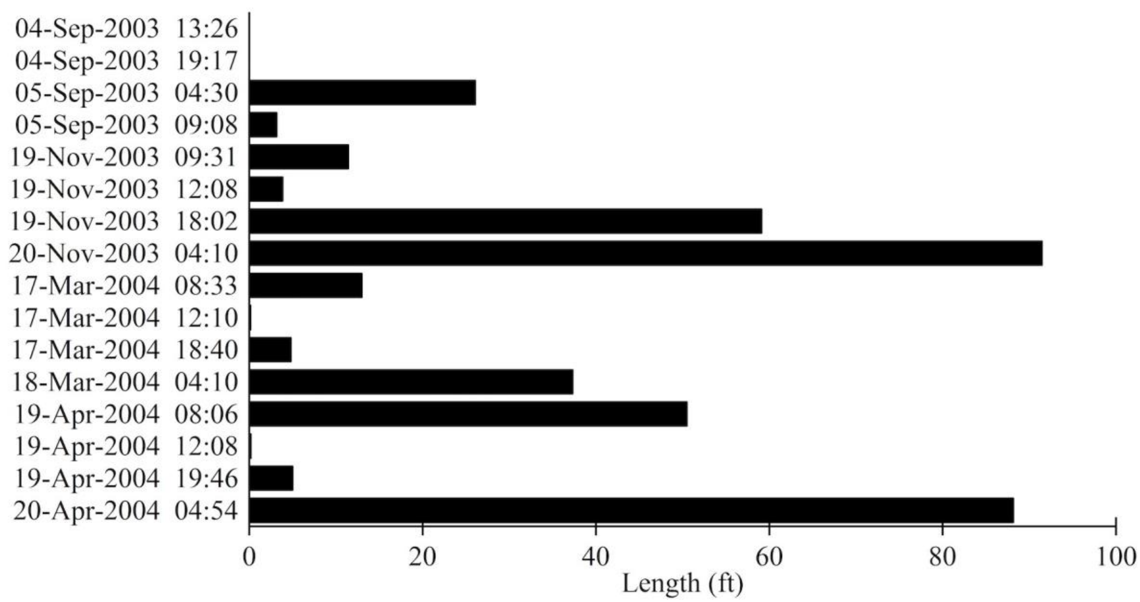

Source: FHWA.

Figure 376. Graph. Total ALR length of section 200202 for the right wheel path.

Figure 377 shows the total ALR length for the right wheel path in each visit to section 200205 using a base length of 25 ft and a roughness threshold of 125 inches/mi. Slabs within this section were curled downward. Within each seasonal group, total ALR length and overall IRI were the highest for the midafternoon visit and lowest for visits prior to 10:00 a.m.

Figure 377 includes evidence of potential seasonal changes in ALR length. By seasonal group, September 2003 measurements had the lowest ALR length and March 2004 measurements had the highest. Higher temperatures or greater moisture under the slabs in autumn and lower temperatures or lower moisture under the slabs in the spring may explain the difference. However, the true seasonal change is difficult to distinguish from diurnal effects.

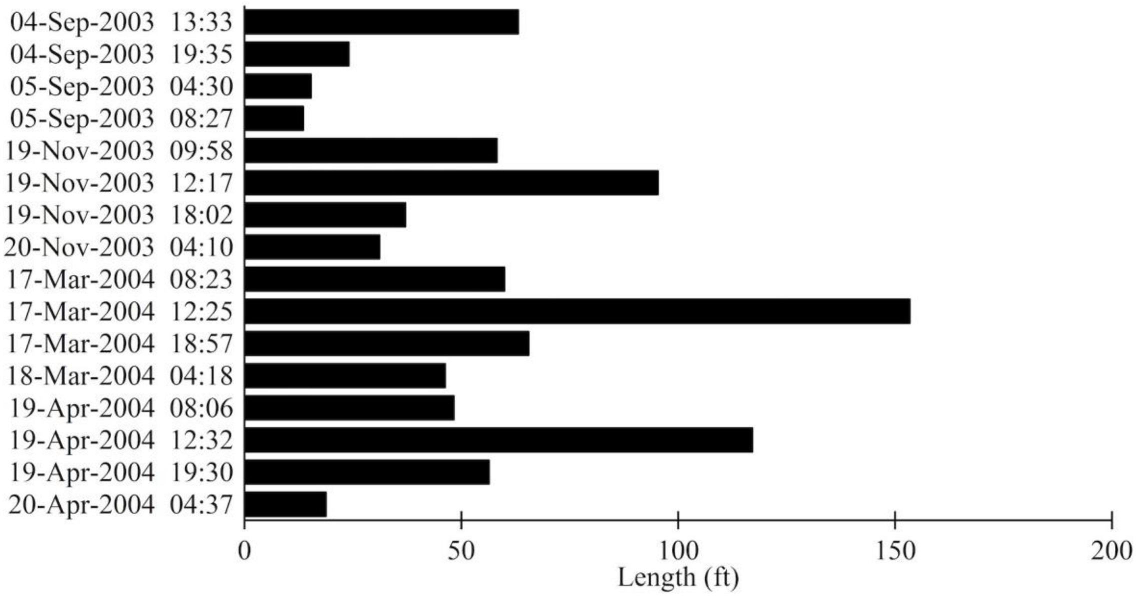

Source: FHWA.

Figure 377. Graph. Total ALR length of section 200205 for the right wheel path.

Figure 378 shows the total ALR length for the right wheel path in each visit to section 390204 using a base length of 25 ft and a roughness threshold of 125 inches/mi. In the portions of the test section that account for most of the ALR, slabs were curled upward. Figure 378 shows ALR length was largest in autumn and winter. Within those seasonal groups, ALR length was largest in the predawn visits and after-dawn visits prior to 10:00 a.m. ALR length was much smaller (or zero) in summer and autumn.

Figure 379 compares ALR behavior of the predawn visit on 25-Jan-2004 to the predawn visit on 16-Jun-2004. The figure shows the total ALR length from the right wheel path versus roughness threshold for one pass from each visit using a base length of 25 ft. The change of roughness threshold associated with a given ALR length did not appear as a uniform shift in the traces shown in Figure 375. Instead, a greater range of roughness existed throughout the section for the profile measured in January 2004. The tail of the total ALR length distribution at high roughness values corresponds to the most severe ALRs.

The increase in overall roughness and ALR in winter is caused by an increase in upward slab curl. However, the change was not uniform throughout the section. The difference in upward curl in January 2004 appeared as severe uplift at specific joints within the last 200 ft of the section when compared to profiles collected in June 2004. The slab curl and the resulting roughness changed less in the first 300 ft of the section, and the severity of the downward fault shown in Figure 358 did not change.

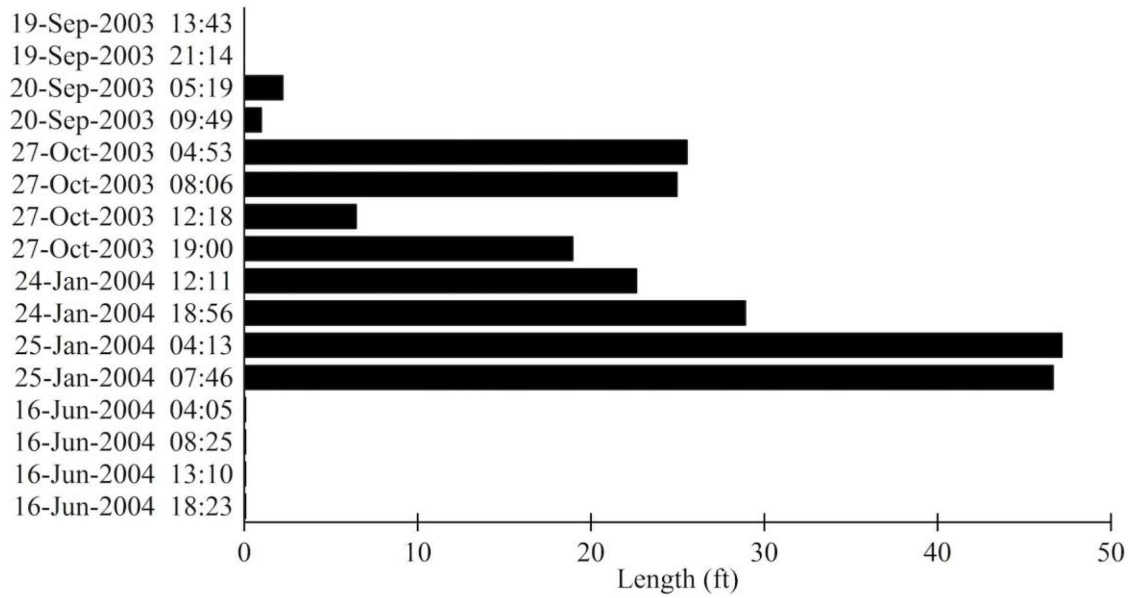

Source: FHWA.

Figure 378. Graph. Total ALR length of section 390204 for the right wheel path.

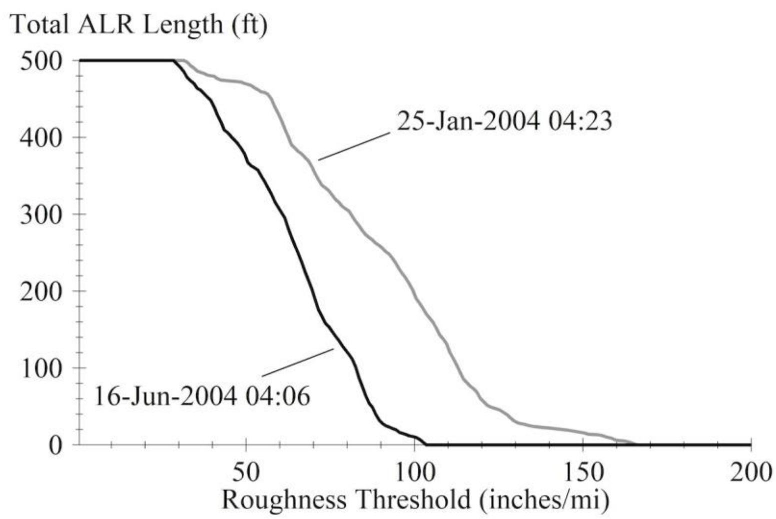

Source: FHWA.

Figure 379. Graph. Cumulative ALR length of section 390204 for the right wheel path.

The examples in this section address short-term changes in total ALR length. On most test sections, short-term changes in ER follow the same qualitative trends as total ALR length. However, the quantitative changes in ER are typically larger in terms of percentage.

Table 69 lists the average ER in the right wheel path for the five repeat passes selected from each diurnal and seasonal series. These values correspond to a base length of 25 ft and a roughness threshold of 125 inches/mi.

LONG-TERM CHANGES

This research examined long-term changes in ALRs for 78 LTPP SPS-2 test sections and 5 LTPP GPS-3 test sections. Data were collected for the LTPP program as described in appendix B. Profile data were collected approximately once per year since the open to traffic date at the SPS-2 sites. GPS-3 sections were monitored in at least 12 and at most 39 visits since 1989. Three GPS-3 sections and three SPS-2 sections were in the LTPP SMP. Profile data were collected over some seasonal cycles and at various times of day at SMP sections. In addition, data were collected at various times during a 24-hour cycle at each SPS-2 site in 2014.

No common long-term trend in ALR length or severity emerged among the 83 test sections. However, when researchers examined the test sections using a base length of 25 ft and roughness thresholds of 125 inches/mi and 160 inches/mi, most test sections exhibited one or more of the following behaviors:

- Little or no ALR: In many cases where overall IRI remained low relative to the roughness threshold throughout the monitoring period, little or no ALR appeared.
- Stable ARL: Several test sections included a similar length of ALR throughout the monitoring history. ALRs typically appeared as a discrete, persistent set of rough profile features on these sections. In some cases, the severity of each ALR was also consistent over time.
- ALR growth with age: Several test sections included little or no ALR in the earliest monitoring visits, but ALR length and severity increased as distress and other sources of roughness increased over time.
- Confounded ALR growth: On some test sections, ALR length and severity increased over time. However, the trend was confounded by seasonal and diurnal fluctuations in curl and warp.

This section presents ALR length, severity, and locations over the monitoring history for eight test sections. These sections represent typical long-term trends for test sections that included ALR for threshold values of 125 inches/mi or higher. For each example, three graphs are provided:

- Bar charts, total ALR length: These figures show the total length for all ALR within the test section at the date and time of each measurement visit. Values of length are the average for the (typically five) repeat profile measurements from each visit.
- Bar charts, ALR severity: These figures show the ER within the test section at the date and time of each measurement visit. Values of ER are the average for the (typically five) repeat profile measurements from each visit. ER is the contribution to the overall IRI of all roughness above the threshold within the roughness profile.
- ALR map: These figures show the range of ALR for each profile-measurement pass. ALRs are marked with a line over the corresponding range, and no markings appear in ranges without localized roughness. Passes are grouped by profile-measurement visit to compare the locations of ALR borders between repeat passes.

All three graphs display the dependent variable (length, severity, or locations) along a horizontal axis. Measurement visits are stacked vertically and are arranged in order of occurrence with the earliest visit at the top. The interval between visits is not consistent for the eight test sections. In some cases, visits are a year or more apart. In others, up to four monitoring visits occurred in one year or over one 24-hour cycle.

Figure 380 through Figure 382 characterize the long-term trend in ALR for the right wheel path of section 040223 using a base length of 25 ft and a roughness threshold of 125 inches/mi. ALR length and ER increase over time. Both quantities are higher in the final monitoring visits than in the earliest monitoring visits. However, diurnal changes in slab curl cause greater variation in roughness than long-term changes.

The largest observations of ALR length and ER occurred between midnight and 3:00 a.m. on 13-Aug-2006 and 20-Sep-2008. This was when upward curl had the highest magnitude, which increased the average roughness to values near the threshold (Figure 380). Many of the ALR are not localized because their peak values did not exceed the average roughness for the section by more than 40 percent. As a result, ALR length stands out relative to other visits more so than ER because peak value at each ALR is not extreme compared to the average.

Four visits starting on 06-Feb-2014 demonstrate diurnal changes in ALR on section 040223 linked to upward slab curl. The roughness, ALR length, and ER were highest at night and early morning when the pavement surface was coolest and lower in the early afternoon and midafternoon when the pavement surface was warm.

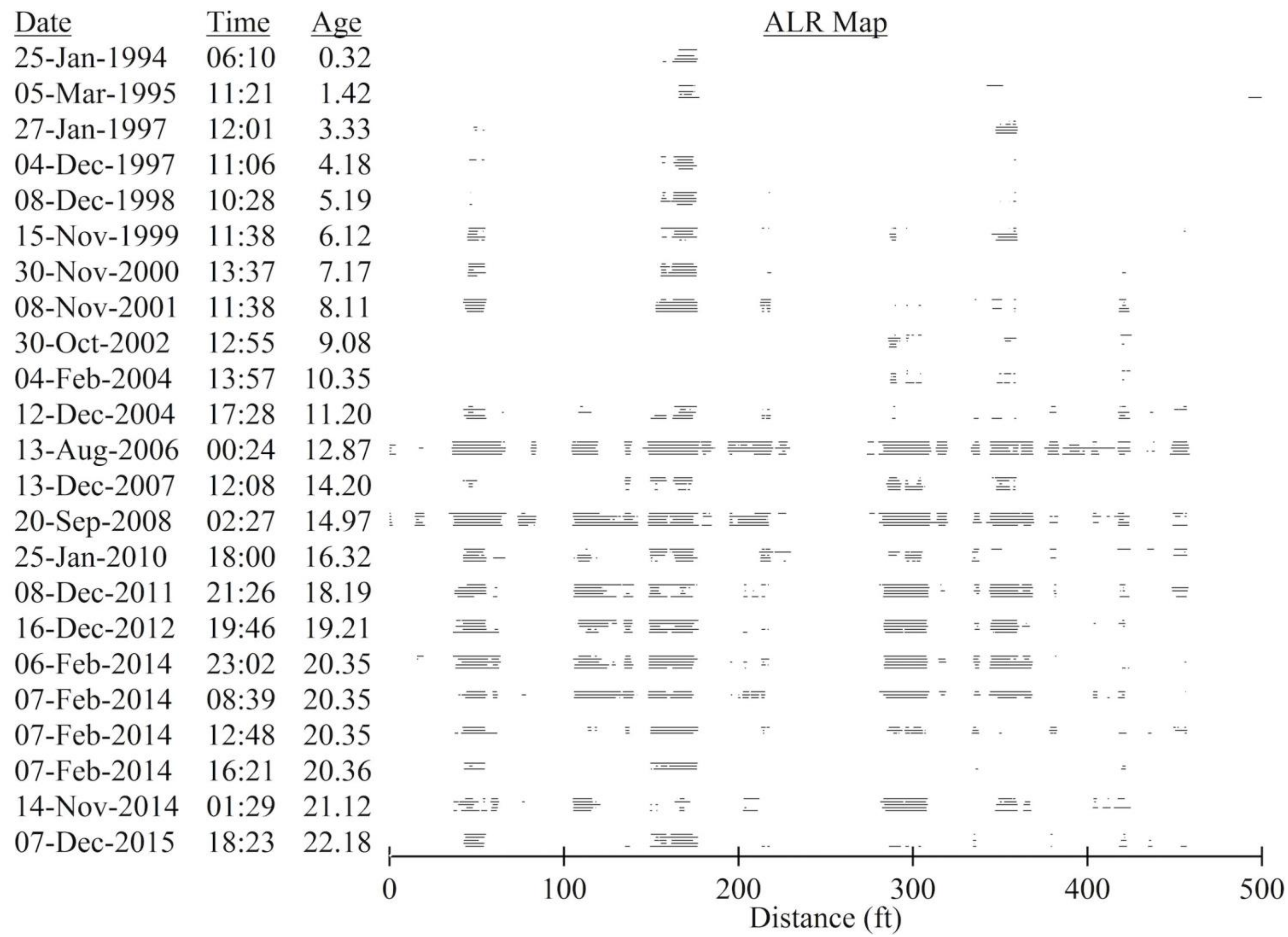

Source: FHWA.

Figure 380. Graph. ALR map of section 040223 for the right wheel path.

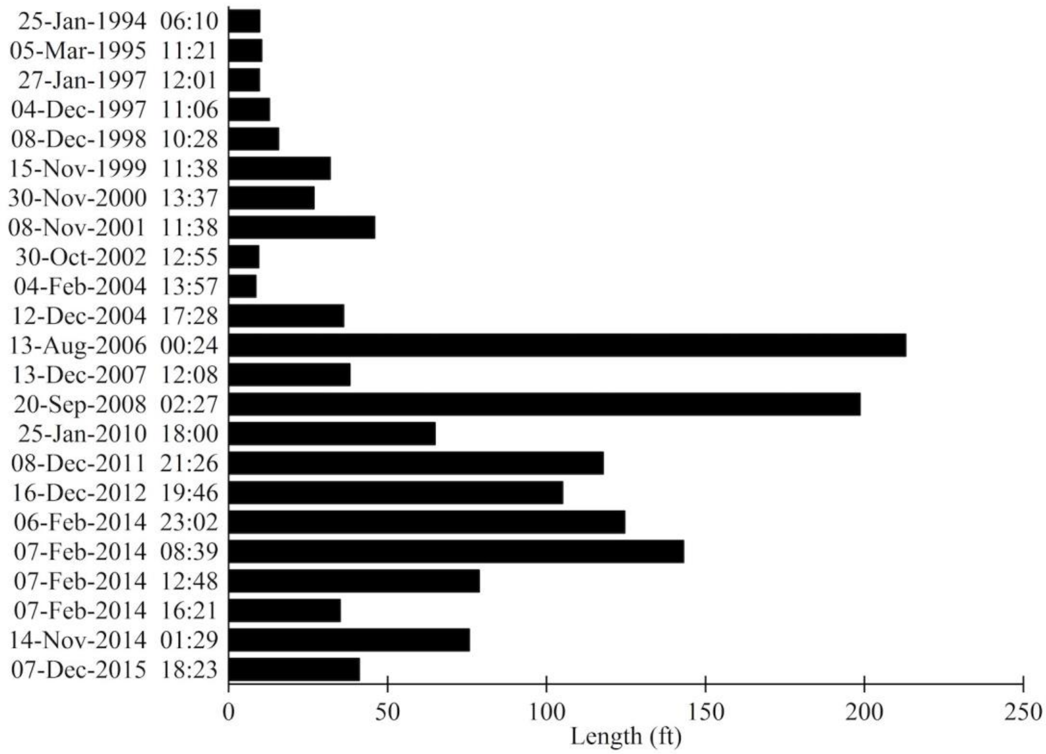

Source: FHWA.

Figure 381. Graph. Total ALR length of section 040223 for the right wheel path.

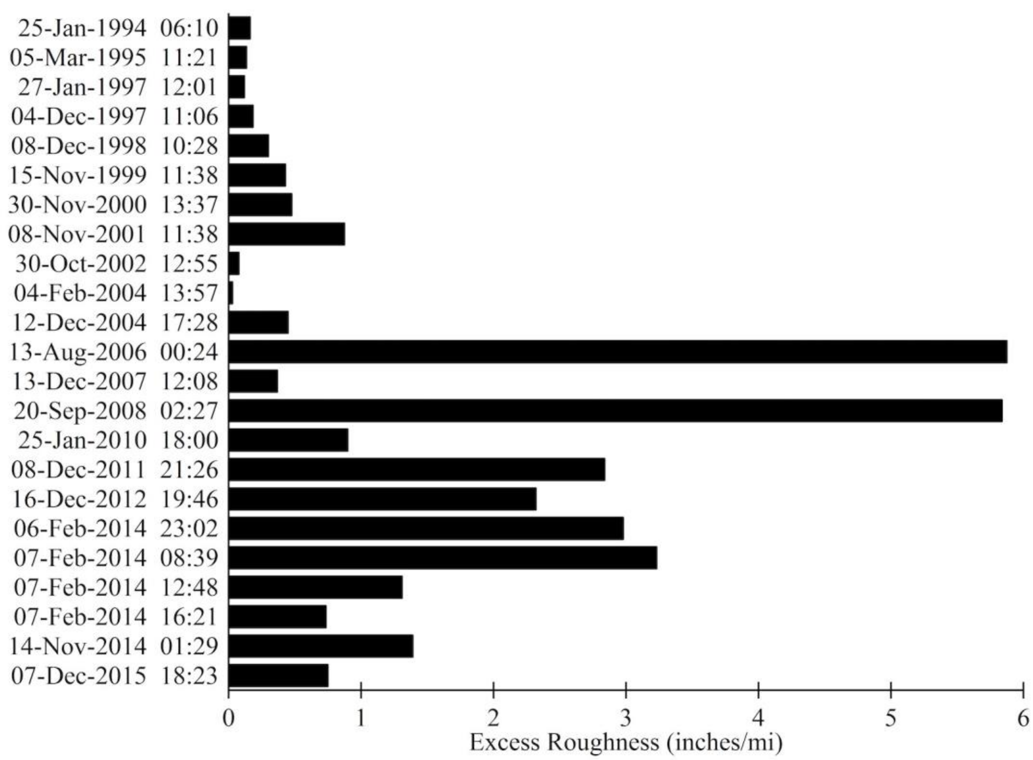

Source: FHWA.

Figure 382. Graph. ER of section 040223 for the right wheel path.

Figure 383 through Figure 385 characterize the long-term trend in ALR for the right wheel path of section 370202 using a base length of 25 ft and a roughness threshold of 125 inches/mi. ALR length and ER may have undergone a modest long-term increase. However, cyclic changes in roughness caused by slab curl and warp obscure the long-term trend.

Monitoring visits to section 370202 include measurements in five consecutive seasons starting in October 1997. In the first four seasons, all profile measurements were collected between 10:30 a.m. and 3:15 p.m. For these visits, the average level of slab curl was neutral (PSG near zero) and the overall roughness in the right wheel path only varied from 81.9 to 83.0 inches/mi. (The range of age from 3.27 to 4.06 years is detailed in Figure 207 and Table 71.) In November 1998, profile measurements began at 8:45 a.m. For this visit, most of the slabs were curled upward. The ALR length and ER were much greater for this visit, and the overall roughness increased to 110.9 inches/mi in the right wheel path. Similar onset of upward curl and commensurate increases in roughness were observed for measurements at about 9:00 a.m. on 14-Jul-2001 and 11-Oct-2001.

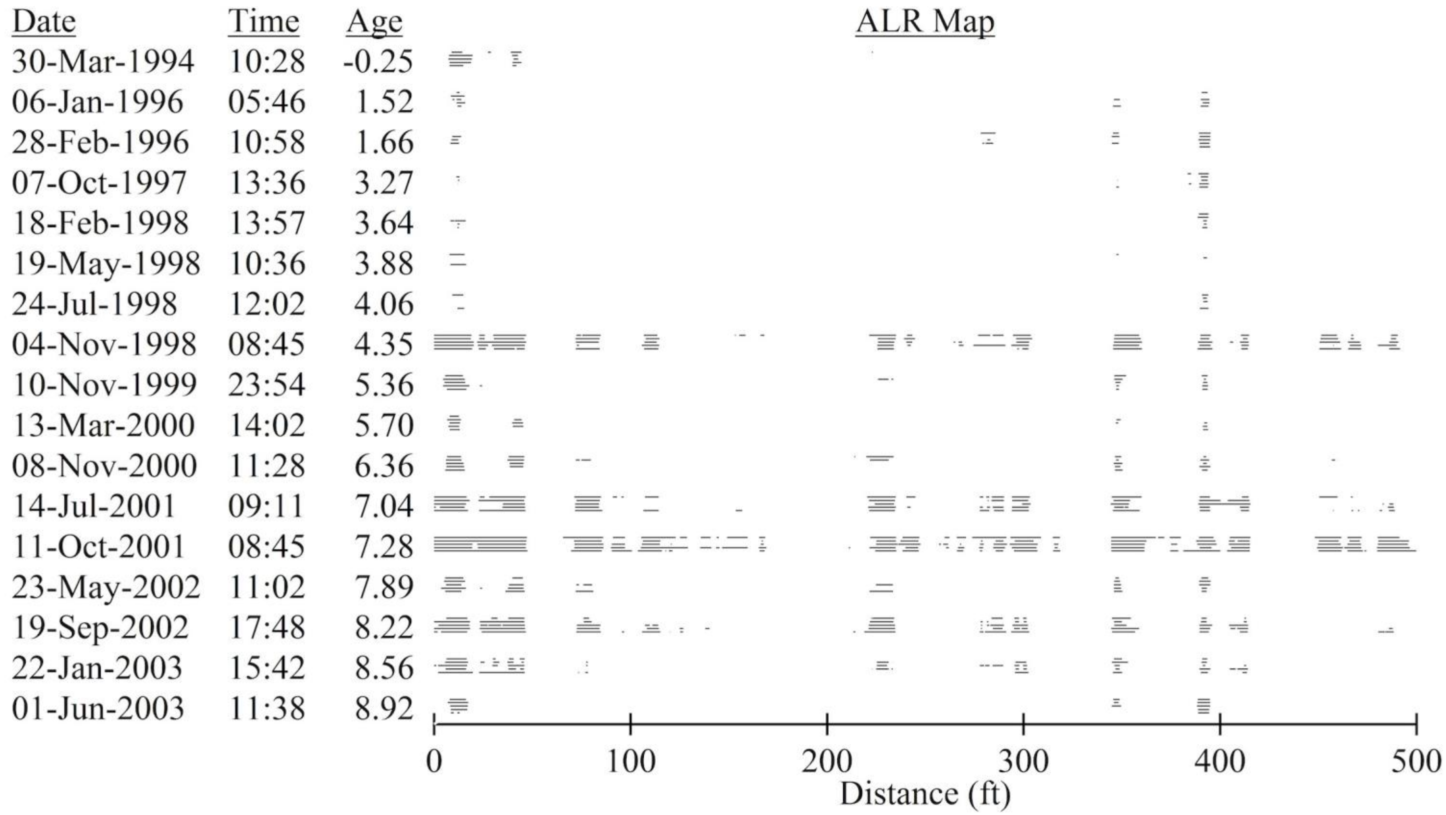

Source: FHWA.

Figure 383. Graph. ALR map of section 370202 for the right wheel path.

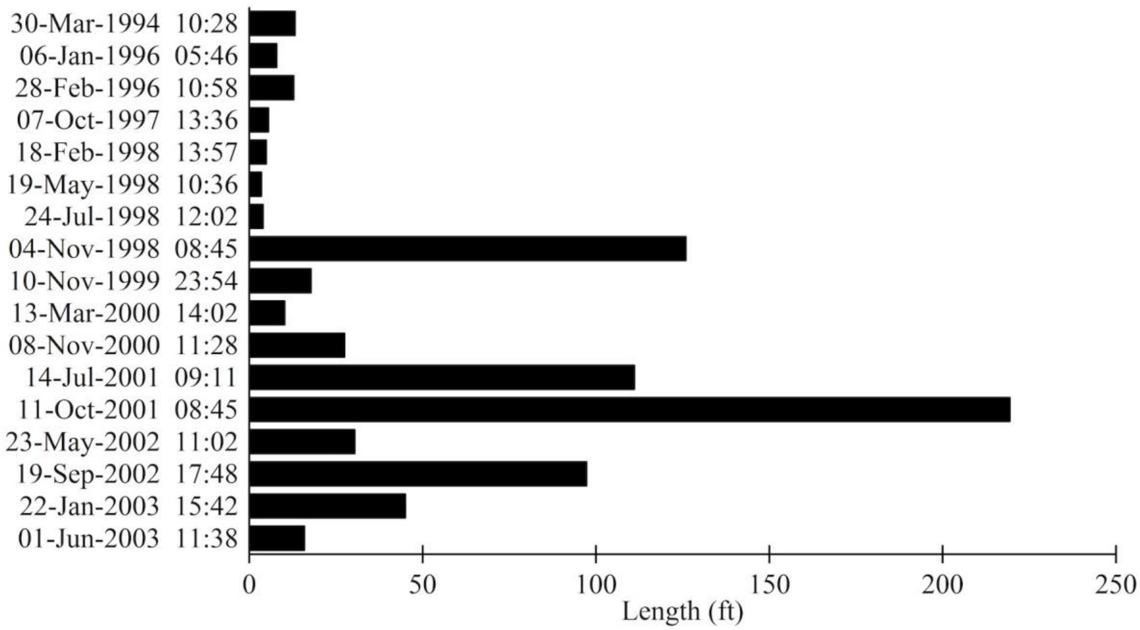

Source: FHWA.

Figure 384. Graph. Total ALR length of section 370202 for the right wheel path.

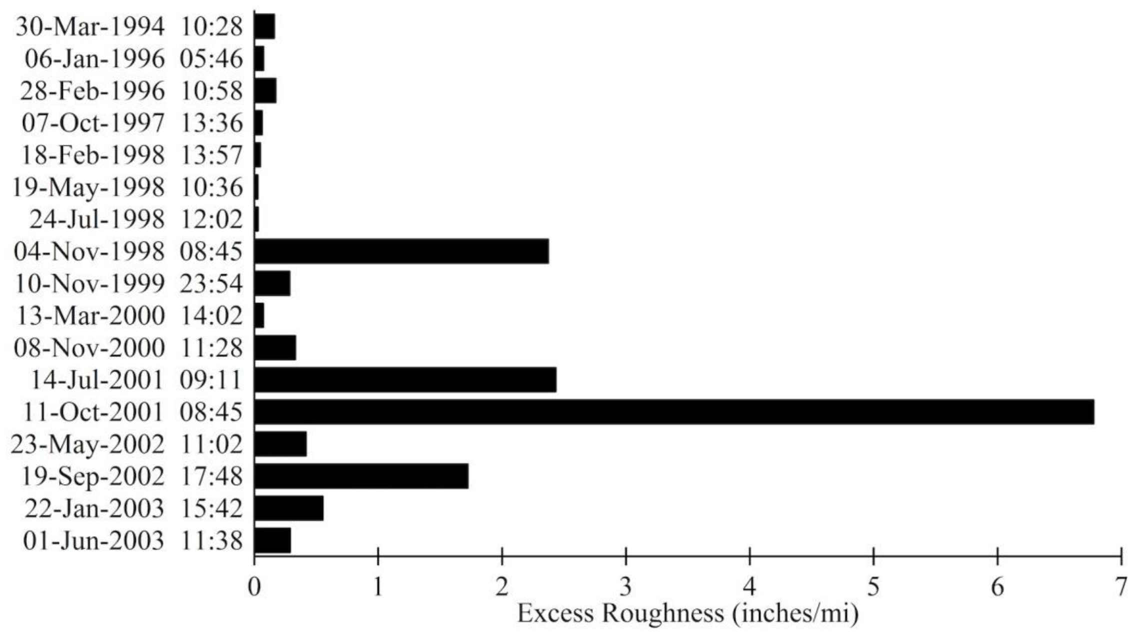

Source: FHWA.

Figure 385. Graph. ER of section 370202 for the right wheel path.

Figure 386 through Figure 388 characterize the long-term trend in ALR for the right wheel path of section 370208 using a base length of 25 ft and a roughness threshold of 160 inches/mi. ALRs appeared in three specific locations in the earliest visits and remained throughout the monitoring history. Four additional ALRs appeared as the pavement aged. No distress was recorded at the locations of these ALRs, and the specific sources of roughness were difficult to discern by viewing the profiles.

Section 370208 provides another example of seasonal and diurnal changes in slab curl making the long-term trend in ALR difficult to identify. Plots for this section were provided because the monitoring history includes two pairs of visits from the same day (28-Feb-1996 and 17-May-2001), measurements over a 24-hour cycle (starting 24-Jun-2014), and multiple visits per year from 2000 through 2003.

The slabs within section 370208 exhibit a modest level of upward curl. In early morning or late evening visits, the length and severity of ALR increased because of an increase in the prevailing levels of upward curl. The increase in upward curl did not introduce new ALR, but it increased the range and severity of the existing ALR.

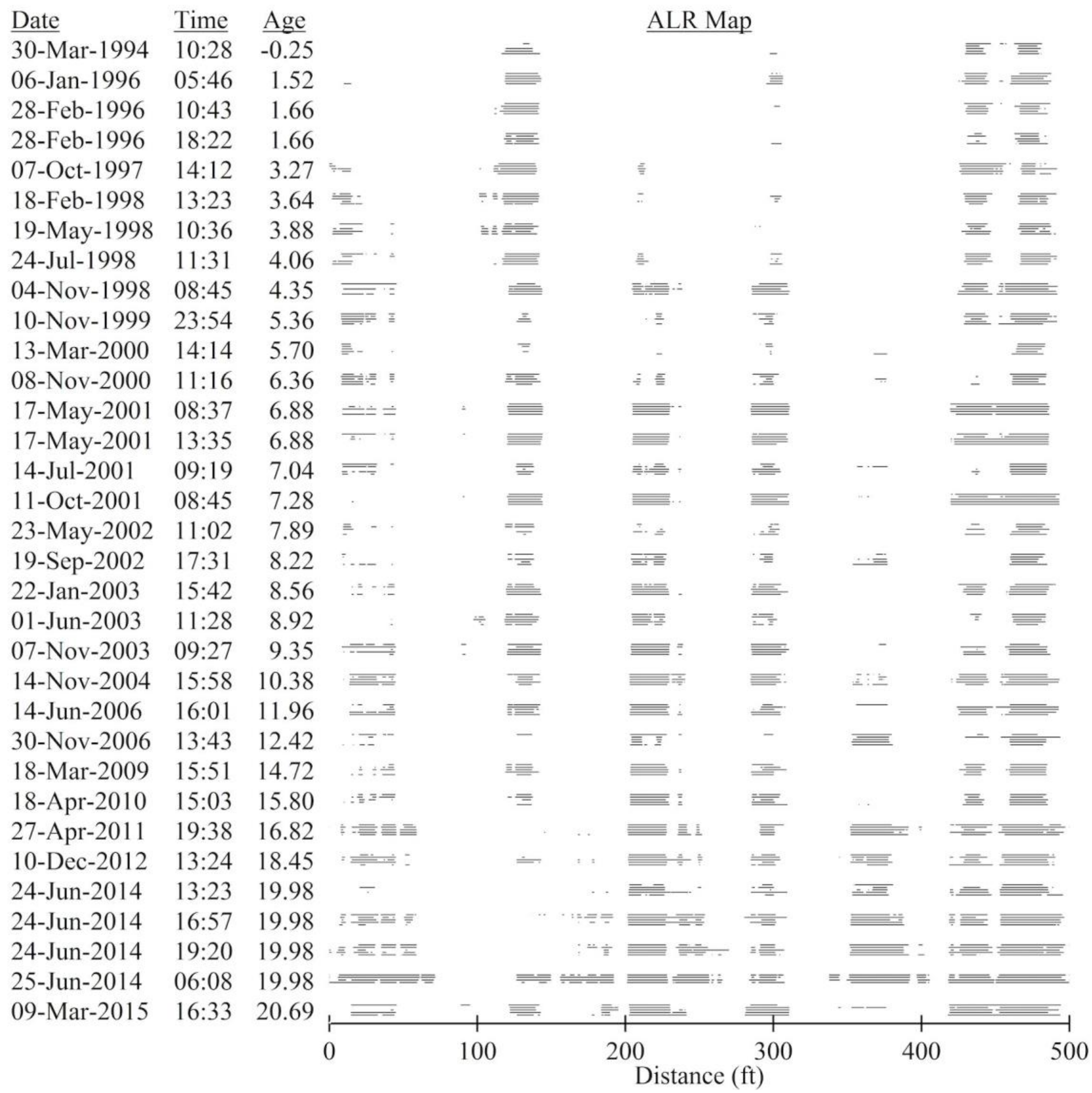

Source: FHWA.

Figure 386. Graph. ALR map of section 370208 for the right wheel path.

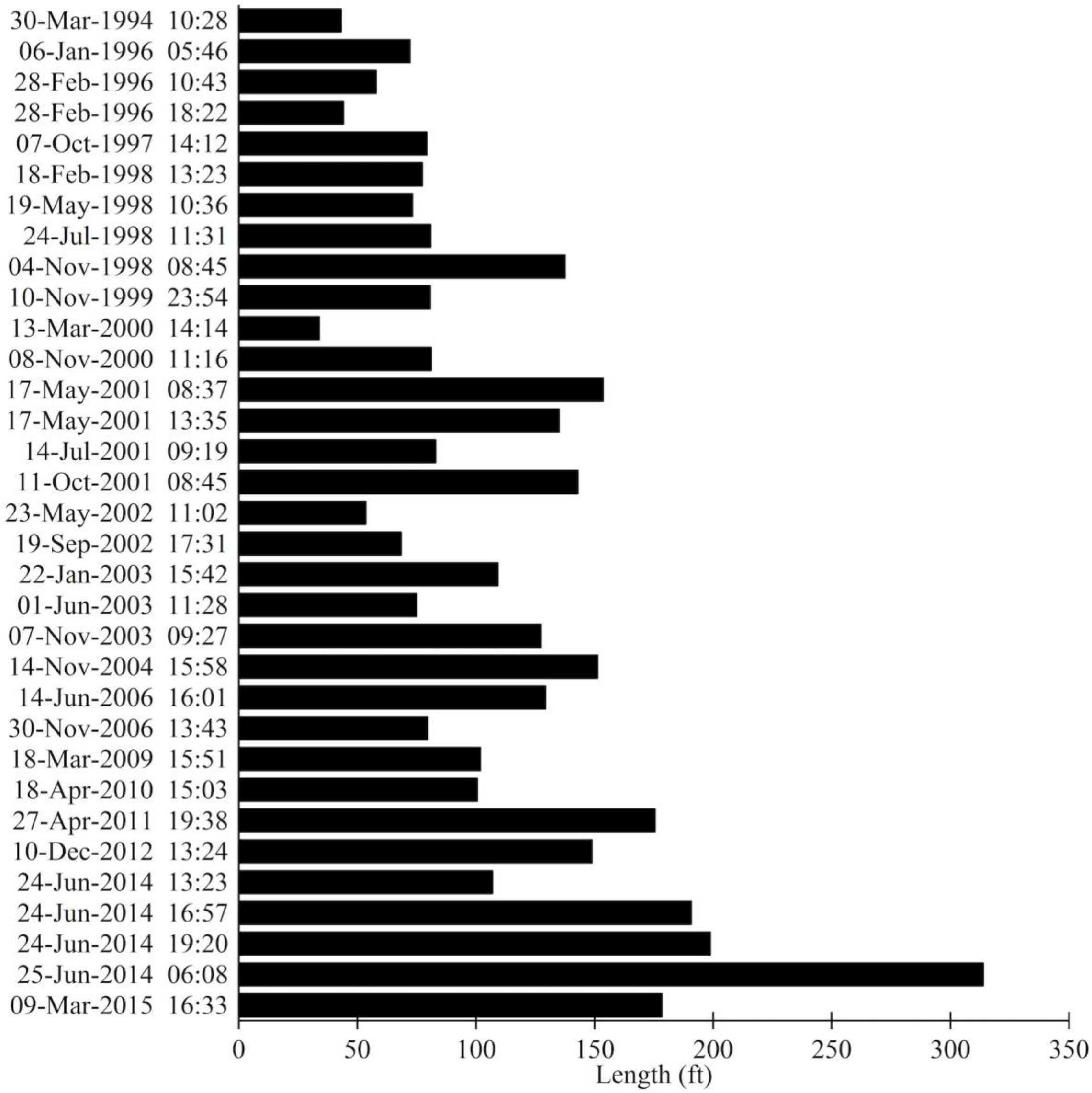

Source: FHWA.

Figure 387. Graph. Total ALR length of section 370208 for the right wheel path.

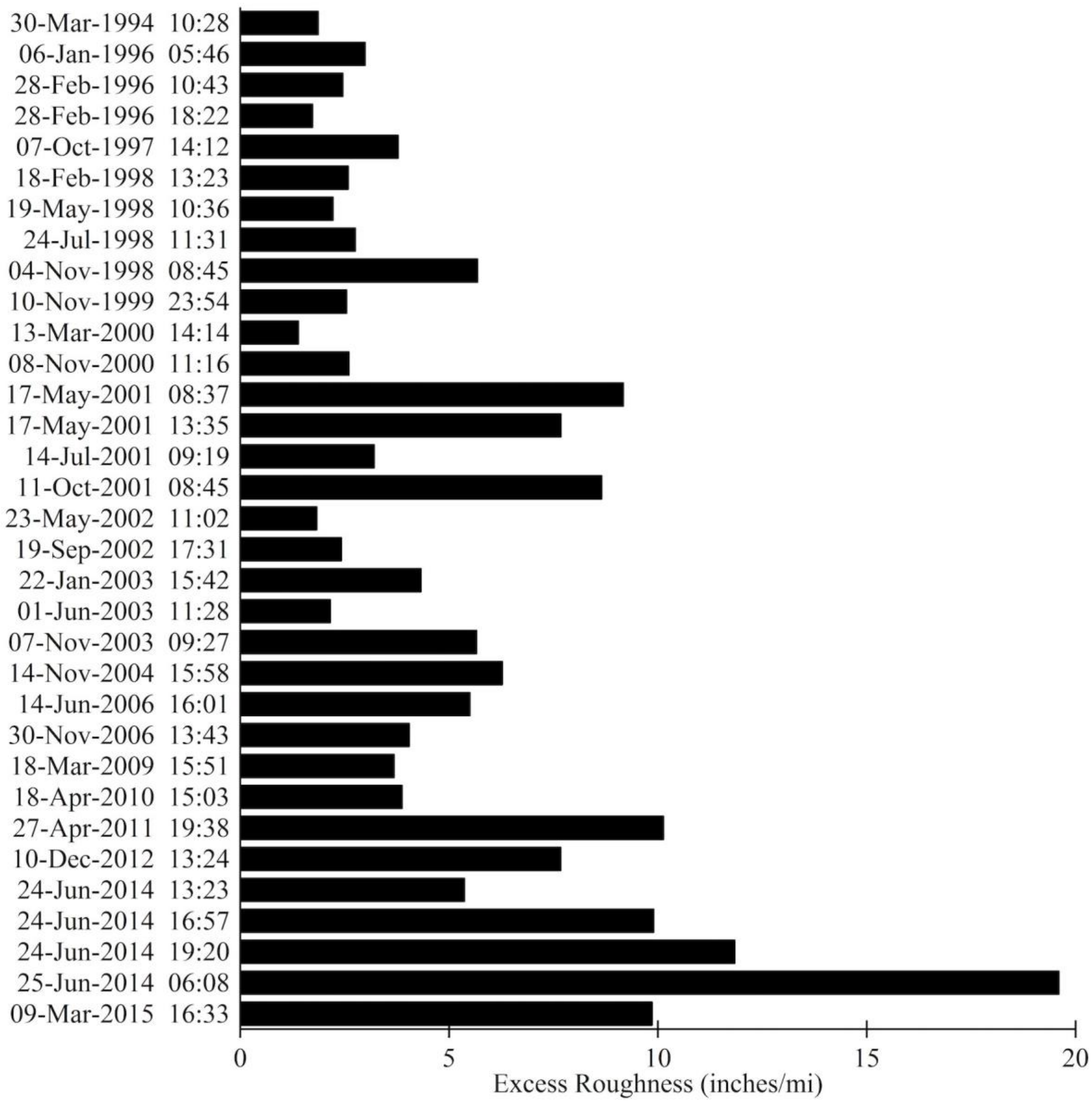

Source: FHWA.

Figure 388. Graph. ER of section 370208 for the right wheel path.

Figure 389 through Figure 391 characterize the long-term trend in ALR for the right wheel path of section 200201 using a base length of 25 ft and a roughness threshold of 125 inches/mi. Three ALRs exist within this section early in its life. Inspection of the profiles showed that ALRs were caused by a slope break between an area of decreasing elevation and a flat area at 170 ft, two narrow bumps in the range from 285 to 300 ft, and a slope break between an area of decreasing elevation and a flat area at 430 ft.

ALR length and ER increased unsteadily throughout the life of section 200201. Two distressed slabs with faulting caused ALRs in the last 50 ft of the section. Slabs in this area were replaced in 1995. Replacement slabs were not flush with the surrounding pavement and cracked transversely. The replacement slabs grew progressively rough until they were replaced in June 2002. (Note the corresponding growth and subsequent reduction in ER in Figure 391.)

The new replacement slabs also caused ALRs. Later in the monitoring history of section 200201, ALRs appear in the right wheel path at distressed joints and at the locations of the joint-repair patches used to address the distress.

Most slabs within section 200201 were curled downward during monitoring visits starting at 7.55 years of age, which caused an increase in ALR length for the midafternoon visits on 06-May-2014 and 05-May-2014 relative to the early morning visits on 06-May-2014. The change in ER for the same visit was proportionately smaller than the change in ALR length because the increased downward curl during the midafternoon visits caused additional ALRs to appear with roughness slightly above the 125-inch/mi threshold.

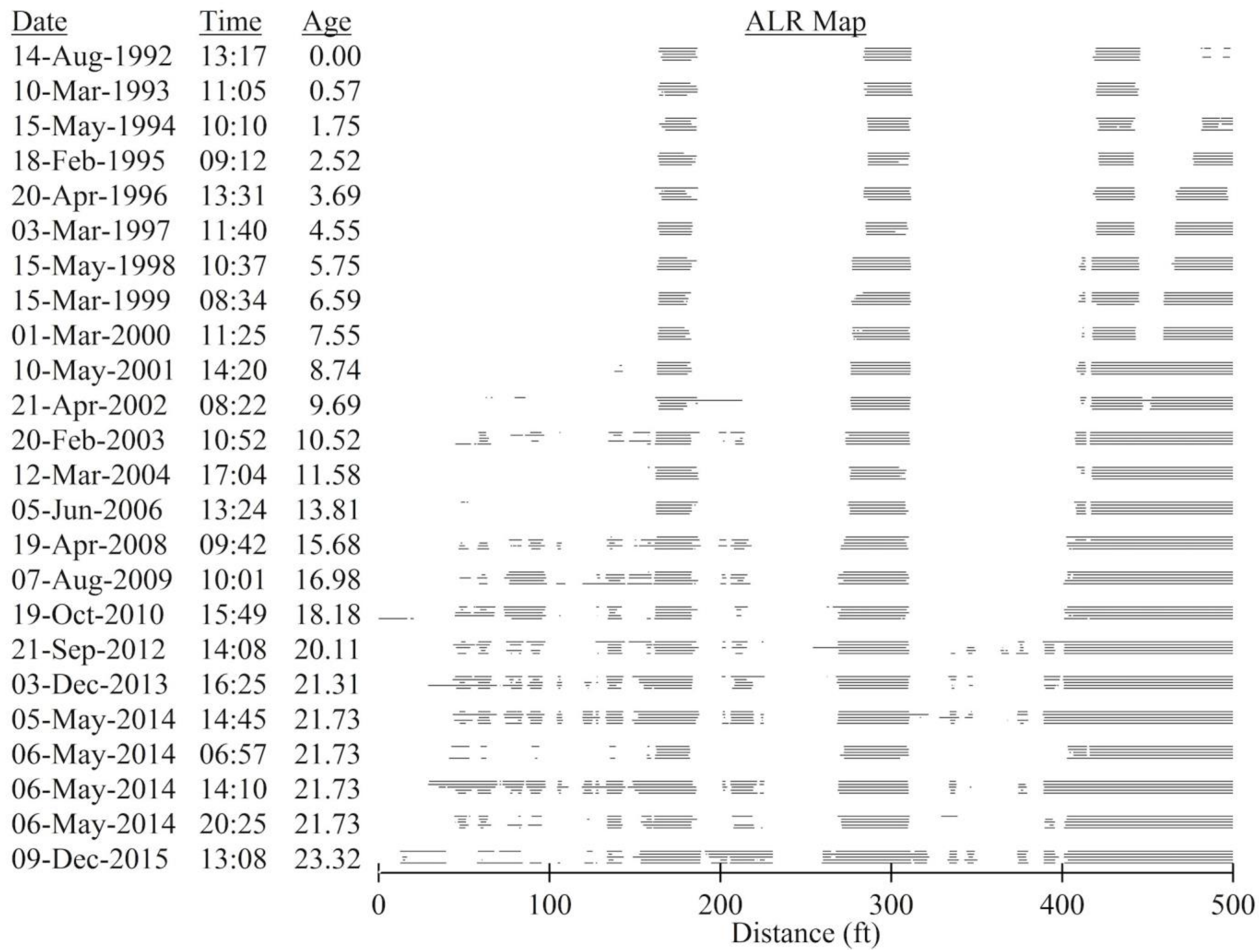

Source: FHWA.

Figure 389. Graph. ALR map of section 200201 for the right wheel path.

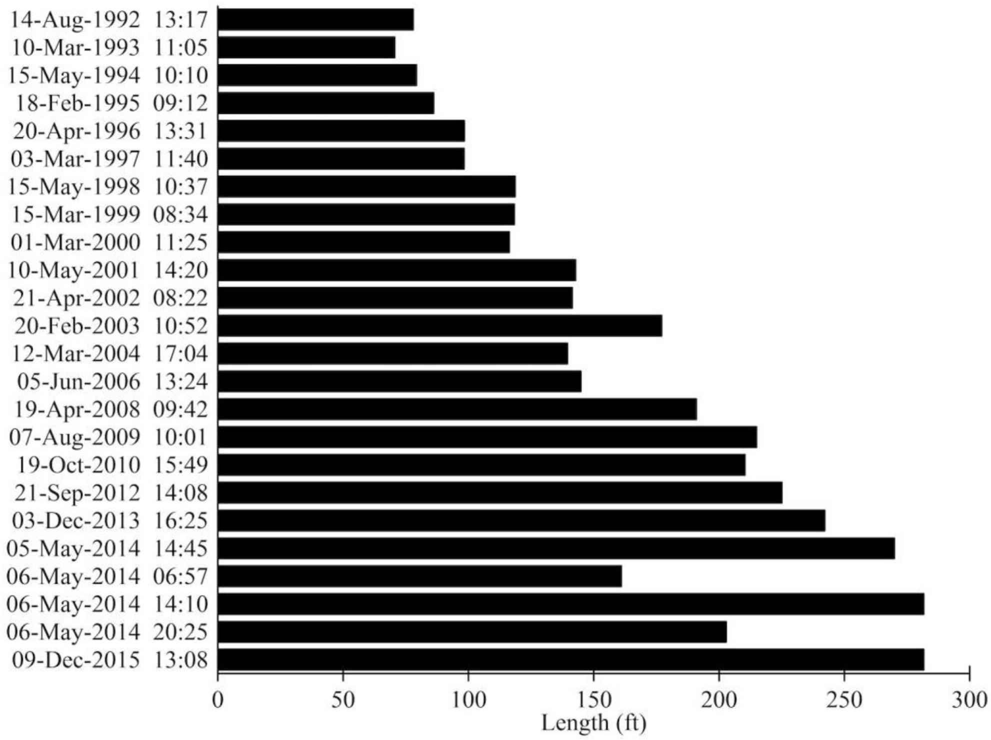

Source: FHWA.

Figure 390. Graph. Total ALR length of section 200201 for the right wheel path.

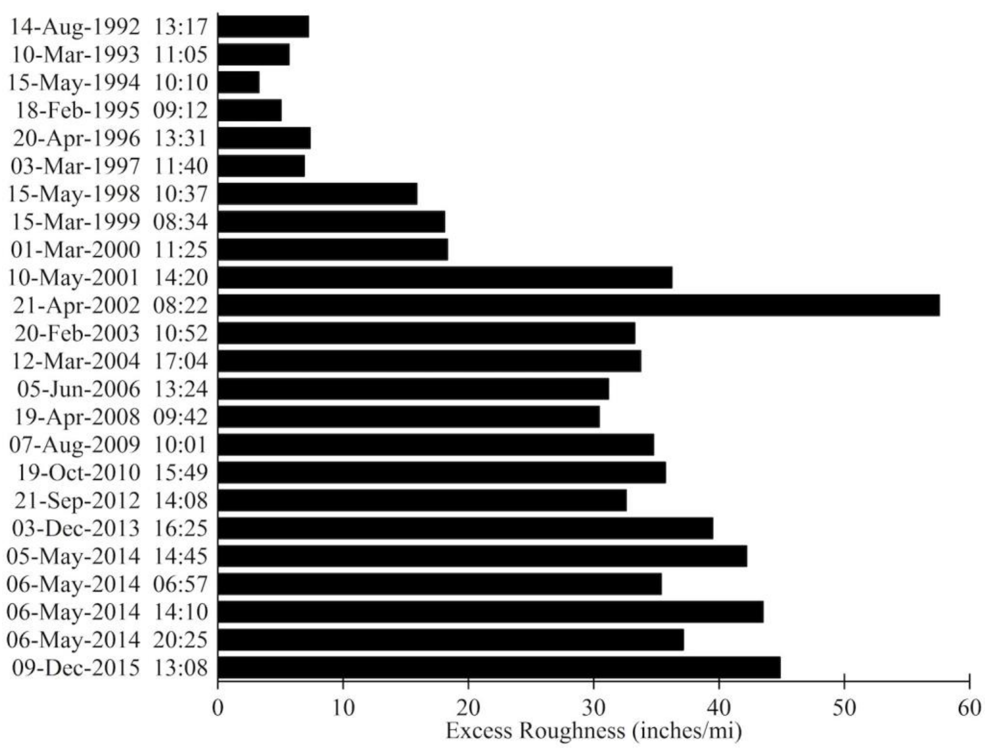

Source: FHWA.

Figure 391. Graph. ER of section 200201 for the right wheel path.

Figure 392 through Figure 394 characterize the long-term trend in ALR for the right wheel path of section 200205 using a base length of 25 ft and a roughness threshold of 125 inches/mi. This section included very little localized roughness early in its life, a somewhat steady increase over the first 12 years, then a more rapid increase after the first 12 years. A single slab with an elevation above the surrounding profile caused the largest ALR in the first 10 years of the history of section 200205.

A long-term increase in downward slab curl contributed to an increase in ALR in the second half of the monitoring history of section 200205. Distress at several joints and roughness at joint-repair patches placed in 2008, 2010, 2011, and 2014 contributed to an increase in ALR, including severe localized roughness in the right wheel path at a joint at 238 ft. Joint distress and joint-repair patches contributed to ER more than downward curl.

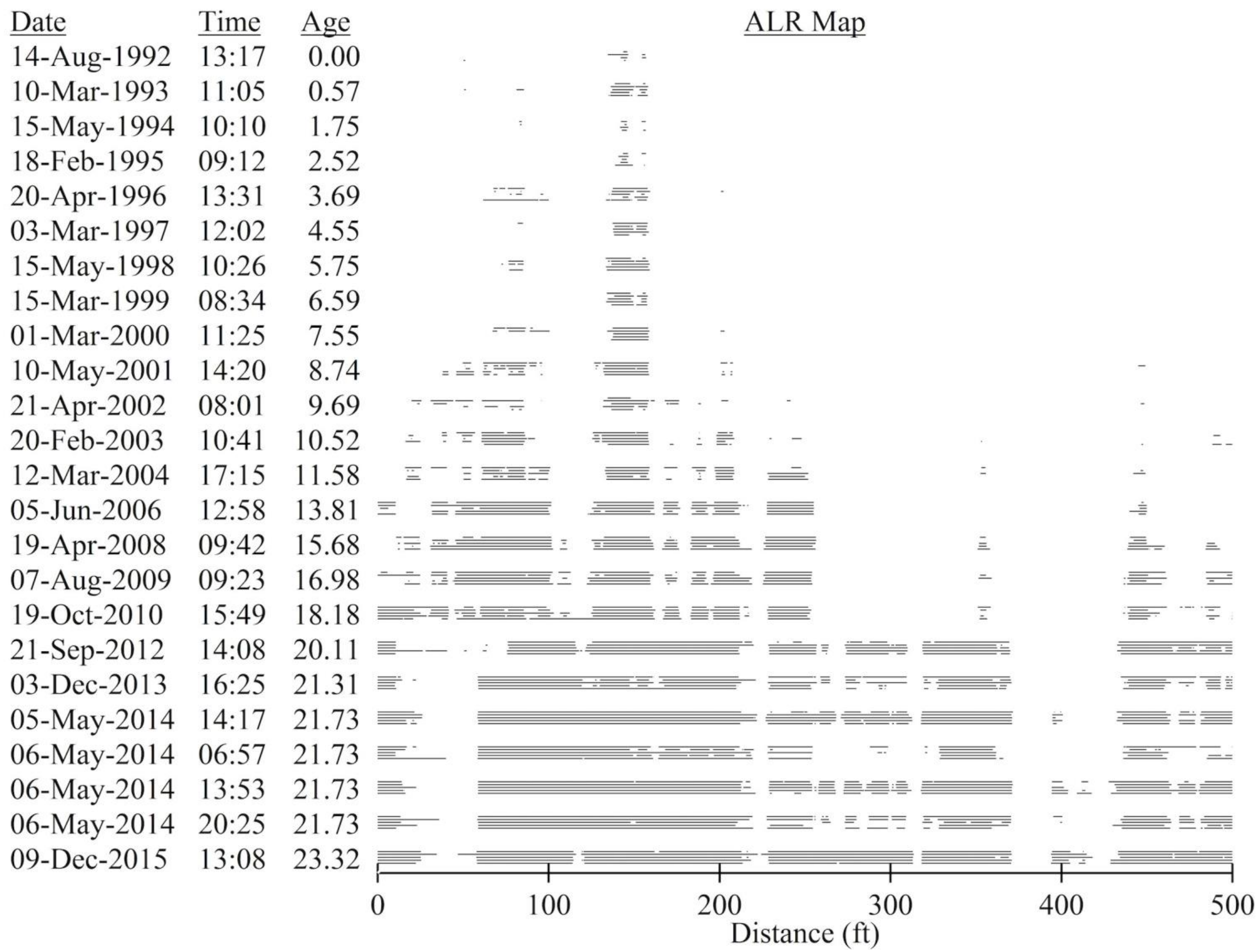

Source: FHWA.

Figure 392. Graph. ALR map of section 200205 for right wheel path.

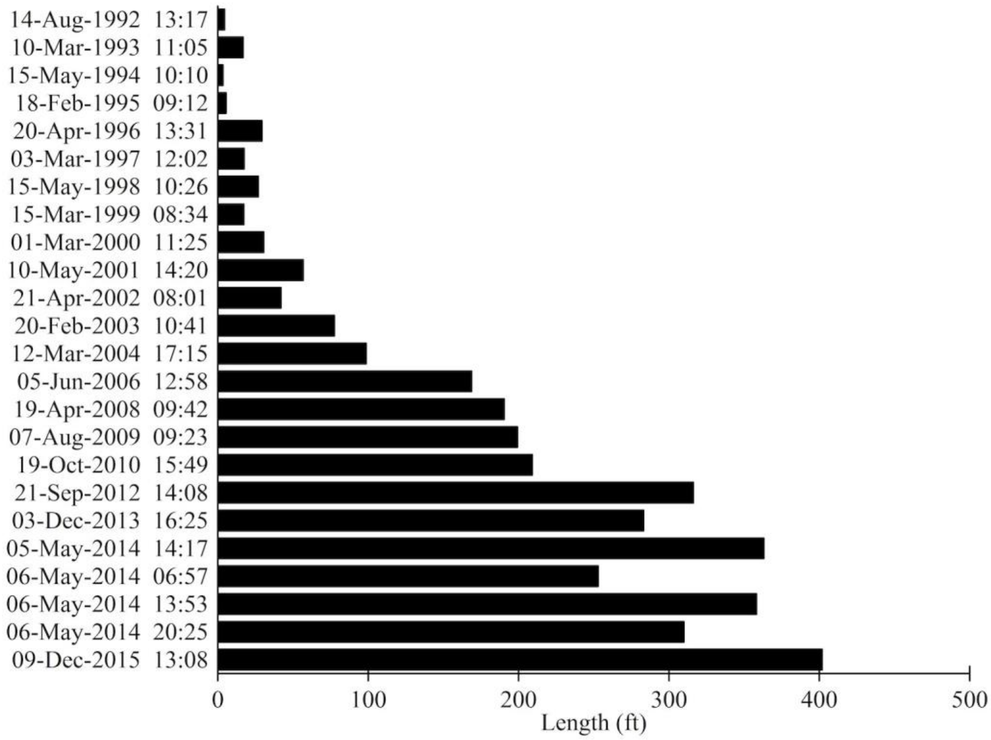

Source: FHWA.

Figure 393. Graph. Total ALR length of section 200205 for the right wheel path.

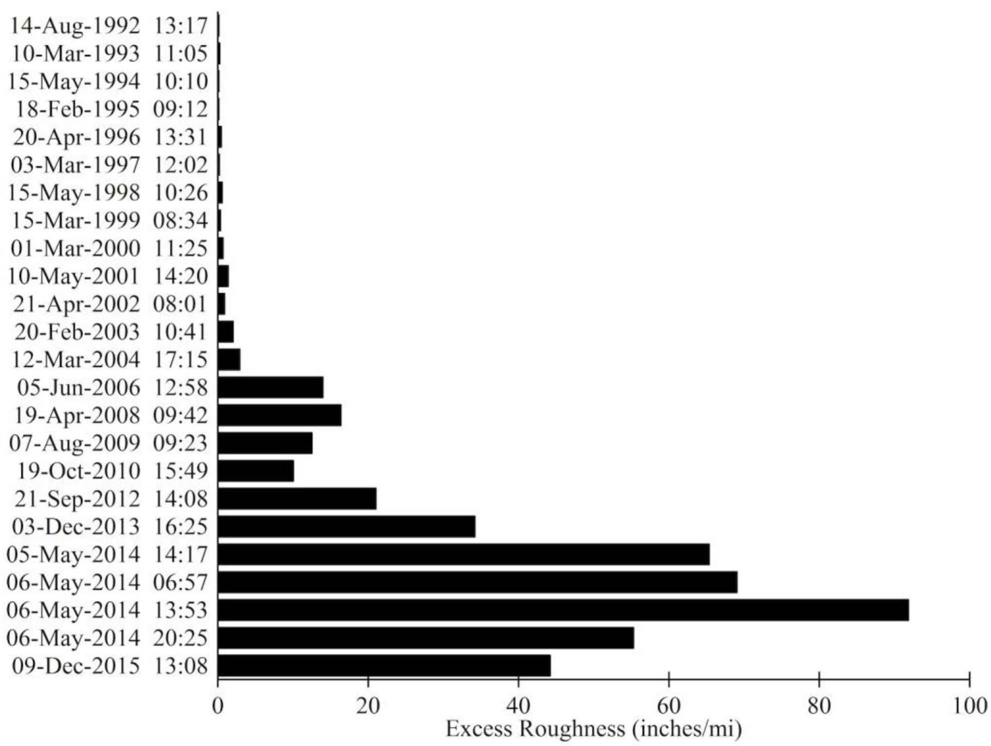

Source: FHWA.

Figure 394. Graph. ER of section 200205 for the right wheel path.

Figure 395 through Figure 397 characterize the long-term trend in ALR for the right wheel path of section 390209 using a base length of 25 ft and a roughness threshold of 125 inches/mi. This section included no ALR in the first monitoring visit and a modest increase in ALR length and ER in the first 10 years. The two ALRs in the first 10 years appeared in the presence of long-wavelength roughness (i.e., long dips that include areas with rapid changes in slope). However, the roughness in these locations did not violate the 125-inch/mi threshold until short-wavelength roughness (i.e., faulting at joints and midslab cracks) appears. Roughness at distressed joints, faulted midslab cracks, and joint-repair patches caused the large increase in ALR length and ER starting at an age of 11.81 years.

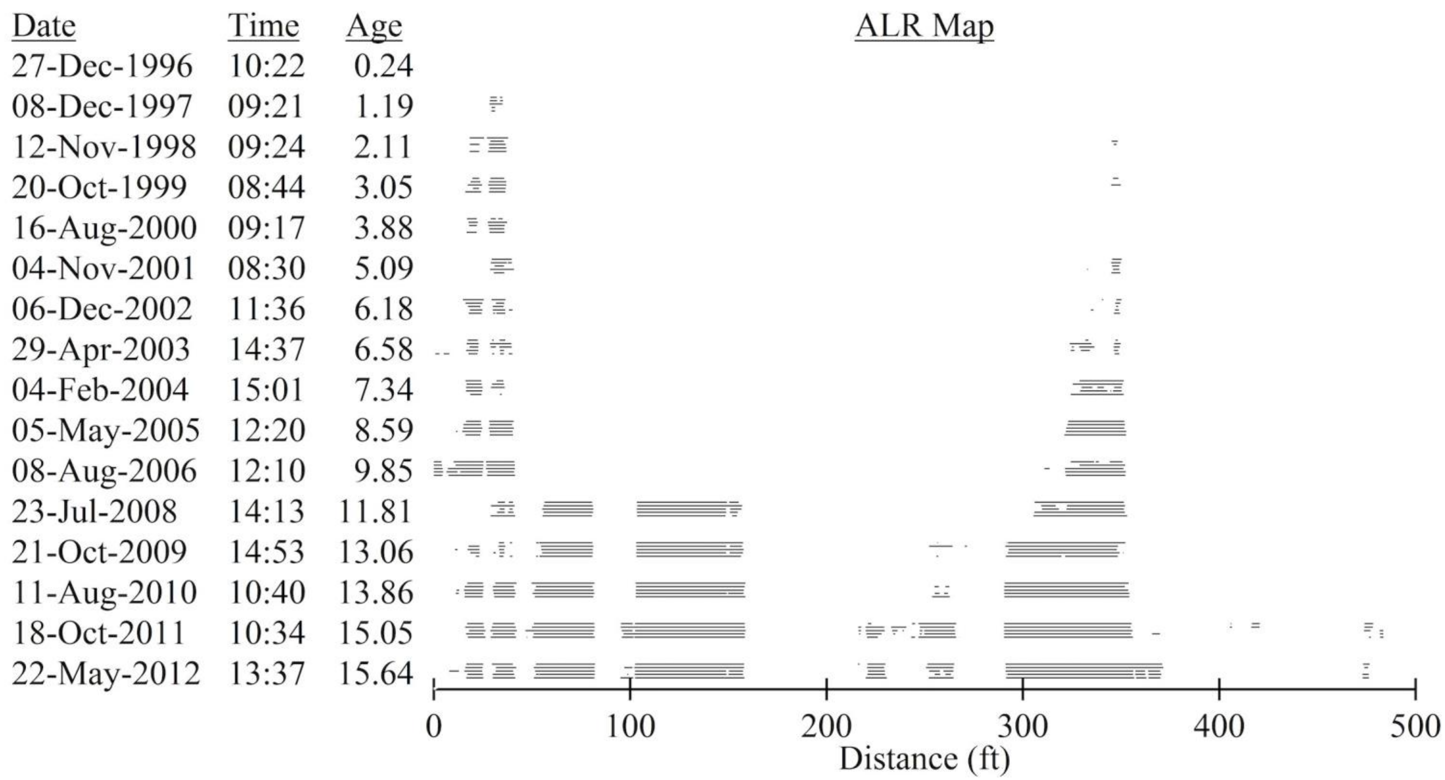

Source: FHWA.

Figure 395. Graph. ALR map of section 390209 for the right wheel path.

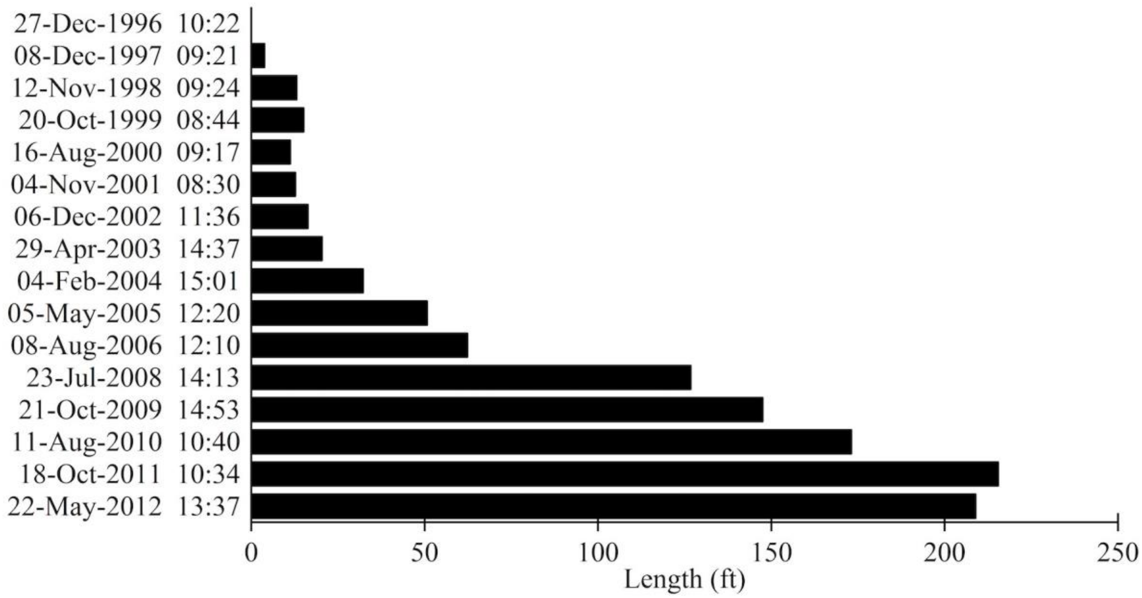

Source: FHWA.

Figure 396. Graph. Total ALR length of section 390209 for the right wheel path.

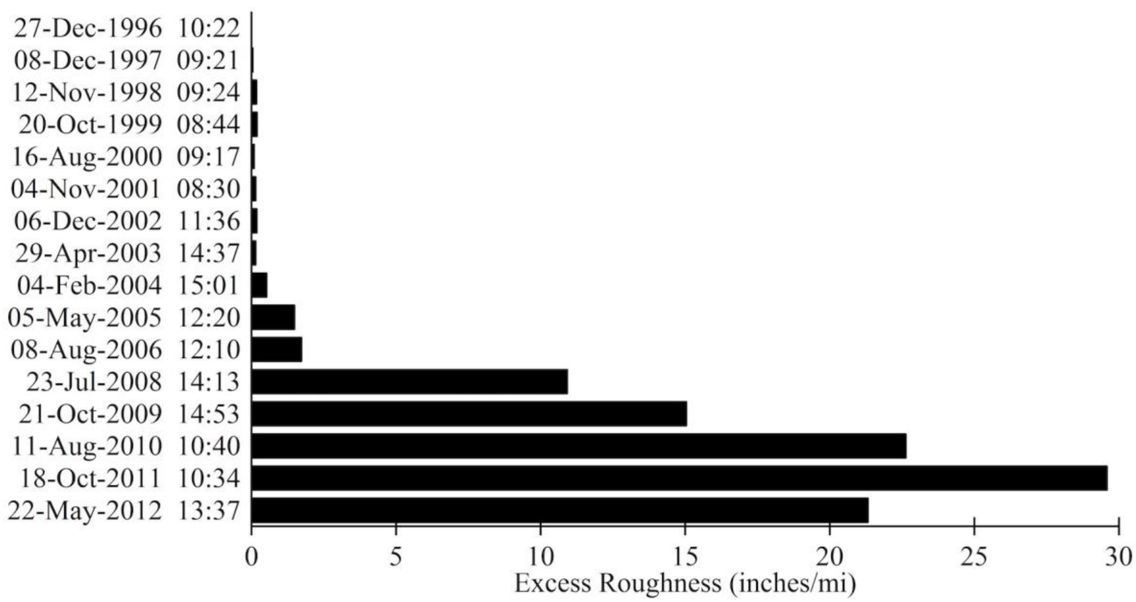

Source: FHWA.

Figure 397. Graph. ER of section 390209 for the right wheel path.

Figure 398 through Figure 400 characterize the long-term trend in ALR for the right wheel path of section 200209 using a base length of 25 ft and a roughness threshold of 125 inches/mi. Two ALRs of low severity appeared in this section throughout its monitoring history. Each ALR appeared at the trailing end of a slab with a larger level of downward curl than the surrounding slabs. Researchers are not clear if structural behavior and environmental conditions caused the downward curling at these slabs or if construction defects caused roughness to appear in the shape of downward curling in these locations.

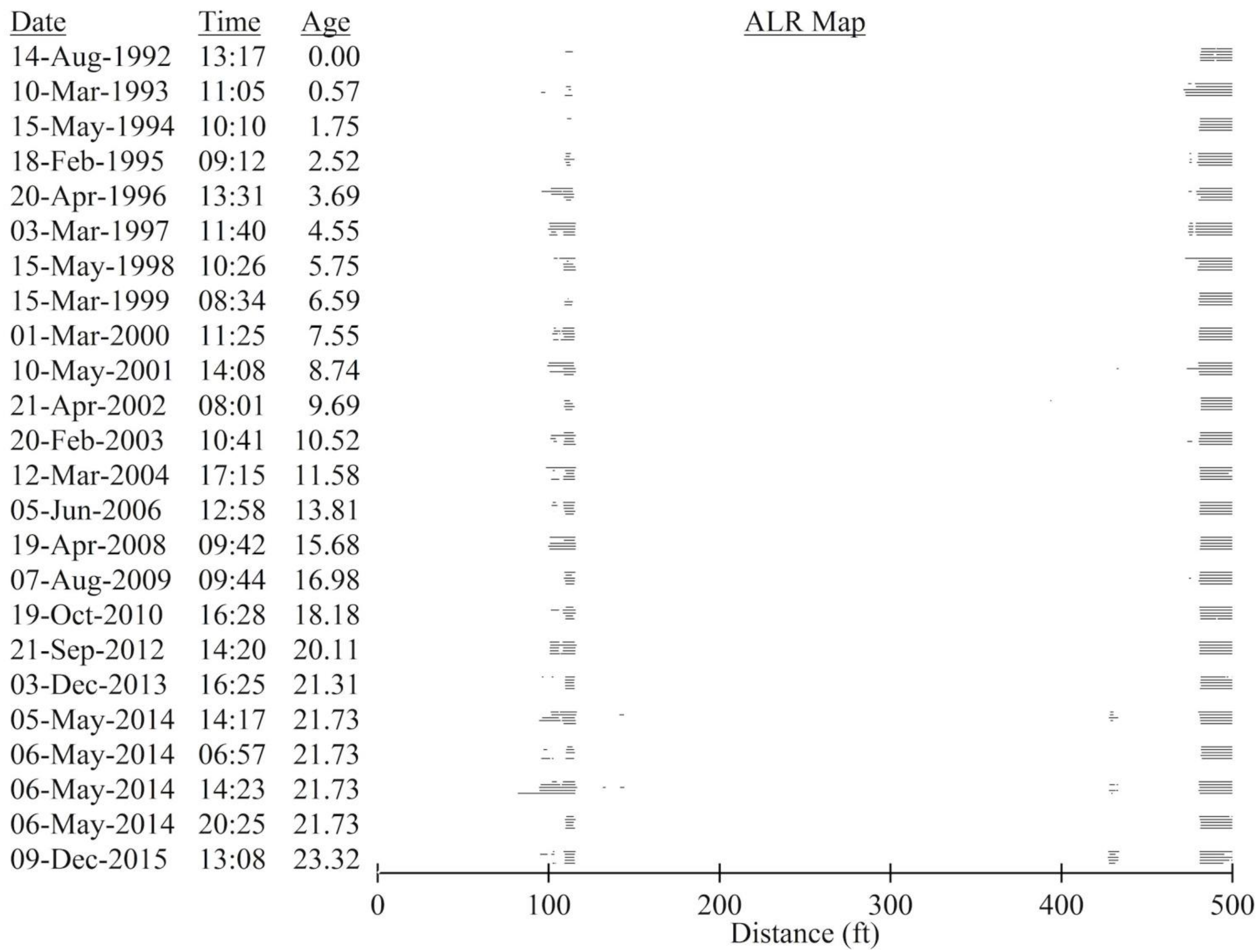

Source: FHWA.

Figure 398. Graph. ALR map of section 200209 for the right wheel path.

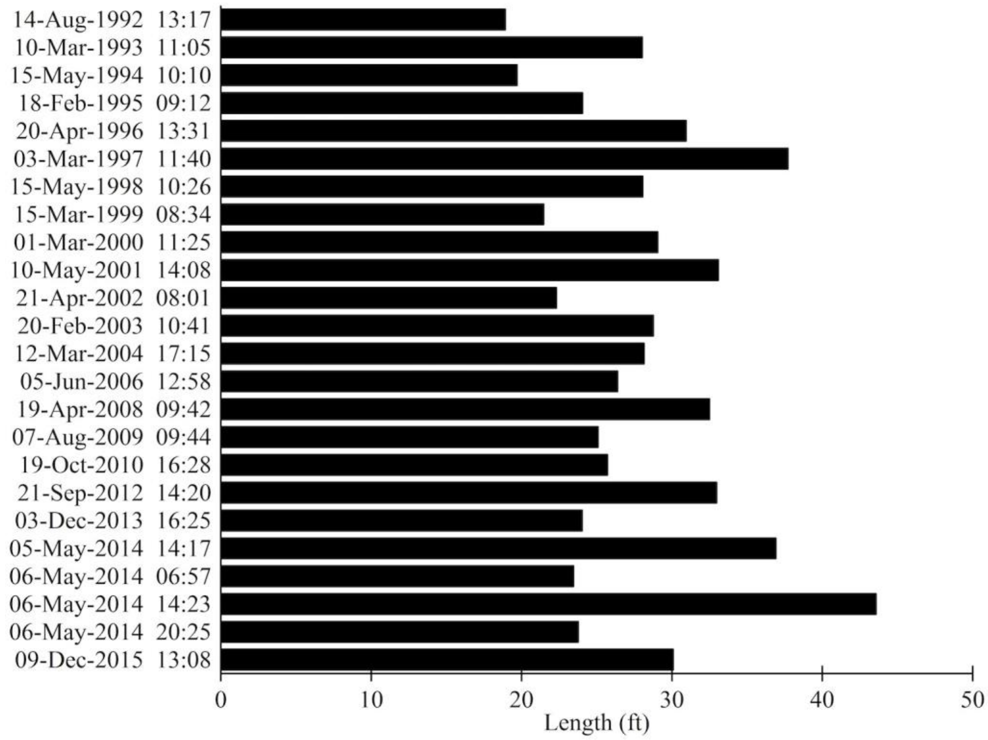

Source: FHWA.

Figure 399. Graph. Total ALR length of section 200209 for the right wheel path.

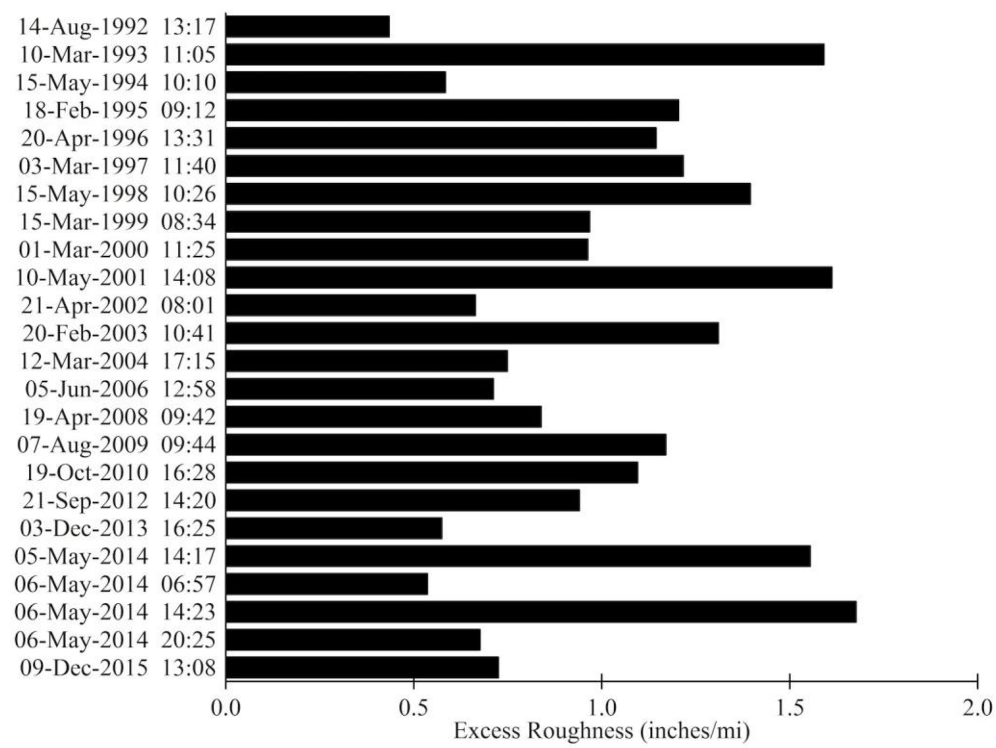

Source: FHWA.

Figure 400. Graph. ER of section 200209 for the right wheel path.

Figure 401 through Figure 403 characterize the long-term trend in ALRs for the right wheel path of section 370260 using a base length of 25 ft and a roughness threshold of 125 inches/mi. Two ALRs appeared early in the life of this section with length and severity that remained stable throughout the monitoring period. A narrow dip at 6 ft caused the ALR at the start of the section. This dip was not severe, and the peak value of the roughness profile was typically 130 to 135 inches/mi. A bump that is more than 0.25 inches high from 310 to 318 ft from the start of the section caused the other ALR. This feature consistently caused peaks in the roughness profile above 200 inches/mi, and it contributed heavily to ER as a result.

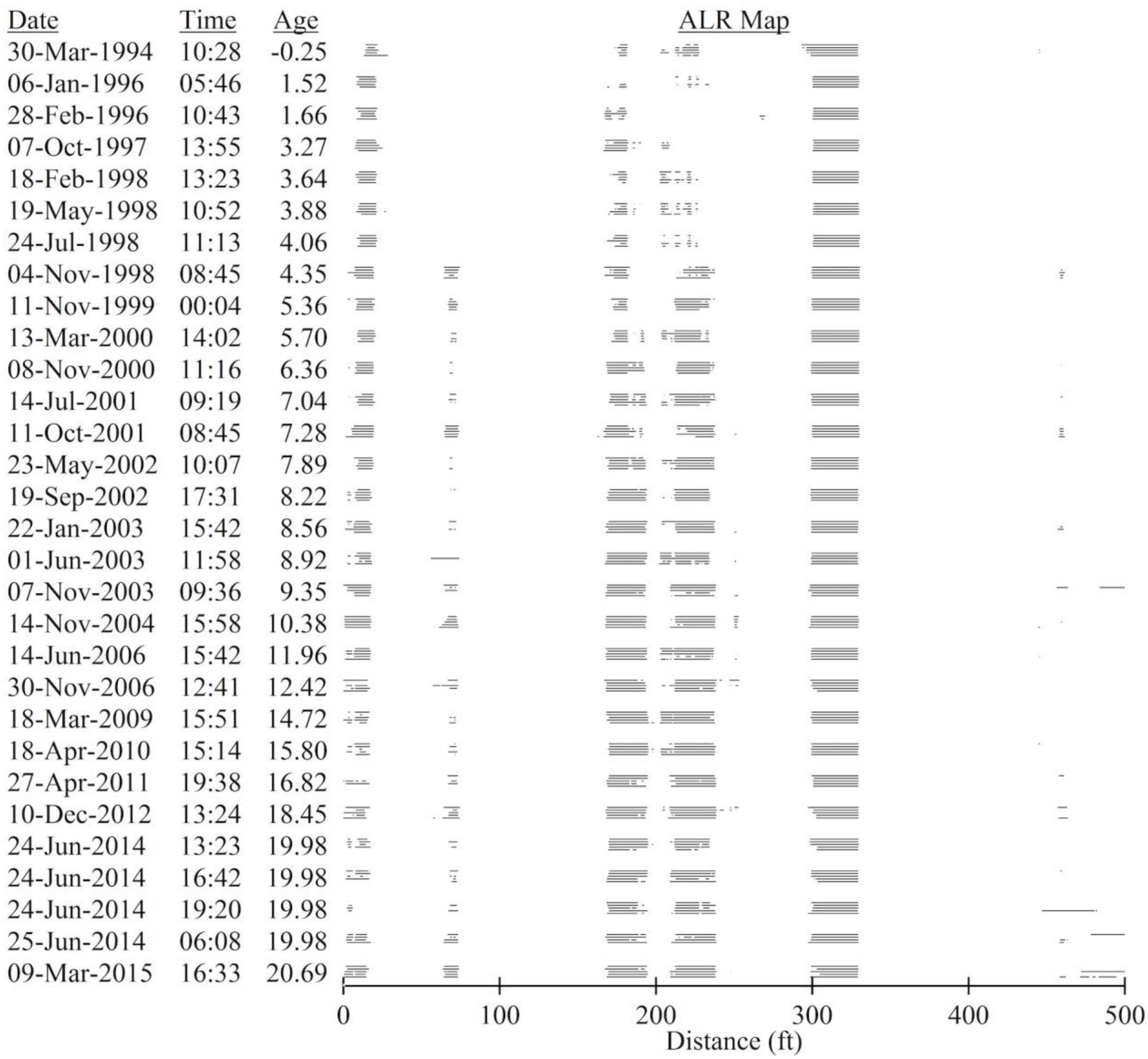

Source: FHWA.

Figure 401. Graph. ALR map of section 370260 for the right wheel path.

Two ALRs appear early in the life of this section that increase in length and severity over the first 8 years, then remain stable for the rest of the monitoring period. The specific source of roughness from 170 to 230 ft is less clear although distress surveys show transverse cracks and joint distress. One ALR appears starting 4.35 years into the life of this section and remains throughout the rest of the monitoring period. Roughness at this feature, however, is barely enough to violate the 125-inch/mi threshold.

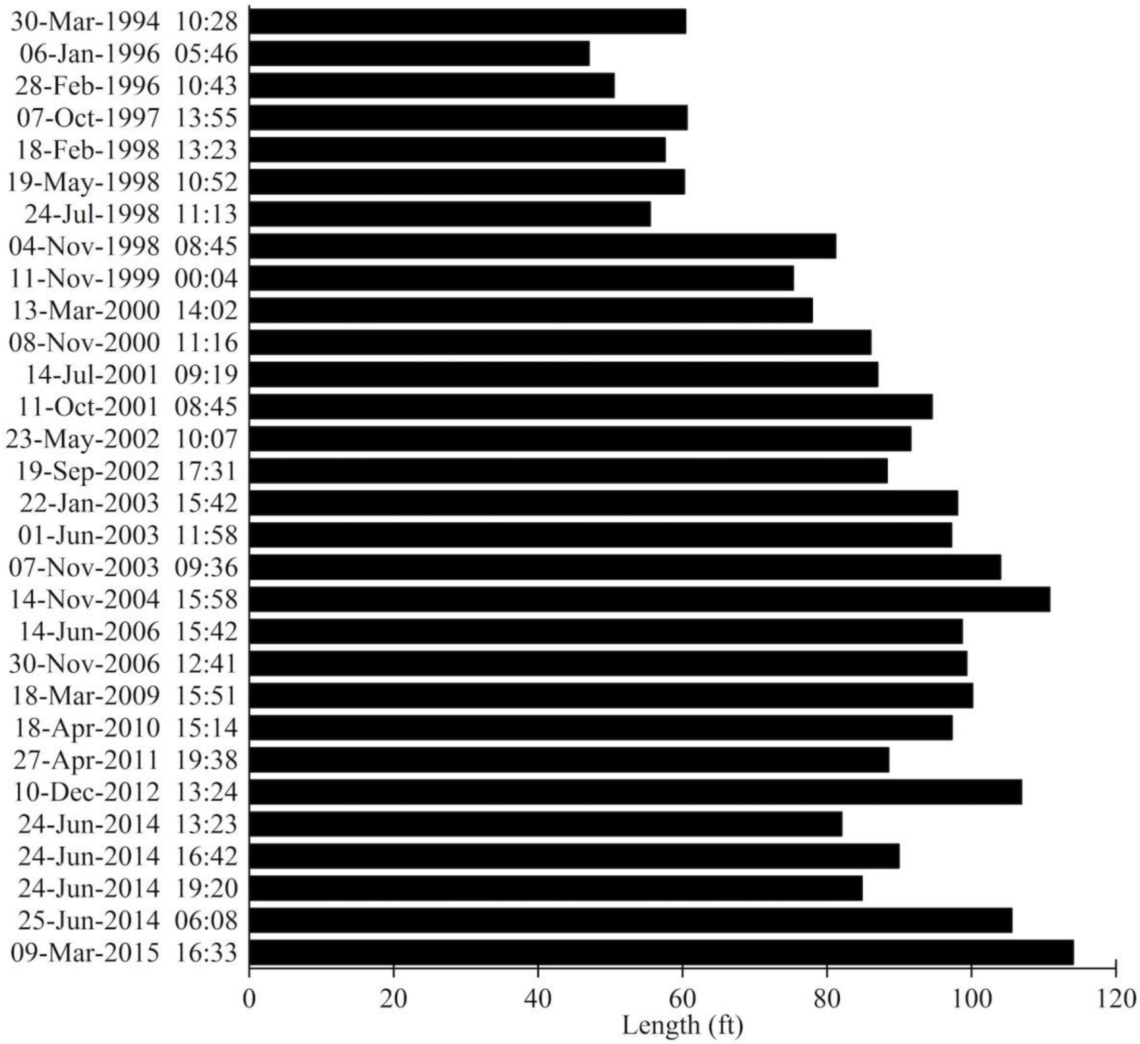

Source: FHWA.

Figure 402. Graph. Total ALR length of section 370260 for the right wheel path.

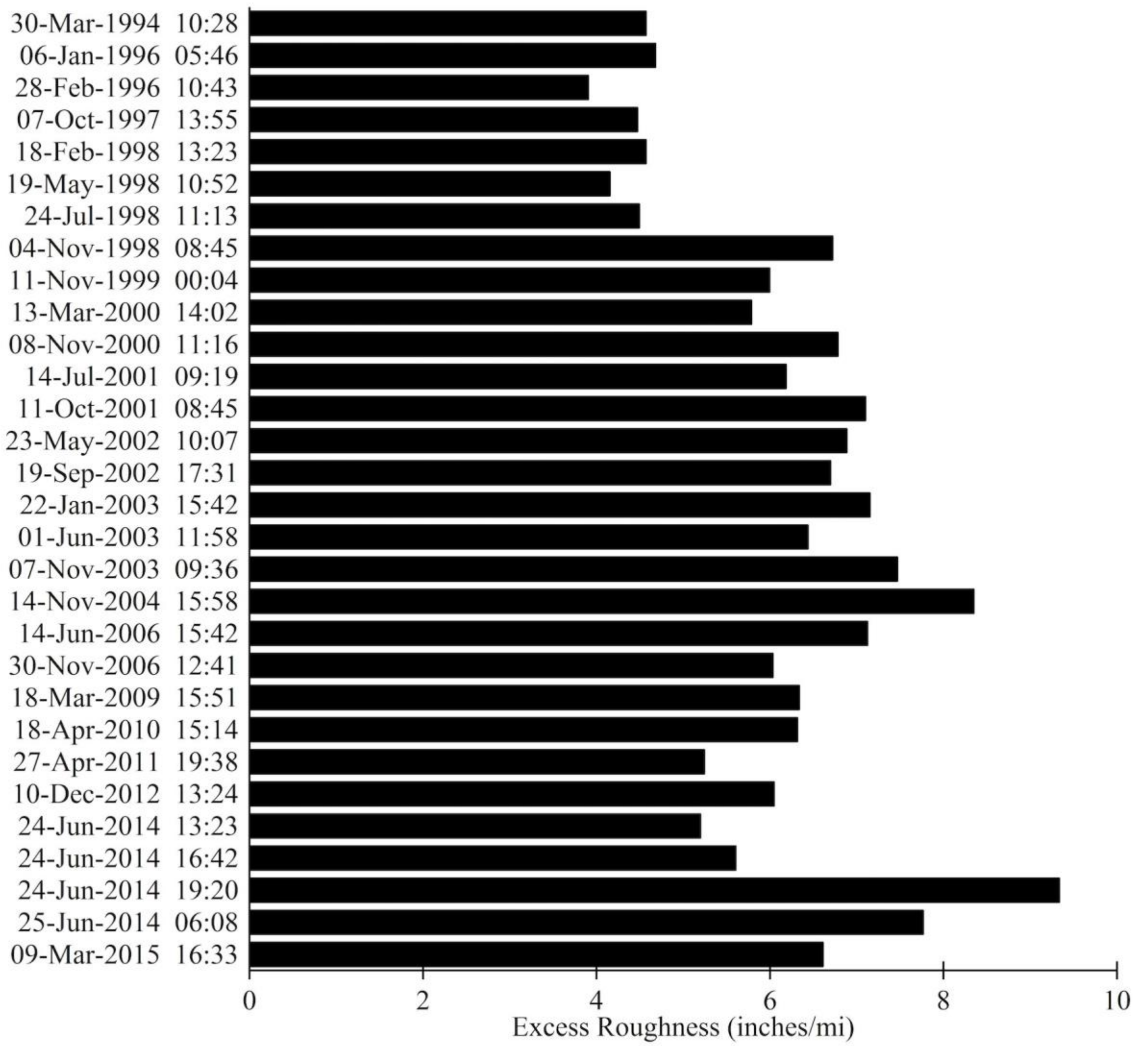

Source: FHWA.

Figure 403. Graph. ER of section 370260 for the right wheel path.

ALR REPEATABILITY

This section presents examples of ALR repeatability using profile measurements collected for the LTPP program. For most profile-monitoring visits, five repeat passes were selected for analysis from a larger set based on agreement in profile features that affect the IRI. Profiles from a specific section were aligned longitudinally over the monitoring history. The alignment process included longitudinal offset adjustment and application of a scale factor to the longitudinal distance interval to improve alignment over the entire length of the section. As such, disagreement within a set of repeat profile measurements corresponds to vertical measurement variations.

Table 70 through

Table 77 present relevant summary statistics for the eight sample sections discussed in the Long-Term Changes section. Repeatability is examined for total ALR length, ER, and ALR placement. The tables list the average IRI, average ALR length, and average ER for each profile-measurement visit. The tables also list the SD of each quantity. The values in the tables are based on five passes per visit except for some visits in 2014 collected for the study of diurnal changes.

ALR length and ER vary more than overall IRI relative to their average values (i.e., the SD of ALR length and ER is greater relative to their average values than overall IRI), which is particularly true when the length and severity of ALR is low or when ALRs appear in some repeat passes. Variations in ALR length and ER are consistent with the observation by Sayers that when using a short base length, the detail within a roughness profile is more difficult to reproduce than the overall IRI.[106]

Table 70 through

Table 77 list the ALR length common to all repeat passes within a given visit. The common length is the ALR length within a test section in which ALR was registered in every pass. Table 70 lists a value of 0.0 ft for the first visit to section 040223. The ALR map in Figure 380 shows that ALR appeared approximately 170 ft from the start of the section. However, the ALR only appeared in four of the five passes. In contrast, ALR appeared in all five passes in the fourth visit, with 8.2 ft of mutual overlap. Figure 380, Figure 383, Figure 386, Figure 389, Figure 392, Figure 395, Figure 398, and Figure 401 show ALR maps that correspond to the "common ALR length (ft)" columns in Table 70 through

Table 77. Typically, ALR with higher severity (i.e., greater ER) registered ALR length more consistently than ALR with peak values barely above the threshold value.

Table 70. ALR repeatability of section 040223 for the right wheel path at 125 inches/mi.

Date	Time	Passes	Average IRI (Inches/mi)	IRI SD (Inches/mi)	Average ALR Length (ft)	ALR Length SD (ft)	Common ALR Length (ft)	Average ER (Inches/mi)	ER SD (Inches/mi)
25-Jan-1994	06:10	5	81.2	2.8	10.0	5.4	0.0	0.2	0.1
05-Mar-1995	11:21	5	80.1	1.5	10.6	7.5	0.0	0.1	0.1
27-Jan-1997	12:01	5	84.8	1.1	10.0	5.3	1.8	0.1	0.1
04-Dec-1997	11:06	5	88.3	2.0	13.1	2.7	8.2	0.2	0.1
08-Dec-1998	10:28	5	92.1	1.3	16.0	4.0	9.0	0.3	0.1
15-Nov-1999	11:38	5	95.4	1.3	32.2	8.6	8.5	0.4	0.2
30-Nov-2000	13:37	5	94.0	0.8	27.1	5.1	17.7	0.5	0.1
08-Nov-2001	11:38	5	99.5	1.0	46.2	3.1	28.6	0.9	0.1
30-Oct-2002	12:55	5	88.6	0.6	9.7	4.3	0.6	0.1	0.1
04-Feb-2004	13:57	5	85.5	1.1	8.8	6.6	0.0	0.0	0.0
12-Dec-2004	17:28	5	99.1	1.0	36.4	10.8	6.8	0.5	0.2
13-Aug-2006	00:24	5	120.8	1.1	213.2	18.2	153.5	5.9	0.7
13-Dec-2007	12:08	5	96.6	1.9	38.4	7.6	6.6	0.4	0.1
20-Sep-2008	02:27	5	118.9	0.7	198.8	17.0	133.1	5.8	0.5
25-Jan-2010	18:00	5	103.2	1.0	65.2	8.7	22.0	0.9	0.2
08-Dec-2011	21:26	5	110.2	1.2	118.0	15.3	72.1	2.8	0.4
16-Dec-2012	19:46	5	107.6	0.8	105.3	6.8	71.0	2.3	0.1
06-Feb-2014	23:02	5	111.5	0.4	124.8	4.2	92.0	3.0	0.1
07-Feb-2014	08:39	3	111.0	2.0	143.3	12.8	0.0	3.2	0.8
07-Feb-2014	12:48	3	106.0	0.7	79.1	4.3	0.0	1.3	0.2
07-Feb-2014	16:21	3	94.3	1.1	35.3	7.7	0.0	0.7	0.2
14-Nov-2014	01:29	5	105.4	0.9	76.0	6.7	39.2	1.4	0.1
07-Dec-2015	18:23	5	99.3	2.0	41.4	13.6	23.2	0.8	0.2

Table 71. ALR repeatability of section 370202 for the right wheel path at 125 inches/mi.

Date	Time	Passes	Average IRI (Inches/mi)	IRI SD (Inches/mi)	Average ALR Length (ft)	ALR Length SD (ft)	Common ALR Length (ft)	Average ER (Inches/mi)	ER SD (Inches/mi)
30-Mar-1994	10:28	5	85.8	0.7	13.5	2.4	7.1	0.2	0.0
06-Jan-1996	05:46	5	86.3	0.9	8.1	2.3	1.0	0.1	0.0
28-Feb-1996	10:58	5	86.5	1.1	13.1	4.5	5.0	0.2	0.0
07-Oct-1997	13:36	5	84.1	0.8	5.7	0.9	3.4	0.1	0.0
18-Feb-1998	13:57	5	84.5	0.7	5.2	2.5	1.6	0.1	0.0
19-May-1998	10:36	5	83.4	1.1	3.7	3.9	0.0	0.0	0.0
24-Jul-1998	12:02	5	83.5	1.3	4.2	3.5	0.0	0.0	0.0
04-Nov-1998	08:45	5	112.5	1.5	126.2	8.6	78.8	2.4	0.3
10-Nov-1999	23:54	5	97.3	0.9	18.0	3.2	10.7	0.3	0.1
13-Mar-2000	14:02	5	87.3	1.2	10.5	3.6	4.7	0.1	0.0
08-Nov-2000	11:28	5	98.7	1.6	27.7	8.5	10.1	0.3	0.1
14-Jul-2001	09:11	5	111.0	2.5	111.3	17.7	64.6	2.4	0.4
11-Oct-2001	08:45	5	123.1	2.7	219.6	30.4	154.8	6.8	1.4
23-May-2002	11:02	5	98.9	2.5	30.6	10.5	12.2	0.4	0.1
19-Sep-2002	17:48	5	107.9	3.0	97.6	26.9	47.6	1.7	0.7
22-Jan-2003	15:42	5	102.7	2.0	45.2	12.5	17.4	0.6	0.2
01-Jun-2003	11:38	5	93.1	1.4	16.2	4.3	8.6	0.3	0.1

Table 72. ALR repeatability of section 200201 for the right wheel path at 125 inches/mi.

Date	Time	Passes	Average IRI (Inches/mi)	IRI SD (Inches/mi)	Average ALR Length (ft)	ALR Length SD (ft)	Common ALR Length (ft)	Average ER (Inches/mi)	ER SD (Inches/mi)
14-Aug-1992	13:17	5	86.4	1.3	78.3	6.0	69.4	7.3	0.3
10-Mar-1993	11:05	5	87.0	3.9	70.9	3.1	61.5	5.7	0.7
15-May-1994	10:10	5	78.7	2.0	79.6	4.9	65.5	3.3	0.8
18-Feb-1995	09:12	5	81.3	0.7	86.4	3.4	75.3	5.1	0.5
20-Apr-1996	13:31	5	90.6	1.2	98.7	2.9	87.2	7.4	0.5
03-Mar-1997	11:40	5	89.1	1.5	98.6	3.0	90.8	7.0	0.5
15-May-1998	10:37	5	104.9	1.9	119.0	2.6	112.6	15.9	0.3
15-Mar-1999	08:34	5	105.8	3.3	118.6	3.5	104.6	18.1	1.1
01-Mar-2000	11:25	5	108.2	0.9	116.6	2.7	108.9	18.4	0.7
10-May-2001	14:20	5	132.3	1.9	143.0	3.6	137.6	36.3	0.4
21-Apr-2002	08:22	5	155.4	4.4	141.7	16.4	124.6	57.6	1.7
20-Feb-2003	10:52	5	134.6	1.5	177.4	13.7	148.4	33.3	0.6
12-Mar-2004	17:04	5	127.3	1.6	139.8	2.2	130.4	33.8	0.7
05-Jun-2006	13:24	5	126.7	1.0	145.1	3.3	140.0	31.2	1.1
19-Apr-2008	09:42	5	136.5	2.3	191.2	22.3	145.9	30.5	0.9
07-Aug-2009	10:01	5	140.8	3.1	215.3	27.5	173.3	34.8	1.3
19-Oct-2010	15:49	5	143.8	2.0	210.6	8.6	173.7	35.8	1.0
21-Sep-2012	14:08	5	144.1	1.7	225.3	16.0	176.9	32.6	1.3
03-Dec-2013	16:25	5	151.1	2.5	242.5	19.5	195.3	39.5	1.3
05-May-2014	14:45	5	156.1	1.0	270.2	15.0	231.4	42.3	0.4
06-May-2014	06:57	5	137.0	2.1	161.2	11.2	143.2	35.4	1.9
06-May-2014	14:10	5	156.8	2.7	282.0	23.4	234.6	43.6	1.6
06-May-2014	20:25	5	145.5	1.9	203.2	13.2	173.5	37.2	1.6
09-Dec-2015	13:08	5	160.2	3.7	282.0	32.1	228.2	44.9	2.8

Table 73. ALR repeatability of section 370208 for the right wheel path at 160 inches/mi.

Date	Time	Passes	Average IRI (Inches/mi)	IRI SD (Inches/mi)	Average ALR Length (ft)	ALR Length SD (ft)	Common ALR Length (ft)	Average ER (Inches/mi)	ER SD (Inches/mi)
30-Mar-1994	10:28	5	110.2	7.2	43.5	12.1	21.9	1.9	0.8
06-Jan-1996	05:46	5	124.1	1.0	72.5	7.2	52.5	3.0	0.3
28-Feb-1996	10:43	5	118.5	1.1	58.2	3.6	46.9	2.5	0.3
28-Feb-1996	18:22	5	114.2	1.2	44.4	10.1	28.1	1.8	0.4
07-Oct-1997	14:12	5	123.2	2.2	79.6	9.2	60.3	3.8	0.3
18-Feb-1998	13:23	5	122.8	2.0	77.7	11.3	50.5	2.6	0.5
19-May-1998	10:36	5	120.9	1.4	73.5	10.1	33.8	2.2	0.3
24-Jul-1998	11:31	5	124.0	2.9	81.2	8.3	53.7	2.8	0.4
04-Nov-1998	08:45	5	137.6	2.1	137.9	10.8	86.4	5.7	0.3
10-Nov-1999	23:54	5	123.7	2.6	81.1	7.3	39.2	2.6	0.3
13-Mar-2000	14:14	5	114.0	3.1	34.3	5.5	18.0	1.4	0.2
08-Nov-2000	11:16	5	125.9	1.1	81.4	4.8	46.4	2.6	0.3
17-May-2001	08:37	5	143.1	2.0	154.0	14.7	131.1	9.2	1.0
17-May-2001	13:35	5	139.2	2.4	135.3	10.5	103.0	7.7	1.2
14-Jul-2001	09:19	5	127.3	3.9	83.2	15.6	39.2	3.2	0.6
11-Oct-2001	08:45	5	140.5	1.3	143.4	6.9	119.8	8.7	1.2
23-May-2002	11:02	5	119.3	1.6	53.8	5.2	15.6	1.8	0.3
19-Sep-2002	17:31	5	125.4	3.5	68.7	20.6	24.6	2.4	0.8
22-Jan-2003	15:42	5	133.5	2.3	109.6	5.8	78.6	4.3	0.8
01-Jun-2003	11:28	5	124.3	1.6	75.4	9.4	45.3	2.2	0.4
07-Nov-2003	09:27	5	139.4	0.8	127.7	15.7	78.8	5.7	0.2
14-Nov-2004	15:58	5	142.6	2.5	151.6	14.6	106.3	6.3	0.8
14-Jun-2006	16:01	5	139.0	2.3	129.6	15.4	73.5	5.5	0.9
30-Nov-2006	13:43	5	126.4	4.7	80.0	20.1	48.5	4.1	0.5
18-Mar-2009	15:51	5	131.6	1.1	102.2	8.2	74.0	3.7	0.4
18-Apr-2010	15:03	5	132.4	1.6	100.9	10.9	64.1	3.9	0.4
27-Apr-2011	19:38	5	149.5	1.2	175.8	9.7	132.3	10.2	0.6
10-Dec-2012	13:24	5	146.2	3.1	149.2	19.4	92.8	7.7	0.5
24-Jun-2014	13:23	5	138.4	4.2	107.3	23.8	52.0	5.4	0.9
24-Jun-2014	16:57	5	152.4	3.2	191.1	27.5	128.5	9.9	1.1
24-Jun-2014	19:20	5	155.8	1.1	199.1	13.2	136.7	11.9	0.8
25-Jun-2014	06:08	4	170.1	2.2	314.2	12.3	0.0	19.6	1.6
09-Mar-2015	16:33	5	147.7	1.6	178.7	11.2	119.4	9.9	1.3

Table 74. ALR repeatability of section 200205 for the right wheel path at 125 inches/mi.

Date	Time	Passes	Average IRI (Inches/mi)	IRI SD (Inches/mi)	Average ALR Length (ft)	ALR Length SD (ft)	Common ALR Length (ft)	Average ER (Inches/mi)	ER SD (Inches/mi)
14-Aug-1992	13:17	5	76.8	1.7	5.0	5.0	0.0	0.1	0.1
10-Mar-1993	11:05	5	83.2	3.1	17.4	4.7	10.0	0.4	0.1
15-May-1994	10:10	5	76.7	0.7	3.9	2.5	0.0	0.0	0.0
18-Feb-1995	09:12	5	75.2	1.0	6.0	2.7	2.3	0.1	0.1
20-Apr-1996	13:31	5	85.9	3.8	29.8	16.2	5.5	0.6	0.3
03-Mar-1997	12:02	5	82.8	0.9	18.0	4.4	10.7	0.3	0.1
15-May-1998	10:26	5	81.0	2.2	27.4	6.0	13.8	0.7	0.2
15-Mar-1999	08:34	5	80.6	0.9	17.8	1.4	11.5	0.4	0.1
01-Mar-2000	11:25	5	86.7	2.3	31.0	12.5	20.4	0.8	0.3
10-May-2001	14:20	5	94.9	1.0	57.3	9.7	30.4	1.5	0.3
21-Apr-2002	08:01	5	90.9	6.2	42.5	30.3	11.4	1.0	0.7
20-Feb-2003	10:41	5	99.7	1.9	78.0	4.3	48.9	2.1	0.4
12-Mar-2004	17:15	5	101.6	2.7	99.1	22.3	42.5	3.0	0.9
05-Jun-2006	12:58	5	118.0	1.1	169.2	13.4	125.1	14.1	1.3
19-Apr-2008	09:42	5	126.0	4.3	191.0	25.2	131.0	16.5	2.1
07-Aug-2009	09:23	5	121.4	2.1	199.7	16.8	137.9	12.6	1.1
19-Oct-2010	15:49	5	120.0	1.4	209.7	12.1	155.3	10.1	0.7
21-Sep-2012	14:08	5	137.3	4.1	316.8	24.3	252.8	21.1	2.7
03-Dec-2013	16:25	5	150.3	5.4	283.6	41.5	202.2	34.3	4.0
05-May-2014	14:17	5	185.3	7.2	363.6	20.6	309.2	65.5	7.4
06-May-2014	06:57	5	181.3	20.9	253.4	41.4	178.0	69.1	22.3
06-May-2014	13:53	5	212.2	19.3	358.7	11.9	305.8	91.9	19.3
06-May-2014	20:25	5	171.7	4.5	310.4	34.0	221.0	55.4	4.6
09-Dec-2015	13:08	5	165.6	5.3	402.3	17.4	371.4	44.3	4.7

Table 75. ALR repeatability of section 390209 for the right wheel path at 125 inches/mi.

Date	Time	Passes	Average IRI (Inches/mi)	IRI SD (Inches/mi)	Average ALR Length (ft)	ALR Length SD (ft)	Common ALR Length (ft)	Average ER (Inches/mi)	ER SD (Inches/mi)
27-Dec-1996	10:22	5	61.7	0.6	0.0	0.0	0.0	0.0	0.0
08-Dec-1997	09:21	5	62.8	0.3	4.1	1.8	1.9	0.0	0.0
12-Nov-1998	09:24	5	68.5	1.4	13.3	3.4	6.9	0.2	0.1
20-Oct-1999	08:44	5	70.6	1.3	15.4	3.4	10.2	0.2	0.1
16-Aug-2000	09:17	5	66.4	0.6	11.5	2.4	4.8	0.1	0.1
04-Nov-2001	08:30	5	73.7	0.9	13.0	3.1	8.1	0.2	0.1
06-Dec-2002	11:36	5	72.6	0.8	16.6	2.7	10.1	0.2	0.1
29-Apr-2003	14:37	5	78.9	0.5	20.7	7.1	7.1	0.2	0.1
04-Feb-2004	15:01	5	73.6	0.7	32.5	4.4	18.7	0.6	0.2
05-May-2005	12:20	5	83.2	1.1	51.0	1.4	47.4	1.5	0.2
08-Aug-2006	12:10	5	85.5	1.0	62.6	6.3	45.4	1.8	0.2
23-Jul-2008	14:13	5	105.3	1.3	127.0	4.2	112.1	11.0	0.4
21-Oct-2009	14:53	5	114.8	1.3	147.8	5.5	132.1	15.1	0.9
11-Aug-2010	10:40	5	126.8	1.4	173.3	3.3	162.1	22.7	1.2
18-Oct-2011	10:34	5	142.3	2.2	215.7	7.4	191.7	29.6	1.7
22-May-2012	13:37	5	131.8	1.3	209.2	7.4	188.8	21.3	0.9

Table 76. ALR repeatability of section 200209 for the right wheel path at 125 inches/mi.

Date	Time	Passes	Average IRI (Inches/mi)	IRI SD (Inches/mi)	Average ALR Length (ft)	ALR Length SD (ft)	Common ALR Length (ft)	Average ER (Inches/mi)	ER SD (Inches/mi)
14-Aug-1992	13:17	5	71.3	0.1	19.0	2.0	16.6	0.4	0.0
10-Mar-1993	11:05	5	83.9	3.5	28.1	3.3	21.3	1.6	0.6
15-May-1994	10:10	5	67.2	0.6	19.7	0.9	19.0	0.6	0.0
18-Feb-1995	09:12	5	74.2	1.0	24.1	1.6	21.8	1.2	0.2
20-Apr-1996	13:31	5	80.1	1.8	31.0	6.7	21.5	1.1	0.3
03-Mar-1997	11:40	5	79.1	0.8	37.8	2.3	32.5	1.2	0.1
15-May-1998	10:26	5	81.0	2.7	28.1	6.1	20.4	1.4	0.5
15-Mar-1999	08:34	5	76.1	1.6	21.5	2.3	19.1	1.0	0.1
01-Mar-2000	11:25	5	78.9	0.8	29.1	2.0	25.1	1.0	0.1
10-May-2001	14:08	5	85.5	1.6	33.1	4.0	25.1	1.6	0.3
21-Apr-2002	08:01	5	77.6	3.7	22.4	2.0	18.3	0.7	0.1
20-Feb-2003	10:41	5	79.7	1.1	28.8	3.0	24.0	1.3	0.3
12-Mar-2004	17:15	5	75.4	1.1	28.2	5.2	21.5	0.8	0.2
05-Jun-2006	12:58	5	76.2	1.1	26.4	1.8	23.8	0.7	0.0
19-Apr-2008	09:42	5	79.4	1.8	32.5	3.7	25.0	0.8	0.1
07-Aug-2009	09:44	5	79.6	1.7	25.1	1.4	22.6	1.2	0.4
19-Oct-2010	16:28	5	81.3	1.1	25.8	3.1	22.4	1.1	0.4
21-Sep-2012	14:20	5	80.2	0.5	33.0	1.3	30.7	0.9	0.2
03-Dec-2013	16:25	5	77.9	1.3	24.1	0.3	20.8	0.6	0.1
05-May-2014	14:17	5	87.0	2.5	37.0	5.8	25.4	1.6	0.3
06-May-2014	06:57	5	75.4	2.1	23.5	3.5	17.9	0.5	0.1
06-May-2014	14:23	5	88.8	0.6	43.6	7.7	29.1	1.7	0.3
06-May-2014	20:25	5	76.0	1.7	23.8	1.0	21.7	0.7	0.1
09-Dec-2015	13:08	5	81.4	0.7	30.1	2.6	22.7	0.7	0.1

Table 77. ALR repeatability of section 370260 for the right wheel path at 125 inches/mi.

Date	Time	Passes	Average IRI (Inches/mi)	IRI SD (Inches/mi)	Average ALR Length (ft)	ALR Length SD (ft)	Common ALR Length (ft)	Average ER (Inches/mi)	ER SD (Inches/mi)
30-Mar-1994	10:28	5	101.2	0.9	60.5	3.9	44.9	4.6	0.5
06-Jan-1996	05:46	5	99.1	0.5	47.2	3.9	39.5	4.7	0.1
28-Feb-1996	10:43	5	97.4	1.1	50.6	1.7	41.7	3.9	0.2
07-Oct-1997	13:55	5	98.7	0.5	60.7	4.7	49.1	4.5	0.3
18-Feb-1998	13:23	5	100.9	0.3	57.7	4.0	46.4	4.6	0.2
19-May-1998	10:52	5	99.6	1.3	60.4	4.9	46.0	4.2	0.2
24-Jul-1998	11:14	5	98.6	0.5	55.6	2.1	44.1	4.5	0.1
04-Nov-1998	08:45	5	106.1	0.8	81.3	6.1	59.6	6.7	0.1
11-Nov-1999	00:04	5	102.8	0.4	75.4	4.0	61.8	6.0	0.4
13-Mar-2000	14:02	5	102.8	1.8	78.0	5.3	65.1	5.8	0.2
08-Nov-2000	11:16	5	104.1	1.1	86.2	4.4	74.5	6.8	0.3
14-Jul-2001	09:19	5	102.7	1.1	87.1	6.3	66.0	6.2	0.6
11-Oct-2001	08:45	5	107.2	1.2	94.7	2.8	75.8	7.1	0.3
23-May-2002	10:07	5	103.7	1.2	91.7	1.2	80.2	6.9	0.3
19-Sep-2002	17:31	5	104.6	0.3	88.4	2.1	81.7	6.7	0.2
22-Jan-2003	15:42	5	104.8	0.4	98.2	5.9	86.0	7.2	0.4
01-Jun-2003	11:58	5	103.4	1.3	97.3	8.7	80.2	6.4	0.3
07-Nov-2003	09:36	5	105.7	2.2	104.2	17.1	75.3	7.5	0.8
14-Nov-2004	15:58	5	108.2	0.9	110.9	4.5	100.8	8.4	0.4
14-Jun-2006	15:42	5	105.2	0.7	98.8	8.3	79.2	7.1	0.3
30-Nov-2006	12:41	5	102.4	3.0	99.4	13.2	70.5	6.0	1.0
18-Mar-2009	15:51	5	103.4	1.1	100.3	4.7	85.7	6.3	0.5
18-Apr-2010	15:14	5	104.4	1.2	97.4	3.1	80.5	6.3	0.3
27-Apr-2011	19:38	5	101.0	1.2	88.6	6.1	69.2	5.3	0.4
10-Dec-2012	13:24	5	102.8	2.3	107.0	12.1	85.2	6.1	1.0
24-Jun-2014	13:23	5	100.9	2.9	82.1	14.2	54.2	5.2	1.1
24-Jun-2014	16:42	5	101.9	2.4	90.1	7.3	61.3	5.6	1.0
24-Jun-2014	19:20	5	105.0	10.5	84.9	20.1	64.2	9.3	8.5
25-Jun-2014	06:08	4	107.2	1.6	105.7	11.5	0.0	7.8	1.2
09-Mar-2015	16:33	5	104.1	4.1	114.2	16.2	89.9	6.6	2.1

ACKNOWLEDGMENTS

The team appreciates the ongoing support of Mr. Larry Scofield of the International Grinding and Grooving Association; he is a true champion of applied research.

REFERENCES

1. National Research Council. 1990. *Specific Pavement Studies, Experimental Design and Research Plan for Experiment SPS-2, Strategic Study of Structural Factors for Rigid Pavements*. SHRP, NRC, Washington, DC.

2. Karamihas, S.M., and K. Senn. 2012. *Curl and Warp Analysis of the LTPP SPS-2 Site in Arizona*, Report No. FHWA-HRT-12-068. Washington, DC: Federal Highway Administration.

3. Chang, G., S.M. Karamihas, R.O. Rasmussen, D. Merritt, and M. Swanlund. 2008. "Quantifying the Impact of Jointed Concrete Curling and Warping on Pavement Uneveness." Presented at the *6th Symposium on Pavement Surface Characteristics*. Portorož, Slovenia: World Road Association.

4. American Association of State Highway and Transportation Officials (AASHTO). 1993. *AASHTO Guide for Design of Pavement Structures*. Washington, DC: AASHTO.

5. Von Quintus, H.L., C. Rao, and L. Irwin. 2015. *Long-Term Pavement Performance Program Determination of In-Place Elastic Layer Modulus: Backcalculation Methodology and Procedures*. Report No. FHWA-HRT-15-036. Washington, DC: Federal Highway Administration.

6. Chang, G.K., S.M. Karamihas, R.O Rasmussen, D.K. Merritt, and M. Ruiz. 2007. *Impact of Temperature Curling and Moisture Warping on Jointed Concrete Pavement Performance, Volume II. Data Analysis and Model Development*. Washington, DC: Federal Highway Administration.

7. Jiang, Y.J., and M.I. Darter. 2005. *Structural Factors on Jointed Plain Concrete Pavements: SPS-2—Initial Evaluation and Analysis*. Report No. FHWA-RD-01-167. Washington, DC: Federal Highway Administration.

8. Federal Highway Administration. n.d.. "LTPP InfoPave™" (website). https://infopave.fhwa.dot.gov/, last accessed March 15, 2016.

9. Simpson, A.L., P.N. Schmalzer, and G.R. Rada. 2007. *Long Term Pavement Performance Project Laboratory Materials Testing and Handling Guide*. Report No. FHWA-HRT-07-052. Washington DC: Federal Highway Administration.

10. Hall, K.T., M.I. Darter, T.H. Hoerner, and L. Khazanovich. 1997. *LTPP Data Analysis Phase I: Validation of Guidelines for k-Value Selection and Concrete Pavement Performance Prediction*, Report No. FHWA-RD-96-198. Washington, DC: Federal Highway Administration.

11. Karamihas, S.M. 2007. *Profile Analysis of the LTPP SPS-1 Site in Arizona*. Report No. UMTRI-2007-16. Ann Arbor, MI: University of Michigan Transportation Research Institute.

12. Karamihas, S.M., and K. Senn. 2009. “Profile Analysis of Arizona Specific Pavement Studies 5 Project.” *Transportation Research Record*, no. 2095: 144–152.

13. Karamihas, S.M. and K. Senn. 2010. *Profile Analysis of the LTPP SPS-6 Site in Arizona*. Report No. UMTRI-2010-17. Ann Arbor, MI: University of Michigan Transportation Research Institute.

14. Perera, R.W., and S.D. Kohn. 2005. *Quantification of Smoothness Index Differences Related to Long-Term Pavement Performance Equipment Type*. Report No. FHWA-HRT-05-054. Washington DC: Federal Highway Administration.

15. Johnson, A. 1993. *SPS-2 Construction Report: I–70 Near Abilene, Kansas*. St. Paul, MN: Braun Intertec Pavement, Inc.

16. Nichols Consulting Engineers. 1997. *Construction Report on Site 530200*. Reno, NV: Nichols Consulting Engineers.

17. Pozsgay, M.A. 1998. *Construction Report for Ohio SPS-2*. Washington, DC: Federal Highway Administration.

18. Rutka, A. 1994. *Construction Report on SPS-2, Project 370200, 1993, US RTE 52 SB, Lexington By-Pass*. Report No. FHWA-RD-94-3701. Washington, DC: Federal Highway Administration.

19. Szrot, R.B. 1994. *Construction Report for Experiment SPS-2*. Reno, NV: Nichols Consulting Engineers.

20. Westergaard, H.M. 1927. “Analysis of Stresses in Concrete Roads Caused by Variations of Temperature.” *Public Roads*, *8*(3): 54–60.

21. National Aeronautics and Space Administration Goddard Space Flight Center. n.d. “Modern-Era Retrospective Analysis for Research and Applications (MERRA)” (website). https://gmao.gsfc.nasa.gov/reanalysis/MERRA, last accessed July 6, 2017.

22. RStudio. n.d. “RStudio: Integrated Development for R. RStudio, Inc.” (website). http://www.rstudio.com/, last accessed October 18, 2018.

23. LAW PCS. 2000. “LTPP Manual for Falling Weight Deflectometer Measurements: Operational Field Guidelines, Version 3.1.” Washington, DC: Federal Highway Administration.

24. American Association of State Highway and Transportation Officials (AASHTO). 2018. *Standard Practice for Accepting Pavement Ride Quality When Measured Using Inertial Profiling Systems*. AASHTO R 54-14. Washington, DC: AASHTO.

25. Stanton, T.E. 1944. *First Report on the Experimental Concrete Pavement Constructed in Ventura County During October 1941 as a Part of the Investigation of Joint Spacing in*

Concrete. Report No. R-00194. Sacramento, CA: State of California Department of Public Works, Division of Highways.

26. Hveem, F.N. 1949. *A Report of an Investigation to Determine Causes for Displacement and Faulting at the Joints in Portland Cement Concrete Pavements.* Sacramento, CA: California Division of Highways, Materials and Research Department,.

27. Hveem, F.N. 1951. "Slab Warping Affects Pavement Joint Performance." *Journal of the American Concrete Institute* 22 no. 10: 797–808.

28. Hveem, F.N. 1952. *Ten Year Report Investigational Concrete Pavement in California Cooperative Research Project in Joint Spacing.* Sacramento, CA: California Division of Highways, Sacramento.

29. Tremper, B., and D.L Spellman. 1963. "Shrinkage of Concrete—Comparison of Laboratory and Field Performance." *Highway Research Record* 3: 30–61.

30. Moyer, R.A. 1950. "Report of Committee on Antiskid Properties of Road Surfaces." *Highway Research Board Bulletin*, no. 27: 1–13.

31. Housel, W.S. 1962. "Cumulative Changes in Rigid Pavements with Age in Service." *Highway Research Board Bulletin*, no. 328: 1–23.

32. State Highway Commission of Kansas. 1949. *Kansas Experimental Concrete Pavement*. Construction Project 10–13 PWS 2. Topeka, KS: State Highway Commission of Kansas.

33. Evans, M., Jr., and W.B. Drake. 1959. *17-Year Report on the Owensboro-Hartford Co-operative Investigation of Joint Spacing in Concrete Pavements*. Lexington, KY: Commonwealth of Kentucky Department of Highways, Highway Materials and Research Laboratory.

34. Highway Research Board. 1962. *The AASHO Road Test. Report 5. Pavement Research*. Washington DC: National Academy of Sciences, National Research Council.

35. Yu, H.T., L. Khazanovich, M.I. Darter, and A. Ardani. 1998. "Analysis of Concrete Pavement Response to Temperature and Wheel Loads Measured from Instrumented Slabs." *Transportation Research Record*, no. 1639: 94–101.

36. Jeong J.H., and D.G. Zollinger. 2004. "Early-Age Curling and Warping Behavior: Insights from a Fully Instrumented Test-Slab System." *Transportation Research Record*, no. 1896: 66–74.

37. Ardani, A. 2006. *Implementation of Proven PCCP Practices in Colorado.* Report No. CDOT-DTD-R-2006-9. Denver, CO: Colorado Department of Transportation.

38. Lowrie, C., and W.J. Nowlen. 1960. "Progress Report: Colorado Concrete Pavement and Subbase Experiment Project." *Highway Research Board Bulletin 274*, *Concrete Pavement Design and Performance Studies,* 150–161, National Research Council, Washington, DC.

39. Spellman, D.L., J.R. Stoker, and B.F. Neal. 1970. *California Pavement Faulting Study. Interim Report.* Report No. M&R 635167-1. Sacramento, CA: State of California, Division of Highways, Materials and Research Department.

40. Rao, S., and J.R. Roesler. 2005. "Characterizing Effective Built-In Curling from Concrete Pavement Field Measurements." *Journal of Transportation Engineering* 131, no. 4: 320–327.

41. Rao, S. 2006. "Characterizing Effective Built-In Curling and its Effect on Concrete Pavement Cracking." Ph.D. dissertation. University of Illinois at Urbana-Champaign. https://www.ideals.illinois.edu/handle/2142/29960, last accessed May 13, 2020.

42. Armaghani, J.M., T.J. Larsen, and L.L. Smith. 1987. "Temperature Response of Concrete Pavements." *Transportation Research Record*, no. 1121: 23–33.

43. Goldsberry, B.M. 1988. "Thermal Effect Curling of Concrete Pavements on U.S. 23 Test Road." Master's Thesis. Ohio University.

44. Poblete, M., R. Salsilli, R. Valenzuela, A. Bull, and P. Spratz. 1988. "Field Evaluation of Thermal Deformations in Undoweled PCC Pavement Slabs." *Transportation Research Record*, no. 1207: 217–228.

45. Yu, H.T., and L. Khazanovich. 2001. "Effects of Construction Curling on Concrete Pavement Behavior." Presented at the *7th International Conference on Concrete Pavements*. Lake Buena Vista, FL: International Society for Concrete Pavements.

46. Rao, S., and J.R. Roesler. 2005. "Nondestructive Testing of Concrete Pavements for Characterization of Effective Built-In Curling." *Journal of Testing and Evaluation* 33, no. 5: 356–363.

47. Teller, L.W., and E.C. Sutherland. 1935. "The Structural Design of Concrete Pavements. Part 1—A Description of the Investigation." *Public Roads 16*, no. 8: 145–158.

48. Teller, L.W., and E.C. Sutherland. 1935. "The Structural Design of Concrete Pavements. Part 2—Observed Effects of Variations in Temperature and Moisture on the Size, Shape and Stress Resistance of Concrete Pavement Slabs." *Public Roads 16*, no. 9: 169–197.

49. Kim, S., H. Ceylan, and K. Gopalakrishnan. 2007. "Initial Smoothness of Concrete Pavements Under Environmental Loads." *Magazine of Concrete Research 59*, no. 8: 599–609.

50. Ceylan, H., S. Kim, K. Gopalakrishnan, and K. Wang. 2007. "Environmental Effects on Deformation and Smoothness Behavior of Early-Age Jointed Plain Concrete Pavements." *Transportation Research Record*, no. 2037: 30–39.

51. Pradena, M., and L. Houben. (2017). "Ride Quality Stability of Jointed Plain-Concrete Road Pavements with Short Slabs." *Proceedings of the Institution of Civil Engineers – Transport, 171*, 3, 1–8, London, UK.

52. Rao, C., E. Barenberg, M.B. Snyder, and S. Schmidt. (2001). “Effects of Temperature and Moisture on the Response of Concrete Pavements.” *Proceedings*, *7th International Conference on Concrete Pavements*, 23–38, International Society for Concrete Pavements, Lake Buena Vista, FL.

53. Hansen, W., D.L. Smiley, Y. Peng, and E.A. Jensen. 2002. “Validating Top-Down Premature Transverse Slab Cracking in Jointed Plain Concrete Pavement.” *Transportation Research Record*, no. 1809: 52–59.

54. Beckemeyer, C.A., L. Khazanovich, and H.T. Yu. 2002. “Determining the Amount of Built-in Curling in Jointed Concrete Pavement.” *Transportation Research Record*, no. 1809: 85-92.

55. Vandenbossche, J.M. 2003. “Interpreting Falling Weight Deflectometer Results for Curled and Warped Portland Cement Concrete Pavements.” Ph.D. dissertation, University of Minnesota.

56. Wells, S.A., B.M. Phillips, and J.M. Vandenbossche. 2006. “Quantifying Built-in Construction Gradients and Early-Age Slab Deformation Caused by Environmental Loads in a Jointed Plain Concrete Pavement.” *International Journal of Pavement Engineering* 7, no. 4: 275–289.

57. Asbahan, R., and J. Vandenbossche. 2011. “Effects of Temperature and Moisture Gradients on Slab Deformation for Jointed Plain Concrete Pavements.” *Journal of Transportation Engineering* 137 no. 8: 563–570.

58. Kim, S. 2006. “Early Age Behavior of Jointed Plain Concrete Pavements Subjected to Environmental Loads.” Ph.D. dissertation, Iowa State University.

59. Ceylan, H., D.J. Turner, R.O. Rasmussen, G.K. Chang, and J. Grove. 2007. *Impact of Curling, Warping, and Other Early-Age Behavior on Concrete Pavement Smoothness: Early, Frequent, and Detailed (EFD) Study. Phase II Final Report.* Report No. FHWA DTFH61-01-X-00042. Washington, DC: Federal Highway Administration.

60. Chen, Z., S. Nassiri, and J. Uhlmeyer. 2016. “Quantifying Effective Built-in Temperature Difference for Decades-Old Jointed Plain Concrete Pavements in Eastern Washington State.” Presented at the *11th International Conference on Concrete Pavements*. San Antonio, TX: International Society for Concrete Pavements.

61. Hogentogler, C.A. 1923. “Apparatus Used in Highway Research Projects in the United States. Results of a Census.” *Bulletin of the National Research Council* 6, no.4: 35, 47–49.

62. Pope, C.S. 1938. “Concrete Pavement Slab Warp and Prevention.” *California Highways and Public Works* 16, no.3: 20–22.

63. Ceylan, H., R.F. Steffs, K. Gopalakrishnan, S. Kim, and S. Yang. 2016. *Development and Evaluation of a Portable Device for Measuring Curling and Warping in Concrete Pavements*. Ames, IA: Institute for Transportation, Iowa State University.

64. Lederle, R.E., R.W. Lothschutz, and J.E. Hiller. 2011. *Field Evaluation of Built-In Curling Levels in Rigid Pavements*. St. Paul, MN: Minnesota Department of Transportation.

65. Lederle, R.E. 2011. "Accounting for Warping and Differential Drying Shrinkage Mechanisms in the Design of Jointed Plain Concrete Pavements." Master's Thesis. Michigan Technological University.

66. Ceylan, H., S. Yang, K. Gopalakrishnan, S. Kim, P. Taylor, and A. Alhasan. 2016. *Impact of Curling and Warping on Concrete Pavement*. Report No. IHRB Project TR-668. Ames, IA: Institute for Transportation, Iowa State University.

67. Darlington, J.R., and P. Milliman. 1968. "A Progress Report on the Evaluation and Application Study of the General Motors Rapid Travel Road Profilometer." *Highway Research Record,* no. 214: 50–67.

68. Sayers, M.W., and S.M. Karamihas. 1996. *Interpretation of Road Roughness Profile Data*, Report No. FHWA-RD-96-101. Washington, DC: Federal Highway Administration.

69. Perera, R.W., C. Byrum, and S.D. Kohn. 1998. *Investigation of Development of Pavement Roughness*. Report No. FHWA-RD-97-147. Washington, DC: Federal Highway Administration.

70. Karamihas, S.M., T.D. Gillespie, S.D. Kohn, and R.W. Perera. 1999. *Guidelines for Longitudinal Pavement Profile Measurement*. Report No. NCHRP Report 434. Washington, DC: Transportation Research Board.

71. Perera, R.W., S.D. Kohn, and S. Tayabji. 2005. *Achieving a High Level of Smoothness in Concrete Pavements Without Sacrificing Long-Term Performance*. Report No. FHWA-HRT-05-068. Washington, DC: Federal Highway Administration.

72. Perera, R.W., and S.D. Kohn. 1994. *Road Profiler Data Analysis and Correlation, Road Profiler User Group Fifth Annual Meeting, Harrisburg, Pennsylvania*. Report No. 92-30. Plymouth, MI: Soil and Materials Engineers, Inc.

73. Karamihas, S.M., R.W. Perera, T.D. Gillespie, and S.D. Kohn. 2001. "Diurnal Changes in Profile of Eleven Jointed PCC Pavements." Presented at *7th International Conference on Concrete Pavements*. Lake Buena Vista, FL: International Society for Concrete Pavements.

74. Johnson, A.M., B.C. Smith, W.H. Johnson, and L.W. Gibson. 2010. *Evaluating the Effect of Slab Curling on IRI for South Carolina Concrete Pavements*. Report No. FHWA-SC-10-04. Columbia, SC: South Carolina Department of Transportation.

75. Byrum, C.R. 2000. "Analysis by High-Speed Profile of Jointed Concrete Pavement Slab Curvatures." *Transportation Research Record* no. 1730: 1–9.

76. Sixbey, D., M. Swanlund, N. Gagarin, and J.R. Mekemson. 2001. "Measurement and Analysis of Slab Curvature in JCP Pavements Using Profiling Technology." Presented at the

7th International Conference on Concrete Pavements. Lake Buena Vista, FL: International Society for Concrete Pavements.

77. Byrum C.R. 2001. *A High-Speed Profiler Based Slab Curvature Index for Jointed Concrete Pavement Curling and Warping Analysis*. Ph.D. dissertation. University of Michigan.

78. Byrum, C.R. "The Effect of Locked-in Curvature on PCC Pavement," in *Long-Term Performance Program: Making Something of It: Papers from the International Contest on LTPP Data Analysis 1998–1999*, ed. R. G. Hicks and J. B. Sorenson (Reston, Va.: American Society of Civil Engineers), 1–20.

79. Sayers, M.W., and S.M. Karamihas. 1998 *The Little Book of Profiling: Basic Information About Measuring and Interpreting Road Profiles.* Ann Arbor, MI: University of Michigan Transportation Research Institute.

80. W. Hudson, D. Halbach, J. Zaniewski, and L. Moser, "Root-Mean-Square Vertical Acceleration as a Summary Roughness Statistic," in *Measuring Road Roughness and Its Effects on User Cost and Comfort*, ed. T. Gillespie and M. Sayers (West Conshohocken, PA: ASTM International, 1985), 3–24.

81. Byrum, C.R. 2006. "Evaluation of Pavement Slab Rocking and Pumping with Elevation Profile Data." *Transportation Research Record*, no. 1947: 28–35.

82. Byrum, C.R. 2010. "Evaluating Effectiveness of Dowels in Jointed-Concrete Pavements with Faulting Data from Rapid-Travel Profilers." *Transportation Research Record*, no. 2154: 32-43.

83. Byrum, C.R. 2009. "Measuring Curvature in Concrete Slabs and Connecting the Data to Slab Modeling Theory." *Transportation Research Record*, no. 2094: 79–88.

84. Gagarin, N., and J.R. Mekemson. 2006. "Analysis of Surface Profiles Measured on Jointed Portland Cement Concrete Pavements." *Journal of the ASTM International* 3, no. 4: 27–38.

85. Chang, G.K., D.K. Merritt, S.M. Karamihas, R.O. Rasmussen, and D.J. Turner. 2007. *Impact of Temperature Curling and Moisture Warping on Jointed Concrete Pavement Performance, Volume I Data Collection*. Washington, DC: Federal Highway Administration.

86. Ruiz, J.M., A.G. Miron, G.K. Chang, R.O. Rasmussen, and X. Qinwu. 2008. "Use of Slab Curvature and ProVAL to Identify the Cause of Premature Distresses." *Transportation Research Record*, no. 2068: 87–96.

87. Merritt, D.K., G.K. Chang, H.N. Torres, K. Mohanraj, and R.O. Rasmussen. 2015. *Evaluating the Effects of Concrete Pavement Curling and Warping on Ride Quality*. Report No. CDOT-2015-07. Denver, CO: Colorado Department of Transportation.

88. Siddique, Z.Q. 2004. "Finite Element Simulation of Curling on Concrete Pavements." Ph.D. dissertation. Kansas State University.

89. Adu-Gyamfi, Y.O., N.O. Attoh-Okine, and A.Y. Ayenu-Prah. 2010. "Analysis of Different Hilbert-Huang Algorithms for Pavement Profile Evaluation." *Journal of Computing in Civil Engineering* 24, no. 6: 514–524.

90. Gagarin, N., N.E. Huang, M.E. Oskard, D.G. Sixbey, and J.R. Mekemson. 2004. "The Application of the Hilbert-Huang Transform to the Analysis of Inertial Profiles of Pavement." *International Journal of Vehicle Design* 36, no. 2/3: 287–301.

91. Franta, D.P. 2012. "Computational Analysis of Rigid Pavement Profiles." Master's thesis. University of Minnesota.

92. Dufalla, N., K. Senn, and P. Schmalzer. 2016. *Development of an SPS-2 Pavement Preservation Experiment*. Report No. TPF-5(291). Reno, NV: Nichols Consulting Engineers.

93. Karamihas, S.M. 2004. "Development of Cross Correlation for Objective Comparison of Profiles." *International Journal of Vehicle Design* 36, no. 2/3: 173–193.

94. Sayers, M.W. 1989. "Two Quarter-Car Models for Defining Road Roughness: IRI and HRI." *Transportation Research Record*, no. 1215: 165–172.

95. Karamihas, S.M., T.D. Gillespie, and S.M. Riley. 1995. "Axle Tramp Contribution to the Dynamic Wheel Loads of a Heavy Truck." Presented at the *4th International Symposium on Heavy Vehicle Weights and Dimensions*. Ann Arbor, MI.

96. American Association of State Highway and Transportation Officials (AASHTO). 2017. *Standard Practice for Evaluating Faulting of Concrete Pavements.* AASHTO R 36-13. Washington, DC: AASHTO.

97. Chang, G., J. Watkins, and R. Orthmeyer. 2012. "Practical Implementation of Automated Fault Measurement Based on Pavement Profiles." *American Society for Testing and Materials STP*, no. 1555: 219–237. West Conshohocken, PA: ASTM International.

98. Mississippi Department of Transportation. 2010. *BATCHCALCFAULT Software User Guide 3.00*. Jackson, MS: Mississippi Department of Transportation.

99. Nazef, N., A. Mraz, I. Shivprakash, and B. Choubane. 2009. "Semi-Automated Faulting Measurement for Rigid Pavements." *Transportation Research Record*, no. 2094: 121–127.

100. Agurla, M., and S. Lin. 2015. *Long-Term Pavement Performance Automated Faulting Measurement*. Report No. FHWA-HRT-14-092. Washington, DC: Federal Highway Administration.

101. Khazanovich, L., S.D. Tayabji, and M.I. Darter. 2000. *Backcalculation of Layer Parameters for LTPP Test Sections, Volume I: Slab on Elastic Solid and Slab on Dense-Liquid Foundation Analysis of Rigid Pavements*, Report No. FHWA-RD-00-086. Washington, DC: Federal Highway Administration.

102. Smith, K.D., M.J. Wade, D.G. Peshkin, L. Khazanovich, and H.T. Yu. 1998. *Performance of Concrete Pavements. Volume II–Evaluation of Inservice Concrete Pavements*, Report No. FHWA-RD-95-110. Washington, DC: Federal Highway Administration.

103. Hall, K.T. and A. Mohseni. 1991. "Backcalculation of Asphalt Concrete–Overlaid Portland Cement Concrete Pavement Layer Moduli." *Transportation Research Record*, no. 1293: 112–123.

104. Press, W.H., B.P. Flannery, S.A. Teukolsky, and W.T. Vetterling. 1986. *Numerical Recipes: The Art of Scientific Computing*. Cambridge, UK: Cambridge University Press.

105. Perera, R.W., and S.M. Karamihas. 2017. *2015 Evaluation of High-Speed Inertial Profilers*. Report No. FHWA-RC-17-0003. Washington DC: Federal Highway Administration.

106. Sayers, M.W. 1990. "Profiles of Roughness." *Transportation Research Record*, no. 1260: 106–111.

107. Swan, M., and S.M. Karamihas. 2003. "Use of a Ride Quality Index for Construction Quality Control and Acceptance Specifications." *Transportation Research Record*, no. 1861: 10–16.

108. Sayers, M.W. 1995. "On the Calculation of International Roughness Index from Longitudinal Road Profile." *Transportation Research Record*, no. 1501: 1–12.

109. Karamihas, S.M., M.E. Gilbert, M.A. Barnes, and R.W. Perera. 2019. *Measuring, Characterizing, and Reporting Pavement Roughness of Low-Speed and Urban Roads*, Report 914. Washington, DC: National Cooperative Highway Research Program.

Recycled
Recyclable

Recommended citation: Federal Highway Administration,
Advancing Profile-Based Curl-and-Warp Analysis Using LTPP Profile Data
(Washington, DC: 2023) https://doi.org/10.21949/1521638

HRDI-30/04-23(WEB)E